

**15th International Conference on
Computer and IT Applications in the Maritime Industries**

COMPIT'16

Lecce, 9-11 May 2016

Edited by Volker Bertram



Technische Universität Hamburg-Harburg
Institut für Entwerfen von Schiffen und Schiffssicherheit
Schwarzenbergstraße 95 Gebäude C D-21073 Hamburg



Sponsored by



DNV·GL

www.dnvg.com

BETTMA
CAE Systems SA

www.beta-cae.gr



www.ndar.com



www.numeca.be

AVEVA
CONTINUAL PROGRESSION

CPU 24|7

www.aveva.com

www.cpu-24-7.com

CD-adapco
www.cd-adapco.com

Dell OEM Solutions

www.dell.com/IoT

SARC
Software and services
for the maritime industry

www.sarc.nl

SpecTec

www.spectec.net

SSI
®

www.ssi-corporate.com

NAPA

www.napa.fi

MARORKA

www.marorka.com

SERTICA

By Logimatic

www.sertica.com

CADMATIC
SOFTWARE SOLUTIONS

www.cadmatic.com

SENER

www.foran.es

INTERGRAPH

www.intergraph.com

PROSTEP

www.prostep.com

This work relates to a Department of the Navy Grant issued by the Office of Naval Research Global. The United States Government has a royalty-free license throughout the world in all copyrightable material contained herein.

15th International Conference on Computer and IT Applications in the Maritime Industries, Lecce, 9-11 May 2015, Hamburg, Technische Universität Hamburg-Harburg, 2016, ISBN 978-3-89220-690-3

© Technische Universität Hamburg-Harburg
Schriftenreihe Schiffbau
Schwarzenbergstraße 95c
D-21073 Hamburg
<http://www.tuhh.de/vss>

Index

Andrea Serani, Emilio F. Campana, Matteo Diez, Frederick Stern <i>A Multi-Objective Optimization: Effects of Potential Flow Formulation and RANS</i>	8
Rodrigo Perez Fernandez <i>Learning Curve and Return of Investment in the Implementation of a CAD System in a Generic Shipbuilding Environment</i>	19
Benoit Mallol, Alvaro Del Toro Llorens, Volker Bertram <i>Trends in CFD Illustrated Exemplarily for Competitive Sailing Yachts</i>	33
Vidar Vindøy, Kristin Dalhaug <i>High-Level Vessel Characterization</i>	42
Lars Lindegaard Mikkelsen, Marie Lützen, Signe Jensen <i>Energy Efficient Operation of Offshore Supply Vessels – A Framework</i>	51
Marco Vatteroni <i>A Standard Protocol for Exchanging Technical Data in the Maritime Industries</i>	64
Scott N. MacKinnon, David Bradbury-Squires, Duane Button <i>Virtual Reality Based Training Improves Mustering Performance</i>	75
Thomas Koch, Sankaranarayanan Natarajan, Felix Bernhard, Alberto Ortiz, Francisco Bonnin-Pascual, Emilio Garcia-Fidalgo, Joan Jose Company Corcoles <i>Advances in Automated Ship Structure Inspection</i>	84
Marco Bibuli, Gabriele Bruzzone, Davide Chiarella, Massimo Caccia, Angelo Odetti, Andrea Ranieri, Eleonora Saggini, Enrica Zereik <i>Underwater Robotics for Diver Operations Support: The CADDY Project</i>	99
Leonard Heilig, Stefan Voß <i>A Holistic Framework for Security and Privacy Management in Cloud-Based Smart Ports</i>	110
Monica Lundh, Steven Mallam, Scott MacKinnon <i>A General Arrangements Visualization Approach to Improve Ships' Design and Optimize Operator Performance</i>	123
Thomas DeNucci, Andrew Britton, Michael Daeffler, Greg Sabra, Hans Hopman <i>Multi-Objective Design Study for Future U.S. Coast Guard Icebreakers</i>	130
Giulia De Masi, Manuela Gentile, Roberta Vichi, Roberto Bruschi, Giovanna Gabetta <i>Corrosion Prediction by Hierarchical Neural Networks</i>	146
Gianandrea Mannarini, Nadia Pinardi, Giovanni Coppini <i>VISIR: A Free and Open-Source Model for Ship Route Optimization</i>	161
Louisa Stewart, John Duncan <i>International Replenishment at Sea: Verification and Validation of a Maritime Simulation Capability</i>	172
Scott Patterson, Andrew Webb <i>Potential Benefits of Augmented Reality in the Smart Ship</i>	186

Matthias Roth <i>Recording As-Built via an Open and Lightweight Solution Supplemented by a Process Evaluation Model</i>	195
Donald MacPherson, Stefan Harries, Simon Broenstrup, Joseph Dudka <i>Real Cost Savings for a Waterjet-driven Patrol Craft Design Using a CAESES-NavCad Coupled Solution</i>	204
Wolfgang Gentzsch, Aji Purwanto, Matthias Reyer <i>Cloud Computing for CFD based on Novel Software Containers</i>	218
Denis Morais, Mark Waldie, Nick Danese <i>Open Architecture Applications: The Key to Best-of-Breed Solutions</i>	223
Kohei Matsuo <i>Augmented Reality Assistance for Outfitting Works in Shipbuilding</i>	234
Hans van Vugt, Edward Sciberras, Leo de Vries, Jonathan Heslop, Anthony P. Roskilly <i>Ship Power System Modelling for the Control & Optimisation of Multiple Alternative Energy Sources On-Board a Ship</i>	240
Elisa Berrini, Bernard Mourrain, Yann Roux, Guillaume Fontaine, Eric Jean <i>Parametric Shape Modeler for Hulls and Appendages</i>	255
Joo Hock Ang, Cindy Goh, Yun Li <i>Hybrid Evolutionary Shape Manipulation for Efficient Hull Form Design Optimisation</i>	264
Jesus Mediavilla Varas, Walter Caharija, Renny Smith, Zakirul Bhuiyan, Wasif Naeem, Paul Carter, Ian Renton <i>Autonomous COLREGs Compliant Ship Navigation, Using Bridge Simulators and an Unmanned Vessel</i>	280
Mohamad Motasem Nawaf, Bilal Hijazi, Djamal Merad, Pierre Drap <i>Guided Underwater Survey Using Semi-Global Visual Odometry</i>	288
Anders Dalén, Sandra Haraldsson, Mikael Lind, Niklas Mellegård, Ulf Siwe, Almir Zerem <i>Engineering Requirements for a Maritime Digital Infrastructure - A Sea Traffic Management Perspective</i>	302
Andrea Coraddu, Toine Cleophas, Sandor Ivancsics, Luca Oneto <i>Vessel Monitoring Based on Sensors Data Collection</i>	316
Thomas Mestl, Kay Dausendschön <i>Port ETA Prediction based on AIS Data</i>	331
Rachel J. Pawling, Alexander S. Piperakis, David J. Andrews <i>Applications of Network Science in Ship Design</i>	339
Mary Etienne, Anthony Sayers <i>The Internet of Things for Smarter, Safer, Connected Ships</i>	353
Ørnulf Jan Rødseth, Lokukaluge Prasad Perera, Brage Mo <i>Big Data in Shipping - Challenges and Opportunities</i>	361

George Korbetis, Serafim Chatzimoisiadis, Dimitrios Drougkas <i>Design Optimization using Fluid-Structure Interaction and Kinematics Analyses</i>	374
David Thomson, Andrew Gordon <i>Maritime Asset Visualisation</i>	387
Kjetil Nordby, Stian Børresen, Etienne Gernez <i>Efficient Use of Virtual and Mixed Reality in Conceptual Design of Maritime Work Places</i>	392
Hideo Orihara, Hisafumi Yoshida, Ichiro Amaya <i>Enhanced Voyage Support System based on Detailed Weather and Performance Monitoring</i>	401
Olivia Chaves, Henrique Gaspar <i>A Web Based Real-Time 3D Simulator for Ship Design Virtual Prototype and Motion Prediction</i>	410
Arno Bons, Meeuwis van Wirdum <i>Big Data and (Inland) Shipping: A Sensible Contribution to a Strong Future</i>	420
Jan Furustam <i>On Ways to Collect and Utilize Data from Ship Operation in Naval Architecture</i>	430
Richard Ramsden, Pete Lelliot, Jeremy Thomason, Duncan van Roermund <i>Project Helm: Insights from AIS, Fouling Control and Big Data</i>	439
Kristine Bruun Ludvigsen, Levi Kristian Jamt, Nicolai Husteli, Øyvind Smogeli <i>Digital Twins for Design, Testing and Verification throughout a Vessel's Life Cycle</i>	448
Pero Prebeg, Smiljko Rudan, Jerolim Andrić <i>Evaluation of Surrogate Models of Internal Energy Absorbed by Oil Tanker Structure during Collision</i>	458
Stefan Gunnsteinsson, Jacob Wiegand Clausen <i>Enhancing Performance through Continuous Monitoring</i>	471
Seth Fireman, Angela Lossa, David Singer <i>Fuzzy Logic Single-Objective Optimization Using Multiple Criteria to Understand Human Factors on Early Stage Design</i>	481
Index of authors	491
Call for Papers for next year	

A Multi-Objective Optimization: Effects of Potential Flow Formulation and RANS

Andrea Serani, CNR-INSEAN, Rome/Italy, andrea.serani@insean.cnr.it

Emilio F. Campana, CNR-INSEAN, Rome/Italy, emiliofortunato.campana@cnr.it

Matteo Diez, CNR-INSEAN, Rome/Italy, matteo.diez@cnr.it

Frederick Stern, The University of Iowa, Iowa City/USA, frederick-stern@uiowa.edu

Abstract

The paper investigates on the effects of the hydrodynamic solver on the multi-objective hull-form optimization of the DTMB 5415 model in calm water. Potential flow and RANS are compared. The former is formulated and implemented using two linearization approaches (Kelvin and Dawson), combined with two methods for the wave resistance. The Pareto fronts for the reduction of the resistance at two speeds are obtained by a multi-objective particle swarm optimization and are significantly affected by the potential flow formulation. A correlation analysis with RANS is shown, in order to suggest the most effective potential flow formulation for the present case.

1. Introduction

Simulation-based design optimization (SBDO) integrates optimization techniques, design modification methods and simulation tools in order to support the design decision process. In this context, computer simulations are used extensively as models of real systems, in order to evaluate objective functions and functional constraints. In hull-form design, high fidelity solvers (such as RANS) have shown their capability to provide accurate solutions to the design problem, *Chen et al.* (2015). The computational cost is a critical issue and metamodels and variable fidelity approaches, based on low and high fidelity solvers, have been applied to reduce the computational time and cost of the SBDO. Low-fidelity solvers (such as potential flow (PF)) have been applied to identify suitable design spaces for RANS-based optimization, *Kandasamy et al.* (2013). Identifying the proper trend of the design objective versus the design variables often represents a critical issue for a low fidelity solver, especially when large design modifications are involved. The choice of a low fidelity solver within SBDO represents a critical issue and should be carefully justified, considering the trade-off between computational efficiency and solution accuracy.

The objective of this work is to investigate the effects of the hydrodynamic solver on the results of a multi-objective SBDO in ship hydrodynamics. Two different linearization approaches for the PF solver are compared, namely Kelvin and Dawson, *Bassanini et al.* (1994), combined with two different methodologies for the calculation of the wave resistance: a standard pressure integral over the body surface and the transversal wave cut method, *Telste and Reed* (1994). The work also presents a sensitivity analysis of the hydrodynamic performance using RANS, in order to compare and correlate PF and RANS trends, and evaluate benefits and drawbacks of the PF formulations within SBDO.

The application presented is the hull-form optimization of a USS Arleigh Burke-class destroyer, namely the DTMB 5415 model, an early version of the DDG-51. The DTMB 5415 model has been widely investigated through towing tank experiments, *Stern et al.* (2000), *Longo and Stern* (2005), and SBDO studies, including hull-form optimization, *Tahara et al.* (2008). Recently, the DTMB 5415 model was selected as test case for the SBDO activities within the NATO STO Task Group AVT-204, formed to “Assess the Ability to Optimize Hull Forms of Sea Vehicles for Best Performance in a Sea Environment” and aimed at the multi-objective design optimization for multi-speed reduced resistance and improved seakeeping performance, *Diez et al.* (2015a). Here we show a multi-objective SBDO example, aimed at the reduction of the total resistance at 18 kn and 30 kn, corresponding to Froude number $Fr=0.25$ and $Fr=0.41$, respectively. The case considered is a 2DOF problem with free surface. The model advances in calm water and is free to heave (stationary sinkage) and pitch (stationary

trim). An orthogonal representation of the shape modification is used. Specifically, two sets of orthogonal functions are applied for the modification of the hull and the sonar dome shapes, and controlled by a total number of design variables $N_{dv} = 6$. A multi-objective extension of the deterministic particle swarm optimization algorithm (MODPSO) is used, *Pellegrini et al. (2014)*. The constraints include fixed displacement and fixed length between perpendiculars, along with a $\pm 5\%$ maximum variation of beam and draft, and a reserved volume for the sonar in the dome. PF simulations are conducted using the code WARP (WAve Resistance Program), developed at CNR-INSEAN. RANS investigations are performed using the CFDShip-Iowa code, *Huang et al. (2008)*, developed at the University of Iowa.

2. Geometry, conditions and optimization problem formulation

Fig. 1 shows the geometry of a 5.720 m length DTMB 5415 model used for towing tank experiments, as seen at CNR-INSEAN, *Stern et al. (2000)*. The main particulars of the full scale model and tests conditions are summarized in Tables I and II, respectively.



Fig. 1: 5.720 m length model of the DTMB 5415 (CNR-INSEAN model 2340)

Table I: DTMB 5415 model main particulars (full scale)

Description	Symbol	Units	Value
Displacement	∇	t	8636
Length between perpendiculars	L_{PP}	m	142.00
Beam	B	m	18.90
Draft	T	m	6.16
Longitudinal center of gravity	LCG	m	71.60
Vertical center of gravity	VCG	m	1.39

Table II: Test conditions (full scale)

Description	Symbol	Units	Value
Speed	U_1, U_2	kn	18.00, 30.00
Water density	ρ	kg/m ³	998.5
Kinematic viscosity	ν	m ² /s	1.09·10 ⁻⁶
Gravity acceleration	g	m/s ²	9.803

The multi-objective problem is defined as

$$\begin{aligned}
 & \text{minimize} && f_1(\mathbf{x}), f_2(\mathbf{x}) \\
 & \text{subject to} && \mathbf{l} \leq \mathbf{x} \leq \mathbf{u} \\
 & \text{and to} && g_k(\mathbf{x}) \leq 0, \quad k = 1, \dots, N_g
 \end{aligned} \tag{1}$$

f_1 and f_2 are the total resistance (R_T) in calm water at $Fr=0.25$ and $Fr=0.41$; \mathbf{x} is the design variable vector, \mathbf{l} and \mathbf{u} the design variables lower and upper bound vectors, and g_k the geometrical constraints. These include fixed length between perpendiculars ($L_{PP}=142.0$ m), fixed displacement ($\nabla=8636$ t), beam and draft variation within $\pm 5\%$ of the original values ($B=18.90$ m; $T=6.160$ m), reserved volume in the dome for the sonar (4.9 m diameter; 1.7 m height).

3. CFD methods

3.1 Potential flow formulations and simulation setup

Wave resistance computations are based on the linear PF theory, e.g. *Bassanini et al. (1994)*. The simplest linear formulation (Kelvin linearization) is obtained by assuming that the actual flow is slightly perturbed from the free stream, and its potential function is given by $\phi = Ux + \tilde{\varphi}$, which provides the Neumann-Kelvin (NK) problem for the Laplace equation. A further linearization, suggested by *Dawson (1977)*, is based on the assumption that the flow near the body is perturbed around the double model (DM) flow, and its potential function is given by $\phi = Ux + \varphi_d + \tilde{\varphi}$. NK is usually reasonable for slender bodies and high speeds, whereas DM is usually more suitable for wider bodies and low speeds. Herein, once the flow is solved, the wave resistance is evaluated by both a pressure integral over the body surface and the transverse wave cut method, *Telste and Reed (1994)*. The frictional resistance is estimated using a flat-plate approximation, based on the local Reynolds number, *Schlichting and Gersten (2000)*. The steady 2DOF (sinkage and trim) equilibrium is achieved by iteration of the flow solver and the body equation of motion.

The solver used is WARP, and the linearization and the wave resistance estimation methods are combined, producing four different PF formulations: (a) Neumann-Kelvin with pressure integral method (NK-PI), (b) Neumann-Kelvin with transverse wave cut method (NK-WC), (c) double model linearization with pressure integral method (DM-PI), and (d) double model linearization with transverse wave cut method (DM-WC). Numerical implementation and validation of the numerical solvers are given by *Bassanini et al. (1994)*.

Simulations are performed for the right demi-hull, taking advantage of symmetry about the xz -plane. The computational domain for the free surface is defined within 1 hull length upstream, 3 lengths downstream and 1.5 lengths aside. Table III summarizes the associated panel grid used, Fig. 2.

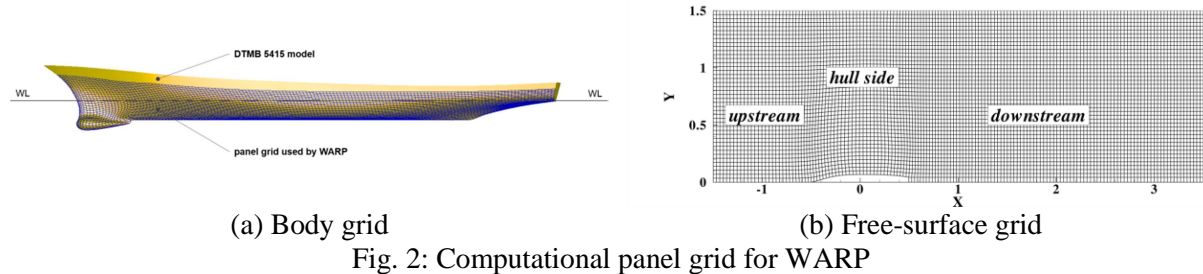


Fig. 2: Computational panel grid for WARP

Table III: Panel grid used for WARP

Hull	Free surface			Total
	Upstream	Hull side	Downstream	
150 × 30	30 × 44	30 × 44	90 × 44	11k

3.2 RANS solver and simulation setup

RANS simulations are performed with the CFDShip-Iowa V4.5 code, which has the capability of a 6DOF simulation and has been developed at IIHR-Hydroscience & Engineering over the past 25 years, for ship hydrodynamics applications. The SST blended $k-\varepsilon/k-\omega$ turbulent model is selected. The free-surface location is predicted by a single phase level set method. A second order upwind scheme is used to discretize the convective terms of momentum equations. For a high performance parallel computing, an MPI-based domain decomposition approach is used, where each decomposed block is mapped to one processor. The code SUGGAR runs as a separate process from the flow solver to compute interpolation coefficients for the overset grid, which enables CFDShip-Iowa to take care of 6DOF with a motion controller at every time step. Only 2DOFs are considered in the current study. Table IV summarizes the associated volume grid used, Fig. 4.

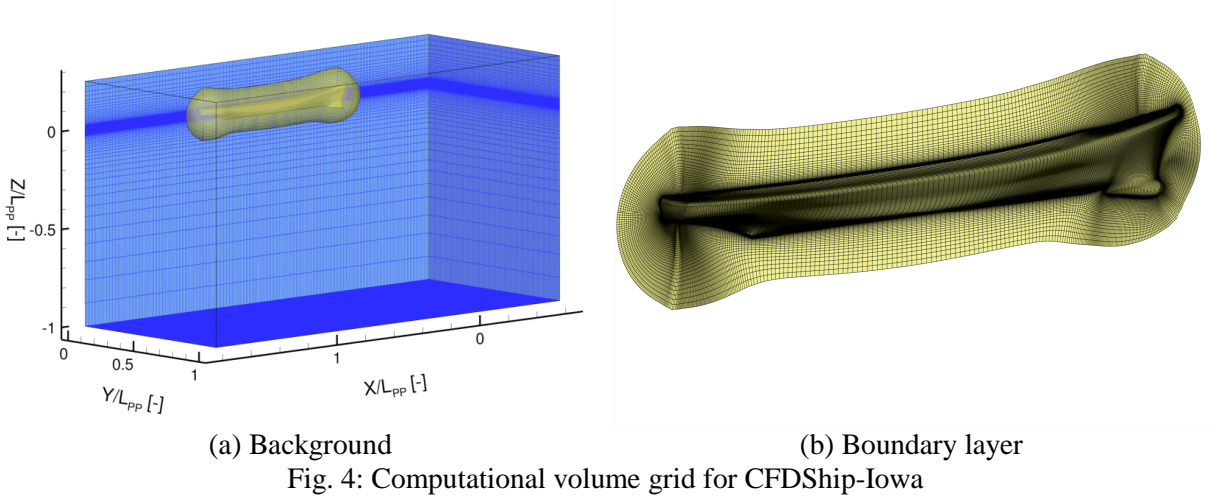


Table IV: Volume grid used for CFDShip-Iowa

Background	Boundary layer	Total
$227 \times 155 \times 115$	$243 \times 71 \times 115$	6M

4. Hull-form modification method

An orthogonal representation of the shape modification is used, *Serani et al. (2015)*, since it is more efficient for shape design optimization, *Diez et al. (2015b)*. Specifically, six orthogonal functions $\Psi_{1,\dots,6}$ are applied for the modification of the hull shape, defined over surface-body patches as

$$\left\{ \begin{array}{l} \Psi_j(\xi, \eta) := \alpha_j \sin\left(\frac{p_j \pi \xi}{A_j} + \phi_j\right) \sin\left(\frac{q_j \pi \eta}{B_j} + \chi_j\right) \mathbf{e}_{k(j)} \\ (\xi, \eta) \in [0; A_j] \times [0; B_j] \end{array} \right. \quad (2)$$

where the coefficient α_j is the corresponding (dimensional) design variable; p_j and q_j define the order of the function in ξ and η direction respectively; ϕ_j and χ_j are the corresponding spatial phases; A_j and B_j define the patch dimension; $\mathbf{e}_{k(j)}$ is a unit vector. Modifications may be applied in x , y or z direction setting $k(j) = 1$, 2, or 3, respectively. Four orthogonal functions ($\Psi_{1,\dots,4}$) and design variables are used for the hull, whereas two functions/variables ($\Psi_{5,6}$) are used for the sonar dome, Fig. 5.

Table V summarized the parameters used here, including upper and lower bounds used for α_j . The results will be presented in terms of non-dimensional design variables $x_j \in [-1,1]$ given by $x_j = 2(\alpha_j - \alpha_{j,\min}) / (\alpha_{j,\max} - \alpha_{j,\min}) - 1$. Details of the design space assessment can be found in *Diez et al. (2015a)*.

Table V: Orthogonal functions parameters

	j	p_j	ϕ_j	q_j	χ_j	$k(j)$	$\alpha_{j,\min}$ [m]	$\alpha_{j,\max}$ [m]
Hull modification	1	2.0	0	1.0	0	2	-1.0	1.0
	2	3.0	0	1.0	0	2	-1.0	1.0
	3	1.0	0	2.0	0	2	-0.5	0.5
	4	1.0	0	3.0	0	2	-0.5	0.5
Sonar dome modification	5	1.0	0	1.0	0	2	-0.3	0.3
	6	0.5	$\pi/2$	0.5	0	3	-0.5	0.5

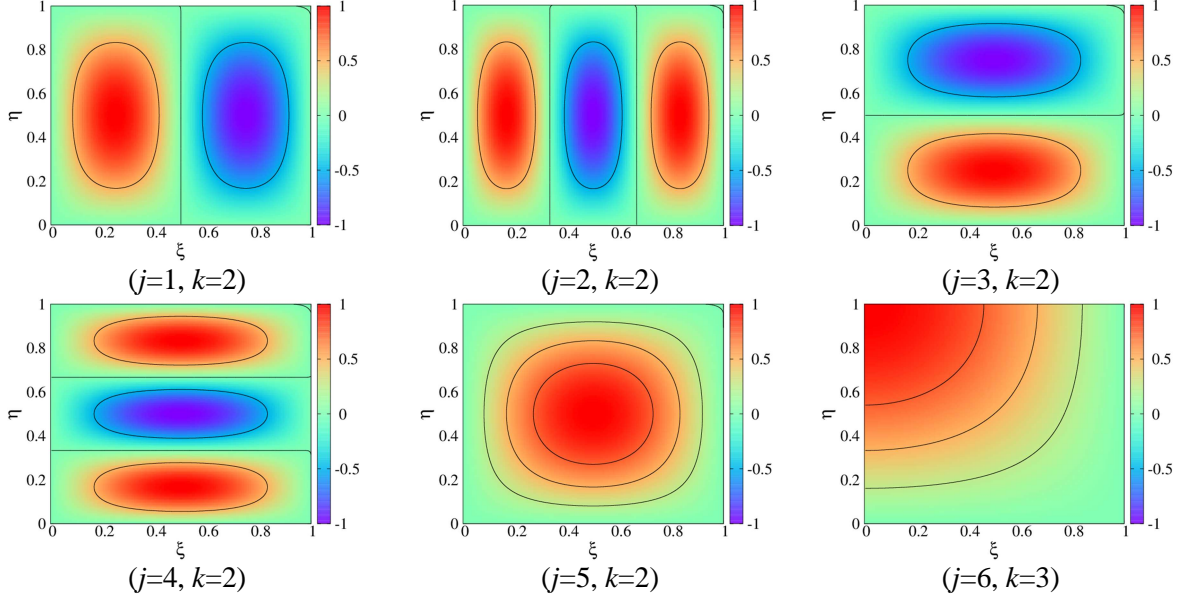


Fig. 5: Orthogonal functions $\psi_j(\xi, \eta)$ for the hull ($j=1, \dots, 4$) and the sonar dome ($j=5, 6$) modifications

5. Multi-objective deterministic particle swarm optimization

Particle swarm optimization (PSO) was originally introduced by *Kennedy and Eberhart (1995)*, based on the social-behaviour metaphor of a flock of birds or a swarm of bees searching for food. PSO belongs to the class of heuristic algorithms for single-objective evolutionary derivative-free global optimization. An efficient deterministic version of PSO (DPSO) is used in this work. Its effectiveness and efficiency in ship SBDO have been shown in *Campana et al. (2009)*, *Serani et al. (2014)*, *Chen et al. (2015)*.

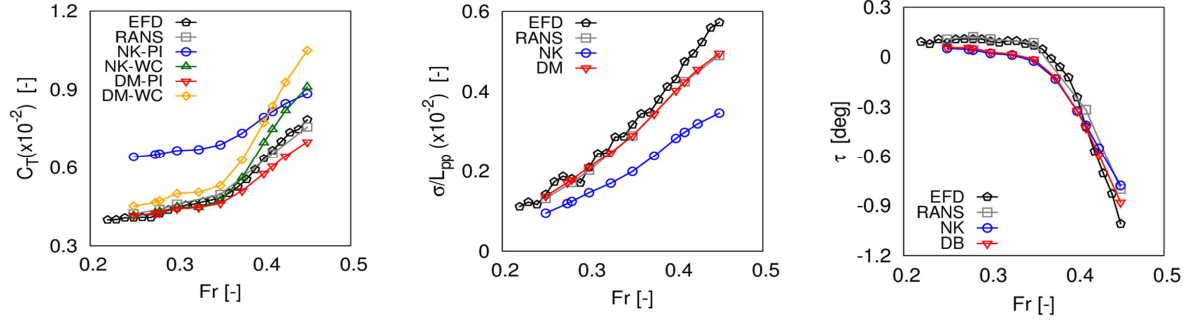
The multi-objective extension of DPSO reads:

$$\begin{cases} \mathbf{v}_i^{k+1} = \chi [\mathbf{v}_i^k + c_1(\mathbf{x}_{i,pb} - \mathbf{x}_i^k) + c_2(\mathbf{x}_{i,gb} - \mathbf{x}_i^k)] \\ \mathbf{x}_i^{k+1} = \mathbf{x}_i^k + \mathbf{v}_i^{k+1} \end{cases} \quad (3)$$

$\mathbf{x}_{i,pb}$ and $\mathbf{x}_{i,gb}$ are respectively the personal (cognitive) and global (social) attractors of the i -th particle. These are defined as the closest point to the i -th particle of the cognitive and social Pareto fronts, respectively. The following setup is used herein, *Pellegrini et al. (2014)*: the number of particles N_p equals 16 times the number of design variables N_{dv} ; the particles initialization includes a Hammersley sequence sampling, *Wong et al. (1997)*, on domain and bounds with non-null velocity, *Chen et al. (2015)*; the coefficients are set as $\chi = 0.6$ and $c_1 = c_2 = 1.7$, *Trelea (2003)*; a semi-elastic wall-type approach is used for box constraints, *Serani et al. (2014)*; a maximum number of function evaluations is set equal to 1,536, which corresponds to $256N_{dv}$.

6. Numerical results

Fig. 6 shows a preliminary validation of PF and RANS simulations versus experimental (EFD) data collected at CNR-INSEAN, *Olivieri et al. (2001)*, for the original DTMB 5415 model ($L_{pp}=5.720$ m). A reasonable trend is shown, especially for low Froude numbers, of total resistance coefficient C_T , sinkage σ , and trim τ , for all formulations but NK-PI for total resistance and NK for sinkage. Fig. 7 shows a preliminary sensitivity analysis in full scale ($L_{pp}=142.0$ m) for each design variable, showing the associated objective function reduction, Δf_1 and Δf_2 . Unfeasible designs are not reported in the plot. Changes in Δf_1 and Δf_2 are found overall significant with each PF formulation. Note how Δf_1 and Δf_2 versus x_1 with NK-PI show an opposite trend compared to the other formulations.



(a) Total resistance coefficient

(b) Sinkage
Fig. 6: Model scale validation for PF and RANS

(c) Trim

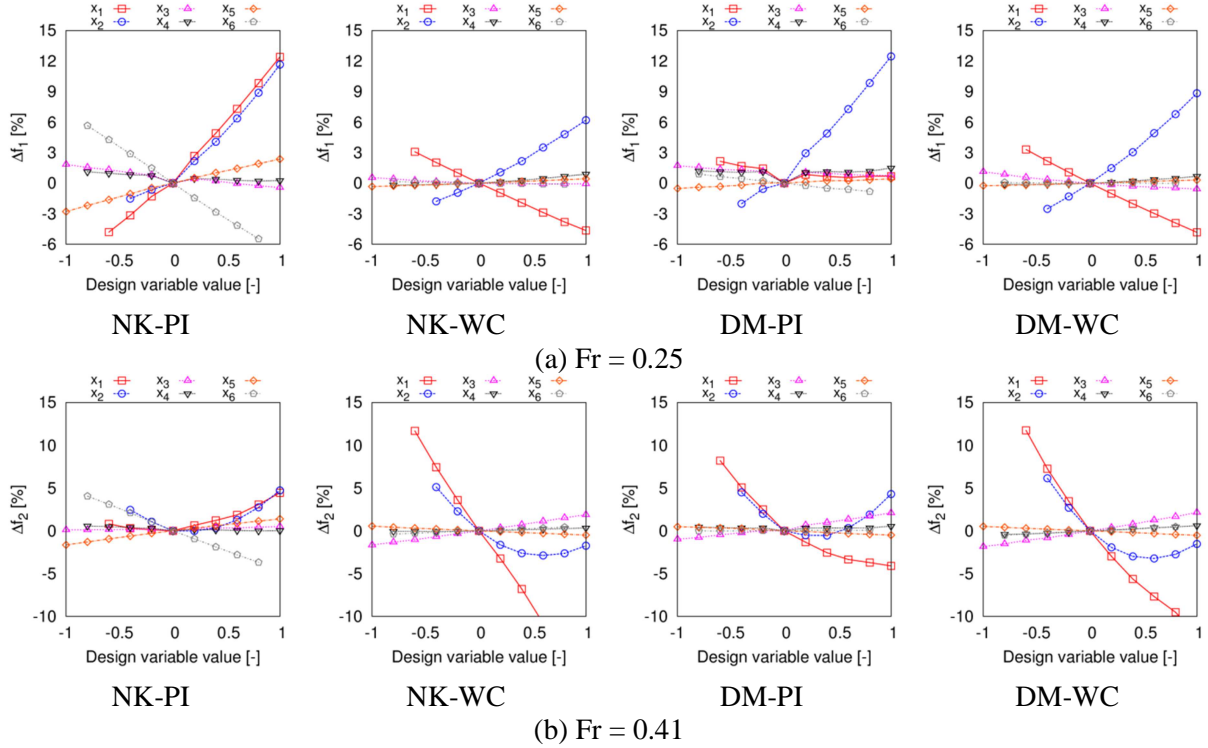


Fig. 7: Preliminary sensitivity analysis with PF

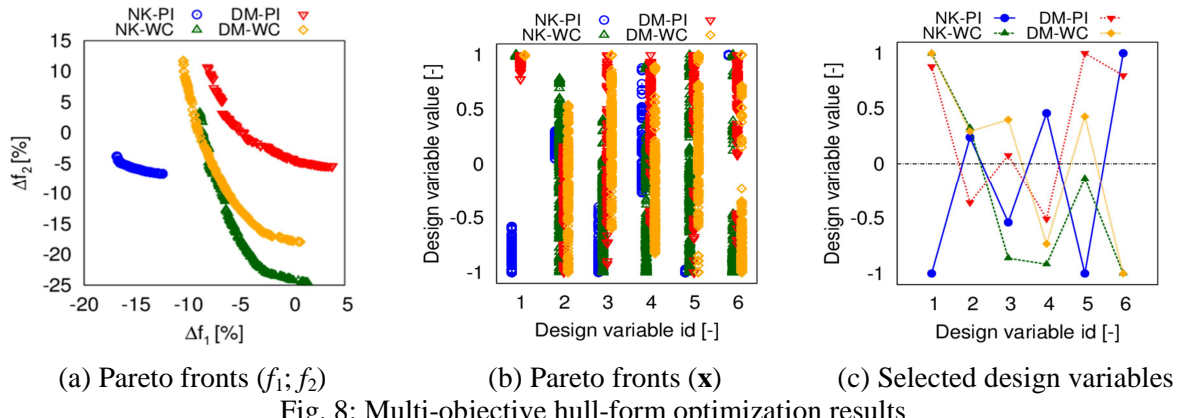


Fig. 8: Multi-objective hull-form optimization results

Fig. 8a shows the Pareto front obtained with each PF formulation. Fig. 8b shows the design variable values of the Pareto front solutions. The best compromise solution between the two objective functions (minimum $\Delta f_1 + \Delta f_2$) is selected, and the corresponding design variable values are shown in Fig. 8c. Different formulations identify different optimal solutions, as also shown in Fig. 9. Table VI

shows the objective function reduction achieved with each PF formulation, for the selected optimal solutions. Except for NK-PI, the reduction of the resistance is consistent with the reduction of the wave elevation pattern, both in terms of transverse and diverging Kelvin waves, for both $\text{Fr}=0.25$ (Fig. 10a) and $\text{Fr}=0.41$ (Fig. 10b). Fig. 11 shows the pressure field of the optimized hulls compared to the original, showing a better pressure recovery towards the stern (except for NK-PI).

Table VI: Hull-form optimization results (selected hulls)

PF formulation	x_1	x_2	x_3	x_4	x_5	x_6	$\Delta f_1(\%)$	$\Delta f_2(\%)$
NK-PI	-1.000	0.239	-0.538	0.458	-1.000	1.000	-16.5	-4.9
NK-WC	0.997	0.325	-0.862	-0.917	-0.136	-0.999	-2.5	-23.0
DM-PI	0.880	-0.358	0.077	-0.505	1.000	0.799	-4.3	-1.1
DM-WC	1.000	0.294	0.399	-0.732	0.427	-1.000	-3.1	-16.3

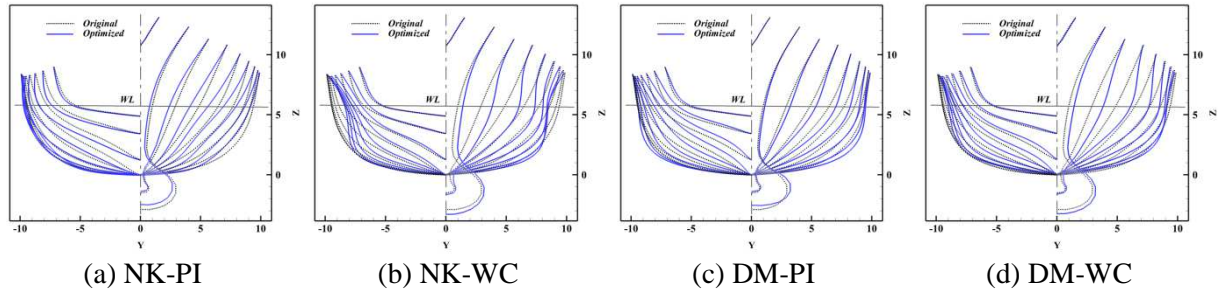


Fig. 9: Selected optimal shapes, compared to the original

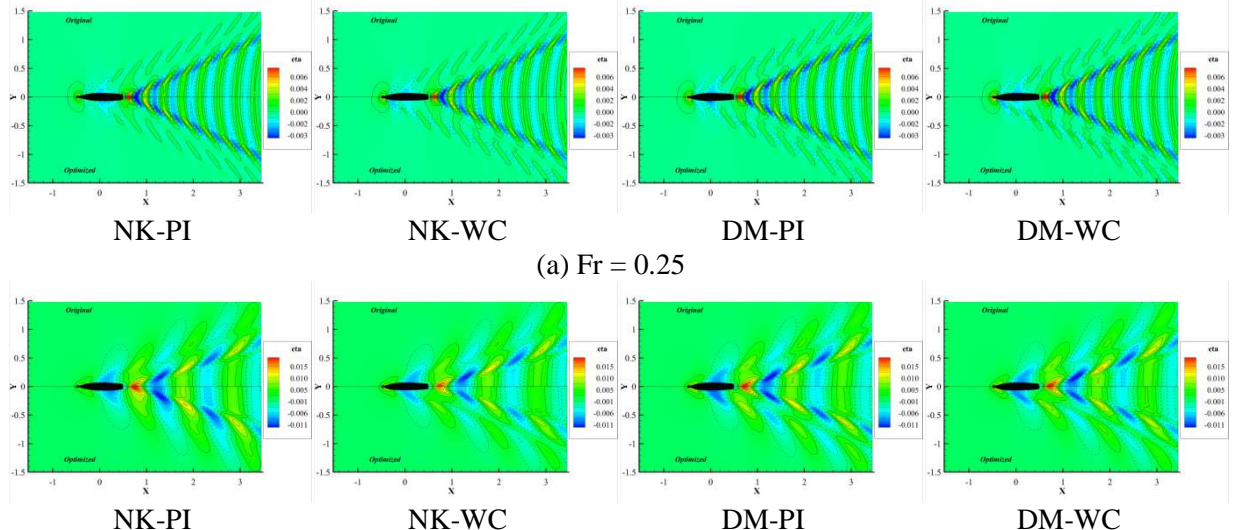


Fig. 10: Wave elevation of the selected optimal hulls, compared with the original

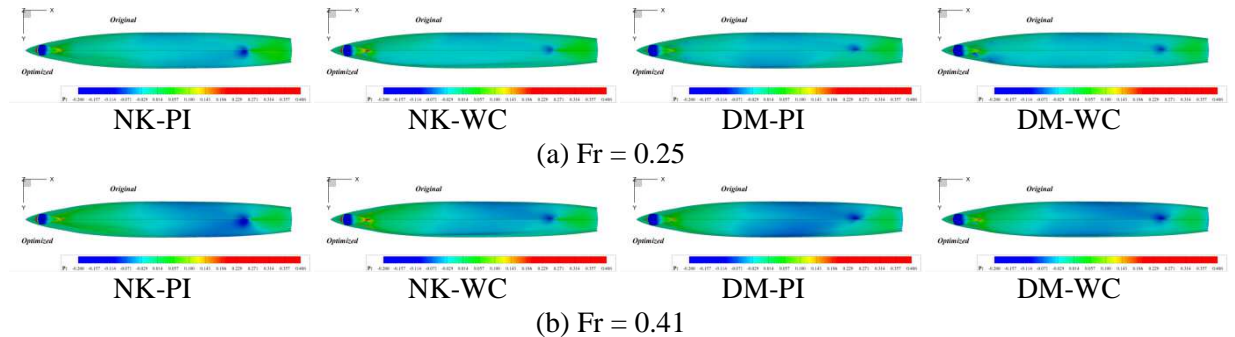


Fig. 11: Pressure of the selected optimal hulls, compared with the original

The heterogeneity of the results obtained with the different PF formulations motivates a further investigation by the RANS solver. Specifically, the sensitivity analysis (in model scale, $L_{PP}=5.720$ m) at $Fr=0.25$ obtained with the PF formulations is compared to RANS for each design variable, Fig. 12.

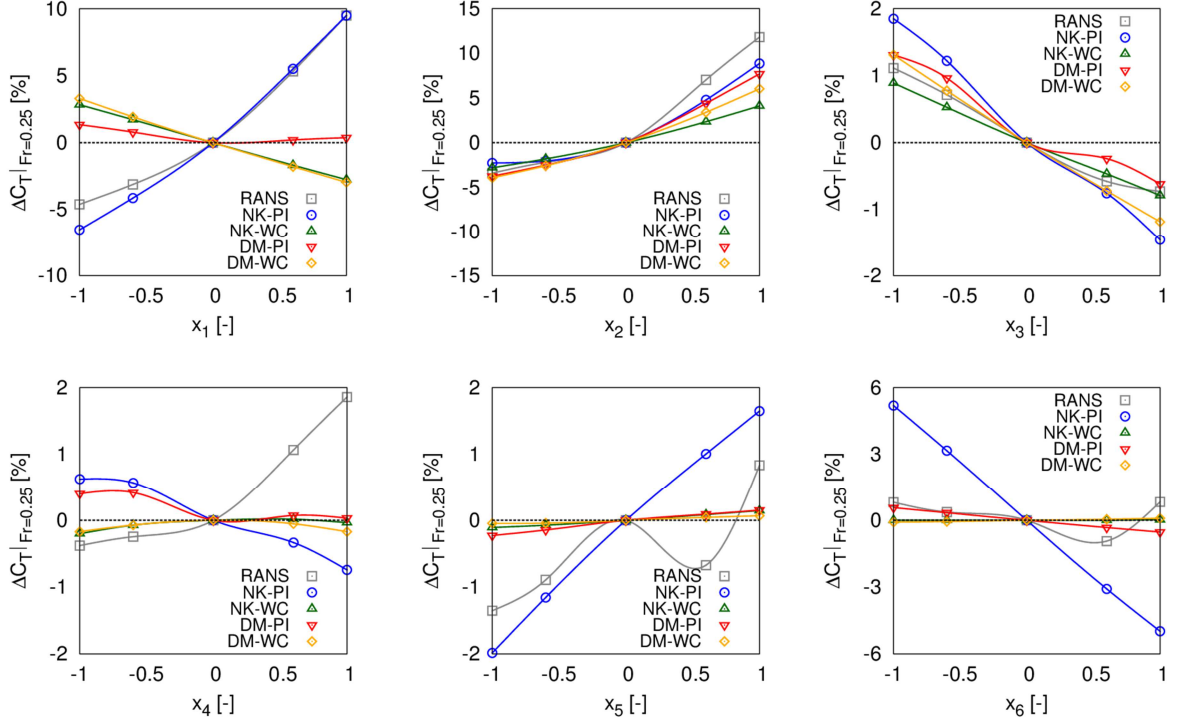


Fig. 12: Comparison of trends between PF and RANS at $Fr=0.25$

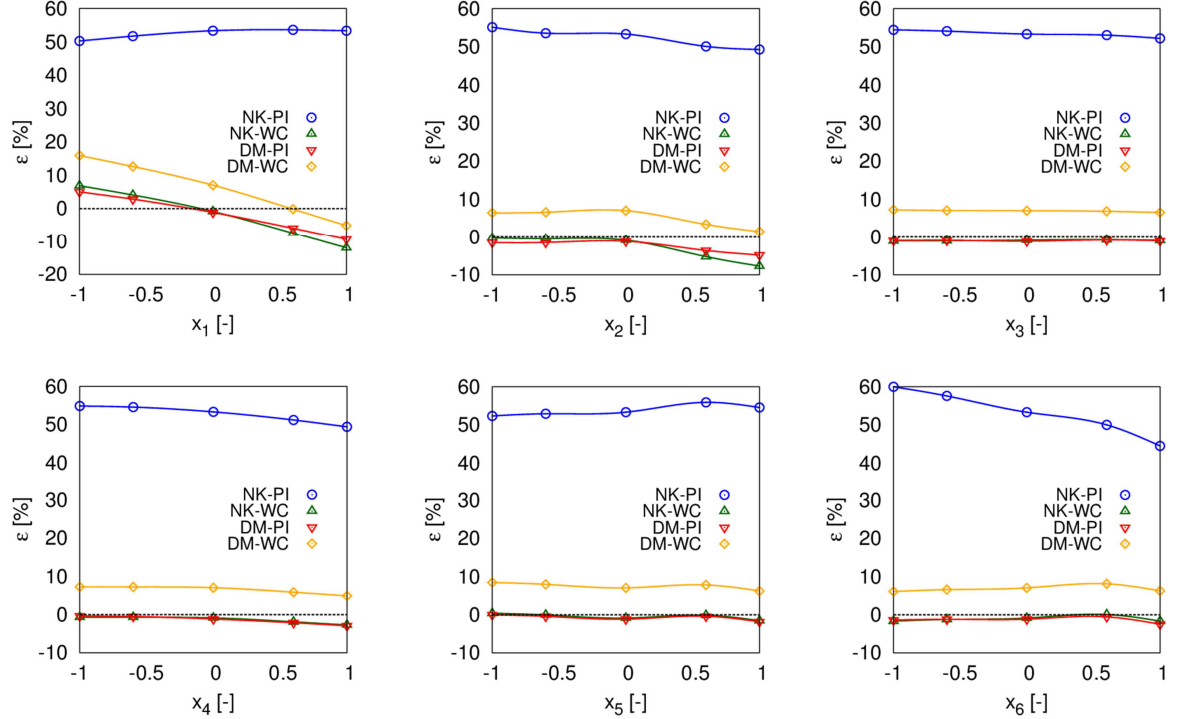


Fig. 13: PF error compared to RANS at $Fr=0.25$

The RANS solutions show several differences compared to the PF formulations. In particular, the trend of the total resistance coefficient is captured only by NK-PI for x_1 , and by all the PF

formulations for x_2 and x_3 , whereas x_4 , x_5 , and x_6 trends are not in agreement with RANS, even if the results are likely within the solution's uncertainty band. Moreover, Fig. 13 shows the error ($\epsilon\%$) between PF formulations and RANS, for each design variable. The NK-PI formulation has the higher error, although almost constant. Table VII summarizes the average absolute errors ($|\bar{\epsilon}| \%$) of the PF formulations. Specifically, the NK-WC and DM-PI formulations have the lowest average error, close to 2%. The analysis of the Pearson's correlation coefficient (r) between PF and RANS results, Table VIII, shows a good correlation between NK-PI and RANS for x_1 , x_2 , x_3 , and x_5 . The other PF formulations have a good correlation for x_2 and x_3 , whereas the correlation for x_4 and x_6 is poor overall, indicating a totally different trend in some case. NK-PI has the better correlation with RANS solutions on average.

Table VII: PF average error compared to RANS

PF formulation	$ \bar{\epsilon} _{x_1}$	$ \bar{\epsilon} _{x_2}$	$ \bar{\epsilon} _{x_3}$	$ \bar{\epsilon} _{x_4}$	$ \bar{\epsilon} _{x_5}$	$ \bar{\epsilon} _{x_6}$	Av.
NK-PI	52.5%	52.3%	53.4%	52.7%	53.8%	53.1%	53.0%
NK-WC	6.3%	2.9%	0.9%	1.4%	0.6%	1.1%	2.2%
DM-PI	4.9%	2.5%	1.0%	1.4%	0.8%	1.4%	2.0%
DM-WC	8.2%	5.0%	7.0%	6.5%	7.5%	6.8%	6.8%

Table VIII: Pearson product-moment correlation coefficient between PF and RANS from Fig. 12

PF formulation	r_{x_1}	r_{x_2}	r_{x_3}	r_{x_4}	r_{x_5}	r_{x_6}	Av.
NK-PI	0.997	0.998	0.993	-0.956	0.826	0.331	0.531
NK-WC	-0.983	0.985	0.994	0.538	0.818	0.482	0.472
DM-PI	-0.622	0.995	0.987	-0.679	0.827	0.335	0.307
DM-WC	-0.979	0.987	0.994	-0.269	0.790	-0.258	0.211

6. Conclusions

A multi-objective deterministic SBDO of the DTMB 5415 model has been shown, using four different PF formulations, combining Kelvin and Dawson linearization with a standard pressure integral and the transversal wave cut method for the wave resistance calculation. The optimization aimed at the reduction of the total resistance in calm water at $Fr=0.25$ and $Fr=0.41$, using six design variables modifying the hull and the sonar dome. A sensitivity analysis at $Fr=0.25$ using RANS has been also shown, for comparison and correlation with the PF solutions.

The results have shown the effects of the PF formulation on the SBDO outcomes. Specifically, the Pareto fronts look quite different and the selected optimal designs fall in different region of the design space, depending on the PF formulation used, Figs. 4 and 5. The following considerations can be made:

- (1) the validation for the original hull shows reasonable trends, but NK-PI for low Fr ;
- (2) DM shows better validation especially for sinkage, compared to NK;
- (3) NK-PI provides significant resistance reductions at low Fr (likely due to an overestimate of the resistance for the original hull) and more limited improvements at high Fr ;
- (4) NK-WC shows a quite opposite trend;
- (5) DM-PI indicates more limited (and realistic) improvements, for both low and high Fr ; it also shows a limited possibility of improving both objectives at the same time;
- (6) DM-WC provides more significant resistance reduction at high Fr ;
- (7) overall, the WC method always indicates greater improvements at high Fr than PI, likely due to an overestimate for the resistance of the original hull;
- (8) NK results seem more affected by the wave resistance estimation method than DM.

These outcomes have motivated further investigations by RANS. Specifically, a sensitivity analysis at $Fr=0.25$ has been conducted and compared with the PF results. This comparison has shown several differences between PF and RANS solutions. Specifically, none of the PF formulations has shown a

reasonable trend for all the design variables, compared to RANS. More in detail, DM-PI, NK-WC, DM-WC, and NK-PI show an average absolute error of 2.0, 2.2, 6.8, and 53.0% respectively (see Table VII). The analysis of the Pearson's correlation coefficient between PF and RANS results (see Table VIII) shows a good correlation between NK-PI and RANS for four out of six variables. For the current test case, NK-PI is the more effective PF formulation.

The present work has shown how the use of low-fidelity solvers in a hull-form optimization problem can lead to inaccurate design solutions. For this reason, the use of high-fidelity solvers (such as RANS or higher) is highly recommended. In order to reduce the computational cost associated to an automatic high-fidelity simulation-based optimization, the use of metamodels with adaptive sampling procedures, *Diez et al. (2015c)* is suggested. Alternatively, multi-fidelity approximations may be used, combining the computational cost of low-fidelity evaluations with the accuracy of high-fidelity simulations, *Pellegrini et al. (2016)*.

Acknowledgements

The present research is partially supported by the US Navy Office of Naval Research, NICOP grant N62909-15-1-2016, under the administration of Dr Woei-Min Lin and Dr Ki-Han Kim and, and by the Italian Flagship Project RITMARE, coordinated by the Italian National Research Council and funded by the Italian Ministry of Education, Research Program 2011-2013. Part of the calculations was performed in collaboration with the NATO RTO Task Group AVT-204 "Assess the Ability to Optimize Hull Forms of Sea Vehicles for Best Performance in a Sea Environment".

References

- BASSANINI, P.; BULGARELLI, U.; CAMPANA, E.F.; LALLI, F. (1994), *The wave resistance problem in a boundary integral formulation*, Surveys on Mathematics for Industry 4, pp.151-194
- CAMPANA, E.F.; LIUZZI, G.; LUCIDI, S.; PERI, D., PICCIALLI, V.; PINTO, A. (2009), *New global optimization methods for ship design problems*, Optimization and Eng. 10/4, pp.533-555
- CHEN, X.; DIEZ, M.; KANDASAMY, M.; ZHANG, Z.; CAMPANA, E.F.; STERN, F. (2015), *High-fidelity global optimization of shape design by dimensionality reduction, metamodels and deterministic particle swarm*, Engineering Optimization 47/4, pp.473-494
- DAWSON, C.W. (1977), *A practical computer method for solving ship-wave problems*, 2nd Int. Conf. Numerical Ship Hydrodynamics, Berkeley, pp.30-38
- DIEZ, M.; SERANI, A.; CAMPANA, E.F.; GOREN, O.; SARIOZ, K.; DANISMAN, D.; GRIGO-ROPOULOS, G.; ALONIATI, E.; VISONNEAU, M.; QUEUTEY, P.; STERN, F. (2015a), *Multi-objective hydrodynamic optimization of the DTMB 5415 for resistance and seakeeping*, 13th Int. Conf. Fast Sea Transportation (FAST), Washington/DC
- DIEZ, M.; CAMPANA, E.F.; STERN, F. (2015b), *Design-space dimensionality reduction in shape optimization by Karhunen–Loève expansion*, Computer Methods in Applied Mechanics and Engineering 283, pp.1525-1544
- DIEZ, M.; VOLPI, S.; SERANI, A.; STERN, F.; CAMPANA, E.F. (2015c), *Simulation-based design optimization by sequential multi-criterion adaptive sampling and dynamic radial basis functions*, Int. Conf. on Evolutionary and Deterministic Methods for Design, Optimization and Control with Applications to Industrial and Societal Problems (EUROGEN), Glasgow
- HUANG, J.; CARRICA, P.; STERN, F. (2008), *Semi-coupled air/water immersed boundary approach for curvilinear dynamic overset grids with application to ship hydrodynamics*, Int. J. Numer. Meth. Fluids 58, pp.591-624

KANDASAMY, M.; PERI, D.; TAHARA, Y.; WILSON, W.; MIOZZI, M.; GEORGIEV, S.; MILANOVIĆ, E.; CAMPANA, E.F.; STERN, F. (2013), *Simulation based design optimization of waterjet propelled Delft catamaran*, Int. Shipbuilding Progress 60/1, pp.277-308

KENNEDY, J.; EBERHART, R.C. (1995), *Particle swarm optimization*, 4th IEEE Conf. on Neural Networks, Piscataway, pp. 1942-1948

LONGO, J.; STERN, F. (2005), *Uncertainty assessment for towing tank tests with examples for surface combatant DTMB model 5415*, J. Ship Research 49/1, pp.55-68

OLIVIERI, A.; PISTANI, F.; AVANZINI, A.; STERN, F.; PENNA, R. (2001), *Towing tank experiments of resistance, sinkage and trim, boundary layer, wake, and free surface flow around a naval combatant INSEAN 2340 model*, Technical report, DTIC Document

PELLEGRINI, R.; CAMPANA, E.F.; DIEZ, M.; SERANI, A.; RINALDI, F.; FASANO, G.; IEMMA, U.; LUCIDI, S.; LIUZZI, G.; STERN, F. (2014), *Application of derivative-free multi-objective algorithms to reliability-based robust design optimization of a high-speed catamaran in real ocean environment*, 4th Int. Conf. Engineering Optimization (EngOpt), Lisbon

PELLEGRINI, R.; LEOTARDI, C.; IEMMA, U.; CAMPANA, E.F.; DIEZ, M. (2016), *A multi-fidelity adaptive sampling method for metamodel-based uncertainty quantification of computer simulations*, European Congress on Computational Methods in Applied Sciences and Engineering (ECCOMAS), Crete

SCHLICHTING, H.; GERSTEN, K. (2000), *Boundary-Layer Theory*, Springer, Berlin

SERANI, A.; DIEZ, M.; LEOTARDI, C.; PERI, D.; FASANO, G.; IEMMA, U.; CAMPANA, E.F. (2014), *On the use of synchronous and asynchronous single-objective deterministic Particle Swarm Optimization in ship design problems*, 1st Int. Conf. in Eng. and Applied Sciences Optimization, Kos

SERANI, A.; FASANO, G.; LIUZZI, G.; LUCIDI, S.; IEMMA, U.; CAMPANA, E.F.; DIEZ, M. (2015), *Derivative-free global design optimization in ship hydrodynamics by local hybridization*, 14th Int. Conf. on Computer Applications and Information Technology in the Maritime Industries (COM-PIT), Ulrichshusen, pp.331-342

STERN, F.; LONGO, J.; PENNA, R.; OLIVIERI, A.; RATCLIFFE, T.; COLEMAN, H. (2000), *International collaboration on benchmark CFD validation data for surface combatant DTMB model 5415*, 23rd Symp. Naval Hydrodynamics, Val de Reuil

TAHARA, Y.; PERI, D.; CAMPANA, E.F.; STERN, F. (2008), *Computational fluid dynamics-based multiobjective optimization of a surface combatant using global optimization method*, J. Marine Science and Technology 13, pp.95-116

TELSTE, J.; REED, A. (1994), *Calculation of transom stern flows*, 6th Int. Conf. Numerical Ship Hydrodynamics, Iowa City, pp.78-92

TRELEA, I. (2003), *The particle swarm optimization algorithm: convergence analysis and parameter selection*, Information Processing Letters 85, pp.317-325

WONG, T.; LUK, W.; HENG, P. (1997), *Sampling with Hammersley and Halton points*, J. Graphics Tools, pp 9-24

Learning Curve and Return of Investment in the Implementation of a CAD System in a Generic Shipbuilding Environment

Rodrigo Perez Fernandez, SENER, Madrid/Spain, rodrigo.fernandez@sener.es

Abstract

The paper shows an analysis performed to provide a clear idea of the Return on Investment of using CAD Systems (in particular, the FORAN system) in a generic shipyard. The Return on Investment analysis for software implementation must consider the changes in productivity during its application period. Those changes in productivity can be generically represented by a transition curve along a learning period. After that period, the standard productivity gain is achieved. The use of a CAD System provides not only a cost reduction in design, but also a cost reduction in production, including two major aspects: savings in materials due to a more accurate definition of components and material management, as well as savings in materials due to a significant reduction of design changes, and consequently reduction of rework in production; and savings of production man-hours due to the reduction of changes and rework.

1. Introduction to CAD Systems

Computer-Aided Design (CAD) Systems help engineers and designers in various industries, designing and building 3D models of airplanes, bridges... and of course, ships, submarines and floating structures. There are other acronyms that are usually accompanying the acronym CAD, such as Computer-Aided Manufacturing (CAM), Computer-Aided Engineering (CAE), and Computer Integrated Manufacturing (CIM), including instructions to Computer Numerical Control (CNC) machines. One could claim that these CAD/CAM/CAE Systems had their origin around the year 350 BC, with the mathematician Euclid of Alexandria. Many of the postulates and axioms used by today's CAD systems are based on Euclidean geometry. Some 2300 years later, many see the birth of 3D CAD with the work of Pierre Bezier, a French engineer working at the Arts et Métiers ParisTech. After his mathematical work concerning surfaces, he developed UNISURF, between 1966 and 1968, to ease the design of parts and tools for the automotive industry. Then, UNISURF became the working base for the following generations of CAD software. Only one decade later, CAD systems were introduced in academic courses. The real breakthrough in CAD systems came, logically, with the development of computers; and during the 1980s the application of CAD systems matured to a similar stage as known today, *Perez and Gonzalez (2015)*.

CAD tools are usually divided into 2D drawing and 3D modelling programs. The drawing tools are based on 2D vector geometric entities such as points, lines, arcs and polygons. In 3D modellers, solids and surfaces are created. In the early stages of the development of CAD systems, the software was running on mainframes, which limited use of CAD systems for manufacturing. With the arrival of workstations and PCs came then widespread use of CAD systems in engineering on a daily base.

2. Why use a CAD/CAM System in ship design?

There are several aspects where CAD systems could, and most likely will, improve in the near future. However, in this section the focus is on functionalities that are being improved right now. E.g. in hull forms definition, the global shape modelling or the advance continuity and capping tools could transform complex surfaces with excellent results, less interaction, high accuracy, and full control. These techniques shorten dramatically the design time, from days to few hours while obtaining excellent results, *Perez and Toman (2014)*.

Another area of improvement concerns one of the most time-consuming tasks in outfitting design, the routing of pipes, *Heat, Ventilation and Air-Conditioning* (HVAC) ducts and cable trays. Automatic routing options will minimise the design man-hours, and at the same time will increase the robustness

of the design. Automatic routing provides simple solutions, with optimisation of material, and several algorithms exist. But the matter is not only to consider existing elements for future routings; it is also necessary to assign priorities, and eventually handle automatic modifications of existing elements as a consequence of new ones. The complexity of the problem explains that there is not yet fully satisfactory solution for the automatic routing in practice. Current solutions provided by CAD systems solve partial problems, offering already significant support.

Another area where the CAD companies are active is Virtual Reality, *Perez and Alonso (2015)*. The objective is to create a user-friendly environment in order to review, audit, obtain metrics such as the progress of a project, etc. This type of review process of the model does not need to use tools for designing, just a simplified tool allowing easy access (“viewer”). Fig. 1 shows a 3D visualization model in a tablet, where the authorized designers/engineers could have all the project information. These navigators allow read-only access to 3D information in order to load the component tree of any design and to obtain information about any item. Other basic tools available in these programs incorporate navigation commands to take action such as measuring distances or angles, creating sections to access internal components, etc. The interface with the program is still via a mouse, but Virtual Reality opens windows of opportunities, with globes, glasses or helmets.

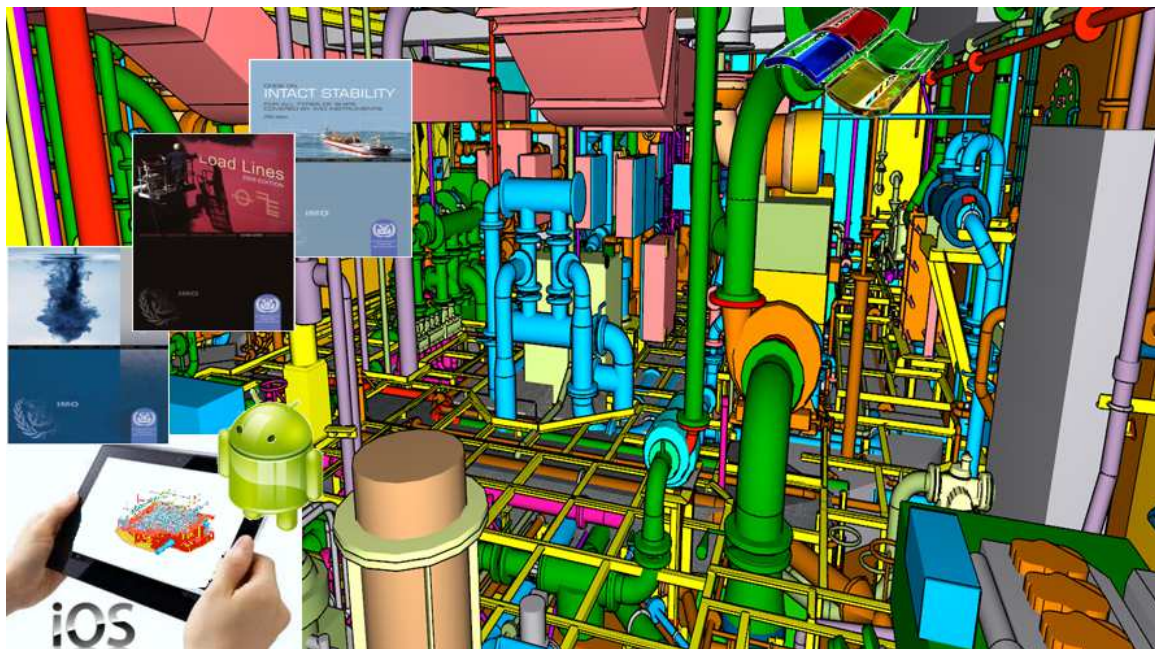


Fig. 1: Marine design future, information in each stage of the ship in electronic devices

Advanced browsers allow incorporating human models in order to study ergonomic aspects, movements of components to perform simulations, etc. Sometimes there is a need to take information from an on-line database and if there is an Ethernet network through the shipyard, it is useful to have viewers that permit connecting to a project. Browsers can connect to the database of a project in order to access information in real time. When there is not an on-line access to the database, viewers should be able to read files with the project information required for 3D modelling of the product and component data with optimal performance. So far it was prevalent to implement viewers on laptops, because laptops are usually equipped with processor and graphics cards that allow navigating through the entire vessel. In recent years there has been a breakthrough in mobile devices like tablets or smartphones. This hardware progressively incorporates new processors that enable enhanced graphics. On the software side, operating systems have been developed specially adapted for such devices (such as Android or IOS) allowing interfacing naturally by touch gestures, *Perez and Gonzalez (2015)*.

The widespread use of these devices nowadays has precipitated its use by software companies. Software developers have taken their time preparing oriented solutions including those that allow to have project drawings or 3D models on tablets or others electronic displays. In modern projects, there is the need, for supervisors, to use these devices to work better, with a quickly access to the 3D model, with all parts information and construction drawings needed. A Wi-Fi connection would allow accessing to an information server to be updating the information needed, mainly in files, as for example: 3D models, classification or production drawings, between others. Another advantage of mobile devices is that the user interface might interact with the project model or parts using gestures just as everybody does every day with smartphones. A development line of navigator's evolution would incorporate augmented reality technology. It would be helpful for production technicians to scroll through the project and pointing the camera of their mobile device to a particular component to obtain information from it and have the actual image of the same 3D design model displayed. This is possible through the use of markers that help the device to position itself within the project and also for the use of Quick Response (QR) codes, *Perez and Gonzalez (2015)*.

CAD systems must handle the information necessary for creating a collision-free design and for generating all production and assembly information, but not only this. The 3D model information is, at the same time, necessary for other activities and other departments involved in the construction of the ship, as planning, purchasing, subcontracting, accounting, etc. Often, several design agents collaborate in the same project; so it is necessary that 3D model information should be shared between them to serve as reference. The paradigm of this problem appears when two or more design agents collaborate in the same project, using different CAD tools. In this case, the CAD systems must provide data exchange capabilities leading to different degrees of integration, like visualization, spatial integration and cross manufacturing, depending on the characteristics and size of 3D model information transferred. At least, it should be geometry and key attributes. A worldwide format for data transfer has not yet been found. Despite recognised international standards, in most cases exist dedicated formats or particular adaptations from standard ones. Transfer of 3D model information could produce degradation of performance due to different geometrical approaches to represent elements in both CAD systems. In this case, special solutions must be adopted in order to minimise this impact.

Another recent milestone is the integration between different CAD systems and Product Lifecycle Management (PLM) tools, e.g. the FORAN Product Lifecycle Management (FPLM) tool with a neutral architecture. In this case, all the information generated in FORAN may be transferred to a PLM and may be subject to all processes: control, configuration and releases lifecycle and process management. FPLM consists of a series of tools and features that enable bidirectional integration between different modules of FORAN and PLM tools, *Perez and Penas (2015)*.

There are many advantages of using CAD in shipbuilding: ease of design, speed of construction, use and reuse of information, etc. It is expected that in the future CAD tools will advance further and allow greater information management and virtual access through smart devices. In general, CAD systems provide tangible benefits while the process is optimized, reducing design time and production, and therefore costs, *Perez et al. (2013)*.

3. Return on investment of FORAN implementation

This paper shows the analyses performed to provide a clear idea of the *Return On Investment* (ROI) of performing a CAD System implementation (in particular, the FORAN System) in a generic shipyard. The analysis on the potential improvements that could be achieved in the different design processes affecting various disciplines in a generic ship design technical office, when working with a specific CAD System(FORAN), provides the necessary inputs to evaluate the productivity gain that are expected. With those inputs, present paper is intended to provide a financial evaluation of the necessary investment, quantifying the benefits and the costs of FORAN implementation in a generic shipyard. The quantification of benefits and costs are analysed along a reasonable time period, generating cash inflows and cash outflows.

This financial analysis includes only those aspects that can be estimated or measured by SENER, company owner of the FORAN System, including also a list of benefits and costs that, although cannot be directly evaluated by SENER, should be also taken into consideration. The information included in this paper has been compiled as a consequence of SENER experience in FORAN implementation in numerous shipyards around the world between 2007 and 2015. The following sections show not only the ratios used to evaluate the ROI, but also analyse the benefits of FORAN implementation, the generated cash flows, the estimated learning process productivity losses, the expected productivity gain, the assumptions taken for the financial analysis, and a sensitivity analysis of the ROI respect to productivity gain and the considered discount rate. The ROI financial analysis included in this paper shows the complete set of cases considered as well as summary tables and charts that helps to the data interpretation.

4. Metrics and ratios for return on investment evaluation

It is highly recommended to have some numbers showing the merits of the investment. There are several valuation tools and methodologies used to describe how good an investment such as the implementation of FORAN is. Those methodologies basically quantify and calculate the different metrics usually used to have a better knowledge of the ROI, because ROI is a standard measure of investment profitability that is based on the calculation of the discounted profits over the life of the project expressed as a percentage of initial investment. Also, ROI is a financial analysis technique used to calculate the benefits of investing. This calculation is based on the following concepts:

Cost: Total amount of money spent on the new system implementation.

$$\sum_{i=1}^n \text{Discounted Costs}_i$$

Benefits: Total amount of money gained from the new system implementation.

$$\sum_{i=1}^n \text{Discounted Benefits}_i$$

Net Present Value (NPV): Discounted cash flows.

$$NPV = \sum_{year=1}^{Years} \left(\frac{\sum_{i=1}^n \text{Benefits}_i - \sum_{i=1}^n \text{Costs}_i}{(1 + \text{DiscountRate})^{year}} \right) - \text{Costs}_0$$

Internal Rate of Return (IRR): Discount rate that makes the Net Present Value zero.

$$IRR = \text{DiscountRate} \leftrightarrow \sum_{year=1}^{Years} \left(\frac{\sum_{i=1}^n \text{Benefits}_i - \sum_{i=1}^n \text{Costs}_i}{(1 + \text{DiscountRate})^{year}} \right) - \text{Costs}_0 \equiv 0$$

Payback Period: Amount of time needed to reach the Break Event Point.

$$PB = year \leftrightarrow \sum_{year=1}^{Years} \left(\frac{\sum_{i=1}^n \text{Benefits}_i}{(1 + \text{DiscountRate})^{year}} \right) = \sum_{year=1}^{Years} \left(\frac{\sum_{i=1}^n \text{Costs}_i}{(1 + \text{DiscountRate})^{year}} \right)$$

Break Event Point (BEP): Value corresponding to the point when benefits meet or exceed cost.

$$BEP = \sum_{year=1}^{Years} \left(\frac{\sum_{i=1}^n Benefits_i}{(1 + DiscountRate)^{year}} \right) = \sum_{year=1}^{Years} \left(\frac{\sum_{i=1}^n Costs_i}{(1 + DiscountRate)^{year}} \right)$$

Profitability Index (PI) or Benefit/Cost Ratio: Ration of benefits to costs.

$$PI = \frac{\sum_{i=1}^n Discounted Benefits_i}{\sum_{i=1}^n Discounted Costs_i}$$

Return on Investment (ROI): Ratio of adjusted benefits to cost.

$$ROI = \frac{\sum_{i=1}^n Discounted Benefits_i - \sum_{i=1}^n Discounted Costs_i}{\sum_{i=1}^n Discounted Costs_i} \times 100\%$$

The ROI calculation results in a value that represents the benefits received from a project against the total costs of the project, being necessary to define costs and benefits on a timeline when they are expected to occur. Therefore, it is necessary to establish a cash flow (outflows = costs and inflows = benefits) in a conservative and reasonable amount.

5. Financial Analysis

5.1. Benefits of Investment of FORAN Implementation

Several shipyards presented its current design process showing a significant complexity, mainly due to the very different data bases and tools used along the process. The use of different data bases drives to a very important effort to maintain their coherence, requiring successive comparison between them (manual and electronic) to maintain data integrity and their consistency. Current modelling process is based in different tools that although stable it is a rather old system with very restrictive development. The implementation of FORAN in a generic shipyard provides obvious benefits, but not all of them can be directly quantified. The obtained benefits can be tangible or intangible, and they can be estimated or not. Benefits can be classified as

- **Tangibles:**
 - Those that can be estimated or measured by SENER.
 - Those that cannot be estimated or measured by SENER, but that can be estimated or measured by the diverse shipyards.
- **Intangibles:** they cannot be inherently estimated or measured.

The present financial analysis takes into account only those aspects that can be estimated or measured by SENER. However, a list of other benefits that cannot be estimated or measured by SENER is also included, as although not quantified, they could be of remarkable importance. The implementation of a software application as FORAN should be supported by an analysis of benefits, activity improvement and business added value. Part of this support can be given with a financial analysis of the necessary investment.

5.2. FORAN Implementation Cash Flow

ROI financial analysis is based on the study of the generated cash flows: cash outflows (costs) and cash inflows (gains). FORAN implementation would have the following tangible cash flows (estimated by SENER):

- **Cash Outflows** (cost):
 - Net Licence cost: single initial cost.
 - Software installation in a generic shipyard computers: single initial cost.
 - Training: single initial cost.
 - Yearly maintenance: annual cost, excluding guarantee of six first months.
 - Technical assistance: First year cost.
 - Implementation/adaptation, coordination and management: First 2 years cost.
 - Loss of productivity during training phase: affecting only to the first year.
- **Cash Inflows** (benefit):
 - Increase of productivity during training phase: affecting only to first year.
 - Increase of productivity once FORAN is fully implemented: affecting the part of the first year in which the FORAN is fully implemented, and the subsequent years.
 - Increase of productivity due to an effective concurrent engineering (all disciplines working with a single database).
 - Reduction of production hours due to reduction of changes and reworks.
 - Reduction of material costs (steel, piping, cables, etc.) due to a most precise definition of items, and reduction of changes and rework during production.

There are other concepts that although tangible, they cannot be estimated or measured by SENER:

- **Potential Cash Outflows** (cost):
 - Information Technology (IT) infrastructure: PCs and necessary basic software.
 - Effort to adapt shipyard structure to the use of FORAN in the design processes.
 - Additional migration costs that cannot be specified by SENER, but that probably can be specified by the shipyard.
- **Potential Cash Inflows** (benefit):
 - Reduction of number of workstations, reduction of maintenance of IT infrastructure.
 - Potential internal structure simplification, and therefore structure optimisation.

In addition, there are other intangible benefits, including:

- Use of a design and modelling tool that includes the state of the art technologies used all over the world for ship design and ship construction. FORAN represents the leading edge CAD/CAE/CAM technology in shipbuilding.
- Use of a tool that is always looking for improvement, developing continuously enhancements, including new functionalities and planning new system improvements.
- Show a better corporate image through the tool used for design and modelling.

5.3. Learning Process

ROI analysis for software implementation must consider the changes in productivity during its implementation period. Those changes in productivity can be generically represented by a transition curve along a training period. After that period, the standard productivity gain is achieved. The transition curve is characterized by a productivity loss during the training courses and some weeks afterwards, characterized by a strong productivity gain progression. After the training courses there is a

maturity period when the designer or modeller gets the adequate skills in a more tended slope curve, achieving finally the standard user skills. The productivity loss at beginning of the implementation is part of the so-called migration costs. Migration costs will be smaller if the implementation is performed in the shortest possible period. Fig. 2 shows the generic design productivity evolution of FORAN implementation for a generic modeller or designer. There is an immediate dip in productivity, as the users get up to speed on the new system. With time, productivity climbs back to where it was with the original system and levels off at a higher point as the new system is fully implemented.

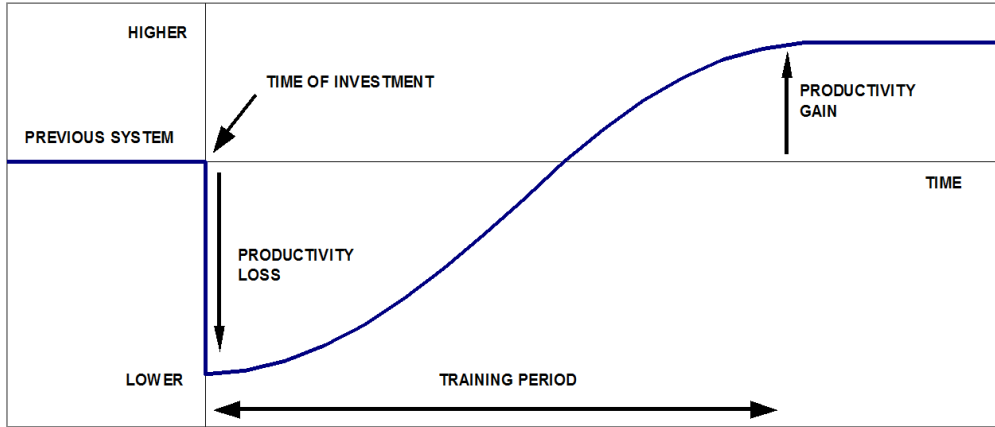


Fig.2: Design productivity evolution of FORAN implementation for a generic modeller or designer

In the case of the ROI analysis for FORAN implementation, the transition curve representing the changes in productivity during the implementation period is characterized by a very short period of loss of productivity (slightly longer than the duration of the training courses), and a short to medium time period to achieve the standard common skills, achieving the old productivity level in a very short time after finishing the training courses.

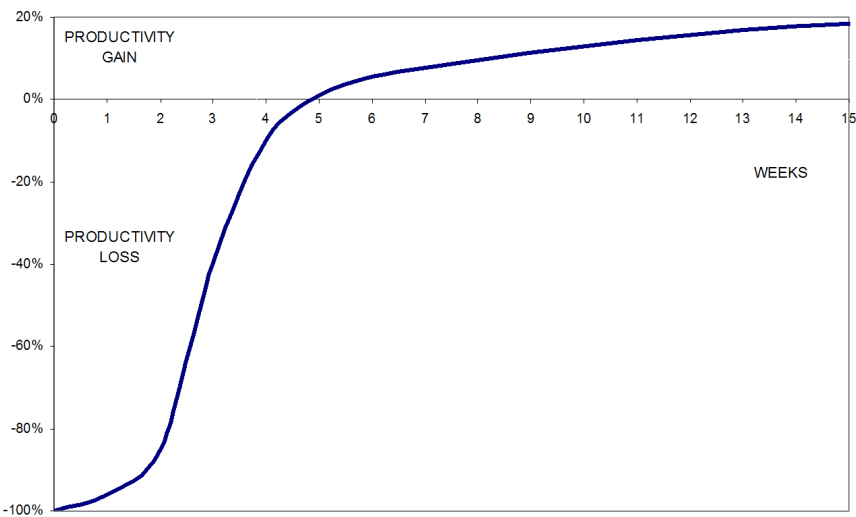


Fig.3: Design productivity evolution of a standard skilled designer, as used in present analysis

After the two or three week training course there is a strong progression in the skills of the users up to four or five weeks, changing to a more tended slope of productivity gain along the following ten to fifteen weeks. Fig. 3 shows the design productivity evolution of a standard skilled designer, as used in present analysis. It is based on a training course of two to three weeks and a post training course period in which the personnel reached the usual skills. We assumed that modellers and designers have a previous standard skill in 3D modelling software packages. Fig. 3 includes SENER experience in the implementation of FORAN in different shipyards. After the training courses, there is a very short period necessary to achieve the previous productivity, and after that there is a period of usually eight weeks after training course when the standard skills are achieved reaching the standard gain in

productivity. Nevertheless, for this analysis, a longer time period has been considered, assuming twelve weeks instead of eight weeks. As the training courses are provided sequentially for several groups of people and for different disciplines along the first year, for present analysis the potential productivity gain in the first year has been reduced to 50%, being that a very conservative assumption. In order to consider a realistic scenario involving all factors, it has been carried out a study about the CAD System learning process in a standard shipyard. Figs. 4 and 5 show the learning curves during the CAD System implementation in the shipyard. During the last two years, data related with hours devoted to design a precise unit (block) with a specific weight were collected in a shipyard. The chosen shipyard was one where FORAN had been implemented for first time. Fig. 4 shows the learning curve during the design of the first ship, Fig. 5 for the second ship design.

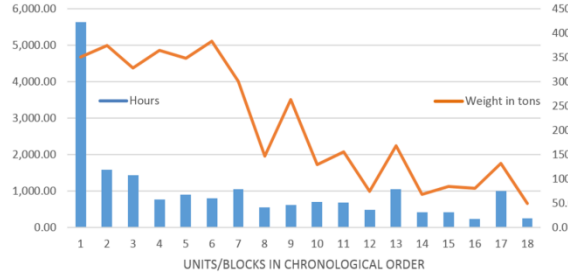


Fig.4: Learning curve with FORAN for first ship

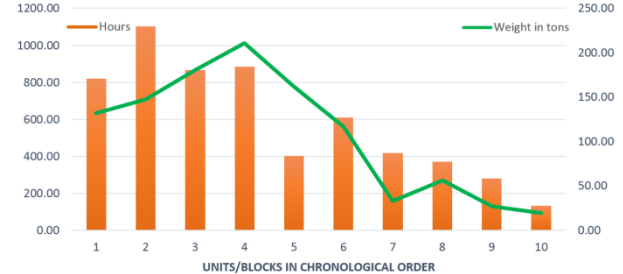


Fig. 5: Learning curve for second ship

5.4. Expected Increase of Productivity

SENER experience indicates that an increase of productivity from 10 % to 20 % is very common when implementing FORAN in shipyards. In present case corresponding to the implementation of FORAN in a generic shipyard, an estimate has been performed by discipline, including weighting factors to obtain a global productivity increase rate. Table I shows disciplines, the weighting factors, and the considered productivity increase rate. These weighting factors, and considered productivity increase rates are only estimates based on impressions obtained from the meetings maintained with different shipyards people. SENER would recommend a detailed quantitative re-assessment once quantitative data from the shipyard is available. In a generic shipyard, the analysis of the different design processes and disciplines drives us to estimate a design productivity increase of 12 % to 18 %.

Table I: Disciplines, the weighting factors, and the considered productivity increase rate

Discipline	Weighting Factor	Productivity Gain	
		Relative	Subtotal
Structure	20 %	14 %	2.80 %
Electrical	15 %	18 %	2.70 %
Piping Routed Systems	30 %	21 %	6.30 %
HVAC Routed Systems	15 %	10 %	1.50 %
Design Area Integration	10 %	11 %	1.10 %
Accommodation /Outfit	5 %	11 %	0.55 %
Miscellaneous Applications	5 %	8 %	0.40 %
Overall Process Productivity Gain			15.35 %

However, the ROI financial analysis includes cases with productivity gains of 6%, 9%, 12%, 15%, and 18%.

5.5. Assumptions for ROI Financial Analysis

A ten years' time frame is going to be considered for the FORAN implementation financial analysis, as FORAN is a strategic long-term tool. Residual cash flows have not been considered in this analysis. This ROI financial analysis takes into account the time value of money, considering an escalation

rate of 3%. The financial analysis includes sensitivity analysis respect to discount rate and to expected increase of productivity rate. For the discount rate the following values are used: 3%, 6%, 9%, 12% and 15%. For the increase of productivity rate the following values are used: 6%, 9%, 12%, 15% and 18% (see expected increase of productivity in previous section). Although taxes and depreciation can also have an impact in the financial analysis, they have not been considered in the present analysis.

5.5.1. Savings in Design, Materials and Production

Savings in design as a function of productivity gain are estimated as follows:

- Design personnel hourly rate cost (and associated indirect costs) that is going to work with FORAN is assumed to be 45 €/h. This number may differ depending of region, country, etc.
- Assumed yearly man production hours: 1760 h/year. As before, this amount could vary.
- Number of designers involved with FORAN is 100. This figure was chosen as an average.
- Different productivity gains considered are: 6%, 9%, 12%, 15%, and 18%.

The use of FORAN will provide not only a reduction of changes, but a more accurate definition of the components of the different systems. It means not only a cost reduction in design, but also a cost reduction in production, including two major aspects:

- Savings in materials due to a more accurate definition of components and material management, as well as savings in materials due to a significant reduction of design changes, and consequently reduction of rework in production.
- Savings of production man-hours due to the reduction of changes and rework.

The estimate of material savings has been done as follows:

- Steel:
 - Steel elaboration: 10000 t/year. This figure has been chosen as an average.
 - Steel price: 600 €/t. This price could change according to several factors.
 - A steel saving rate of 0.5% is assumed, meaning 30000 €/year.
 - This saving is assumed to be effective from the third and subsequent years.
- Other materials: pipes and cables:
 - The annual cost of such materials is assumed to be about 2 m€/year.
 - Materials saving rate is estimated to be about 1 %, meaning 20000 €/year.
 - This saving is assumed to be effective from the third and subsequent years.

Savings in production due to reduction of changes and corresponding rework is assumed as follows:

- Production personnel cost (and associated indirect costs) is assumed to be 35 €/h.
- Assumed yearly man production hours: 1760 h/year.
- Assumed production personnel rate respect to design personnel: 8 (it means 4000 people in production). Again, this number has been assumed by the author.
- Production hours reduction rate due to reduction of changes and rework is assumed to be about 0.5 %, meaning a production saving of 1230000 €/year.
- This saving is assumed to be effective from the third and subsequent years.

5.5.2. Software License and Services Costs

The costs have not been included in these paragraphs due to it is a confidential information. But although the costs are not included, these have been used for the analysis, and not less important, the concepts of these costs are shown as follow:

- FORAN Licence cost: single initial cost in Euros.

- Software installation in standard computers (sites): single initial cost in Euros.
- Training cost: single initial cost in Euros. For reducing cost, it could be considered that only receive the trainings a group of super users.
- Annual maintenance cost: excluding first months of guarantee.
- First year technical assistance cost: it depends of how many man-weeks will be necessary.
- First year of implementation/adaptation program, coordination and management: it depends of how many man-weeks will be necessary.

5.6. ROI Financial Analysis

The following financial indexes are used to evaluate the implementation of FORAN:

- **Net Present Value (NPV)**: represents the difference between investment market value and its costs (sum of present values of net annual benefits minus the initial investment required). The future cash flows that the FORAN implementation would produce is estimated taking into account outflows (costs, loss of productivity ...) and inflows (cost savings, increase of productivity, other benefits ...). The Discounted Cash Flow (DCF) has been evaluated.
- **Internal Rate of Return (IRR)**: It is the discount rate that makes the NPV of a project equal zero
- **Payback Period** (discounted): It is the amount of time needed for an investment to generate cash flows (discounted) to recover its initial costs.
- **Profitability Index (PI)** or Benefit/Cost Ratio: It is the present value of future cash flows divided by the initial investment.
- **Return on Investment (ROI)**: It represents the relative value of the project's cumulative net benefits (benefits less costs) over the analysis period, divided by the project's cumulative total costs, expressed as a percentage.

The following tables show the results of the financial analysis including a sensitivity analysis respect to Productivity Gain to Discount Rate. Corresponding charts are also included for easier data interpretation. Tables with complete cash flows, discounted cash flows and corresponding financial evaluations are also included for predefined cases (different productivity gains and different discount rates). Table II describes the Net Present Value (NPV) in Euros, which is the difference between the present value of cash inflows and the present value of cash outflows. NPV is used in capital budgeting to analyse the profitability of a projected investment or project. A positive NPV indicates that the projected earnings generated by a project or investment exceed the anticipated costs. This investment has a positive NPV, so it will be profitable.

Table II: Net Present Value in Euros

Discount Rate	Productivity Gain				
	6 %	9 %	12 %	15 %	18 %
3 %	10,702,675	21,817,329	32,931,983	44,046,636	55,161,290
6 %	7,823,812	17,259,347	26,694,883	36,130,419	45,565,954
9 %	5,575,061	13,668,480	21,761,899	29,855,318	37,948,737
12 %	3,804,320	10,813,417	17,822,513	24,831,609	31,840,705
15 %	2,399,755	8,523,872	14,647,990	20,772,108	26,896,226

Fig. 6 shows the NPV. Determining the value of a project is a challenging exercise because there are different ways to measure the value of future cash flows. Because of the time value of money, money in the present is worth more than the same amount in the future. This is both because of earnings that could potentially be made using the money during the intervening time and because of inflation. In other words, Euro earned in the future will not be worth as much as one earned in the present.

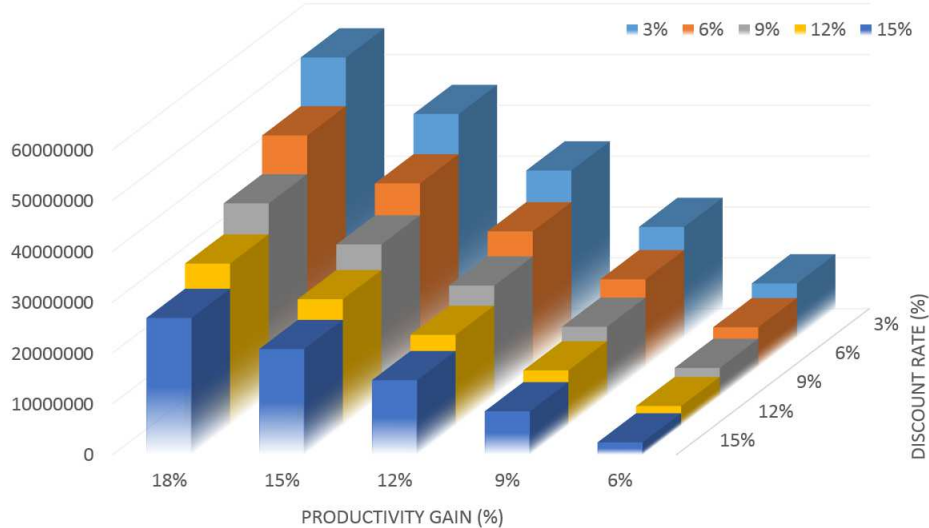


Fig.6: Net Present Value in Euros

Table III describes the Discounted Payback Period (DPP), which is a capital budgeting procedure used to determine the profitability of a project. In contrast to an NPV analysis, which provides the overall value of a project, a DPP gives the number of years it takes to break even from undertaking the initial expenditure. Future cash flows are considered are discounted to time zero. This procedure is similar to a payback period; however, the payback period only measure how long it take for the initial cash outflow to be paid back, ignoring the time value of money.

Table III: Discounted Payback Period in years

Discount Rate	Productivity Gain				
	6 %	9 %	12 %	15 %	18 %
3 %	5.4	3.8	3.0	2.5	2.2
6 %	5.7	3.9	3.1	2.6	2.2
9 %	6.1	4.1	3.1	2.6	2.3
12 %	6.6	4.2	3.2	2.7	2.3
15 %	7.2	4.4	3.3	2.7	2.3

The payback period is the time required to recover the cost of an investment. The payback period of a given investment or project is an important determinant of whether to undertake the position or project, as longer payback periods are typically not desirable for investment positions. Ship design projects that have a negative net present value will not have a DPP, because the initial outlay will never be fully repaid. This is in contrast to a payback period where the gross inflow of future cash flows could be greater than the initial outflow, but when the inflows are discounted, the NPV is negative.

Table IV: Profitability Index related to productivity gain and discount rate

Discount Rate	Productivity Gain				
	6 %	9 %	12 %	15 %	18 %
3 %	2.47	4.00	5.52	7.05	8.57
6 %	2.07	3.36	4.65	5.94	7.23
9 %	1.76	2.86	3.96	5.06	6.16
12 %	1.52	2.47	3.42	4.36	5.31
15 %	1.32	2.15	2.98	3.80	4.63

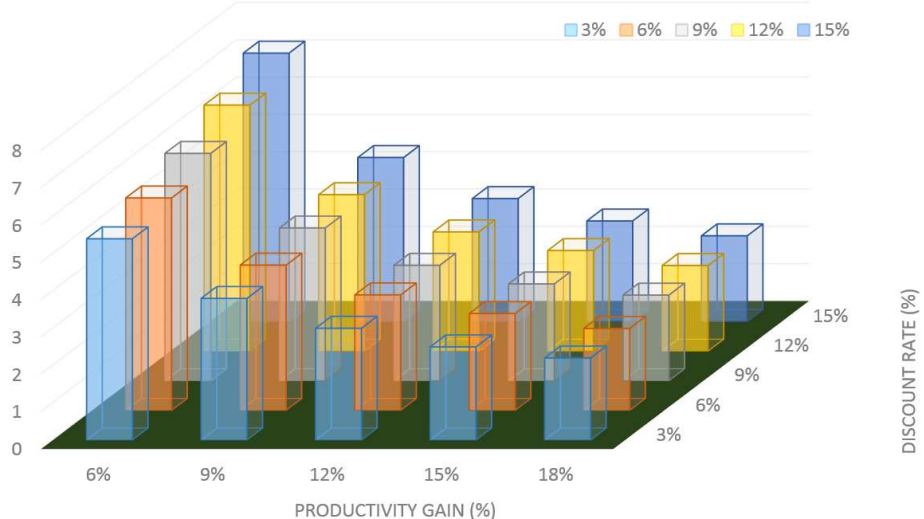


Fig.7: Discounted Payback Period in years

Fig. 7 shows the DPP in years, considering different productivity gains and different discount rates. Table IV describes the Profitability Index (PI), which is an index that attempts to identify the relationship between the costs and benefits of a proposed project through the use of a ratio calculated as the coefficient between the present value of future cash flows and the initial investment. A ratio of 1.0 is logically the lowest acceptable measure on the index. Any value below 1.0 indicates that the project's present value is less than the initial investment.

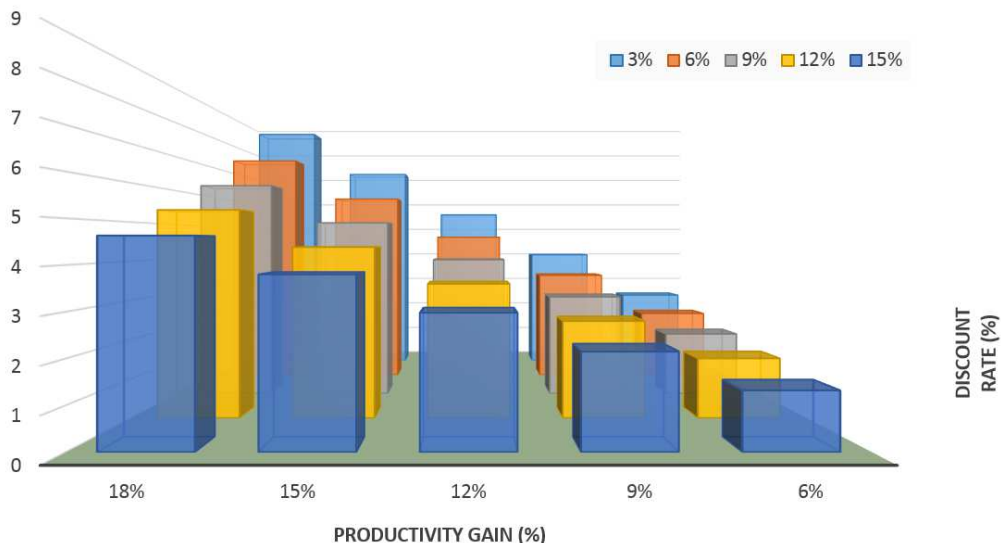


Fig.8: Profitability Index related to productivity gain and discount rate

Table V: Return On Investment (ROI) in percentage

Discount Rate	Productivity Gain				
	6 %	9 %	12 %	15 %	18 %
3 %	147%	300%	452%	605%	757%
6 %	107%	236%	365%	494%	623%
9 %	76%	186%	296%	406%	516%
12 %	52%	147%	242%	336%	431%
15 %	32%	115%	198%	280%	363%

Fig. 8 shows the PI, considering different productivity gains and different discount rates. Table V describes the ROI, which is the benefit to the investor resulting from an investment of some resource. A high ROI means the investment gains compare favourably to investment cost. As a performance measure, ROI is used to evaluate the efficiency of an investment or to compare the efficiency of a number of different investments. In purely economic terms, it is one way of considering profits in relation to capital invested. Fig. 9 shows the ROI, considering different productivity gains and different discount rates.

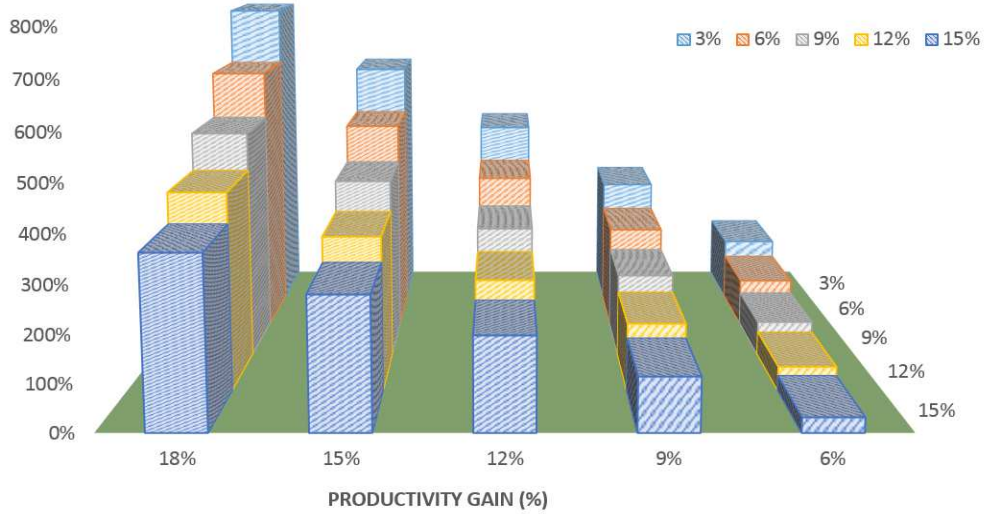


Fig.9: Return On Investment related to productivity gain and discount rate

Investment is buying an asset with the expectation of capital appreciation, dividends (profit), interest earnings, rents, or some combination of these returns. This may or may not be backed by research and analysis. Most forms of investment involve some form of risk, such as investment in equities, property, and even fixed interest securities which are subject to e.g. inflation risk. It is indispensable for project investors to identify and manage the risks related to the investment. Investment and investing is distinguished from other uses of money (such as saving, speculation, donation, gifting), in that the deployment of money is done for the purposes of obtaining a positive expected return.

7. Conclusions

In the light of the results of the ROI financial analysis and sensitivity analysis, we can state that the implementation of FORAN in a generic shipyard has a reasonable justification. The expected benefits are considerably much higher than the costs incurred, even with high variability of productivity gain. As mentioned before, in addition to the factors considered in this ROI analysis, there are others (intangibles or tangibles, but not estimated by SENER), that could have an important impact in the decision making process. The assumptions considered in this ROI financial analysis are mainly based on qualitative information obtained during the meetings with different shipyards. Therefore, it is highly recommended to recalculate this ROI analysis with more accurate data, if available.

Table VI: Internal Rate of Return (IRR) in percentage

Productivity Gain				
6 %	9 %	12 %	15 %	18 %
22.5%	40.8%	59.6%	79.5%	100.9%

Table VI describes the Internal Rate of Return (IRR) related with the productivity gain. The IRR (a.k.a. discounted cash flow rate of return) is the rate of return used in capital budgeting to measure and compare the profitability of investments. It is important to obtain the IRR of the CAD System implementation versus the productivity gain, so it will provide its degree of lucrativeness.

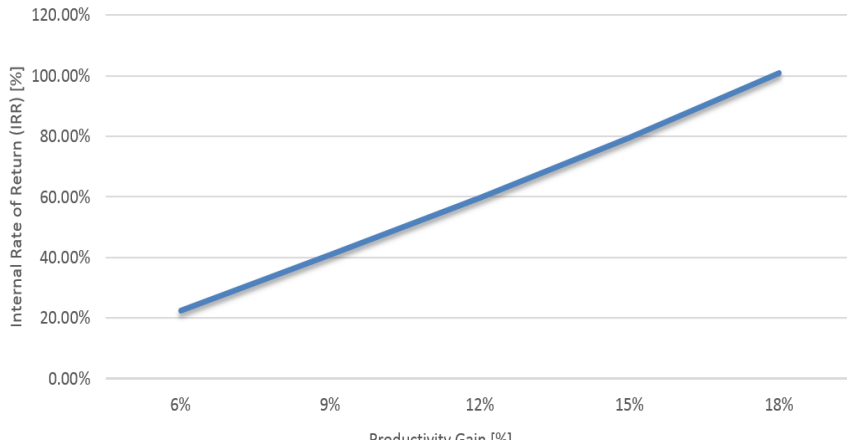


Fig.10: Internal Rate of Return in percentage

Fig. 10 illustrates Table VI, where with an 18% of productivity gain, the IRR will exceed of 100%. IRR for the calculations here has been used to evaluate the desirability of CAD System investments in the shipyards. The higher a CAD System investment's IRR, the more desirable is investment in a new CAD tool. Assuming all CAD System investments require the same up-front investment, the CAD System investment with the highest IRR would be considered the best and undertaken first. Another key aspect of this paper, is the analysis of the learning curve of a new CAD System implemented in a generic shipyard. The data, hours expended designing blocks and units of different weights, collected for this paper during a couple of years from a generic shipyard, have been a fantastic tool for analyzing the factors that affect a learning curve process. One of this key factor is the designers' mobility, which explains why the curve has peaks, so a well-trained and experienced draftsman could leave the shipyard, and another less skilled designer needs time to learn the new CAD System.

References

- LEE, D.J.; CEBOLLERO, A.; PÉREZ, R. (2013), *New approach to design transition in Korean production environment*, ICCAS, Busan, pp.109-118
- PEREZ, R.; GONZALEZ, C. (2015), *History and Evolution of Shipbuilding Oriented CAD Tools*, 14th COMPIT, Ulrichshusen, pp. 8-21
- PEREZ, R.; PENAS, R. (2015). *Integration between shipbuilding CAD Systems and a generic PLM tool in naval projects*. Computer Science and Applications 2/5, pp. 181-191
- PEREZ, R.; TOMAN, M. (2014), *An innovative approach for hull surface fairing stages*, 13th COMPIT, Redworth, pp.32-40
- PEREZ, R.; ALONSO, V. (2015), *Virtual Reality in a Shipbuilding Environment*, Advances in Engineering Software 81, pp. 30-40
- PEREZ, R.; ALONSO, V.; VALDERRAMA, A. (2013), *The use of a 3D CAD system for early design in shipbuilding*, Ship Production Symposium (SPS), Bellevue, pp. 545-553
- TORROJA, J. (1999), *The role of advanced communications in ship engineering*, ICCAS, Cambridge, pp.183-196

Trends in CFD Illustrated Exemplarily for Competitive Sailing Yachts

Benoit Mallol, NUMECA, Brussels/Belgium, benoit.mallol@numeca.be
Alvaro del Toro Llorens, NUMECA, Brussels/Belgium, alvaro.deltorollorens@numeca.be
Volker Bertram, DNV GL, Hamburg/Germany, volker.bertram@dnvgl.com

This paper describes trends in CFD (computational fluid dynamics) techniques for simulation-based design and simulation-based operation. The general trends are illustrated by applications from NUMECA's experience with competitive sailing yachts. Trends include automated work processes, adaptive schemes, systematic parameter variations (in concept exploration and optimization), high-performance computing, hybrid computational strategies for faster response times, multi-phase flows, multi-physics analyses (most notably for fluid-structure interaction), and advanced turbulence models. The progress in CFD capabilities has already led to abandoning model tests altogether for America's Cup yachts. It is reasonable to expect that we will see a similar fading out of model tests for ship design for other ship types.

1. Introduction

The improvements in computing power have allowed using CFD (computational fluid dynamics) to simulate ship hydrodynamic performance more accurately and faster than ever before. The industry's ability to handle complex geometries with all relevant details has also greatly improved. Many aspects have advanced and continue to advance the wide acceptance of CFD as a design and optimization tool. The increase in hardware performance combined with progress in various aspects of algorithms permit an even wider scope of applications, e.g. Peric and Bertram (2011), Bertram and Peric (2013).

The America's Cup (AC) is for the maritime industry what Formula 1 is for the automotive industry: the avant-garde technology driver and magnet for media (and therefore public) attention. The "Defender" yacht, which won the first America's Cup, has little in common with the latest catamaran designs for the America's Cup, Fig.1, except that the finest materials and engineering of its time went into the design and construction of these yachts. CFD has played a fundamental role within AC design process ever since the "Stars and Stripes" effort to bring the Cup back to America. More recently, NUMECA's FINE™/Marine CFD software, <http://www.numeca.com/en/products/finetmmarine>, has been the choice for almost all AC yacht design teams.

Some key trends in CFD applications for marine applications will be discussed in the following.



Fig.1: America's Cup yachts have driven technology spanning almost two centuries; "Defender" (1895) (left), Groupama Team France's foiling catamaran AC 2015 (right)

2. Overview of trends

2.1. Improved physics

2.1.1. Full-scale computing

Model tests cannot respect all similarity laws; thus in some aspects, the flow around a ship model in a model basin differs from that around the real ship, *Hochkirch and Mallol (2013)*. For example, the boundary layer thickness is relatively thinner at full scale, leading e.g. to very different behavior of propulsion improving devices. Another important scale effect (i.e. difference between model scale and full scale) appears for wave breaking, which is particularly important for intermediate drafts in ships. This is important in various aspects, e.g. hull optimization for realistic operational scenarios, trim optimization and performance monitoring. Therefore, we increasingly see full-scale simulations instead of model-scale simulations: “numerical sea trials” replace the “numerical towing tank”.

2.1.2. Multi-phase flows

Ships and sailing yachts operate at the interface between water and air. Correspondingly, free-surface flows are of prime interest for naval architects. Interface-capturing methods (volume of fluid, two-phase flow, level set, etc.) allow the simulation of highly nonlinear free-surface flows. Special numerical schemes allow maintaining sharp free-surface interface over the course of a simulation. Arbitrary free-surface deformation, including breaking waves with detaching droplets, can be adequately modelled as long as gravity and surface-tension effects are included, Fig.2.

10 years ago, many free-surface simulations around ships still showed rapidly decaying wave patterns, unable to reproduce typical Kelvin patterns with crisp wave crests. Increased grid density (especially with adaptive grids) and higher-order differencing schemes have overcome these problems for most practical applications, e.g. *Larsson et al. (2015)*. Similarly, ventilation prediction and cavitation models have matured and are in standard industry applications for propeller and water-jet design.

For seakeeping problems, coupled simulations of flows and flow-induced motions of floating bodies (ships or offshore structures) are desired. These simulations should be implicit, as implicit simulations pose no restrictions on the time-step size. Such 6 DoF (Degrees of Freedom) rigid-body motions of freely moving vessels have been presented for a variety of applications. For sailing yachts, at least the effect of sails on roll damping has to be included as external body force if the sails are not directly modelled.

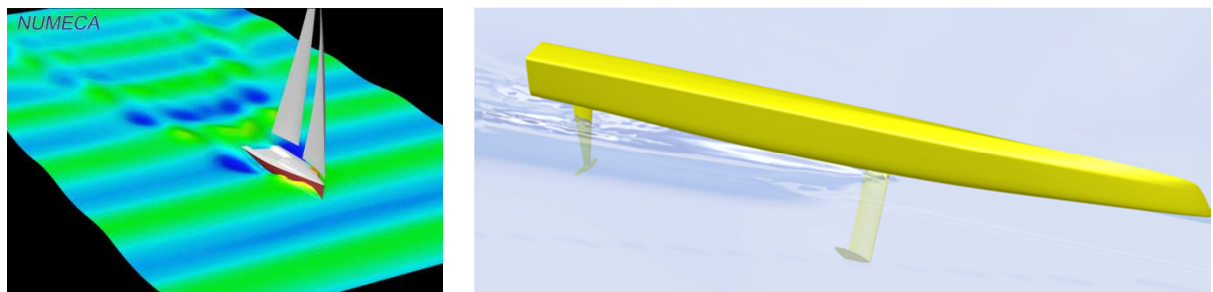


Fig.2: Wave patterns around sailing yachts, conventional (left) and Emirates Team New Zealand’s America’s Cup yacht 2013 (right)

2.1.3. Multi-physics analyses

Coupled simulation of flow and flow-induced deformation of solid structures have evolved more recently for marine applications. Fluid-structure interaction (FSI) is important for relatively flexible structures, most notably for sails, but also for masts. So far, coupling of RANSE codes and finite-element codes (for the structural analyses) is usually explicit, making the computations inefficient to

the point where they are not applicable to most practical problems. Implicit coupling (as already in place for rigid-body motions in waves) is required for robustness and computational efficiency. R&D is active in this field and efficient FSI simulations are only a matter of time.

Bergsma et al. (2013) give a typical example for sailing yacht, coupling FINE™/Marine with the finite-element code Femap to determine the deformation of the sail subject to the aerodynamic load.

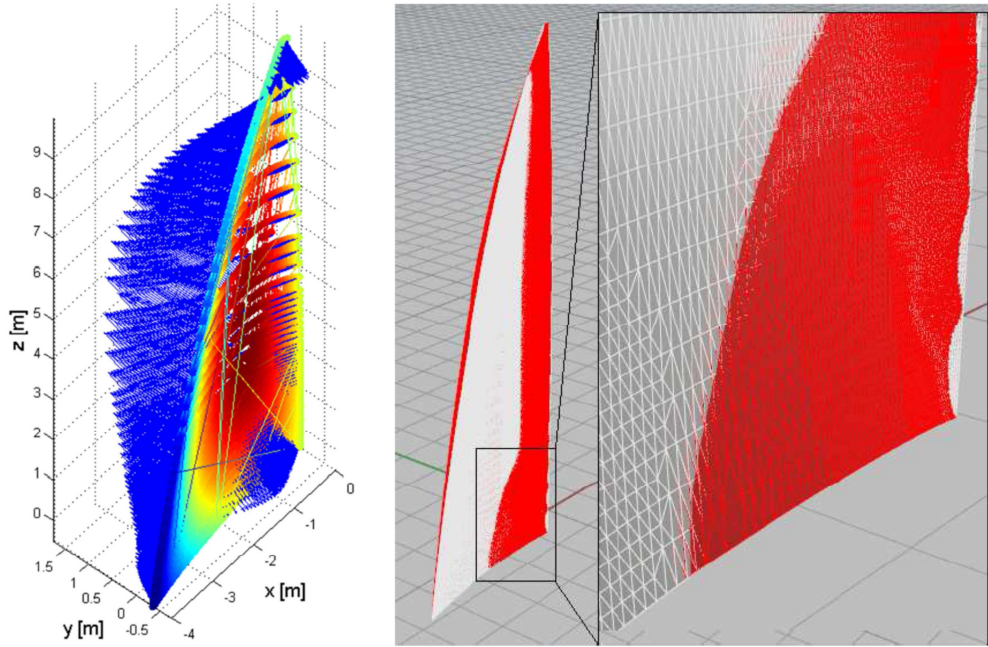


Fig.3: Displacement vectors of deformed shape in FSI analysis (left) with ripples appearing near leading edge (right), *Bergsma et al. (2013)*

Durand et al. (2013) give another example of coupling FINE™/Marine with K-Epsilon's code ARA for sails deformation. The solver ARA was developed during the project VOILEnav. One aim of the code is to model the dynamic behavior of sailboat rigs: sails, mast and cables.

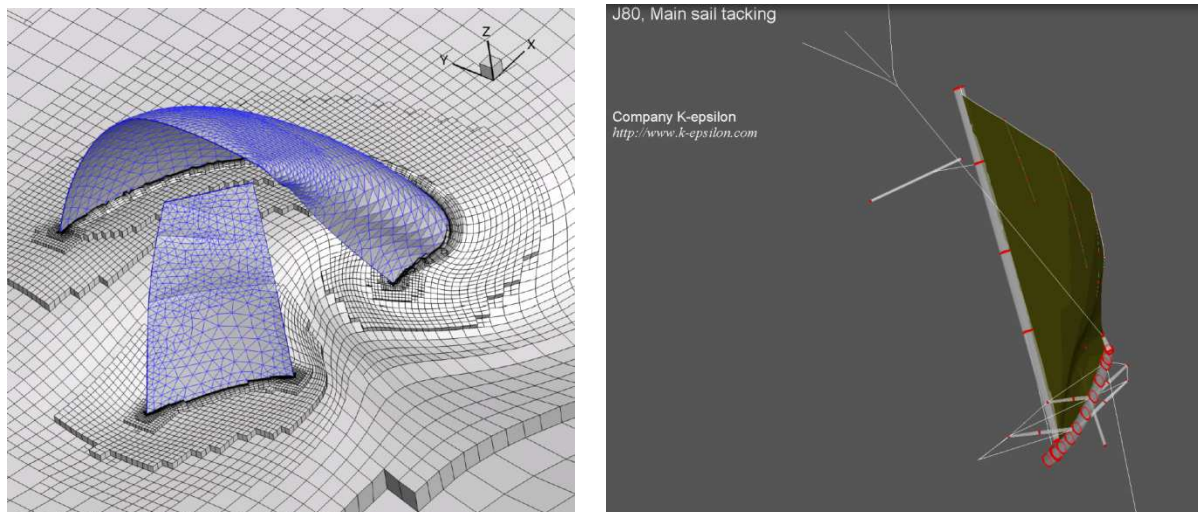


Fig.4: Mesh deformation technique for sails deformation *Durand et al. (2013)* (left) and rigs modeling with ARA (right)

2.1.4. Advanced turbulence models

The standard CFD approach in industry is based on solving the time-averaged Navier-Stokes equations (RANSE = Reynolds-averaged Navier-Stokes equations). The RANSE approach requires external turbulence models to couple the Reynolds stresses (terms from the turbulent fluctuations) to the time-averaged velocities in order to close the set of equations. Turbulence modelling is important for resistance and vortex formation e.g. at appendages. Turbulence modelling has progressed significantly in the past 30 years, from linear one or two-equation models (Spallart-Allmaras, K- ϵ , K- ω , etc.) to non-linear algebraic two equations models (EASM), RSM (Reynolds stress models) and most recently DES. DES (Detached eddy simulation) combines RANSE in the near-wall region with LES (large eddy simulation, i.e. direct resolution of larger characteristic turbulence structures in space and time combined with a sub-grid turbulence model). This approach often yields similar accuracy levels as pure LES with remarkably reduced computational costs and may become the best-practice turbulence model choice of the next decade.

2.2. Systematic parameter variations

Growing computer power and fully automatic procedures have opened the door for systematic variations as the next natural step beyond simulation-based design. Various approaches are used in industry projects, *Bertram and Hochkirch (2015)*. In concept exploration, a.k.a. “design of experiment” (DOE), a large set of candidate solutions is generated by varying design variables. Each of these solutions is evaluated in key performance indicators and stored. Concept exploration thus generates a “map” of the unknown design space. Using suitable graphical displays, the designer gets a feeling of how certain variables influence the performance of the design.

In optimization, parametric models are varied automatically and a formal optimum is found automatically for a given objective function subject to given constraints. In practice, formulating the objective function and the constraints is not often easy. Multi-objective optimization combines concept exploration and optimization. The concept exploration helps in defining objective functions and constraints. CFD-based optimization of hull and appendages has become by now a standard design tool in the marine industry, but research continues to push the limits, *Hochkirch and Bertram (2012)*.

Optimization software, e.g. *Harries (2014)*, *Harries et al. (2015)*, is available to guide an automated simulation process towards an optimum design, combining automatic generation of parameterized geometry, mesh generation, CFD simulation, and subsequent design adaptation. Such optimization may be used for design (hull, appendages, sails, etc.) or operation (hull trim, sail trim, course, etc.), e.g. *Knudsen (2013)*. *Paulin et al. (2015)* describe an application of such operational optimization for competitive sailing yachts. They present a Velocity Prediction Program (VPP) combining CFD results for the hydro- and aerodynamic forces on a hydro-foil sailing catamaran. Using the developed VPP model, realistic velocity prediction can be carried out.

2.3. More efficient computations

High-level CFD simulations in the maritime field are challenging due to numerous computationally very expensive features, such as 6 DoF motions, wave breaking, or relative motion of multiple bodies (e.g. hull, propeller, and rudder). In turn, various developments make CFD projects more efficient, opening the door to even more sophisticated applications.

2.3.1. Automated work processes

In practice, a lot of time has been spent/wasted in interfacing software, data passing (with required conversion and checking) and manual handling of different software, *Bertram (2012)*. This issue has seen considerable progress, although there is still room for improvement. Integrated software environment with seamless interfaces for data passing have supported the progress in this field. As an

example, FINETM/Marine is a complete CFD tool chain, described e.g. in *Visonneau et al. (2012)*, incorporating the following modules:

1. Mesh generator HEXPRESSTM: A full hexahedral unstructured mesh generator which produces body fitted meshes with a high-quality boundary layer resolution.
2. Flow solver ISIS-CFD: The flow solver inside FINETM/Marine is an incompressible free-surface RANSE code, *Duvigneau et al. (2003)*, *Queutey and Visonneau (2007)*. Several turbulence models are implemented ranging from the simple Spalart-Allmaras closure to more advanced models such as the EASM (Explicit Algebraic Stress Model) and hybrid RANSE-LES formulations, *Duvigneau et al. (2003)* and *Deng et al. (2005)*. Free-surface flow is represented by a VOF (Volume of Fluid) technique with an interface capturing approach, allowing representation of breaking waves with crisp and accurate surface capturing schemes, *Queutey and Visonneau (2007)*. Furthermore, the flow solver features 6 DoF motion for the simulation of freely moving ships, *Leroyer and Visonneau (2005)*.
3. Flow visualization system CFViewTM: This system incorporates also marine specific plug-ins. Characteristic features such as wave patterns, free surface and wetted surface are visualized by a mouse-click. Similarly forces, moments and angles can be displayed as single values or time histories.

The whole pre-processing step including mesh and computation setup for complete matrix of simulations are fully automated inside the C-Wizard of FINETM/Marine for many applications including among others, the resistance of sailing yachts with appendages.

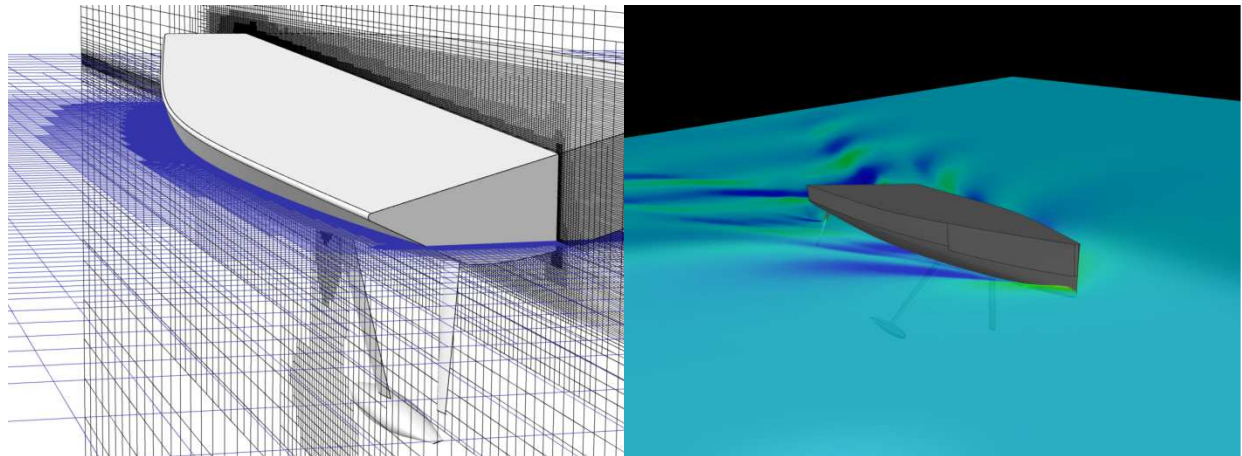


Fig.5: Pre-processing in FINETM/Marine

Fig.6: Post-processing in FINETM/Marine

2.3.2. Adaptive schemes

Numerical accuracy is driven by a number of factors. Grid resolution and numerical scheme are two of these factors which are well suited for adaptivity. Adaptive schemes adjust grids (or other elements such as the order of numerical differencing schemes) in order to obtain a sufficiently good overall result with the least computational effort, *Hildebrandt and Reyer (2015)*. Grids are then refined in regions of high flow gradients and coarsened in regions of low flow gradients.

High velocity gradients appear near the ship hull, the propeller blades and the free surface. Similar to spatial gradients, temporal gradients exist in unsteady flow fields. To ensure an equal processor load even with adapting meshes, the newly created cells have to be distributed automatically between the partitions by the flow solver. Hence the total number of cells on each processor is comparable and an efficient usage of all processors is achieved. Several refinement criteria are available (free-surface criterion, gradient criteria, Hessian based criteria) and can be selected separately, combined or in suc-

cession of each other according to the task at hand. The techniques adopted in FINE™/Marine are described in more detail in *Wackers et al. (2010, 2014)*.

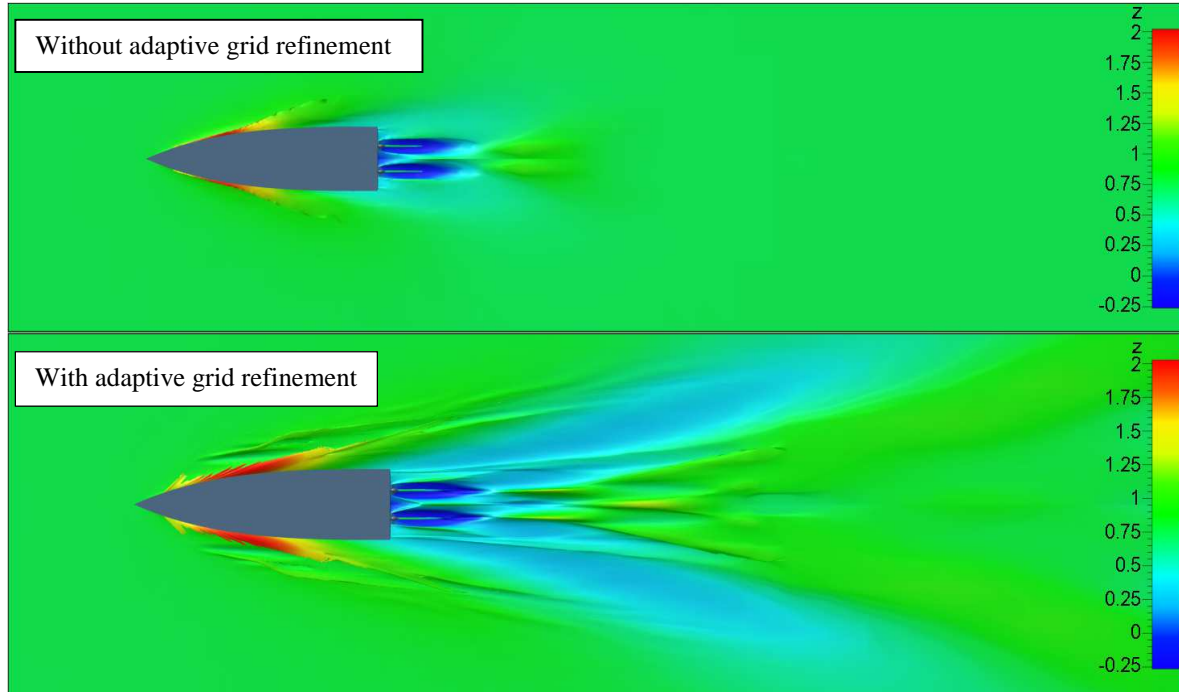


Fig. 6: Wave pattern without (top) and with (bottom) mesh adaptation

The efficiency of adaptive mesh refinement is highlighted in Fig. 7. In this case, the adapted mesh has only about 40% more cells than the initial mesh but the wave pattern is considerably much more detailed showing features which do not appear in the original mesh. Numerical experiments have shown that similar or even better resolution of flow features can be obtained on properly adapted grids, having not even a fifth of the mesh count compared to a fine mesh without adaptation.

2.3.3. High-performance computing (HPC)

The exponential growth in computing power has been based in the past mainly on miniaturization of chips. We just cannot continue making chips infinitely smaller. Once we reach thickness values of a few molecules, we have reached limits where we need other strategies to make computers faster. In short, the key word is “parallelization” instead of “miniaturization”. The architecture of future supercomputers will be much more parallel than in the past. These new computer architectures will require new algorithms (or computing strategies).

(Nearly) full parallelization is relatively simple of fixed grids, but more challenging for adaptive grids. In non-adaptive calculations, usually a domain-decomposition is performed before the computation is initialized. The decomposed regions (partitions) of the grid are then distributed over the available cores, which may even have different individual performances. The number and size of the decomposed regions depend on the number and performance of the computing nodes. Each domain is then put on one core. For adaptive grids, a new decomposition and redistribution over the parallel hardware becomes necessary after each adaptation step. FINE™/Marine uses automatic dynamic load balancing which redistributes the refined grid over the allocated cores when some regions have been refined or coarsened.

In exceptional cases, CFD simulations for ships (numerical propulsion tests) with 200.000 cores have been successfully demonstrated, *Nishikawa (2015)*. In our practice, applications are more moderate, but demonstrate the trend towards using increasing numbers of cores. The trend is towards flexible access to hardware and software. The “NUMECA on Demand” concept combines arbitrarily scalable

HPC resources with an online license management for FINE™/Marine, *Hildebrandt and Reyer (2015)*. Moreover, an UberCloud application software container helps to effectively eliminate the need to maintain in-house HPC expertise as stated by CCTO in *Gentzsch et al. (2016)*.

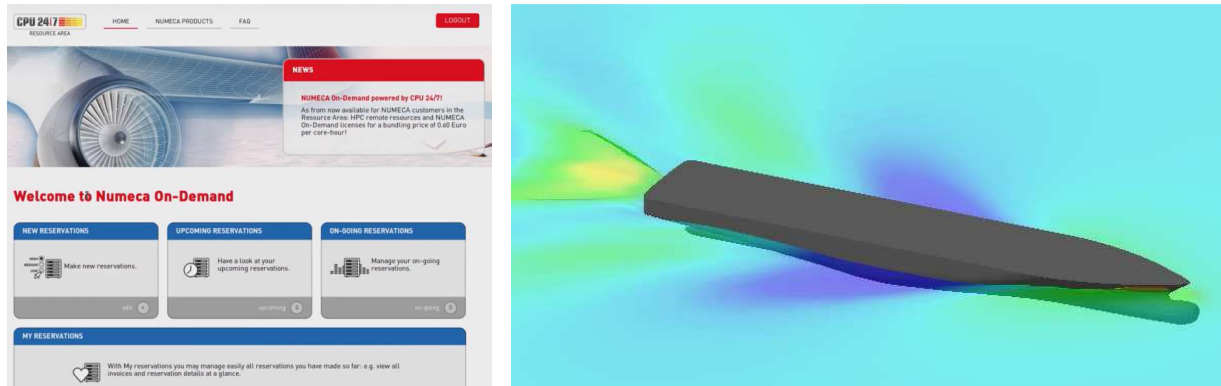


Fig.7: “NUMECA on Demand” at CPU 24/7 and CCTO case study results on UberCloud

2.3.4. Hybrid computing

Hybrid computing mixes low-fidelity approximations (e.g. potential flow solvers or coarse-mesh CFD) and high-fidelity approximations (CFD with fine meshes) to get accurate solutions efficiently. The low-fidelity simulations are then used in regions of secondary interest, for initialization of high-fidelity simulations, or in optimization projects to determine regions of interest for more sophisticated searches.

For example in ship hull optimization, DNV GL employs its in-house wave resistance code for a first-stage selection of hull variants, then FINE™/Marine with medium-grid resolution for the actual optimization (especially of the stern region) and finally a fine-grid RANSE simulation for the power prediction of the determined best hull.

3. Conclusions

Progress in hardware and software have resulted in CFD surpassing model tests as the preferred approach for many applications in the maritime industry. America’s Cup projects are already exclusively CFD-based. There are first proponents of purely CFD-based ship design for commercial shipbuilding, e.g. *Schrooyen et al. (2014)*. The development of CFD capabilities shows no signs of slowing down. We expect that trends seen now for America’s Cup yachts will be followed by the marine industry for general ship design with maybe 5-10 years delay.

Acknowledgement

We thank our colleagues and customers for their support for this paper: Emirates Team New Zealand, Groupama Team France, Van Oossanen, K-Epsilon and CCTO.

References

BERGSMA, F.M.J.; MOERKE, N.; ZAAIJER, K.S.; H.W.M. HOEIJMAKERS (2013), *Development of computational fluid-structure interaction method for yacht sails*, 3rd Int. Conf. Innovation in High Performance Sailing Yachts, Lorient

BERTRAM, V. (2012), *Practical Ship Hydrodynamics*, Butterworth & Heinemann, Oxford

BERTRAM, V.; HOCHKIRCH, K. (2015), *Optimization for ship hulls – Design, refit and operation*, 6th Int. Conf. Computational Methods in Marine Engineering (MARINE), Rome, pp.210-217

BERTRAM, V.; PERIC, M. (2013), *Advanced simulations for offshore industry applications*, 12th Conf. Computer and IT Applications in the Maritime Industries (COMPIT), Cortona, pp.7-20

DENG, G.B.; QUEUTEY, P.; VISONNEAU M. (2005), *Three-dimensional flow computation with Reynolds stress and algebraic stress models*, In W. Rodi and M. Mulas, editors, *Engineering Turbulence Modelling and Experiments 6*, pp 389–398. ELSEVIER

DURAND, M.; LOTHODE, C.; HAUVILLE, F.; LEROYER, A.; VISONNEAU, M.; FLOCH, R.; GUILLAUME, L. (2013), *FSI investigation on stability of downwind sails with an automatic dynamic trimming*, INNOVSAIL, Lorient

DUVIGNEAU, R.; VISONNEAU, M.; DENG, G.B. (2003), *On the role played by turbulence closures in hull shape optimization at model and full scale*, J. Marine Science & Technology 8/1, pp.1-25

GENTZSCH, W.; YENIER, B. (2016), *Prediction of barehull resistance curve of a day-cruise ship in the cloud*, <http://www.theubercloud.com/>

HARRIES, S. (2014), *Practical shape optimization using CFD*, Whitepaper CAESES, Potsdam

HARRIES, S.; ABT, C.; BRENNER, M. (2015), *Upfront CAD – Parametric modeling techniques for shape optimization*, 11th Int. Conf. Evolutionary and Deterministic Methods for Design, Optimization and Control with Applications to Industrial and Societal Problems (EUROGEN), Glasgow

HILDEBRANDT, T.; REYER, M. (2015), *Business and technical adaptivity in marine CFD simulations - Bridging the gap*, 14th Conf. Computer and IT Applications in the Maritime Industries (COMPIT), Ulrichshusen, pp.394-406

HOCHKIRCH, H.; BERTRAM, V. (2012), *Hull optimization for fuel efficiency – Past, present and future*, 11th Conf. Computer and IT Applications in the Maritime Industries (COMPIT), Liege, pp.39-49

HOCHKIRCH, K.; MALLOL, B. (2013), *On the importance of full-scale CFD simulations for ships*, 12th Conf. Computer and IT Applications in the Maritime Industries (COMPIT), Cortona, pp.85-95

KNUDSEN, S.S. (2013), *Sail Shape Optimization with CFD*, Master Thesis, Danish TU, Lyngby

LARSSON, L.; STERN, F.; VISONNEAU, M.; HINO, T.; HIRATA, N.; KIM, J. (2015), *Proceedings Tokyo 2015 Workshop on CFD in Ship Hydrodynamics*, Chalmers TU, Gothenburg

LEROYER, A.; VISONNEAU, M. (2005), *Numerical methods for RANSE simulations of a self-propelled fish-like body*, J. Fluid & Structures 20/3, pp.975-991

NISHIKAWA, T. (2015), *Application of fully resolved large eddy simulation to self-propulsion test condition of double-model KVLC2*, 14th Conf. Computer and IT Applications in the Maritime Industries (COMPIT), Ulrichshusen, pp.191-200

PAULIN, A.; HANSEN, H.; HOCHKIRCH, K.; FISCHER, M. (2015), *Performance Assessment and Optimization of a C-Class Catamaran Hydrofoil Configuration*, 5th High Performance Yacht Design Conf., Auckland

PERIC, M.; BERTRAM, V. (2011), *Trends in industry applications of CFD for maritime flows*, 10th Conf. Computer and IT Applications in the Maritime Industries (COMPIT), Berlin, pp.8-19

QUEUTEY, P.; VISONNEAU, M. (2007), *An interface capturing method for free-surface hydrodynamic flows*, Computers & Fluids 36/9, pp.1481-1510

SCHROOYEN, I.; RANDLE, K.; HERRY, B.; MALLOL, B. (2014), *Methodology for quick and accurate CFD Calculations of self-propelled ships using sliding grids and dynamic RPM control*, 13th Conf. Computer and IT Applications in the Maritime Industries (COMPIT), Redworth, pp.49-60

VISONNEAU, M.; QUEUTEY, P.; DENG, G.B.; WACKERS, J; GUILMINEAU, E.; LEROYER, A.; MALLOL, B. (2012), *Computation of free-surface viscous flows around self-propelled ships with the help of sliding grids*, 11th Conf. Computer and IT Appl. Maritime Ind. (COMPIT), Liege, pp.344-358

WACKERS, J.; DENG, G.B.; VISONNEAU, M. (2010b), *Tensor-based grid refinement criteria for ship flow simulation*, 13th Numerical Towing Tank Symp. (NuTTS), Duisburg

WACKERS, J.; GUILMINEAU, E.; PALMIERI, A.; QUEUTEY, P. (2014), *Hessian-based grid refinement for the simulation of surface-piercing hydrofoils*, 17th Numerical Towing Tank Symp. (NuTTS), Marstrand

High-Level Vessel Characterization

Vidar Vindøy, DNV GL, Oslo/Norway, vidar.vindoy@dnvgl.com
Kristin Dalhaug, DNV GL, Oslo/Norway, kristin.dalhaug@dnvgl.com

Abstract

This paper presents a proposal for a high-level characterization of vessels. The proposal is based on the use of 5 basic variables. The proposal will enable the continued use of ‘vessel type’ lists, by defining each vessel type based on the basic variables.

1. Introduction

1.1. Terminology

The term ‘vessel’ is used to denote any kind of watercraft, e.g. ships, craft, offshore units.

1.2 Vessel related references at DNVGL

As a basis for DNVGL’s class and statutory services, a set of about 50 reference standards relating to vessels have been developed and are in daily use. Our standardized description of the vessel and its equipment is formulated in the ‘Generic product model’, *Vindøy (2010)*. In this paper, the references used to characterize the vessels on a high level are presented.

1.3 Need for high level characterisation

A high-level characterization of vessels is fundamental to most technical and commercial topics within the maritime industry. Nevertheless, no universally adopted standard for this exists. Most organizations working in the maritime industry relate to one or more propriety defined lists of ‘ship types’. This situation prevents an effective exchange of information.

2 Problems with existing ‘ship type’ lists

2.1 Uniqueness constraint

Most ‘ship type’ lists operate under the unspoken constraint that one vessel may have only one ‘ship type’. In order to characterize vessels with more than one purpose, combination types must be made, e.g. ‘Fire fighter and supply vessel’.

2.2 Lack of consistence

Many ‘ship type’ lists mix different characteristics of the vessels as their purpose, structural design type or regulatory framework into one list. Together with the uniqueness constraint, this prevents the setting of all relevant characteristics.

2.3 Granularity

Different uses will require different granularity. In commonly used ‘ship type’ lists, the number of items in a list varies from 8 to more than 500.

2.4 Vessel size

Some ‘ship type’ lists differentiates upon size characteristics, such as tonnage, length or cargo carrying capacity.

3. Vessel characterization by basic variables

In our experience, most vessels may be adequately characterized by the use of 4 discrete variables relating to physical properties of the vessels. In addition, a variable relating to the regulatory framework that vessels operate under has been found to be useful. Examples of possible lists defining the 5 variables are included in the appendices. Sizing variables can be used in addition.

3.1 Vessel purpose

By vessel purpose is meant the tasks that the vessel is designed to perform, e.g. oil carriage, passenger carriage, towing, drilling etc. The vessel purposes may be set up in a hierarchical structure. The vessel purposes is the variable that in most respects resembles current ‘ship types’. Each vessel must have one main purpose, but may have additional purposes.

3.2 Structural design type

By structural design type is meant e.g. monohull ship, catamaran, column-stabilized unit, self-elevating unit. Each vessel must have one and only one structural design types.

3.3 Propulsion principle

By propulsion principle is meant the method(s) used in order to enable the vessels movement through the water. Each vessel must have one main propulsion principle, and may have additional propulsion principles.

3.4 Cargo handling principles

By cargo handling principle is meant the method(s) used in order to loan and/or unload cargo. Each vessel must have at least one cargo handling principle.

3.5 Regulatory regime

By regulatory regime is meant the regulatory framework under which the vessel is supervised. Each vessel must have one and only one regulatory regime.

4. Proposal

4.1 Standardization of basic variables

The 5 variables defined in 3 should be defined in a suitable reference library in an international standard. The definitions should include

- codes
- names
- hierarchical structure
- definitions of each term

4.2 Application to vessels

Maritime databases should include specification of the basic variables for each vessel covered by the database.

4.3 Use of vessel types

List of vessel types may be defined through relations to the basic variables, and where needed also to sizing variables. The granularity of any vessel type list may be tailored to its use through the hierarchy inherent in the basic variables.

Reference

VINDØY, V. (2010), *A Functionally Oriented Vessel Data Model Used as Basis for Classification*, PDT Europe 2010, Reading, pp.60-69

Appendix 1 – Vessel purposes

Vessel purpose			Assign to vessels
Code	Name	Definition	
10	Liquid and gas bulk cargo carriage	Bulk carriage of liquid and gas cargoes	FALSE
11	Oil carriage	Bulk carriage of oil and oil products	FALSE
11.1	Crude oil carriage	Bulk carriage of crude oil	TRUE
11.2	Oil product carriage, low flashpoint (< 60 °C)	Bulk carriage of refined petroleum products, either clean or dirty with flashpoint < 60 °C	TRUE
11.3	Oil product carriage, high flashpoint (>= 60 °C)	Bulk carriage of oil or oil products with flashpoint >= 60 °C, other than asphalt or bitumen	TRUE
11.4	Oil products carriage at high temperature	Bulk carriage of oil products, e.g. asphalt or bitumen at temperatures between 50 and 200 °C	TRUE
12	Chemical carriage	Bulk carriage of cargoes listed in IBC Code chapter 17	FALSE
12.1	Chemical carriage, low flashpoint (< 60 °C)	Bulk carriage of flammable chemicals with flashpoint < 60 °C	TRUE
12.2	Chemical carriage, high flashpoint (>= 60 °C)	Bulk carriage of flammable chemicals with flashpoint >= 60 °C	TRUE
12.3	Chemical carriage, non flammable	Bulk carriage of non flammable chemical products	TRUE
13	Gas carriage	Bulk carriage of gas	FALSE
13.1	Liquefied gas carriage, flammable	Bulk carriage of flammable liquefied gas	FALSE
13.11	Liquefied natural gas carriage	Bulk carriage of liquefied natural gas	TRUE
13.12	Liquefied petroleum gas carriage	Bulk carriage of liquefied petroleum gas	TRUE
13.2	Liquefied gas carriage, non flammable	Bulk carriage of non flammable liquefied gas	TRUE
13.23	Liquefied CO2 carriage	Bulk carriage of liquefied CO2	TRUE
13.3	Compressed gas carriage, flammable	Bulk carriage of compressed flammable gas	FALSE
13.31	Compressed natural gas carriage	Bulk carriage of compressed natural gas	TRUE
13.32	Compressed petroleum gas carriage	Bulk carriage of compressed petroleum gas	TRUE
14	Liquid carriage, non-oil, non-chemical	Bulk carriage of cargoes listed in IBC Code chapter 18	FALSE
14.1	Liquid carriage, low flashpoint (< 60 °C)	Bulk carriage of non-oil, non-chemical, low flashpoint (< 60 °C) liquids	TRUE
14.2	Liquid carriage, high flashpoint (>= 60 °C)	Bulk carriage of non-oil, non-chemical, high flashpoint (>= 60 °C) liquids	TRUE
14.3	Liquid carriage, non flammable	Bulk carriage of non flammable liquids	FALSE
14.31	Liquid carriage, non flammable	Bulk carriage of non flammable liquids, other than fruit juice, wine, molasses, beer or water	TRUE
14.32	Fruit juice carriage	Bulk carriage of fruit juice	TRUE
14.33	Wine carriage	Bulk carriage of wine	TRUE
14.35	Molasses carriage	Bulk carriage of molasses	TRUE
14.36	Beer carriage	Bulk carriage of beer	TRUE
14.37	Water carriage	Bulk carriage of water	TRUE
20	Dry bulk cargo carriage	Bulk carriage of dry cargo	FALSE
21	Dry bulk cargo carriage, general	Bulk carriage of dry cargo	FALSE
21.0	Dry bulk cargo carriage	Bulk carriage of dry cargo	TRUE
21.1	Grain carriage	Bulk carriage of grain	TRUE
21.3	Fertilizer carriage	Bulk carriage of fertilizer, e.g. urea	TRUE
21.4	Sugar carriage	Bulk carriage of refined sugar	TRUE
21.5	Powder carriage	Bulk carriage of powder	TRUE

21.6	Dry bulk forest products carriage	Bulk carriage of forest products	TRUE
21.7	Log / lumber carriage	Bulk carriage of log or lumber	TRUE
21.8	Wood chips carriage	Bulk carriage of wood chips	TRUE
22	Heavy dry bulk cargo carriage	Bulk carriage of heavy dry cargo	FALSE
22.0	Heavy dry bulk cargo carriage	Bulk carriage of heavy dry cargo	TRUE
22.1	Ore carriage	Bulk carriage of ore	TRUE
22.2	Cement carriage	Bulk carriage of cement	TRUE
22.3	Stone carriage	Bulk carriage of stone	TRUE
22.4	Sand carriage	Bulk carriage of sand	TRUE
30	General cargo carriage	Carriage of unitized dry cargo	FALSE
31	General cargo carriage	Carriage of unitized dry cargo	FALSE
31.0	General cargo carriage	Carriage of unitized dry cargo	TRUE
31.1	Pallet carriage	Carriage of unitized dry cargo stored on pallets	TRUE
31.3	Barge carriage	Carriage of purpose built barges (lighters) loaded with cargo. Also known as 'Lighter aboard ship vessels' (LASH).	TRUE
31.4	Nuclear fuel carriage	Carriage of nuclear fuel	TRUE
31.5	Pulp carriage	Carriage of paper pulp	TRUE
32	Container carriage	Carriage of containers	TRUE
33	Vehicle carriage	Carriage of cars, trains or other vehicles. As well new vehicles as vehicles in use, e.g. ferries.	FALSE
33.1	Car carriage	Carriage of cars. As well new cars as cars in use, e.g. ferries.	TRUE
33.2	Train carriage	Carriage of trains. As well new trains as trains in use, e.g. ferries.	TRUE
33.3	Military vehicle carriage	Carriage of military vehicles	TRUE
34	Refrigerated cargo carriage	Carriage of refrigerated cargo	TRUE
36	Sea product carriage	Carriage of sea products	FALSE
36.1	Fish carriage	Carriage of fish and fish products	TRUE
36.2	Live fish carriage	Carriage of live fish	TRUE
36.3	Pearl shell carriage	Carriage of pearl shells	TRUE
39	Unitized cargo carriage, other	Carriage of other types of unitized cargoes that those described in 31 -36	FALSE
39.1	Livestock carriage	Carriage of livestock	TRUE
40	Passenger carriage and accommodation	Carriage of passengers, crew or troops; accommodation, yachting or leisure	FALSE
41	Passenger carriage	Carriage of passengers on vessels certified to carry more than 12 passengers	TRUE
42	Crew and troop carriage	Carriage of crew or troops	FALSE
42.1	Troop carriage	Carriage of troops	TRUE
42.2	Crew carriage	Carriage of crew to or from vessels or installations	TRUE
43	Accommodation	Provision of accommodation for those working on other vessels or installations	TRUE
44	Yachting	Yachting	TRUE
49	Passenger carriage and accommodation, other	Carriage of passengers, crew or troops; accommodation, yachting or leisure other than those described in 41 - 44	FALSE
49.1	Hospital	Equipped to serve as a hospital	TRUE
49.2	Leisure	Exhibitions, trade fairs, catering and the like	TRUE
49.4	Pilot carriage	Carriage of pilots	TRUE
49.5	Training	Training	TRUE
50	Sea product handling	Capability to handle sea products	FALSE
51	Sea product catching	Capability to catch sea products	FALSE
51.1	Fishing	Capability to catch fish	TRUE
51.2	Sealing	Capability to catch seals	TRUE
51.3	Whaling	Capability to catch whales	TRUE

52	Sea product processing	Capability to perform refrigerating, processing or canning of sea products	TRUE
53	Harvesting	Capability to harvest sea resources	FALSE
53.1	Kelp dredging	Capability to harvest kelp seaweed	TRUE
53.2	Mining	Capability to perform mining operations, e.g. for diamonds	TRUE
60	Offshore and coastal operation	Capability to perform offshore and coastal operations	FALSE
61	Offshore operations	Capability to perform offshore operations including supply, support, standby, rescue, anchor handling, salvage, towing, pushing and diving	FALSE
61.1	Supply operations	Capability to perform supply, support, standby, rescue, anchor handling, salvage operations, oil recovery, low flashpoint liquid carriage or well stimulation.	FALSE
61.11	Supply	Capability to perform transportation of stores, liquids and goods to offshore units or installations	TRUE
61.12	Support	Capability to perform support of offshore units or installations	TRUE
61.13	Standby	Capability to perform safety standby duties for offshore units or installations including facilities for rescue, reception and initial care of survivors from accidents	TRUE
61.14	Rescue	Capability to perform search and rescue operations	TRUE
61.15	Anchor handling	Capability to provide assistance to mooring or anchoring operations for other vessels	TRUE
61.16	Salvage	Capability to perform salvage of e.g. grounded vessels	TRUE
61.17	Oil recovery	Equipped for the purpose of pollution control, including oil-spill recovery and pollution and debris collection	TRUE
61.18	Low flashpoint liquid supply	Capability to supply flammable liquids with flashpoint < 60 °C	TRUE
61.19	Well stimulation	Capability to stimulate oil or gas production from subsea wells	TRUE
61.2	Towing and pushing	Capability to tow and push other vessels	FALSE
61.21	Towing (active)	Capability to tow other vessels in harbour or in open sea, and with manoeuvring capabilities to assist vessels to berth or unberth in ports	TRUE
61.22	Towing (passive)	Capability to being towed by another vessel, e.g. by a tug	TRUE
61.23	Pushing (active)	Capability to push other vessels, e.g. barges or pontoons	TRUE
61.24	Pushing (passive)	Capability to being pushed by another vessel, e.g. by a pusher	TRUE
61.3	Diving support	Capability to provide support of diving operations and life support for divers	TRUE
61.4	Tank cleaning	Capability to perform cleaning of the tanks or removal and transport of slops for other vessels	TRUE
61.5	Servicing	Capability to perform servicing or support of marine installations, e.g. wind farms.	TRUE
62	Oil and gas production and storage	Capability to control production rates from an oil field or a gas field and to store oil or gas produced prior to its transfer to a pipeline or another vessel for transportation	FALSE
62.1	Oil production and storage	Capability to control production rates from an oilfield and to store oil produced prior to its transfer to a pipeline or another vessel for transportation	FALSE
62.11	Oil production	Capability to control production rates from an oilfield	TRUE
62.12	Oil storage	Capability to store oil produced prior to its transfer to a pipeline or another vessel for transportation	TRUE
62.2	Gas production and storage	Capability to control production rates from a gas field, and to store gas produced prior to its transfer to a pipeline or another vessel for transportation	FALSE
62.21	Liquefied gas production	Capability to control production rates from an gas field, and to liquefy the produced gas	TRUE
62.24	Liquefied gas storage	Capability to store produced gas in liquefied form prior to its transfer to a pipeline or another vessel for transportation	TRUE

62.4	Offshore unloading	Unloading of produced oil or gas to a transportation vessel at an offshore location	TRUE
63	Drilling and well operation	Capability to perform drilling, intervention, testing or stimulation of subsea oil or gas wells	FALSE
63.1	Drilling	Capability to perform drilling operations on subsea oil or gas wells, including obtaining of cores for research purposes	TRUE
63.2	Well intervention	Capability to perform interventions of subsea wells	TRUE
63.3	Well testing	Capability for testing the quality and amount of oil or gas produced by subsea wells	TRUE
64	Research	Capability to perform research or survey at sea, e.g. oceanographic, hydrographical, fishery or biological research or survey	FALSE
64.1	Seismic exploration	Capability to perform geophysical research or survey at sea	TRUE
64.2	Oceanographic / hydrographical research	Capability to perform oceanographic or hydrographical research or survey at sea	TRUE
64.4	Fishery research	Capability to perform fishery research or survey at sea	TRUE
65	Marine operations	Capability to perform marine operations, e.g. ice breaking, fire fighting, crane operation, sea bottom operation, docking or repair	FALSE
65.1	Ice breaking	Capability to clear a passage through ice	TRUE
65.2	Fire fighting	Capability to fight fires on other vessels or installations	TRUE
65.3	Crane operation	Capability to perform lifting operations by use of crane	TRUE
65.4	Sea bottom operations	Capability to perform sea bottom operations, e.g. pipe laying, cable laying, dredging, mass depositing or trenching support	FALSE
65.41	Pipe laying	Capability to lay solid or flexible pipes on the sea bed	TRUE
65.42	Cable laying	Capability to lay or repair underwater cables	TRUE
65.43	Dredging	Capability to obtain material from the sea bed	TRUE
65.44	Mass depositing	Capability to carry stones and aggregates and to deliver them on to the sea bed, e.g. in order to bury pipes or cables	TRUE
65.45	Trenching support	Capability to operate submersibles for digging trenches on the sea bed, e.g. for pipes or cables	TRUE
65.5	Docking	Capability to dry-dock other vessels whilst afloat	TRUE
65.6	Repair	Capability to perform general work and repair operations	TRUE
69	Offshore and coastal operation, other	Offshore and coastal operations other than those described in 61 - 68	FALSE
69.1	Lighthouse	Capability to operate as a lighthouse	TRUE
69.3	Wind turbine installation and operation	Capability to install or operate wind turbines	TRUE
69.4	Waste disposal	Capability to perform transportation, treatment or discharge at sea of waste material	TRUE
69.5	Utility operations	Capability to perform general utility operations	TRUE
69.6	Supply tendering	Capability to perform transportation of stores and goods to remote communities	TRUE
69.7	Rocket launching	Capability to launch rockets	TRUE
70	Navy and coast guard operation	Capability to perform naval and coast guard operations	FALSE
71	Naval operations	Capability to perform naval operations	FALSE
71.0	Naval operations	Capability to perform naval operations	TRUE
71.1	Beaching and offshore docking	Capability to perform beaching and offshore docking operations	TRUE
71.2	Combat	Capability to combat	TRUE
72	Patrol operations	Capability to patrol	TRUE
79	Navy and coast guard operation, other	Capability to perform naval and coast guard operations, other than those described in 71 - 78	TRUE

Appendix 2 – Structural design types

Structural design types			Assign to vessels
Code	Name	Definition	
BU	Buoy	A floating body, normally of a cylindrical shape.	TRUE
CS	Column-stabilised unit	Floating unit or installation dependent on the buoyancy of columns and pontoons.	TRUE
CY	Cylindrical unit	Floating unit or installation of cylindrical shape.	TRUE
DD	Deep draught installation	Floating structure having a relatively deep draught to obtain high heave eigenperiod avoiding resonance responses. A deep draught unit or installation can have single or multi-vertical columns, with or without moonpools.	TRUE
SE	Self-elevating unit	Unit or installation with hull of sufficient buoyancy for safe transit which is operation is elevated above sea surface by legs resting on the sea bed.	TRUE
SM	Submarine		TRUE
SS	Ship	A floating structure designed to move efficiently through water e.g. for transport of people and goods.	FALSE
SS.01	Monohull ship	A ship with a single hull.	TRUE
SS.03	Catamaran	A ship with two hulls.	TRUE
SS.04	Trimaran	A ship with three hulls.	TRUE
SS.06	Surface effect ship	A multihull ship where the hulls together with skirts provide the boundaries for an air cushion.	TRUE
SS.07	Air cushion vehicle	A monohull ship with skirts providing the boundaries for an air cushion.	TRUE
TL	Tension leg installation	Buoyant installation connected to a fixed foundation by pre-tensioned tendons.	TRUE

Appendix 3 – Propulsion principles

Code	Name	Definition	Assign to vessels
C	Conventional propulsion	Propulsion by means of one or more drivers connected to one or more propulsion lines with a propeller in the vessel's stern.	FALSE
C.CE	Conventional propulsion - combustion engine	Conventional propulsion where at least one of the propulsion lines is driven by a combustion engine.	TRUE
C.EL	Conventional propulsion - electric	Conventional propulsion where at least one of the propulsion lines is driven by an electric motor.	TRUE
C.GT	Conventional propulsion - gas turbine	Conventional propulsion where at least one of the propulsion lines is driven by a gas turbine.	TRUE
C.HY	Conventional propulsion - hydraulic motor	Conventional propulsion where at least one of the propulsion lines is driven by a hydraulic motor.	TRUE
C.RS	Conventional propulsion - reciprocating steam engine	Conventional propulsion where at least one of the propulsion lines is driven by a reciprocating steam engine.	TRUE
C.ST	Conventional propulsion - steam turbine	Conventional propulsion where at least one of the propulsion lines is driven by a steam turbine.	TRUE
NO	None	No propulsion or propulsion not sufficient for the vessel's service area.	TRUE
SA	Sails	Propulsion by means of sails.	TRUE
T	Thruster propulsion	Propulsion by means of one or more thrusters. The term thruster includes pods and waterjets.	FALSE
T.CE	Thruster propulsion - combustion engine	Thruster propulsion where at least one of the thrusters is driven by a combustion engine.	TRUE
T.EL	Thruster propulsion - electric	Thruster propulsion where at least one of the thrusters is driven by an electric motor.	TRUE

T.GT	Thruster propulsion - gas turbine	Thruster propulsion where at least one of the thrusters is driven by a gas turbine.	TRUE
T.HY	Thruster propulsion - hydraulic motor	Thruster propulsion where at least one of the thrusters is driven by a hydraulic motor.	TRUE
T.RS	Thruster propulsion - reciprocating steam engine	Thruster propulsion where at least one of the thrusters is driven by a reciprocating steam engine.	TRUE
T.ST	Thruster propulsion - steam turbine	Thruster propulsion where at least one of the thrusters is driven by a steam turbine.	TRUE

Appendix 4 – Cargo handling principles

Code	Name	Definition
BL	Blowing	The cargo is loaded or unloaded by use of fans or compressors or by pressure differences.
CA	Carrying	The cargo is loaded or unloaded by walking on its own legs. The cargo is humans, cattle or sheep walking on or off the vessel, or the cargo is carried on or off the vessel.
CO	Conveying	The cargo is loaded or unloaded by use of conveying belts.
DU	Dumping	The cargo is unloaded by opening the vessel's bottom and dumping the cargo into the sea.
FL	Floating	The cargo is loaded or unloaded by floating the cargo on or off the vessel.
LI	Lifting	The cargo is loaded or unloaded by use of any type of lifting arrangements.
NO	None	There is no cargo handling.
PU	Pumping	The cargo is loaded or unloaded by use pumps. The cargo may be liquids suitable for pumping or the cargo may be dissolved or undissolved in the pumping media.
RO	Rolling	The cargo is loaded or unloaded by use of any type of rolling machinery, e.g. cars, trucks or fork lifts, including cargo lifting by air cushion or similar arrangements.

Appendix 5 – Regulatory regimes

Code	Name	Definition
HSLC	High speed, light craft	Vessels supervised by a flag authority and engaged in international or national trade, constrained to reach a safe refuge under certain predefined environmental conditions. The supervision is based upon: - International Code of Safety for High-Speed Craft (HSC), or - Code of Safety for Dynamically Supported Craft (DSC), or - National regulations.
INV	Inland navigation vessels	Vessels supervised by a flag authority and engaged in inland or coastal trade. The supervision is based upon: - Regional regulations, or - National regulations.
Naval	Naval vessels	Vessels supervised by a naval flag authority. The supervision is based upon: - Naval Ship Code (NSC), or - National regulations.
Offshore	Offshore units	Vessels supervised by a flag authority or costal state and engaged in exploration for or exploitation of resources beneath the sea-bed such as liquid or gaseous hydrocarbons. The supervision is based upon: - Code for the Construction and Equipment of Mobile Offshore Drilling Units (MODU), or - National regulations.
Ship	Ships	Vessels supervised by a flag authority and engaged in international or national trade. The supervision is based upon: - International Convention for the Safety of Life at Sea (SOLAS), or - National regulations.
Yacht	Yachts	Pleasure vessels in private use or engaged in trade. The vessels may be supervised by a flag authority based on international or national regulations.

Energy Efficient Operation of Offshore Supply Vessels – A Framework

Lars Lindegaard Mikkelsen, University of Southern Denmark, l1mi@iti.sdu.dk

Marie Lützen, University of Southern Denmark, mlut@iti.sdu.dk

Signe Jensen, Svendborg International Maritime Academy, Denmark, sje@simac.dk

Abstract

Most performance systems in the market have been developed for long distance sailing and cannot be used directly at working vessels having unpredictable and flexible operation profiles. The aim of this paper is to present a framework that describes the overall decision structures in connection with energy optimisation of offshore supply vessels. Modelling a framework like this requires a deep insight into the operation of ships and therefore a high level of crew involvement has taken place.

1. Introduction

For many years, there has been a growing focus on energy efficient operation of vessels. Stakeholders in the maritime industry have identified several methods to improve energy efficiency and a large number of studies estimating ways to improve cost-effectiveness have been performed. The increasing pressures from environmental problems, human health and global climate change have also resulted in new legislation for reduction in greenhouse gas emissions.

Despite the fact that knowledge of ways to improve cost-effectiveness are well understood in the industry, there is only minor emphasis on energy efficient operation on board many offshore vessels of today. Optimising energy efficiency on these vessels can be very difficult; the vessels are known to be involved in many different operations and therefore they have a very complex operation profile, which is difficult to evaluate and to compare. Furthermore, safety issues and optimising the time available for performing offshore work has been a topic of focus for many years. The offshore work is normally very time consuming and well paid compared to the fuel oil costs.

The regulatory framework is also mostly focused on safety issues, and international regulations on energy efficiency are not applicable for offshore supply vessels. The International Maritime Organisation (IMO) has introduced guidelines for calculating energy efficiency during both the design and operation phases through the Energy Efficiency Design Index (EEDI), *IMO (2012a)*, the Ship Energy Efficiency Management Plan, SEEMP, *IMO (2012b)* and the Energy Efficiency Operational Indicator EEOI, *IMO (2009)*. The regulation entered into force in January 2013 with the adoption of amendments to MARPOL Annex VI – adding a new chapter on Regulations on energy efficiency for ships, *IMO (2011)*. Where EEDI sets the design limits for new vessels, the intention of the SEEMP is to improve daily operation on-board. The SEEMP is mandatory for all vessels, and also non-transport vessels operating as working vessels, whereas only cargo carrying vessels are included in the EEDI approach of today. The conventional transport vessels operating as container vessels, tankers and bulk carriers are easy to categorise – they are intended for one purpose with a single design point specified with a given cargo load and design speed. The more specialised vessels such as e.g. offshore supply vessels are not covered by the regulations as propulsion type, speed and operations are varying, and it is difficult to define a fixed design point. EEOI is a voluntary guidance tool for existing ships that can help to identify best practices for fuel-efficient operation. The EEOI is based on transport work (cargo transported per nautical mile per ton of fuel), which makes it unusable for most working vessels such as e.g. offshore supply vessels. Lately the European Union has pushed forward an EU-wide legal framework for monitoring, verification and reporting MRV of CO₂ emissions from maritime transport, *EU (2015)*. This regulation, which was adopted on 29th April 2015, applies to larger vessels (over 5000 gross tonnage) calling at EU ports from 1st January 2018 to collect and later publish data on CO₂ emissions; most offshore vessels are below 5000 GT and therefore not included in the regulation.

Guidelines for offshore marine operations, such as *G-OMO (2013)* and regulations like the ISM code, *IMO (2014)* and the safety management system (SMS), which is an important part of the ISM code, are introduced to establish good practice for safe operations, and concerns regarding energy efficiency are not included. These considerations and initiatives must be implemented by the shipping company itself. Furthermore, many offshore vessels are operated on a time charter basis meaning that the capital and the operational costs including the investment in fuel efficiency of the vessel are paid by the owner, whereas the voyage cost including the fuel are paid by the charter. This, which is also called the spit incentives problem, does not promote the energy efficiency initiative either.

The number of offshore vessels is increasing; *OECD (2015)* concludes that in the period from 2014 to 2025 there will be a growing demand for energy, which will have an effect on the offshore shipping market. For example, the demand in offshore support vessels engaged as installation supply vessels is expected to grow by 50% and the demand for wind turbine installations vessels by 117%. The numbers are at present challenged by the fall in the oil prices but long-term studies show that there will be a growing demand.

The total CO₂ emissions for offshore and service vessels is estimated to be 6% of the total emissions from ships, *Smith et al. (2015)*. Therefore, there is a need for a special focus on these vessels and on the development of systems that help the crew and ship-owner to optimise operations and to reduce energy consumption.

2. Methods and Framework

The aim of this section is to present a framework that describes the overall structure of a system for energy optimisation of offshore supply vessels. The process of developing the framework is described briefly. Data collected, people involved, analyses and finally the framework connecting the findings from the analysis is presented.

2.1. Data Collection

Data used for the present study includes a wide range of qualitative data - documentary data, interviews, workshops and observations on board a vessel. Technical data is generated by studying ship drawings, and collecting information from system configurations, technical specifications and layout. Specific company information including policies, operational guidelines and procedures from the Safety Management System (SMS) and other internal documents and HSQE programs etc. were studied. The content of the ship's energy efficiency management plan (SEEMP) together with the use of the plan was also examined in greater detail.

As the study requires a deep insight into the operation of a ship, there has been a high level of involvement of people having operational knowledge during the process of developing a model for the framework. A shipping company, operating an offshore supply vessel, has been involved. 21 interviews, 4 with represents from both technical and HSQE departments and 17 interviews with the crew, have been carried out. The initial model idea was presented and discussed, and the knowledge obtained was used to re-define and update the model. Three workshops with experienced officers have been conducted. The officers were specially invited to assist with development and validation of the framework. Voyage and work descriptions were discussed in detail, and their technical experience and knowledge was used to define technical systems on-board.

2.2. Analysis – Operational Findings

From the initial literature review and during interviews and workshops it was found that an energy management system for these vessels requires a thorough description of the working pattern – the modes, the work done in each mode and a clear description of the transition between modes. Furthermore, it was also found that decisions taken or requirements set by both internal and external actors, including the ship owner, charter, costumer and authorities, have a large influence on the daily

operation of the vessel. Finally, yet importantly, if the system shall be regarded as a support system, it must be meaningful for the crew and fit to the vessel and the technical installations on board.

2.2.1. Modes and Operations

From interviews and workshops with the experienced officers it was found, that the phases of a typical voyage for a working vessel can be described by four main modes. The first three modes, which have been denoted as, harbour, manoeuvring and passage will be equally described for most vessels, whereas the last mode denoted as offshore work will characterise the special purpose of a vessel.

- Harbour: The vessel is alongside the harbour, moored with lines, with the engine and thrusters stopped.
- Manoeuvring: The vessel is manoeuvring in the harbour or in a restricted area. Propulsion and manoeuvring systems including the engine, thrusters and maybe DP (dynamic positioning) are running.
- Passage: The vessel is on passage between fixed positions.
- Offshore work: The vessel can be involved in a number of different types of offshore work depending on the ship's characteristics. The work is described by one or more operations performed in the specific mode. Operations related to offshore work could be cargo transfer, anchor handling, towing, or acting as a standby vessel.

2.2.2. Activity State

One of the main findings from the analysis was the importance of having a clear set of detailed definitions of the transitions between modes and also attaching an activity state to each mode. Three main activity states were defined; namely, active, preparation and waiting.

- Active: The vessel is performing as pre-described. If the involved operation tasks are taken into account, it is possible to compare active modes of the same type. Noticing systems running and the amount of equipment started, together with the load rates and the energy consumption will give a clear picture of the energy efficiency and possible energy saving opportunities.
- Preparation: Preparing the vessel for a mode is a necessary task. To start-up engines, pumps and thrusters takes time. It is un-productive but necessary time used.
- Waiting: Waiting is un-productive time. When, who or what causes these delays – and furthermore, how they can be avoided – must be analysed.

2.2.3. Requirements

Requirements for operating a vessel are laid down by a number of different actors. In the present model, these actors have been separated into three groups: the authorities, the shipping company, and external stakeholders as a possible charterer or the customers. The authority group covers regulations from international and national regulators including IMO and national authorities; this could be regulations on minimum requirements to stability, ballast water handling, when and how to conduct drills, or environmental regulations applying to special emission control areas such as ECA. Regulations laid down by authorities are mandatory and must be fulfilled. The other group of requirements is laid down by the shipping company itself. These requirements will always be stricter than requirements set by the authorities. These requirements could include procedures on how to handle the ship in extreme weather e.g. specific requirements for stability and speed, or it could be procedures for start-up of engine equipment in relation to special operations. External stakeholders, mostly the charterer, can have special requirements regarding e.g. readiness, speed or time of arrival. It is important to notice from whom the requirement is set – requirements set by the company or the charterer are not mandatory and can be evaluated, discussed or negotiated, if it is found that they conflict with improved energy efficiency.

2.2.4. Systems and Equipment

In order to establish a model for determining the energy efficiency of a vessel, it is necessary to have knowledge of design and technical systems on-board. Energy consuming systems running in modes such as systems for propulsion, ballast water, manoeuvring and the underlying equipment such as pumps, generators and steering gear must be mapped and described in detail.

2.2.5. The Framework

The concept model describes the problem based on results from the analysis and findings. The model provides an overview of a whole voyage of the vessel and describes the connection between different actors, requirements, modes, operations, technical systems etc. Fig. 1 depicts the conceptual model, in which the outer boundary – the voyage – indicates that the system covers a complete voyage. The next layer – the vessel – is influenced by the requirements of authorities, the shipping company or external stakeholders and from fixed or variable environmental conditions such as wind, sea, water depth etc. The core of the vessel layer is organised into three main columns, namely “Operational Objectives”, “Technical systems” and “Equipment” – a terminology known by the crew. The two columns “Technical ship systems” and “Equipment” are determined by the ship’s design, whereas the “Operational Objectives” are a combination of the requirements and operations given for each mode in relation to the voyage. Inside the vessel layer is also the crew – it is the crew that, in the end, based on requirements, ship design and environmental conditions, makes the decision how to operate the vessel. By organising the model into columns, it is possible to show the connections and dependencies, which influence the decision processes.

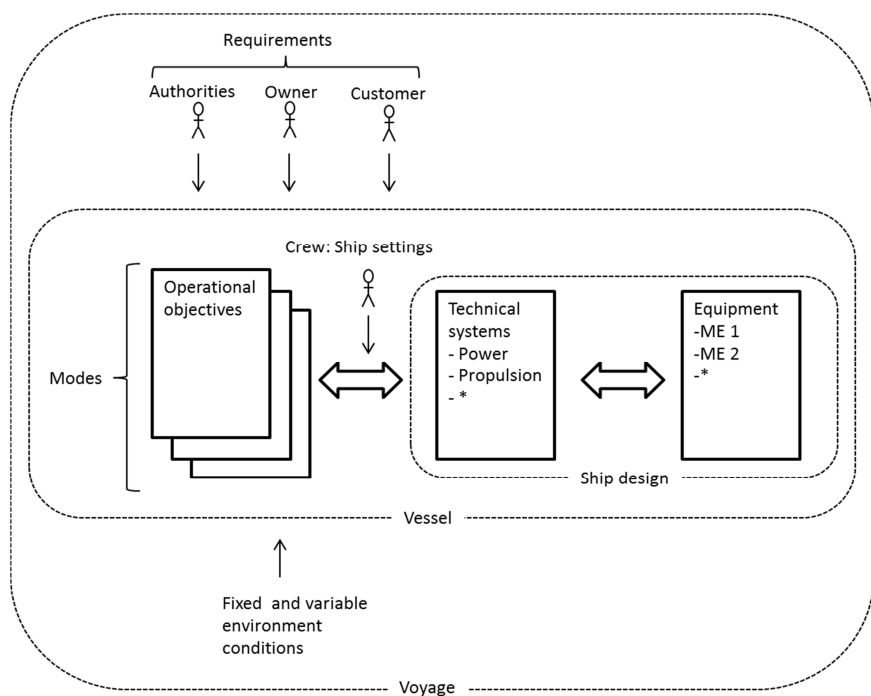


Fig.1: The framework

3. Case Study

The problem of operating and handling vessels having a very flexible working pattern is illustrated by a case describing a voyage for an offshore supply vessel. The section begins by providing a short description of offshore vessels and an introduction to the case. The voyage is described in detail. A clear description of what the vessel is doing during the voyage is given together with comments on the activity state and the transition between different modes. Potential energy savings are mentioned and commented upon.

The term ‘offshore vessels’ covers vessels supporting the industry of energy exploration and production activities offshore. The group consists of a variety of supply and service vessels assisting oil and gas installations and offshore wind farms. These vessels can be employed with towing and anchor handling (AHTS), cable laying, bringing supply (PSV), transferring crew to and from offshore areas, performing maintenance, and acting as standby vessels outfitted with safety and fire-fighting equipment. The vessels can be designed for multiple functions, and often a ship can change purpose, from e.g. AHTS to PSV repeatedly during its lifecycle. The primary purpose of the vessels is the work they perform at sea, and the work has therefore to be taken into account when a model for energy efficiency management is developed. The exploration activities are limited to the continental shelf relatively near to the coast and the sea passages will therefore be of limited length - this is contrary to energy efficient models for transport vessels such as container vessels where the sea passage will be in focus. Safety is an important factor in the offshore industry and special considerations are taken when offshore vessels enter exploration activity areas. Normally, a distance of 500m from the site is considered to be a safety zone, and vessels entering this zone must be extra careful. Offshore vessels working inside the 500m zone are required to follow special procedures, in many cases based on the G-OMO guidelines requiring backup on propulsion and manoeuvring systems.

The offshore vessels have a very complex and flexible working pattern and can, during one trip or voyage, perform many different operations. The detailed planning of a voyage is performed by the crew on-board the vessel, whereas the overall planning is performed by the shipping company or the charterer. The time schedule is based on the work to be carried out and therefore, for this kind of vessel, the time schedule will normally be determined by the charter.

One of the main findings from the analysis in Section 2 was the importance of having a clear set of detailed definitions of the transitions between modes, and attaching an activity state to each mode. To reflect the activity state and the transition between modes a flowchart has been developed, see Fig. 2. This figure depicts modes and states. The arrows indicate the transitions between the states inside a mode and between the modes. Modes, states, and transitions need to be clearly defined and known by the crew. In the case description, modes are marked with bold whereas activity states are in italics.

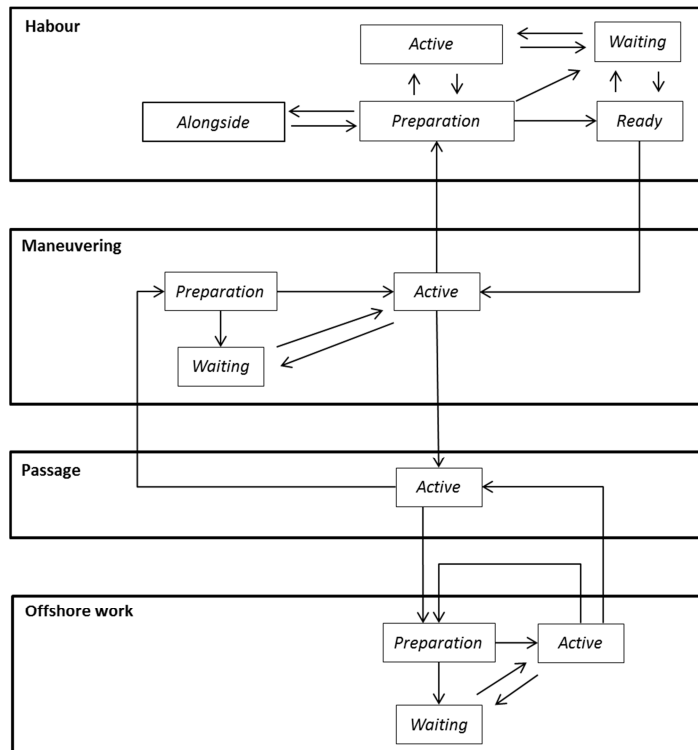


Fig. 2: Mode/state flowchart

Fig. 3 depicts the voyage flowchart with the involved modes. The numbers 1-15 are used to identify the modes in the voyage description, and the dashed lines around mode 4 and 11 indicate that these two modes are unplanned activities at the beginning of the voyage, and are therefore not a part of the voyage planning. The voyage is described in detail in the following description. A clear description of what the vessel is doing in the particular mode is given together with comments on the activity state and the transition between modes. Potential energy saving is also mentioned and commented in each description. If modes are repeated during the voyage, the detailed description is only included the first time the mode is described.

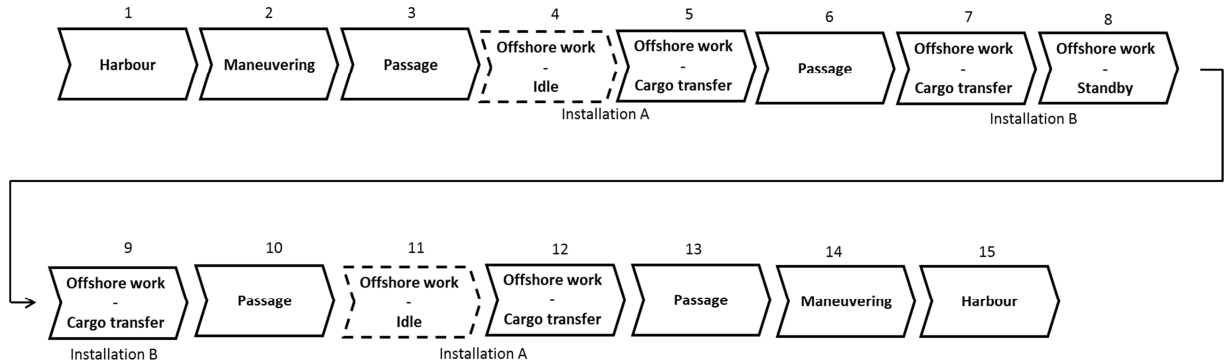


Fig. 3: Voyage flowchart

For each mode, technical systems and the underlying equipment required for running the operation safely and in an energy efficient way must be described. This leads to the introduction of the dependency diagram shown in Fig. 4, where dependencies between operational objectives, technical systems and equipment are modelled. The two columns “Technical ship systems” and “Equipment” are determined by the ship design and technical layout, whereas the “Operational objectives” are a collection of objectives directly related to the given mode and operations. The dashed lines in Fig. 4 indicate the possibility to start up extra equipment i.e. if extra energy is needed.

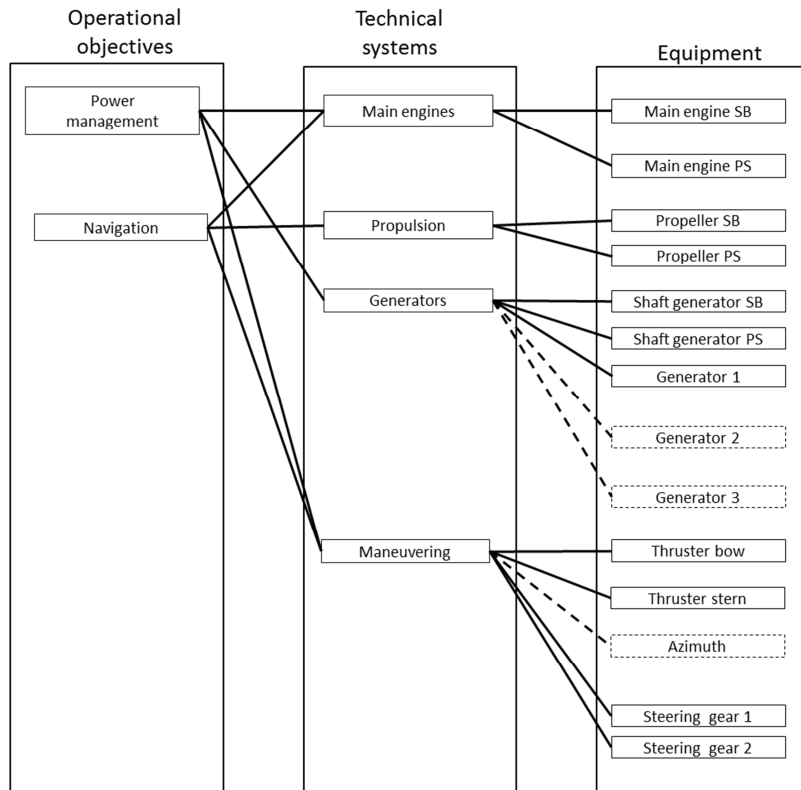


Fig. 4: Dependency diagram – Operational objectives, technical system and equipment on-board

3.1 The Case

The problem of operating and handling working vessels is illustrated by a case describing a single voyage for an offshore supply vessel. The vessel is on a time charter contract covering voyages between the shore base in a harbour and a number of fixed offshore oil and gas production installations. The voyage starts alongside the harbour, the ship is fully loaded and ready to let go of the mooring lines.

The planned tasks for the voyage are as follows: Cargo transfer from the harbour to installation A, cargo transfer from installation A to installation B, be standby vessel at installation B for a shorter period, cargo transfer from installation B to installation A and then returning to port with empty containers and garbage. An unplanned activity occurs during the voyage where a broken pump from installation A is sent ashore for repair.

3.1.1. Harbour (1)

The vessel is *alongside*, fully loaded and *preparation* for departure begins. During the *preparation* state, the bridge and the engine room are made ready for departure, following company procedures and checklists from the safety management system (SMS); this preparation takes approximately half an hour. Bridge and engine systems including radar, engines, and thrusters are made ready for operation. When all preparations are completed and checklists are filled out, the vessel is *ready* for departure and the port control is advised. The transition from **Harbour** mode to **Manoeuvring** mode occurs when the crew start to let go of the mooring lines.

Energy saving – comments: The vessel can be delayed after the preparations are finished, due to late arrival of cargo, delayed paperwork, waiting for other vessels leaving or entering port etc. This causes non-productive *waiting* time and extra energy consumption as equipment such as the main engines are running.

3.1.2. Manoeuvring (2)

The vessel is in the *active* state and the crew starts manoeuvring the vessel, which will bring it from the quay to a specific position outside the harbour area. In the present case, the vessel leaves the port without *waiting*. In the **Manoeuvring** mode, the engine room will be manned and there will normally be an extra officer at the bridge; the manning demand is described by procedures in the SMS system. Propulsion and manoeuvring systems such as engines, thrusters, and steering gear are running. The navigation must normally be performed with caution as the ratio between draft and water depth is often low, the opportunity for deviating from course is therefore limited.

Energy saving – comments: It is, from an energy efficiency perspective, always important to consider the amount of equipment needed for a particular task. Here, a number of objectives must be taken into account, such as the requirements from the owner or charter, weather conditions, complexity of the harbour area, competences of the crew etc. For some vessels, the amount of equipment that is running will be controlled by pre-described SMS procedures determined by the shipping company, as an example, the number of running thrusters in many cases is based on a worst-case scenario set for reasons of safety.

3.1.3. Passage (3)

When the vessel is outside the harbour area, thrusters are stopped and engines transferred to bridge control, this is the transition between the modes **Manoeuvring** and **Passage**, and the vessel is now *active* in the passage mode. Arrival time at the offshore installation A is set by the charter for the next morning at 7 a.m. The crew on board calculates and proceeds at the lowest necessary speed. Upon arrival at installation A, it turns out that the installation is not ready to receive cargo before 10 a.m. The charter's representative at the installation informs the vessel to wait until further information is

given. This leads to an additional unplanned mode, here denoted as the **Offshore Work - Idle** mode.

Energy saving – comments: If the charter had sent an updated time for arrival, the speed could have been adjusted accordingly and thereby energy could have been saved.

3.1.4. Offshore work – Idle (4)

The waiting will be done outside the 500m safety zone, so the only *preparation* is reducing speed and changing course to compensate for wind and sea.

Energy saving – comments: If the weather is calm, the main engines can be stopped and the installed azimuth propeller can be used to keep the vessel outside the 500m safety zone. Using the azimuth instead of the main engines will reduce energy consumption.

3.1.5. Offshore Work – Cargo Transfer (5)

Transferring cargo to the offshore installation requires entering the 500m safety zone of the installation. Before entering the zone, the crew will perform the preparation procedure and fill out the checklists, the vessel goes from *active* in the **Offshore Work – Idle** mode to *preparation* for the **Offshore Work - Cargo Transfer** mode. Depending on owner or charters requirements, the configuration of the vessel can differ due to weather conditions and e.g. crane reach out at the installation. In some cases, an active DP system (Dynamic Positioning) is required before entering the safety zone. Building up the DP model takes about half an hour, which is considered to be a part of the *preparation*. Inside the safety zone, it is a requirement that the engine room is manned and two officers are present at the bridge. When the preparation checklist for entering the 500m safety zone is completed and the DP system is started, the vessel is ready for the *active* state under the crane. Unfortunately, it turns out that installation A is not ready for cargo transfer, and the vessel enters the *waiting* state.

Energy saving – comments: *Waiting* alongside the installation due to interruptions in crane operations is unproductive time and must be avoided by better planning at the installation. In this particular case, the active DP system is not required and the half hour used for initialising the system can be saved. Being inside the 500m safety zone, procedure guidelines require backup on propulsion and manoeuvring systems, meaning that extra equipment is running. Time used inside the zone must be minimised as energy costs are increased; advantageously the vessel should stay outside the zone as long as possible.

3.1.6. Passage (6)

After the cargo transfer at installation A is completed, the next task will be cargo transfer at 9 a.m. the next day at installation B. The passage to installation B is short which allow ultra-slow steaming.

Energy saving – comments: The vessel is equipped with two main engines, but also with an azimuth propeller, which can be used for ultra-slow steaming in calm weather; this will reduce the energy consumption.

3.1.7. Offshore Work – Cargo Transfer (7)

As the ETA was estimated correct, the vessel went directly from **Passage** *active* state to *preparation* state in the **Offshore Work – Cargo Transfer**. Installation B is normally unmanned and the embarking of people is, due to safety reasons, done by helicopter. The schedule for the helicopter gives the required time of arrival for the vessel. The crew transferred to the installation will, during the day, handle the cargo transfer and perform other maintenance tasks at the installation. The crew at the vessel have to perform the same preparations for transition to the **Offshore Work – Cargo Transfer** mode as described in mode 5. When alongside the offshore installation the cargo, i.e. tools

and equipment for today's work, is transferred, before the vessel leaves the 500m safety zone again. The vessel is now standby vessel at the installation.

3.1.8. Offshore Work – Standby (8)

Even though the vessel now is in a waiting position, the state for **Offshore Work– Standby** is *active*, as this is a part of the requested work. Here, the standby mode is split into two – work outside and inside the 500m safety zone, respectively. The first part is done outside the safety zone; the vessel is then called inside the zone for being standby due to outboard work at the installation. Before entering the 500m safety zone the vessel has to perform the same preparations as described in mode 5.

Energy saving – comments: The time the vessel is inside the 500m safety zone must be limited, as extra machinery equipment is required. The vessel has to run the procedure for preparation for entering the 500m zone twice. In situations like this, the crew must carefully consider whether they shall leave or stay inside the zone.

3.1.9. Offshore Work – Cargo Transfer (9)

After the work at the platform is finished, the cargo and crew is returned to the vessel. No *preparation* is needed as the vessel is already inside the zone. After the work has been performed, the vessel leaves the safety zone; non-necessary equipment and DP is stopped and engines are transferred to bridge control. This is the transition between the **Offshore Work** and **Passage** modes; the vessel is now *active* in the passage mode.

3.1.10. Passage (10)

At the **Passage** from installation B to A the vessel is requested by charter to use normal cruise speed. Unfortunately, the installation cannot receive cargo transfer before the next day, which results in unplanned waiting for the vessel. The installation plans are not forwarded to the ship, meaning that the vessels will enter the **Offshore work – Idle** mode upon arrival.

Energy saving – comments: Ultra-slow steaming on azimuth propellers could have been used if the vessel had been informed about the work plan of the installation. The energy consumption would have been reduced.

3.1.11. Offshore Work – Idle (11)

The vessel will be waiting outside the safety zone at the installation. Due to calm weather conditions, it is decided to stop the main engines and start the azimuth propeller.

Energy saving – comments: Using azimuth propellers instead of the main engines saves energy.

3.1.12. Offshore Work – Cargo Transfer (12)

The next day the vessel will be prepared for the cargo transfer at installation A. Before entering the 500m safety zone, the preparations described in mode 5 are performed. Alongside the installation, the vessel is loaded with empty containers and a broken pump. The pump is important for production and the vessel is requested by the charter to sail to port as fast as possible with the pump for repair.

3.1.13. Passage (13)

The request from the charter results in steaming at maximum speed.

Energy saving – comments: Maximum speed does not leave room for energy saving, but it is

important for the vessel to observe states of wind and wave and the ratio between draft and water depth in order to adjust the speed and course to avoid using energy without gaining speed.

3.1.14. Manoeuvring (14)

Outside the harbour area, the vessel goes into the **Manoeuvring** preparation state. The engine room is manned and there is an extra officer at the bridge. Thrusters are started and everything is made ready for manoeuvring – procedures described in the SMS system are followed and checklists are filled out. When all preparations on the bridge and in the engine room are performed, the vessel enters the *active* state and manoeuvring into the harbour and the quay can start.

3.1.15. Harbour (15)

The vessel is now alongside, mooring lines are fastened and engines stopped. The vessel is ready for unloading.

4. Discussions

Despite the fact that knowledge of cost-effective improvements are well known in the industry, energy efficient operation is only a minor or even neglected topic on board many working vessels of today. In the present section, the case study from Section 3 will be used as basis for discussing the problem. The case, which describes the problem of operating and handling vessels with a very flexible working pattern, is a simple example but the problems related to energy efficient operation are well known across the industry.

The case, which is built upon statements and comments from the crew on-board a supply vessel and discussions with experienced officers invited for workshops (see Section 2), shows that the reasons for not running a ship in the most energy efficient way can generally be separated into two main reasons, namely un-productive time and unnecessary equipment running. These two topics will be discussed in the following discussion. The sections end with a short summary and an introduction to possible ways forward.

4.1. Un-productive Time

The main reasons for un-productive time (waiting) are related to ineffective planning or poor communication. Waiting relates mostly to external factors such as requests from charter, and the crew on-board the vessel has often no influence. A very common situation may occur when a vessel arrives on time to the specified destination to discover that the harbour or installation is not ready. This situation has been experienced many times by both crew and officers interviewed in Section 2. This demonstrates the same problem as seen in the case study described in Section 3. A non-productive waiting at arrival to the destination may occur when the vessel is forced to go from the **Passage** mode to **Offshore work – Idle**; because the installation is not ready, see mode 4 and 11 in the case study. Time spent in this mode can be seen as time wasted due to poor planning or bad communication. The too early arrival request from the installation will cause the vessel to proceed at high speed with unnecessary extra fuel consumption during the passage. It could be argued that **Offshore - Idle** should be part of the mode **Offshore work - cargo transfer** in mode 5 and not be given a separate mode, but this would conceal the time wasted due to planning errors. Mode 4 and 11 could both have been avoided with better planning; introducing the extra mode makes the problem more visible for charter and owner.

In some cases, it might be necessary for the vessel to wait, and entering the mode **Offshore work–idle** could be a good choice. This is illustrated in the case in mode 5 where the vessel starts preparation for **Offshore work - cargo transfer**. The installation is not ready which results in unnecessary waiting time with all engines running, resulting in an increased energy consumption. In other situations it might be better that the vessel is ready and waiting with engines running, but it is only if

the waste of time and energy is identified that it is possible to make a well-founded choice. Statements from experienced officers working in companies where installation and vessel are part of the same company shows that there has been a movement towards a situation where installations have to be ready when the vessel arrives, otherwise the supply transferee has to wait until the next time the vessel arrives at the installation. This will probably lead to more careful planning and communication. If the time spent in **Offshore work – Idle** mode was visible to owner and charter they could discuss this issue and probably find a solution. Fuel costs are paid by the charter, which in most cases is the owner of the installation - knowing that fuel could be saved with a more precise arrival would probably facilitate communication and cooperation between the ship and the installation.

4.2. Unnecessarily Start-up of Equipment

The appraisal of what equipment is necessary in a certain situation is done by the crew on-board the vessel, and often it is a decision made only by the captain. In some situations, the safety management system will provide guidance to the crew and captain as to what the owner sees as necessary equipment. This guidance is often based on fleet experiences and near-miss reports. The interviews performed in relation to the present study have shown that the captain on-board the vessel tends to have more engines and other equipment running than necessary, so if one engine sets out, the redundant one can take over. The modes **Manoeuvring** and **Offshore work** are the two modes where this reflection between safety, or the need for redundancy, and energy efficiency are most pronounced. *Bonavita et al. (2008)* uses the concept of a comfort zone in the context of oil and gas production. The comfort zones are the bands between production constraints and the actual production values. In the oil and gas production industry the operators should strive to minimise the comfort zones and thereby increase production and at the same time reduce energy consumption. The concept of a comfort zone can also be used in this context i.e. if unnecessary equipment is running during operation where neither external requirements nor weather conditions requires it, the comfort zone is too wide. A number of factors incite the crew for the increased comfort zone and procedures and regulations tend to promote safety behaviour ignoring the energy efficient operation of the vessel. Many procedures are built on worst-case scenarios and the main purpose of the SMS is to make sure that the vessel is running in a safe manner i.e. guidelines for navigating a supply vessel in the 500m safety zone only focus on safety. Furthermore, many offshore vessels are operated on a time charter basis meaning that fuel is paid by the charter, which does not promote energy efficiency initiatives, the extra fuel cost is not taken into account.

4.3. The Way Forward

To increase awareness of the energy efficiency of supply vessels it is important to focus on the above-mentioned topics. The problems must be visible and presented for the crew, owner and charter and it must be possible to analyse a given situation.

If the vessel goes into waiting, when, who and what that causes it must be analysed - and furthermore, how this can be avoided. Running equipment must be registered together with practical need in the present situation. If more equipment than necessary is running, it must be possible to gain information about the reason. Is it due to regulations from authorities that are mandatory and therefore must be followed, procedures from owner or charter that may be evaluated for the given situation or is it the captain that runs more equipment because external factors such as wind and sea demand it for safety reasons.

To support the crew, charter and owner, the introduction of a decision support system must be introduced. The system should provide all parties with a transparent decision process and show the consequences to ensure that the crew only starts up necessary equipment and the owner and charter focuses on precise planning to avoid un-productive time. The system should also show the impact on the present situation caused by procedures set by charter and owner.

5. Conclusions

A framework that describes the overall decision structure in connection with energy efficient operation offshore supply vessels has been presented. The framework provides an overview of a whole voyage and describes the connections between different actors, requirements, modes and technical systems on-board. Modelling a framework like this requires a deep insight into the operation of a vessel, therefore a high involvement of people having operational knowledge has taken place. Workshops with experienced officers and 21 interviews with crew and office employees from a shipping company have been conducted.

From interviews and workshops, it was found that a typical voyage for working vessels can be separated into four modes, the first three apply to all kinds of vessels whereas the last mode denoted offshore work characterises the special purpose of a working vessel. One of the main findings from the analysis was the importance of having a detailed description of the transition between modes and attaching an activity state to each mode, as this allows monitoring of the vessels' operational patterns and identification of waiting time. Analysis of statements and comments from crew and officers shows that main reasons for not running a ship in the most energy efficient manner can generally be separated into two main topics, namely un-productive time and unnecessary equipment running.

The findings from the present analysis can be used for the development of a decision support system. The system should provide all parties, i.e. the crew, the owner and the charter, with a transparent decision process and show the consequences of this, to ensure that the crew only starts up necessary equipment and the owner and charter focuses on precise planning to avoid un-productive time.

Acknowledgements

The authors would like to acknowledge funding support from the Danish Maritime Fund and Innovation Fund Denmark.

The authors would like to thank crew and employees from the shipping company Esvagt for participating in interviews and for sharing valuable information about operating offshore supply vessels. Also thanks to the three experienced officers Søren Nikolai Kyndi, Jeppe Billeschou and Morten Meldgaard Petersen for sharing their experiences about operation of working vessels, and for giving valuable comments to the developed model.

The present study was carried out during a project carried out under Blue INNOship – a Danish societal partnership focusing on creating growth and employment in the Blue Denmark through development of green and energy-efficient solutions.

References

BONAVITA, N.; BIRKEMOE, E.; SLUPPHAUG, O.; STORKAAS, E. (2008), *Operational performance excellence through production optimization in the upstream industry*, 10th Mediterranean Petroleum Conf. (MPC08), Tripoli

EU (2015), *Regulation (EU) 2015/757 of the European parliament and of the council of 29 April 2015, on the monitoring, reporting and verification of carbon dioxide emissions from maritime transport, and amending Directive, 2009/16/EC*

G-OMO (2013), *The International Guidelines for Marine Operations*, G-OMO working group, <http://www.g-omo.info>

IMO (2009), MEPC.1/Circ.684, *Guidelines for voluntary use of the ship energy efficiency operational indicator (EEOI)*

IMO (2011), *Amendments to the annex of the protocol of 1997 to amend the international convention for the prevention of pollution from ships (Inclusion of regulations on energy efficiency for ships in MARPOL Annex VI)*, Resolution MEPC.203(62),

IMO (2012a), *Guidelines on the method of calculation of the attained Energy Efficiency Design Index (EEDI) for new ships*, Resolution MEPC.212(63)

IMO (2012b), *Guidelines for the development of a Ship Energy Efficiency Management Plan (SEEMP)*, Resolution MEPC.213(63)

IMO (2014), *International Safety Management Code* (ISM Code), ISBN 978-92-801-15901

OECD (2015), *Offshore Vessel, Mobile Offshore Drilling Unit and Floating Production Unit Market Review*, C/WP6 (2015)5/FINAL, OECD, www.oecd.org/sti/shipbuilding

SMITH, T.W.P.; JALKANEN, J.P.; ANDERSON, B.A.; CORBETT, J.J.; FABER, J.; HANAYAMA, S.; O'KEEFFE, E.; PARKER, S.; JOHANSSON, L.; ALDOUS, L.; RAUCCI, C.; TRAUT, M.; ETTINGER, S.; NELISSEN, D.; LEE, D.S.; NG, S.; AGRAWAL, A.; WINEBRAKE, J.J.; HOEN, M.; CHESWORTH, S.; PANDEY, A. (2015), *Third IMO GHG Study 2014*, International Maritime Organization (IMO), London

A Standard Protocol for Exchanging Technical Data in the Maritime Industries

Marco Vatteroni, Shipdex Consulting Ltd, mv@shipdexconsulting.com

Abstract

Shipdex (www.shipdex.com) is an independent, non-proprietary and free-of-charge standard protocol, open to all shipping players who wish to adopt it. It is a collection of “business and writing rules” developed to standardize and improve the production and the exchange of technical information. Shipdex also intends to decrease the traditional effort and costs in managing and importing technical data into corporate IT systems like ERP (Enterprise Resource Planning) or CMMS (Computerized Maintenance Management System). Shipdex can also be used to create the corporate Technical Publications repository, called Common Source DataBase (CSDB), shared by the technical staff in the ship-owner/ship manager office. Shipdex is based on xml mark-up language employing a neutral data exchange format. It allows export in different formats (as pdf, Html, IETP) without changing the data.

1. Introduction

The scope of Shipdex Protocol is to replace paper (or pdf) technical manuals with advanced, electronic and standardized Technical Publications. The reason to develop a common and standardized Protocol for producing and exchanging data resides on the fact that shipping companies are receiving from manufacturers technical manuals in different formats (Word, Pdf, Html, etc.), different structures (chapters, paragraphs, etc.), different layouts (manufacturers layouts) and different data quality based on manufacturers organization and policy. This means that manufacturers are providing end users with “pages of information” that are very difficult to be handled electronically. This situation created several troubles to end users in terms of information comprehension and electronic usage.

Shipdex drives the makers to produce electronic technical information focusing the attention to the content of the manual and forgetting the manual composition and layout. The technical manuals (in different formats and distribution media) must be considered just as an output from the data developed in accordance with the Shipdex Protocol. In other words, Shipdex allows manufacturers to provide end users with “information” instead of “pages of information”.



Fig. 1: The Shipdex (R)evolution

The Shipdex Protocol is also the perfect solution for shipyards, ship-owners and ship managers to receive electronic and standardized data in Shipdex format. Every Shipdex package of data (called dataset) has the same internal structure (based on mandatory xml schemas) regardless who is the maker and which the equipment is. In addition, Shipdex offers end users the opportunity to eliminate or reduce the traditional pain and high costs in storing and retrieving technical information and

loading ERP (Enterprise Resource Planning) and CMM (Computerized Maintenance Management) Systems with technical manual contents.

Shipdex is the S1000D (www.s1000d.org) customization for the shipping community. The S1000D (www.s1000d.org) is an international specification for the production of technical publications, issued in the early 1980s under the name of AECMA (Association Européenne des Constructeurs de Matériel Aérospatial) Spec 1000D to cover the European aerospace market. Since the beginning of 2000s, the S1000D specification is worldwide recognized as the international Technical Publication Specification for the military and civil aviation communities and it covers air, land and sea environments.

The S1000D specification is sponsored by:

- ASD Aerospace and Defence Industries Association of Europe
- AIA Aerospace Industries Association of America
- ATA Air Transport Association e-Business program

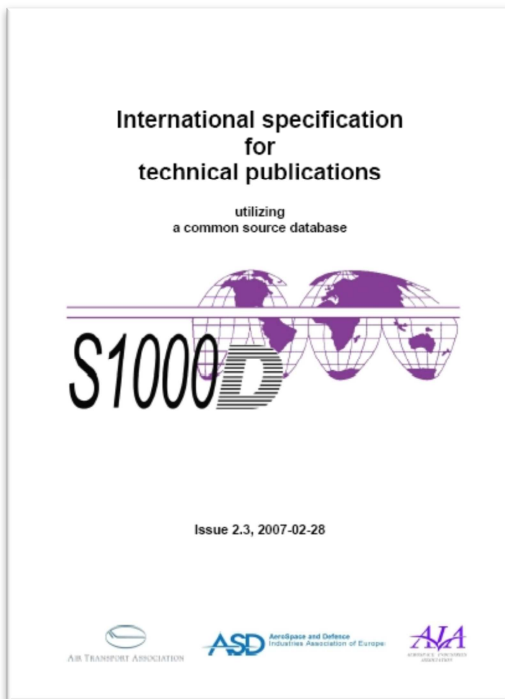


Fig. 2: S1000D specification

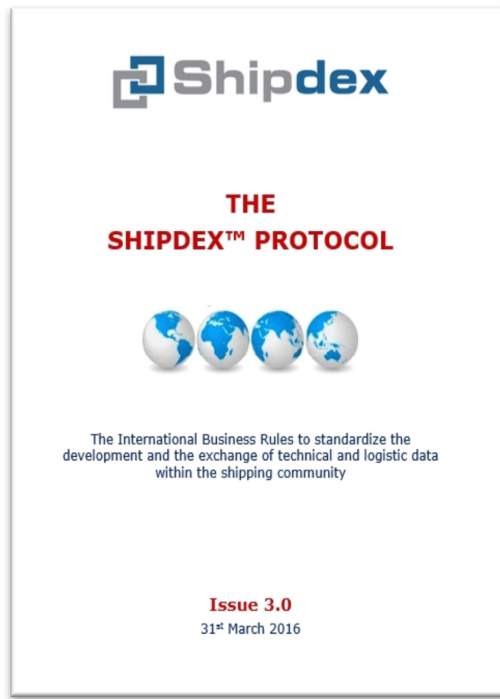


Fig.3: Shipdex specification

Shipdex has been granted an Observer status at S1000D Steering Committee, evidence that Shipdex has been well recognised and accepted by the S1000D community.

2. Who developed Shipdex

2.1. The Story

On 27-28 March 2007 a meeting was organized in Naples at Grimaldi Compagnia di Navigazione premises with the participation of some ship-owners and their most important suppliers together with an IT company with an expertise in Electronic Technical Manuals. That meeting was held to confirm the will to develop a common and shared Data Exchange Protocol whose name was decided to be Shipdex (Ship data exchange) and the NON-PROFIT Shipdex organization was created to cover the whole shipping supply chain.

All the below companies (the Founder Members) agreed to develop the Shipdex Protocol:

- Grimaldi Compagnia di Navigazione (Chairman)
- Intership Navigation
- Alfa Laval
- MacGREGOR
- MAN Diesel & Turbo
- SpecTec Group Holdings
- Yanmar
- Mastermind Shipmanagement
- Shipdex Consulting

2.2. Shipdex organization

The Shipdex organization is composed of the following working groups:

- The Shipdex Protocol Steering Committee (SPSC)
The SPSC is composed of the Founder Members listed in Section 2.1. The main mission of the SPSC is to conduct the overall governance of the Shipdex development and decide the “road map”. The role is to provide the vision for the specification, the direction to the Maintenance Group (SPMG) and a general promotion of the use of the Shipdex. The Shipdex Chairman governs the SPSC.
- The Shipdex Protocol Maintenance Group (SPMG)
The SPMG is a working group composed of the SPSC members and some “supporting companies” (admitted by the SPSC) who have a common interest in developing and maintaining the Shipdex Protocol. Currently, the SPMG is composed of the following companies:
 - Alfa Laval
 - Grimaldi Group
 - MacGregor
 - Man Diesel & Turbo
 - Mastermind Shipmanagement
 - Shipdex Consulting (Technical Manager)
 - Yanmar
 - Furuno
 - Rolls-Royce Marine

The role of the Maintenance Group is to maintain the currency of the specification by processing and accepting or rejecting the Change Proposal Forms (CPFs) coming from the shipping operators. The accepted Change Proposals will be incorporated into new issues of the specification, taking also into account the visionary direction of the SPSC. The Shipdex Technical Manager governs the SPMG.

3. Shipdex Protocol

3.1. Shipdex main principles

Information produced in accordance with Shipdex Protocol is achieved in a modular form called "Data Module". A data module is defined as a standalone information unit and can contain descriptive, catalogues, procedural, operational and troubleshooting data for a platform, system or a component. It is produced in such a form that it can be stored and retrieved from a Common Source DataBase (CSDB) by using the Data Module Code (DMC) as the identifier. Data Modules are produced in xml format, according to specific xml schemas that are provided together with the specification. Shipdex defines all the modularization rules to build the Data Modules.

The Shipdex main principles are summarized here below:

- Modularization of the data (Data Module concept)
- No duplication of the data (Data Module concept)
- Re-usability of the data (WORM principle: Write Once Read Many)
- Standardization (all the data are produced in accordance with mandatory S1000D compliant templates called “xml schema”)
- Hardware oriented information (Shipdex data shall be related to physical components in a given configuration)

A Shipdex dataset is the collection of all the information related to a given product in a given configuration and contains:

- Data Modules, in xml format
- Illustrations, drawings, multimedia objects in different formats (jpg, cgm, svg, avi, etc.)
- External documents (pdf, MS Office)

A Shipdex dataset can be composed of the following “information sets”:

- Description and operation
- Maintenance procedures
- Troubleshooting
- Illustrated parts data (IPD)
- Service Bulletin (the way to automatically update Shipdex manuals)
- Maintenance Planning

A standard Shipdex dataset is structured into the following two sections, Fig. 4:

- The “Source technical data” section contains all the technical information related to a given product configuration. A manufacturer can re-use this section every time the same product is supplied to a customer.
- The “Contract Data” section contains specific information related to a specific supply. It contains the list of the physical components delivered to the customer. Every physical component must be identified with its Part Number and, when available, its Serial Number.

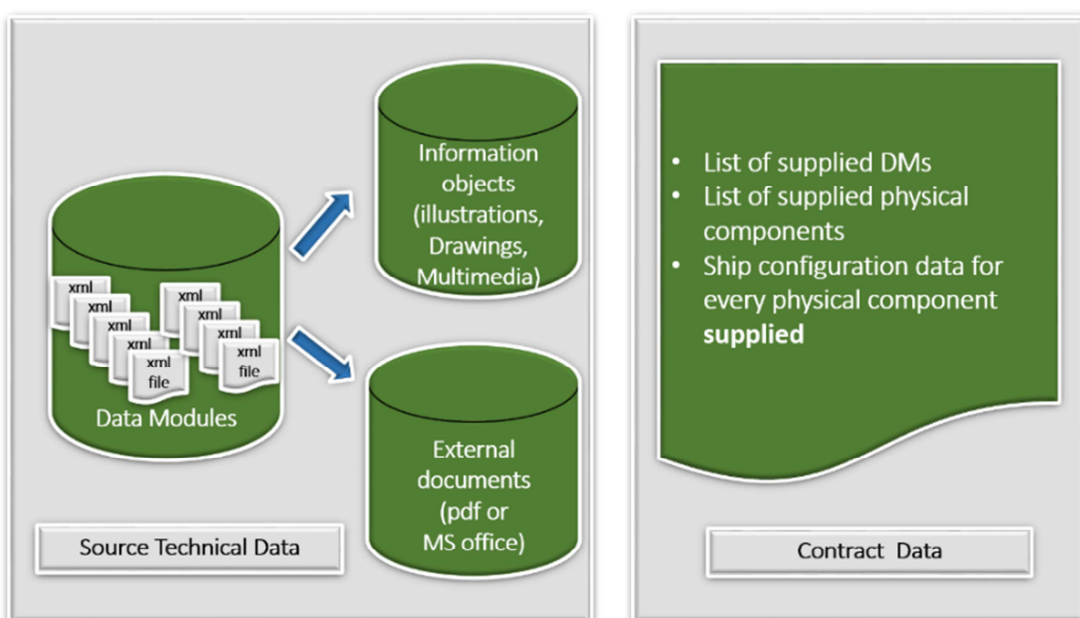


Fig. 4: The standard structure of a Shipdex dataset

3.2 Shipdex Information Sets

3.2.1 Description and operation information set

This information set covers the requirements for the exchange of information that will enable skilled personnel to understand the construction, function, operation and control of a physical component.

3.2.2 Maintenance Procedures information set

This information set covers the requirements for the exchange of information that will enable skilled maintenance personnel to perform maintenance tasks on the Product and its installed components. The information should enable personnel to:

- connect and disconnect test equipment and power supplies
- use any special tools and support equipment
- maintain and service the Product and its systems/components
- do tests which will show whether systems and components meet their minimum acceptable performance standards
- rectify failures
- remove and install all systems/components in the minimum time

3.2.3 Troubleshooting information set

This information set covers the requirements for the preparation of information applicable to troubleshooting which will enable skilled personnel to analyse reports provided by:

- the centralized monitoring systems of the Product
- the crew/operators and/or maintenance personnel
- the result of post mission inspections
- According to the level of accuracy of the data, analysis may be followed by:
 - an inspection, check and/or test
 - a corrective action or a fault isolation procedure

3.2.4 Illustrated Parts Data (IPD) information set

This information set covers the requirements for the preparation of information applicable to Illustrated Parts Data (IPD) related to:

- Spare Parts catalogues
- Support Equipment catalogues
- Consumables/Supplies catalogues

3.2.5 Service Bulletin information set

This information set covers the requirements for the preparation and coding, where appropriate, of Data Modules for Service Bulletin. The Shipdex Service Bulletin (SSB) must be used to distribute:

- Information to apply a change, a special and/or temporary inspection to an in-service Product or part of the Product (SSB Type A)
- Changes to technical information already supplied in Shipdex format (SSB Type B).

3.2.6 Maintenance Planning information set

This information set covers the requirements for the preparation and coding of “customizable” maintenance planning information. The most important advantages using the Maintenance Planning information set are listed below.

Advantages for Customers:

- To receive from Manufacturers simpler and better organized maintenance plans in order to understand and optimize the whole on-board maintenance process
- To group different tasks with the same periodicities, in order to be performed together
- To group different tasks for type, zone, skill, support equipment, etc. in order to increase maintenance efficiency and reduce the life cycle cost
- To generate less work orders into corporate CMMS
- In addition, Customers could develop their own specific Maintenance Planning data modules to be in accordance with internal maintenance policy or quality requirements, for instance:
 - Applying different periodicities
 - Removing some tasks
 - Adding new tasks (e.g. to be in accordance with internal standards or with Class Societies requirements)

Advantages for Manufacturers:

- It encourages the re-usability of Procedural Data Modules (maintenance tasks) that can be developed in a more generic and neutral form because they:
 - Could be related to higher breakdown levels (e.g. at product level or main components level)
 - Could not contain a specific periodicity
 - Could be referred into many different Maintenance Planning data modules without duplications. This feature allows to re-use generic tasks into different Maintenance Planning data modules
- Reduce the effort to develop and maintain the “same” Procedural data modules for different components. It would be enough to create generic/neutral tasks (just once) and include them into Maintenance Planning data modules related to different products/components
- Suggest the customer the most efficient maintenance process and allowing a better understanding of the maintenance policy

3.3 Shipdex data production

Manufacturers shall generate their own “product breakdown structures” composed of all the physical components until the “last significant maintainable item” in such a way to allow the production of an optimized Maintenance Plan. The information related to a given product configuration is collected into several data modules in xml format. The number of Data Modules to be developed for every single “product dataset” is based on well-defined modularization rules. The collection of all the Data Modules developed for a given product configuration is contained into the product dataset.

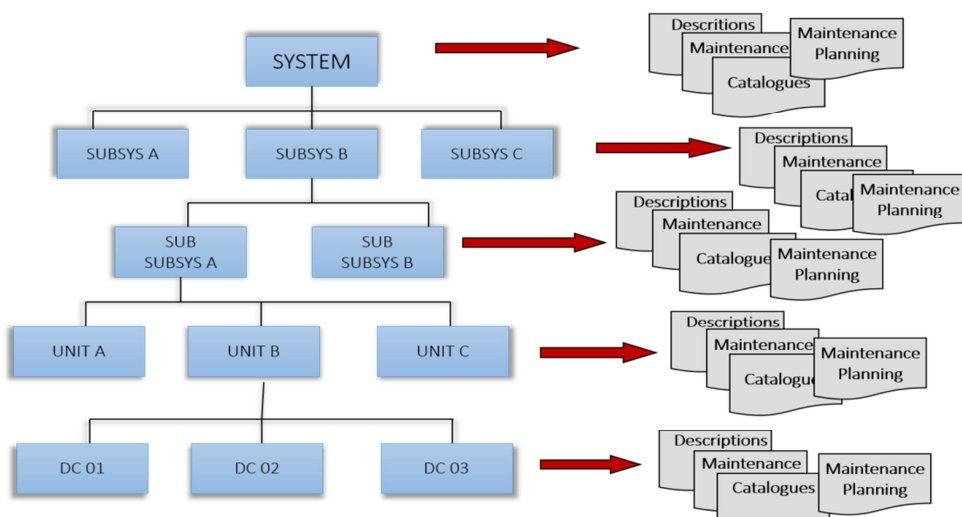
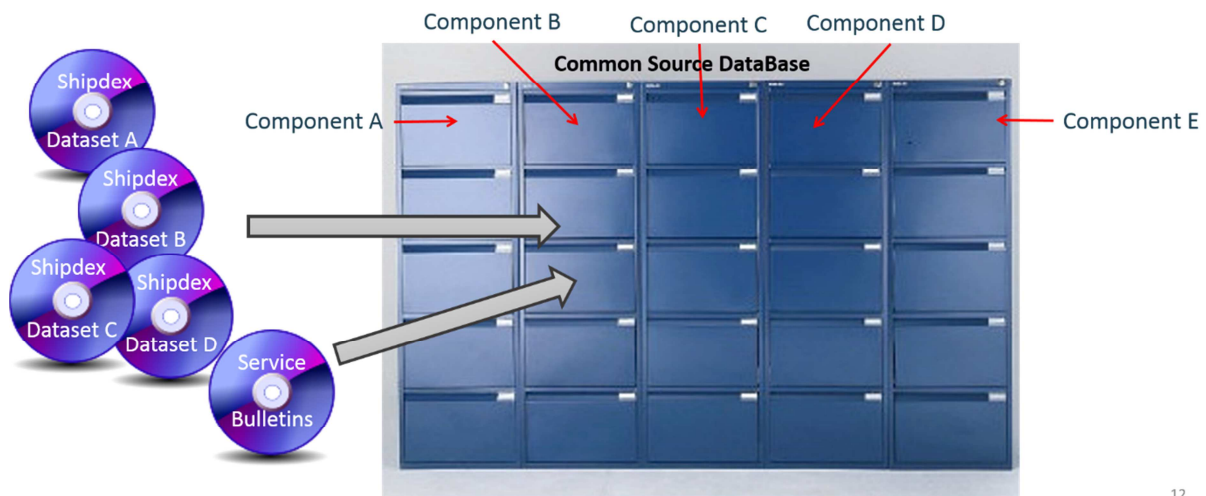


Fig. 5: Simple product breakdown structure and relevant data modules

Every product dataset can re-use already existing data modules (e.g. safety precautions, general warnings, common maintenance tasks, common catalogues, etc.) to avoid data duplication. Another big advantage comes when the maker needs to update information applicable to different products; it is enough to change the relevant data modules and all the datasets could be updated automatically.

4. The Common Source DataBase (CSDB)

The Common Source DataBase is the “place” where all the Shipdex data (xml data modules, illustrations, drawings, multimedia objects and external documents) should be stored for management and use under configuration and quality control along the whole life cycle of a platform, a system or a component. The information, in the form of data modules, is closely related to the relevant physical components.



12

Fig. 6: Shipdex Common Source DataBase (CSDB)

The information stored and managed into the CSDB can be simply and quickly retrieved from the CSDB, using a set of appropriate filters, for the following main purposes:

- Update the information and release the new issues
- Create a Shipdex dataset for a given product configuration
- Assemble a new technical manual to be published in the form of:
 - Pdf manual
 - Interactive Electronic Technical Publication (IETP)
- Import the data into Corporate IT databases as ERP, CMMS, etc.
- Create Computer Based Training (CBTs)

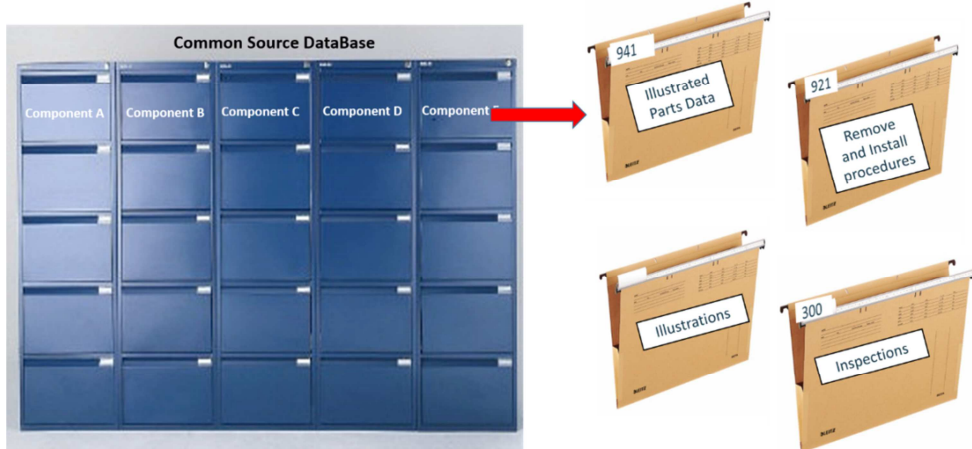


Fig. 7: Retrieving information from the Shipdex CSDB

5. Main benefit adopting Shipdex

Data benefits:

- Interoperability at data level, with mandatory and well-defined xml schemas
- Meta Data, consistently applied across the Shipdex datasets
- Data Dictionary, standardisation of naming conventions
- Non-proprietary, based on open standards
- Ease of data exchange, small xml based files structures
- Can be linked with source data (e.g. engineering databases), and can be used to enhance integrated data environment
- Permits the addition of extra documentation features such as link mechanisms to illustrations, multimedia objects, etc., enabling better end-user experience
- Delimits objects of information, rather than the traditional paper bound constraints, allowing more focused data
- The data module concept can be applied to legacy data as well

Authoring Benefits:

- Re-use of data, the modular concept allows data re-use up to 40%
- Reduction in update costs, due to use of data module concept of up to 30%
- Defined Document Structures (xml schemas) to define authoring structure within programs
- Module Uniqueness (Task /Description), allows task orientated definition
- Toolkit, standard toolkits available
- Compliant Authoring tools available, multiple vendor support

Training Benefits:

- Single User Interface, eases end-user acceptance
- Single Document Construct, eases standardisation
- Single Method of Production, eases synergy within and across organisations

Lifecycle Cost Benefits

- Reduced creation costs, due to data re-use
- Lower document distribution costs, multiple methods of delivery available
- Lower footprint costs, e.g. warehousing
- Wider access and more efficient retrieval of the documentation by the end user, multiple methods of delivery available
- Easy filtering of information (e.g. search and retrieval by applicability, through the use of metadata and content in searching)
- Increased operational readiness through reduced Mean Time To Repair (MTTR), thanks to more focused maintenance information
- Increase in data integrity and in the generation of better quality documents, through data integration and data module concept

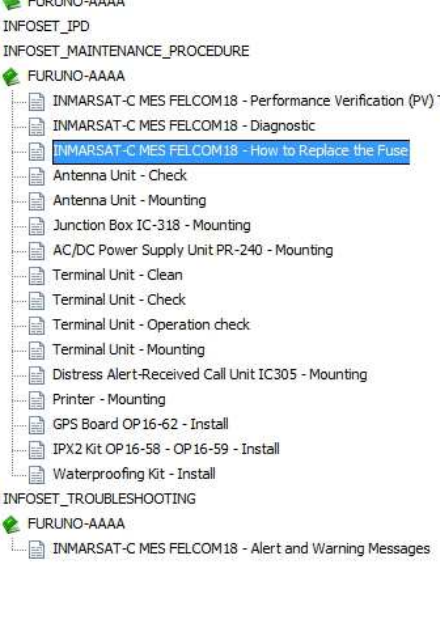
6. How to “navigate” through the Shipdex datasets, retrieve and print information

The free-of-charge Shipdex Viewer is a powerful browser that offers the following main features:

- Select from your file system and “open” a Shipdex dataset
- 2 tree-structures available to display the “Table of Content” (TOC):
 - Ordered by Information Set, Fig. 8
 - Ordered by physical component, Fig. 9
- Select from the TOC the piece of information (every TOC element refers a specific data module) to be displayed, Figs. 10 to 13
- Filter and retrieve the information using advanced filters
- Convert the data into pdf format:
 - A single data module, Fig. 14
 - A selection of data modules

- The whole dataset. In this case a whole “technical manuals” is created with automatic and interactive:
 - o Table of content
 - o List of tables
 - o List of illustration

Table of Content



- S0622#00001#FELCOM18#2-1
 - INFOSET_DESCRIPTION_OPERATION
 - FURUNO-AAAA
 - INFOSET_IPD
 - INFOSET_MAINTENANCE_PROCEDURE
 - FURUNO-AAAA
 - INMARSAT-C MES FELCOM18 - Performance Verification (PV) Test
 - INMARSAT-C MES FELCOM18 - Diagnostic
 - INMARSAT-C MES FELCOM18 - How to Replace the Fuse**
 - Antenna Unit - Check
 - Antenna Unit - Mounting
 - Junction Box IC-318 - Mounting
 - AC/DC Power Supply Unit PR-240 - Mounting
 - Terminal Unit - Clean
 - Terminal Unit - Check
 - Terminal Unit - Operation check
 - Terminal Unit - Mounting
 - Distress Alert-Received Call Unit IC305 - Mounting
 - Printer - Mounting
 - GPS Board OP16-62 - Install
 - IPX2 Kit OP16-58 - OP16-59 - Install
 - Waterproofing Kit - Install
 - INFOSET_TROUBLESHOOTING
 - FURUNO-AAAA
 - INMARSAT-C MES FELCOM18 - Alert and Warning Messages

Fig. 8: TOC ordered by Information Set

Table of Content

- INMARSAT-C MES FELCOM18 - Set the IMN
- INMARSAT-C MES FELCOM18 - Set external Equipment
- INMARSAT-C MES FELCOM18 - Set Alarm Contact
- INMARSAT-C MES FELCOM18 - Set up the AMS
- INMARSAT-C MES FELCOM18 - Select Position-fixing Equipment
- INMARSAT-C MES FELCOM18 - Set up for 2nd DTE
- INMARSAT-C MES FELCOM18 - System status Monitor
- INMARSAT-C MES FELCOM18 - Current position Log
- INMARSAT-C MES FELCOM18 - Performance Verification (PV) Test
- INMARSAT-C MES FELCOM18 - Diagnostic
- INMARSAT-C MES FELCOM18 - Alert and Warning Messages
- INMARSAT-C MES FELCOM18 - How to Replace the Fuse
- INMARSAT-C MES FELCOM18 - Spare Parts
- INMARSAT-C MES FELCOM18 - Support Equipment
- INMARSAT-C MES FELCOM18 - Supplies
- Antenna Unit - Cable Connector at the Terminal Unit
- Antenna Unit - Outline Drawing
- Antenna Unit - Check
- Antenna Unit - Mounting
- Alarm Unit - Wiring
- Alarm Unit - Outline Drawing
- Junction Box IC-318 - Wiring
- Junction Box IC-318 - Outline Drawing
- Junction Box IC-318 - Mounting
- AC/DC Power Supply Unit PR-240 - Change specifications
- AC/DC Power Supply Unit PR-240 - Outline Drawing
- AC/DC Power Supply Unit PR-240 - Mounting
- Terminal Unit - Outline Drawing
- Terminal Unit - Clean
- Terminal Unit - Check
- Terminal Unit - Operation check
- Terminal Unit - Mounting
- Distress Alert-Received Call Unit IC305 - Wiring
- Distress Alert-Received Call Unit IC305 - Outline Drawing
- Distress Alert-Received Call Unit IC305 - Mounting
- Printer - Outline Drawing
- Printer - Mounting

Fig. 9: TOC Ordered by physical component

Fig. 10: How to select and display a Descriptive data module

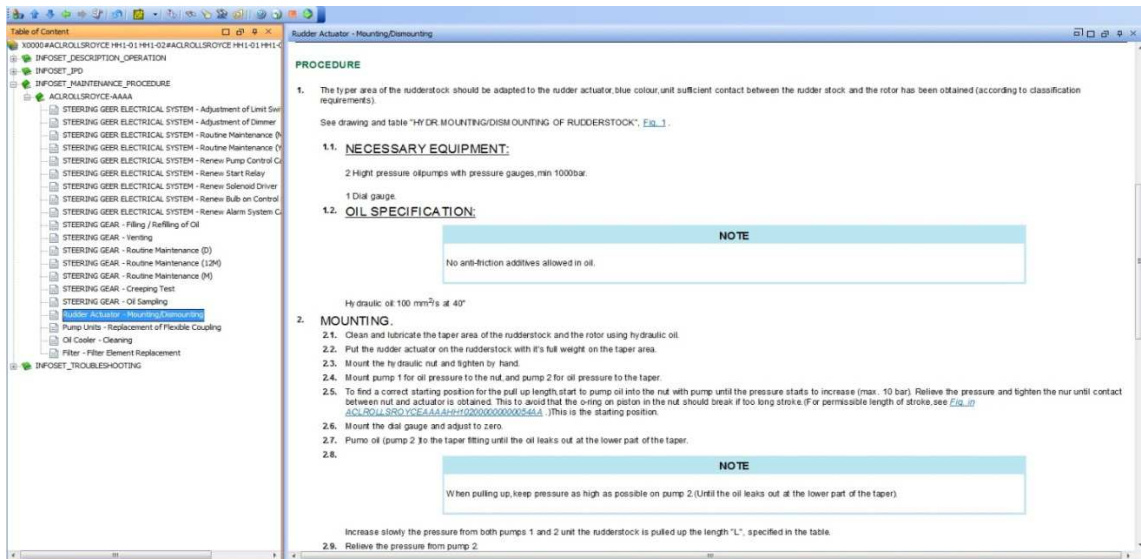


Fig. 11: How to select and display a Maintenance Task data module



Fig. 12: How to select and display a Spare Parts Catalogue data module

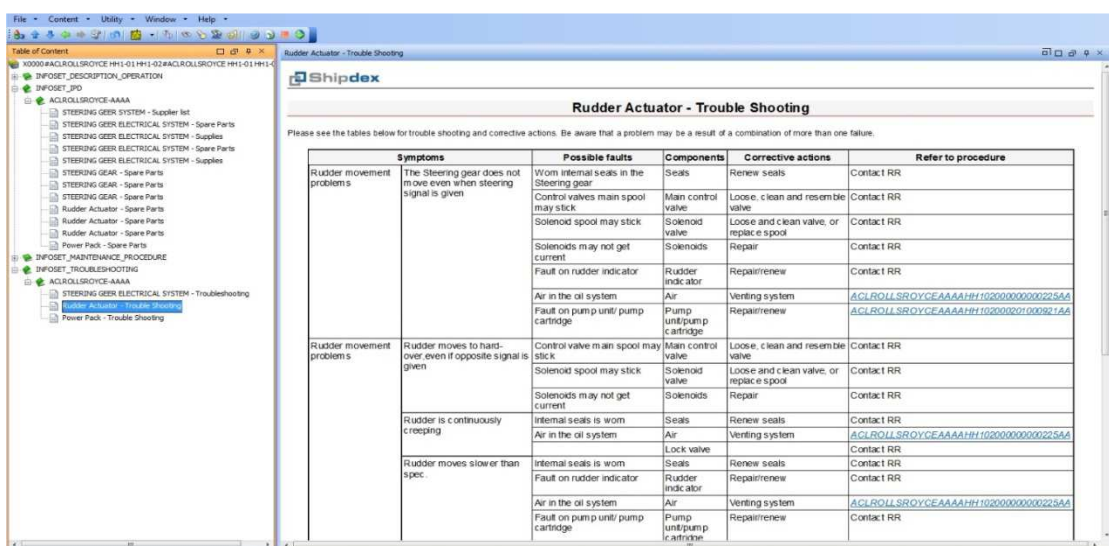


Fig. 13: How to select and display a Troubleshooting data module

- 3.6. => Actuate the hydraulic unit until bubble-free oil flows out through set screws 19.
Close set screws.

CAUTION



The jack is marked with its MAX. STROKE of 30 mm. The tie rod elongation (ΔL) can be controlled by means of pin 20 as a reference of the piston position.

Relief valve 18 is provided as stroke limiter relieving the pressure in case the max. stroke is exceeded. The relieve valve must be checked for tightness if it has been activated. A leaking valve has to be replaced.

- 3.7. => Operate the hydraulic unit up to 1900 bar and maintain this pressure.

CHECK

Using a feeler gauge inserted through slot 'KO' and check if there is any clearance between upper tie rod nut 3 and intermediate ring 2.

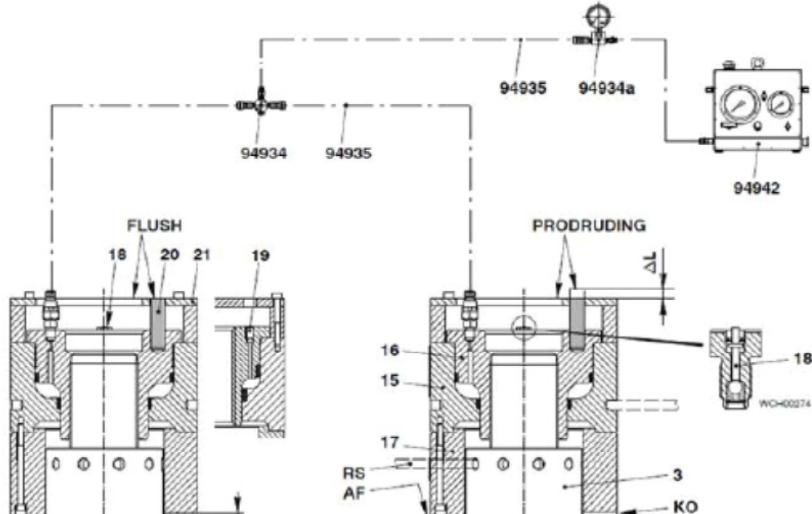


Fig. 14: A Shipdex data module automatically converted to pdf format

The Shipdex Viewer can be downloaded from the Registered Members Area on the Shipdex website (www.shipdex.com). In addition, the manufacturers are allowed to provide it to their customers together with a Shipdex dataset.

References

S1000D issue 2.3 (www.s1000d.org)

Shipdex issue 3.0 (www.shipdex.com)

Virtual Reality Based Training Improves Mustering Performance

Scott N. MacKinnon, Memorial University, St. John's/Canada, smackinn@mun.ca

David Bradbury-Squires, Memorial University, St. John's/Canada, djbs32@mun.ca

Duane Button, Memorial University, St. John's/Canada, dbutton@mun.ca

Abstract

Evacuation training under realistic situations is practically impossible due to the high degree of risk. The objectives of this study were to determine the effectiveness of different modes of learning on task performance during simulation training (ST) in a virtual environment (VE) of an offshore oil installation. Naïve participants were assigned to two learning groups (Active and Active/Passive). The Active learner was able to explore the virtual environment while the Active/Passive learner followed a prescribed tour of the most efficient routes to the muster station. Each participant undertook three scenarios requiring mustering to a defined station. “Active” learners demonstrated superior mustering performance. Future research should investigate how ST using a VE transfers to similar, real-world environments.

1. Introduction

Offshore oil installations are often situated hundreds of kilometers from land, located in harsh environments and employ hundreds of people at any given time. Emergency situations on these installations can be highly complex, dynamic and often involve underspecified problems, which must be resolved under time-pressure constraints while interacting within a large socio-technical system, *Dahlstrom et al. (2008)*. Over the last three decades, several disasters have occurred on offshore installations. In 1980, the Alexander Kielland platform in the North Sea capsized, with only one successful lifeboat being launched as 123 of the 212 personnel onboard were killed, *Skogdalen et al. (2012)*. Two years later, the Ocean Ranger capsized and sank off the coast of Newfoundland. All 84 personnel did not survive, none reaching deployed lifeboats, *Hickman (1984)*. The Deepwater Horizon drilling unit resulted in 11 worker casualties and the accident reports portrayed the scene onboard as being “out of control”, stating that “there was a sense of urgency” and that “people were frozen up”. The crew reported the evacuation as being unorganized, with lifeboats being launched prematurely and some crew members ignoring evacuation procedure and jumping off the platform, concluding that “the consequences of human error in an offshore emergency can be severe” and that “it is important that emergency drills include worst case scenarios to prepare for emergency, evacuation, and rescue (EER) operations during major accidents,” *Skogdalen et al. (2012)*. In a risk-based analysis, *Norazahar et al. (2014)* suggested that administrative controls regarding training and crew-competencies were significant factors in the root cause of this tragedy.

Traditional occupational training methods meant to complement classroom teaching often take place under benign conditions. An evacuation exercise normally occurs in the daytime with no time pressure or emerging hazards to influence evacuation performance. While these methods may effectively teach personnel the required spatial and procedural knowledge regarding the installations egress routes, it is clear that employees won’t necessarily be exposed to training designed to increase participant stress. Since stress increases the likelihood of human error, *Skogdalen et al. (2012)*, stress-inducing training (which prepares employees to perform effectively in stressful environments) is necessary to fill the current training gap. As *Burian et al. (2005)* stated: “The degree to which training truly reflects real-life emergency and abnormal situations, with all of their real-world demands, is often limited.”

Simulation Training (ST) can be used to complement traditional training methods, *Saus et al. (2010)*. ST complements classroom and on-site training by allowing individuals to gain “artificial” experience undergoing stress-inducing scenarios, *Musharraf et al. (2016)*. Since placing employees in these situations in the real world is impossible due to ethical, logistical and financial concerns, *Veitch et al.*

(2008), virtual environments (VE's) are used to allow employees to develop naturalistic decision-making heuristics in a controlled environment, *Klein (1999)*. While offshore installation evacuations are often caused by blowouts, extreme weather conditions or process accidents, *Skogdalen et al. (2012)*, there exists an infinite amount of evacuation situations that conventional training methods cannot possibly prepare personnel. ST within VE's can provide these enhanced training opportunities.

In an evacuation situation, an employee must travel to a predetermined muster station to await instructions from the offshore installation manager. To do so, the employee must navigate a highly complex environment with many floors, congested with co-workers and surrounded by potentially hazardous materials. To arrive at a muster station safely and efficiently, a high level of spatial knowledge regarding the installation is necessary. In ST, spatial learning occurs by navigating a VE then encoding and subsequently retrieving information regarding the VE and ones orientation within it, *Peruch and Wilson (2004)*. In VE's, the extent of spatial learning can be quantified by task performance, such as the time to complete a task or number of errors made while completing a task, *van Baren and Ijsselsteijn (2004)*. Improvements in task performance are considered to represent improvements in spatial learning. Thus, if an individual demonstrates exemplary task performance, that individual is considered to have a large amount of spatial knowledge about the VE. Although spatial learning can be acquired through the use of maps, videos, descriptions, or navigations of the real-world environments, using a VE for ST may offer advantages in spatial learning that traditional forms of training cannot provide *Aggarrwal et al. (2005)*, *Gallagher et al. (2005)*, *Scalese et al. (2007)*. However, it is unclear whether ST involving active exploration, passive exploration, or a combination of both is the best way to acquire task performance, such as mustering proficiency. Establishing the mode of learning that induces the greatest increases in task performance may allow for the creation of ST protocols designed to maximize spatial learning. Better ST protocols may lead to increases in operator competency during EER situations, subsequently decreasing human error-related maritime accidents, thus saving resources and most importantly, human lives.

The objective of this research is to determine the effectiveness of different modes of learning (active learning and combined active and passive learning) on task performance during ST in a VE of an offshore oil installation. It is hypothesized that participants who participate in active learning will perform better on task performance measurements than participants who participate in a combined active and passive learning modality.

2. Methodology

Forty-six participants volunteered to participate in this study. Participants were verbally informed of all procedures and the overall goal of the experiment, but were naïve concerning the specific hypotheses and testing conditions. None of the participants had previous experience with the VE used in this experiment or with navigating the real-world environment (i.e. offshore oil and gas installation) modeled in the VE. This study was approved by Memorial University of Newfoundland's Interdisciplinary Committee on Ethics in Human Research. An independent measures (between groups) experimental design was used. Participants were randomly assigned to one of two groups: 1) an active exploration group (A) or 2) a hybrid active and passive exploration group (AP). Participants were required to attend four sessions (three training sessions and one testing session) on four separate days, with a minimum of 24 and a maximum of 48 hours between sessions. The first training session lasted approximately 50 minutes, the second and third training sessions lasted approximately 35 minutes, and the testing session lasted between 45 and 70 minutes. The total exploration time for each group was 30 minutes per training session, for a total of 90 minutes of exploration.

A graphic PC-based desktop workstation was used to create a VE of an actual, nine-level 3-D offshore oil installation, Fig. 1. An approximate scale of 1:10 was used to represent the exterior platforms included several staircases, a helicopter pad, a drilling deck, and a lifeboat deck and had a total area of 16,762 m². The total area of the interior platforms (representing the total area of floors and not the actual area of the corridors and rooms) totaled 8,169 m², for a total playable area of 24,931 m².



Fig. 1: Depiction of the Virtual Environment (VE) of the offshore platform

Three non-interactive videos were created for the AP group by capturing footage of gameplay in the VE. The lengths of the videos were 3.42, 4.93 and 3.6 minutes for navigational routes one, two and three respectively. The audio narration was recorded separately and overlayed on the video.

Participants controlled movement in the VE by using a wired game controller. Three movement options were given: 1) no movement, 2) walking (at a speed of 4.8 km/h), and 3) running (at a speed of 12 km/h), *Bohannon* (1997). Possible movements in the VE were: forward/backward translation, left/right translation, up/down rotation, and left/right rotation. It was possible to move in one direction while looking in another. To determine backtracking, a detection algorithm was parameterized with a horizontal range and a vertical range. The backtracking time was calculated by summing the differences of a backtracking point's time stamp from its predecessor.

2.1. Procedure

A five-minute pre-training period was used to allow the participant to familiarize him or herself with the controller and user interface. The participant was given a controller schematic and stayed on the top floor of the structure to avoid any additional opportunity for active learning but long enough to become proficient with the game controller. Each group was provided with a set of floor plans and each participant was allowed to self-select the degree to which these were used. These floor plans were only used in the training sessions and were not given to participants in the testing session. All the training and testing sessions started on the top floor of the structure. The goal for each group was to learn to navigate to the assigned muster and lifeboat platform located on the bottom floor of the structure.

Participants in Group A were instructed to freely explore the environment with the constraint that they stay on task and try to learn how to navigate to the muster and lifeboat platform as quickly as possible. Group AP watched three videos of an avatar following a predetermined path from the top floor of the structure to the lifeboat platform. Each video demonstrated a different navigational route and the avatar stopped several times along each route to discuss the landmarks located on each floor (i.e. “the games room is located on this floor.”). The avatar also discussed alternate routes to take in the event that a stairway or hallway was blocked. After watching a video, the participant attempted to imitate the route taken by the avatar. This process continued for the entire 30 minute time period, with the order of the videos being randomized for each session. Training sessions two and three began with a standardized briefing similar to that of the first training session. After the briefing, participants in each group completed a 30-minute training session.

2.2. Testing Session

The objective for the participant during the testing session was to reach the lifeboat platform as quickly as possible. Three testing conditions were completed in a randomized order: 1) Day, 2) Night and 3) Hazardous events. The Day condition mimicked the training scenarios and was characterized with normal levels of visibility. The Night condition was similar to the Day condition, except visibility was greatly reduced, however, participants could deploy a virtual flashlight to increase visibility (although not to the level of visibility in the Day condition) if they remembered how to operate their flashlight as described in the training sessions. The Hazard condition had daytime levels of visibility, but had several routes blocked by virtual hazards that included a jet fire, an electrical fire, and heavy smoke.

The task performance measurements used to quantify spatial learning were: 1) time to evacuation muster, 2) distance travelled during evacuation and 3) backtracking time during evacuation and 4) backtracking distance travelled during evacuation.

2.3. Statistical Analyses

Three participants withdrew from the study and in the A Group. Four females were determined to be outliers, with one female unable to complete the Hazard condition. In the AP group, one male was an outlier. A Shapiro-Wilk test of normality indicated non-parametric statistics were required for the subsequent analyses. To determine the effects of group on task performance, two-sample Kolmogorov-Smirnov Tests were performed. To determine within-group differences in the A and AP groups between the three conditions, Friedman's tests were performed. A Spearman's rho (ρ) correlation coefficient was used for all reported correlations. All tests were two-tailed. An alpha level of $p < 0.05$ was used to determine statistical significance. Results include all 38 participants unless otherwise stated.

3. Results

The average number of videos watched per session by the AP group was 4.38 ± 0.23 videos. Thus, the AP group spent 14.45 minutes (58% of each training session) in passive exploration and 12.55 minutes (42% of each training session) in active exploration.

Figs. 2 to 5 illustrate the effect of group on task performance. In the Hazard condition, time to evacuation, distance travelled during evacuation, backtracking time, and backtracking distance travelled were significantly ($p < .05$) higher in the A-P group by approximately 43, 35, 103, and 102% respectively, compared to the A group. In the Day condition, backtracking time and backtracking distance travelled was significantly ($p < .05$) higher in the A-P group by approximately 72 and 20%, respectively compared to the A group.

In the A group, the Hazard condition time to evacuation, distance travelled during evacuation backtracking time, and backtracking distance travelled significantly ($p < .001$) increased by approximately 235, 194, 2500, 2197%, respectively compared to the Day and Night conditions. In the AP group the Hazard time to evacuation, distance travelled during evacuation, backtracking time, and backtracking distance travelled significantly ($p < .001$) increased by approximately 340, 298, 2961, and 3722% respectively compared to the Day and Night conditions. Furthermore, in the AP group time to evacuation and distance travelled during evacuation significantly ($p < .05$) increased by approximately 9 and 7%, respectively from the Day to Night condition. To summarize, differences between the Day and Night conditions were minimal, regardless of group. However, during the most challenging condition (Hazard), the A group demonstrated better performance compared to the AP group.

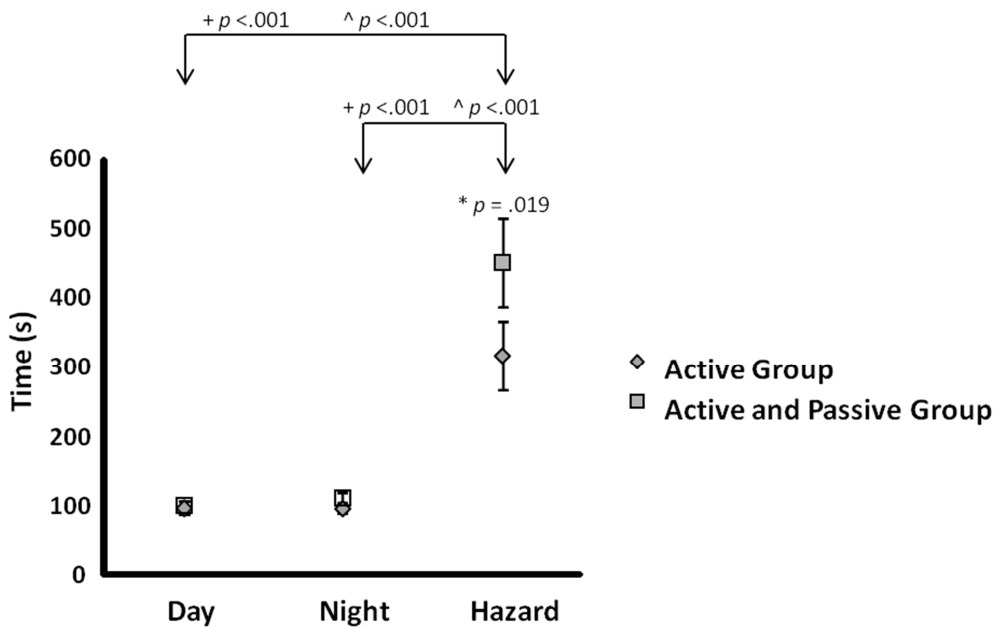


Fig. 2: Time to evacuation; Error bars represent standard error (SE). + = active group within-group difference; \wedge = active & passive group within-group difference; * = between group difference

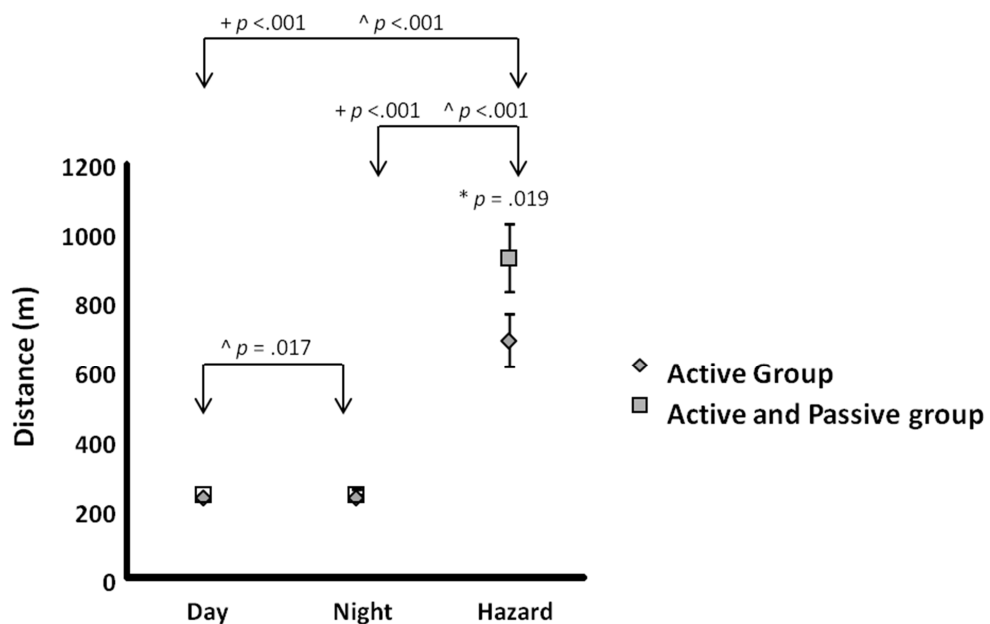


Fig. 3: Distance travelled during evacuation; Error bars represent standard error (SE). + = active group within-group difference; \wedge = active & passive group within-group difference; * = between group difference

4. Discussion

The most significant finding of this study was that Active Learning resulted in better task performance compared to combined Active and Passive Learning. Analyses of the task performance measures indicate that the Day and Night conditions were relatively equal in difficulty, whereas the Hazard condition was much more difficult as indicated by the decline in task performance. Although the Night condition was supposed to present a relative increased challenge, it appears that decreasing visibility does not substantially impact task performance in a multi-task VE. The Hazard condition imposed task performance decrements, and thus could be replicated in future VE's as a criterion measure for benchmark performance.

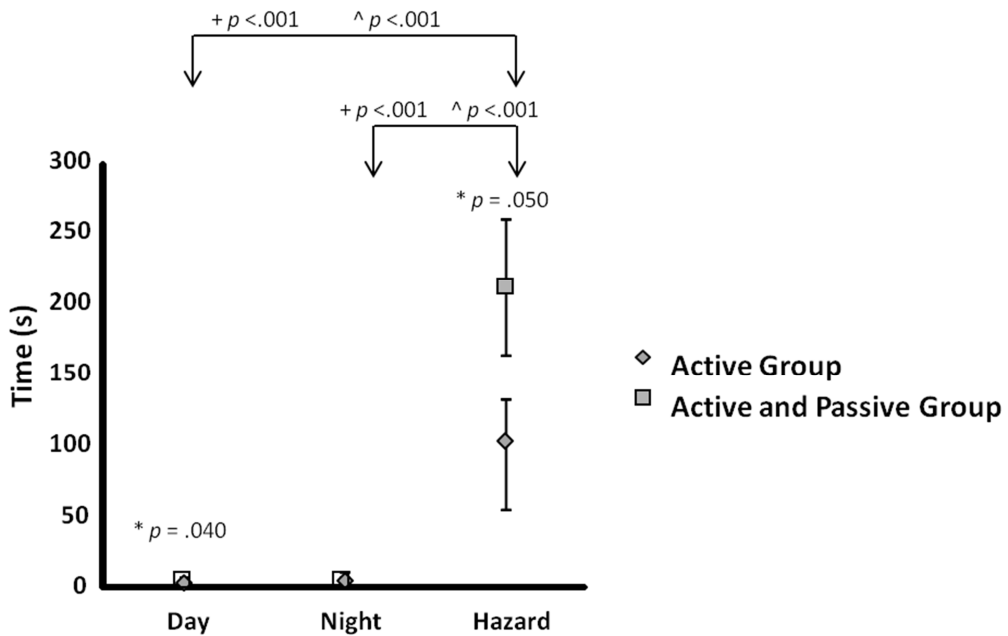


Fig. 4: Backtracking time during evacuation; Error bars represent standard error (SE). + = active group within-group difference; ^ = active and passive group within-group difference; * = between group difference

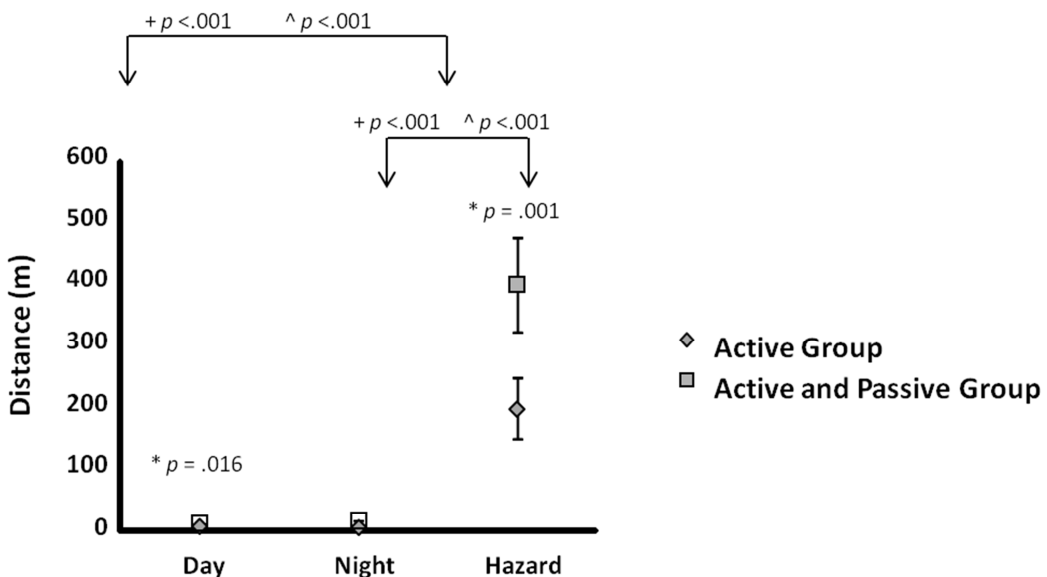


Fig 5: Backtracking distance travelled during evacuation; Error bars represent standard error (SE). + = active group within-group difference; ^ = active and passive group within-group difference; * = between group difference

To determine an appropriate “moderate” difficulty condition, future studies should decrease visibility further (or not allow for use of the flashlight) to determine if decreasing visibility affects task performance in the absence of other changes.

To effectively implement VE’s during ST, spatial learning (the process of encoding and retrieving information about one’s environment and orientation within that environment, *Peruch and Wilson (2004)*) must occur. The A Group demonstrated improved (35-103%) task performance compared to the AP Group in all four task performance measures during the most challenging (Hazard) condition. Since the A group was exposed to 58% more active exploration time compared to the AP group, it

appears that active exploration facilitated greater spatial learning than a combined active and passive learning approach.

The time to evacuation, Fig. 2, and distance travelled during evacuation, Fig. 3, tasks can be considered as surrogates for a wayfinding task. Furthermore, backtracking time, Fig. 4, and backtracking distance, Fig. 5, are added evidence of the advantages of an Active Learning approach. The task performance results of this study are in agreement with similar studies which found that active explorers demonstrated better wayfinding task performance and greater spatial knowledge on subjective route analysis and route drawings, *Peruch et al.* (1995), *Carassa et al.* (2002). However, the task performance results contrast with other studies which found no active-passive differences in the following tasks: pointing towards the origin, *Wilson et al.* (1997), *Gaunet et al.* (2001), scene recognition, *Christou and Bulthoff* (1999), *Gaunet et al.* (2001), route drawings, *Gaunet et al.* (2001), time to locate/number of errors made while locating a target, *Wilson et al.* (1997), and making distance estimates, *MacKinnon et al.* (2009).

In studies where an active learning advantage is found, it was hypothesized that active exploration resulted in a more survey-type representation, *Peruch et al.* (1995), *Carassa et al.* (2002). When no active-passive difference is found, the results are generally attributed to task-specific differences and similar attention levels between groups. It appears that for wayfinding/time to completion tasks (such as the time to evacuation task used in this study) active exploration results in better performance than passive exploration. The study by *Wilson et al.* (1997) was the only study using a wayfinding task that found no active-passive difference, however the active group in that particular study was not truly “active” since the experimenter guided them. To efficiently complete the Hazard condition, it would appear that a survey-type representation would be most beneficial since novel routes may need to be navigated to evacuate. The environment used in the present study had 8 and 7 more floors and was 1492 and 1627% larger in area compared to similar studies by *Wilson et al.* (1997) and *Carassa et al.* (2002), respectively. If active exploration created a more survey-type representation as hypothesized by the current study and others, *Hazen* (1982), then perhaps the advantages of survey representation (such as the ability to link together distant places to create a global overview, *Carassa et al.* (2002)), are more pronounced in larger, more complex environments. Thus, not only may there be a task-specific (wayfinding/time to completion) advantage of active exploration, then there may also be an environment-specific advantage, as suggested by *Peruch and Wilson* (2004).

It has been suggested that attention to the spatial environment is more important than mode of exploration for spatial learning in a VE, *Peruch and Wilson* (2004) and that no active-passive exploration differences exist if both groups equally attend to the spatial properties of the environment, *Peruch and Wilson* (2004), *Chrastil and Warren* (2012). However, it may be more difficult to sustain attention during passive learning compared to active learning. Increased autonomy over exploration allows active explorers to plan and subsequently test the consequences of their decisions during exploration, affecting their resulting view of the environment, *Chrastil and Warren* (2012), and potentially facilitating a survey-type representation. Although attention was not directly measured in the present or the above-mentioned studies, the A group may have had greater attentional allocation to relevant (i.e. routes, landmarks, relationships between landmarks, etc.) features of the VE during ST. This greater attentional allocation may have resulted in a more survey-type representation, allowing the A group to more efficiently navigate the complex Hazard condition. Therefore, more time spent in active exploration results in better task performance.

5. Conclusions

Since task performance is a measure of spatial learning in VE's, the results suggest that the A group demonstrated increased spatial learning as compared to the AP group. Active exploration may result in a more survey-type representation, potentially due to greater attentional allocation to spatial properties of the VE.

Even with technological improvements in navigation, processing, safety and evacuation equipment, accidents related to human error still represent a substantial risk to the health and safety of employees on offshore installations, *Saus et al. (2010)*. ST using VE's can be used as a complement to traditional training methods by allowing employees to gain experience with dangerous and stressful scenarios which would normally be impossible due to financial, ethical, and logistical concerns, *Veitch et al. (2008)*.

Although the aviation industry has been at the forefront in their use of ST over the past number of years, marine industries are beginning to research and develop similar training protocols. To be effective, ST must train the appropriate skills in suitable environments so that individuals can practice complex tasks in a manner that could transfer to similar tasks in real-world environments, *Gallagher et al. (2005)*. However, before marine industries invest large sums of money and time implementing ST, it is important to determine which mode of learning is most effective.

The current study provides evidence that while using a multi-task VE for ST, active exploration results in increased spatial knowledge within a VE compared to combined active and passive exploration. Subjective and objective measures of presence are rarely correlated with each other and presence is not related to task performance within the VE. Future research should investigate how different modes of learning and different levels of presence transfer to task performance in real-world environments.

References

- AGGARRWAL, R.; BLACK, S.; HANCE, J.; DARZI, A.; CHESHIRE, N. (2005), *Virtual reality simulation training can improve inexperienced surgeon's endovascular skills*, Eur. J. Vasc. Endovasc. Surg. 31, pp.588-593
- BOHANNON, R.W. (1997), *Comfortable and maximum walking speed of adults aged 20-79 years: Reference values and determinants*, Age and Ageing 26, pp.15-19
- BURIAN, B.K.; BARSHI, I.; DISMUKES, R.K. (2005), *The challenges of aviation emergency and abnormal situations*, N.A.R. Center, Editor Moffett Field
- CARASSA, A.; GEMINIANI, G.; MORGANTI, F.; VAROTTO, D. (2002), *Active and passive spatial learning in a complex virtual environment: The effect of efficient exploration*, Cognitive Processing 3(4), pp.65-81
- CHRASTIL, E.R.; WARREN, W. (2012), *Active and passive contributions to spatial learning*, Psychon. Bull. Rev. 19, pp.1-23
- CHRISTOU, C.G.; BULTHOFF, H. (1999), *View dependence in scene recognition after active learning*, Memory & Cognition 27(6), pp.996-1007
- DAHLSTROM, N.; DEKKER, S.; VAN WINSEN, R.; NYCE, J. (2008), *Fidelity and validity of simulator training*, Theoretical Issues in Ergonomics Science 10(4), pp. 305-314
- GALLAGHER, A.G.; RITTER, E.; CHAMPION, H.; HIGGINS, G.; FRIED, M.; MOSES, G.; SMITH, C.; SATAVA, R. (2005), *Virtual reality simulation for the operating room: Proficiency-based training as a paradigm shift in surgical skills training*, Annals of Surgery 241(2), pp.364-372
- GAUNET, F.; VIDAL, M.; KEMENY, A.; BERTHOZ, A. (2001), *Active, passive and snapshot exploration in a virtual environment: Influence on scene memory, reorientation and path memory*, Cognitive Brain Research 11, pp. 409-420

HAZEN, N.L. (1982), *Spatial exploration and spatial knowledge: Individual and developmental differences in very young children*, Child Development 53, pp. 826

HICKMAN, T.A. (1984), *Report one: The loss of the semisubmersible drill rig Ocean Ranger and its crew*, Royal Com. on the Ocean Ranger Matter Disaster

KLEIN, G. (1999), *Sources of Power: How People Make Decisions*, First MIT Press

MacKINNON, S.; EVELY, K.A.; ANTLE, D. (2009), *Does mariner experience effect distance judgments of visual targets in virtual marine environments?*, The Interservice/Industry Training, Simulation and Education Conf., Orlando

MUSHARRAF, M.; SMITH, J.; KHAN, F.; VEITCH, B.; MacKINNON, S. (2016), *Assessing off-shore emergency evacuation behavior in a virtual environment using a Bayesian Network approach*, Reliability Engineering and System Safety 152, pp.28-37

NORAZAHAR, N.; KHAN, F.; VEITCH, B.; MACKINNON, S. (2014), *Human and organizational factors assessment of the evacuation operation of BP Deepwater Horizon accident*, Safety Science 70

PERUCH, P.; VERCHER, J-L.; GAUTHIER, G.M. (1995), *Acquisition of spatial knowledge through visual exploration of simulated environments*, Ecological Psychology 7(1), pp.1-20

PERUCH, P.; WILSON, P.N. (2004), *Active versus passive learning and testing in a complex outside built environment*, Cogn. Process 5, pp. 218-227

SAUS, E.-R.; JOHNSEN, B.H.; EID, J. (2010), *Perceived learning outcome: The relationship between experience, realism, and situation awareness during simulator training*, Int. Marit. Health 61(4), pp. 258-264

SCALESE, R.J.; OBESO, V.T.; ISSENBERG, S.B. (2007), *Simulation technology for skills training and competency assessment in Medical Education*, J. Gen. Intern. Med. 23(1), pp.46-49

SKOGDALEN, J.E.; KHORSANDI, J.; VINNEM, J.E. (2012), *Evacuation, escape, and rescue experiences from offshore accidents including the Deepwater Horizon*, J. Loss Prevention in the Process Industries 25, pp.148-158

VAN BAREN, A.; IJSELSTEIJN, A.W. (2004), *Measuring presence: A guide to current measurement approaches*, OmniPres Project

VEITCH, B.; BILLARD, R.; PATTERSON, A. (2008), *Emergency Response Training Using Simulators*, Offshore Technology Conf., Houston

WILSON, P.N.; FOREMAN, N.; GILLETT, R.; STANTON, D. (1997), *Active versus passive processing of spatial information in a computer simulated environment*, Ecological Psychology 9(3), pp.207-222

Advances in Automated Ship Structure Inspection

Thomas Koch, Atlantec Enterprise Solutions, Hamburg/Germany, thomas.koch@atlantec-es.com

Sankaranarayanan Natarajan, Felix Bernhard, DFKI Robotics Innovation Center,

Bremen/Germany, {sankar.natarajan, felix.bernhard}@dfki.de,

Alberto Ortiz, Francisco Bonnin-Pascual, Emilio Garcia-Fidalgo, Joan Jose Company Corcoles,

University of Balearic Islands, Palma de Mallorca/Spain,

{alberto.ortiz, xisco.bonnin, emilio.garcia, joanpep.company}@uib.es

Abstract

Inspection of ship-board structures by humans is a time-consuming, expensive and commonly hazardous activity, creating the need to search for better solutions. Simultaneously the desire for broader and intensified data acquisition grows to provide a better basis for refined condition assessment. As the implementation of automated and increasingly autonomous robotic platforms for everyday use becomes more realistic, we have realised various approaches to robotic ship inspection, which are based on advances in multiple dimensions: light-weight robotic platform development, complex data pre-processing functions and large-scale data analytics. Results of investigations carried out as part of a project for enhanced ship safety are presented.

1. Introduction and background

Inspections on-board sea-going vessels are regular activities being initiated not only due to applicable classification and statutory regulations, but also performed for ship operators to assess the condition of a vessel's structure and to ensure its integrity. Since unexpected disruptions of vessel service availability tends to be very costly, ship operators have a vested interest to monitor the condition of the structure at a required level of detail. Unfortunately, continuous monitoring of stress and strain conditions, identification of defects or assessment of corrosion is not trivial and quite expensive. Since inspections are and will be an important source of information for structure condition assessment, it seems necessary to try to reduce the effort and cost related to these activities.

With the constant progress that can be observed in the field of robotics and automation, the introduction of automated tools for support of inspections appears to be a logical step to improve the efficiency and cost of inspections. However, some challenges must be overcome in this field of application, such as dealing with the harsh operating environment, complying with the safety requirements and managing the limited access and space. This has led to the research approach of using different robotic platforms and a wide range on sensors to determine useful combinations of technology for different operational scenarios. On the other hand, automated devices can still only cover part of the activities carried out during inspections. Critical (and usually limiting) design factors are: in-situ data processing capability, energy supply vs. payload, sensor sensitivity and reliability, signal quality, autonomy and fail-safe operation. Therefore, it is essential to combine the actual robotic devices with a carefully configured support system that provides functions for control, data acquisition and data post-processing.

The application of automated tools is intended to provide various important benefits. An important starting condition is that the overall cost of the robotic platforms is already quite low and will continue to decrease, eventually reaching more or less the commodity level. This will enable ship operators to equip vessels with a tailored set of inspection devices, which are instantly available for operation. This will lower the entry barrier considerably for ad-hoc inspections of limited scope, which are more easily arranged with less impact on operations of the vessel. As in many other industrial application areas, the use of automated tools will substantially reduce the exposure of operating staff to hazardous conditions. Due to the automated data acquisition, the hull structure coverage can be extended both in terms of area/volume as well as in number of parameters collected.

Being able to collect data and assess a structure's condition more easily will contribute to building up a wealth of processed data. It will help to establish a more detailed time history of various condition parameters, enabling or improving the use of advanced analytics for structure condition assessment leading to new possibilities for forecasting and damage prevention. This paper describes the automation efforts pursued within the framework of the EU-funded project INCASS, *INCASS* (2013), in accordance to the aforementioned.

2. Robotic systems for on-board inspection

In the recent years, advanced technological devices are finding their way into the marine vessel's inspection area. In this respect, the INCASS project considers the inspection of interior areas of a vessel, e.g. cargo holds, by means of robotic platforms. The two robotic devices which are available, namely an aerial platform and a magnetic crawler, are the result of the re-design of two platforms developed to accomplish the objectives of project MINOAS, *MINOAS* (2009), in accordance to the feedback received from vessel surveyors during several field trials at the end of that project. In short, they are intended to be lightweight and fast deploying vehicles capable of reaching points several meters high above the ground. The main parameters of both platforms can be found in Table I. They both are reviewed in more detail in the following sections.

Table I: Main technical specification of the INCASS robotic platforms

	Aerial platform (Pelican)	Magnetic crawler
Size (L x W x H)	650 mm × 650 mm × 270 mm	330 mm × 300 mm × 130 mm
Weight	1700 g	1230 g
Speed	0.5 – 2 m/sec	0.5 m/sec on vertical adhesive walls
Propulsion	<ul style="list-style-type: none"> • 4 × 160 W brushless motors • 10" propellers 	<ul style="list-style-type: none"> • 2 × 12V DC geared motors with encoders
Sensors	<ul style="list-style-type: none"> • 3-axis IMU • Laser scanner / optical flow • Height meter • 2 Mpx still camera • 12 Mpx Full HD video camera 	<ul style="list-style-type: none"> • Motor encoders • HD 720p USB camera • 3-degree of freedom accelerometer
Auxiliary components	<ul style="list-style-type: none"> • 2 × LED spotlights (3W) 	<ul style="list-style-type: none"> • 3 x LED • Lithium-Polymer saver
Communication & interaction	<ul style="list-style-type: none"> • Dual 2.4 - 5GHz Wi-Fi LAN • Joystick / gamepad 	
Power	11.1V, 4500mAh, 3-cell Lithium-Polymer	11.1V, 800mAh, 3-cell Lithium-Polymer

2.1 Aerial platform

2.1.1. Platform overview

In line with the robotic platform developed for the MINOAS project, the INCASS aerial vehicle is based on a multi-rotor design. The control software has been configured to be hosted by any of the research platforms developed by Ascending Technologies (the quadcopters Hummingbird and Pelican, and the hexacopter Firefly), although it could be adapted to other systems. The AscTec vehicles are equipped with an inertial measuring unit (IMU), which comprises a 3-axis gyroscope, a 3-axis accelerometer and a 3-axis magnetometer, and two ARM7 microcontrollers. Attitude stabilization control loops linked to the on-board IMU and thrust control run over the main ARM7 microcontroller as part of the platform firmware. The manufacturer leaves almost free an additional secondary ARM7 microcontroller which can execute on-board higher-level control loops.

All platforms are fitted with a navigation sensor suite that allow them to estimate the vehicle state,

which comprises 3-axis speed (v_x , v_y , v_z), the flying height z and the distances to the closest obstacles in different orientations, e.g. left (d_l), right (d_r) and forward (d_f). These estimations can be performed by means of different sensor combinations leading to different weight, volume occupied and power consumption. This permits preparing for the inspection application either vehicles of low payload capacity (lower-cost platform) or vehicles able to lift a heavier sensor suite (higher-cost platform). As example, Fig. 1 shows a Hummingbird platform, fitted with two lightweight optical-flow sensors for speed estimation, ultrasound sensors for obstacle detection and an infrared height-meter, and a Pelican platform fitted with a laser scanner for speed estimation and obstacle detection, and a laser-based height-meter.

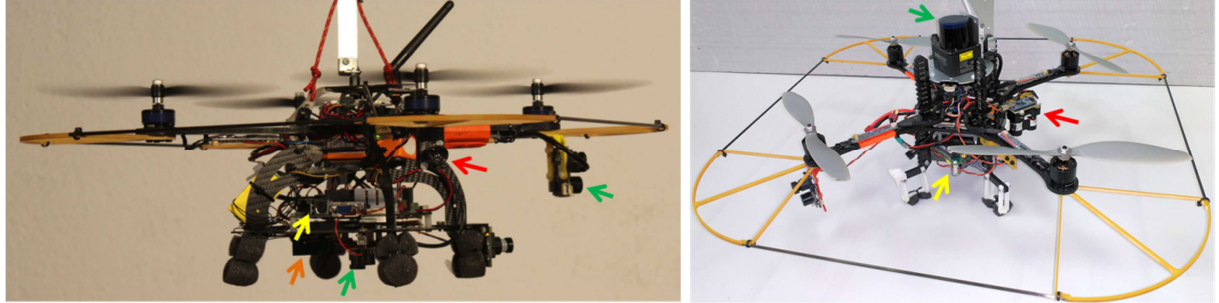


Fig. 1: [left] Hummingbird platform with optical flow sensors (green), infrared height-meter (orange), and ultrasound sensors (red). [right] Pelican platform with laser scanner (green) and laser-based height-meter (red). The embedded PC is indicated by a yellow arrow in each case.

Besides the navigation sensor suite, all platforms carry, in accordance to their payload capacity, one or several cameras for collecting the expected visual inspection data. To finish, apart from the two ARM7 microcontrollers integrated in the flight control unit of the AscTec platforms, all vehicles carry an embedded PC, which avoids sending sensor data to a base station, but process them on-board and, thus, prevent communications latency inside critical control loops. Once again, the different platforms are fitted with boards compatible with their payload limits, e.g. the Hummingbird of Fig. 1 features a Commell LP-172 Pico-ITX board fitted with an Intel Atom 1.86 GHz processor and 4 GB RAM, while the Pelican carries an Intel NUC D54250WYB with an Intel Core i5-4250U 1.3 GHz processor and 4 GB RAM.

2.1.2. Control software

The aerial platforms integrate a control architecture that follows the supervised autonomy (SA) paradigm, *Cheng and Zelinsky (2001)*. This is a human-robot framework where the robot implements a number of autonomous functions, including self-preservation and other safety-related issues, which simplify the intended operations for the user, so that he/she, which is allowed to be within the general platform control loop, can focus in accomplishing the task at hand. Within this framework, the communication between the robot and the user is performed via qualitative instructions and explanations: the user prescribes high-level instructions to the platform while this provides instructive feedback. In our case, we use simple devices such as a joystick or a gamepad to introduce the qualitative commands and a graphical user interface (GUI) to receive the robot feedback. Joystick commands and the GUI are handled at a base station (BS) linked with the MAV via a Wi-Fi connection.

The control software is organized around a layered structure distributed among the available computational resources. On the one hand, the low-level control layer implementing attitude stabilization and direct motor control executes over the main microcontroller as the platform firmware provided by the manufacturer, *Gurdan et al. (2007)*. On the other hand, mid-level control, running over the secondary microcontroller, comprises height and velocity controllers which map input speed commands into roll, pitch, yaw and thrust orders. Lastly, the high-level control layer, which executes over the embedded PC, implements a reactive control strategy coded as a series of ROS (Robot Operating System (www.ros.org)) nodes running over Linux Ubuntu, which combine the user desired speed command with the available sensor data $-v_x$, v_y , and v_z velocities, height z and distances to the closest obstacles

d_l , d_r and d_f , to obtain a final and safe speed set-point that is sent to the speed controllers.

Speed commands are generated through a set of robot behaviours organized into a hybrid competitive-cooperative framework, Arkin (1998). I.e., on the one hand, higher priority behaviours can overwrite the output of lower priority behaviours by means of a suppression mechanism taken from the subsumption architectural model. On the other hand, the cooperation between behaviours with the same priority level is performed through a motor schema, where all the involved behaviours supply each a motion vector and the final output is their weighted summation. An additional flow control mechanism selects, according to a specific input, among the outputs provided by two or more behaviours.

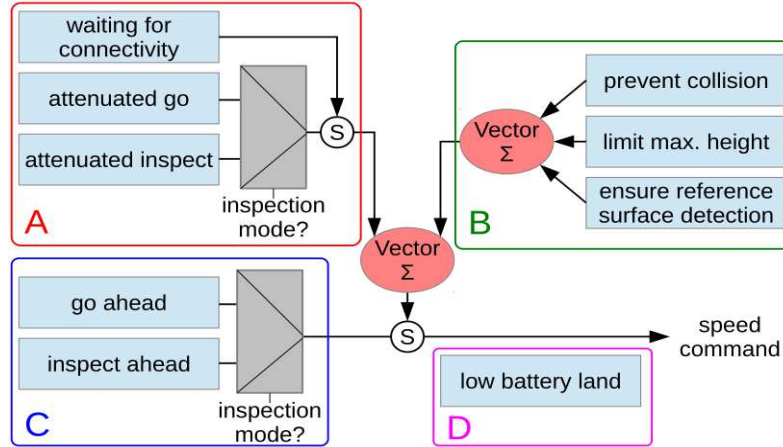


Fig. 2: Behaviour-based upper control layer

Fig. 2 details the behaviour-based architecture, grouping the different behaviours depending on its purpose. A total of four general categories have been identified for the particular case of visual inspection: (a) behaviours to accomplish the user intention, which propagate the user desired speed command, attenuating it towards zero in the presence of close obstacles, or keeps hovering until the Wi-Fi link is restored after an interruption; (b) behaviours to ensure the platform safety within the environment, which prevent the robot from colliding or getting off the safe area of operation; (c) behaviours to increase the autonomy level, which provide the platform with higher levels of autonomy to both simplify the operation and to introduce further assistance during inspections; and (d) behaviours to check flight viability, which checks whether the flight can start or progress at a certain moment in time. Some of the behaviours in groups (a) and (c) can operate in the so-called inspection mode. While in this mode, the vehicle moves at a constant and reduced speed (if it is not hovering) and user commands for longitudinal displacements or turning around the vertical axis are ignored. In this way, during an inspection, the platform keeps at constant distance/orientation with regard to the front wall, for improved image capture.

2.2 Magnetic crawler

2.2.1. Platform overview

The main aim for developing the magnetic crawler is to get a closer visual inspection. The use of magnets or suction pads to locomote on the inspection surface of a marine vessel is already available in research and also industry robots, CROMSCI, Jung *et al.* (2010), MagneBike, Tache *et al.* (2010), MARC, Bibuli *et al.* (2012). As marine vessels are made of solid steel using magnetic wheels or magnetic tracks system offers an efficient solution for both locomotion and also for traction. In this section the hardware design and software architecture of the magnetic crawler is explained. The first design concept of this magnetic crawler was described in Eich and Voegele (2011). During the development of the current magnetic crawler the surveyor's recommendations are included in the design criteria. Fig. 3 shows the newly developed magnetic crawler. The main design criteria for the magnetic crawler are to be lightweight; deployment does not require any extra installation, capable of

teleoperating and semi-autonomous navigation, wireless communication, tiltable camera system and easy to use for the surveyor.



Fig. 3: Lightweight magnetic crawler (source: DFKI GmbH)

The magnetic crawler is controlled and data are processed by an Odroid-U3 single-board computer with a quad-core processor. The computer has a 2GB RAM, 3 high speed USB port, Ethernet and GPIO/UART/I2C ports. The magnetic crawler is equipped with the sensors like accelerometer, high definition camera and two motor encoders. A custom designed printed circuit board was developed based on a PIC board housing an ADXL345 accelerometer, a DC/DDC converter, a USB-IO board. A 720p high definition USB based camera is mounted on a tilt unit and it is installed in front of the crawler. This tilt unit is controlled by a micro-servo motor. The tiltable camera is advantageous over a static camera as it will be helpful to navigate the crawler by tilting the camera in the crawler moving direction. In order to get a close-up image the camera can be tilted downwards. Adequate light is always an issue in taking inspection images in the marine vessel. It is not always possible to illuminate an entire tank or a cargo hold for acquiring image during the inspection. There might be certain areas which were not properly illuminated due to lack of light source near the target area or due to the shadow caused by the crawler. To overcome this issue the crawler is fitted with two sets of LEDs, one set is fixed in front of the crawler and the other set is fixed below the crawler. All these components are controlled through the USB-IO board. The crawler is equipped with a wireless local area network (WLAN) which is used in transmitting camera data such as images and videos and also for communicating with the crawler.

The magnetic crawler is actuated by two 12 V DC motors that drive the two magnetic wheels. In order to increase the crawler stability while climbing on corrugated metal structures, a flexible tail is attached on the rear part of the crawler through passive joints. A neodymium permanent magnet ring is fixed to the end of the tail. The magnetic wheel is one of the most challenging parts in the development of the crawler. Instead of fitting the magnets directly in to the wheel, a soft wheel-belt was designed to hold the magnet around the wheel frame. The cups-like structure in the soft wheel belt holds the magnets in place and also helps in preventing the magnets losses. The soft wheel belt was manufactured by developing a negative mould out of CNC-milling-wax and then casting a positive mould with a flexible polyurethane casting system, Fig. 4. The magnets were glued with a two-component epoxide glue into the roughened polyurethane cups, their adhesion pulled them to the bottom direction (iron sheet) while drying.



Fig. 4: Wax mould with the casted polyurethane stripes (left). Polyurethane stripes with integrated magnets (middle). Wheel-CAD model (right) (source: DFKI GmbH)

2.2.2. Control Software

A graphical overview of the magnetic crawler's control architecture is shown in Fig. 5. The crawler consists of several hardware and software components. The Robot Operating System (ROS) is used as a software framework in the crawler. To maintain the light weight, only low level software components such as motor controller, driver for camera, accelerometer, and camera servo motor are running in the crawler computer. As self-localisation is not feasible by using only crawler's on-board sensors, an external tracking unit is also used along with crawler's on-board sensors. The external tracking unit consists of a camera, a laser-based distance measurement unit and two dynamixel servos. The bright LED light which is fitted on the top of the crawler for tracking purpose will be detected by the tracking unit camera. With the help of the two servo motors the tracking unit controller is capable of tracking the moving crawler. A detailed design and the control of the tracking unit were described in *Eich and Voegele (2011)*. The crawler can be teleoperated by an operator with a help of a joystick. A graphical user interface (GUI) is developed to provide a surveyor an overview of the crawler's current status and also for sending higher level commands. The crawler's current status such as current pose, image from the camera are shown in the GUI. The surveyor can also use this GUI for controlling the crawler movement, sending the inspected image along with its pose value to the database, controlling the tilt angle of the camera and for turning ON/OFF the LED light.

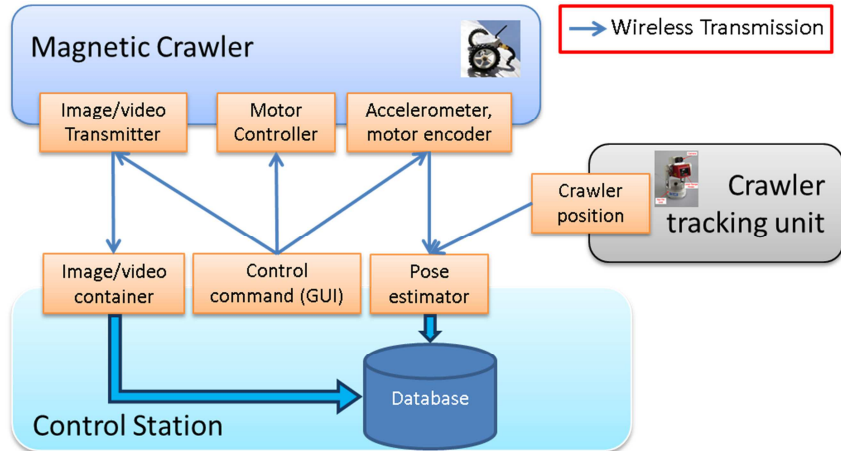


Fig. 5: Overview of the software architecture of the lightweight magnetic crawler

3. On-site data collection

As described above, the main purpose of the two robotic platforms is to serve as remote sensors of inspection data. In this section, we describe the sort of data collected as well as any processing that is performed.

3.1 Aerial platform

During flight, any of the aerial platforms can collect pictures on demand or at a fixed rate, e.g. 10 fps, as well as log flight data. The latter includes the vehicle pose, i.e. 3D position and 3D attitude, the vehicle speeds and the distances to the closest obstacles. Of particular relevance is the vehicle pose, which permits associating a 3D position to the defects found. For this purpose, two simultaneous and localization methods (SLAM) have been integrated on-board the aerial platforms given their different payload capacities. One adopts a laser-based SLAM strategy while the other is a visual single-camera SLAM solution: while the first one aligns consecutive laser scans to estimate the vehicle motion from one time instant to the next, the second solution matches image features across consecutive images, projects them in 3D and determines the corresponding 3D transformation. Depending on the robot on-board computational capabilities, the latter process can run on-line or off-line, after flight. By way of example, Fig. 6 (top) shows the paths estimated by the laser-based approach for two flights, as well as illustrates the defect localization process after visual inspection through the projection, as different

coloured boxes, of the bounding boxes of the defects found during a flight. Fig. 6 (bottom) shows the robot during a visual inspection on board an oil tanker and one of the images captured.

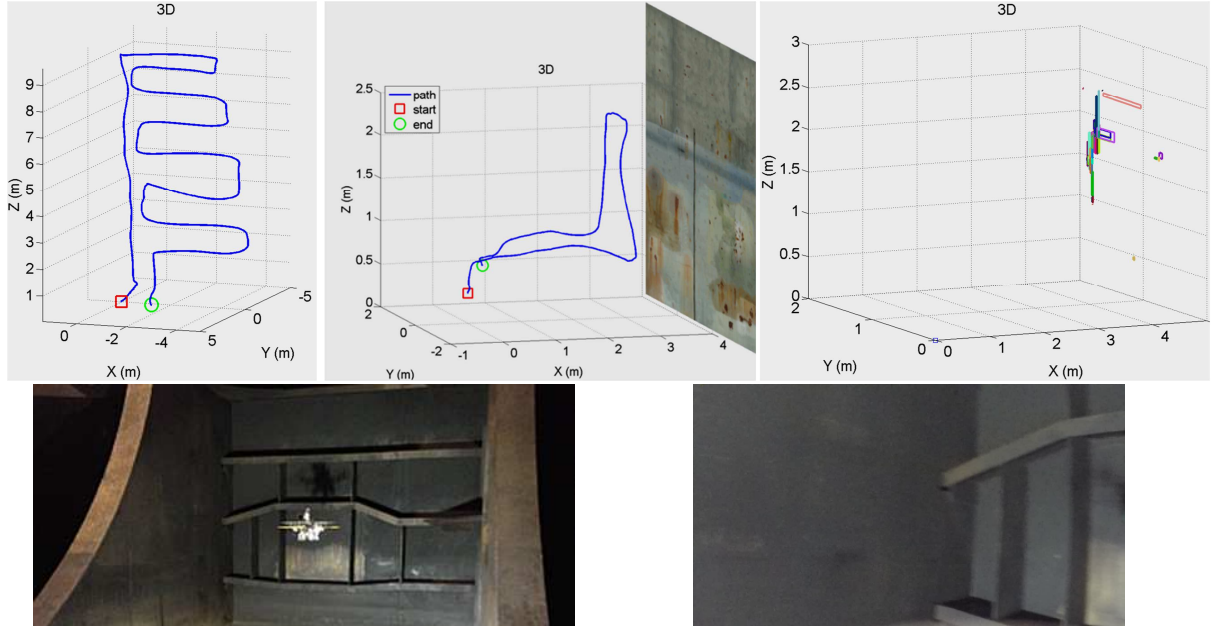


Fig. 6: Paths estimated after a flight and illustration of defect localization process after visual inspection (top). Visual inspection inside an oil tanker and one of the images collected (bottom)

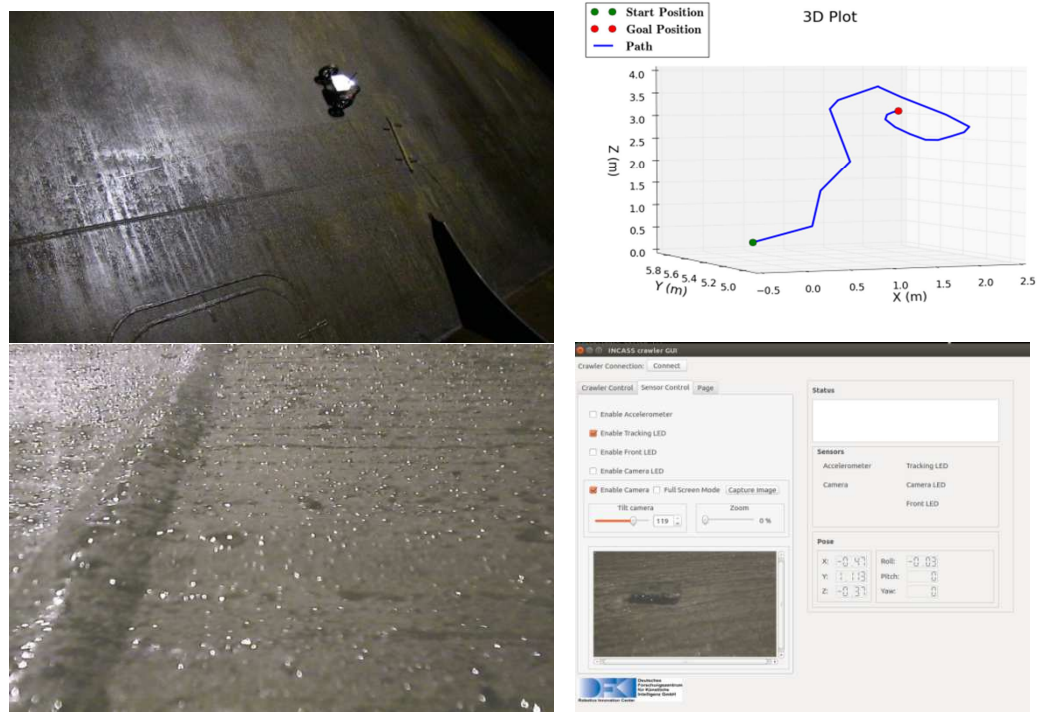


Fig. 7: Visual inspection inside an oil tank (top, left). Path followed by the crawler (top, right). Sample image during inspection (bottom, left). GUI showing an image and its pose (bottom-right).

3.2 Magnetic crawler

During the visual inspection, the surveyor needs, besides the visual data, the actual position of the visual data with respect to a reference frame. A pose estimator module running on the control station is responsible for estimating the crawler's position along with its orientation with respect to a

reference frame. Since the position information sent by the crawler's tracking unit and crawler's orientation and odometry information are transmitted separately, the pose estimator module needs to synchronise all the incoming data based on the timestamps before estimating the crawler's current pose. The visual data along with its corresponding pose value are stored in a database on the crawler's control station. The inspection information is all saved in a XML file. Fig. 7 shows the inspection area, the path followed by the crawler, and a sample inspection image.

4. Image analysis and defect assessment

In this work, we consider defects as rare phenomena that may appear on a regular surface or structure. Since they are rare, the probability that an area is affected by a defect is rather low. This low probability can be used as an indicator of image saliency, and thus highlight image areas suspicious of being defective. Next sections describe saliency computation as well as the performance attained.

4.1 Bayesian Approach for Saliency Computation

Similarly to *Zhang et al. (2008)*, we make use of a Bayesian approach to compute a saliency map Σ_{ij} :

$$\Sigma_{ij} = \frac{1}{p(F=f_{ij})} p(F=f_{ij}|T=\delta). \quad (1)$$

where f_{ij} is the value of the feature F found at an image location (i, j) , and T stands for the target class, i.e. the defect class δ in our case. Hence, equation (1) combines top-down information with bottom-up saliency to find the pointwise mutual information between the feature and the target. Using this formulation, the saliency at a given image point decreases as the probability of feature value f_{ij} gets higher, and increases as the probability of feature value f_{ij} for the defect class δ increases.

4.2 Contrast-based Saliency

As said before, we consider defects as rare phenomena that catch the visual attention of the observer during visual inspection. Following this idea, we describe defects by means of features typically used in cognitive models to predict human eye fixations. To this end, we make use of one of the most influential saliency computational models based on contrast, described in *Itti et al. (1998)*. In this model, the contrast levels in intensity, colour and orientation are computed as centre-surround differences between fine and coarse scales over image pyramids of up to 7 levels; that is to say, the difference between each pixel on a fine (or centre) scale c and its corresponding pixel in a coarse (or surrounding) scale s is calculated as $M(c, s) = |M(c) \otimes M(s)|$, where \otimes is the centre-surround operator, $c \in \{1, 2, 3\}$ and $s = c + \lambda$, with $\lambda \in \{3, 4\}$. Given an RGB colour image, this process is performed over: (\oplus denotes the across-scale addition operator)

- the intensity channel $I = (r + g + b)/3$, with r, g and b as the original red, green and blue channels, to build the intensity conspicuity map $IM = \bigoplus_{c=2}^4 \bigoplus_{s=c+3}^{c+4} N(I(c, s))$;
- the colour channels RG and BY defined as $RG = R - G$ and $BY = B - Y$, with $R = r - (g + b)/2$ for red, $G = g - (r + b)/2$ for green, $B = b - (r + g)/2$ for blue and $Y = (r + g)/2 - |r - g|/2 - b$ for yellow (negative values are set to zero for all channels), to build the colour conspicuity map $CM = \bigoplus_{c=2}^4 \bigoplus_{s=c+3}^{c+4} N(RG(c, s)) + N(BY(c, s))$; and
- the orientation channels $O(\theta)$, calculated by convolution between channel I and Gabor filters at orientations $0^\circ, 45^\circ, 90^\circ$ and 135° , to build the orientation conspicuity map $OM = \sum_{\theta \in \{0^\circ, 45^\circ, 90^\circ, 135^\circ\}} N\left(\bigoplus_{c=2}^4 \bigoplus_{s=c+3}^{c+4} N(O(c, s, \theta))\right)$.

The map normalization operator $N(*)$ highlights saliency peaks in maps where a small number of strong peaks of activity (conspicuous locations) are present, while globally suppressing peaks when

numerous comparable peak responses are present. To this end: (1) the map is normalized to a fixed range, (2) the global maximum M is found, (3) the local maxima average m is determined, and (4) the map is multiplied by $(M - m)^2$.

Finally, the three conspicuity maps are normalized and summed into the final output:

$$\Sigma_{ij} = \frac{1}{3}(N(IM) + N(CM) + N(OM)) \quad (2)$$

4.3 Performance Assessment

Fig. 8(a) shows probability density functions (PDFs) for contrast, i.e. $p(F = \text{contrast}_{ij})$, and contrast conditioned on the presence of defects, i.e. $p(F = \text{contrast}_{ij}|T = \delta)$, both determined by means of the Parzen windows method, *Theodoridis and Koutroumbas (2009)*, and a training image set comprising surfaces and structures containing cracks, coating breakdown and corrosion.

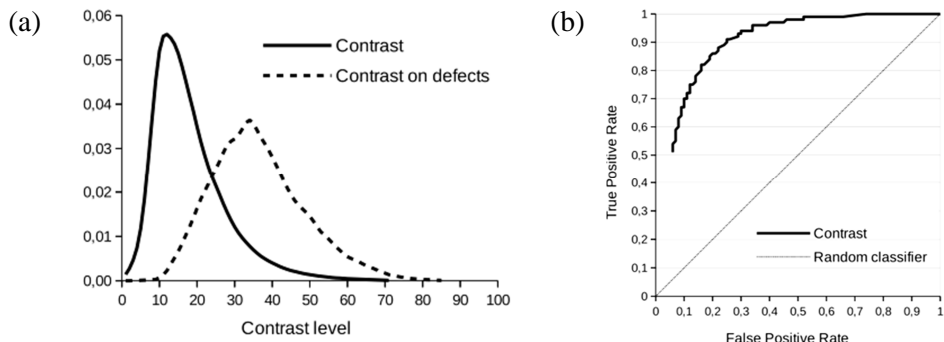


Fig. 8: (a) PDFs for contrast (b) ROC curve for the defect detector [AUC = 0.88]

Fig. 9 shows detection results for a number of images after the training performed. Moreover, we have evaluated the detection approach using leave-one-out cross-validation, *Duda et al. (2000)*: one image is selected from the dataset, while the rest is used to obtain the feature PDFs that make up the defect detector (training step), the selected image is next used to validate the detector, and the process is repeated for each image in the dataset. Global performance is shown in Fig. 8(b) in the form of a ROC curve relating true positive rate (TPR) and false positive rate (FPR). (FPR, TPR) points result from thresholding the defect maps at different contrast levels and comparing the resulting binary image with a ground truth. The area under the curve (AUC) metric, *Fawcett (2006)*, for this detector was assessed as 0.88, which is quite above the performance of a random classifier.

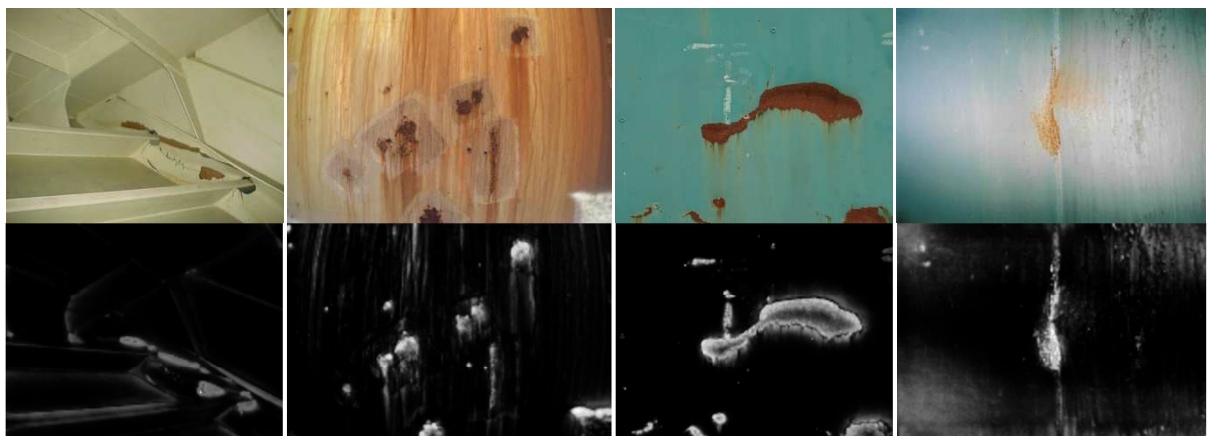


Fig. 9: Real images containing defects and corresponding defect maps (whiter means more salient)

5. Data transfer

The robotic platforms can feed a number of different data streams depending on the number of sensors and image capturing devices used. Every connected data acquisition platform can output different data collections for further processing. However, the internal data structures for the data acquisition operation may vary widely. It can be expected that in future production applications a considerable range of different robotics-based data acquisition systems will be available, offering a confusing number data formats to work with. To be able to deliver this data efficiently and reliably, a commonly established data transfer method seems necessary.

The purpose of the Hull Condition Monitoring (HCM) data exchange standard, *HCM (2016)*, is to provide such a data transfer model and format for easy and yet powerful exchange of thickness measurement results from inspections. It is therefore an important means for capturing information needed to analyse and assess the structural status of a vessel. HCM defines an XML schema based data model that is originally influenced by ISO 10303-218, *ISO (2004)*, to cover description of structure models but adds a range of entities to handle inspection related data. It therefore defines a focussed and compact model suitable for description of ship structures as required for inspection purposes, e.g. as defined by *IACS (2006,2009)*. Based on this, inspection results are captured by means of campaign data that can hold all relevant details about the findings. Most importantly, HCM also provides an extension mechanism which supports transport of additional data for use case specific contexts. This mechanism has been used in our implementation work to satisfy additional requirements demanded by automated inspection activities.

As illustrated above, common inspection tasks do not only involve thickness measurement readings, but may also include data sources such as ultrasonic readings or visual inspection imaging and image analysis. For automated visual inspections image and video data is essential, but after post-processing various kinds of condition assessments will also be available and need to be communicated. To satisfy these demands, three extensions for HCM have been developed:

- VisualInspectionCampaign – allows the transfer of imaging data directly linked to the HCM structure model
- HullSurvey – captures the condition assessment data such as identified cracks and common types of deformations
- CoatingCondition – provides a model for describing the coating and corrosion condition encountered during an inspection

The following excerpt from an exchange unit utilising the HullSurvey extension demonstrates the application for describing the geometry of identified crack geometry and the link to the captured image which has been used for this assessment:

```
<Extension id="hs1" status="in progress" xsi:type="HullSurvey">
<SurveySession id="session-1" status="in progress">
<Defects>
  <Crack length="0.16539" name=" session-1.defect1">
    <Shape>
      <Vertex x="0.91963" y="0.30105" z="1.601"/>
      <Vertex x="0.92056" y="0.27804" z="1.601"/>
      <Vertex x="0.92056" y="0.27804" z="1.4372"/>
      <Vertex x="0.91963" y="0.30105" z="1.4372"/>
    </Shape>
    <Attachments>
      <DocumentReference refId="doc0"/>
    </Attachments>
  </Crack>
```

```
...      </SurveySession>
...
</Extension>
```

6. Data management and processing

During ship inspections, surveys and monitoring activities using automated devices results in a considerable amount of “raw” data being collected. This data has to be processed and stored to capture and extract as much relevant information as possible. Automation allows inspecting an increased quantity of sampling locations during available time slots using various sensors more or less concurrently, thus additionally amplifying this demand. Data volume is further multiplied as inspection and monitoring is supposed to occur more frequently during the full operational life time of the vessel. Previously acquired data must be made available for further (re-)processing and (re-)assessment. Support functions for visual inspection by human operators including thorough evaluation performed by experts or application of advanced analysis using distinct (and rapidly developing) collections of algorithms (some of which will inevitably require access to sufficiently powerful computing resources) depend on easy access and efficient querying and retrieval. With such large sets of data, a foundation is established to apply new or refined analytical methods, which are essential for automating (part of) the assessment activities (e.g. defect pre-identification) and to prepare the data in the best possible way for final judgement by human experts.

Despite the fact that inspection devices carry considerable embedded processing capabilities, immediate post-processing capacity is nevertheless limited and thus further substantial post-processing occurs after actual acquisition but before finally storing the data for long-term reference. During this process the objective is to capture as much raw information as possible during acquisition and then to reduce the data volume using closely linked post-processing steps without losing any valuable information.

Such post-processing steps may include:

- Filtering (e.g. removing noise, detecting out-of-bounds recordings, and performing other quality checks)
- Data compression (e.g. removing redundancy or combining many samples into a compact storage format)
- Data fusion (e.g. combining image data, structure model data, thickness measurements to create part status information)
- Data attribution (e.g. linking image information with location and orientation data)
- Information generation (e.g. defect identification from image processing)

As shown in the system architecture, Fig. 10, processing is distributed to different system components: operations that depend on raw data and/or are specific to individual robotic platforms are implemented as part of portable data acquisition systems, which will be closely located and linked to the robotic units. The output from these systems is suitable for compact storage and transfer using the extended HCM and VoyageLog data exchange formats. These data can be asynchronously processed by the information management system (IMS) using appropriate adapters which prepare and convert the HCM and VoyageLog data for persistent data storage. Once it is stored, the data will be available for any type of inquiry, reporting and analytic operation.

Within the information management system, data entities such as the following are being stored for processing and evaluation:

- Vessel details: general particulars, class notation, time line
- Compartmentation data
- Hull structure details down to physical part level

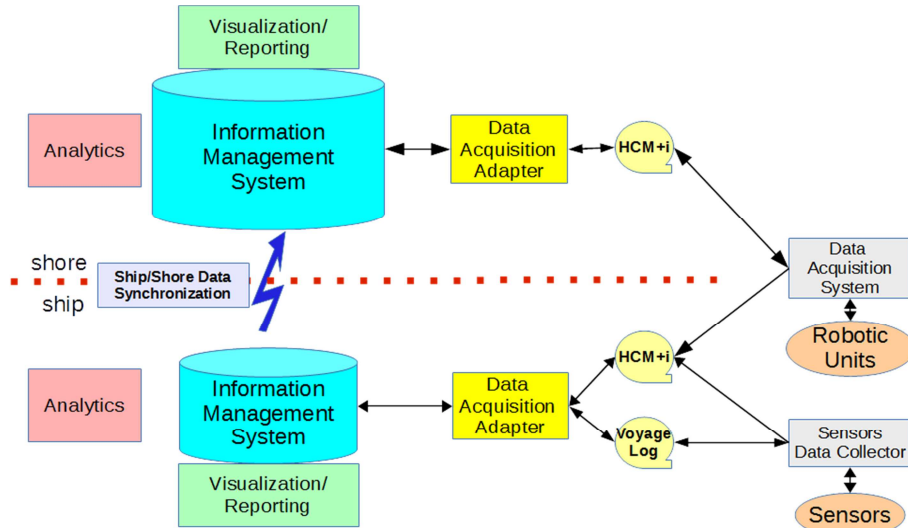


Fig. 10: System architecture for information management system

- Analytical models: finite element models, hydrodynamic models, reliability models
- Life cycle history: voyage tracking, loading conditions, inspection events
- Repairs: activity records and replaced parts
- Inspection data:
 - Bulk data
 - Thickness measurements
 - Images, videos
 - Post-processed data
 - Coating condition assessment
 - Corrosion assessment
 - Structure defects: cracks, buckling, general deformations
- Monitoring data: time series data for strain gauges, accelerometers, vibration and shock sensors
- Analytics results

The information management system has been implemented based on the Topgallant Information Server (TGIS), <http://www.atlantec-es.com/topgallant-product-is.html>, which provides specific support for complex structured engineering type data and can operate on top of different storage engine platforms.

Considering the wide range of data management requirements in this application, it was determined that scalability of the information management system is a critical design parameter. This has been achieved by employing three different storage platforms for different usage scenarios, all of which are operated via the same single data management API available in TGIS:

- A small footprint embedded single-process engine that utilizes a configurable in-memory database cache to ensure high performance on smaller platforms and requires minimal configuration but provides full persistence and transaction capabilities. This engine allows prototyping as well as operating in moderately sized and portable support tools, e.g. as they may be used on-board vessels.
- A client-server engine that operates as a multi-user networked database layer. It is intended to cover common scenarios of multi-client operation against a storage server. This configuration is suitable for use in larger on-board configurations. However it is primarily targeting mid-range on-shore configurations.
- A distributed, highly scalable engine implementing a NOSQL storage paradigm. This engine provides “big data” processing power, capable of handling multi-Terabyte data volumes with

selectable data redundancy and availability levels. Since this platform can involve a large amount of hardware (including options to operate as a cloud-based system), more advanced configuration considerations apply. It is expected that with continued advances in commodity hardware and virtualisation techniques this may well become the standard operational platform.

For complex analytics and continued (re-)processing of the data, the system supports the dynamic integration on externally provided calculation modules, as described in Koch *et al.* (2015). Using this method, a variety of processing capabilities can be provided ranging from visualisation (e.g. image rendering) and reporting (e.g. graphs) to analytics and reporting.

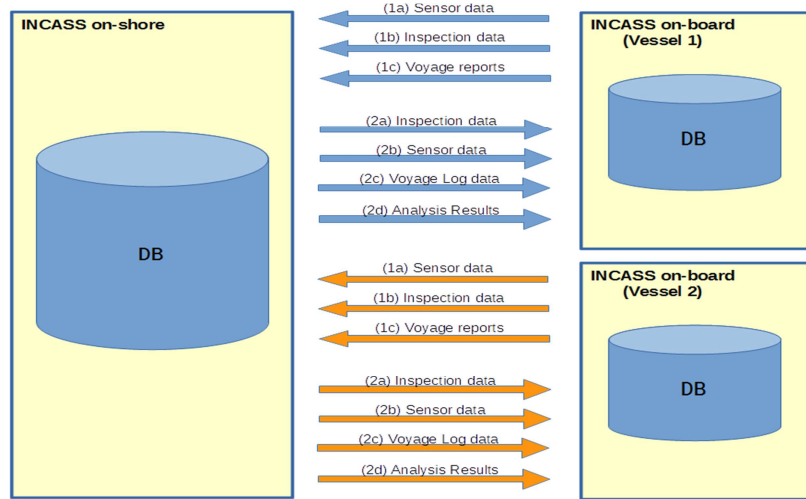


Fig 11: Ship-Shore communication data streams

Finally, some attention had to be given to the communication requirements of the overall system configuration, Fig. 11. Since the data acquisition occurs almost exclusively on board the vessel and quite a range of useful functions can be provided on board based on those data, it seems logical to have an on-board installation of the information management components which can be used as a connection point by the robotics data acquisition systems. At the same time, ship operators will want to have access to the same data on shore, and the known data about a particular vessel should always – at least eventually – be synchronised between these installations. This requires a reliable data communication path between on-board and on-shore components.

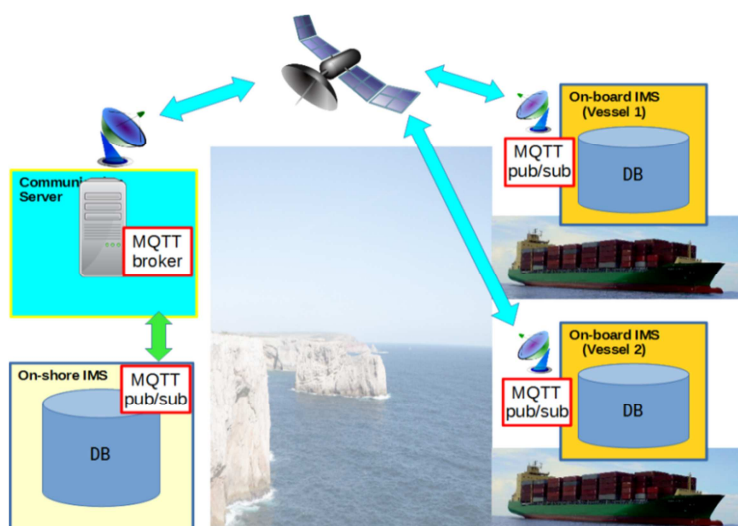


Fig 12: Reliable communication via MQTT messaging

Constraints for such a communication path are well known: while technology advances rapidly in terms of available ship-shore bandwidth and reliability, it will – for a foreseeable future – lag behind pure on-shore solutions in both these parameters, and this must be taken into account. For this application, a messaging sub-system based on the MQTT protocol has been put in place, what ensures a fault-tolerant and reliable operation, Fig. 12, *OASIS* (2014). By including an independently operating message broker, which supports guaranteed message delivery, data synchronisation can be accomplished via optimised combined message publisher/subscriber end points in the IMS installations.

7. Conclusions and Outlook

Due to the high cost of inspections of ship-board structures, given the recent advances in robotics and automation, better methods for these tasks seem feasible. However, the operating environment as well as the variety and complexity of the inspection processes pose a challenge. In this paper, we have discussed some developments that demonstrate how different platforms and approaches may be used and how they could operate effectively in combination and with support from appropriate software components. Results indicate that – at least for the foreseeable future – a well-tuned combination of different robotic tools may be a very promising solution. Another important aspect (just about to be fully realised) is the fact that automated data acquisition needs to be complemented by adequate post-processing and data management capabilities.

Remaining challenges that need to be addressed in the near future comprise the incorporation of further developments on industry standard data formats for inspection data transfer, as well as the development of enhanced software for embedded large volume data acquisition. Further assessment of the robotic platforms performance will also take place in the near future in order to identify limitations and ways of improvement in all hardware and software components.

Acknowledgements

Work described in this paper has been supported with funding from the 7th Framework Programme of the European Commission under Grant Agreement FP7- SST.2013.4-2, CP-605200 (INCASS - Inspection Capabilities for Enhanced Ship Safety). It reflects only the authors' views and the European Union is not liable for any use that may be made of the information contained therein. The authors also wish to thank the partners of the INCASS Project for their input and support.

References

- ARKIN, R. (1998), *Behavior-based Robotics*, MIT Press
- BIBULI, M. et al. (2012), *MARC: Magnetic autonomous robotic crawler development and exploitation in the MINOAS Project*, Int. Conf. Computer and IT Appl. Maritime Ind. (COMPIT), Liege, pp.62-75
- CHENG, G.; ZELINSKY, A. (2001), *Supervised autonomy: A framework for human-robot systems development*, Autonomous Robots 10/3, pp. 251-266
- DUDA, R.; HART, P.; STORK, D. (2000), *Pattern Classification*, Wiley-Interscience
- EICH, M; VOEGELE, T. (2011), *Design and control of a lightweight magnetic climbing robot for vessel inspection*, IEEE Mediterranean Conf. Control & Automation, pp.1200-1205
- FAWCETT, T. (2006), *An introduction to ROC analysis*, Pattern Recogn. Letters 27/8, pp.861-874
- GURDAN, D. et al (2007), *Energy-efficient autonomous four-rotor flying robot controlled at 1 kHz*, IEEE Int. Conf. Robotics & Automation, pp.361-366

HCM (2016), OpenHCM Consortium: Sourceforge repository, http://sourceforge.net/projects/open_hcmstandard/files/Schema_xsd_files_and_corresponding_descriptions/

IACS (2006), UR Z *Survey and Certification. Requirements concerning Survey and Certification*, Int. Association of Classification Societies, London, <http://www.iacs.org.uk>

IACS (2009), PR19 *Procedural Requirement for Thickness Measurements*, Int. Association of Classification Societies, London, <http://www.iacs.org.uk>

INCASS (2013), *Description of Work*, FP7-TRANSPORT-2013-MOVE-1; SST.2013.4-2. Inspection capabilities for enhanced ship safety (GA 605200)

ISO (2004), ISO 10303-218:2004: *Industrial automation systems and integration -- Product data representation and exchange -- Part 218: Application protocol: Ship structures*, Intl. Organization for Standardization, Geneva

ITTI, L.; KOCH, C.; NIEBUR, E. (1998), *A model of saliency-based visual attention for rapid scene analysis*, IEEE Trans. Pattern Analysis and Machine Intelligence 20/11, pp.1254-1259

JUNG, M.; SCHMIDT, D.; BERNS, K. (2010) *Behavior-based obstacle detection and avoidance system for the omnidirectional wall-climbing robot CROMSCI*, Emerging Trends in Mobile Robotics, pp.73-80

KOCH, T.; SMITH, M; TANNEBERGER, K. (2015), *Improving Machinery & Equipment Life Cycle Management Processes*, Int. Conf. Computer and IT Appl. Maritime Ind. (COMPIT), Ulrichshusen, pp.101-115

MINOAS (2009), *Description of Work*, FP7-SST-RTD-1; SST.2008.5.2.1. Marine INspection rObotic Assistant System (GA 233715)

OASIS (2014), BANKS, A.; GUPTA, R. (eds.), MQTT Version 3.1.1, OASIS Standard <http://docs.oasis-open.org/mqtt/mqtt/v3.1.1/os/mqtt-v3.1.1-os.html>

TACHE, F. et al. (2010); *MagneBike: Compact Magnetic Wheeled Robot for Power Plant Inspection*, Intl. Conf. Applied Robotics for the Power Industry, pp.1-2

THEODORIDIS, S.; KOUTROUMBAS, K. (2008), *Pattern Recognition*, Academic Press

ZHANG, L. et al. (2008), *SUN: A Bayesian framework for saliency using natural statistics*, J. Vision 8/7, pp.1-20

Underwater Robotics for Diver Operations Support: The CADDY Project

Marco Bibuli, CNR-ISSIA, Genoa/Italy, marco.bibuli@ge.issia.cnr.it

Gabriele Bruzzone, CNR-ISSIA, Genoa/Italy, gabriele.bruzzone@ge.issia.cnr.it

Davide Chiarella, CNR-ISSIA, Genoa/Italy, davide.chiarella@ilc.cnr.it

Massimo Caccia, CNR-ISSIA, Genoa/Italy, massimo.caccia@ge.issia.cnr.it

Angelo Odetti, CNR-ISSIA, Genoa/Italy, angelo.odetti@ge.issia.cnr.it

Andrea Ranieri, CNR-ISSIA, Genoa/Italy, ranieri@ge.issia.cnr.it

Eleonora Saggini, CNR-ISSIA, Genoa/Italy, eleonora.saggini@ge.issia.cnr.it

Enrica Zereik, CNR-ISSIA, Genoa/Italy, enrica.zereik@ge.issia.cnr.it

Abstract

This paper describes the EU project “CADDY – Cognitive Autonomous Diving Buddy” which aims at developing a cooperative autonomous underwater robotic system to improve monitoring, assistance, and safety of the diver’s operations. The paper presents key results related to the gesture recognition system, developed to enhance the interaction between diver and robot, and autonomous functionalities provided by the robotic framework to support the diver operations. Some experimental results obtained by field trials are also reported.

1. Introduction

Since January 2014 the FP7 CADDY project (<http://caddy-fp7.eu>) has been developed in order to pursue collaborative R&D work aimed at enhancing cognitive robotics in the underwater arena; specifically, to develop robots capable of cooperating with divers. The main motivation for the CADDY project was the fact that divers operate in harsh and poorly monitored environments in which the slightest unexpected disturbance, technical malfunction, or lack of attention can have catastrophic consequences. They manoeuvre in complex 3D environments and carry cumbersome equipment while performing their missions. To overcome these problems, CADDY aims to establish an innovative set-up between a diver and companion autonomous robots (underwater and surface) that exhibit cognitive behaviour through learning, interpreting, and adapting to the diver’s behaviour, physical state, and actions. A complete overview of the project is reported in Miskovic *et al.* (2015).

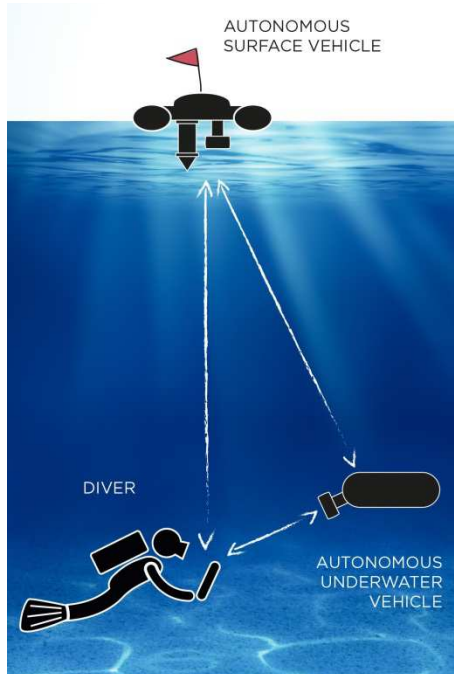


Fig. 1: CADDY concept: autonomous underwater and surface vehicle interacting with the diver

The main CADDY concept is shown in Fig. 1 where three components are illustrated: an autonomous surface vehicle, autonomous underwater vehicles, and the diver. The autonomous surface vehicle has the function of communicating with the diver and the autonomous underwater robot, as well as serving as a communication relay link to the command centre. It also plays the key role of navigation aid for the underwater agents – it must adapt its motion to optimize communication efficiency and navigational accuracy of agents. The autonomous underwater vehicle, on the other hand, manoeuvres in the proximity of the diver, and exhibits cognitive behaviour with regard to the diver actions by determining the diver's intentions and the state of the diver's body.

The CADDY project replaces a human buddy diver with an autonomous underwater vehicle and adds a new autonomous surface vehicle to improve monitoring, assistance, and safety of the diver's mission. The resulting system plays a threefold role similar to those that a human buddy diver should have: i) the buddy "observer" that continuously monitors the diver; ii) the buddy "slave" that is the diver's "extended hand" during underwater operations performing tasks such as "do a mosaic of that area", "take a photo of that" or "illuminate that"; and iii) the buddy "guide" that leads the diver through the underwater environment.

This envisioned threefold functionality will be realized through S&T objectives which are to be achieved within three core research themes: the "Seeing the Diver" research theme focuses on 3D reconstruction of the diver model (pose estimation and recognition of hand gestures) through remote and local sensing technologies, thus enabling behaviour interpretation; the "Understanding the Diver" theme focuses on adaptive interpretation of the model and physiological measurements of the diver in order to determine the state of the diver; while the "Diver-Robot Cooperation and Control" theme is the link that enables diver interaction with underwater vehicles with rich sensory-motor skills, focusing on cooperative control and optimal formation keeping with the diver as an integral part of the formation.

This paper presents an overview of the activities that have taken place during the first year of the project – the partners have made substantial progress in both technological as well as scientific objectives that were set in the project, including the following:

1. Development of a cooperative multi-component system capable of interacting with a diver in unpredictable situations and supporting cognitive reactivity to the non-deterministic actions in the underwater environment.
2. Establishing a robust and flexible underwater sensing network with reliable data distribution, and sensors capable of estimating the diver pose and hand gestures.
3. Achieving full understanding of the diver behaviour through interpretation of both conscious (symbolic hand gestures) and unconscious (pose, physiological indicators) nonverbal communication cues.
4. Defining and implementing cognitive guidance and control algorithms through cooperative formations and manoeuvres in order to ensure diver monitoring, uninterrupted mission progress, execution of compliant cognitive actions, and human-machine interaction.
5. Developing a cognitive mission (re)planner that relies on interpreted diver gestures that make more complex words.

2. Overall CADDY framework

The CADDY framework is realized through the integration of different modules in such a way to provide an innovative and advanced system for diver operations support. The framework comprises a set of heterogeneous robotic platforms that share a number of both hardware and software interface, so to improve the modularity and the interchange capability. The primary surface vehicle used in CADDY experiments is MEDUSAs, Fig. 2, a light, streamlined vehicle with 2 thrusters, 1035 mm long, and weighing 23-30 kg. The backup surface vehicle is PlaDyPos, Fig. 3, Nad *et al.* (2015), an omnidirectional autonomous vessel with 4 thrusters in X configuration 0.7 x 0.7 m, and weighing around 30 kg.



Fig. 2: MEDUSA robotic platform



Fig. 3: PlaDyPos robotic platform

In the underwater segment, the primary underwater vehicle is BUDDY, Fig. 4, an AUV built specially for CADDY purposes, *Stilinović et al. (2015)*. BUDDY is equipped with an underwater tablet as a means of interaction with the diver. In addition, it is equipped with a stereo camera, a monocular camera, and a multi-beam sonar that are all used for "seeing the diver". The backup underwater vehicles is R2 ROV, Fig. 5, a fully actuated underwater robotic platform with 4 horizontal and 4 vertical thrusters, 1.3 (length) x 0.9 (width) x 1.0 (height) m, rated up to a depth of 500 m.

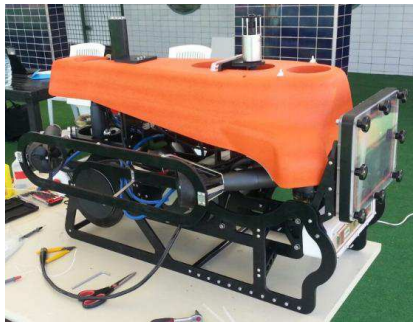


Fig. 4: BUDDY AUV robotic platform



Fig. 5: R2 ROV robotic platform

The third agent in the CADDY system is the diver. In order to allow interaction between robotic vehicles and the diver, a commercially available tablet enclosed in a waterproof housing and fully operational underwater, is used as an interface. The android application developed in CADDY that runs on the tablet shows the diver position in the underwater environment, and enables messaging with the surface while the diver is underwater.

To enable reliable underwater positioning and acoustic communication between CADDY components, novel miniature underwater modem and USBL devices have been developed within the project measuring 160 x 55 mm. In addition to highly reliable spread spectrum based communication, algorithms have been developed to simultaneously obtain accurate and repeatable positioning information from a USBL array transducer with element spacing of only 20mm, Fig. 3, *Neasham et al. (2015)*. The hardware platform is based on a powerful and flexible ARM processor device, providing a software upgrade path for higher data rates and improvements in positioning.

3. Gesture recognition

The gesture recognition module is based on the processing of images gathered by a stereo-camera system (based on the PointGrey BumbleBee XB3 device). A large amount of video data with divers wearing artificially marked gloves has been collected during CADDY experimental trials. The gloves shown in Fig. 6 were designed to provide easier and more reliable process of the automatic hand gesture recognition. The data recorded using a stereo camera covered a variety of gestures belonging to the specific language (CADDIAN) developed for the project, which is based on diver symbolic language. More than 40 commands/messages that allow diver-robot communication within the scope of CADDY project were defined. Stereo camera imagery was used to produce 3D point clouds, Fig. 7.



Fig. 6: Gesture execution during swimming pool trials. Marked gloves allow easier detection of diver gestures even under challenging light conditions and turbid waters.



Fig. 7: Resulting point clouds from stereo images collected. Diver contours are visible, but due to lack of texture on the wetsuit, most of the diver is not properly reconstructed in 3D.

As a first step towards gesture classification, hand detection algorithms suited for real-time computation were developed. Haar classifiers are used to detect possible locations of the hands in the monocular image. Then stereo imagery is used to compute a disparity map and to filter all possible clutter in the image by depth information. Under the assumption that the diver is the closest “object” to the camera, the background can be thresholded. The second hypothesis is that diver's hands are closer to the camera than the rest of the diver's body, Fig. 8. These assumptions are mainly used as heuristics to focus attention to particular parts of the image to enable fast processing.

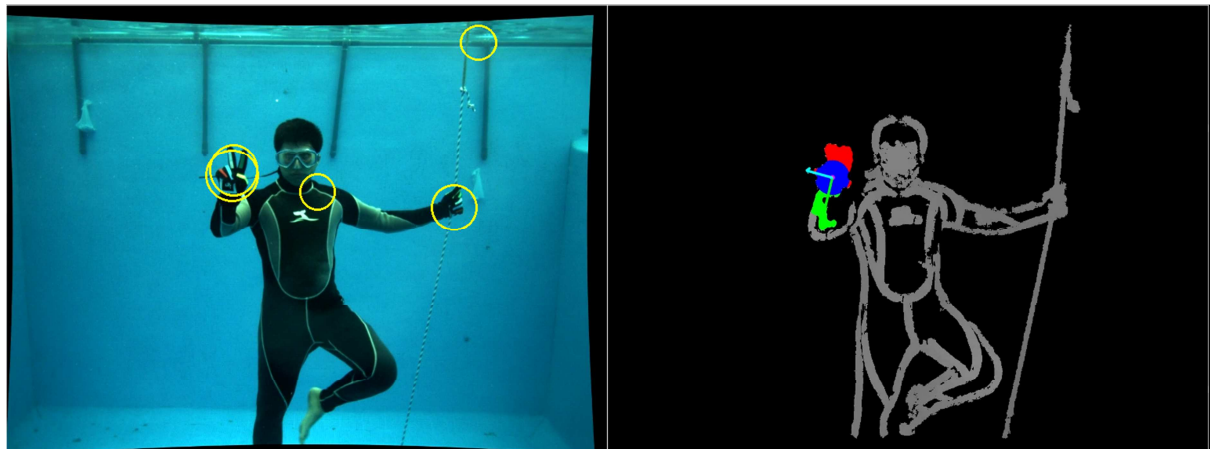


Fig. 8: (Left) Monocular image with the hand candidate patches output by the Haar classifier. (Right) Disparity image with the detected hand segmented.

The next step represents the novel image processing techniques that have been developed for hand gesture classification in the underwater environment. Due to camera noise and the fact that the disparity processing relies on image feature matching which is not always 100% accurate, the hand candidates are evaluated by a new variation of a Random forest classifier, namely a Multi-Descriptor Nearest Class Mean Random Forest (MD-NCMF). A large number of CADDY gestures have been successfully detected during validation trials; some are shown in Fig. 9.

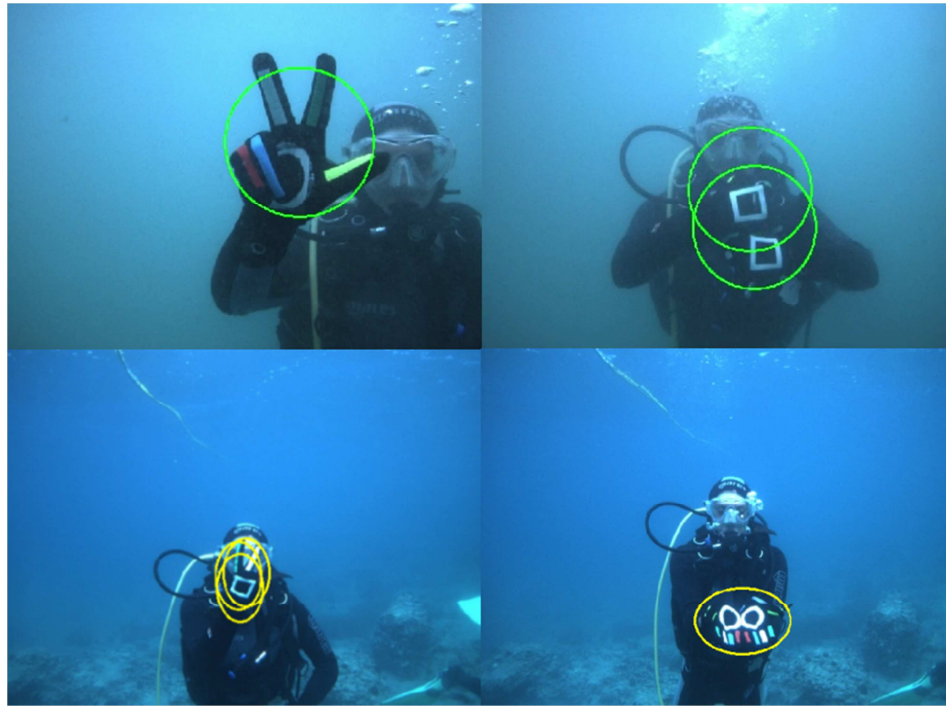


Fig. 9: Detected gestures (starting top left, then clockwise): take a photo, carry equipment, start communication, go to the boat.

4. Interpretation of gestures

CADDIAN language is based on diver symbolic gestures and it has been developed together with a precise syntax used to describe complex scenarios that are required in the scope of the CADDY project, Chiarella *et al.* (2015). The developed syntax has also been extended with CADDY "slang" that utilizes simple gestures defined by the diving community. In order to interpret and validate longer gesture sequences, a gesture sequence interpretation has been implemented through the realization of a parser, which accepts commands or messages belonging to CADDIAN language. Each message/command is a sequence of symbols/gestures delimited, at the beginning, by a symbol of "Start communication" and, at the end, by the same symbol or by a symbol of "End of communication", Fig. 10.

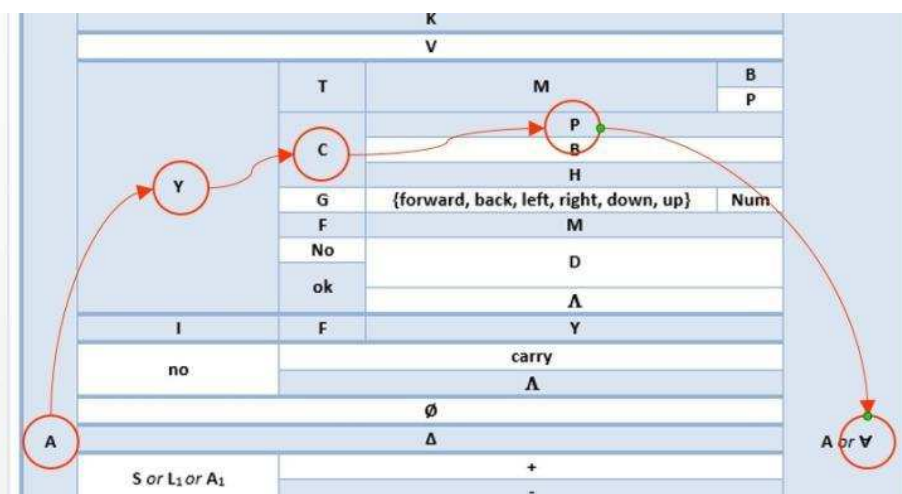


Fig. 10: "Table of possible sequences" - the table representation of the command "A Y C P √" ("Come to the point of interest"). After the "C" gesture only "P" or "B" or "H" can follow in a semantically correct message: and after them only "A" (i.e. a sequence of commands) or "√" (i.e. the sequence of commands/the message ends).

Fig. 11 shows the relation between performed gesture sequence and interpreted meaning by means of the developed module.

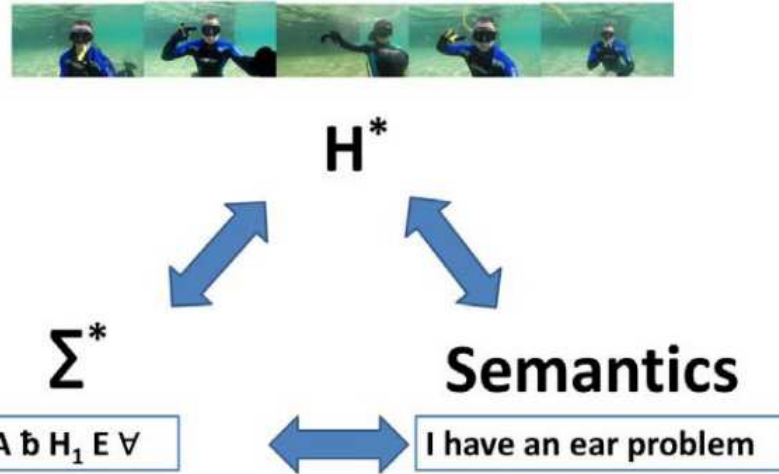


Fig. 11: Relation between performed gesture sequence and interpreted meaning

6. Robot's compliant reaction

On the basis of the issued command or request by the diver, the robot has to promptly react in order to fulfil the required actions. To achieve this goal, a reliable and efficient mission control architecture has been developed. Following consolidated approaches such as *Caccia et al. (2004)* and *Bibuli et al. (2008)*, already exploited and validate during at field campaigns, a Petri Net based specific mission controller has been developed to automatically execute the following operations:

- provide a high-level interface between primitives for diver support (e.g. follow me, guide me, take photo, etc.) and low level specific robotic tasks;
- select and activate the proper task needed to fulfil the required actions, keeping into account the specific robot capabilities and resolving the possible task conflicts;
- execute the selected tasks, setting the proper reference signals and complying with the safety constraints.

The aim of providing a compliant behaviour of the overall robotic system, with respect to the operations undertaken by the diver, is made available through the development of an automatic selection system for the execution of the proper autonomous robotic tasks.

First of all, the basic CADDY functionalities have to be mapped into subsets of tasks that can be provided by the robotic platforms. In order to define the primitives-tasks matching, an additional high-level task set has to be defined as cross-interface between the primitives and robotic task sets. A preliminary definition of the three sets is reported in Fig. 12, where:

- functional primitives represent the macro-actions that the robotic platform has to carry out in order to support the diver operation and that are strictly related to the current functional mode (slave, guide, observer);
- high-level logical tasks are the interface between the primitives and the operative task provided by robot. This logical task set is common in the overall architecture and will provide the required functionalities activating the proper low-level tasks that are currently made available by the employed robotic platform;
- low-level robotic tasks are the actual implemented autonomous functionalities on the target robot, e.g. speed regulators, heading and depth controller, etc. Depending on the low-level task availability, the CADDY compliant mission control system will properly select which

high-level functionalities can be activated allowing, in turn, the enabling of the required primitives to fulfil the mission operations.

Functionality primitives	High-level logical tasks	Low-level robot tasks
Stand (slave)	go_to_depth (depth z)	depth_control (z z_force)
Look at me (observer)	go_to_altitude (altitude z)	altitude_control (z z_force)
Follow me (slave)	turn_towards (orientation ψ)	heading_control (ψ torque)
Guide me (guide)	go_to_2D_point_fa (x, y u, v)	surge_control (u u_force)
Take photo (slave)	follow_path_fa (P, s u, v)	sway_control (v v_force)
Make mosaic (slave)	use_camera (_ mode)	camera_trigger (mode cam)
	use_light (_ i)	light_trigger (i lgh)

Fig. 12: Primitives and tasks definition

For the automatic selection, activation and inter-task conflict management, a Petri net based execution control system, inherited from the CNR-ISSIA robotic framework, is under current development. The system is configured by means of a set of configuration files that specify, on one side, the capabilities of the robot in terms of autonomous tasks and, on the other side, the set of high level functionalities that the CADDY system has to provide for the diver support. A real-time Petri net engine models the logical interconnections among the tasks and primitives and, depending on the specific actions commanded by the diver, automatically handle the activation/deactivation of the proper task sets.

As an example, Fig. 13 (left) reports the case of activation of the "Follow me" primitive; such a primitive requires the system to turn on the following functionalities: "go_to_depth" to reach and maintain a desired depth (i.e. the same of the diver); "go_to_2D_point_fa" is the procedure to track a 2D point (the diver position) for fully-actuated (fa) platforms, that generates proper horizontal velocities for point tracking; "turn_towards" enabling the auto-heading capability to always look towards the diver.

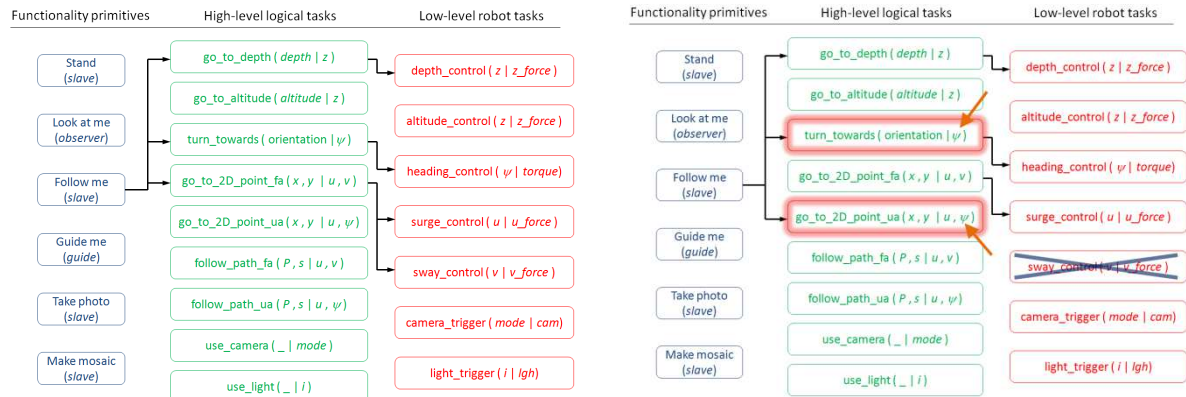


Fig. 13: Example of "follow me" primitive activation for fully-actuated robot (left) and for under-actuated robot (right) with inter-task conflict management

In turn, each of the high-level tasks has to be linked with one or more low-level tasks in order to physically execute the required actions:

- "go_to_depth" requires the activation of a depth_controller;
- "go_to_2D_point_fa" requires the activation of surge and sway velocity regulators;
- "turn_towards" enables the auto-heading controller.

The logical links between the high- and low-level layers are set on the basis of the input/output variables: the output generated by a high-level task is the input for one or more low-level tasks, e.g. "go_to_2D_point_fa" generates the u and v speed reference signals that feed the low-level speed controllers.

If, as a second exemplificative case, an under-actuated platform is employed, it implies in turn that the "sway_speed" controller is not available (due to under-actuation, e.g. of a rudder based vehicle). The unavailability of this latter low-level task reflects on the inhibition of the "go_to_2D_point_fa". Anyway to fulfil the "follow me" primitive requirements, the system can automatically switch to the "go_to_2D_point_ua" that can drive the robotic platform towards the desired point generating proper surge velocity and heading signals. The activation of the "go_to_2D_point_ua" task goes in conflict with the "turn_towards" one, given the generation of the ψ reference signals by both the tasks. Detecting this logical conflict, Fig. 13 (right), the system deactivates the execution of the "turn_towards" (that, by user definition, has a lower priority with respect to the "go_to_2D_point_ua" in relation to the "follow me" primitive).

7. Experimental results

Two experimental campaigns have been carried in 2015, one in Biograd Na Moru (Croatia) in October and a second one in Genoa (Italy) in November. Both the trials were focused on the validation of the interaction capabilities, mostly related to the gesture recognition and compliant robot reaction to the desired commands.

Divers performing the gestures are shown in the next images in different type of environments to emphasize the different challenges which need to be solved to output a correct classification. For example, the first image (Fig. 14) shows a diver facing the light source and a diver giving his back to it. This causes the colours to have less contrast and more attenuation, it can be seen that the red colour of the gloves in the right image is close to be black.



Fig. 14: Data collection and testing in Biograd Na Moru (left) and Genoa (right). This includes the teaching process of the CADDIAN language to the divers.

The second image (Fig. 15), shows how the diver can vary greatly his relative pose with respect to the camera; which in consequence causes the hand's pose and size to change. This happened during the Biograd Na Moru trials when the divers could not keep a static position due to the weather conditions that created strong waves in the sea.

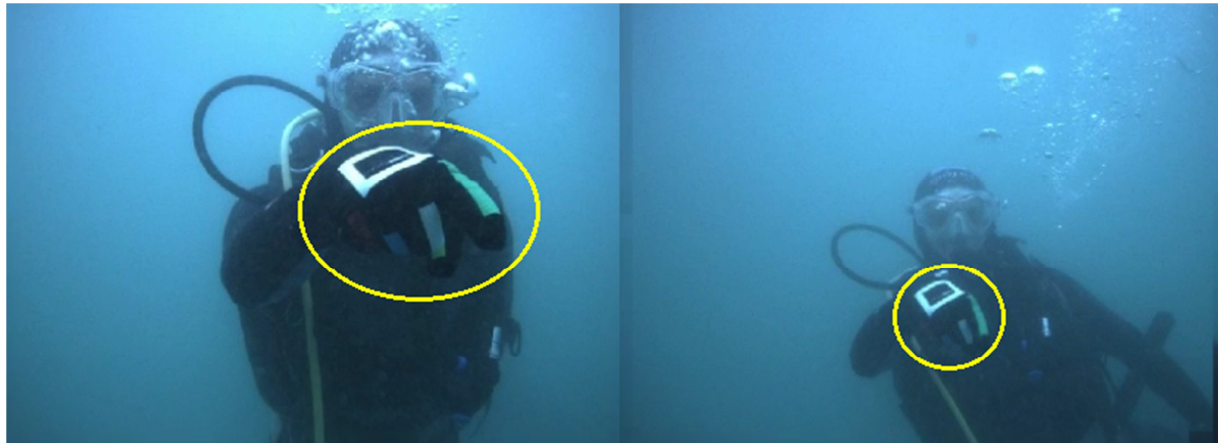


Fig. 15: Data collection and testing in Biograd Na Moru (left) and Genoa (right). This includes the teaching process of the CADDIAN language to the divers.

The third image (Fig. 16) shows also a difference of the diver's position regardless of the fact that the same gesture is performed. Furthermore, this also proves that the localization of the hands cannot totally depend on the localization of other parts of the body e.g. the head, which is commonly done in other standard RGB-D gesture recognition approaches. In this image, we can also see the difference in colour with respect to the previous ones: it seems to have a stronger blue component. This last image is from the Genoa trials, and the previous ones from Biograd Na Moru; the different types of water (salt/sweet), weather conditions and background imagery cause these changes in colour.

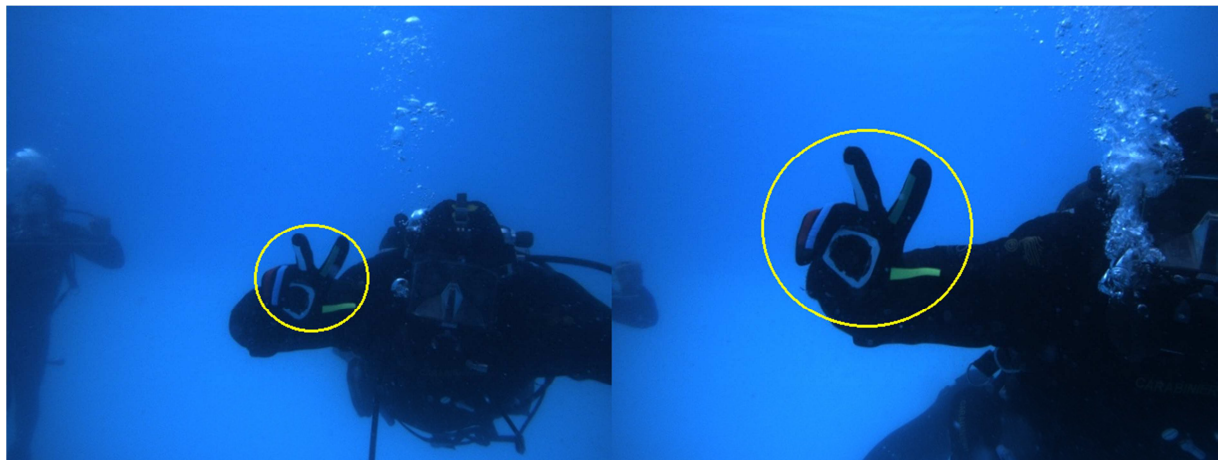


Fig. 16: Data collection and testing in Biograd Na Moru (left) and Genoa (right). This includes the teaching process of the CADDIAN language to the divers.

All of the previous proves that the classifier has to be robust against rotations, changes in illumination and different scales. It is difficult for one type of descriptor to be invariant to all these image changes: for this reason a multi-descriptor classifier was adopted as mentioned.

In a first stage, the target of the trial was the validation of single gesture recognition; a single gesture is a quick command used by the diver for communicating direct commands (as for instance “go up” or “move backward”) or physical situations (pain, cold, or any other emergency related to the diver feeling). Single gestures are used as a “slang” inside the wider CADDY language; being related to harmful situation of quick commands to be executed, they have to be reliably recognized and the corresponding actions have to be promptly carried out. In Fig. 17 an exemplificative set of the tested single gestures is reported.

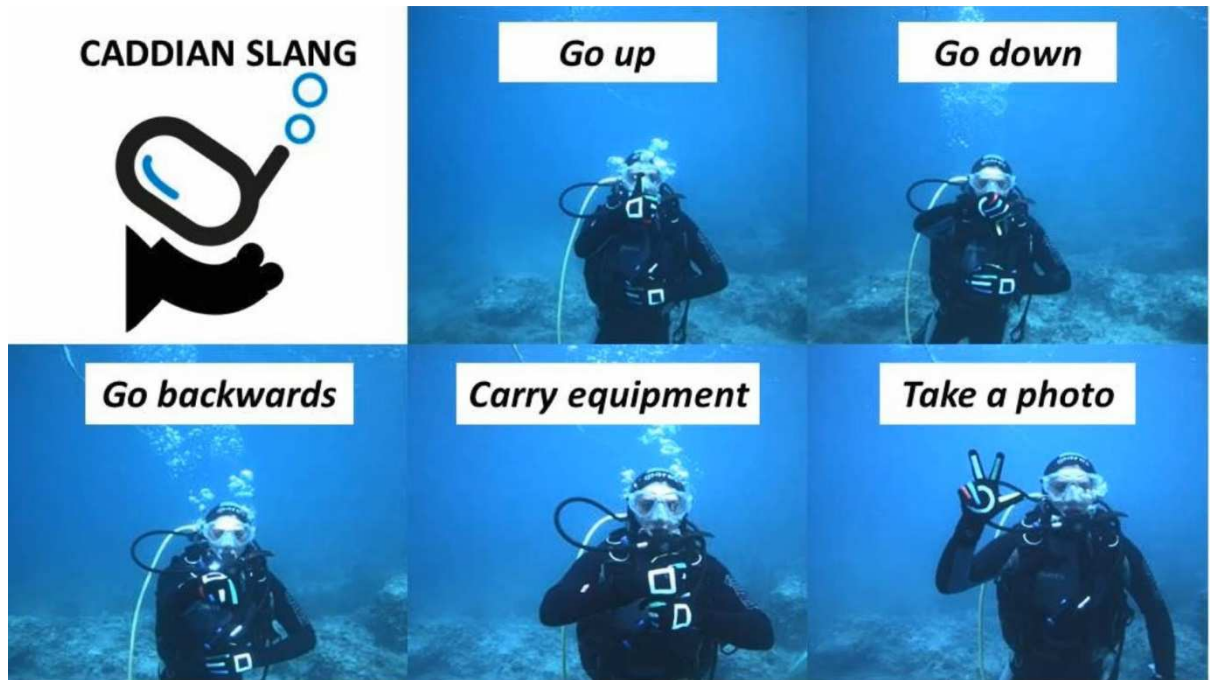


Fig. 17: CADDY slang gestures tested during 2015 validation trials

The system is able to promptly react to the gesture commands, recognizing in real-time (1-2 s) the issued hand signs and in turn executing the related actions. Fig. 18 shows the behaviour of the robot executing a “go up” command after successful gesture recognition and interpretation.



Fig. 18: Robot executing a “go up” command

Extensive tests were carried out during a second phase of the trial, focused on the complex gesture sequence recognition. Complex sequences are enriched set of gestures that represent dialogs or sentences containing more information that the robot has to recognize, separate and interpret in order to achieve the desired goal required by the diver. Example of complex sequences are “Go to boat and carry equipment here” or “Execute a mosaic of N x M meters”. Also for complex sequences, a number of tests were carried out in order to evaluate the reliability and success rate of the system, obtaining good results in terms of recognition capabilities. An example of a complex sequence executed by a diver is the “Go down 2 m” shown in Fig. 19.



Fig. 19: “Go down 2 m” gesture sequence executed during trials

8. Conclusions

At the current stage of development and with still one year until the end, the CADDY project has collected many successful results: the underwater robot is now able to detect and recognize different hand gestures performed by the diver; single or sequences of gestures are mapped into simple up to more complex actions that the robotic system has to execute to support the specific diver operation. The cooperative guidance executed by surface/underwater vehicles allows following or guiding the diver in the exploration of the underwater environment.

The achievement of such results requires strong efforts by all the partners involved that, during each project meeting and at-field integration & test phases, put their equipment and personnel into play, combined with their knowledge and invaluable experience.

The complete system integration and final validation trial will take place next October 2016 in Biograd Na Moru (Croatia) to demonstrate the feasibility and reliability of this cutting-edge project and sparking new ideas for a project follow-up in the direction of industrial and societal exploitation.

Acknowledgements

The research leading to these results has received funding from the European Union Seventh Framework Programme (FP7/2007-2013) under grant agreement n° 611373.

References

- MISKOVIC, N.; BIBULI, M.; BIRK, A.; CACCIA, M.; EGI, M.; GRAMMER, K.; MARRONI, A.; NEASHAM, J.; PASCOAL, A.; VASILJEVIC, A.; VUKIC, Z. (2015), *Overview of the fp7 project "CADDY - Cognitive Autonomous Diving Buddy"*, MTS/IEEE Oceans, Genoa
- CHIARELLA, D.; BIBULI, M.; BRUZZONE, G.; CACCIA, M.; RANIERI, A.; ZEREIK, E.; MARCONI, L.; CUTUGNO, P. (2015), *Gesture-based language for diver-robot underwater interaction*, MTS/IEEE Oceans, Genoa.
- CACCIA, M.; COLETTA, P.; BRUZZONE, G.; VERUGGIO, G. (2004), *Execution control of robotic tasks: a Petri net-based approach*, Control Engineering Practice 13/8, pp.959-971
- BIBULI, M.; BRUZZONE, G.; CACCIA, M. (2008), *Mission control for unmanned underwater vehicles: functional requirements and basic system design*, IFAC Navigation Guidance Control of Underwater Vehicles Conf., Killaloe
- NAD, D.; MISKOVIC, N.; MANDIC, F. (2015), *Navigation, guidance and control of an over-actuated marine surface vehicle*, Annual Reviews in Control 40, pp.172-181
- NEASHAM, J.A.; GOODFELLOW, G.; SHARPHOUSE, R. (2015), *Development of the "Seatrac" miniature acoustic modem and USBL positioning units for subsea robotics and diver applications*, MTS/IEEE Oceans, Genoa

A Holistic Framework for Security and Privacy Management in Cloud-Based Smart Ports

Leonard Heilig, University of Hamburg, Hamburg/Germany, leonard.heilig@uni-hamburg.de
Stefan Voß, University of Hamburg, Hamburg/Germany, stefan.voss@uni-hamburg.de

Abstract

The efficiency of seaports depends, to a great extent, on the cooperation of companies handling the flow of cargo between the sea- and landside. Real-time information exchange is essential for the coordination of activities and decision making in smart ports. In a big data era, emergent information technologies increasingly facilitate the collection of different types of business-critical data from different sources including sensors, mobile devices, and operating systems. However, a core problem is still the willingness to share information among competing and non-competing organizations. In this paper, we develop a framework for data security and privacy management in smart ports.

1. Introduction

After decades of streamlining port operations, ports still experience process and coordination problems due to a lack of information exchange and decision support. In particular ports with scarce space capacities are affected by increasing traffic and environmental problems. In general, these problems have immediate consequences on the competitiveness of seaports, e.g. Wiegmans *et al.* (2008). Since the 1980s, major ports have undergone several stages of digital transformation, also referred to as IT or information systems enabled business transformation, e.g. Venkatraman (1994), to cope with new business requirements, Heilig *et al.* (2016b). The primary focus of those digital transformations was on two main aspects: the information exchange between port actors to facilitate an improved hand-over of cargo based on Electronic Data Interchange (EDI) and the automation of activities in container terminals, where those aspects influence each other. Although these transformations established a foundation for streamlining port operations and achieving important competitive advantages, it is assumed that activities within sub-processes are performed autonomously by each involved port actor and that inter-organizational information are only required at certain “checkpoints” during the planning and operation of port processes (e.g. at the terminal gate to manage import and export cargo flows carried out by drayage truck companies). The use of advanced information technology (IT) and information systems enable the collection of masses of actual data about moving and non-moving objects, like vehicles and infrastructure, respectively. The integration of these various sources of contextual information enormously increases the visibility in port operations and related global supply chains. In today’s big data era, new methods further facilitate an efficient processing of this data in order to discover detailed, contextualized, and relevant insights into port operations, e.g. Chen *et al.* (2012). Moreover, the connectivity among embedded systems creates new forms of infrastructure control and location-based services (LBS) allow to use real-time personal and contextual information to assist port actors during operations. Altogether, those IT innovations shape port processes and trigger modernization of ports, Heilig *et al.* (2016b).

Due to their potential to support the enhancement of cargo flows and the reduction of environmental burdens, major ports established the concept of smart ports. In comparison to traditional third-generation ports, UN (2002), procedures in smart ports are able to flexibly respond to changing circumstances and to consider economic and ecologic impacts of actions by exploiting various integrated sources of information used to support (near) real-time decision analytics, Heilig *et al.* (2016b). The main aim is to increase efficiency, safety, and ecological sustainability by enhancing planning, coordination, and collaboration in ports. This implies that sub-processes cannot be performed autonomously by port actors anymore, but firstly need to take into account external information to perform activities in accordance with changing conditions and, secondly, to share information to frequently inform other involved actors. In practice we observe, however, that these two requirements lead to two main barriers to implementation, respectively: First, port actors need to transform their business

processes to benefit from those new opportunities. In this regard, the quality of information is a crucial factor for the acceptance. Second, the willingness to share information in an ecosystem constrained by a culture of limited cooperation and competition needs to be established to achieve the benefits of increased information sharing in seaports. IT security and privacy management thus plays an essential role for establishing the trust and preserving interests of stakeholders in establishing a central information system (i.e. platform) used to facilitate data gathering, integration, processing, exchange, and decision analytics in smart ports. Furthermore, a secure, integrated, and standardized central information platform represents a single window and thus builds a basis to cope with increasing reporting obligations and regulatory requirements of national single window (NSW) systems in ports, e.g. *Tsen (2011)*.

In this paper, we propose a consistent and holistic framework for security and privacy management in smart ports. We present a generic system architecture to explain the different levels and services for information processing in smart ports. The generic system architecture combines several concepts, like mobile cloud computing, internet of things, and LBS. Moreover, a prototype of the proposed system architecture is presented to emphasize the role of central information platforms in smart ports. Based on the generic system architecture, we identify security and privacy requirements in such environment by looking into literature surveys of related research areas. From the identified requirements, we derive common levels and domains of security and privacy management and link them to possible approaches from the literature. Therefore, the framework will help to implement smart port solutions and consider important aspects and methods on several levels. As such, it represents an essential basis for an increased trust and willingness to share information in smart ports.

2. Cloud-based Data Processing in Seaports

As an underlying concept, we apply the idea of mobile cloud computing (MCC) proposed by *Dinh et al. (2013)*. The main objective of MCC is to integrate cloud computing with mobile environments to overcome performance (battery life, storage, and bandwidth), environment (e.g. heterogeneous access, scalability, availability), and security issues (e.g. reliability and privacy). (For a detailed overview on the mobile cloud computing architecture, applications, and approaches, the reader is referred to *Dinh et al. (2013)* and *Fernando et al. (2013)*.) Besides mobile technologies, sensor and actuator networks as well as identification technologies play an essential role in smart ports as they allow to automatically identify and gather relevant information about movable and non-movable objects (like movable bridges, traffic lights, etc.), respectively. In *Heilig and Voß (2015)*, we propose a cloud-based service-oriented architecture (SOA) to integrate cloud, sensor and actuator networks, and identification technologies in the context of port operations. In this work, we abstract from technical details and extend the system architecture with mobile technologies in order to provide a generic system architecture used to identify the relevant areas for IT security and privacy management. In the end of this section, we present an implementation of this generic architecture in form of a mobile cloud platform prototype.

2.1. Architectural Setting

The proposed generic system consists of four main environments, Fig. 1. While component services are applied to movable and non-movable objects in the ports, the remaining services are hosted in an accessible, scalable, and on-demand cloud environment. In the following, we briefly explain the different types of services.

1) Component Services

An essential foundation for a smart port is the seamless integration of physical objects into IT systems in order to allow a contextual measurement and control, commonly referred to as internet of things (IoT). Moreover, data on physical objects, environmental aspects, and related supply chain operations might also be managed by third-party IT systems.

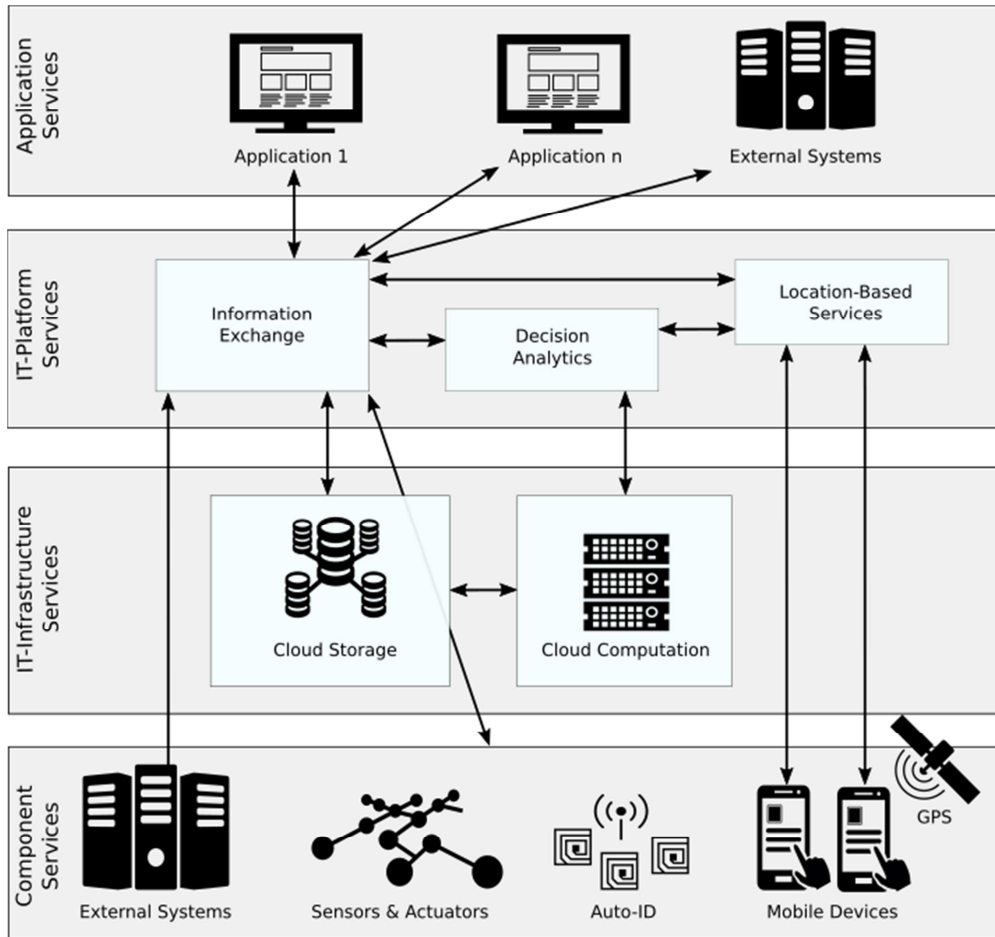


Fig. 1: Generic smart port system architecture

In the following, we briefly explain the main component services used in smart ports. Note that we provide a categorization and an extensive overview on IT systems and information systems in seaports in *Heilig and Voß (2016)*.

- Sensors and actuators: Devices measuring all kinds of contextual data of objects (e.g. position, temperature, noise, pollution, etc.) and allowing to act upon an environment or object. Wireless sensor networks (WSN) are used, for example, to monitor large areas of interest. The capabilities of related devices range from basic sensing and actuator functionality to powerful processing and storage capacities.
- Auto-ID: Enables an automatic identification of objects. Radio-frequency identification (RFID) is already used in supply chains and seaports for supporting several activities, for example, to allow identifying and securing containers (e.g. RFID-based electronic seals).
- Mobile devices: Equipped with a rich set of embedded sensors, communication capabilities, and a human interface, mobile devices allow a contextual measurement and interaction with the owner. Consequently, the ubiquitous use of mobile devices offers many opportunities in the logistics sector and specifically in smart ports.
- External systems: Facilitates the integration of (real-time) information provided by other third-party information systems (e.g. weather and traffic services, port community systems). This might also include information of other ports.

2) IT-Infrastructure Services

The proposed system architecture uses on-demand computing resources of a cloud. This can be either a private cloud exclusively used by the port community or a public cloud. If a public cloud is used, we have to consider that some management tasks regarding data security and privacy management are

outsourced to a third-party cloud provider. Basically, a cloud provides flexible access to virtualized computing services, e.g. in form of virtual machines (VMs) and storage capacities. The scalability of cloud systems enables an adjustment of the IT infrastructure according to the current demand. In public clouds, costs are normally calculated on the actual usage of services and thus involve operational expenses (OpEx) rather than capital expenses (CapEx). For an extensive overview on cloud computing and related research topics, the reader is referred to *Armbrust et al. (2010)* and *Heilig and Voß (2014)*.

3) IT-Platform Services

The platform services build the core of the system architecture and contain functionality to improve the communication, coordination, performance, and visibility in smart ports. The logic for providing information services to the users is implemented with three main components.

- Information exchange: Integrates the component services and application services and implements functionality to store, access, and exchange data in real-time. Moreover, it coordinates the access to the decision analytics services and LBS.
- Decision analytics: Encompasses different decision support functionality for supporting both planning and operations, including optimization modules (e.g. route planning) and predictive analytics modules to make predictions about future events (e.g. travel times, transport demands). The different modules might interact with each other.
- LBS: Integrates the location or position of a mobile device with other information in order to provide added value to a user, *Spiekermann (2004)*. Therefore, LBS components interact with information exchange and decision analytics components in order to offer individual information and decision support services, respectively.

4) Application Services

The application services implement different interfaces to access the functionality of the cloud-based information platform. This includes dedicated software applications, implemented as software as a service (SaaS) application, such as order and fleet management services, as well as application programming interfaces (APIs) to manage the access and information exchange with external systems. These external systems are operated by stakeholders (e.g. port/supply chain actors) that may use the cloud-based information platform to improve their own business processes. Depending on the business model, the users might be charged for using the application services. In this regard, the pricing model can range from hourly on-demand pricing to monthly subscription-based pricing.

2.2. Prototype

A prototype of the proposed generic system architecture, referred to as port-IO, has been implemented in previous studies, *Heilig et al. (2016a)*. The mobile cloud platform allows the coordination of truck movements within the port area based on the current positions of trucks and traffic situation. Transport orders can also be outsourced to subcontractors with free capacities in the port area, if considered as economically reasonable. Truck drivers with smartphones are able to receive order information and are assisted in accessing the port area. The mobile cloud platform contains all functionality to enable real-time information exchange and planning. For the latter, it implements different methods to optimize the related inter-terminal truck routing problem (ITTRP), aiming to reduce the transport costs while reducing empty trips. By coordinating transports, the number of empty trips can be reduced considerably. Consequently, port-IO is an example of a smart port application used to trigger the digital transformation in seaports in order to enhance port operational excellence and quality of service.

For the implementation of the platform services, we use the Google App Engine (GAE), <https://cloud.google.com/appengine/>, which is the platform as a service (PaaS) provided by the Google Cloud Platform. Therefore, the underlying IT infrastructure services are completely managed by the cloud provider. As the platform services are implemented following a modular design, means to horizontally scale components can be applied. Moreover, we use a distributed memcache to accelerate data access for the optimization component. The implemented platform services facilitate both the information exchange and coordination in port operations. To implement the component layer, we develop an Android mobile application and further integrate the Google Maps API. The latter serves as an external system providing forecasts on travel times, route information, and maps. The mobile application contains received transport orders, routing information, and messenger functionality. An application service in form of a web-based SaaS application can be used for managing operations in the port. Besides basic functionality, it includes components for fleet management, order management, and route planning. Fig. 2 shows main parts of the mobile cloud platform.

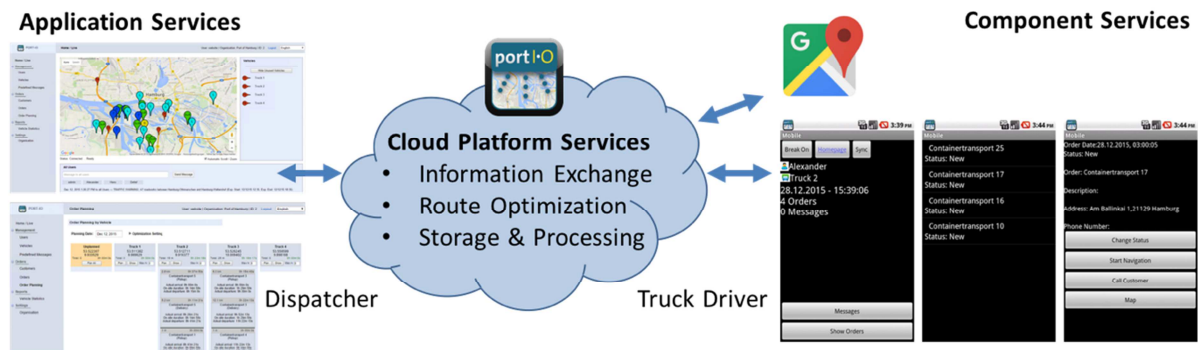


Fig. 2: Implementation of the generic system architecture in port-Io

3. The holistic security and privacy management framework

The proposed centralized cloud-based information platform for smart ports involves several technologies and systems that are affiliated with different streams of research including, but not limited to, research topics related to IT governance, cloud computing, MCC, IoT, physical devices (e.g. RFID, WSN), and LBS. As security and privacy play an essential role in related environments, a significant amount of research has been undertaken to address individual security and privacy requirements of novel IT innovations and applications. To combine the complementary technologies and systems as proposed in our system architecture, however, a holistic view on security and privacy aspects becomes essential for an efficient management of the related information platform. Based on an extensive review of well-recognized survey papers from related research streams, we collect important security and privacy requirements and some approaches how to address them. By this, we can identify numerous overlaps and develop a holistic framework covering major security and privacy aspects of the proposed system architecture, aimed at supporting the concept of smart ports.

3.1. Related literature surveys

In this subsection we summarize the reviewed literature surveys related to security and privacy in RFID, WSN, IoT, cloud computing (CC), MCC, and LBS. Table I gives an overview on possible threats and countermeasures.

The overview of literature surveys indicates that several threats and countermeasures overlap or influence each other. Therefore, a consistent and holistic security and privacy management becomes essential for avoiding losing control and to build up trust in information services provided in a smart port.

Table I: Literature surveys

Source	Area	Possible Threats	Possible Countermeasures
<i>Juels (2006)</i> <i>Rieback (2006)</i>	RFID	<ul style="list-style-type: none"> • Unauthorized tracking and inventorying • Tampering of tags (e.g. spoofing) • Counterfeiting attacks (e.g. tag cloning) • Eavesdropping (e.g. sniffing) • Replay attacks • Denial of service 	<ul style="list-style-type: none"> • Privacy protection mechanisms • Authentication mechanisms • Integrity mechanisms (e.g. digital signing tag data) • Cryptographic schemes (e.g. minimalist cryptography, data encryption) • Renaming of tag identifiers • Detection mechanisms • Temporary deactivation
<i>Wang et al. (2006)</i>	WSN	<ul style="list-style-type: none"> • Transmission disruption (e.g. jamming) • Tampering of nodes • Denial of service • Communication attacks (e.g. collisions) • Network attacks (e.g. spoofed, altered, or replayed routing information) 	<ul style="list-style-type: none"> • Tamper-proofing mechanisms • Authentication mechanisms • Monitoring • Cryptographic schemes • Intrusion detection and prevention • Access control mechanisms
<i>Weber (2010)</i> <i>Roman et al. (2013)</i>	IoT	<ul style="list-style-type: none"> • Physical damage of nodes • Tampering of nodes • Denial of service • Eavesdropping • Unauthorized controlling of nodes 	<ul style="list-style-type: none"> • Protocol and network security • Authentication and identity management • Privacy protection mechanisms • Fault tolerance mechanisms • Intrusion detection and prevention
<i>Takabi et al. (2010)</i> <i>Subashini and Kavitha (2011)</i> <i>Zisis and Lekkas (2012)</i>	CC	<ul style="list-style-type: none"> • Cross-site scripting • Data / privacy breaches • Distributed denial of service • Impersonation • Eavesdropping 	<ul style="list-style-type: none"> • Authentication and identity management • Certificate-based authorization • Access control mechanisms (e.g. role-based access control) • Cryptographic schemes • Monitoring • Policy-evolution management • Audit management • Risk management • Cyber insurance • Organizational security management • Fault tolerance mechanisms • Intrusion detection and prevention
<i>Khan et al. (2012)</i>	MCC	<ul style="list-style-type: none"> • Data breaches • Impersonation • Man-in-the-middle attacks • Use of a mobile device by a non-legitimate person • Eavesdropping • Identify, location, and status privacy breaches • Application tampering 	<ul style="list-style-type: none"> • Authentication and identity management • Access control • Cryptographic schemes • Anti-tamper mechanisms • Mobile-masquerader detection (e.g. behavioural authentication) • Data masking / obfuscation

<i>Duckham and Kulik (2006)</i> <i>Krumm (2009)</i>	LBS	<ul style="list-style-type: none"> • Identify, location, and status privacy breaches (e.g. tracking of users) • Disclosure of intrusive inferences / sensitive information (e.g. personal information, confidential business information) • Data disclosure to third parties • Location-based spam (e.g. unsolicited product marketing) 	<ul style="list-style-type: none"> • Data-centric access control / location privacy data specifications • Policy verification • Spatial and temporal cloaking schemes (e.g. <i>K</i>-anonymity) • Pseudonym generation mechanisms • Need-to-know principle / data obfuscation (e.g. data quality degradation, proximity- or region-based visibility mechanisms)
--	------------	---	--

3.2. Framework levels and domains

As a result of an extensive requirements analysis, we present a holistic framework that consists of three main levels: governance level, platform level, and physical level, Fig. 3. In the following, we briefly describe the role of each level and give more details about associated management domains.

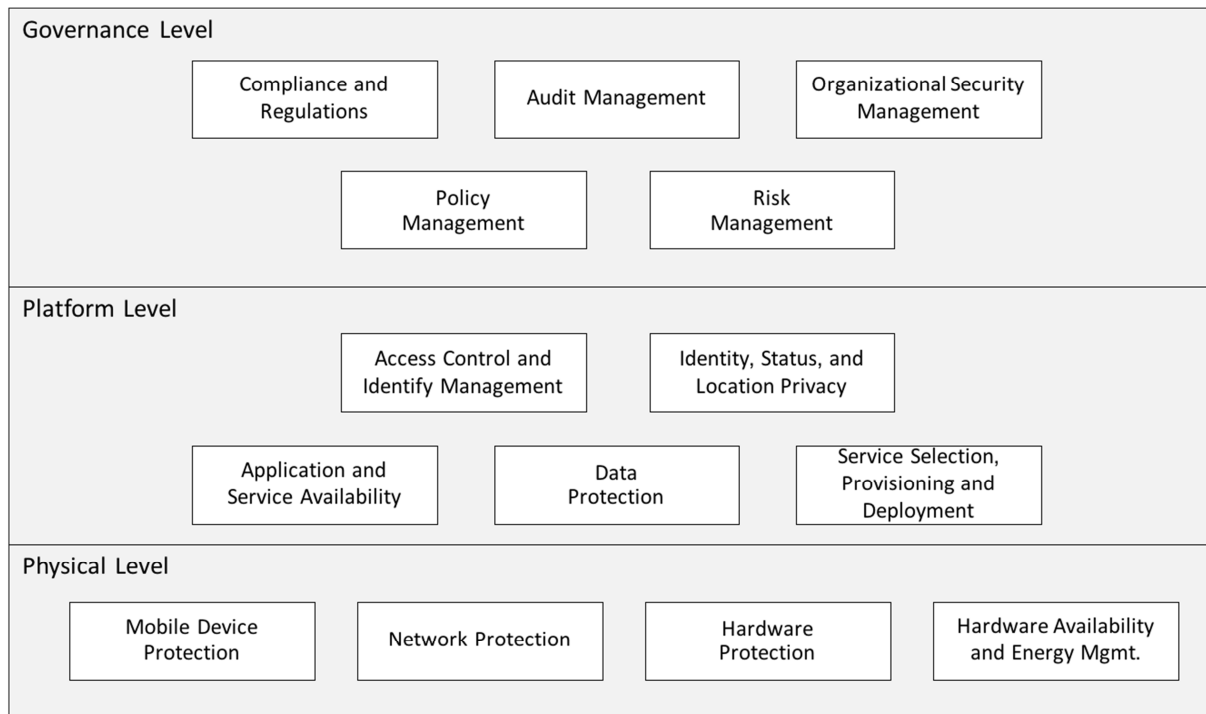


Fig. 3: Framework for security and privacy management in smart ports

3.2.1. Governance Level

The governance level defines policies, processes, and organizational structures taking into account risks, regulatory, and legal requirements. It further includes activities for ensuring that audit directives are implemented efficiently and thus controls the implementation of security and privacy measures. Focusing on information security and privacy management, it is a part of the overall information governance. As such, it builds an essential prerequisite for the proper implementation of security and privacy management. In a broader perspective, it assures that the use of IT is aligned with corporate objectives (including stakeholder interests) in order to gain business value.

- **Compliance and Regulations**
Involves management processes for creating and improving transparency, accountability, and control over compliance with corporate and external policies, procedures, laws, and regula-

tions. For deriving related requirements and regulations to be implemented in port processes, all important stakeholders need to be involved. Internal and external audits assess the implementation of requirements.

- Audit Management
Defines and organizes internal and external audit processes. In particular, in cloud environments, related management processes assure that cloud providers meet the corporates' and legal requirements by evaluating and testing the implemented processes and techniques.
- Organizational Security Management
Existing security and privacy management life-cycle models change through the adoption of cloud computing, *Takabi et al. (2010)*, as the responsibility for implementing requirements is shared among the platform service provider and the cloud provider(s). The distribution of different devices and embedded systems furthermore require metrics and measures to monitor and control the security and risks in those environments, for instance, in a port control centre. In this regard, the proposed centralized approach will help to collect and aggregate measurement data from both cloud resources and integrated devices and systems. Nevertheless, the development of standards and a re-evaluation of best practices is necessary, *Takabi et al. (2010)*, as well as the definition of roles, responsibilities, decision rights, and accountability in a shared environment.
- Policy Management
Regarding the variety of general and specific security and privacy requirements (see Table I), policy management processes ensure consistency between internal policies and regulatory requirements. Moreover, it controls the policy evolution and makes sure that current requirements are considered. This further involves the definition of corporate standards, for example, regarding the use of cryptographic standards that may change over time (e.g. when broken). Therefore, it is necessary to keep track of the implementation of policies in the overall environment.
- Risk Management
Identifies, evaluates, and controls security risks resulting from the implementation of IT systems. This includes an assessment of the impact of security and privacy breaches, for instance, in terms of user satisfaction and financial losses. In this regard, cyber insurance coverage can be used to hedge against the risk of damage or loss of digital assets, e.g. *Takabi et al. (2010)*.

3.2.2. Platform Level

The platform level involves concrete implementation of measures to manage the security and privacy in centralized information systems (*i.e.*, platforms) comprising several IT hardware and software systems. In the proposed system architecture, these systems are hosted in a virtualized cloud environment.

- Access Control and Identity Management
The heterogeneity of devices and services require fine-grained access control policies that capture dynamic, context, or attribute- or credential-based access requirements, *Takabi et al. (2011)*. In port environments, access control services must support efficient information sharing between port actors according to the principle of least privilege. The latter could mean, for instance, that drayage trucking subcontractor companies obtain only temporal admission to services and receive information according to the need-to-know principle. Secure and consistent authentication mechanisms must be implemented in all service layers to prevent attacks like data breaches, impersonation, and unauthorized control over actuators. In the context of mobile cloud computing, several schemes for controlling and securing the access to

shared data have been proposed, e.g. *Khan (2012)*. To support port operations, it must be further differentiated between data sharing in coalitions and general purpose data aggregation. While the former supports efficient information sharing between companies involved in common port or supply chain processes, the latter intends to increase the overall visibility and efficiency in port environments. Consequently, access control for further processing of granular data becomes increasingly important. Given access control policies, a secure and consistent identity management system must be implemented supporting the authentication of users and objects (e.g. RFID tags, sensor nodes) based on credentials and characteristics, e.g. *Bertino et al. (2009)*.

- Identity, Status, and Location Privacy

Due to specific security and privacy concerns, the application of LBS must be considered separately. The transmission and storage of identity and contextual information of users (e.g. status, location) as well as the access to this information must comply with users' privacy requirements and need to be protected against fraudulent use. In particular, data-centric sharing policies and obfuscation mechanisms have been proposed in the literature. While the former involves the development of standards for attaching usage rights to contextual information (e.g. "GeoPriv", *Peterson (2005)*), the latter consists of several methods to limit the visibility or to degrade the quality of contextual information by applying mechanisms for increasing its inaccuracy, imprecision, and vagueness, e.g. *Snekkenes (2001)*; *Duckham and Kulik (2005)*. However, the degree of degradation has an effect on the quality of LBS. Another option is to geographically limit the visibility of location-based information. The transmission of contextual information could be limited to certain areas (e.g. based on port boundaries) or dependent on the proximity of the user to other authorized parties, e.g. *Duckham and Kulik (2006)*, *Beresford and Stajano (2003)*. For example, the location of drayage trucks may only be visible within the port area for the port authority. Given specific access control policies, this visibility might be further limited for other port actors according to the need-to-know principle. Moreover, pseudonym generation mechanisms could be applied to protect the identity of users and companies as long as it is not important for an efficient collaboration between companies. For example, analysing traffic and emissions in the port area based on location and sensor information of trucks generally does not require the collection of identities.

- Application and Service Availability

The availability of business-critical applications and services need to be guaranteed continuously to ensure seamless and efficient business operations. Application testing and monitoring is essential to detect faults and outages. Scaling capabilities of cloud systems enable a flexible adjustment of the underlying IT infrastructure according to application and service loads. Updates are managed and implemented centrally so that users always use the latest version of the application.

- Data Protection

Data protection mechanisms, protecting the integrity, confidentiality, and availability of data, are an important pillar for establishing trust in information platforms. Therefore, data storage and transmission need to be protected against unauthorized usage, modifications, and disclosures. In the proposed system architecture, data is physically stored and exchanged in distributed component services and central IT infrastructure services. While data is collected for further processing and future usage in the cloud platform, the storage of data in component services can be temporary (e.g. sensor measurements) and persistent (e.g. RFID tags). Cryptographic mechanisms need to be applied in both environments to prevent data breaches and leakages. For energy-constrained devices, several energy-efficient approaches have been presented in the literature, for instance, involving a trusted third party to offload processing of encryption, decryption, and authentication operations, e.g. *Yang et al. (2011)*, *Hsueh et al. (2011)*, *Zhou and Huang (2012)*. Using public clouds, data is stored outside the enterprise boundaries. Therefore, it must be assured that strong encryption techniques and fine-grained

authorization to control access to data are implemented at the cloud provider's site, *Subashini and Kavitha (2011)*. Data owners should have the possibility to track changes and accesses on data records, *Takabi et al. (2010)*. Moreover, the cloud provider needs to ensure that data is regularly backed up to facilitate recovery in case of failures and disasters, *Subashini and Kavitha (2011)*.

- Service Selection, Provisioning, and Deployment

Cloud computing allows the on-demand selection and scaling of computing resources according to actual computational demands. Scaling allows increasing the reliability and availability of services and applications by flexibly allocating redundancy. On the other hand, the selection of third-party cloud resources must comply with security and privacy requirements. The geographical location, for example, has an impact on data protection regulations. Risk and financial aspects have to be considered when selecting cloud providers. The selection and provisioning of computing resources must satisfy all user, application, and compliance requirements.

3.2.3. Physical Level

The physical level contains all physical devices and embedded systems that are attached to movable and non-movable real-world objects (i.e. “things”, people) and establish a communication link to send and retrieve information to and from other systems, respectively. In the proposed generic system architecture, we refer to them as component services. Consequently, the physical level involves all activities to manage security and privacy aspects in those systems.

- Mobile Device Protection

Mobile devices, such as smartphones or tablets, may contain sensitive information and provide access to unauthorized users when not protected sufficiently. Therefore, it is important to define policies and preventive measures against unauthorized mobile device use, such as appropriate authentication mechanisms (e.g. biometric authentication) and means to remotely delete data if the device is stolen or lost. Another possible approach is referred to as mobile-masquerader detection. That is, classification methods are used to detect an impersonation by analysing mobile user behaviour, e.g. *Mazhelis (2006)*.

- Hardware Protection

Deployed hardware devices and systems need to be protected against physical damage and tampering. For a large number of hardware, this can only be assured by implementing automatic techniques for detecting intrusions and damages. Intrusion detection mechanisms and rules, e.g. making use of data mining methods, can be applied to detect outliers and intrusion attempts, *Roman et al. (2013)*. Moreover, existing container inspection technologies, such as OCR (Optical Character Recognition), could be used to record the physical conditions of devices attached to movable objects. In general, the physical access to hardware systems should be constrained, which is normally the case in dedicated port areas. Moreover, the quality of hardware systems has an impact on the durability, reliability of measurements, and other important aspects, resulting in a trade-off between costs and quality of service.

- Network Protection

Heterogeneous and interconnected network environments need to be protected against several types of attacks with an impact on availability, integrity, and confidentiality. It is important to use state-of-the-art routing protocols and cryptography approaches that adequately fulfil the security and privacy requirements. As the transmission of data in networks of devices with scarce energy resources accounts for a large part of the energy consumption, it is further advisable to apply secure data aggregation protocols, *Wang et al. (2006)*. Supplementary to the monitoring of hardware systems, intrusion detection systems may help to identify anomalies and deviations, including injected false information by compromised hardware systems.

Nowadays, major public cloud providers allow to establish a virtual private network (VPN) in order to securely connect geographically separated IT infrastructures as well as mobile devices (referred to as mobile VPN).

- **Hardware Availability and Energy Management**

To monitor the availability of resource-constrained devices (e.g. sensors), often densely deployed in harsh environments, their status needs to be constantly checked with periodic and energy-efficient heartbeat signals. As some devices rely on battery power, means to reduce and monitor energy consumption needs to be implemented. For critical systems where failures have severe safety or economic consequences, fault tolerance mechanisms must be implemented in order to increase the reliability of systems. This applies in particular to actuators that automatically control movable and non-movable equipment.

4. Conclusion and Outlook

Current projects and initiatives in major seaports emphasize the essential role of smart ports for improving port operations. The main prerequisite for smart ports is an efficient utilization of available sources of information. As this rises security and privacy concerns of involved port actors, security and privacy management becomes increasingly important for promoting the willingness of sharing information.

We have presented a holistic framework for security and privacy management in smart ports. The framework is linked to a generic system architecture enabling the integration of physical objects, mobile devices, and external IT systems with a scalable cloud environment supporting information exchange and decision analytics in smart port environments. The mobile cloud platform prototype port-IO has been presented to demonstrate the idea of the proposed system architecture in a real smart port environment. Given this foundation, main security and privacy requirements are considered on different levels and domains of the proposed framework. As such, the framework on the one hand represents a guideline for practitioners aiming to implement a smart port information platform. On the other hand, it gives an overview of related research approaches and implemented standards and methods.

The framework provides a basis for developing a comprehensive criteria catalogue used to evaluate compliance of smart port information platforms. For further research, the development of the framework can be extended by creating a maturity level model. This might help to identify security and privacy lacks and could be used to prioritize projects. Moreover, a maturity model could further help external parties, e.g. cyber insurance companies, in evaluating the risks in smart port information platforms. To improve the identity, status, and location privacy in port-IO, we aim to apply and evaluate security and privacy measures in future versions of the mobile cloud computing platform.

References

ARMBRUST, M.; FOX, A.; GRIFFITH, R.; JOSEPH, A.D.; KATZ, R.; KONWINSKI, A.; LEE, G.; PATTERSON, D.; RABKIN, A.; STOICA, I.; ZAHARIA, M. (2010), *A view of cloud computing*, Communications of the ACM 53/4, pp.50-58

BERESFORD, A.R.; STAJANO, F. (2003), *Location privacy in pervasive computing*, IEEE Pervasive Computing 2/1, pp.46-55

BERTINO, E.; PACI, F.; FERRINI, R. (2009), *Privacy-preserving digital identity management for cloud computing*, IEEE Computer Society Data Engineering Bulletin, pp.1-4

CHEN, H.; CHIANG, R.H.; STOREY, V.C. (2012), *Business intelligence and analytics: From big data to big impact*, MIS Quarterly 36/4, pp.1165-1188

DINH, H.T.; LEE, C.; NIYATO, D.; WANG, P. (2013), *A survey of mobile cloud computing: architecture, applications, and approaches*, Wireless Communications and Mobile Computing 13/18, pp.1587-1611

DUCKHAM, M.; KULIK, L. (2006), *Location privacy and location-aware computing*, Dynamic and Mobile GIS: Investigating Change in Space and Time, CRC Press, pp.35-51

FERNANDO, N.; LOKE, S.W.; RAHAYU, W. (2013), *Mobile cloud computing: A survey*, Future Generation Computer Systems 29/1, pp.84-106

HEILIG, L.; LALLA-RUIZ, E.; VOSS, S. (2016a), *port-IO: A mobile cloud platform supporting context-aware inter-terminal truck routing*, 24th European Conf. Information Systems (ECIS), Istanbul

HEILIG, L.; SCHWARZE, S.; VOSS, S. (2016b), *An analysis of digital transformation in the history and future of modern ports*, Working Paper, Institute of Information Systems, University of Hamburg

HEILIG, L.; VOSS, S. (2014), *A scientometric analysis of cloud computing literature*, IEEE Trans. Cloud Computing 2/3, pp.266-278

HEILIG, L.; VOSS, S. (2015), *A cloud-based SOA for enhancing exchange and decision support in ITT operations*, Computational Logistics, Lecture Notes in Computer Science 8760, Springer, pp.112-131

HEILIG, L.; VOSS, S. (2016), *Information systems in seaports: A categorization and overview*, Working Paper, Institute of Information Systems, University of Hamburg

HSUEH, S.C.; LIN, J.Y.; LIN, M.Y. (2011), *Secure cloud storage for conventional data archive of smart phones*, 15th Int. Symp. Consumer Electronics (ISCE), Singapore

JUELS, A. (2006). *RFID security and privacy: a research survey*, IEEE J. Selected Areas in Communications 24/2, pp.381-394

KHAN, A.N.; MAT KIAH, M.L.; KHAN, S.U.; MADANI, S.A. (2013), *Towards secure mobile cloud computing: A survey*, Future Generation Computer Systems 29/5, pp.1278-1299

KRUMM, J. (2009), *A survey of computational location privacy*, Personal and Ubiquitous Computing 13/6, pp.391-399

MAZHELIS, O. (2006), *One-class classifiers: a review and analysis of suitability in the context of mobile-masquerader detection*, South African Computer J. 36, pp.39-48

PETERSON, J. (2005), *A presence-based GEOPRIV location object format*, Technical Report, Internet Engineering Task Force (IETF), <http://tools.ietf.org/html/rfc4119>

RIEBACK, M.R.; CRISPO, B.; TANENBAUM, A.S. (2006), *The evolution of RFID security*, IEEE Pervasive Computing 5/1, pp.62-69

ROMAN, R.; ZHOU, J.; LOPEZ, J. (2013), *On the features and challenges of security and privacy in distributed internet of things*, Computer Networks 57/10, pp.2266-2279

SNEKKENES, E. (2001), *Concepts for personal location privacy policies*, 3rd ACM Conf. Electronic Commerce, Tampa, pp.48-57

SPIEKERMANN, S. (2004), *General aspects of location-based services*, Location-based services, Morgan Kaufmann, pp.9-26

SUBASHINI, S.; KAVITHA, V. (2011), *A survey on security issues in service delivery models of cloud computing*, J. Network and Computer Applications 34/1, pp.1-11

TAKABI, H.; JOSHI, J.B.D.; AHN, G.-J. (2010), *Security and privacy challenges in cloud computing environments*, IEEE Security & Privacy Magazine 8/6, pp.24-31

TSEN, J.K.T. (2011), *Ten years of single window implementation: Lessons learned for the future*, Global Trade Facilitation Conf., UN Economic Commission for Europe (UNECE), pp.1-30.

UN (2002), *Value-added services of logistics centres in port areas*, Technical Report, Commercial Development of Regional Ports as Logistics Centres, United Nations, pp.19-34

VENKATRAMAN, N. (1994), *IT-enabled business transformation: From automation to business scope redefinition*, Sloan Management Review 35/2, pp.73-87

WANG, Y.; ATTEBURY, G.; RAMAMURTHY, B. (2006), *A survey of security issues in wireless sensor networks*, IEEE Communication Surveys & Tutorials 8/2, pp.2-32

WEBER, R.H. (2010), *Internet of things – new security and privacy challenges*, Computer Law & Security Review 26/1, pp.23-30

WIEGMANS, B.W.; VAN DER HOEST, A.; NOTTEBOOM, T.E. (2008), *Port and terminal selection by deep-sea container operators*, Maritime Policy & Management 35/6, pp.517-534

YANG, J.; WANG, H.; WANG, J.; TAN, C.; YU, D. (2011), *Provable data possession of resource constrained mobile devices in cloud computing*, J. Networks 6/7, pp.1033-1040

ZHOU, Z.; HUANG, D. (2012), *Efficient and secure data storage operations for mobile cloud computing*, 8th Int. Conf. Network and Service Management, Laxenburg, pp.37-45

ZISSIS, D.; LEKKAS, D. (2012), *Addressing cloud computing security issues*, Future Generation Computer Systems 28/3, pp.583-592

A General Arrangements Visualization Approach to Improve Ships' Design and Optimize Operator Performance

Monica Lundh, Chalmers Univ. of Technology, Gothenburg/Sweden, monica.lundh@chalmers.se
Steven Mallam, Chalmers Univ. of Technology, Gothenburg/Sweden, steven.mallam@chalmers.se

Scott MacKinnon, Chalmers Univ. of Technology, Gothenburg/Sweden, scottm@chalmers.se

Abstract

Working on ships is considered a high risk occupation. Slip, trips and fall represent one of the major risks on board. By visualizing ergonomic principles and analytic methods in a virtual design tool the discussion of different design solutions and the impact they have on the operators' performance is facilitated. Ergonomic Ship Evaluation Tool, E-SET provides a platform where different stakeholders can discuss the optimal design of the engine room. Optimized equipment layout, task demands that can be effected early in the design stages will likely result in construction cost savings, optimized task performance and an overall improved work environment.

1. Introduction

The shipping industry is a highly competitive business which has most recently undergone major technical changes. Ships have become more specialized, technologically advanced while crew complement has decreased as ships have become more complex and automated, *Bloor et al. (2000)*, *Mårtensson (2006)*, *Mallam (2014)*. Designing a ship is a complex activity involving many stakeholders and partners. The focus of the design process is the type of ship, its purpose and the operational safety including stability criteria and sea worthiness, *Veenstra and Ludema (2006)*, *Dokkum (2011)*. The preliminary design of a ship consists of an outline specification, which is a brief technical description of the vessel, together with the General Arrangement Drawings (GAD), *Dokkum (2011)*. The GAD plan gives a side and top view of the ship basically showing the arrangement of relevant spaces on board but with few details, Fig. 1.

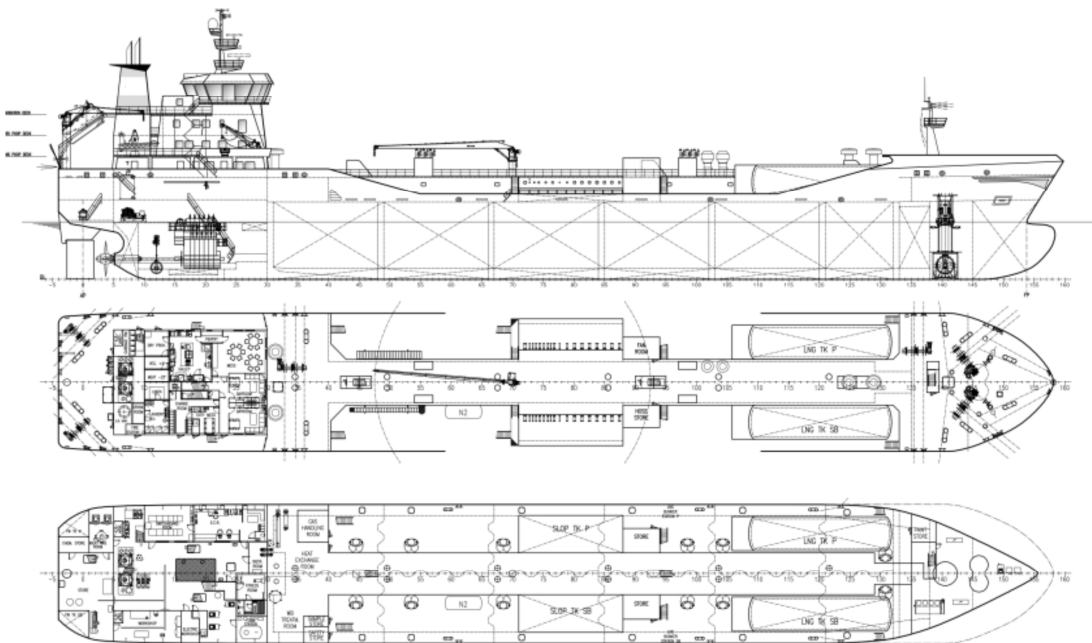


Fig. 1: Example of a General Arrangement Drawing

The cargo hold is the part of the ship which generates money and to make the cargo handling optimal and as efficient as possible the design of the cargo hold has highest priority. This risks creating a

conflict with other spaces, such as the allocated space for the engine department, *Veenstra and Ludema (2006), Lundh (2010)*. The International Maritime Organization (IMO) is appointed by the United Nations as a specialized agency which is responsible for regulating shipping by issuing mandatory conventions and guidelines. The mandatory regulations mainly addresses the safety issues and technological specifications of the ship, *IMO (2001)*. The guidelines governing the design of the engine department are not mandatory and provide few details to support the designers, *IMO (1998)*.

The detailed design and build of the engine department has to comply with the rules of the Classification Society and the actual build of these systems are usually sub-contracted by the ship yard, *Dokkum (2011)*. This is a costly (a rule of thumb is 10% of the total building price) and time consuming procedure involving a lot of person hours and, more often than not, different subcontractors deal with the different mechanical, hydraulic, pneumatic and electrical systems, *Dokkum (2011)*. Thus, several sub-contractors who all likely work towards a profit margin, a ship yard working towards a delivery date and an owner anxious to realize a speedy return on investment lead to a situation where fast and cheap trump quality, especially related to providing the crew-member with an efficient and safe work environment. Hence, a tool that can provide these stakeholders with optimized design, with a goal of minimizing the physical effort of crew-members is necessary, specifically providing specifications during the design phase and guidance during the construction period.

2. Working on board

The work environment on board has always been challenging, especially in the engine department, *Ivergård et al. (1978), Lundh et al. (2011)*. Working on board ships is in general regarded as a high risk occupation where the mortality and risk of injury is higher than average, *Hemmingsson et al. (1997), Bloor et al. (2000), Forsell et al. (2007), Orosa and Oliviera (2010)*.

A reduction in the number of crew members on board creates fewer hands available to manage the manual work on board. Despite down-sizing of crew, maintenance and repair work still have to be performed by the crew onboard. Parts of this work include the logistics of moving pieces of machinery, spare parts and crew around the engine department and the vessel itself. Lifting aids, such as overhead trolleys and lifting eye bolts, are present but not covering the whole work space, *Lundh et al. (2011)*. The design of a ship is going to influence how the crew can and will perform their tasks. Awkward work postures, noisy and warm environments, confined spaces and multi-level work areas are a part of the daily work on board, *Seif et al. (2003), Mallam (2014)*. Once the ship is built and put into operation, any design changes tend to become costly and time consuming. Rather than making alterations on board, the crew adapt to the context and put themselves at risk while executing their tasks, such as slip, trips and falls and an increased risk of exposure of oils and chemicals, *Forsell et al. (2008), Lundh (2010), Mallam (2014)* concludes that the physical design of a ship must reduce the crew's exposure to traditional and environmental hazards.

2.1. Slip, trips and falls

The IMO guidelines MSC/Circ. 834 addressing the design of the engine department are not mandatory and make generalized recommendations, *IMO (1998)*. However slip, trips and falls are indirectly addressed in two subsections:

6.4.4 A non-skid coating or covering should be provided for decks, platforms and ladder treads to prevent slipping.

6.4.5 Tripping, falling and bumping hazards, such as the top and bottom of ladders, stanchions, sills and low overheads, should be vividly marked to call their attention to personnel working in the engine-room.

Slip, trips and falls (STF) are recognized as a major work hazard in many domains. A study performed in Sweden investigated 1600 accident reports from occupational groups with high incident

rates of STF. Their results stated that although different occupational groups were included, the work place hazards were common to all, *Kemmlert and Lundholm (2001)*. Among the major causes of STF injuries are slips due to lack of orderlies (e.g. wet/greasy floor, obstacles) and miss-step/loss of footing on floor/ground were mentioned as two of the major causes.

Among injuries on board, STF are one of the main causes for injuries on ships, *Jensen et al. (2005)*. Apart from the human cost and even risk of death these also involve significant costs for the ship owners and insurance companies. This problem has been recognized by different stakeholders such as classification societies (e.g. Bureau Veritas and Lloyd's Register) and interest group organizations (e.g. The Nautical Institute). Fig. 2 exemplifies STF hazards in the form of uneven surfaces and obstacles in the engine room.



Fig. 2: Example obstacles in the engine room and bottom of ladder

3. Integrating Human Factors knowledge into the design process

A lot of the design issues can be easily and cost effectively managed from General Arrangement Drawings (GAD), but requires that human factors considerations are brought into the design process at an early stage, *Mallam (2014)*, *Mallam et al. (2015)*. Participatory ergonomics is regarded as the workers' active involvement in implementing ergonomic knowledge and procedures in their workplace, *Nagamachi (1995)*. This methodology has been used in several work contexts addressing both mental and physical workload to improve the work situation, *Nagamachi (1995)*, *Vink et al. (1995)*, *Vink et al. (2006)*. Recent research has also addressed the importance of involving the end user and applying the principles of participatory ergonomics in ships' design process, *Mallam (2014)*, *Costa (2016)*. Traditionally ergonomics and human factors are not included into the training of naval architects, *Costa (2016)*. By using simple methods which are easy to grasp and involving both upfront and end-users a lot of information about the work environment can be identified and incorporated. To be able to determine how the design best can support the crew in their performance of tasks all analyses need to start with an understanding of the tasks to be performed, what is done, in what order and how.

3.1. Focus groups

Conducting Focus Group interviews using subject matter experts (SMEs) and end users can give a variety of perspectives and ideas on a given topic, *Patton (2002)*. 3-5 SME participants can be asked to describe their tasks and how they perform them. Design solutions can then be evaluated and approved by the SMEs during a second Focus Group, Fig. 3.



Fig. 3: Example of focus group interviews using a model to guide discussions about changes in design

3.2. Hierarchical Task Analysis

The work of integrating human factors into a work place design starts with a description of the task to be performed. The end user(s) describe their work using a Hierarchical Task Analysis (HTA). The task can be divided into subtasks, choosing the required level of detail. The relationship between main task and the subtasks tasks is described in a plan which also contains the specific goal for each subtask, its input conditions and actions required to attain the goal, Fig. 4, *Arnett (2003)*.



Fig 4: Example of a Hierarchical Task Analysis

3.3. Link Analysis

Once the task is determined and divided up into tasks and subtasks, a Link Analysis method can be used to provide a graphic representation of the work space layout, *Stanton et al. (2013)*, Fig. 5. The Link Analysis is used to get a deeper understanding of the task helping to point out frequency and importance of the different task and subtasks within a geographic space.

4. Ergonomic Ship Evaluation Tool, E-SET

The Ergonomic Ship Evaluation Tool (E-SET) is an interactive visualization tool that uses GAD to evaluate different design solutions, work procedures and how these are affected by design. In this tool, GAD options can be tested and evaluated by naval architects, shipping companies, other stakeholders and end users.

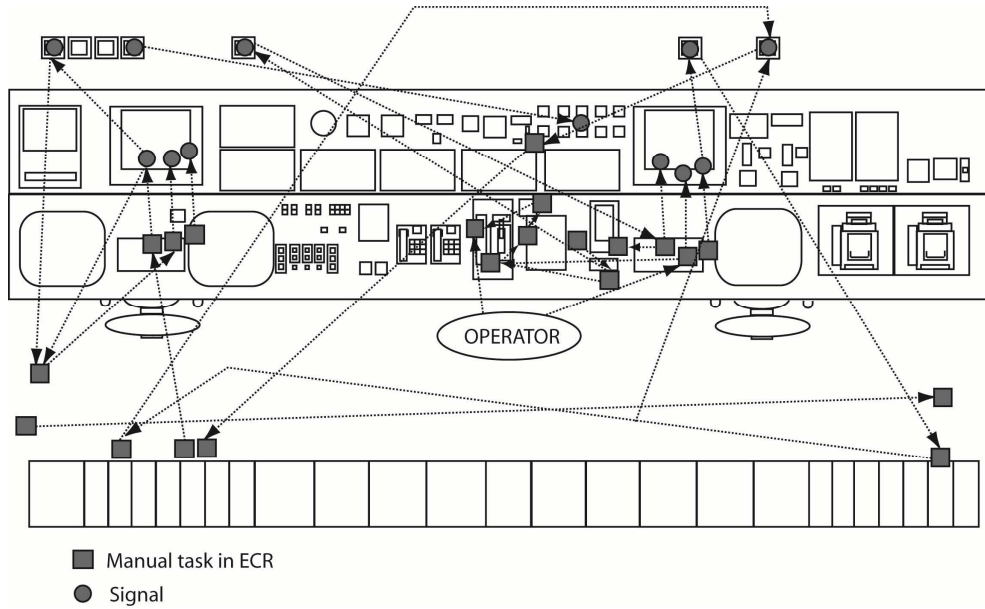


Fig. 5: Example of a Link Analysis

A number of tasks and task descriptions are identified by SMEs during a Focus Group session(s). The results of these are entered into E-SET and tasks are divided into different sequences. Information about at what location the different sequences occur, at what deck and a description about the event is also entered, Table I.

Table I: An example of task description in E-SET

Sequence	Location	Deck	Event
1	Engine Control Room	4	Alarm signal – port seawater chest blocked
2	Seawater Chest	1	Onsite inspection
3	Work Shop	2	Collection of appropriate tools/equipment
4	Seawater Chest	1	Manual maintenance tasks – dirty seawater filter inspected and removed
5	Washing Area	1	Transport of seawater filter to washing areas
6	Storage Area	1	New filter transported from storage area to sea water chest
7	Sea water chest	1	Installation of new filter
8	Workshop	2	Tools/equipment returned
9	Engine control room	4	Confirmation of success in the remote monitoring and alarm system
10	Washing area	1	Clean dirty seawater filter
11	Storage area	2	Transport cleaned seawater filter to storage area

Using the E-SET tool every sequence is marked on a GAD and the programs visualizes the link analysis and calculates movement time, Fig. 6. The results can be scrutinized deck by deck but also from a side view. When analyzing potential risk of STF, congested areas and vertical movements are of particular interest. Obstacles can be entered into the program that will generate a recalculation of movement tracts, much like a car's GPS system will suggest alternative routes because of construction or accident. By suggesting alternative locations associated with the different tasks and entering these into E-SET, a relative comparison of time and thus the efficiency of the task can be attained. Congested areas and vertical movements can be optimized to find the best solution. The remaining risk areas are early in the design process identified and can be monitored through the building of the ship. Rather than following the recommendations in the MSC/Circ. 834 to vividly mark STF hazards to draw the crew's attention to this, uneven surfaces and/or obstacles can be avoided.

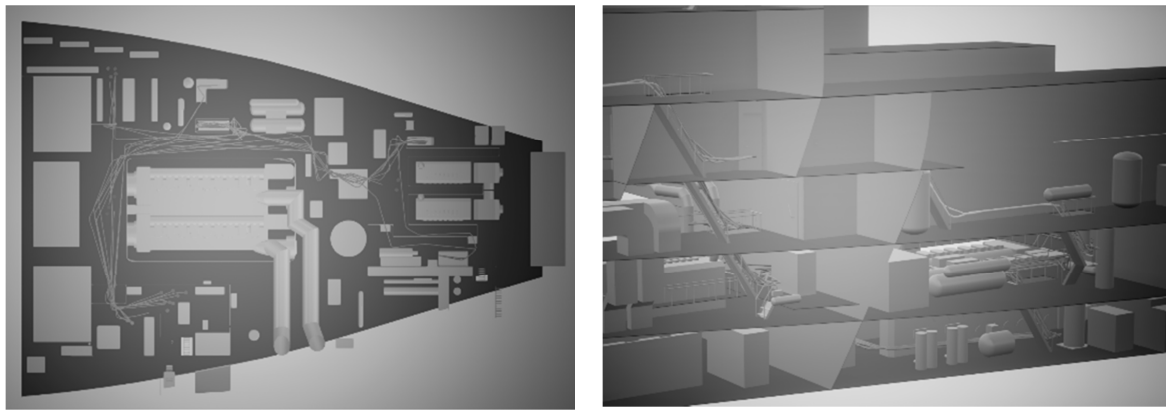


Fig. 6: Example of an E-SET link analysis

5. Conclusions

Visualizing basic ergonomic principles and simple analytic methods in a virtual design tool facilitates the discussion of different design solutions and the impact they have on the operators' performance, efficiency and safety in task performance and the work environment on board. E-SET provides a platform where different stakeholder and end users can meet and discuss the optimal design of the engine room without previous knowledge and training in ergonomics. Optimized equipment layout, task demands that can be effected early in the design stages will likely result in construction cost savings, optimized task performance and an overall improved work environment.

Acknowledgement

We thank the Swedish Merchant Mercantile Foundation for supporting this work.

References

- ARNETT, J. (2003), *Hierarchical Task Analysis*, Handbook of Cognitive Task Design, CRC Press
- BLOOR, M.; THOMAS, M.; LANE, T. (2000), *Health Risks in the Global Shipping Industry: An Overview*, Health, Risk & Society 2(3)
- COSTA, N. (2016), *Human Centered Design for Maritime Safety: A User Perspective on the Benefits and Success Factors of User Participation in the Design of Ships and Ship Systems*, Lic. Thesis, Dept. of Shipping and Marine Technology, Chalmers University of Technology, Gothenburg
- DOKKUM, K. (2011), *Ship Knowledge*, Dokmar Maritime Publishers BV
- FORSELL, K.; HAGBERG, S.; NILSSON, R. (2007), *Lung cancer and mesothelioma among engine crew - Case reports with risk assessment of previous and ongoing exposure to carcinogens*, International Maritime Health, 58, pp.1-4
- FORSELL, K.; HAGBERG, S.; NILSSON, R. (2008), *Ansamling av cancerfall på en passagerarfärja. Rapport från Arbets- och miljömedicin nr 117 (Accumulation of Cases of Cancer on board a Passenger ferry, Rep. Occupational and Environmental Medicine No 117)*, Göteborgs Universitet
- HEMMINGSSON, T.; LUNDBERG, I.; NILSSON, R.; ALLEBECK, P. (1997), *Health-related selection to seafaring occupations and its effects on morbidity and mortality*, Am. J. Ind. Med. 31(5)
- IMO (1998), *MSC/Circ.834 Guidelines for Engine- Room Layout, Design and Arrangement*, IMO
- IMO (2001), *SOLAS The International Convention for the Safety of Life at Sea*, IMO

IVERGÅRD, T.; EKELIN, A.; LUNDBERG, M.; NORBERG, L.; SVEDUNG, I. (1978), *Arbetsmiljö inom sjöfarten - en kartläggning (Work Environment in the Shipping Industry - a Survey)*, Sjöfartens arbetarskyddsnämnd (SAN), Stockholm

JENSEN, O.C.; SØRENSEN; J.F.L.; CANALS, M.L.; HU, Y.; NICOLIC, N.; MOZER, A.A., et al. (2005), *Non-Fatal Occupational Injuries Related to Slips, Trips and Falls in Seafaring*, American J. Industrial Medicine 47, pp.161-171

KEMMLERT, K.; LUNDHOLM, L. (2001), *Slip, trip and falls in different work groups - with reference to age and from a preventing perspective*, Applied Ergonomics 32, pp.149-153

LUNDH, M. (2010), *A Life On the Ocean Wave - Exploring the interaction between the crew and their adaption to the development of the work situation on board Swedish merchant ships*, PhD Thesis, Chalmers University of Technology

LUNDH, M.; LÜTZKHÖFT, M; RYDSTEDT, L.; DAHLMAN, J. (2011), *Working Conditions in the Engine Department - A qualitative study among engine room personnel onboard Swedish merchant ships*, Applied Ergonomics 42, pp.384-390

MALLAM, S. (2014), *The Human Element in Marine Engine Department Operation: Human Factors & Ergonomics Knowledge Mobilization in Ship Design & Construction*, Lic. Thesis, Dept. Shipping & Marine Technology, Chalmers University of Technology, Gothenburg

MALLAM, S.; LUNDH, M.; MACKINNON, S. (2015), *Integrating Human Factors & Ergonomics in large-scale engineering projects: Investigating a practical approach for ship design*, Int. J. Industrial Ergonomics 50, pp. 62-72

MÅRTENSSON, M. (2006), *Sjöfarten som ett socialt system - Om handelssjöfart, risk och säkerhet (The Shipping Industry as a Social System - About the Merchant Navy, Risk and Safety)*, PhD Thesis, Techn. Univ. Luleå

NAGAMACHI, M. (1995), *Requisites and practices of participatory ergonomics*, Int. J. Industrial Ergonomics 15, pp.371-377

OROSA, J; OLIVIERA, A. (2010), *Assessment of Work-Related Risk Criteria Onboard a Ship as an Aid to Designing its Onboard Environment*, J. Marine Science and Technology 15

PATTON, M. (2002), *Qualitative Research & Evaluation Methods*, Sage Publications Inc.

SEIF, M.; DEGIULI, N.; MUFTIC, O. (2003), *Ergonomical Valorization of Working Spaces in Multipurpose Ships*, Collegium Antropologicum 27(1), pp.391-402

STANTON, N. (2013), *Human Factors Methods - A practical Guide for Engineering and Design*, Ashgate Publishing Ltd.

VEENSTRA, A. W.; LUDEMA, M. V. (2006), *The Relationship Between Design and Economic Performance of Ships*, Maritime Policy & Management 33(2), pp.159-171

VINK, P.; KONINGSVELD, E.; MOLENBROEK, J. (2006), *Positive outcome of participatory ergonomics in terms of higher comfort and productivity*, Applied Ergonomics 37, pp.537-546

VINK, P.; PEETERS, M.; GRÜNDEMANN, P.; DUL, J. (1995), *A participatory ergonomics approach to reduce mental and physical workload*, J. Industrial Ergonomics 15, pp. 389-396

Multi-Objective Design Study for Future U.S. Coast Guard Icebreakers

Thomas DeNucci, U.S. Coast Guard Academy, New London/USA, thomas.w.denucci@uscga.edu
Andrew Britton, U.S. Coast Guard Academy, New London/USA, Andrew.a.Britton@uscga.edu
Michael Daeffler, U.S. Coast Guard Academy, New London/USA, michael.s.daeffler@uscga.edu
Greg Sabra, U.S. Coast Guard Academy, New London/USA, gregory.k.sabra@uscga.edu
Hans Hopman, Delft University, Delft/Netherlands, j.j.hopman@tudelft.nl

Abstract

This paper describes an optimization study for USCG icebreakers. TU Delft's 2.5-D packing-based synthesis model was used to investigate the icebreaker design space. Using a concept operational requirements document (ORD) and input from subject matter experts, a polar icebreaker design model was developed. To properly size the propulsion plant, a combinatorial catalogue-based prime mover selection and optimization algorithm was developed to consider operational requirements, size constraints and icebreaking capability for each variant. A description of the icebreaker design space, key trade-offs and performance limits as well as a discussion of results and insights gained in this design study will be presented.

1. Introduction

As a leading global maritime force, the U.S. Coast Guard is charged with protecting the interests of the United States in the Polar Regions.

The Arctic region is a primary focus in the U.S. geopolitical spotlight as climate change reduces multi-year ice and creates more extensive areas of open water. These environmental changes, coupled with the emergence of previously undiscovered natural resources, have led commercial entities to push the bounds of their economic and technological interests in the region. Sovereignty claims in this region exacerbates the problem, as Arctic nations vie to establish a national presence in these waters. The U.S. also has national interest in the Antarctic region. In addition to supporting National Science Foundation (NSF) research activities in the Antarctic, U.S. icebreakers perform an annual resupply mission to McMurdo Station, the large Antarctic research station located near the Ross Ice Shelf.

Currently, the Coast Guard's most significant obstacle to fulfilling its statutory icebreaking mission is the growing obsolescence of the current vessels and the resulting capability gap caused by their increasingly limited operations, *Caldwell (2011)*. To remedy this, the Coast Guard is actively investigating options to recapitalize its icebreaking fleet. The current U.S. Coast Guard congressional authorization act provides up to \$14 million (USD) for pre-acquisition activities for a new polar icebreaker over the next two years.

The issue for Congress is whether to approve, reject, or modify the Administration's plans for sustaining and modernizing the polar icebreaking fleet, *O'Rourke (2016)*. Congress's decisions on this issue could affect Coast Guard funding requirements, the Coast Guard's ability to perform its polar missions and the U.S. shipbuilding industrial base.

One of the key issues at hand concerns the acquisition strategy of the new icebreakers. While many within the service argue that the Coast Guard should design its own icebreaker, there are a growing number of activists lobbying towards either the purchase or lease of an icebreaker. While this approach may reduce risk, it often results in ship designs that do not sufficiently meet operational requirements.

The goal of this project is to explore the icebreaker concept design space to better understand the requirements, design lanes and trade-offs associated with the project and share insights and recommendations on the acquisition strategy.

2. Current Status of USCG Icebreaking Fleet

The operational U.S. polar icebreaking fleet currently consists of one heavy icebreaker, POLAR STAR, and one medium icebreaker, HEALY, Fig. 1. The 107.3m (10,800 LT) Polar class icebreaker was commissioned in the late 1970's. These combined diesel electric or gas turbine (CODLOG) vessels produce 16,000 hp in diesel electric mode and 60,000 hp with gas turbines. The *Polar* class was designed to break 2m (6ft) of ice continuously at 3 knots. Scientific support, including laboratories and science systems, were an afterthought in this design and added once the design was delivered to the USCG.

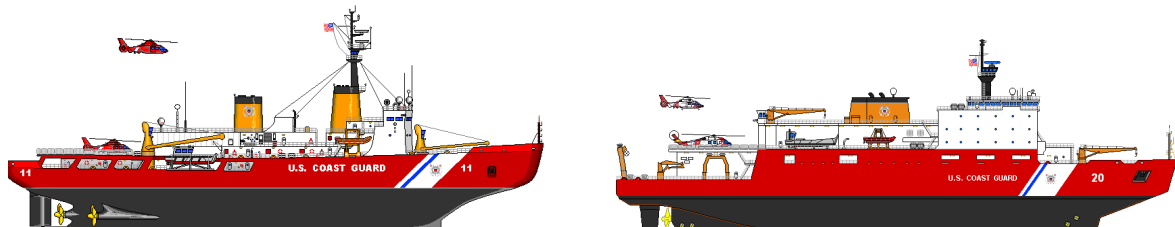


Fig. 1: Current USCG Polar Icebreakers. The Polar class icebreaker appears on the left and the HEALY class icebreaker appears on the right.

The 128m (16,000 LT) HEALY class icebreaker was commissioned in 1999. The diesel electric AC/AC cycloconverter propulsion plant produces approximately 30,000 hp. HEALY was designed to break 1.4m (4.5ft) of ice continuously at 3 knots. Science support systems, including a wet lab, meteorological lab, main science lab, climate control chambers and science staging areas were design from the earliest stages of design.

2.1 Challenges in Icebreaker Design

Some of the more typical process challenges inherent in naval ship acquisition projects exist in the icebreaker replacement project. Generally speaking, these challenges include a protracted design timeline, conflicting and inconsistent requirements, a high level of complexity and limited research and development investment (relative to other industries). Class specific challenges include infrequent design, a traditionally small fleet size (one-class ship), hull forms (open water vs. ice breaking), complex machinery and propulsion plants, extended range and operation in extreme climates.

Despite these challenges, numerous technological breakthroughs have ushered in a new and exciting era of icebreaker design. During the past half-century, icebreaker design has been subject to improved hydrodynamics, cost and propulsion options, *Keinonen et al. (2010)*. The advent of ice model testing in the late 1960's, resulted in a transition from rounded hull shapes with sharp stems (low open water resistance) to hull shapes with angles specifically optimized for low ice resistance. In the 1980's, as the offshore industry invested in oil and gas exploration in ice covered waters, the design focus shifted from vessel performance to the overall cost of the vessel. This transition provided new hull shapes that were simple, inexpensive and efficient. Vertical flat sides, parallel mid-body and hard chines all contributed to a less expensive hull form. During this time, icebreakers also tended to become more "boxy", due to their required square deck areas. Most recently, new and innovative propulsion plants, including electric ship configurations and azimuthing thrusters, have offered opportunities to introduce new propulsion technology in icebreaker design.

2.2 Design Synthesis

In order to explore the icebreaker design space, elucidate requirements and provide insight on design trade-offs, a packing-based ship synthesis model was used to create icebreaker designs. To mitigate the challenges outlined above, and to capitalize on current technologies in icebreaker design, a collection of different icebreaker hull forms were used to predict open water and icebreaking resistance. The design impact of propulsion plant selection was captured by a combinatorial catalogue-based prime

mover selection algorithm was developed. The cost model incorporates a weight-based labor and material cost estimating relationship (CER) and considers both risk and production adjustments to predict costs for each concept design, *DeNucci et al. (2015)*.

3. Approach

The design approach is centered on TU Delft's 2.5-D packing-based ship synthesis model coupled with a genetic search algorithm. This approach rapidly generates a large and diverse set of technically feasible 2.5-D dimensional ship designs that cover a wide range of user-defined trade-offs. Computer processing time is saved in the 2.5-D case (vs. 3-D), given that transverse object locations are collapsed on a centerline plane.

The model uses a concurrent combined bin-packing and wrapping approach that provides the ship description and parametric variation during early stage design. Using the initial location of the space as genes, a NSGA-II genetic algorithm optimizes the chromosomes of the object's coordinates using tournament selection, simulated binary crossover and mutation. The algorithm searches for balanced designs meeting a set of non-negotiable constraints. Details on this approach can be found in *Van Oers and Hopman (2012)*, *Van Oers (2012)* and *DeNucci (2012)*.

Once the packing routine places all objects within the hull envelope, a synthesis model calculates a variety of numerical values to evaluate ship performance and fitness. Parameters such as metacentric height (GM), draft, freeboard, weight and centers (KG / TCG / LCG) are used for design constraints while values of cost, resistance and operability are used as design optimization goals.

3.1. Icebreaker Model

USCG subject matter experts provided the majority of the input for the operational and design requirements of the vessel. The general parameters of the icebreaker design were:

- Length: 100m-150m
- Range: ~24,000 nm @ 15 knots, preferably 80-90 days
- Icebreaking Capability: > 2m
- Science Support
- Twin shaft / screw
- Propulsion System:
 - Diesel
 - Turbine
 - Combine Diesel and Gas Turbine (CODAG)
 - Diesel Electric
 - Turbine Electric

A library of icebreaker objects (systems and spaces) were derived from a USCG indicative design as well as from general arrangement plans of the *Polar* and *HEALY* classes. Over 170 objects were developed in this research to accurately describe the icebreaker ship structure, machinery, mission support systems, human support systems and tanks. A suite of dedicated science support systems, such as a meteorology lab, wet lab, chemical lab, science winch staging and biology lab were included in this model.

Each object definition includes data on its size (minimum and maximum area/volume), its weight (actual weight or weight density) and its geometry, i.e., whether object functionality would be lost with shape deformation. Overlap and connection constraints, packing routine rules to satisfactorily place objects, are also defined. Unfortunately, the object library cannot dynamically change, i.e., objects are predefined, but each object has the ability to change shape to fit the hull envelope.

The icebreaker model includes five different hull forms. In addition to the *POLAR* and *HEALY* hull forms, the USCG Academy designed concept hull forms for a naval arctic patrol vessel (the NOSIB) and two commercial arctic offshore supply vessels (AOSV). Fig. 2 shows three of the icebreaker hull models used in this research.



Fig. 2: Hull forms developed to support the generation of icebreaker designs

3.2. Weight and Cost Estimation

A Ship Work Breakdown Structure (SWBS) weight formulation was based on general arrangements and specific weight-deck area formulation. Each SWBS group, classified by systems and equipment with similar functionalities, is shown in Table 1. Weight data was calculated for each specific three-digit component of SWBS groups using a combination of first principles, e.g., calculation of hull and structure weight, ratiocination formulas, and weight densities, e.g., specific weight and compartment area statistics to achieve area-dependent weight estimates. Because of the added hull structure required for icebreaking, first-principles, in addition to ABS Guidance on icebreaker hull design (specifically ice belt thickness) was used to estimate the weight of SWBS 100. Weight validation was performed using a USCG icebreaker indicative design and was found to be within 10% of the estimate.

Table 1: SWBS Classification

SWBS Group Number	Description
100	General Hull Structure
200	Propulsion Plant
300	General Electric Plant
400	Command & Surveillance (C4ISR)
500	Auxiliary Systems
600	Outfit & Furnishings
700	Armament

A parametric cost model was used to predict the non-recurring costs, recurring costs, and cost risk for the user-defined ship systems in each feasible design. The model produces a cost matrix that includes the total cost of the design, as well as the specific cost for each SWBS group. Cost model input comprises five different cost factors that estimate key parameters for each cost element; planning/planning labor, direct labor, material, functional, and profit costs. Specific details of this approach can be found in *DeNucci et al. (2015)*.

The cost model was updated to reflect additional expenses accrued in icebreaker design. A new Cost Estimating Relationship (CER) was applied to SWBS 100 group. Because the weight of the hull structure is so significant in ice breaker design, an updated material and labor rate was applied to this group. Because of the extreme temperatures in the Polar Regions, most C4ISR systems require military rated temperature specifications (operations below -25.5°C); as such, the cost of this group increased. Similarly, SWBS 500, Auxiliary Equipment, also requires additional costs associated with cold weather operation, e.g., required heating elements for topside hydraulic systems. Updated material and labor rates were developed for these groups to factor costs associated with cold weather operation.

As part of this research, the costs associated with SWBS group 200 were calculated using the manufacturer cost estimates instead of a weight-deck area formulation. All other SWBS groups scaled well using ratios and weight-deck area formulation applied in non-icebreaker designs.

3.3. Model Resistance

To enable proper propulsion selection, both open water and icebreaking resistance must be calculated. Various open water resistance methods were analyzed to determine which would prove most accurate in determining a hull resistance of an icebreaker. In open-water, an icebreaker's behavior is similar to a tow boat or tug's behavior; the power used to propel the vessel at top speed is not the same as the maximum installed power of the vessel. The Holtrop resistance series was used to estimate open water resistance because it includes the largest variety of ship types (including tugs and combatants) and has parameters which are within the typical icebreaker hull form. Past tow tank model tests at the U.S. Coast Guard Academy with icebreaker hull forms corroborate this approach.

Although there are numerous algorithms for icebreaking resistance prediction and class guidance, the Lewis Method for Ice Breaking Resistance provided the best approximation of first order resistance predictions, as it was the least hull form dependent and allows for the variation of the icebreaking speed of the vessel.

3.3.1 Open Water Resistance

The total open water resistance of a vessel was broken down into the following components:

$$R_{ow} = R_F(1 + k_1) + R_{App} + R_W + R_{TR} + R_A$$

Where: R_F = Frictional resistance from ITTC-1957
 $1 + k_1$ = Form Factor
 R_{App} =Appendage Resistance
 R_W = Wave Resistance
 R_{TR} = Transom Immersion Resistance
 R_A = Correlation Allowance

During this calculation, it was assumed that a bulbous bow would not be considered on the icebreaker and that a stern shape was of "normal" form, if for no other reason than to accommodate over the stern science equipment. To validate this methodology, principal dimensions and coefficients were obtained from the USCG National Security Cutter (NSC). Using these dimensions, the Holtrop open water resistance was calculated by the ship synthesis model and compared to the resistance prediction in NavCad, a well-established ship resistance program, across various speeds. There was an average percent error of 8% found between the two methods.

3.3.2 Icebreaking Resistance

Determining a vessel's icebreaking resistance during preliminary design is extremely difficult compared to other calculative methods of resistance. While regression-based models of open water hull resistance are being challenged by CFD analysis, icebreaker resistance prediction is a more complex phenomenon and can be challenging to effectively predict in the preliminary stages of design. Most ice resistance prediction methods vary with the level of ship detail and require an assortment of ship parameters. Ice resistance calculation input can include the performance of the hull in all types of ice, thrust and torque characteristics of suitable propellers, and the interaction of the propellers between the hull, propeller and ice, *Lewis et al. (1982)*. These physical parameters are further compounded by the complexity of the ice field, e.g., type of ice, thickness of ice, layout of ice, and method of breaking ice, i.e., backing and ramming versus continuous breaking that make preliminary predictions inaccurate versus actual performance. However, a well-recognized resistance calculation formula was developed by Lewis et al which accounts for preliminary hull design information, estimated ramming speed, and estimate ice thickness to reliably predict the estimated resistance.

The Lewis method uses the following equation to estimate ice resistance:

$$R_i = \rho_w g B h^2 (C_0 + C_1 \frac{\sigma_f}{\rho_w g h} + C_2 \frac{V}{\sqrt{gh}} \frac{(L/h)}{(B/h)^{1/2}})$$

Where: R_i : Total Ice Breaking Resistance (N)

ρ_w : Mass Density of Water (1025 kg/m³)

g : Acceleration of gravity (9.81 m/s²)

B : Maximum beam at operating water line (m)

h : Ice Thickness (m)

σ_f : Ice Flexural Strength (kPa)

V : Ship Speed (m/s)

L : Length at operating water line (m)

C_0 : Constant (valued determine from linear regression 3.8989)

C_1 : Constant (valued determine from linear regression 0.0123)

C_2 : Constant (valued determine from linear regression 0.223)

Where ice flexural strength as determined by *Timco et al. (1996)* is:

$$\sigma_f = 1,750 * e^{(-5.88\sqrt{v_b})}$$

v_b : Brine volume as calculated in *Frankenstein and Garner (1967)* with a mean value of 0.04 for multi-year ice

To calculate the total resistance during icebreaking operations, the total hull resistance (at the ice-breaking ship velocity) would be:

$$R_T = R_i + R_{ow}$$

For calculative values in the model, a speed of 3 knots (1.54 m/s) was chosen as the continuous icebreaking speed with an ice thickness of 2m. The IACS Unified Requirements for Polar Ships would identify this as a PC-3 designation, which means the vessel can operate year-round in first year ice that may include old ice inclusions. This classification would satisfy the typical condition for a USCG icebreaker conducting a break-out operation in the Antarctic.

3.4 Powering Calculations

Once effective power predictions were calculated from resistance data, propulsion efficiencies were estimated to determine the necessary installed power to reach desired speeds. However, as mentioned in the previous section, there are considerable adjustments to the propulsive efficiencies during ice breaking. Given that ice breaking does not occur at a vessel's top rated speed (which is typically where most prime movers are designed to operate), two calculations are required to determine the installed power of the prime mover: an open water powering calculation at top speed and an ice-breaking powering calculation at ice breaking speed. The higher of these two parameters is then designated as the required installed power for the design.

For open water calculations, a vessel's wake fraction with a block coefficient of 0.5 was estimated to be approximately 0.1, *Molland et al. (2011)*. For ice breaking powering requirements, there is considerable change to the wake fraction, thrust deduction fraction, and the open water efficiency. In an effort to determine the correct values for icebreaking, an extrapolation of the data presented in *Lewis et al. (1982)* was used to estimate typical values during ice breaking. Table 2 compares the estimated propulsion efficiencies and margins between open-water and icebreaking used to produce the necessary Installed BHP.

Table 2: Open-water and icebreaking propulsive efficiencies and margins

Parameter	Open Water	Ice Breaking
Thrust Deduction Fraction	0.15	0.05
Wake Fraction	0.10	0.10
Open Water Efficiency	0.65	0.20
Relative Rot. Efficiency	0.95	0.98
Behind Efficiency	0.618	0.196
Installed Power Margin	0.85	0.85

Using these efficiencies and margins, a required horsepower to reach 6 various speeds was produced to find a BHP vs Vessel Speed curve. To compare the curves calculated for both open water and ice breaking power, known hull designs utilized. The U.S. Coast Guard's National Security Cutter (NSC) was used for open water power, while the POLAR STAR and CGC HEALY were used for ice breaking power.

To achieve 30 knots the required maximum horsepower of the NSC, according to the coded Holtrop Method, was found to be 51,900. This power curve correlates well to the actual installed horsepower on the NSC. The NSC operates on a CODAG propulsion plant configuration with two 10,000 horsepower MDEs and a 30,000 horsepower gas turbine. The total published plant power of the NSC provides 50,000 horsepower for a maximum speed of 28 knots.

For icebreaking, the resistance and installed power for the CGC HEALY and CGC POLAR STAR were calculated based on the methodology explained in the resistance section. For each ice breaker, there were unique requirements for ice thickness; for example, POLAR can break thicker ice than HEALY. Based upon the above efficiencies, the calculated values were within 10% of the actual installed power, which validated the above wake, thrust, and open water efficiencies chosen.

3.5 Prime Mover Selection

Regardless of being time consuming and cumbersome, it is extremely important to select the proper type of icebreaker propulsion system. In terms of cost, U.S. icebreaker propulsion plant selection (and associated systems, e.g., fuel) will often be the greatest lifecycle cost, in some instances even more expensive than crew costs. In addition, it is often difficult to conduct meaningful trade studies to determine the optimal propulsion configuration suitable for further analysis. This paper uses combinatorial optimization to select a valid propulsion system from a library of various engines and generator sets. The term “prime mover” is used in this paper to describe either the engine or generator set that is consuming fuel and producing either electrical or mechanical power for propulsion.

3.5.1 Prime Mover Selection Process

In order to explore propulsion design space, diesel engines, gas turbines, diesel generator sets and gas turbine generator sets were cataloged into a library for optimization. This library includes information on each engine's manufacturer, model, power output (kW), horsepower (hp), rated speed (rpm), length, width, height, total volume, dry weight, specific fuel consumption (SFC) and estimated cost. Some of these factors serve as the basis for this optimization; the others were included for future improvements. The catalog resulted in 81 total prime movers, 37 diesel engines, 10 gas turbines, 27 diesel engine generator sets, and 7 gas turbine generators sets all derived from 8 different manufacturers. Power output ranged from 500hp to 50,000hp. Dual fuel generator sets were also cataloged in the library to accommodate the potential for future Emission Control Areas (ECA) in the Polar Regions. The engine library is used in a constrained single objective bounded combinatorial optimization algorithm to select prime movers with the lowest acquisition cost.

A modified approach to the greedy approximation solution as described in *Dantzig (1957)* was examined for rapid optimization; however, this methodology could not provide a sufficiently optimized design given the hard constraints and bounded nature of this problem. Instead, a more robust method was required to evaluate all possibilities of combinations against predefined hard constraints prior to optimizing over cost; three hard constraints were used in the optimization process. First, the power delivered by the prime mover combination must be greater than or equal to the required power for the design. Second, the total area of the engines, including maintenance envelopes, must be less than the available engine room footprint from the space allocation algorithm and lastly the number of prime movers in the combination must be less than or equal to a predefined limit. Additionally, using a more robust approach will allow future improvements with multi-objective optimization.

$$\begin{aligned}
 & \min \sum_{i=1}^n n_i C_i \\
 & \sum_{i=1}^n n_i P_i \geq \text{Require Power} \\
 & \sum_{i=1}^n n_i \leq \text{Maximum Prime Movers} \\
 & \sum_{i=1}^n n_i (A_i + ME) \leq \text{Alloted Area} \\
 n_i & = \min \left(\text{Maximum Prime Movers}, \left\lceil \frac{\text{Required Power}}{P_i} \right\rceil \right)
 \end{aligned}$$

where: n_i – quantity of the i^{th} engine model included in that combination

C_i – estimated cost of the i^{th} engine model

P_i – maximum power output

A_i – area footprint

ME – maintenance envelop (held at 1m in each direction)

The combination generation was bounded to combinations of engines between 0 and n_i .

The power and area constraints discussed above are physical parameters that are required to be met in order to achieve a valid ship design. In order to limit the number of combinations, three additional restrictions were imposed. The first was the maximum prime mover constraint mentioned above; without applying this constraint, the combinatorial output in the 30 MW range resulted in over 100 quintillion (100×10^{18}) prime mover solutions and thus became practically and computationally prohibitive. The selection of the maximum prime mover limit is a heuristic value based on designer knowledge and the customer's willingness to accept the complexities that can arise from having additional prime movers connected in the propulsion plant. Even with the maximum number of prime movers constrained, over a quadrillion (1×10^{15}) combinations were possible for some inputs.

In order to further reduce the number of combinations, the library was first split then truncated. Each portion of the library was split by manufacturer such that the optimization could not create combinations with prime movers from multiple manufacturers, i.e., it would not select a Wartsila 8L-26 with a Caterpillar 8M32C. This restriction was imposed based logistics support strategies which generally have all prime movers selected from the same manufacturer. The library was then truncated to remove prime movers with a power output below a minimum limit. The lower limit of engine power is derived from the powering information above and an estimated operational profile. This value should be thought of as power required for open water transit. In the case of electric drive vessels this would mean that any single generator could be on line in normal open water transit condition. With gear driven vessels, it would indicate that any single engine could propel the ship during open water transits. The engine optimization process is shown as Fig. 3.

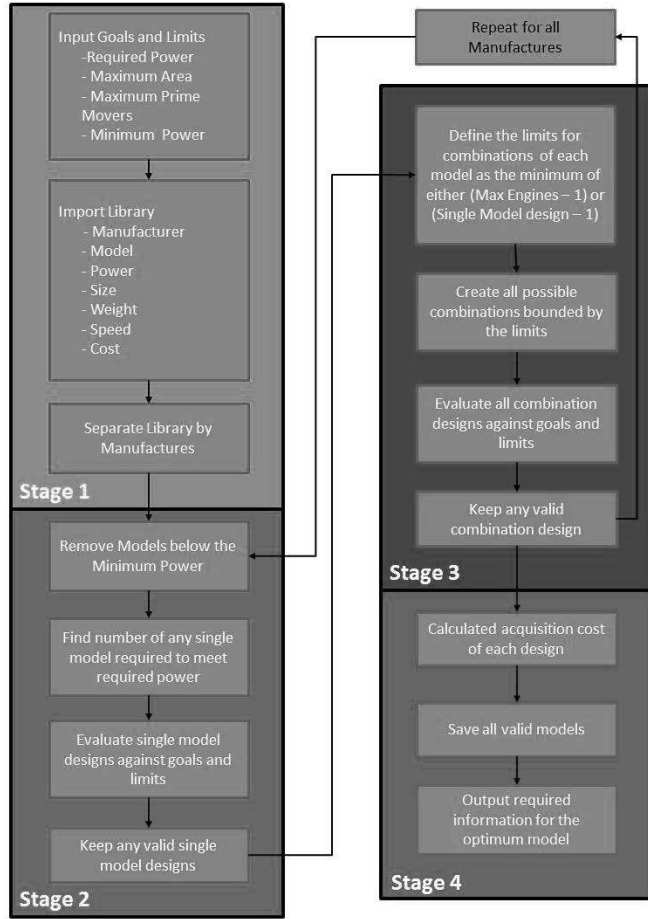


Fig. 3: Engine optimization process

The optimization algorithm is blind to overall propulsion plant configurations or even the type of prime mover that it optimizes over. Given inputs of the set of prime movers to optimize over, a required power, minimum power, maximum number of engines and allotted area, the optimization occurs in four stages:

1. Inputs are processed, the applicable prime mover catalog is loaded and the prime movers are categorized by manufacturer.
2. The manufacture specific prime mover catalog is truncated to remove prime movers below the minimum power threshold. Each prime mover model is evaluated to determine a single model design, i.e., 3 Rolls Royce 4500 GT Generators. This process determines the required number of each single prime mover to meet the goal of the required power. Each single model design point is evaluated against the above defined limits (power, area and maximum prime movers). All acceptable design points are retained for later optimization in Stage 4.
3. Multiple model design combinations are generated using a semi-intelligent method to generate a robust set of possible combinations from the truncated data set. Depending on the number of prime movers for that manufacturer, this can exceed one billion design points. Due to computational complexity and memory requirements for data set this large, these design points may be evaluated piecewise in groups of up to 10 million at a time. Again, all designs that satisfy the constraints are retained for optimization. Note that Stage 2 and Stage 3 repeat consecutively for each manufacturer.
4. Stage 4: Acquisition cost and weight is calculated for each valid design point. The design with the lowest cost is selected as the optimum propulsion configuration and all the pertinent data is fed back to the NSGA-II genetic algorithm.

4. Test Case Analysis

With multiple objectives to analyze, it is critical to select those parameters that will be the most effective in aiding the selection of a final design. For a typical Coast Guard cutter, the most important metrics considered during design selection are mission effectiveness and cost per operating hour. Ideally, the goal is to increase the mission effectiveness while decreasing the cost to operate the vessel. For an icebreaking vessel, mission effectiveness can be defined in several different ways and is often challenging to measure, e.g., icebreaking capability, time to “groom” ice channels or scientific mission support, time on location, etc. To compound this challenge, the calculation of cost per operating hour is extremely difficult during concept design because it requires detailed information, e.g., crew costs, maintenance costs, fuel costs, etc.

As a starting point, this paper focused on the design parameters that influence both mission effectiveness and cost during concept design. This involved consideration of four multi-objective design studies:

- Resistance vs. Cost: The goal in the designing the hull of a ship is to reduce the total resistance caused by friction and wave making components, thereby decreasing power requirements. With less installed power, there is a decrease in the acquisition cost of the vessel. It would be expected that a decrease in the overall resistance of the vessel will reduce the total cost of the vessel.
- Horsepower vs. Hull Type: When developing an icebreaker hull versus an open water hull, additional power is typically required depending upon how effective the hull is in clearing and breaking ice, as well as principal dimensions (such as beam) which can impact how effective the hull is in clearing ice. It is expected that an icebreaker hull form would require less total horsepower for icebreaking operations than a hull designed for open water transit, and a hull designed for open water transit would require less total horsepower for open water transit than a hull designed for icebreaking. The goal is to determine whether the hull form has an impact on the total horsepower required.
- Prime Mover vs. Ice Capability: Prime mover selection greatly impacts the effectiveness and methods to conduct ice breaking missions; in addition, the thickness of ice needed to be broken greatly impacts the power requirements of the vessel. When selecting prime movers, factors such as size, weight, and power are the primary factors. The goal would be to determine the optimal prime mover combination.
- Sea Keeping vs. Cost: Sea keeping of an open ocean vessel is a major concern for structural strength and for operability of the vessel. Typical relationships between sea keeping and design show that vessels that are larger tend to have better sea keeping properties; however, length tends to drive up cost. The goal would be to determine what the optimal solution between cost and sea keeping.

4.1 Resistance and Cost

In order to establish a cost baseline and principal dimensions of the concept icebreaker, the first design study considered both resistance and cost. To accomplish this, a Gas Turbine (GT) Electric plant, with the requirement to break 2m of ice at 3 knots, was selected as the design variant in this study. The results varied in size and hull form to ultimately drive cost and resistance to a minimum. Fig. 4 shows some initial results from this research. The algorithm converges on a set of designs with minimum length and beam to reduce both cost and resistance. The volume and area requirements of the design can be achieved with principle dimension much smaller than those currently considered by the USCG. In fact, if hull lengths as small as 70m are considered in the synthesis program, designs which resemble the 1950’s era Windlass icebreakers can be realized,

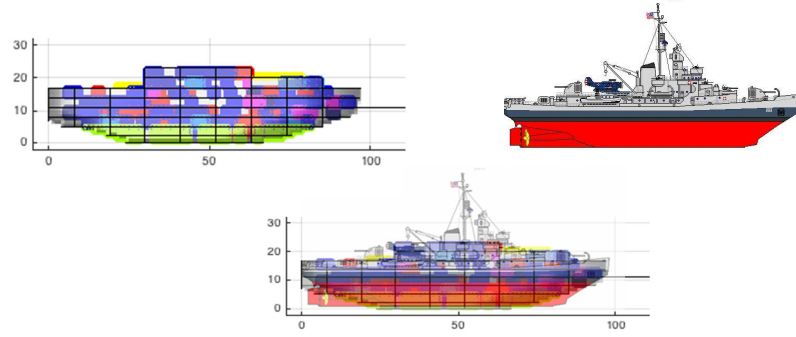


Fig. 5: Windclass icebreaker and concept design. Vessels have length of ~82m and beam of ~19m

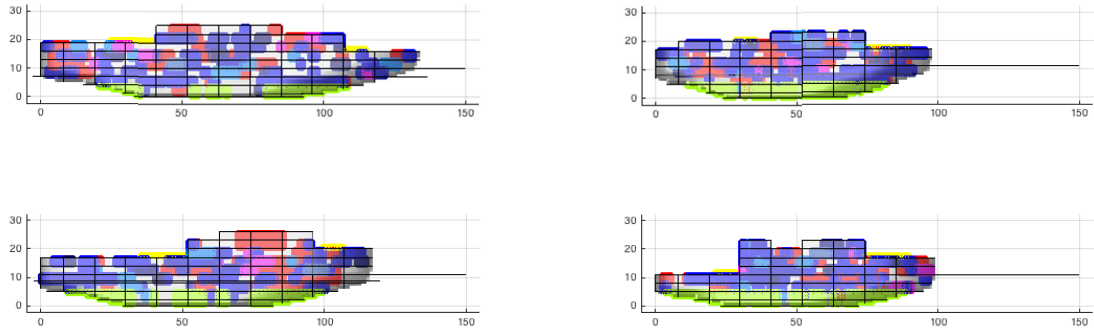


Fig. 4: Samplings of initial results

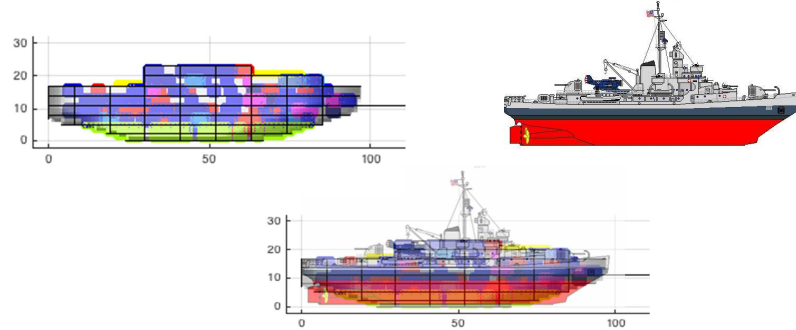


Fig. 5: Windclass icebreaker and concept design. Vessels have length of ~82m and beam of ~19m

Using the given operational and design requirements discussed in Section 3.1, the vessel designs require approximately 35,000hp for icebreaking as shown in Fig. 6. However, for open water requirements, shown in the left graph in orange, there are three distinct bands of required horsepower. It is unclear if all three bands have an ice breaking horsepower around the minima or if some of those bands correlate to the higher ice breaking horse power. A ratio of the ice breaking power and open water power also show the same three distinct bands. It appears even though the ice breaking power between hulls is the same there are certain hull forms which require about ~15% less lower power for open water travel. Though it is not currently considered, the difference in open water power requirements creates a noticeable fuel cost difference over a vessel's life cycle; this is especially prevalent in longer range icebreakers which must travel to reach the Antarctic from the United States.

Fig. 6 illustrates that the lowest cost designs (~\$603 million USD) also have the lowest icebreaking resistance and smallest hull volume. In addition to the hull volume, the superstructure volume also significantly contributed to the cost variation for different ship designs. Examples of designs with similar principle dimensions, but with very different superstructure sizes, show appreciable cost difference (see DeNucci, *et al.* (2015) for graphical examples).

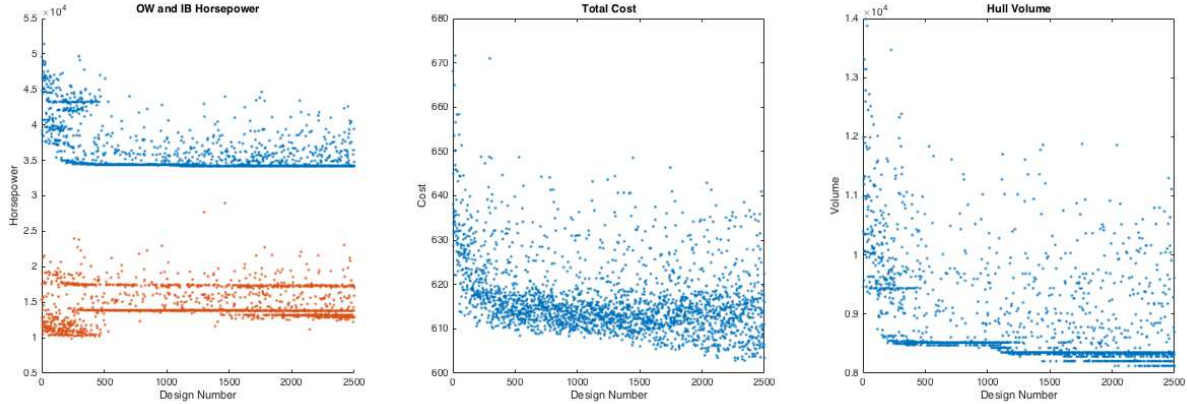


Fig. 6: Resistance (open water in orange, ice breaking in blue), cost, and hull volume calculation of concept icebreaker designs

SWBS group 500 (auxiliary systems) contains a substantial number of objects in the group's system definition which have the ability to deform shape and size within user-defined deck area or volume requirements. As a result, these systems can have significant cost variation. Examples of these spaces include living and engineering spaces, storage rooms, and tanks. Not only does SWBS group 500 have the largest cost difference between high and low cost designs, this group also contributes to ~20% of the total cost for each design meaning it is the cost driver in some icebreaker designs.

One comparable icebreaker of interest to the U.S. is the Canadian icebreaker CCGS John G. Diefenbaker. This ship, if used as a parent hull, would be the largest in the Coast Guard fleet and rank just below the largest Russian nuclear icebreakers in terms of displacement and icebreaking capability. A comparison between the Diefenbaker and the concept design ship produced in this study is shown below in Table 3.

Table 3: CCGS John G. Diefenbaker and a feasible icebreaker design produced in this research

Parameter	Diefenbaker	Concept Design
Length	150 m	120 m
Beam	28 m	14 m
Displacement	~23,100 t	~16,900 t
Max. Power	42,000 hp	35,000 hp
Icebreaking Capability	2.5 m	2.0 m
Cost	~710 m\$	~600 m\$

Based on the results of the optimization model, a case can be made for acquiring a much smaller vessel which can provide a 15% cost savings and meet the same mission requirements. To date, the general trend within the Coast Guard has been to purchase larger vessels; however, there is the possibility to achieve the same mission impacts with significant cost savings. Based on the results of the model, the volumetric requirements did not drive the size of the vessel (including prime mover selection). The only trade-off to be considered is the sizeable difference in ship beam, which from an operational perspective, would require additional passes to clear channel ice.

4.2 Resistance and Hull Type

Fig. 7 shows trends in open water and icebreaking horsepower requirements across different icebreaker hull forms. As an arctic patrol vessel, the NOSIB hull was specifically designed with a lower open water resistance in mind, and icebreaking capability as a secondary requirement. Conversely, the AOSV hull was optimized for icebreaking. For each hull form, and in each case, a ~5,000 HP difference is realized, depending on whether the hull is optimized for higher open water

efficiency or icebreaking. Fig. 7 shows that the AOSV (optimized for icebreaking) required more power for open water transit, but less power for icebreaking. On the other hand, the NOSIB (optimized for open water) required less power for open water, but more power for during icebreaking operations. In the end, the model accurately captures hull form characteristics unique to icebreaker design, i.e., power requirement variance during open water and icebreaking operations.

The larger question is whether this power difference matters. For both hull forms, the icebreaking power requirements ranges between 35,000 and 40,000 HP; a variation of only 5,000 HP (15%) is relatively minor during preliminary design. As a result, the decision to optimize for speed versus open water will not significantly impact the final powering results; in the end, the hull form can be optimized in a later stage of the design, and should not significantly impact the key parameters of the vessel during concept design.

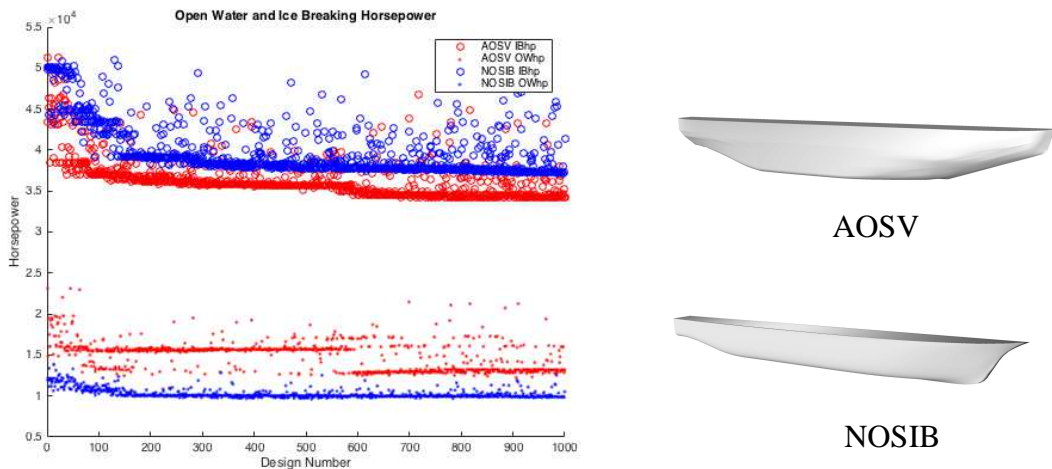


Fig. 7: Horsepower requirements across different icebreaker hull forms

4.3 Prime Mover vs. Ice Capability

Due to the need for high torque at low speed for icebreaking, electric drive propulsion plants were the primary focus of the prime mover design study. Electric propulsion options consisted of the following components:

1. Three different types of generators, i.e., diesel engine driven generators, gas turbine driven generators and combined diesel and turbine generator-sets.
2. Source of hotel power, i.e., integrated propulsion systems (IPS) or non-IPS (separate ship service generators).

Given these parameters, six different electric propulsion combinations were possible. Fig. 8 shows the optimized propulsion plant configurations for an icebreaker designed to break 2 m of ice.

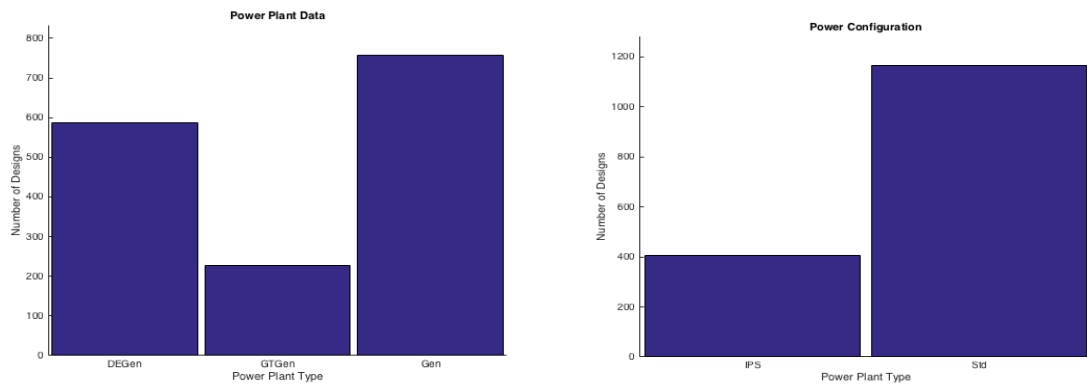


Fig. 8: Propulsion selection results for a concept Polar icebreaker

Following 150 design generations, the combined diesel engine and gas turbine generator set was the propulsion system most often selected from the aforementioned electric propulsion configurations. Additionally, the non-IPS plant configuration was heavily favored throughout the design iterations. In order to explore this relationship further, 10% of the designs with the lowest cost estimates were further analyzed. Fig. 9 indicates that the lowest cost propulsion plant in this data set favored diesel engine generators with non-IPS hotel loads. If there were no constraints on number of prime movers or engine room area, the algorithm would likely always select a diesel engine generator set or combination of sets due to their lower cost to power ratio.

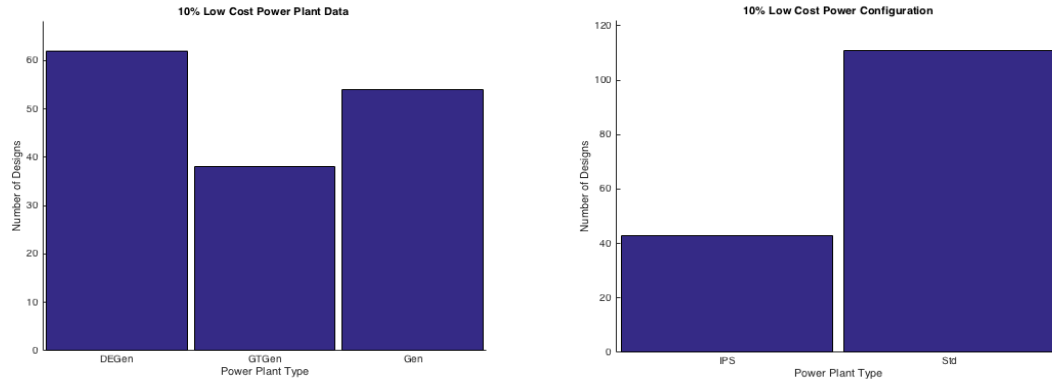


Fig. 9: Lowest cost option for a Polar icebreaker propulsion plant

The primary benefits of using a turbine generator set are attributed to the higher power to weight as well as power to volume ratios of these systems. As the optimization routine generated designs with lower and lower installed power requirements, it was possible to meet the maximum prime mover constraint and area limits with strictly diesel engine generator sets. For the IPS solution (includes hotel loads), there were no valid diesel engine generator combinations that would satisfy the power requirements; therefore, gas turbine generators were selected, resulting in a more expensive propulsion system.

Next, these propulsion preferences were compared to those that resulted from ships with higher ice breaking capability (3m). As expected, results yielded higher ice breaking resistance (70,000 HP). This increase in required horsepower showed a much stronger preference towards a combined gas turbine generator and diesel generator non-IPS plant configuration. This utilized the higher power gas turbine generators more frequently than in the 2 m ice thickness data.

The engine selection process was optimized for lowest acquisition cost, without factoring lifecycle cost considerations. As a result, the combined gas turbine and diesel engine generator configuration provided discrete increments of installed horsepower; installing a propulsion plant which provided the minimum horsepower still meeting powering requirements ultimately resulted in lowering the expected acquisition costs.

Moving forward, incorporating cost per operating hour data would more accurately reflect the positives impacts of limiting number of engines selected. Limiting the number of installed engines, while considering maintenance as well as operational costs, would certainly impact the decision to incorporate a non-IPS diesel and gas turbine generator system.

4.4 Motions

Generally speaking, U.S. icebreakers, especially those focused on a mission in the Antarctic, are concerned about the ship motions when transiting 9,500 miles from Seattle to the South Pole. Traditional icebreaker hulls, such as those found in the Polar class vessels, are notoriously rough riding in an open seaway. In order to investigate the role of ship motions in icebreaker design, a cursory investigation into the trade-off between seakeeping and cost was performed. The sea keeping

(operability) approach was presented in *DeNucci, et al. (2015)*. Fig. 10 shows that seakeeping performance of icebreakers can be improved, but with a penalty of increased length requirements of the vessel. Designs with poor seakeeping performance were less than 110 m long and featured superstructures with a disproportionately large freeboard. The weight distribution of these vessels showed allocation forward of the ship's longitudinal centre of gravity, which again, was attributed to a decrease in ship operability. Designs with the best seakeeping performance were approximately 142 m in length and the superstructure volume and weight was distributed over the length of the design (albeit cost disadvantageous), contrasting the short and tall superstructures found on designs with poorer motions. The weight distribution of the designs with improved seakeeping performance was distributed across the entire length of the ship, instead of being concentrated at one location. It is interesting to note that for a fixed vessel length, weight distribution can play a significant role in the reduction of motions (reducing accelerations by one-third).

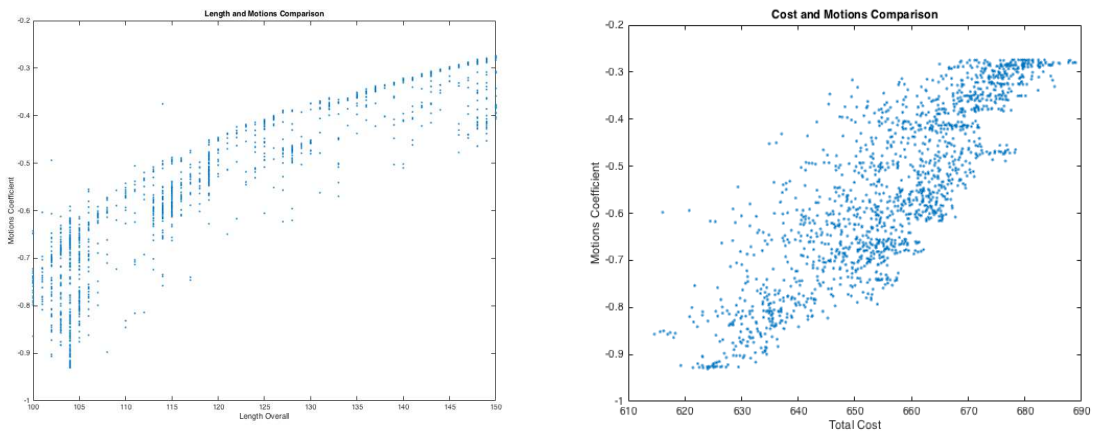


Fig. 10: Seakeeping vs. cost in icebreaker designs

5. Observations & Conclusions

This paper presents an overview an initial foray into icebreaker design using a computer-based synthesis model and genetic algorithm. The observations and main results are outlined below.

- “Bigger is better” is a bad acquisition strategy for icebreakers. Icebreakers are notoriously designed with too much volume. Concept design requires a careful analysis of the requirements, and specific to icebreakers, the volume and area requirement associated with those requirements. Results showed that much smaller and less expensive vessels can meet the same mission requirements as larger icebreakers.
- Target and threshold requirements for icebreaker principle dimensions should be carefully reviewed. Historically, icebreaker height requirements were governed by the location of the aloft conning station while icebreaker beam requirements were typically governed by ice “grooming” lanes and the transverse width of propulsion system. Technological improvements can reduce the footprint of the ship in all dimensions without a loss in capability.
- Ship superstructure has a significant influence on both ship acquisition cost and seakeeping performance. Superstructures should be minimally sized, and their weight should equally distributed over and slightly forward of the ships' longitudinal center of gravity. Auxiliary systems had a more pronounced role in icebreaker acquisition costs than originally anticipated.
- The current prime mover selection process provides a good cursory insight into the icebreaker propulsion plant design space. Since acquisition cost is the primary objective of the optimization process, propulsion systems outside of traditional ship design convention are selected.
- Buying designs – while reducing risk and potentially shortening the acquisition time frame – often result in unnecessary and expensive requirements.

6. Future Considerations

- The beam of the concept icebreakers were limited by the position space of the model (~15m). Despite showing that a functional icebreaker exists at this beam, an increased positioning space for the beam would allow designs that are closer in displacement to icebreaker replacements currently considered by the Coast Guard.
- Future work in propulsion plant optimization includes using an objective function that could include system complexity based costing, total life cycle cost of the propulsion based on maintenance cost per operational hour, fuel cost, reduction gear sizing. Updates to stage 4 of the engine selection process would allow optimization based on maintenance, complexity, efficiency, emissions or life cycle cost depending on available data and requirements.
- Future work will look into dual and Liquefied Natural Gas (LNG) fuelled vessels. This would require LNG tank definition and overlap requirements coincident with the topside placement of storage tanks.

References

- CALDWELL, S. (2011), *Observations on Arctic Requirements, Icebreakers and Coordination with Stakeholders*, U.S. Government Accountability Office Report, Washington, D.C.
- DANTZIG, G. (1957), *Discrete-Variable Extremum Problems*, Operations Research 5(2), pp.266-288
- DENUCCI, T.; SIMIONE, L.; HOPMAN, J., (2015), *Investigating Cost and Operability Optimization in Computer Generated Designs*, 14th COMPIT, Ulrichshusen
- DENUCCI, T. (2012), *Capturing Design: Improving Conceptual Design through the Capture of Design Rationale*, PhD Thesis, Delft University of Technology
- FRANKENSTEIN, G.; GARNER, R., (1967), *Equations for determining the brine volume of sea ice from -0.5°C to -22.9°C*. J. Glaciol. 6(48), pp.943–944
- LEWIS, J.W.; DEBOARD, F.W.; BULAT, V.A., (1982), *Resistance and propulsion of ice-worthy ships*, SNAME Trans. 90, pp-249-276
- KEINONEN, A.; MARTIN, E.; BERROW, D., BROWN, J.; REVILL, C.; SMITH, N. (2010), *Icebreaker Vessel Technologies for USCG Missions*, Tech. Rep. prepared for USCG, Victoria
- MOLLAND, A.; TURNOCK, S.; HUDSON, D. (2011), *Ship Resistance and Propulsion*, Cambridge University Press, pp. 106
- O'Rourke, R. (2016), *Coast Guard Polar Icebreaker Modernization: Background and Issues for Congress*, Congressional Research Service, Washington, D.C.
- TIMCO, G.; FREDERKING, R.M.W. (1996), *A review of sea ice density*, Cold Region Science Technology 24(1), pp.1–6
- VAN OERS, B.J. (2012), *A Packing Approach for the Early Stage Design of Service Vessels*, PhD Thesis, Delft University of Technology
- VAN OERS, B.J.; HOPMAN J.J. (2012), *Simpler and Faster: A 2.5D Packing-Based Approach for Early Stage Ship Design*, Int. Marine Design Conf., Glasgow, pp. 297-316

Corrosion Prediction by Hierarchical Neural Networks

Giulia De Masi, Saipem, Fano/Italy, giulia.demasi@saipem.com

Manuela Gentile, Saipem, Fano/Italy, manuela.gentile@saipem.com

Roberta Vichi, Saipem, Fano/Italy, roberta.vichi@saipem.com

Roberto Bruschi, Saipem, Fano/Italy, roberto.bruschi@saipem.com

Giovanna Gabetta, eni, San Donato Milanese/Italy, giovanna.gabetta@eni.com

Abstract

Internal corrosion of pipelines transporting hydrocarbons is a growing challenge for Oil & Gas industry. The progress in time of internal corrosion, the location along the route and across the pipe section, the development pattern and the depth of the loss of metal are a complex issue: high damage in some sections of pipelines may occur, while in adjacent sections no active corrosion is detected. Being the corrosion phenomenon likely due to different mechanisms, a deterministic approach is not able to predict with enough accuracy the sections more exposed to risk of failure. In the present study, a data-driven model that integrates the analysis of products, transport conditions over the operating lifespan, process fluid-dynamics, pipeline geometrical configuration and the most important deterministic corrosion models produces quite good predictions of section more exposed to corrosion. A multi-scale approach is proposed, based on a cascading set of neural networks that allows corrosion prediction from macro to fine spatial scales.

1. Introduction

Corrosion is one of the principal causes of degradation to failure of marine structures: external sea water corrosion is prevented by the use of an external coating (passive protection) and by cathodic protection (active protection). In addition in a closed sea or in deep water the occurrence of anaerobic condition with the proliferation of sulphate reducing bacteria requires a very clean steel and a strictly control of hardness. While for long transportation pipelines the gas is normally dry and the internal corrosion is not an issue, for flowlines and inter-field lines transporting untreated fluids, internal corrosion plays a crucial role for structure integrity. This is a growing and challenging problem for the Oil & Gas industry, since the age of plants and components is worldwide increasing. Moreover, new frontiers of Offshore Engineering are ultra-deep waters, where remote treatment is performed on floating processing units: in this case, also integrity of flowlines and risers has to be assessed. In order to increase the environmental protection, it is necessary to prevent failures of all these components, *LaQue (1975)*.

Internal corrosion shows a very complex phenomenology due to interaction of different mechanisms. Water and electrochemistry, protective scales, flow velocity, steel composition and localized bacteria attacks are the most relevant, *Palmer and King (2008)*.

While it is reasonably easy to understand a corrosion event “retrospectively” with failure analysis methods, a large degree of uncertainty is associated with the attempt of quantifying a prediction for the future evolution of damage.

Relevant engineering analysis is multi-disciplinary and includes different tasks: analysis of products, transport conditions over the operating lifespan, process fluid-dynamics and pipeline configuration on the real seabed, *Bruschi et al. (2013)*.

An effective corrosion modelling methodology would be based on fundamental laws and first principles since analyses could be performed over a wide range of conditions with some degree of confidence. But corrosion mechanisms are not yet understood well enough to develop purely first-principles mechanistic models, although this is the final goal of research on corrosion. For this reason semi-empirical and empirical models have been studied. Unfortunately, due to its complexity, the

localized corrosion process is hardly reproduced even by semi-empirical models proposed in literature, *De Waard and Lotz (1993), De Waard et al. (1995), Norsok Standard (1998)*.

Field data, nowadays increasingly available, e.g. from internal line inspections (ILI) by intelligent pigs, allows the development of data-driven fully empirical models that can be useful to process corrosion data, *National Research Council (2011)*. Integrity assessment of specific pipeline during operation, *NACE (2010)* may benefit from analysis and processing of field data from ILI. Given that the uncertainties related to measurements of remaining wall thickness in an intelligent pig are very low, this allows to accurate estimate volume loss and corrosion rate along a specific pipeline.

Among several expert systems and data driven modelling, in this paper artificial neural networks (ANN) have been chosen, *Haykin (1999)*. Given that ANNs are capable of approximating any continuous function, and thus explicit functional relationships among different parameters are not necessary, they are here implemented to recognize pattern of internal corrosion inside the pipeline depending on hydrocarbon characteristics, process fluid-dynamics and pipeline configuration. More notably, ANNs can be useful to build explanatory models, because they explore data sets in a search for relevant variables or groups of variables; the results of such explorations can facilitate the process of model building. This approach certainly requires large data collection, as recently emphasized by *Li et al. (2015)*.

While application of ANNs has already been demonstrated to be very useful for internal corrosion prediction, *Zangari et al. (2006), Liao et al. (2012), Hernandez et al. (2005)*, differently from other publications, the scope of the present paper is to identify along the pipelines *where* the sections with high risk of corrosion are located, *De Masi et al. (2014)*. Analysis of fluid properties (e.g. fluid dynamics, production and transported fluids) along lifetime is crucial to identify critical locations where different corrosion mechanisms might be relevant. Analyses should be performed at different spatial scales, being the phenomenon partially global on the whole length of the pipe (generalized corrosion), partially medium scale (corrosion due to increase/decrease of fluid-velocity or passage of slugs), partially very local scale (for instance, stagnant water regions).

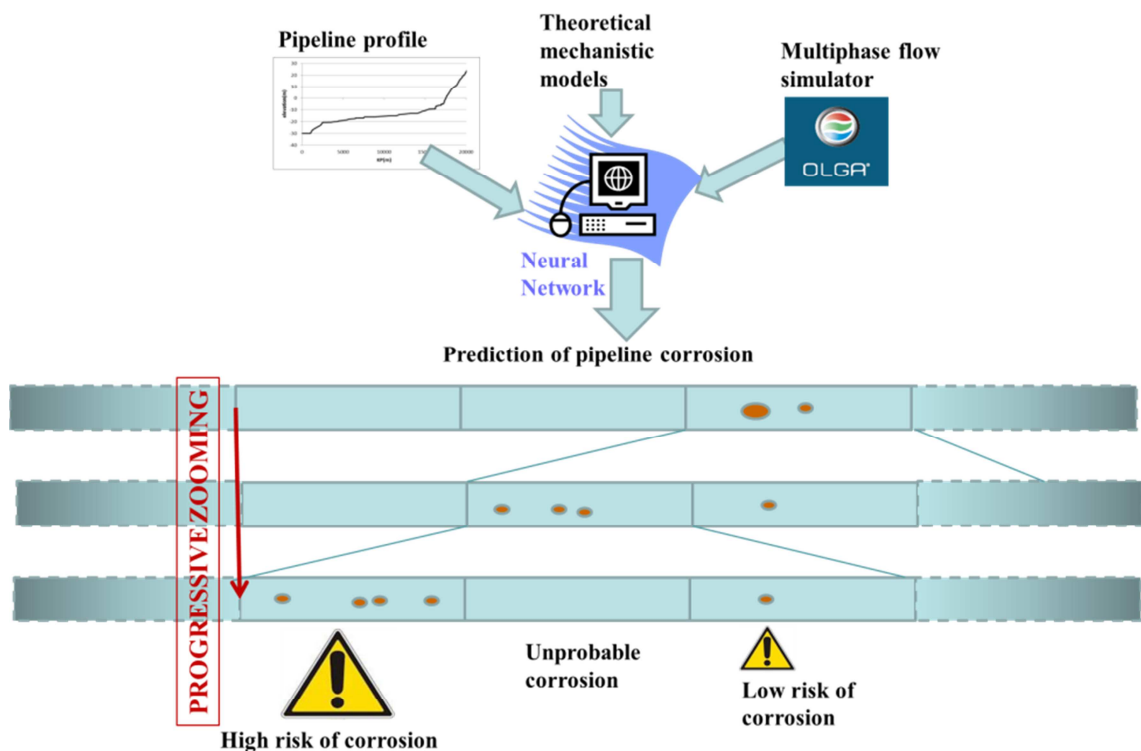


Fig. 1: Scheme of the model

A detailed scale of 10 m (close to 12 m, the average length of pipe joints) is considered an appropriate scale, because integrates information of all defects observed in each 10 m sector, automatically making less important isolated pits that can be due to different reasons (like defects of material) and automatically removing possible shifts and misalignments of instruments. It is also suitable from the point of view of integrity assessment in order to identify the pipe joints where to do more specific integrity measurements.

As in *De Masi et al. (2015)*, the ANN learns from field corrosion data and integrates this information with corrosion estimation by mechanistic models, fluid-dynamic simulations and pipeline geometry, in order to identify sections more exposed to corrosion. In the present paper, a further development, based on a multi-scale approach, has been adopted, as reported in Fig. 1: a set of cascading ANNs, each one representing the phenomenon at a different spatial scale, has been designed. A progressive zoom on three scales has been implemented from coarse to fine, being each scale 1/10 of the superior one. Each network, except the one representing the coarse scale, has an additional input, which is the average volume loss predicted at the superior scale sector of pertinence. This multi-scale approach allows obtaining good prediction at 10 m scale.

2. Methodology

2.1. Product characterization and historical data collection

In the first phase, it is required to collect and then organize all existing, relevant, essential, historic and current operating data about the pipeline segments and/or regions relevant to corrosion distribution.

The types of data collected are typically available in design and construction records (e.g. routes, material, flow rates, design pressures and temperatures, fluid composition and microstructure), operating and maintenance histories, corrosion survey records, gas and liquid analysis reports, and inspection reports from prior integrity evaluations or maintenance actions.

2.2. Multiphase flow regimes

Once identified a representative scenario of fluid-dynamic boundary conditions, multiphase flow modelling is done using OLGA software, OLGA Ver.7.2. As the operating conditions vary along the route, this program determines temperature profile along the pipeline, pressure profile, velocity profiles of each phase, hold-ups and flow regimes, given boundary pressure, temperature values and flow composition.

The profile of fluid dynamic variables like flow regimes and hold-ups is extremely useful in order to categorize locations along a pipeline for susceptibility to and severity of corrosion damage. In our specific case, regime is usually stratified or slug. Water can be considered a phase separated from gas, at the bottom of pipe. Water wetting of the pipe wall plays a crucial role for this kind of corrosion.

Moreover, pressure, temperature, liquid flow velocity, wall shear stress and so on, are used in the corrosion rate calculations, i.e. as input parameters of the available corrosion models. The factors contributing to the distribution of corrosion within each flow regime are identified by the ANN model and the locations of different corrosion damage severity can be predicted (e.g. deposits of formation water, or condensed water, high flow velocities, etc.).

2.3. Geometric profile

The choice of a significant profile and consequently inclination and concavity to set as input for ANN inputs is a very crucial issue. Generally, a profile, i.e. KP vs. Elevation, provided by an ILI inspection is quite accurate: the spacing among the samples may be very low, in order of 20 – 30 cm. So the number of points to describe kilometres of pipelines may be huge (hundreds of thousands). At the

same time, the variations of geometrical sizes among adjacent points are quite small (flat trend). In order to reduce this number and obtain significant variations of the geometrical variables, a filtering of the profile has been performed. The filter is chosen such that the final profile is representative of main spatial variations, without having too much detail.

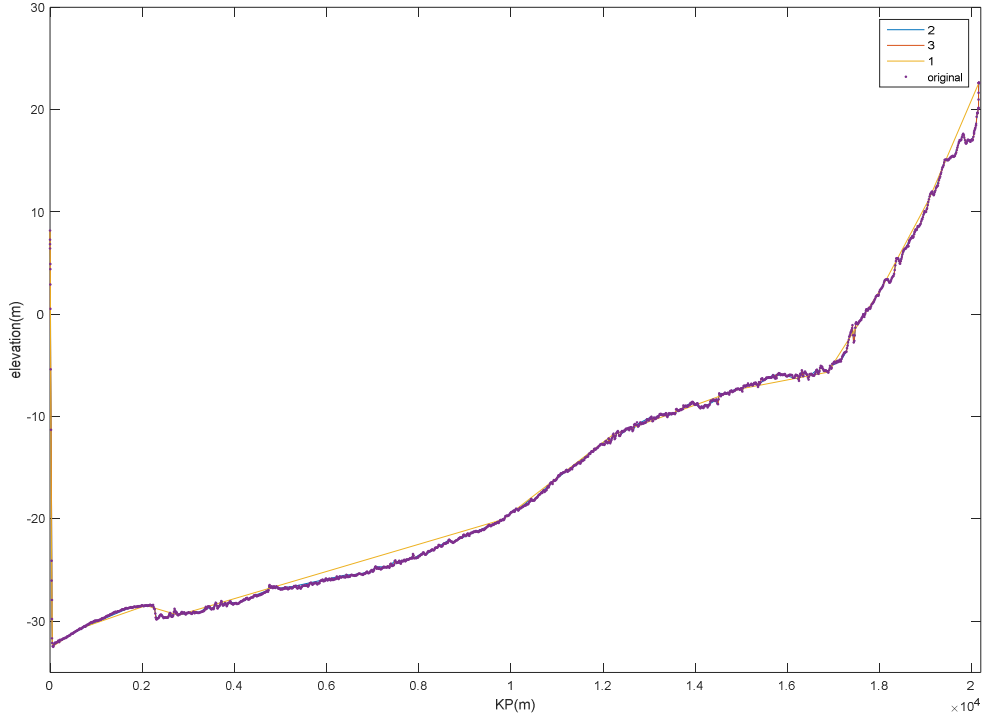


Fig. 2: Original profile and three filtered profile at different resolutions: Profile 1 represents macro scale, profile 2 intermediate, profile 3 fine scale

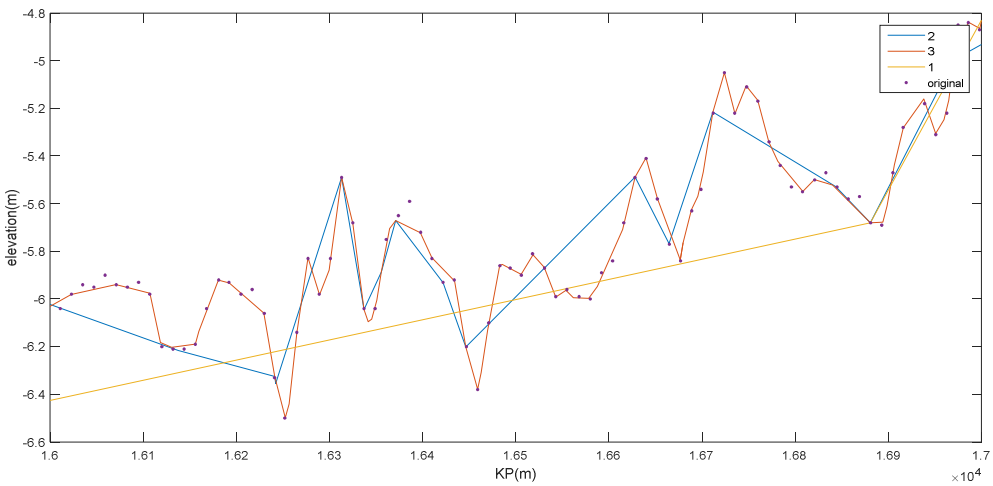


Fig. 3: Zoom on KP=16-17

Filtering procedure allows capturing geometrical variation at scales predetermined by operator. Fig.2 and Fig.3 show original profile and three filtered profiles at different resolutions for a specific pipeline. Evidently, different filters highlight geometrical variations at different scales, from local to macro-scale.

After profile selection, the pipeline has been characterized by its geometrical features: elevation, inclination and concavity. Inclination is demonstrated to play an important role in corrosion process, since water holdups and therefore risk of corrosion increases above certain critical angles. Concavity is expected to be important as well, determining water accumulation.

Inclination (I) is related to pipeline elevation (e). In the point \hat{x} it is defined as:

$$I(\hat{x}) = \arctg\left(\frac{e(\hat{x}+h)-e(\hat{x})}{h}\right) \quad (1)$$

Whereas concavity C is defined as:

$$C(\hat{x}) = \frac{e(\hat{x}+h)-2e(\hat{x})+e(\hat{x}-h)}{h^2} \quad (2)$$

2.4 Deterministic models

Two deterministic models selected by company experience are integrated in the artificial intelligence model here proposed. The first one is *De Waard and Lotz (1993)* model, which correlates corrosion rate (V_{cor}) to temperature (t) and CO_2 partial pressure ($p\text{CO}_2$), by the following relationship:

$$\log(V_{cor}) = 5.8 - \frac{1710}{273+t} + 0.67 \cdot \log(p\text{CO}_2) \quad (3)$$

The second model is proposed by *NORSOK (1998)*: CR is an empirical function of temperature t , CO_2 , pH, wall shear stress. For temperature between 20°C and 120°C:

$$CR_t = K_t \cdot f_{\text{CO}_2}^{0.62} \cdot \left(\frac{s}{19}\right)^{0.146+0.0324 \cdot \log(f\text{CO}_2)} \cdot f(\text{pH})_t \quad (4)$$

For $t=15^\circ\text{C}$

$$CR_t = K_t \cdot f_{\text{CO}_2}^{0.36} \cdot \left(\frac{s}{19}\right)^{0.146+0.0324 \cdot \log(f\text{CO}_2)} \cdot f(\text{pH})_t \quad (5)$$

At temperature 5°C

$$CR_t = K_t \cdot f_{\text{CO}_2}^{0.36} \cdot f(\text{pH})_t \quad (6)$$

2.5. Multi-scale analysis

Corrosion phenomena show double multi-scale properties: temporal as well as spatial. From the temporal point of view, while single electron transfer at metallic surface occurs within femtoseconds and multiple oxide layers require minutes to form via diffusion and multiple reaction cascades, the macroscopic corrosion and decomposition of metallic structures proceeds over decades and even over hundreds of years. In the present study, the time is assumed fixed because only a snapshot of corrosion pattern is provided corresponding to ILI: this is the cumulated effect of corrosion from pipeline installation to ILI occurrence. Therefore, here only the spatial multi-scale behaviour is under investigation.

As reviewed by *Gunasegaram et al. (2014)*, multi-scale behaviour of localized corrosion ranges from 1000km to 1nm. Here a smaller range is investigated: from 20km (average length of the pipeline) to 10m (length of the bar), that can be considered a reliable length to get significant value of volume loss. Furthermore, from a practical point of view, to get field information at finer scales is often not possible.

In Fig.4, multi-scale analysis is sketched from whole length of pipeline (top panel) where behavior at 1000 m scale can be identified, zooming to 1 km medium scale (middle panel), where behavior at 100 m can be observed, zooming further to 100 m pipe section (bottom panel) where 10 m scale behavior can be detected.

From the phenomenological point of view, several scales play a role in localised corrosion inside the considered pipelines. Generalized corrosion plays a global action on the whole length of the pipe, while on a medium scale corrosion is due to increase/decrease of fluid-velocity or passage of slugs, finally on a very local scale stagnant water regions activate local corrosion.

Looking at Fig.5, corrosion is observed where discontinuities in pipeline profile and consequently transition regions for fluid variables are present. Furthermore, the largest number of defects falls in the area where at a macroscopic scale there are changes in pressure, flow rate, and elevation. At medium/small scale, the concentration of most defects is evident at the “transition” from a regime mainly slug to another predominantly layered or vice versa.

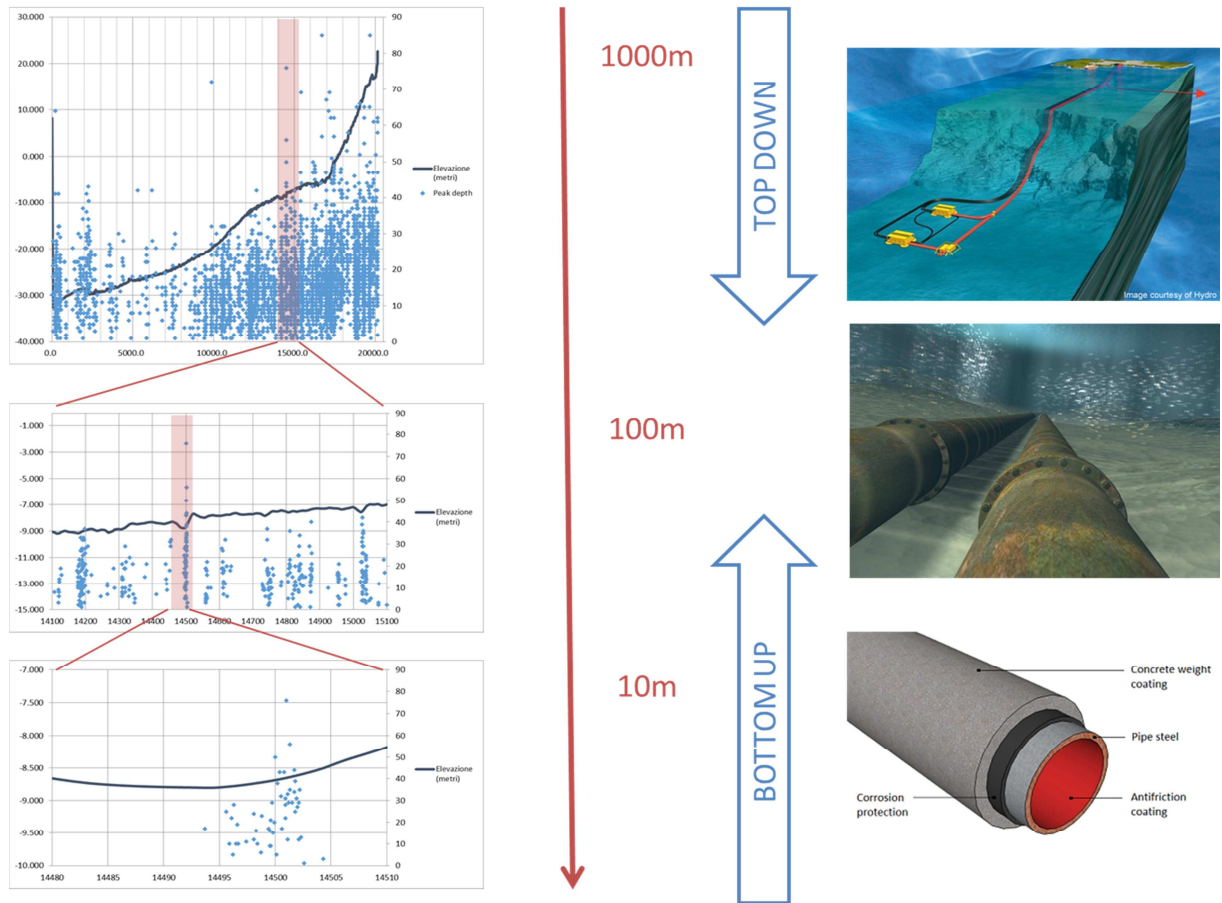


Fig. 4: Multi-scale analysis: geometric profile and defect peak depths, at different scale size (1000 m, 100 m and 10 m).

In order to give an interpretation on where the corrosion is observed, it should be remembered that the ILI observes the corrosion cumulated in several decades, when several fluid-dynamic regimes change and possibly corrosion increased only in particular periods with particular fluid-dynamic conditions. Since geometry remains constant during the operative life of pipeline, it plays a crucial role in the interpretation.

Looking at Fig.4, at macro-scale, corrosion is stronger in sections with change of inclination. Where inclination increases, liquid velocity decreases. A possible explanation is that the liquid, stabilizing and slowing in that area, can create greater corrosion. On the contrary, probably a system more stable and less turbulent allows CO₂ to better solubilize in the liquid and, at the same time, allows the liquid to better wet the wall. Moreover, where inclination changes, slug phenomena are more frequent.

At a medium scale it is evident that corrosion appears in sections with high hold-up and slug regime, where gas velocity is higher and water velocity is lower (see middle panel of Fig. 5). Large wall wetting allowed by high hold-up creates conditions appropriate for corrosion. Slugs can also increase corrosion, by turbulent removal of oxide protection from crevices. Finally, zooming further, at finer scale defects are observed in concave sections (where up-hill rise starts) which correspond to transition to high hold-up, slug regime, decreasing water velocity and increasing gas velocity, all conditions suitable for local corrosion.

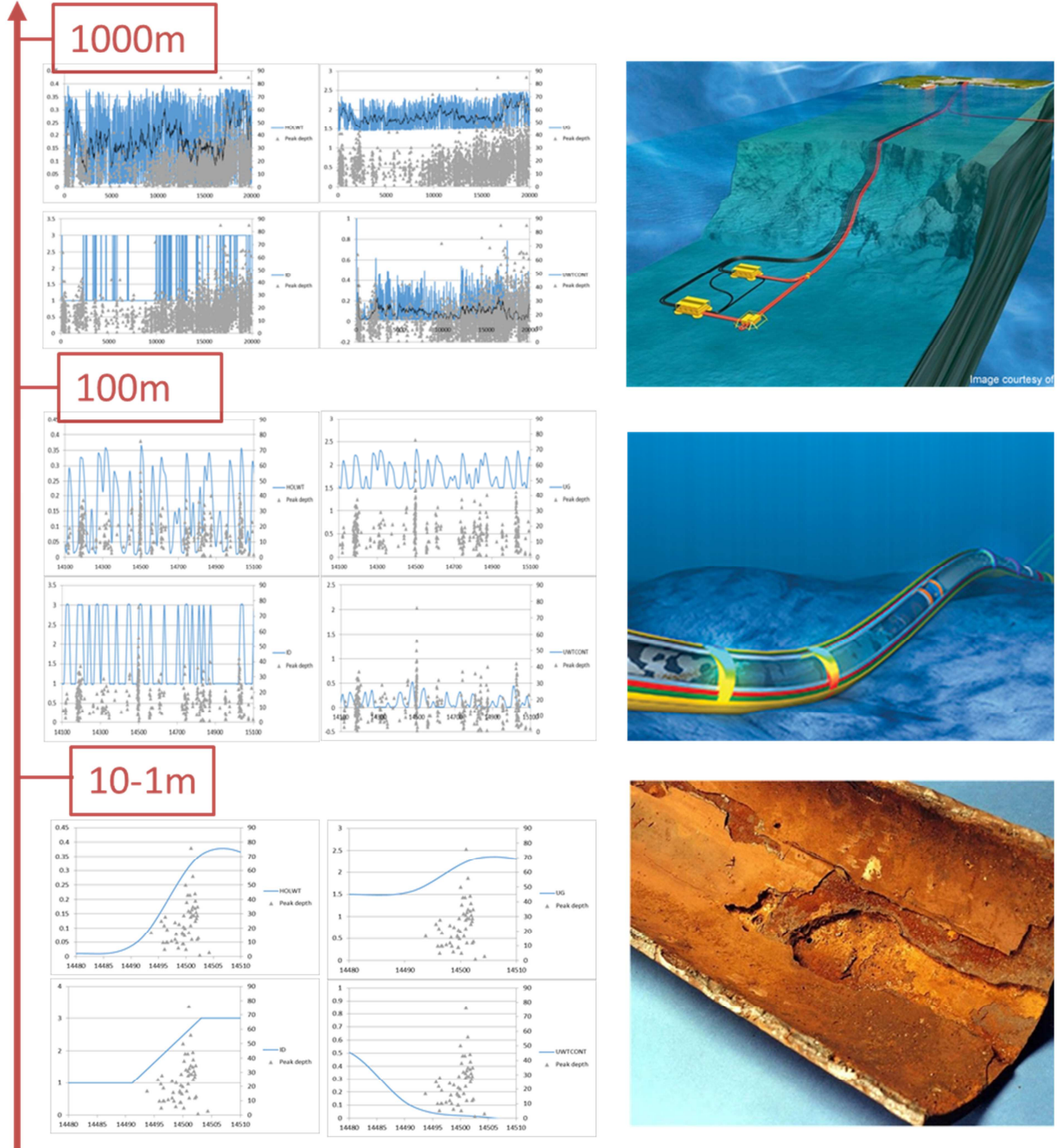


Fig. 5: Multi-scale analysis: defect peak depth (grey dots) and fluid-dynamic significant variables (blue lines), as provided by OLGA, at different scale size (1000 m, 100 m and 10 m): hold-up (HOLWT), regime (ID), gas velocity (UG) and water velocity (UWTCNT) along the pipeline

2.6. Neural Network model

In the present study, a hierarchical cascading set of fitting neural networks, each one representing the phenomenon at a different spatial scale, is implemented. An ensemble approach is adopted to improve the prediction. A detailed description of the model is reported step by step: 1) description of fitting networks; 2) realization of an ensemble; 3) hierarchical model, which is the core of the present paper.

2.6.1. Fitting neural networks

Fitting networks (FNN) are feedforward neural networks used to fit an input-output relationship, Haykin (1999). From literature it has been demonstrated that two (or more) layer fitting networks can fit arbitrarily well any finite input-output nonlinear relationship, given enough hidden neurons. The network structure is reported in Fig. 6.

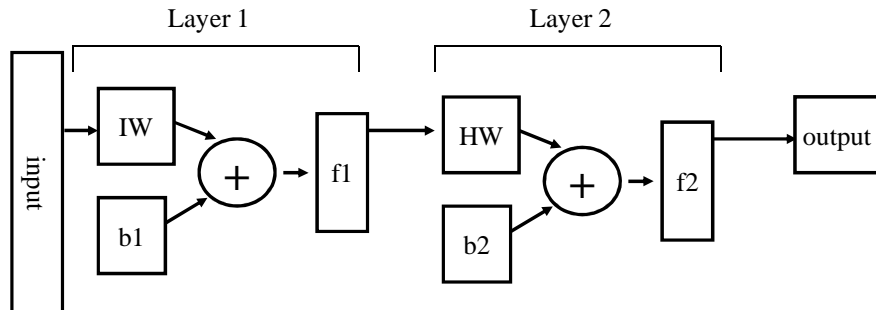


Fig.6: Feed forward ANN architecture

In the present study, input variables are of five types, Fig. 7:

- Historical data: here only the pipeline operative life has been reported
- Hydrocarbon characteristics (CO_2 partial pressure)
- Geometrical pipeline characteristics (elevation, inclination, concavity)
- Fluid dynamic multiphase variables (flow regime, pressure, gas flow, total flow, liquid velocity, gas velocity)
- Deterministic models (de Waard and NORSOOK)

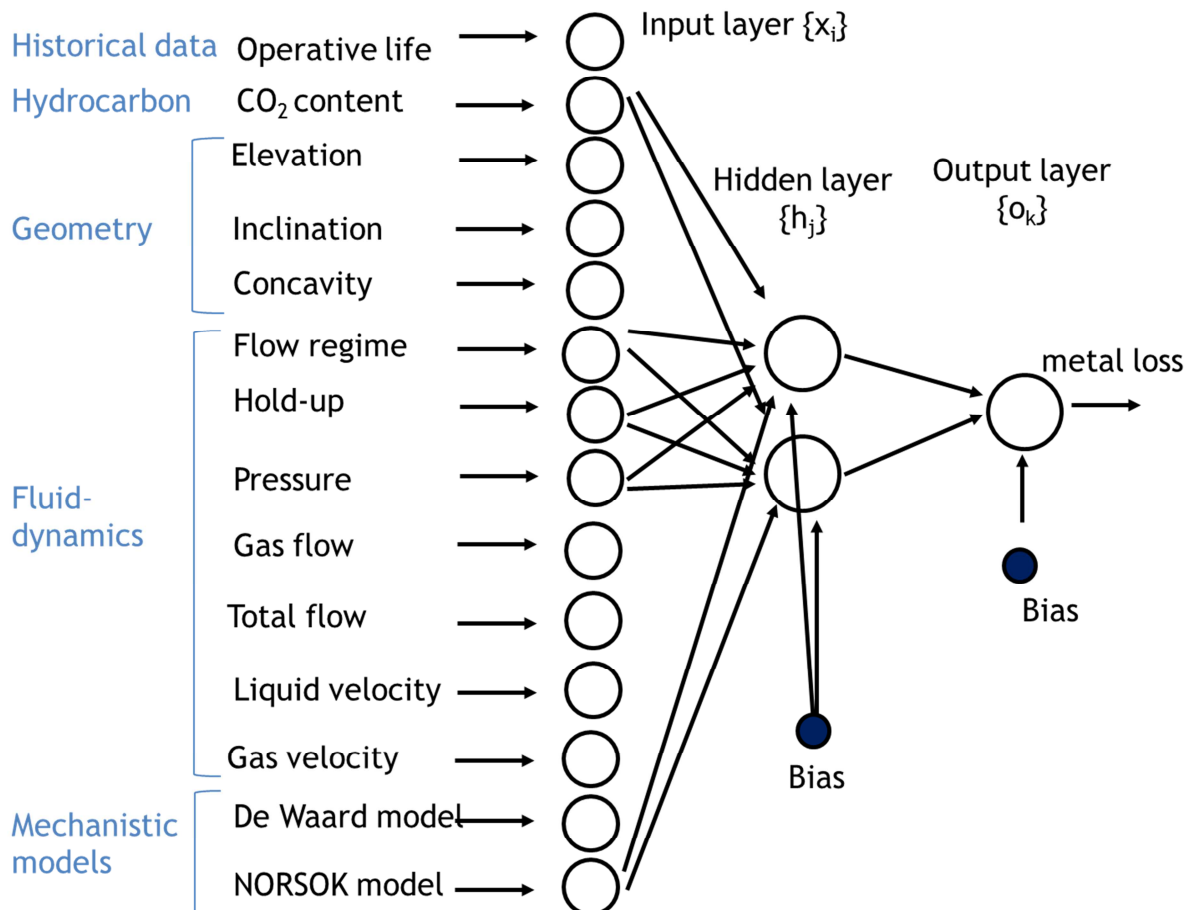


Fig.7: FNN architecture with all inputs and alternative outputs (intermediate arrows are not indicated)

Each network has only one output, the total metal loss on the representative sections (1000 m, 100 m and 10 m for the first, second and third cascading ANN, respectively).

The optimal configuration of weights and biases is obtained by a training algorithm, minimizing an error function between the observed and predicted series. Several training algorithms have been tested; finally the Levenberg-Marquardt back propagation algorithm was selected as the one producing best prediction. By a sensitivity study, it has been previously demonstrated that 20 hidden neurons produce the best network performance, *De Masi et al. (2013)*.

2.6.2 Ensemble of neural networks

Given the obvious importance of connection weights in assessing the relative contributions of the independent variables, the optimal connections weights configuration has to be identified. During the optimization process, it is necessary that the network converges to the global minimum of the fitting criterion (e.g. prediction error) rather than to one of the many local minima. Connection weights in networks that have converged to a local minimum will differ from networks that have globally converged, thus resulting in the misinterpretation of variable contributions. In order to overcome this problem, a possible approach consists in combining different local minima rather than choosing between them, for example, by averaging the outputs of networks using the connection weights corresponding to different local minima, *Perrone and Cooper (1993), Naftaly et al. (1997)*. Therefore, an ensemble of ANNs is generated, obtaining better performances than any individual model, because the models errors "average out."

The network ensemble is a solution to the bias–variance tradeoff (or dilemma), that is the problem of simultaneously minimizing two sources of error that prevent supervised learning algorithms from generalizing beyond their training set: i) the bias is the error from erroneous assumptions in the learning algorithm. High bias can cause an algorithm to miss the relevant relations between features and target outputs (under-fitting); ii) the variance is the error from sensitivity to small fluctuations in the training set. High variance can cause overfitting, i.e. modeling the random noise in the training data, rather than the intended outputs.

To solve this dilemma, the theory of ensemble averaging relies on two properties of ANNs: i) In any network, the bias can be reduced at the cost of increased variance; ii) in a group of networks, the variance can be reduced at no cost to bias.

Ensemble averaging consists in a group of networks, each with low bias and high variance, which are combined into a new model with low bias and low variance. It is thus a solution of the bias-variance dilemma.

A statistical ensemble of equivalent ANNs, differing only for their initial synaptic weights, is realized, as sketched in Fig. 8. All predictions are then averaged out.

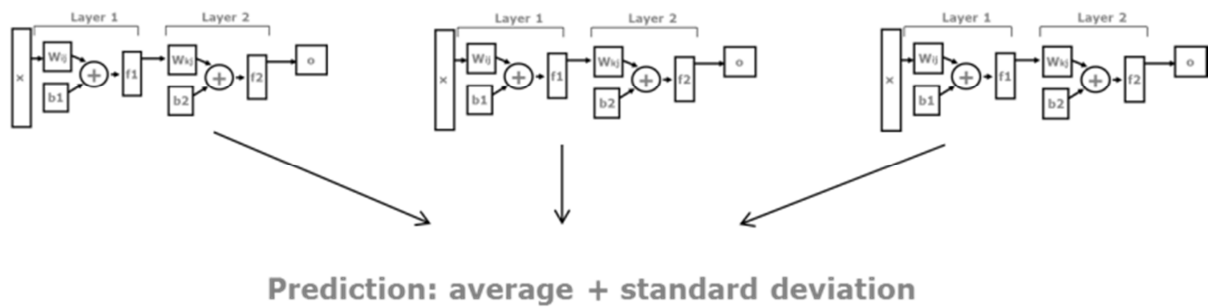


Fig.8: Ensemble of FFNN

2.6.3 Hierarchical Neural Networks

In order to represent multi-scale phenomenology and to obtain prediction of regions more exposed to corrosion also at fine scale (for our purposes 10 m), a hierarchical approach has been adopted: a set of cascading ANNs, each one representing the phenomenon at a different spatial scale (1000 m, 100 m, 10 m) has been designed. A progressive zoom on three scales has been implemented from coarse to fine, being each scale 1/10 of the superior one. Each network, except the one for coarse scale, has an additional input, which is the average volume loss predicted at the superior scale of pertinence.

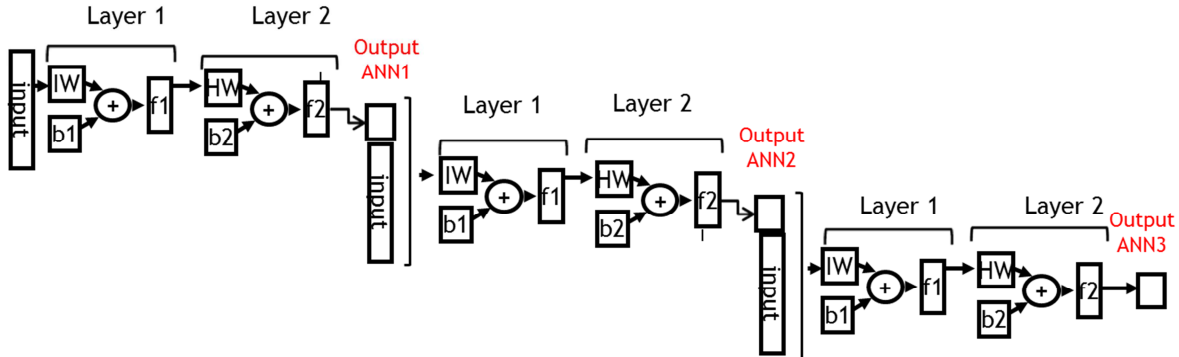


Fig. 9: Hierarchical neural networks

As evident from Fig. 9, the first ANN produces prediction at macro-scale (1000 m) identifying the main factors producing corrosion in the large sections. Its output is fed as an additional input into the second ANN that identifies within the large area which subsections have flow regimes more suitable for corrosion. This second ANN produces a middle-scale (100 m) prediction that is fed as additional input into the third ANN. This ANN, zooming further in smaller subsections, identifies regions of stagnant water and fluid regime transitions, producing prediction at finest scale (10 m).

2.6. Randomization test

A randomization test is done in order to evaluate statistical significance of model results. In particular, using the same input set, the output variable values are randomly permuted. The results obtained under this null hypothesis are compared with results obtained from actual dataset.

3. Application

3.1. Corrosion data

Corrosion database at the moment consists of internal line inspections (ILI) of four pipelines from the same geographic region in Mediterranean Sea. All pipelines transport wet gas and are made with the same carbon steel. Two pipelines are from platform to landfall and two are from platform to platform. All data are used to train the model, distinguishing the two cases of “platform to landfall” and “platform to platform” configurations.

Unfortunately, the datasets do not have same accuracy. One dataset (here called pipeline A) is very accurate, also at very fine scale, both regarding corrosion data and geometric profile, by an advanced internal line inspection by pig with GPS. Even in this case, a prediction below 10 m is not reliable enough, even if declared instrument resolution is much higher.

A second pipeline (B) has good corrosion data but very poor geometric profile, not geographically referenced, produced by two different instruments, because half of pipeline is buried. Poorly geometric definition implies poor fluid-dynamic profile. In this case, even 10 m prediction is not feasible because of difficulties to match pipeline profile with pattern obtained from in-line inspection. Pipeline A and B are around 20 km long and around 30 years old.

The two other pipelines (C and D) are very similar regarding operative life (13 years), length (15 km), geometric profile but show corrosion different by more than one order of magnitude. Also position of defects with respect to geometric profile is very different between the two pipelines. Fig. 10 shows the integration of data from the four pipelines in ANN model.

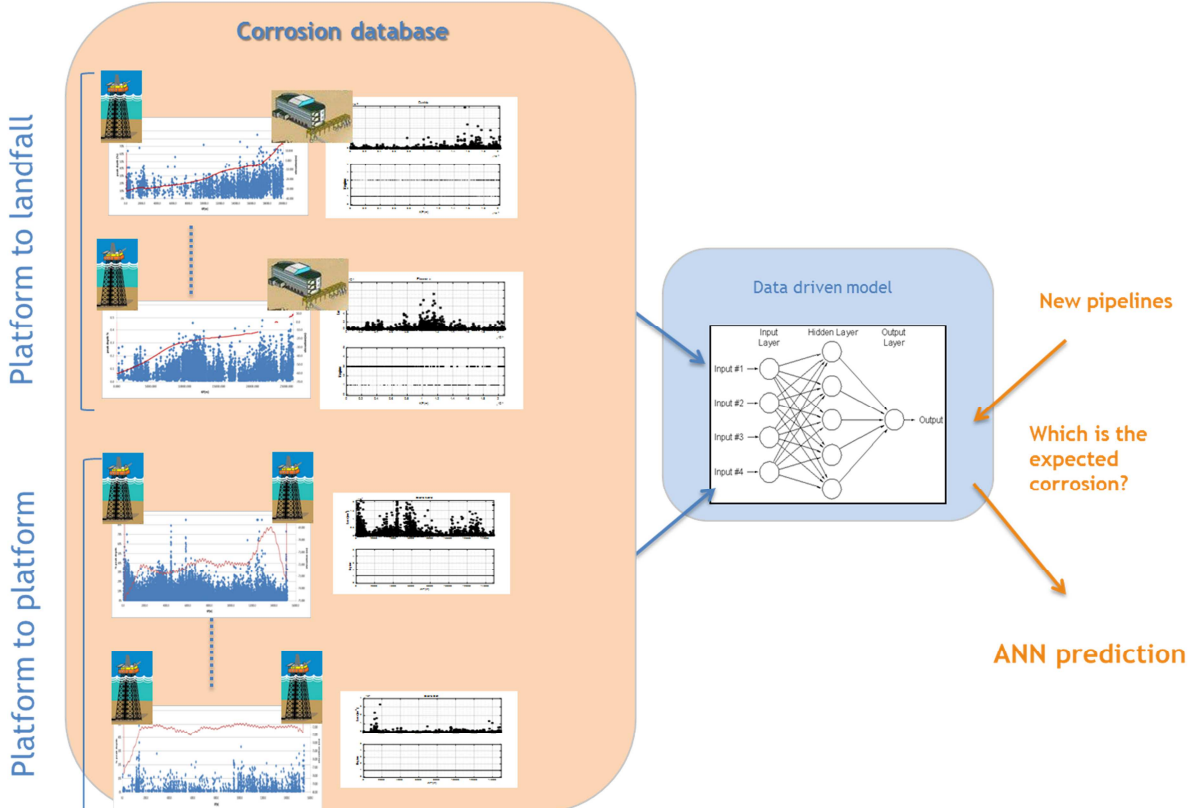


Fig.10: Overall model scheme: for each pipeline are sketched defect depth along the profile (left panel), volume loss (top right panel) and fluid regime (bottom right panel).

Pipelines are grouped as “platform to landfall” and “platform to platform”. For each pipeline, all input data described in Fig. 7 are collected and fed into the ANN model, using corrosion volume loss as a target to train the model.

3.2 Statistical measurements

In order to evaluate performances of ANN predictions some indices have been chosen:

Pearson correlation coefficient (defined between -1 and 1)

$$R = \frac{\sum_{i=1}^N (p_i - \bar{p})(o_i - \bar{o})}{\sqrt{\sum_{i=1}^N (p_i - \bar{p})^2 \sum_{i=1}^N (o_i - \bar{o})^2}}$$

Scatter index (lower bounded to 0: closer values to 0 indicate better agreement between the two series)

$$SI = \frac{RMSE}{\bar{o}}$$

Efficiency Coefficient (upper bounded to 1: closer values to 1 indicate better agreement between the two series)

$$CE = 1 - \frac{\frac{1}{N} \sum_{i=1}^N (p_i - o_i)^2}{\frac{1}{N} \sum_{i=1}^N (o_i - \bar{o})^2}$$

3.3 Results

Considering the dataset with highest resolution (pipeline A), three subsets are randomly defined at macro scale: training set, validation set and testing set (randomly sampled respectively as 70%, 15% and 15% of initial dataset).

Using the hierarchical model (Par.2.5.3), consisting of three cascading ANNs, the goal is to predict total volume loss on the testing set at finest scale: from macro (1000 m), to medium (100 m) to end up to fine scale (10 m).

Results are reported in Fig. 11. The top left panel shows prediction at macro scale (1000 m) produced by the first ANN, the central panel prediction at medium scale (100 m) obtained by second ANN, and the right bottom panel prediction at fine scale (10 m) obtained by the third ANN. Top right panel shows a zoom on a specific sample of testing set (10 m). Prediction is very good, as also evident from statistical measurements reported in the first row of Table I.

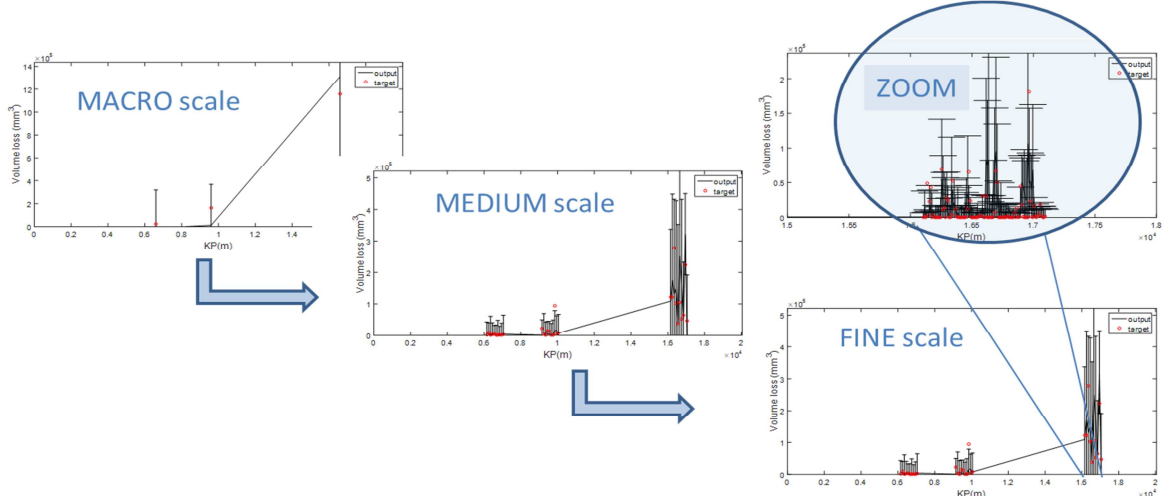


Fig. 11: Results of the multi-scale model. Top left panel shows prediction at macro scale (1000 m), central panel at medium scale (100 m), right bottom panel at fine scale (10 m). Top right panel shows a zoom on a specific sample of testing set (10 m).

Table I: Statistical measurements

Model	SI	R	CE
Hierarchical ANN (10 m)	0.6	0.85	0.65
ANN ensemble (100 m)	1.3	0.8	0.2
ANN ensemble (10 m)	2.9	0.7	-0.8
Single ANN(100 m)	2.3	0.6	0
Null hypothesis(100 m)	2.5	0.5	-5.6

Table I reports a comparison of statistical measurement among the present model (Hierarchical ANN) with past different models:

- a) Single scale ANN ensemble for sections 100 m long
- b) Single scale ANN ensemble for sections 10 m long, producing not very good results
- c) Single ANN
- d) Null hypothesis model

Models (a), (c) and (d) were developed for 100 m long sections, *De Masi et al.* (2015); results at lower scale were not acceptable: see e.g. very poor results of the ensemble model developed for 10 m sections (indicated by b). On the contrary, the present hierarchical model strongly improves prediction performance at 10m scale, producing also the best results among all the past models.

4. Conclusions

The prediction of internal corrosion along the pipeline route is a critical issue for the Oil & Gas industry. Corrosion assessment during the design phase has a great impact on the material selection (the choice between carbon steel, stainless steel or alloys) and therefore on pipeline costs. A reliable prediction of pipeline sections where corrosion risk is higher, would help pipeline integrity management. Furthermore, given the worldwide increasing number of old pipelines, this issue is particularly relevant also to avoid pipeline failures and their health, safety and environmental impact.

Since the corrosion phenomenon is due to different mechanisms, a deterministic approach is not able to reproduce the corrosion rate and the defects distribution observed during pigging activity. Furthermore, it is practically impossible to formulate a functional relationship between relevant parameters, which may cover all potential mechanisms. For this reason, a Machine Learning data-driven method based on artificial neural networks (ANN) has been adopted. The model integrates different kinds of information that play a crucial role for corrosion development: product characteristics, transport conditions over the operating lifespan, process fluid-dynamics and pipeline configuration on the real seabed.

In a previous work, *De Masi et al.* (2015), an artificial intelligence model has been proposed, considering several contributions to corrosion and several network inputs: geometrical pipeline features, fluid dynamic multiphase variables and deterministic models. The model obtained good predictions at 100 m scale. In the present paper, the methodology is further improved, in order to obtain prediction at finer scales (10 m). For this purpose, a hierarchical approach has been adopted in order to represent the inherently multi-scale phenomenology: a set of cascading ANNs, each one representing the phenomenon at a different spatial scale has been designed. A progressive zoom on three scales has been implemented from coarse (1000 m) to fine (10 m), being each scale 1/10 of the superior one. Each network, except the one for coarse scale, has an additional input, which is the average volume loss predicted at the above scale sector of pertinence. In particular, the first ANN identifies the main factors producing corrosion in the large sections (1000 m). The second ANN identifies, within the large area, which subsections have flow regimes more suitable for corrosion, producing a middle-scale (100 m) prediction. The third ANN, zooming further in smaller subsections, identifies regions of stagnant water and fluid regime transitions, producing prediction at finest scale (10 m).

Field measurements derived from internal line inspections of four pipelines have been processed. The analysed pipelines are affected by CO₂ corrosion and possibly bacteria activity. The observed corrosion pattern is very complex, showing high damage in some sections of pipelines, while in near sections no active corrosion is detected. Despite this large complexity, the multi-scale model seems to capture main evidences of local corrosion, providing a promising methodology for crucial assessment.

Predictions can be further improved in the future considering larger datasets (with several pipeline cases and different flow conditions). This would allow:

- to improve the generalization capability of the model;
- to extend the model to different conditions;
- to perform sensitivity analysis to properly identify the most important variables at each scale, without possible biases related to small dataset.

Further developments regard the temporal dynamic investigation of corrosion pattern formation, assuming different hydrocarbon boundary conditions representative of the pipeline life span, *Din et al.*

(2015). The long term goal of the research is the prediction of internal corrosion risk for non-piggable pipelines: the identification of pipeline sections with higher risk of corrosion will indicate where performing localized inspections and direct assessment. The final instrument can be used as an assistance tool for any decision in direct assessment of pipelines.

References

- BRUSCHI, R.; CHERUBINI, P.; VICHI, R.; GENTILE, M. (2013), *Integrity management on pipeline affected by corrosion*, IBP1471_13, Rio Pipeline Conf. & Exposition, Rio de Janeiro
- DE MASI, G.; VICHI, R.; GENTILE, M.; BRUSCHI, R.; GABETTA, G. (2014), *A neural network predictive model of pipeline internal corrosion profile*, IEEE SIMS (Systems Informatics, Modelling and Simulation), Sheffield
- DE MASI, G.; VICHI, R.; GENTILE, M.; BRUSCHI, R.; GABETTA, G. (2015), *Machine learning approach to corrosion assessment in subsea pipelines*, IEEE Oceans, Genoa
- DE WAARD, C.; LOTZ, U.; DUGSTAD, A. (1995), *Influence of liquid flow velocity on CO₂ corrosion: A semi-empirical model*, NACE, Corrosion 1995, Paper N°128
- DE WAARD, C.; LOTZ, U. (1993), *Prediction of CO₂ corrosion of carbon steel*, NACE Corrosion, Houston, Paper N°69
- DIN, M.M.; ITHNIN, N.; ZAIN, A.; NOOR, N.; SIRAJ, M.; RASOL, R. (2015), *An artificial neural network modelling for pipeline corrosion growth prediction*, ARPN J. Eng. and Applied Sciences 10/2
- GABETTA, G.; TRASATTI, S.P. (2006), *Analysis of CO₂ corrosion model by Neural Networks*, Eurocorr, Maastricht
- GUNASEGARAM, D.R.; VENKATRAMAN, M.S.; COLE, I.S. (2014), *Towards multiscale modelling of localised corrosion*, Int. Materials Reviews 59(2)
- HAYKIN, S. (1999), *Neural Networks, A Comprehensive Foundation*, Prentice Hall
- LAQUE, F. L. (1975), *Marine Corrosion: Causes and Prevention*, Wiley
- LI, X.; ZHANG, D.; LIU, Z.; LI, Z.; DU, C.; DONG, C. (2015), *Share Corrosion Data*, Nature 527, pp.441-442
- HERNÁNDEZ, S.; NESIC, S.; WECKMAN, G.; GHAI, V. (2005), *Use of Artificial Neural Networks for Predicting Crude Oil Effect on CO₂ Corrosion of Carbon Steels*, NACE Corrosion Conf., Houston, Paper No. 05554
- NAFTALY, U.; INTRATOR N.; HORN, D. (1997), *Optimal ensemble averaging of neural networks*, Network: Comput. Neural Syst. 8, pp. 283–296
- NACE, *Wet Gas Internal Corrosion Direct Assessment Methodology for Pipelines* (2010), NACE SP0110-2010, Item No. 21146
- NATIONAL RESEARCH COUNCIL (2011), *Research Opportunities in Corrosion Science and Engineering*, Committee on Research Opportunities in Corrosion Science and Engineering
- NESIC, S.; NORDSVEEN, M.; MAXWELL, N.; VRHOVAC, M. (2001), *Probabilistic modelling of CO₂ corrosion laboratory data using neural networks*, Corrosion Science 43/7, pp.1373-1392

NORSOK Standard N°M-506 (1998), *CO₂ Corrosion Rate Calculation Model*, Rev.1, Norwegian Technology Standards Institution, <http://www.nts.no/norsok>

OLGA, Multiphase Flow Simulator, by ScandPower Petroleum Technology, Ver.7.2.

PALMER, A.C.; KING, R.A. (2008), *Subsea Pipeline Engineering*, PennWell Books

PERRONE, M.P.; COOPER, L.N. (1993), *When networks disagree: Ensemble methods for hybrid neural networks*, Artificial Neural Networks for Speech and Vision, Chapman and Hall, pp.126-147

ZANGARI, G.; GABETTA, G.; TRASATTI, S.P. (2006), *Analysis of CO₂ corrosion models by neural networks*, Eurocorr, Maastricht

VISIR: A Free and Open-Source Model for Ship Route optimization

Gianandrea Mannarini, Centro Euro-Mediterraneo sui Cambiamenti Climatici, Lecce/Italy,
gianandrea.mannarini@cmcc.it

Nadia Pinardi, Università di Bologna, Bologna/Italy, n.pinardi@sincem.unibo.it

Giovanni Coppini, Centro Euro-Mediterraneo sui Cambiamenti Climatici, Lecce/Italy,
giovanni.coppini@cmcc.it

Abstract

VISIR (discoVerIng Safe and effIcient Routes) represents an attempt to build a fully open ship routing model. This is achieved through a GPL licensing of the source code and detailed model documentation on open-access journals. This way, numerical optimization methods, hydrodynamic effects considered, approximations used, and their ranges of application are documented and made available to the research, technical, and even business communities. VISIR's main architectural choices, main logical components, and an outline of possible goals for a future community of VISIR developers and users are presented here.

1. Introduction

Several commercial weather routing software programs for ships are currently available. They often have appealing features in terms of vessel modeling and algorithms used for route computation and optimization, *Walther et al. (2014)*. However, as their source code is not available and related technical documentation is poorly published, such products partially act as “black boxes” with respect to how the nominal product features are actually implemented. This situation is likely to hinder possible breakthroughs arising from a collaborative scientific environment, or an “open science” paradigm, *Pontika (2015)*. Given the global significance of maritime transportation and the push for increasing its overall efficiency and in particular for reducing its environmental impact, *Mannarini (2015a)*, such further developments should be more than fostered.

As an outcome of publicly funded research (projects TESSA <http://tessa.linksmt.it>, IONIO <http://www.ioniproject.eu/>, AtlantOS <http://atlantos-h2020.eu/structure/overview/>), VISIR ([vi'zi:r], discoVerIng Safe and effIcient Routes) represents an attempt to build a fully open ship routing model. This includes a copylefted (GPL v.3) free and open-source code, www.visir-model.net, *Mannarini et al. (2015b)*, and an open review of related scientific publications on open access journals. This way, hydrodynamic effects, numerical methods, approximations used, and their ranges of application are extensively documented and made publicly available.

It is not just the research and technical community that benefits from this approach, but possibly also the business community. As a matter of fact, the open setup of the VISIR model did not prevent the building of an operational, user-oriented Decision Support System for safer and efficient navigation in the Mediterranean Sea, *Mannarini et al. (2016)*.

Whether for science or for business, numerical code quality remains a top priority in the agenda of maritime stakeholders, as it may indirectly affect the safety of navigation, *Lee and Alexander (2013)*. This is why in the construction of the VISIR source code we attempted to follow the best practices from software engineering, *Wilson et al. (2014)*, though we recognize that the system is still far from being a full-featured industrial product. Nevertheless, we are glad to offer the best of our efforts for enabling and easing further improvements of VISIR.

2. Ship route optimization

VISIR aims at optimizing nautical routes in the presence of both static and dynamic constraints arising from the ocean topology and environmental conditions, *Mannarini et al. (2015b)*.

Motor vessels with displacement hulls are considered in the first version of the model (VISIR-I). Friction and form resistance can be parameterized as polynomials in the Froude number. The peak value of wave added resistance is assumed to scale linearly in terms of Froude number and as a power-law with respect to the principal particulars (length, beam, draught), *Alexandersson* (2009). The spectral and angular dependence of the wave added resistance is neglected in VISIR-I.

Vessel intact stability is considered through checks for the activation of parametric roll, pure loss of stability, and surf-riding/broaching-to conditions, *Belenky et al.* (2011).

The optimization algorithm is based on a graph search method by *Dijkstra* (1959). The graph itself is represented as a list of edges and, for enhancing computational performance, the algorithm uses a “forward star” data structure, *Ahuja et al.* (1988). Furthermore, VISIR allows for voluntary speed reduction whenever useful in order to skip route diversions arising from the safety checks.

VISIR is suited for use in the presence of complex topology: routes can be optimized even in sea domains containing peninsulas, islands, and archipelagos. Besides a shoreline and a bathymetry database, the model needs an input forecast or analysis fields of sea state (significant wave height, wave period, and direction). In the current version of the software, they are provided through netcdf files from operational runs of the Wave Watch-III model in the Mediterranean Sea, *Tonani et al.* (2014).

3. Code quality and structure

VISIR model was designed to ingest operational meteo-oceanographic forecasts and eventually become the engine of a new operational Decision Support System, *Mannarini et al.* (2016). Thus, the model had to be robust enough to handle diverse and extreme field values from the operational data feeds. This is why in developing the code attention was given not just to the scientific soundness of the output, *Mannarini et al.* (2015b), but also to the quality of the computer program and its layout, to aid future development by multiple programmers. In the next two subsections we provide more information regarding these topics.

3.1. Best coding practices

VISIR-I is coded in Matlab®. The code of VISIR was designed and implemented with an effort to follow the guidelines from software engineering manuals and collections of best practices in scientific programming, such as those reported by *Wilson et al.* (2014). Nevertheless, VISIR-I is not an industrial product stemming from consolidated requirements. Rather, it is research software developed and re-designed on the fly while at least part of the user-requirements was still being collected, and literature analysis and community interaction were in progress. Thus, some of the best practices have strictly been followed since the beginning, while others are left for the forthcoming development of the code. In general, compliance with principles, *Lee and Alexander* (2013), and ISO norms (especially ISO/IEC 9126) of software quality assurance should be pursued for any (and especially for) safety-related software products, such as those for maritime applications.

In VISIR we considered and implemented following principles:

- Modularity. The code is organized into high-level modules, accessed by the main function and corresponding to the main logical steps of execution (Tier #1 functions in Fig.1). Each module is further structured, including four total tiers of functions, from the level of the principal functions, down to the utility functions. A “design by contract” approach was applied at least for the more general functions. There are in total more than one hundred functions making up the VISIR distribution and their average size is about 70 LOC, Table I.
- Semantic consistency. The backbone of the VISIR filesystem is the set of input, code, and output directories shown in Fig.1. The choice of array names and functions (e.g. *_edges, *_Inset, readout_*.m, write_*.m) is meant to be self-consistent. Furthermore, Matlab® structures are used to store nature constants (e.g. “const.rho_water” or “const.g0” in settings.m) and various software parameters.

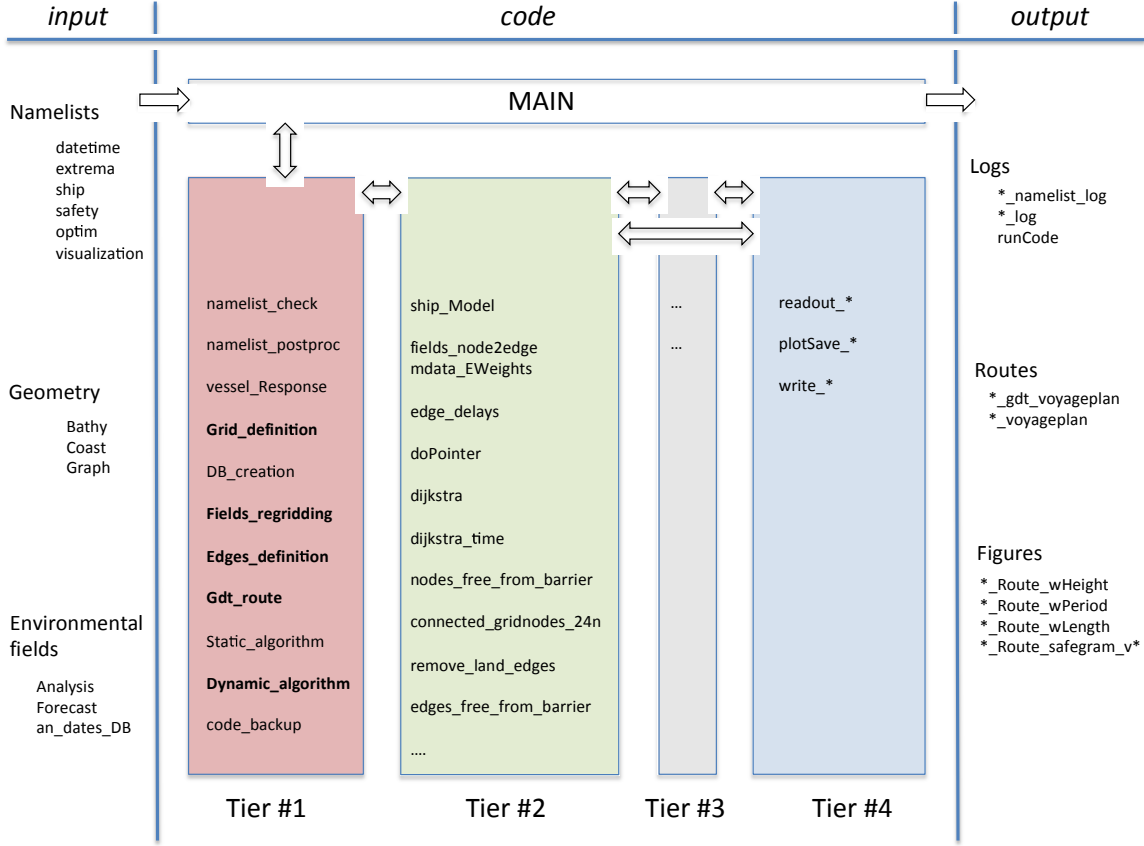


Fig. 1: Scheme of VISIR package structure. Arrows indicate the information flow direction. MAIN is the function where code execution starts and ends. Names in bold within Tier#1 indicate principal functions. File extensions are omitted. The Tiers are defined in Section 3.2.

Children (called functions)

Function Name	Function Type	Calls	Total Time	% Time	Time Plot
Edges_definition	function	1	35.399 s	53.9%	
Dynamic_algorithm	function	1	13.644 s	20.8%	
Gdt_route	function	1	12.495 s	19.0%	
Fields_regridding	function	1	2.571 s	3.9%	
Grid_definition	function	1	0.847 s	1.3%	
code_backup	function	1	0.207 s	0.3%	
vessel_Response	function	1	0.114 s	0.2%	
close	function	1	0.094 s	0.1%	
readout_namelists	function	1	0.029 s	0.0%	
namelist_check	function	1	0.016 s	0.0%	
clearvars	function	1	0.011 s	0.0%	
strcat	function	4	0.011 s	0.0%	
eta_Job	function	1	0.004 s	0.0%	
namelist_postproc	function	1	0.004 s	0.0%	
num2str	function	1	0.003 s	0.0%	
settings	function	1	0.002 s	0.0%	
Self time (built-ins, overhead, etc.)			0.267 s	0.4%	
Totals			65.719 s	100%	

Fig. 2: Profiling of VISIR execution for $N=39\ 780$, with Tier#1 functions ranked by computing-time consumption. Self time is time spent within a given function, excluding time spent within its child functions. Self time also includes overhead resulting from the process itself of profiling.

Table I: VISIR code metrics

		notes
Number of Functions	128	
Lines of Code (LOC)	10 902 (8 952)	Including all comments and blank lines (Excluding 15 lines of license header per file)
Average lines per function	85.2 (69.9)	``
Disk space occupation	1088 kB	

- DRY (“Don’t Repeat Yourself”) principle. There is a single place in the code where each constant quantity is defined. Hardcoded information is deprecated, and it is grouped into external “namelist” files (see Fig.1 and Table II) or in the namelist_postproc.m and settings.m functions.
- Checks. The user-defined parameter space is quite large and the code cannot provide a correct answer for any input value. E.g. departure date cannot be earlier than the first time step in the forecast file used and ship length cannot be a negative quantity. This and similar checks are performed within the namelist_check.m function and on derived variables in the body of the code (see e.g. the checks ending with exit() in readout_envFields.m or Grid_definition.m).
- Tracking. The initial development of the code spanned a relatively long time (about three years) and the capacity to track changes and recover previous states was crucial, even though a full-featured versioning system was not employed. Thus, for each VISIR run, all input parameters, names of used files, and even the run code suite are saved to the output directory of the job run (*_namelist_log.txt, *_log.txt, runCode.tar).
- Regression tests. For the aforementioned reason, it is essential to always have tested runs, whose output files act as a reference. Some of them are provided along with the VISIR distribution.

Table II: Namelist files driving VISIR code execution

Namelist file name	purpose
extrema_pars.txt	Start/end position, bufferzone of bounding box, minimum offshore distance
datetime_pars.txt	departure date and time
ship_pars.txt	vessel parameters
safety_pars.txt	flags for intact stability constraints
optim_pars.txt	optimization options
visualization_pars.txt	rendering options

- Oracles. Any possible comparison with benchmarks is exploited. For the shortest path routine an analytical result is available for a specific spatial configuration of ship speeds, *Mannarini et al. (2015b)*. It served as a validation for the code development, and it is left in the distribution as a tool for checking that the core code is not corrupted (see forcing.analytic flag in namelist_postproc.m).
- Profiling. Once the code reached maturity, its performance was profiled in order to highlight bottlenecks. E.g. Figs. 2 and 3 show that, for larger simulations, the most time consuming part is the preprocessing of the graph quantities (“edges”), followed by the calls to shortest path routine. Not just CPU resources but also RAM memory requirements were profiled, and an example is provided in Fig. 4.
- Portability. The code was developed on a workstation and a laptop computer and it is meant to be run operationally on a supercomputing facility. Thus, code portability has been a must from its inception. An installation wizard eases the porting of the distribution (though just *nix systems are supported by us, an extension to Windows systems is possible).
- Documentation. The internal code documentation is focused on the interfaces rather than on individual method descriptions. Though documentation is not yet fully developed with respect to the design-by-contract standards, a compact user manual is provided along with the code distribution. It is complemented by other open-access resources such as the present paper and, for a technical description of the ship routing model, by *Mannarini et al. (2015b)*.

3.2. Package organization and performance

The organization of the VISIR package and its performance documented here correspond to the code version of 2016-02-09 and to the results achieved on an iMac with 3.5 GHz Intel Core i7 processor with 32 GB RAM memory (1600 MHz DDR3). The code suite is organized into input, code, and output folders, see Fig.1. There are input subfolders containing static and dynamic databases (shoreline, bathymetry, and graph connectivity information: “geometry/” and environmental field forecasts: “fields/”), as well as subfolders containing the namelists (see Table II) relative to the individual job runs (“in/<job_name>”). There are then output subfolders matching the input ones (“out/<job_name>”). The code functioning starts and ends within the MAIN.m function. Tier 1 functions are those directly called by MAIN.m and include, for instance, the reading of the namelist and environmental field files, the basic-level checks, the graph pre-processing, and the calls to the shortest path routine, Fig. 1. Tier 2 functions are those directly invoked by Tier 1 functions. Tier 4 is made up of utilities that are called both by Tier 3 and Tier 2 functions.

VISIR computing time depends on route length, through the graph size N , Fig. 3. The log-log scale and the polynomial fits of the performance, Table III, indicate that there is a linear regime for small N and a quadratic one for large N . The main contributors to such time expenditure are the graph edge preparation and the two calls (geodetic and optimal route) to the shortest path routine. As seen from Table III, the edge preparation outweighs the sum of the geodetic and optimal route computation time. Furthermore, the computational cost for edge preparation is dependent on actual sea conditions: the rougher the sea, the lower the sustained ship speed, and consequently the longer the route duration. This results in a larger number of forecast time steps needed, and, in turn, a longer edge pre-processing time. Furthermore, edge preparation is quite a memory consuming process, and memory allocation may grow significantly for large graphs, Fig. 4. The output consists in log files and the actual route information (for both the geodetic and the optimal route, Table IV). Furthermore, a geographical rendering based on third party software libraries (m_map package) is provided along with the VISIR distribution. The output file names contain a prefix indicating whether VISIR was run using a static (0_) or a time-dependent (2_) version of the shortest path routine.

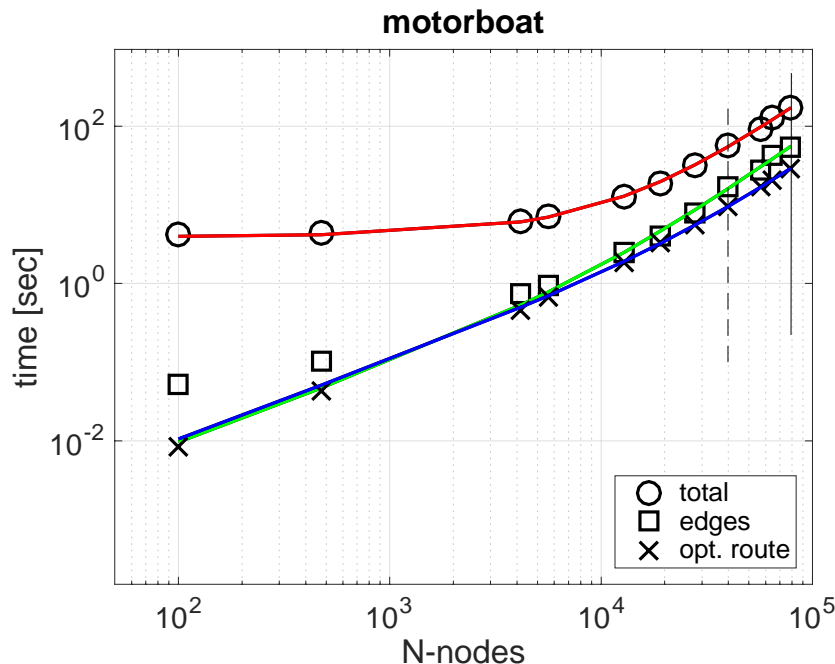


Fig. 3: VISIR code performance as function of the number N of graph grid points within the selected bounding box. The fit model and the parameters of the fitted curves are provided in Table III. The vertical dashed (solid) line indicates results obtained for value $N=39\ 780$ ($N= 79\ 068$), corresponding to the CPU time and RAM memory profiling shown in Figs. 2 and 4, respectively.

A few key technical choices made for the VISIR code are highlighted in the following:

- Use of a vessel Look-Up-Table (LUT). Sustained ship speed in various sea states and engine throttle values is computed within `ship_Model.m`. The LUT is then interpolated to the actual sea state corresponding to the various (time – dependent) edges, speeding up computations.
- Use of a limited spatial domain. As in any graph search method, grid size N is the key factor affecting the CPU time for computing the routes (see Fig.3 and Table III). In order to reduce the time, just a limited subset of the environmental fields is used. The user specifies the extent of such “bounding box” through four parameters for the buffer zone around the box, with departure and arrival as vertices (see `extrema_pars.txt` in Table II). This way, the number of gridpoints is easily reduced from about 10^6 (whole Mediterranean Sea grid at 1 nautical mile resolution, see *Mannarini et al. (2015b)*) to typically a few 10^4 .
- Search of sea-next grid point. Even in case that the VISIR user specifies a departure or an arrival point located on the landmass, the code recovers the next sea grid point, compatible with a positive Under Keel Clearance (UKC) and the minimum offshore distance set by the user. In order to do so, VISIR computes a joint mask, accounting for both vessel UKC and shoreline distance (`Grid_definition.m`).

Table III: Performance of VISIR components shown in Fig. 3. The fit model for the computing time τ is: $\tau = c_0 + c_1 N + c_2 N^2$. The parameter c_0 is constrained to 0, except for the fitting of the total job performance.

	c_0 [s]	c_1 [s]	c_2 [s]	R^2 [%]	RMSE [s]
opt	0	1.1e-04	3.3e-09	99.9	0.1
edges	0	9.6e-04	7.7e-09	98.9	2.1
tot	3.8	4.2e-04	2.2e-08	99.4	4.9

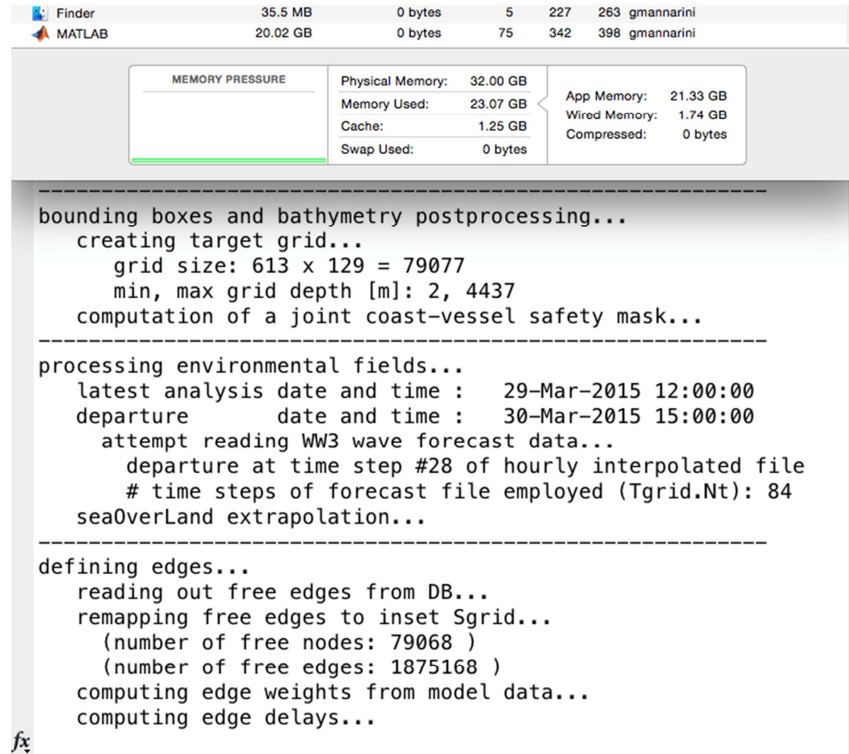


Fig. 4: VISIR RAM-memory usage at peak and excerpt of the messages output to the command line. The number of graph grid-points used in this route computation was $N= 79068$.

- Use of pointers for the graph edges. In exact graph search methods such as Dijkstra’s algorithm, there is an unavoidable work load due to the scan of all the edges for checking the

“complementary slackness conditions” *Bertsekas (1998)*. In particular, they are checked sequentially for each candidate node on the shortest path. In order to speed up the computations, it is convenient to adopt the viewpoint of the edges emanating from a given node (“forward star”, see *Ahuja et al. (1988)*). In the absence of a corresponding data structure available in Matlab®, the forward star is implemented through an explicit provision of pointers to each node in the list of graph edges. They are prepared in the doPointer.m function and then employed in both the dijkstra.m (static algorithm) and dijkstra_time.m (time-dependent algorithm) optimization functions.

4. Example of results

In order to illustrate the results that can be obtained via VISIR, we provide here a full-featured description of a relatively long sea route, in the presence of a complex domain (coastline, islands, and a strait) and rough enough seas. This highlights the time-dependent structure of the algorithm, its capacity to retrieve the route in a complex topology, and the strategic savings it offers.

The route is set in the Ligurian and Tyrrhenian Seas, between Cannes (France) and Porto Cervo (Italy), during a typical Mistral event. It starts on 2016-02-19 at 17:00 UTC. Sea state forecasts from Wave Watch-III model stemming from an analysis for 2016-02-19 at 12:00 UTC provide the significant wave height, period, and direction of the peak wave spectrum component. A vessel with parameters from Table V is employed for the computations.

The route job, excluding maps and time series rendering, took (on the same computer described in Sect.3.2) $\tau = 47 \pm 1$ s, with a peak Matlab® RAM memory allocation of about 4.7 GB.

Table IV: Route model stored by VISIR. The column “Type” specifies the graph element to which the attribute refers (n: node; e:edge). The index-like attributes (last 3 rows) are available for the geodetic route only.

Attribute	Description	Units	Format	Type
WP	Waypoint index	-	integer	n
ISO_date	Date and time	-	ISO 8601	n
lon	longitude	deg E	real	n
lat	latitude	deg N	real	n
cum_dist	cumulative distance	NM	real	n
course	Course over ground	deg	real	e
throttle	Engine throttle	%	real	e
speed_out	Speed over Ground	kn	real	e
alpha	wave-ship relative direction	deg	real	e
T_E	Encountered wave period	s	real	e
redLambda	Wavelength divided by ship length	-	real	e
swh	Significant wave height	m	real	e
UKC	Under Keel Clearance	m	real	e
parRoll	Parametric roll index	-	integer	e
pureLossStab	Pure Loss of Stability index	-	integer	e
surfRid	Surf-riding index	-	integer	e

The four panels in Fig. 5 (a-d) display four snapshots of both the significant wave height and direction fields, and the progress of both the geodetic and optimal route computed by VISIR. The geodetic route minimizes spatial distance between departure and arrival. It considers the shoreline, checks for the condition $UKC > 0$, and uses the sea state information just for computing the sustained speed at each route leg. The optimal route, besides checking for both shoreline distance and $UKC > 0$, keeps into account vessel intact stability as a constraint, and total time of navigation as an optimization objective (see Section 2). It is seen that the different objectives and constraints for the two routes lead to quite different paths. In fact, one route keeps Corsica to the port side (geodetic), while the other to

starboard (optimal). This way, the optimal route is significantly longer in distance than the geodetic one, but still 7% shorter in navigation time (see Table VI). This is due to the calmer sea experienced east of Corsica, the consequent reduction in wave added resistance, and involuntary vessel speed loss. The kinematics of the routes is further explored in Fig. 6(a-d).

The time series for sustained speed clearly shows that, for the optimal route, when the vessel is navigating in calm seas in the lee of more than 1000 m a.s.l. high mountains, Fig. 5b-c), there is a sudden rise of sustained speed, up to the top speed c (Fig. 6a at $\Delta t > 13$ h after departure). Along the optimal route, speed is up to four knots larger than along the geodetic one, and this allows for overall savings in navigation time, despite a longer sailed path.

Panel Fig. 6b monitors the wavelength λ with respect to vessel length L . In fact, a specific value of the λ/L ratio is one of the necessary conditions for the loss of intact stability, *Mannarini et al. (2015b)*. This occurs along the geodetic route at $\Delta t > 25$ h, Fig. 6d). However, it cannot occur along the optimal route, since route legs leading to stability loss cannot be employed by the optimization algorithm, per construction (if corresponding flags in the safety_pars.txt namelist are set to 1, Fig. 1).

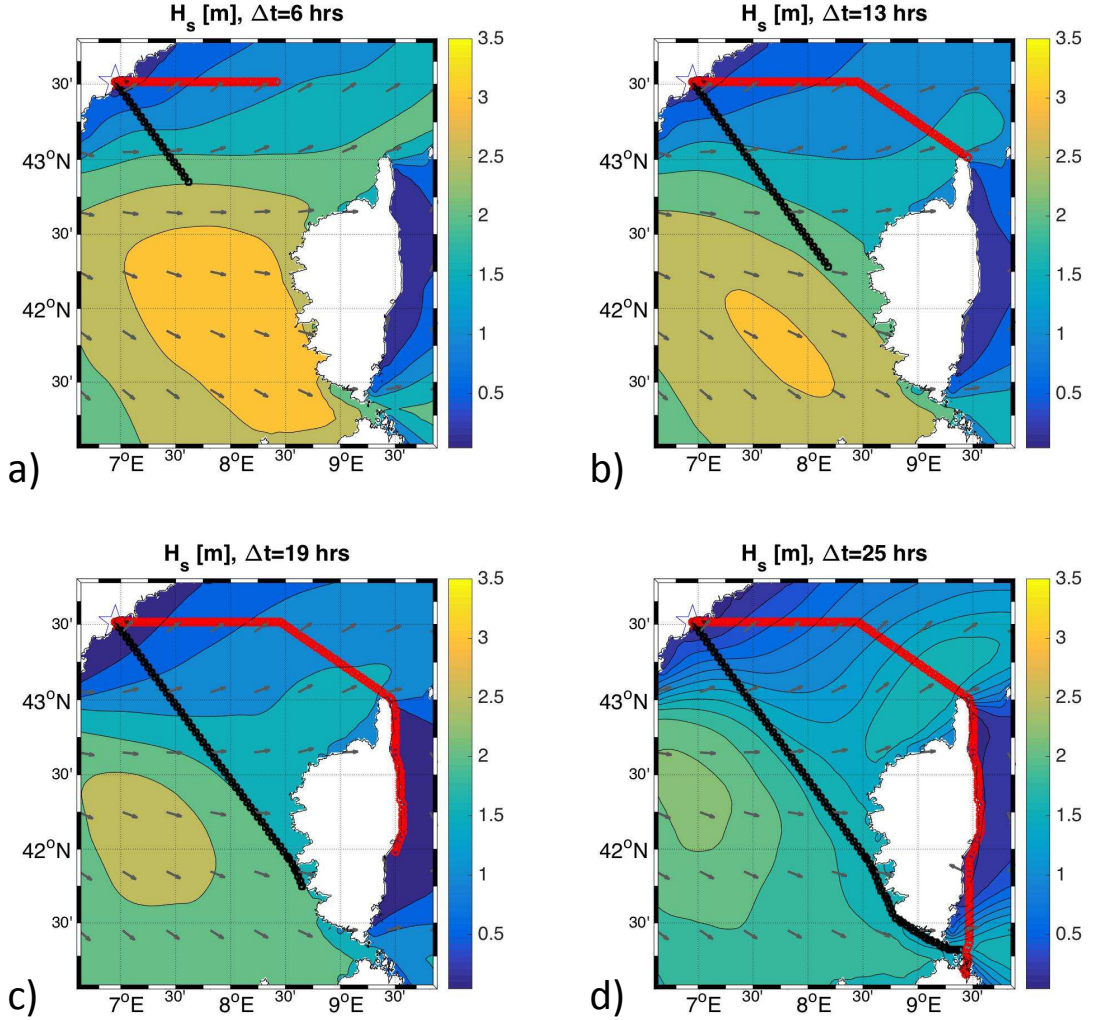


Fig.5: Geodetic (black markers) and optimal (red markers) route from Cannes (France) to Porto Cervo (Italy) for a displacement hull vessel with the parameters from Table V and departure on 2016-02-19 at 17:00 UTC. Panels (a-d) refer to various time steps after departure. Significant wave height forecast fields H_s are displayed by coloured shadings and wave directions by arrows. The graph generated by VISIR for solving this route optimization task has a size $N=27927$.

Finally, the chosen route also demonstrates VISIR's capacity to suggest a voluntary speed reduction. This occurs at $\Delta t = 25$ h along the optimal route, Fig. 6c. The algorithm suggests reducing the engine throttle to 85% for a few minutes long to avoid stability loss. The possible route diversion to avoid throttle reduction and keep from stability loss in fact would lengthen the route, which would not offset the time saving due to keeping engine throttle at its maximum value.

Table V: Values of the ship parameters used for the VISIR routes shown in this manuscript

1	Maximum engine brake power	650	hp
2	top speed	10.7	kt
3	length at waterline	22	m
4	beam (width at waterline)	6	m
5	draught	1.9	m
6	natural roll period	5.4	s

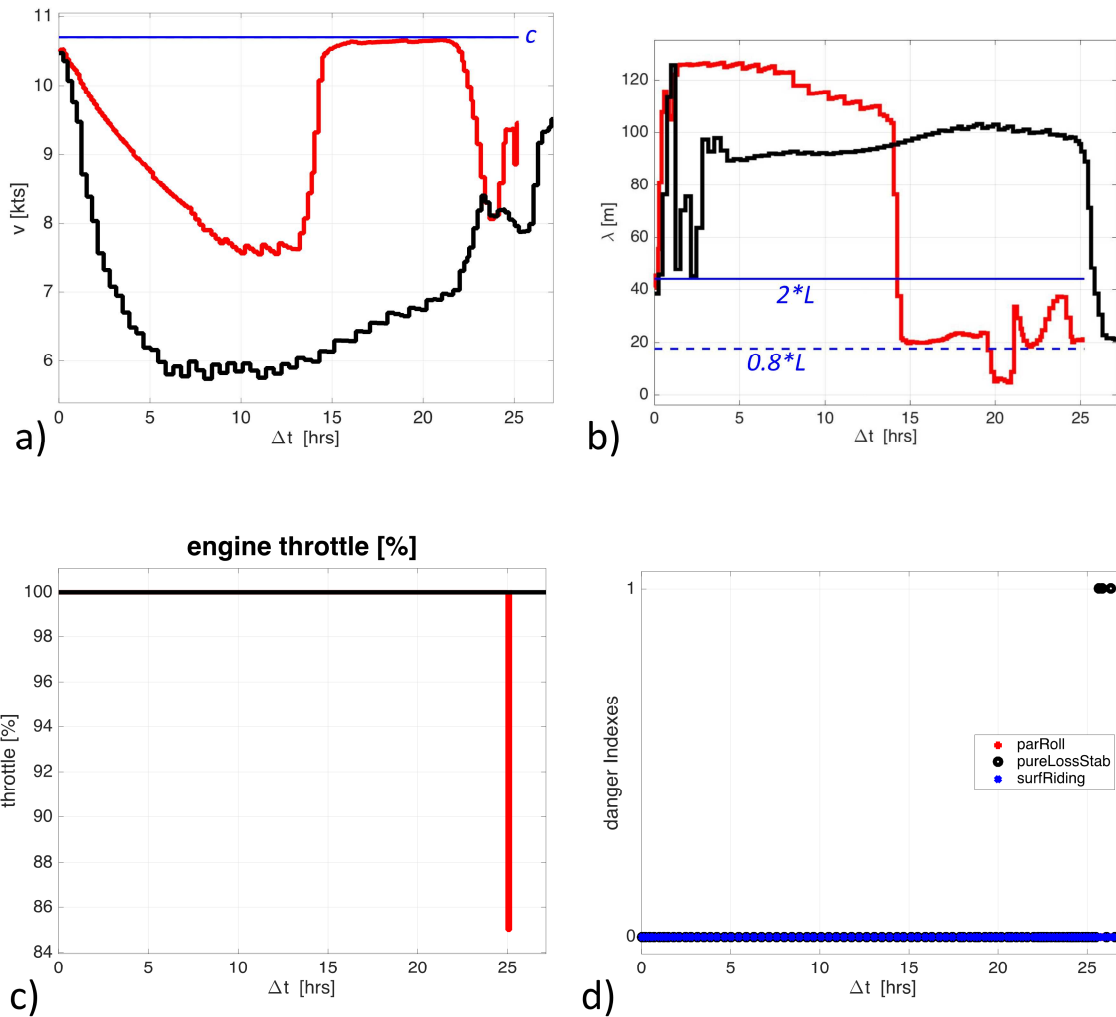


Fig. 6: Information along geodetic (black) and optimal (red) route of Fig. 5. Δt is time elapsed after departure. (a) sustained speed v and reference line at maximum speed c ; (b) wavelength λ and reference lines at vessel length multiples $0.8L$ and $2L$; (c) engine throttle; (d) danger indices along geodetic route, 0: safe; 1: dangerous.

Table VI: Summary metrics for the route computation shown in Fig. 5 and Fig. 6. The relative differences are computed as $\Delta = 100 * (\text{Optimal}/\text{Geodetic} - 1)$.

	<i>Units</i>	<i>Geodetic</i>	<i>Optimal</i>	$\Delta \square \square \square$
Length	NM	187.38	233.56	+24.6
Duration	hh:mm:ss	27:08:31.1	25:14:37.4	-7.0
Average speed	kt	6.90	9.25	+34.0

5. Conclusions

This paper presents some features of the numerical code of ship routing model VISIR. The model is made free and open-source, and its documentation is open-access. This should enable the formation of a community of users and developers.

A few principles of robust scientific programming were adopted. Even before adding new functionalities or better parameterizations of vessel response, there is certainly room left for code performance optimization (see e.g. discussion about edge pre-processing in Section 3.2), redesign by-contract, and internal documentation. Full compliance with code quality standards such as ISO/IEC 9126 or ISO/IEC 25010:2011 would be also beneficial. Refactoring into an object-oriented language is an attractive option and a research activity in this direction has already been started at CMCC.

Furthermore, the authors foster the creation of a VISIR developer consortium and a large community of users. Non-commercial agreements with companies are also possible. Cooperation with the industry would be especially useful for collecting feedback from the maritime end-users, while the research community might consider VISIR as an open platform for testing optimization methods, vessel response parameterizations, and the impact of various types of environmental data relevant to navigation.

References

- AHUJA, R.K.; MAGNANTI, T.L.; ORLIN, J.B. (1988), *Network Flows*, MIT, Cambridge
- ALEXANDERSSON, M. (2009), *A study of methods to predict added resistance in waves*, Master thesis, KTH Centre for Naval Architecture, Stockholm
www.kth.se/polopoly_fs/1.151543!/Menu/general/column-content/attachment/Alexandersson.pdf
- BELENKY, V.; BASSLER, C.G.; SPYROU, K.J. (2011), *Development of Second Generation Intact Stability Criteria*, 5 Tech. Rep., DTIC Document
<http://www.uscg.mil/hq/cg5/cg5212/docs/dtmb-2ndgen-is-rpt2011.pdf>
- BERTSEKAS, D.P. (1998), *Network Optimization: Continuous and Discrete Models*, Athena Scientific, http://web.mit.edu/dimitrib/www/netbook_Full_Book.pdf
- DIJKSTRA, E.W. (1959), *A note on two problems in connexion with graphs*, Num. Math. 1.1, pp.269-271
- LEE, S.; ALEXANDER L. (2013), *Software Quality Assurance Issues Related to e-Navigation*, Marine Navigation and Safety of Sea Transportation: Advances in Marine Navigation, CRC Press
- MANNARINI, G. (2015a) *The twofold aspect of climate change on navigation: the search for new maritime routes and the challenge of reducing the carbon footprint of ships*, CMCC Research Paper RP0252, <http://www.cmcc.it/wp-content/uploads/2015/03/rp0252-opa-03-2015.pdf>
- MANNARINI, G.; PINARDI, N.; COPPINI, G.; ODDO P.; IAFRATI A. (2015b), *VISIR-I: small vessels, least-time nautical routes using wave forecasts*, Geosci. Model Dev. Discuss. 8, pp.7911-

7981, <http://www.geosci-model-dev-discuss.net/8/7911/2015/gmdd-8-7911-2015.pdf>

MANNARINI, G.; TURRISI, G.; D'ANCA, A.; SCALAS, M.; PINARDI, N.; COPPINI, G.; PALERMO, F.; CARLUCCIO, I.; SCURO, M.; CRETÌ, S.; LECCI, R.; NASSISI, P.; TEDESCO, L. (2016), *VISIR: Technological infrastructure of an operational service for safe and efficient navigation in the Mediterranean Sea*, Nat. Hazards Earth Syst. Sci. Discuss. 32, pp.1-19
<http://www.nat-hazards-earth-syst-sci-discuss.net/nhess-2016-32/nhess-2016-32.pdf>

PONTIKA, N., KNOTH, P., CANCELLIERI, M., PEARCE, S. (2015), *Fostering open science to research using a taxonomy and an eLearning portal*, 15th Int. Conf. on Knowledge Technologies and Data-driven Business, ACM, p.11, http://libeprints.open.ac.uk/44719/2/kmi_foster_iknow.pdf

TONANI, M., ODDO, P., KORRES, G., CLEMENTI, E., DOBRICIC, S., DRUDI, M., PISTOIA, J., GUARNIERI, A., ROMANELLO, V., GIRARDI, G., GRANDI, A., BONADUCE, A., PINARDI, N. (2014), *The Mediterranean Forecasting System: recent developments*, Geophys. Res. Abstr., EGU2014-16899-1, EGU General Assembly, Vienna. 7939
<http://www.tandfonline.com/toc/tjoo20/current#aHR0cDovL3d3dy50YW5kZm9ubGluZS5jb20vZG9pL3BkZi8xMC4xMDgwLzE3NTU4NzZYLjIwMTUuMTA0OTg5MkBAQDE=>

WALTHER, L.; BURMEISTER, H.C.; BRUHN, W. (2014), *Safe and efficient autonomous navigation with regards to weather*, 13th Int. Conf. on Computer and IT Applications in the Maritime Industries, Redworth, pp. 303–317,
http://data.hiper-conf.info/compit2014_redworth.pdf

WILSON, G.; ARULIAH, D.; BROWN, C.T.; HONG, N.P.C.; DAVIS, M.; GUY, R.T.; HADDOCK, S.H.D.; HUFF, K.D.; MITCHELL, I.M.; PLUMBLEY, M.D.; WAUGH, B.; WHITE, E.P.; WILSON, P. (2014), *Best practices for scientific computing*, PLoS Biol. 12/11
<http://iacs-courses.seas.harvard.edu/courses/cs207/resources/BestPractices.pdf>

International Replenishment at Sea: Verification and Validation of a Maritime Simulation Capability

Louisa Stewart, Systems Engineering & Assessment Ltd, Bristol/UK, louisa.stewart@sea.co.uk
John Duncan, UK MoD Defence Equipment & Support, Simulation Based Acquisition, Bristol/UK

Abstract

This paper presents an overview of the UK perspective on the International Replenishment at Sea simulation, with a focus on verification and validation of the capability. Development was via a NATO inspired Memorandum of Understanding Project Arrangement to create and validate a modular simulation to be made available to all participating nations. A short summary of the developed capability is presented, and then a description and assessment of the overall verification and validation process, which has been completed via a range of activities carried out by the UK and other project participants.

1. Introduction

The International Replenishment at Sea (IRAS) simulation capability uses the High Level Architecture (HLA) framework, and provides a set of federates that can be used to construct a modular simulation of replenishment at sea (RAS) manoeuvres and activities. A federate is a simulation module that is HLA-compliant, and can take part in an HLA federation. The NATO inspired Memorandum of Understanding (MoU) Project Arrangement (PA) under which the work has been conducted ran for several years, and covered the design, development, verification and validation (V&V) of the complete capability.

The HLA federates were developed in accordance with the IRAS federation design, produced by the UK and Canada in consultation with the other contributing nations: Germany, Italy and France. In addition to jointly leading the design, the UK contribution consisted of a set of participating federates as well as verification and validation evidence based on multiple data sets collected over several years. Fig. 1 shows a visualisation of the IRAS simulation, which includes the RAS rig conducting a load transfer; this version of the simulation is constructed entirely of UK federates. Verification & validation of such a simulation capability is challenging; individual federates must be verified at component level, validated where appropriate, and then the federation as a whole, including different international variants, must also undergo a V&V process. This paper describes the approach taken to V&V within the UK as part of the IRAS program, summarises the results obtained, and reviews the process of constructing a set of evidence demonstrating that the federation is fit for purpose.



Fig. 1: Screenshots of simulation visualisation showing two ships in station keeping positions and a load transfer between supply and receiving ships

2. The IRAS Objectives

The overall objectives for the IRAS project are defined in the IRAS Project Arrangement. The requirement is to be able to simulate, at a high level of fidelity, the performance of RAS manoeuvres and transfers, and the stated objective is to:

‘...deliver a set of fully-tested, validated interoperable HLA federates that can be used to construct a fully-functional, validated HLA federation that can be used internationally to simulate ship-to-ship highline transfer of liquids and solids for:

- a. Any pair of ships
- b. Any sea state
- c. Any type of transfer rig
- d. Any size of solids load
- e. Any type of liquid
- f. Any flow rate of liquids transfer.’

As the IRAS simulation has been designed as a modular, HLA-based federation, it enables different conditions, ship combinations, transfer rigs and transfer types to be simulated. Additionally, the PA aims to:

- ‘...provide an enduring set of maintained federates and supporting tools which could form the basis of a common NATO repository
- ... improve and standardise the methods for modelling the hydrodynamics of ship-to-ship interactions.
- ... validate the hydrodynamic codes for ship-ship interaction against real-world data.’

The overall design and development process carried out was therefore conducted in a way that enabled the verification and validation of federates and federations, to ensure that the capability was able to be maintained in the future, and to meet the objectives relating to hydrodynamics methods and codes.

3. The IRAS Simulation Capability: Design and Development

Planning and execution of a successful V&V strategy begins at the design stage, and continues through development; the overall approach must be tailored to the structure and content of the capability. This section reviews the structure of the IRAS software, and briefly describes the available simulation federates.

3.1 Overview

The UK IRAS contribution is part of a broader Virtual Ships simulation capability intended for use in simulating various maritime activities and operations involving multiple ships or other vessels. Available components are as follows:

- The Flexible Modelling Framework (FMF)
Provides simulation management functionality and manages HLA wrappers if present
- HLA Wrapper Functions
Optional, provides HLA interfaces for all federates that are included in a specified federation
- HLA Execution Manager
Optional, provides execution manager if simulation is executed as an HLA federation
- Generic Components
Simulation components that are used in multiple federation types:
 - Ship motion federate
 - Hydrodynamics federate

- Aerodynamics federate
- Environment federate
- Lead helm federate
- Visualisation federate
- IRAS Components
Simulation components specific to the IRAS federation:
 - Transfer system federate
 - Following helm federate

Fig.2 shows the overall structure of an IRAS federation constructed using these components.

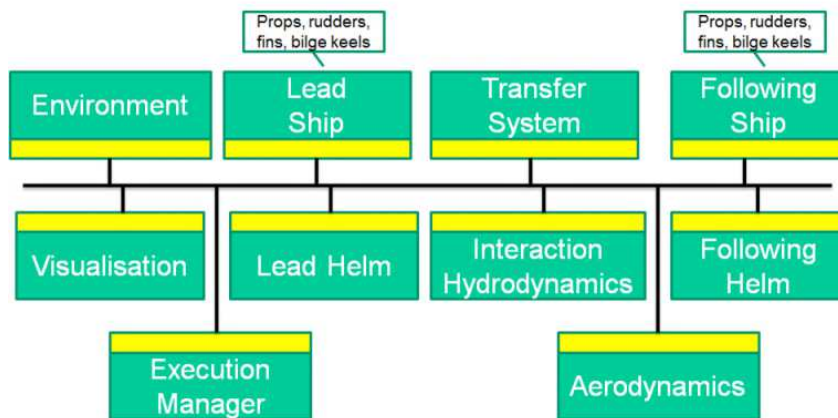


Fig. 2: Components used to construct an IRAS simulation capability; the UK has developed a version of all of the federates shown in the diagram; other nations have supplied their own versions of a subset of these to the IRAS PA.

As the structure is modular, the UK simulation can be used in three different ways:

- To run an IRAS federation, using federates from one or more nations, using HLA as the framework and to provide the simulation manager;
- To run an IRAS simulation consisting of UK federates or plugins only, using either HLA or FMF as the simulation manager;
- To run an HLA or FMF simulation representing other maritime operations while underway, using UK federates or plugins.

3.2. The Flexible Modelling Framework and High Level Architecture

The UK capability includes the Flexible Modelling Framework (FMF) developed by the UK as well as modules known as *plugins* that are used to construct a simulation. FMF provides a simulation manager which can execute a simulation composed of multiple plugins, as shown in Fig. 3.

The interfaces from FMF to the plugins have many similarities with HLA: the simulation interfaces are based on using a publish-subscribe messaging pattern, objects within a simulation are defined using a Federate Object Model (FOM), FMF events are analogous to HLA interactions, time management is based on HLA principles, and the execution manager launches and synchronizes plugins and manages communications in a manner that is completely compatible with the HLA 1.3 and HLA 1516 protocols. Fig. 4 shows how a set of plugins and the FMF simulation manager can participate in a wider HLA federation. The only change required is the addition of an HLA plugin to provide full HLA interfaces, and to enable the simulation execution to be controlled externally via an RTI.

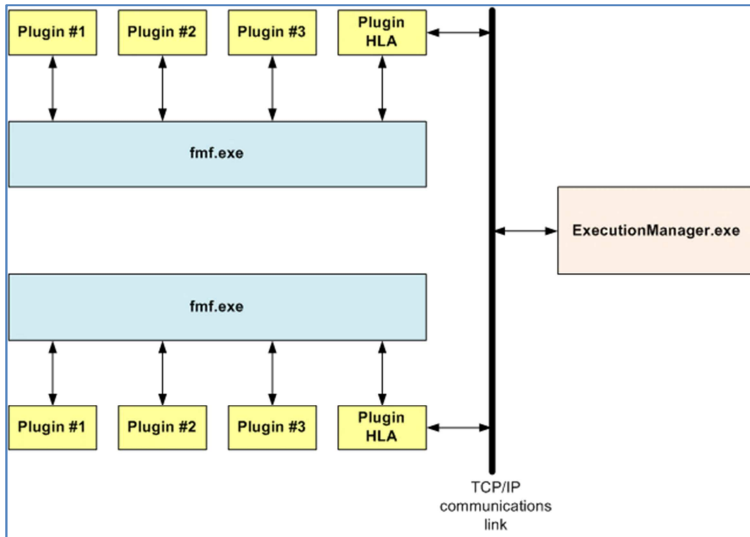


Fig. 3: Structure of the Virtual Ships simulation capability, upon which IRAS is based. Any plugins that adhere to appropriate standards can be added to the simulation; the HLA wrapper plugin will create and manage interfaces for all other plugins if the HLA option is selected.

The overall structure of the UK Virtual Ships simulation capability and IRAS are therefore interchangeable from a UK perspective; verification and validation evidence can be used for all types of simulation performed by the capability. As the UK uses its generic simulation components in other Virtual Ships simulations as well as for the IRAS capability; this means that V&V evidence for these components generated via other projects can also be used as evidence for the IRAS simulation.

3.3. Generic Components

These components are the core of the simulation, enabling one or more ships and their interactions to be modelled. These plugins are used across the UK Virtual Ships simulation capability.

3.3.1 Ship Motion and Hydrodynamics Federates

The ship motion federate is responsible for updating the ship position and orientation (spatial data) in response to the forces (mechanical, aerodynamic and hydrodynamic) acting on it. A variety of ship federate types can be supported by the federation; in IRAS, the ship federate is a self-contained federate, able to receive hydrodynamic interaction effects due to another ship, and able to receive forces due to attached RAS systems.

The UK hydrodynamics federate calculates isolated hull forces and interaction forces between two ships; the plugin can be set up to supply these separately, or as a total force on each hull. A set of data tables are calculated offline by a hydrodynamics model in a specified format, and then these are used within the simulation to look up forces applied to the hulls at each time step. It is possible to use data generated by any hydrodynamics model, as long as the files comply with the interface specifications supplied within the Virtual Ships Standardisation Agreement (STANAG), NSA (2012). It is important to distinguish between the simulation plugin representing hydrodynamic effects, which require a pre-calculated data set to be provided for use during a simulation, and the methods used to carry out these pre-calculations, which must be separately validated, as described in Section 3.3.2.

3.3.2 Hydrodynamics Methods

The hydrodynamics data file format enables the supply of data points over a range of lateral and longitudinal ship separation distances and speeds. The hydrodynamics federate takes this information, together with accelerations calculated at the current time step, and calculates interpolated values for the forces and moments supplied that are then used to drive the ship motion over the time step.

The basis of the federation design is that it does not matter what hydrodynamic method is used to calculate the data within the tables, as long as it is in the specified format and implements the documented interface to the hydrodynamics plugin. However, this does mean that V&V of the hydrodynamic calculations must be considered. During the IRAS PA, it has frequently been convenient to consider hydrodynamic validation in parallel with federation validation, but the two tasks could be carried out independently. Additional verification and validation would be required if a different hydrodynamic method was used in the future. The current hydrodynamic models are all based on panel methods, which have been demonstrated to produce good results when applied to problems involving ship hulls travelling through water.

3.3.3 Lead Helm Federate

The lead helm federate is responsible for sending rudder and propeller demands for ship helm control in order to maintain a ship's heading and speed. The demands are calculated in response to the ship spatial updates. The performance of the lead helm is entirely dependent on the parameters set in the proportional-integral-derivative (PID) controller that it uses; this federate is verified to confirm that the PID controller is correctly implemented and then performance is tested to demonstrate that it can control the ship appropriately in a range of conditions.

3.3.4 Environment Federate

The environment federate provides the initial (onset) environmental data for the federation, including data representing the wave spectra, current and pressure profile with depth, as well as wind profiles. The environmental data does not change during the federation execution; other federates subscribe to this data and then use it as required. The environment federate itself requires only verification to demonstrate that it is reading and publishing the data; however, there are a number of issues relating to the environmental data supplied to the simulation, which are described in Section 4.4.

3.4 IRAS Components

There are two federates within the IRAS simulation that are specific to IRAS: the transfer rig and the following helm. The transfer rig is a generic system that can represent operation of a range of actual rigs, and can be used with any ship. The following helm implements controllers to enable a supply ship to perform appropriate manoeuvres and station keeping within a RAS simulation.

4. IRAS Verification and Validation in the UK

It is clear from the overall design of the UK Virtual Ships and IRAS capabilities that a flexible and considered approach must be taken to verification and validation. Different elements of the simulation require different treatment, and in cases where multiple federates are used to conduct validation activities, it is important to specify what part of the capability is being validated by a particular exercise.

4.1 Overall Approach to Verification and Validation

Verification and validation covers all elements of proving the simulation capability. In general:

- Verification demonstrates that functionality has been correctly implemented in line with the simulation design;
- Validation demonstrates that the implemented functionality correctly represents the elements of reality being simulated.

All simulation modules have been verified; however, certain simulation components have not been validated, or have limited validation evidence. The environment, aerodynamics, UK transfer rig, and lead and following helm plugins are in this category. This is either because the modules only require

verification, or because appropriate validation data sets are not available. In addition, some federates cannot be validated, as no appropriate data for validation can be collected, but do require performance testing, which provides additional verification evidence that they are fit-for-purpose, and confirms that they can perform a particular task within appropriate bounds. Table I summarises the activities carried out to check and validate individual federates, underlying calculations, and federations following verification.

Table I: Validation activities carried out for different simulation federates

Federate	Activities
Ship motion	Validation via all tank test and sea trials activities
Lead helm	Performance assessment to demonstrate ability to use lead helm to maintain a set course
Following helm	Performance assessment to demonstrate ability of following helm to carry out RAS manoeuvres relative to a lead helm
Hydrodynamics federate	Validation via all tank test and sea trials activities
Hydrodynamics calculations	Validation via comparison of generated forces with constrained tank test data for isolated and interacting hulls
RAS transfer federate	Performance assessment to demonstrate ability to maintain line tensions within specified ranges
Aerodynamics	No further effort beyond verification; no RAS participants have opted to use the aerodynamics module at present due to configuration uncertainties
Environment	Assessment of how the underlying wave spectra used as data within the environment federate affects variation in results and requires results of the simulation to be interpreted in a probabilistic manner
UK federation	Validation via comparison with unconstrained tank test results and sea trials data

4.2 Verification Activities

For all components within the Virtual Ships simulation, their functionality is described within one or more of the design documents. These documents describe the functionality implemented within each module, and are the basis for verification testing.

The general approach to simulation verification has been to:

- make use of simple tests based on the underlying physics of the simulation where possible to verify that these basic equations are correctly implemented;
- make use of simple test data, such as tank tests performed in unidirectional waves, roll decay tests, or turning circle data, to verify that elements of performance based on ship properties and configuration are functioning as expected;
- perform tests to ensure that implemented algorithms are functioning as expected, for example helm controllers;
- perform tests to check that the simulation framework and wrapper modules are managing the simulation and its data as they should.

This approach ensures that as many elements of the simulation as possible are verified using basic checks of functionality, and applies to all simulation components.

4.3 Performance Testing

For certain plugins and federates, validation is inappropriate because the federate is designed to implement a particular algorithm whose performance will depend on the tuning of its parameters, rather than being designed to mimic a specific, physical element of reality. For IRAS, three federates fall into this category: the transfer system, and the lead and following helms

4.3.1. RAS Transfer Module

The RAS transfer module available within the UK simulation was originally intended to model the rigs installed on to UK ships and used for 2-tonne transfers. However, details of the design of that specific rig were not available, and the module therefore implements a generic transfer rig with a controller algorithm that attempts to maintain a fixed force at the winches throughout a transfer.

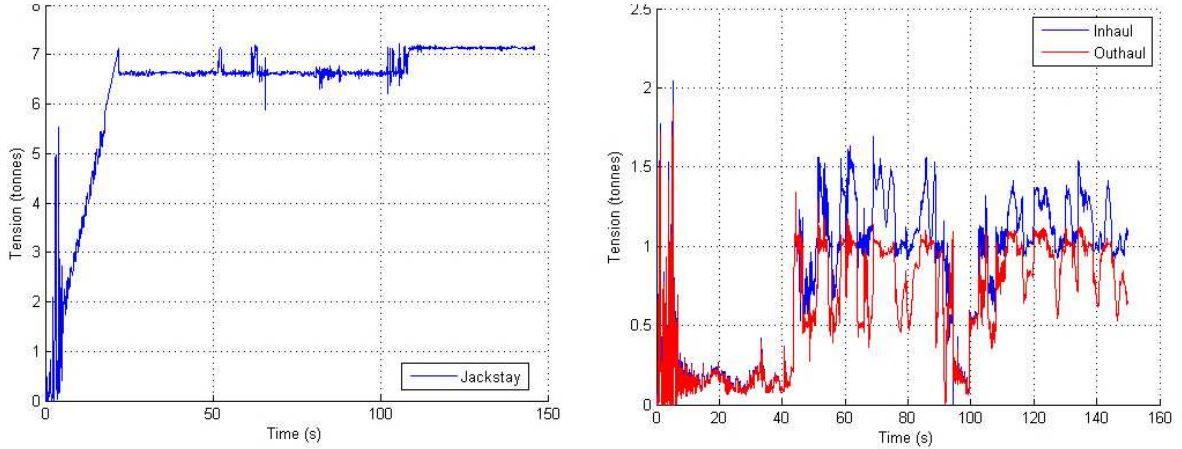


Fig. 4: The generic transfer rig used within the RAS simulation can be set up to maintain a specific tension range throughout a transfer. An appropriate force is applied to both the supply and receiving ship RAS stations throughout the simulation on the jackstay, inhaul and outhaul lines.

Configured appropriately, it will always maintain the specified force; however, it cannot be used to assess the performance of the real rig. Validation is therefore inappropriate; verification is used to check the function of the federate. Fig.4 shows the performance of the transfer system when configured to represent a system which requests a constant tension of 6-7 tons during a transfer; it can be seen that the tension remains within this range during the entire period. This data is taken from a simulation representing a generic solids transfer rig.

4.3.2 Helm Controllers

An IRAS simulation requires controllers for both the lead and following helms. Both helms apply control algorithms that attempt to cause particular behaviour in the simulated ship(s) depending on user-set parameters. The lead helm uses a simple PID controller for propeller and rudder control. The following helm applies sequential PID controllers that act first to set a desired speed and heading based on the current position and orientation of the supply and receiving ships, and then uses the output of these as input to propeller and rudder controllers. We have found that this type of controller can be configured such that it appropriately controls the following helm across a wide range of conditions with a single set of parameters. Single-PID controllers that calculate rudder and propeller settings from ship position and orientation data in a single step must be tuned for each individual case, and are therefore impractical for conducting studies that require large numbers of simulations to be run.

These sequential-PID controllers appear to represent real ship behavior well. Fig. 5 shows the trajectories of two ships during a station-keeping simulation in head and beam seas; we understand from discussion with navigational personnel that the ‘oscillating’ relative position, in both the lateral and longitudinal directions, especially in beam seas, is the expected behaviour for these types of ships.

Both the lead and following helm controllers must be tuned appropriately in all cases; we have found that a simple manual process for this tuning gives sufficiently good results for use in assessing performance. Appropriate tuning of the following helm is critical to the overall performance of the simulation, as without a well-behaved controller, the ship will not perform the approach and station-keeping manoeuvres to its full ability.

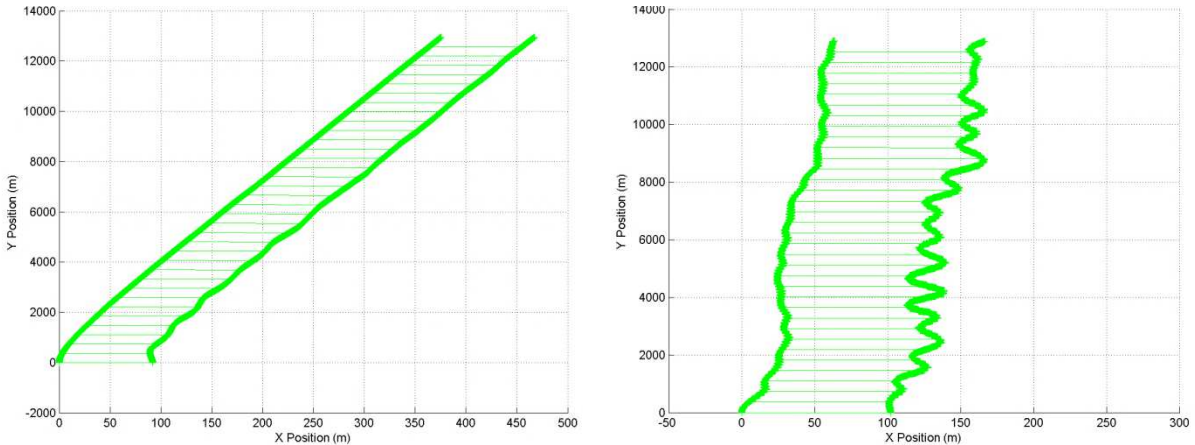


Fig. 5: Trajectories of a simulated lead and following helms during station keeping with a following helm implemented by a dual-PID controller. The lead ship is to port, and the following ship to starboard; the left image is for two ships in head seas; the right in beam seas. The controller successfully maintains position within appropriate lateral and longitudinal limits, but displays appropriate oscillation relative to the lead helm in the more challenging conditions, as would be expected.

Verification of these plugins consists of checking that the control algorithms are implemented as intended. A further test activity involves checking how effective the algorithms are at achieving a specified outcome, in reasonable circumstances, but this falls into the category of performance testing rather than validation as the simulation does not try to replicate any well-defined and specified real world controller.

4.4 Validation Activities

The UK validation program for Virtual Ships and IRAS consisted of a number of different assessments and comparisons using both tank tests and sea trials data. This section reviews the data sets that were used for validation, and the outcome of these validation exercises.

4.4.1 Tank Test Overview

Dedicated tank tests were carried out to collect data to validate both the methods used offline to generate hydrodynamic data, and the full IRAS simulation including the hydrodynamics federates used to calculate forces and moments. Tank tests for this purpose are of great importance because (a) tests can be conducted on models in both constrained and unconstrained configurations, and (b) it is possible, particularly during constrained testing, to record a more comprehensive measurement set than would be the case for full-scale ships participating in sea trials or for unconstrained tank tests. UK tank tests were all carried out in the Towing Tank at the Haslar facility, near Portsmouth, UK. Hydrodynamics is one of the more complex elements of the simulation to test as it consists of a number of components:

1. Checking the accuracy of the underlying data calculated offline using computational methods;
2. Checking the applicability of the methods used to look up and apply forces at runtime;
3. Checking the methods used to apply the hydrodynamic forces to the simulated ships.

In addition to the dedicated tank tests, data from tests carried out to assess performance of both isolated and interacting hulls for UK supply and receiving ships was provided, for cases where the hulls were unconstrained and fully appendaged. In the cases where tests were carried out using interacting hulls performing RAS manoeuvres, GPS and on-board controllers similar to the lead and following helms within the simulation were used to maintain the relative position of the ships throughout the test runs.

4.4.2 Constrained Tank Tests and Other Data for Hydrodynamics Validation

The constrained tank tests carried out for isolated and interacting hulls were primarily carried out to validate the hydrodynamics methods used to generate data to be used within the IRAS simulation. Tank test data collected in a dedicated facility using appropriate bare hull models was a core part of the validation strategy. These tests allow the models to be constrained and specific scenarios run to isolate particular forces and effects, enabling the validation of individual elements of the underlying calculations to be tested. This is particularly useful in assessing the calculation and application of hydrodynamic forces within the simulation. Tests and measurements included:

- Tank test results for yaw-constrained bare hull models;
- Tank test results for side by side constrained bare hull models;
- Theoretically derived Response Amplitude Operators (RAOs) for the supply ship;
- Experimentally derived RAOs for the receiving ship;
- Tank test results for unconstrained models of the ships with appendages.

These data sets were used to conduct various comparisons with simulation results. Two of the most significant analysis exercises were comparisons of measured and simulation forces for isolated constrained hulls and separately, for interacting hulls. Isolated hull test were carried out at various yaw angles, with the ships towed forwards in the tank and forces measured. Fig. 6 shows an example of the type of comparison carried out between simulated and measured data.

Tests carried out using side-by-side hulls to measure interactive forces were the most challenging to conduct. The tests successfully measured the side forces and post loads for both hulls; however, on inspection of the results it is clear that despite the best efforts of the test team, the overall forces included significant spurious contributions, most likely caused by the rig itself. These forces were of a similar order of magnitude to the interactions forces expected to be generated by the ships themselves in some scenarios. A subset of cases where the interaction forces were strongest – in general, where the lateral separation was small, and the smaller supply ship was located within the region affected by the wash from the larger receiving ship – were deemed suitable for use as validation data as the expected interaction forces were sufficiently large. Fig. 7 shows an example set of results for cases carried out at a fixed lateral separation, speed, and wave condition, and varying longitudinal separation. The overall results, when comparing the hydrodynamic forces measured in the tank test against data from the simulation set up to represent the tank test cases, indicate that both the isolated and interacting forces for constrained hulls match well, to within 10-15%, for cases with good measurement data.

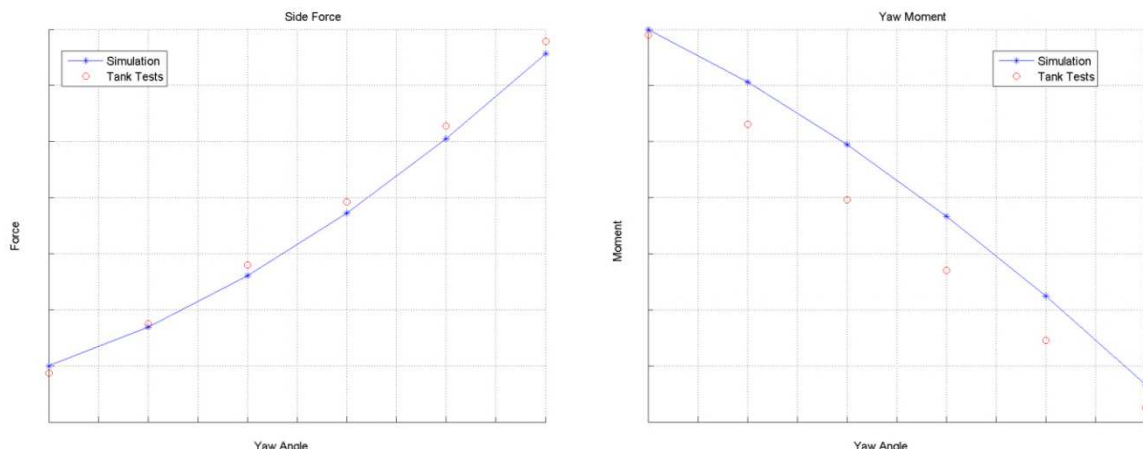


Fig. 6: Measured vs. simulated side force and yaw moment for a supply ship constrained at a given yaw angle and towed at a constant speed in a tank.

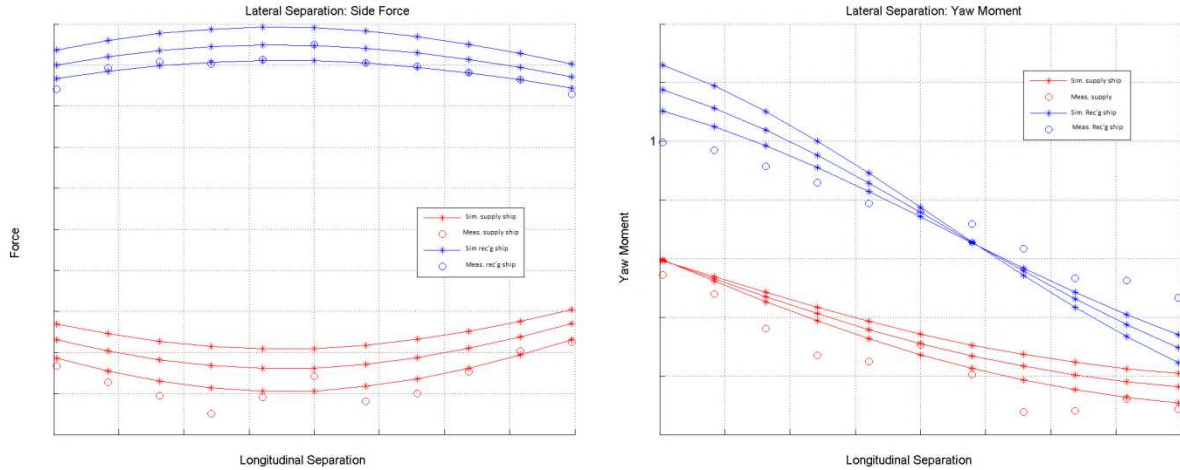


Fig. 7: Measured vs. simulated side force and yaw moment for two ships held side-by-side and constrained in sway, surge, yaw and roll. Lateral separation is held constant; longitudinal separation is varied between cases. Simulated results are shown by the continuous lines at the tank separation, as well as at $\pm 5\text{m}$; measurements are individual points marked by a ‘o’. Results in the upper part of the diagram are for the supply ship, in the lower part for the receiving ship.

4.4.3 Unconstrained Tank Test Data for Simulation Validation

In addition to the constrained tank tests specifically carried out for hydrodynamic validation purposes, data from unconstrained tank tests were also made available for other UK supply and receiving ships. These tank tests were carried out to measure seakeeping and manoeuvring performance including ship motions in waves and calm water, and were used as a validation data set for the complete simulation, minus a RAS rig. Tests were carried out for both isolated hulls, as well as for scenarios in which the two ships maintained station as if they were performing RAS station keeping using GPS and on-board controllers. The comparison between recorded and simulated data consisted of checking the capability of the isolated or side-by-side hulls to perform similar manoeuvres, as well checking the pitch, heave and roll motions during both manoeuvres and seakeeping.

4.4.4 Roll Performance

There are significant difficulties in accurately simulating the roll performance of a ship. The primary issue is the ability to accurately model the roll damping characteristics of a particular appendaged hull. The generally accepted approach to this problem is to either (a) represent roll damping using a polynomial, and tune the parameters appropriately using experimental data, or (b) use an empirically-based model, *ITTC (2011)*, which accounts for multiple linear and non-linear effects and is based on a combination of theoretical models and empirical data. Neither of these methods is ideal; we have found that calibration to real data is difficult to achieve, partly because appropriate and accurate measurements are difficult to obtain, and partly because due to the varied contributions to roll damping caused by different effects, appropriate parameters must be calculated at a range of speeds. The empirical method has been demonstrated to work reasonably well for ships simulated within IRAS in a range of conditions, but a full validation would require more data than we currently have available to us.

4.4.5 Sea Trials for Validation of Generic Components

No dedicated sea trials were carried out in the UK for the IRAS program of work. However, another Virtual Ships program, the NATO Submarine Rescue System (NSRS) simulation, has carried out four different sea trials exercises between 2011 and 2014, using one of two typical NSRS motherships. During these trials, mothership motion and Submersible Rescue Vessel (SRV) motion were recorded, as well as other operational parameters and data only relevant to the NSRS system.

We have used this sea trials data to carry out a number of Virtual Ships simulation validation activities, making use of measurement of both mothership and SRV motion. The data sets include measurements taken in conditions up to and including upper sea state 5. Fig.8 shows which components within this NSRS simulation are also part of the generic Virtual Ships capability, and therefore also part of IRAS.

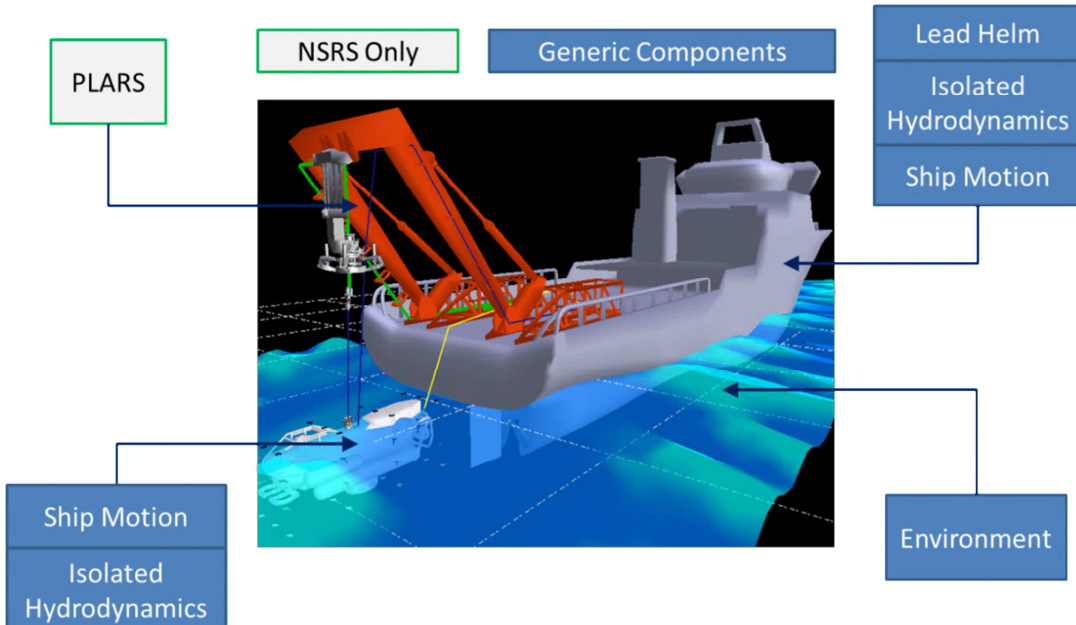


Fig. 8: NSRS simulation based on the same framework and generic components as IRAS; using the same hydrodynamics, ship motion, helm and environment plugins, introducing only one new component to model the Portable Launch and Recovery system (PLARS).

Results from comparisons of sea trials with simulation results have shown that in conditions up to and including sea state 5, the simulated and measured ship motions are statistically similar. This work has also yielded a number of observations about the overall performance of ships within the simulation, and the wave spectra used within the environment federate; these are reviewed in the section below.

4.4.6 The Simulated Environment

In recent years, for validation and trials purposes, we have performed a number of studies using data sets that include actual wave spectra measured using wave buoys. This type of data can be used to generate a wave spectrum that can be used as input to the simulation in the same format as the theoretical spectra. We have found that this gives much better agreement between sea trials data and simulated results, as would be expected. It is generally the case that measured spectra do not match any known theoretical spectra closely in terms of the amplitude profile with frequency. The waves in the simulation are the driving force for the motions; it should therefore be noted that care must be taken to configure any simulations with an appropriate spectra, particularly where results are to be compared with trials or test data.

One of the most interesting aspects of the measured NSRS sea trials data was wave data recorded by wave buoys deployed in the vicinity of the mothership during the trials. The IRAS simulation requires the user to provide a wave spectrum of up to 200 components, which is usually produced using one of the standard theoretical spectra: Bretschneider, Pierson-Moskowitz, or Jonswarp. The wave buoy measurements, which consist of a set of actual measured wave spectrum components plus a statistical measurement of modal period and significant wave height, were collected over the course of multiple sea trials. The measured spectra can be used as a direct input to the simulation; alternatively, the statistics can be used as an input to generate a theoretical weave spectrum.

It is notable that theoretical spectra generated using this statistical data do not match the measured spectra well for the recorded cases. This data was collected over several sea trials, at different times of year, and in different locations. Several examples of measured spectra collected during a single sea trial are shown in Fig.9, alongside example Bretschneider and Jonswap spectra representing similar conditions and used in the simulation.

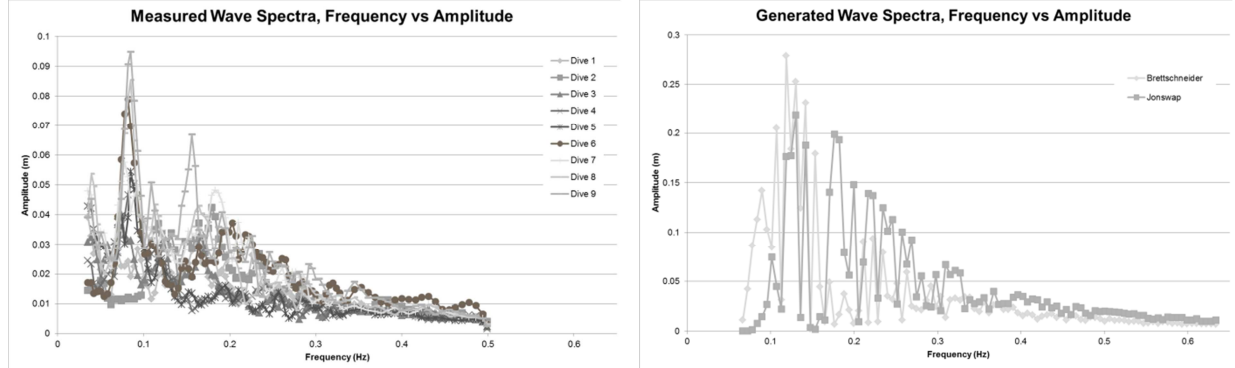


Fig.9: Left: Example measured wave spectra showing calculated frequencies and amplitudes. The profiles of these spectra vary considerably. Right: Generated Bretschneider and Jonswap spectra from a spectrum generator using the same significant wave height and modal period as a typical measured spectrum during the measurements period.

This result is as expected; it does however demonstrate the importance of selecting a representative spectrum or set of spectra, and of treating the problem of simulation validation and performance studies as a probabilistic problem. It is necessary to ensure that the runs carried out are sufficient to yield the full range of representative behaviour, and therefore understand the likelihood of occurrence of particular outcomes, especially in cases where discrete events such as RAS approach manoeuvres are being studied.

4.4.7 UK Validation Summary

The overall result of the validation exercises described above is that we have generated a broad set of data showing good performance for the simulation against a wide range of measurements. Due to the many issues that arose during validation related to measurement accuracy, test reproducibility, performance characterization disparities, and difficulties in simulating some of the behaviour within a RAS system, we conclude that it would not have been possible to validate the simulation using a smaller set of studies; the use of data from both different test and theoretical sources, and for different ship hulls was a crucial part of the overall validation process.

In practical terms, many simulation projects will not be able to spend the time and effort on validation that has gone into the IRAS project. Problems in doing this are generally related to a lack of good quality real-world data, which is expensive and challenging to collect. Some lessons learned during this work are as follows:

- Modular designs and clarity in functionality and interfaces is a key principle when following this type of V&V program. The ability to verify federates separately, in small groups, and as a complete federation makes it possible to perform many different types of tests and comparisons;
- Verification of individual federates and of the federation as a whole should be carried out as early as possible and repeated as necessary as development proceeds. The exchange of validation tests between suppliers of interacting components can be a very useful way of carrying out preliminary integration testing;
- Tank test data forms a core component of the data set required for V&V, in particular constrained hull tests for validation of hydrodynamic models to calculate forces generated by

isolated and interacting hulls. Careful consideration of how to set up and conduct these tests is needed in order to generate a useful data set;

- Sea trials validation is often conducted relatively early in a V&V program. However, it is best used as a final check for the federation once confidence in its physical accuracy is already high. As the measurements taken are usually limited to ship motions, they are an aggregate of all underlying physical effects in an unconstrained scenario, and therefore cannot on their own provide a high degree of confidence in the aggregated results. This also applies to tank test for appendaged, unconstrained hulls;
- An overall validation case can be built up using by combining multiple sets of incomplete data. In particular, the addition of independently collected data sets for validation is of value.

In summary, the process of V&V for complex simulations must be incremental and flexible, and it is important to consider how each individual element is to be verified and validated as well as to consider the simulation as a whole.

5. International Verification and Validation

As part of the IRAS PA, Italy, Germany, Canada and France also submitted validation data and evidence for the federation. This has been combined with the evidence generated by the UK to strengthen the case for validation of the UK and other variants of the IRAS simulation. This section briefly summarises some of the more significant work carried out by other nations.

5.1 Canadian Tank Test Data for Validation of Hydrodynamics Interaction Data

Of particular interest was the submission by Canada of a set of tank test data measuring interaction forces between hulls on Canadian supply and receiving ships, as well as a paper on a validation exercise carried out for the Canadian federation against this data set. This data and analysis joins the UK's tank test data, recording forces and moments for interacting supply and receiving ships within the repository of validation data. This is an important data set, as hydrodynamic interaction forces between two side-by-side hulls are one of the most difficult elements of IRAS to model accurately. The only way of demonstrating that the underlying hydrodynamic calculations are valid is to carry out comparisons with tank test data from experiments that constrain hulls in such a way that these types of forces can be directly measured. In addition, the Canadian data set can be considered to be completely independent of the UK data set: it was collected for different hulls, in a different test facility, with a different team running the tests and collecting the data, *McTaggart et al (2003)*.

The tank test cases were also run using the UK federation to further validate the hydrodynamic model and its integration into the simulation; Fig. 10 shows an example of the results obtained. A further comparison of simulated and measured results was also carried out by Canada using a French data set recorded for two interacting hulls.

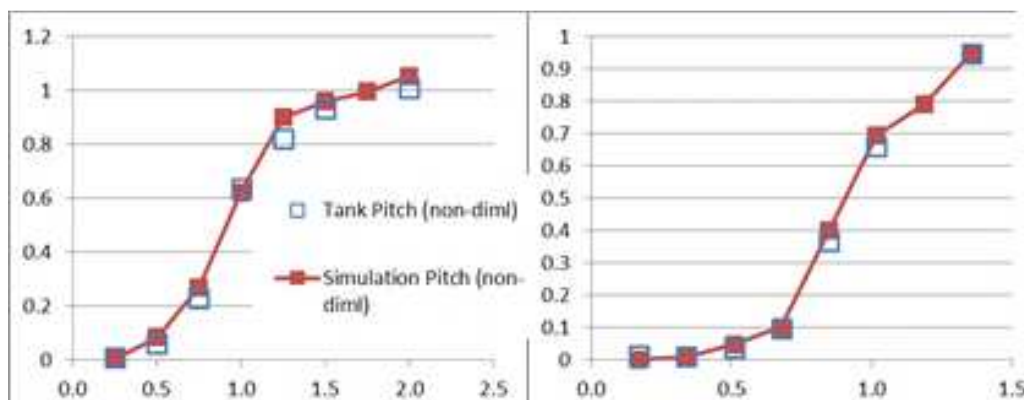


Fig. 10: Normalized pitch results for the isolated hull of the Canadian supply ship, as simulated by the UK IRAS federation and compared with supplied tank test data.

5.2 Italian Demonstration of Equivalence between National Federations

As discussed earlier in this paper, IRAS is an international capability, and each participating nation runs its own federation, based on the core capability but potentially with its own national substitutions or additions. At present, the primary variation between national federations is the ship motion calculation, as Italy, Canada and the UK have all supplied a federate for this purpose. In order to demonstrate their equivalence, Italy has carried out an exercise to run the same simulation cases using all three variants of the IRAS federation. At this point in time, the UK and Italian ‘flavours’ of the federation have been demonstrated to perform similarly.

5.3 German Validation against Sea Trials Data

This exercise compared simulations run using the UK and Canadian ship motion federate against data collected as part of a set of German sea trials. Cases available were turning circles in calm water, and ship motions in pitch, heave and roll collected in waves. This exercise therefore provides additional evidence on the equivalence of the different national federations, as well as an overall validation set for the complete IRAS federation consisting of ship motions. As noted above, overall motions cannot be used in isolation to validate this type of simulation, as they do not provide a precise enough way of checking that all underlying behaviours and calculations are correct. However, sea trials data works well as a high-level validation set to check performance at the end of the V&V process when confidence is high that the federation is behaving correctly in all aspects.

6. Conclusion

The provision and maintenance of this type of simulation capability is a challenging task that requires significant effort to be expended not only in terms of design and development, but also in terms of verification and validation, maintenance, and consideration of how the capability will be used. We believe that the IRAS simulation capability is now a leading example of how to conduct verification and validation for maritime simulation, and demonstrates how to deal with the difficult and complex nature of such a validation process. It is also one of the only programmes of its kind to create a simulation that is available for use internationally.

We have presented an outline of the process by which the UK has participated in the design, development and validation of the IRAS simulation, focussing on the V&V process conducted, which included testing the simulation against theoretically-generated results, tank test data, and sea trials data. We have also provided examples of international collaborations carried out in achieving this. Our intention is now to make full use of the capability to begin analysing RAS scenarios of interest to the UK MoD.

Acknowledgements

The verification and validation activities reported in this paper were significantly enhanced by the support provided from the other participating PA nations Canada, France, Germany and Italy.

References

ITTC (2011), *Numerical Estimation of Roll Damping*, Recommended procedures, International Towing Tank Conference

McTAGGART, K; CUMMING, D.; HSIUNG, C.C; LI, L. (2003), *Seakeeping of two ships in close proximity*, Ocean Engineering 30, pp.1051-1063

NSA (2012), *STANAG 4684 Standards for Virtual Ships*, Draft, NATO Standardization Agency

Potential Benefits of Augmented Reality in the Smart Ship

Scott Patterson, Babcock International, Lichfield/UK, scott.patterson2@babcockinternational.com
Andrew Webb, Babcock International, Lichfield/UK, andrew.webb@babcockinternational.com

Abstract

This paper describes potential benefits of Augmented Reality (AR) technology in merging the physical and digital versions of a vessel in order to help the crew of a future smart ship improve the effectiveness and efficiency of support and operations. The developing challenge around ships and fractured digital solutions is discussed and AR introduced as a potential mitigation. The paper explores a roadmap for AR alongside secure wireless communications (including Li-Fi), wearable and mobile technologies, smart sensors and powerful onboard analytics.

1. Introduction

When a new vessel is delivered it is (ideally) accompanied by a digital version of itself containing all of the information required to keep it safe, effective and available throughout its life. As the physical ship both ages and adapts to new requirements so does the digital one in order to keep pace. The two vessels (one physical and one digital) are linked together but often decidedly separate such as in differences between as designed and as built as items of equipment onboard are upgraded to overcome obsolescence but the documentation and training has not kept pace.

2. The Emerging Challenge

2.1. The Physical Ship

External drivers such as automation and cost savings have reduced crew size, especially for navy vessels. Other factors (such as the demands for increased endurance and capability) have increased the physical size of these vessels. E.g., the Type 45 destroyers have almost doubled in size compared to their predecessor (Type 42) but have a ship's company of just 190 compared to 250 on the older vessel. The Invincible class had a displacement of approximately 22,000 tonnes and a ships company of 650 (not including embarked air wings) whilst the Queen Elizabeth class will have a displacement of approximately 70,600 tonnes and a ship's company of just 679, only increasing to the full complement of 1,600 when the air elements are embarked. The negative effects of this relative reduction have been mitigated by increased levels of automation but exacerbated by the growing technical complexity of that automation and the increasing demands of regulation and compliance.

2.2. The Digital Ship

As well as an increased physical territory for each crew member to cover they also have an increasing range of duties reliant on engaging with the digital version. This is not an easy task with a diverse and fragmented range of systems needing to be engaged frequently throughout every day. The range includes logistics systems, maintenance systems, drawings, administration systems plus all of the operational and communication systems they support. These systems are not well integrated leading to multiple logon accounts, system servers, laptops, software upgrades and swivel chairs between systems. All of this distracts crew members from their core roles and prevents them from becoming more efficient and effective.

2.3. Innovation

An innovative approach is required to help cope with the growing challenge and to bridge the gap between the physical and the digital ship. Solutions are required which make personnel safer and more efficient. As the data from a future smart ship (with greatly increased sensing, automation and

communication) grows it must be capable of empowering the crew, providing the ability to call up assured information seamlessly and on demand. It must also enable unobtrusive data gathering to improve evidence-based decision making and analytics.

3. Augmented Reality

Augmented reality (AR) is a live direct or indirect view of real-world environment whose elements are augmented (or supplemented) by computer-generated input such as sound, video, graphics or GPS data. It is related to a more general concept called mediated reality, in which a view of reality is modified (possibly even diminished rather than augmented) by a computer. As a result, the technology functions by enhancing one's current perception of reality. By contrast, virtual reality (VR) replaces the real world with a simulated one. Augmentation is conventionally in real-time and in semantic context with environmental elements, such as sports scores on TV during a match. With the help of advanced AR technology (e.g. adding computer vision and object recognition) the information about the surrounding real world of the user becomes interactive and capable of being digitally manipulated. Information about the environment and its objects can be overlaid on the real world.



Fig. 1: Using a mobile tablet to augment the real-world view in an industrial context

4. Benefits of Augmented Reality

An understanding of both the technological development of Augmented Reality and in-service support challenges raises some potential benefits in applying the technology:

- Seamless Integration
Merging the physical and the digital ships in real time to exploit the information from both in order to facilitate better decision making.

- Internet of Things
Providing a route for real-time visualisation of the increased data from the smart ship and internet of things to drive more efficient ways of working.
- Hands Free Operation
Through the use of AR Glasses, the maintainer may carry out his tasks unencumbered by laptops or the need to log onto multiple systems to access the information needed to complete each task.
- Live Feedback
Unobtrusive control room access to see what the maintainer is doing in real time and to monitor and record maintenance activities and defects.
- 3D Images
The ability to overlay animated 3-dimensional digital models of the equipment over the physical version in order to provide supplementary information and thus reduce errors and uncertainty when undertaking tasks.
- Multi-Media
Instant access to multi-media training, maintenance, logistics and operations material, provided to the point of need.
- Workflow Approvals
The ability to automate permissions to undertake work from the coal face direct to the correct approver with a full (automated) record of the steps and warnings required and undertaken.
- Unobtrusive Data Capture
Full recording of what was seen in the real ship, what was recorded from sensors, what the wearer of the technology viewed from the digital ship and what decisions can be taken to provide complete auditability.



Fig. 2: Hands-free operation in a support environment

5. Technical Developments and Demonstrations

5.1. Initial Tasking

In early 2015, we were asked by the Ministry of Defence to deliver a proof of concept (PoC) demonstrator to explore the benefits of Augmented Reality for an engineer in the submarine maintenance and support environment. One of our business units had already developed a similar product for a major infrastructure provider but that relied heavily on GPS technology – something that cannot be relied upon inside a submarine.



Fig. 3: Graphic description of the Augmented Reality demonstrator rig

5.2. Phase 1 PoC

Phase 1 was undertaken over an 8 week period from the initial whiteboard session to demonstration of the technology within a mocked-up submarine compartment containing samples of representative hardware in order to create as much of an immersive experience as possible. As the team were dealing with the unknown, an agile development approach was selected with weekly reviews with the customer to check progress and agree next steps. A range of mobile devices was considered from tablets and wearables to glasses. Through early exploration of the use cases, glasses were selected to allow hands free use by the maintainer. Standard positioning methods (GPS, built in accelerometers) were discounted by the operational context and replaced by an ultrasonic tracking system to give the highly accurate positional data required to provide a seamless overlay. Phase 1 was through the demonstration of a scenario where a routine set of rounds was enhanced by Augmented Reality information streamed to the crew member which highlighted a fault on an item of equipment. A specialist maintainer then used the same technology to access training videos, system schematics and parts details through the glasses before viewing an expanding three-dimensional overlay to understand how the equipment should be dismantled.

Once the investigation was complete a faulty o-seal was discovered identified and a replacement manufactured by 3-dimensional printing. The PoC demonstration was successfully demonstrated the potential utility of Augmented Reality but also raised new questions about how and where it would be most useful within wider use case.

5.3. Phase 2 Demonstration

Phase 2 considered the learning from Phase 1 and broadened the scope of the demonstration from just Augmented Reality into developing a future vision for platform support which encompassed all of the enabling technologies to support the use of AR. In addition to improving the Augmented Reality system itself, the team also developed seamless integration with smart sensors to deliver live analytics and mobile applications to demonstrate how communications and workflows might operate between the maintainer, control room and Marine Engineering Officer. Improved and ruggedized hardware was utilised to better demonstrate the practicalities of the environment and other wearable technologies added to demonstrate wider benefits in communicating with technical teams. Phase 2 was demonstrated to the Ministry of Defence at several sites between January and March 2016.

6. Lessons from the Technical Demonstrations

The following lessons were identified so far:

- Phase 1 Lessons
Augmented Reality technology has exciting possibilities but the use cases were not sufficiently clear to determine where the most compelling benefits (and hence return on investment) lay.
- Phase 2 Lessons
By broadening the scope of Phase 2 it was understood that Augmented Reality on its own is not sufficient to improve support performance but that may form part of the eventual answer on the smart ship. The most immediate benefits may be in communication, workflows and unobtrusive data capture, but also instant access to the full range of digital data required to operate and maintain the ship. Augmented Reality may change how personnel undertake their roles onboard; it also places increased emphasis on the fundamentals of Integrated Logistic Support if the full benefits are to be realised. The technology will need to work in conjunction with other supporting technologies and systems onboard (secure wireless, communications systems, Platform Management Systems, Condition Based Monitoring, etc.)

7. Augmented Reality Technology Detail

For Phase 1 of the technical demonstration, Epson Moverio BT-200 glasses were chosen as the Augmented Reality hardware in order to provide hands-free operation to the user. They required significant modification to add an ultrasonic tracking system for sufficient geospatial accuracy for the user to experience seamless integration.



Fig. 4: Unmodified Epson Moverio BT-200



Fig. 5: The modified glasses in use during the first demonstration

The communication system was also enhanced to allow the audience of the demonstration to understand what was taking place as were the background analytics which simulated the smart ship. An expanding 3-dimensional model of the example pump was provided by Skills2Learn and integrated with the solution.



Fig. 6: Unmodified Epson Moverio Pro BT-2000

For Phase 2 an Epson Moverio Pro BT-2000 Smart Headset was obtained to provide a more rugged platform for industrial use and a live camera feed for integration into the ship's systems. Wireless smart sensors, smart watches, RFID tagging, control room screens and mobile tablets were also integrated into the solution to fully demonstrate the benefits within the smart ship.

Due to the emerging nature of the technology, most of the code had to be created from scratch. This included an innovative user interface which explored the potential of controlling the technology through head gestures.

8. Supporting Technologies to enable Augmented Reality in the Smart Ship

The adoption of Augmented Reality technology in the smart ship could dramatically improve the efficiency with which maintenance tasks are undertaken through instant access to the onboard digital library. However, it cannot be implemented without a range of supporting technologies. Many of these technologies are core requirements of the smart ship:

- **Wireless Technology**
Wireless communications technology is the primary enabler to the adoption of Augmented Reality for both positional accuracy and communication. Depending on the operational context it need not be WiFi but could also utilise other technologies such as ultrasonics, Bluetooth or LiFi (communicating wirelessly through the visible light spectrum). Without wireless technology onboard some of the functionality of Augmented Reality may be possible (such as through image recognition) but it is less likely to be successful.
- **Smart Sensors**
Wireless smart sensors would combine the benefits of live information feeds to the Augmented Reality user and fully support a Condition Based Monitoring and maintenance regime. These sensors could create their own maintenance burden (especially if powered by batteries) but developments in harvesting power from host machinery vibration or photovoltaic cells will likely mitigate this in the future.
- **Onboard Analytics**
The user of Augmented Reality devices will not wish to be overwhelmed by data feeds. Onboard analytics, whether simple and rules-based or based upon more complex machine learning should ensure that only relevant information is provided at the point of use. Processing onboard will limit the requirement for communications bandwidth to shore authorities but will also benefit from fleet-wide experience when combined at suitable intervals. The enhancement in unobtrusive data gathering should also improve the quality of data by reducing the opportunity for human bias from the process.
- **Wearables**
Whilst our demonstrations focussed on glasses, a large number of other wearable devices are in production or development and the end user may benefit from utilising a combination of these. As an example; a tap on the wrist from a smart watch may be sufficient to warn a maintainer of a performance issue directly without the need for main broadcast announcements.
- **Integration**
To further release the benefits of the technology, it could be integrated with existing onboard Platform Management Systems and Mission Systems but the data fusion challenge would be considerable if not planned and developed during the early design phase.
- **Others**
If Augmented Reality technology was embedded as part of the onboard communications, administration and operational ecosystems it would also support the implementation of 3-D printing, RFID tagging controls and other initiatives.

9. Obstacles to Implementation

Alongside the positive developments and opportunities for Augmented Reality, there are also considerable obstacles to be overcome which may delay or prevent eventual adoption. The first of these is the embedding of reliable and secure wireless networks onboard due to security and interference issues. Justifying the costs of development and implementation will also be challenging as the benefits are wide and varied, but difficult to prove. It may take considerable patience and commitment to fully realise the potential.

As a new form of communications technology it could increase the number of interfaces and therefore risks of cyber-attack. The practicalities of providing sufficiently robust hardware would need to be overcome. The main manufacturers recognise this and are now producing hardware for industrial customers but have some way to go before becoming ‘jack-proof’. Environmental effects such as vessel movement and inevitable black spots need to be better understood. Current gaps and weaknesses in support solutions would become extremely apparent through gaps in cover through Augmented Reality. The costs to remedy this may be high and unjustified depending on remaining platform life.

10. Other Use Cases

This paper has focussed on the potential benefits of Augmented Reality technology in an onboard maintenance use case but it is recognised that for a technology as immature as Augmented Reality this may not be where it is best or most sustainably utilised. Other use potential cases include in fire-fighting scenarios with reduced visibility due to smoke or on the bridge visual sightings can be augmented by information from navigation and surveillance systems. Training could be accelerated if the name and purpose of complex components was provided during familiarisation. Decision support could be enhanced through live communication and data gathering. Further exploration and study is warranted to better understand these and other uses.



Fig. 7: Potential use case to assist firefighters

11. Conclusion

At the beginning of this paper the challenge of larger, more complex vessels and smaller ships companies was discussed in relation to both the physical ship and the digital twin. Initial developments and demonstrations of Augmented Reality have shown that it has the potential to move these two closer together and make onboard support simpler to perform and safer to control: however, this can only be achieved once the underpinning enabling technologies have been sufficiently de-risked to allow onboard installation. This is the challenge for the next phase of this work which will aim to demonstrate a smart ship concept in a full scale surface ship demonstrator.

Recording As-Built via an Open and Lightweight Solution Supplemented by a Process Evaluation Model

Matthias Roth, Siemens Industry Software GmbH, Cologne/Germany, matthias.roth@siemens.com

Abstract

Siemens PLM Software is taking part in the state-funded German research project ARVIDA - among twenty-one other partners. One of the sub-projects is to support shop floor workers with a tool that provides the backflow of information into the PLM (product lifecycle management) system in an open, lightweight way. The demonstrator aims at the individual manufacturing industry, such as shipbuilding. One of the prerequisites was to enable partners to update their heterogeneous software systems with as-built shop floor information. Also, a benchmark of different ways to assess the possible methods was demanded. In the following paper, the concept of the software is presented as well as the valuation model for the comparison of PLM-supported process landscapes - especially regarding the data formats being used and the reduction of iteration cycles between shop floor level and construction department.

1. Introduction

Supporting the product lifecycle from cradle to grave is one of the keys to a successful product. In a global environment, challenges in shipbuilding are even greater. Reducing production times, increasing complexity, higher demands on the accuracy of the construction documents and extended MRO life cycles – especially when it comes to the constant changes that are inherent to structures as large as ships – all of these give rise to a need for an accurate as-built recording on shop floor level. To face these challenges, subprojects of the German state-funded research project ARVIDA included the target-actual comparison in various industries. One of these subprojects is the recording of the as-built within the heterogeneous system landscape of a partner shipyard. An open and lightweight strategy (OLS) was used, in order to enable the various systems to be fed with the high amount of data. The concept of OLS plays an important role in this matter, as it is a new way to use lightweight data formats such as JT not as “frozen”, Vettermann (2010) data but also as an upstream format. In order to prove the efficiency of the concept, a process valuation model was set up for the comparison of PLM processes – especially with regard to the corresponding data formats and their abilities to fulfil the requirements. In the paper at hand, the software demonstrator as well as the valuation model will be explained in short.

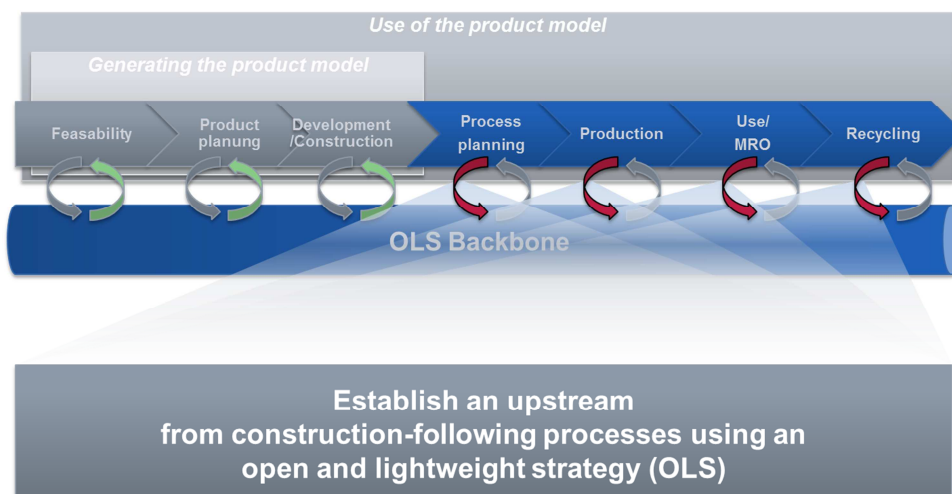


Fig. 1: Establishing an upstream from late PLM processes into the OLS data backbone (red arrows), Roth (2012)

2. Approach: Process analysis and requirements elicitation

The research partner needed an upstream of information from shop floor level to reduce iteration cycles, which partly took place due to the lack of updated data on construction level. Another reason for the need of information upstream was formed by general preconditions in shipbuilding (such as late changes during production or the tolerances in steel welding processes). As the latter one couldn't be changed with a reasonable effort, the first one is a clear objective of advanced PLM solutions. So the main goal was to establish systematic information upstream from shop floor level.

2.1. Process Analysis

The process analysis of the current “problem reporting” process showed that there was no systematic information upstream of the changes taking place on shop floor level. Mainly, an oral information package was passed between worker and principal worker, and then is entered to the ERP system by a third person. Sometimes, there wasn't any information being played back at all. The PLM system often wasn't fed with information at all. In order to give a systematic information flow from shop floor level to the PLM system, an open approach was taken as the historically grown heterogeneous system landscape of the research partner showed the need for it. A lot of iteration cycles took place between shop floor and construction department, partly with time-consuming on-site visits.

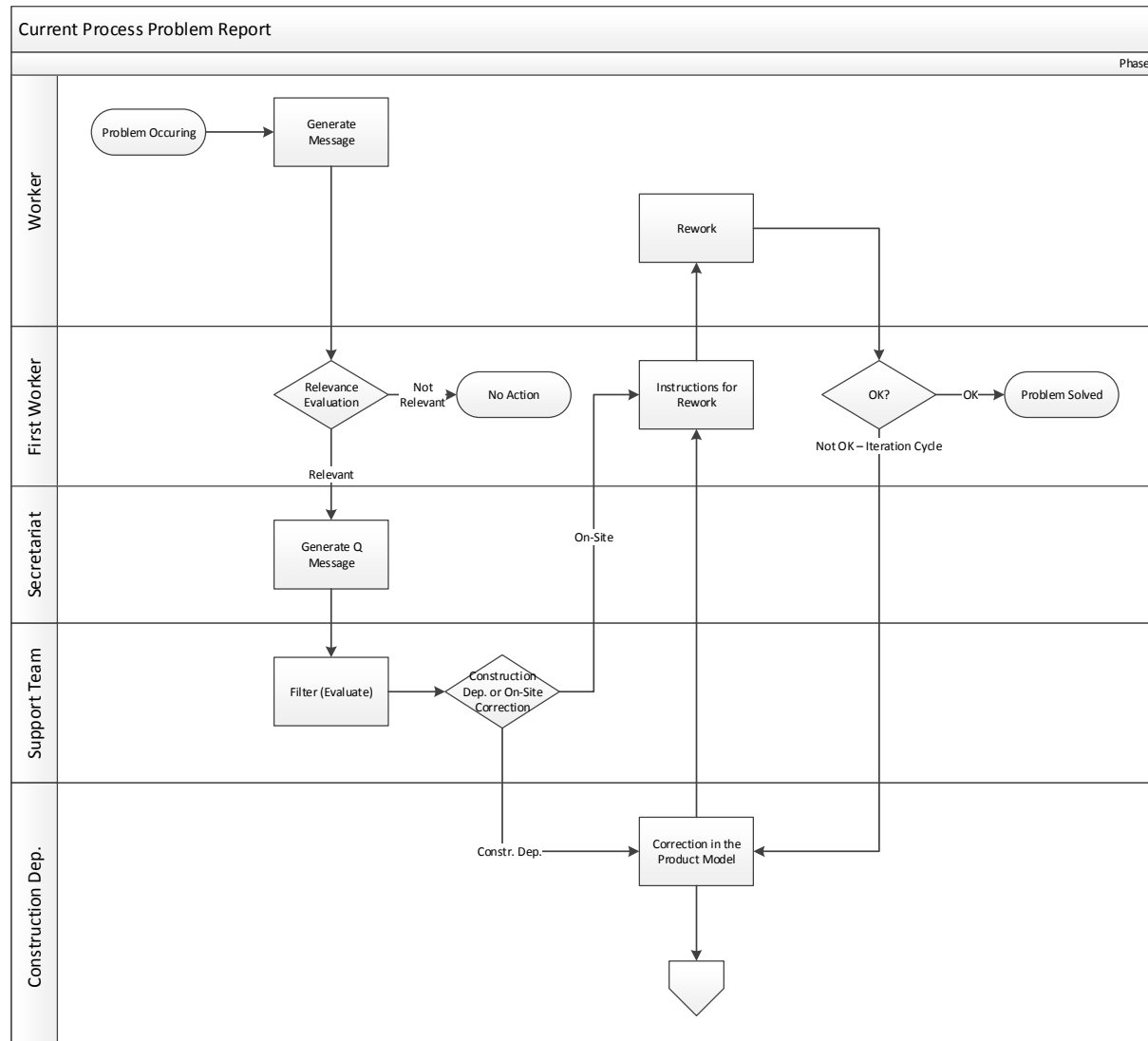


Fig. 2: Simplified swimlane process diagram of the current problem reporting process

2.2. Process Synthesis

Based upon the challenges, a process was designed that enabled the flow of information from the worker on shop floor level to the responsible persons in the construction department. The process incorporates omitting the role of the secretariat as there is no more transition from oral to textual information. The supervisor worker enters the information directly in the tablet with the as-built recording software. Responsible persons in the construction department receive a notification as soon as synchronization takes place. A change process is initiated if needed. Information is being played back.

The consistent use of JT as an open format plays a significant role in getting the information without breaks to the construction department and beyond - e.g. further MRO processes. Also, the time-consuming iteration cycles and on-site visits are much less with the availability of 3D information from shop floor level in the construction department.

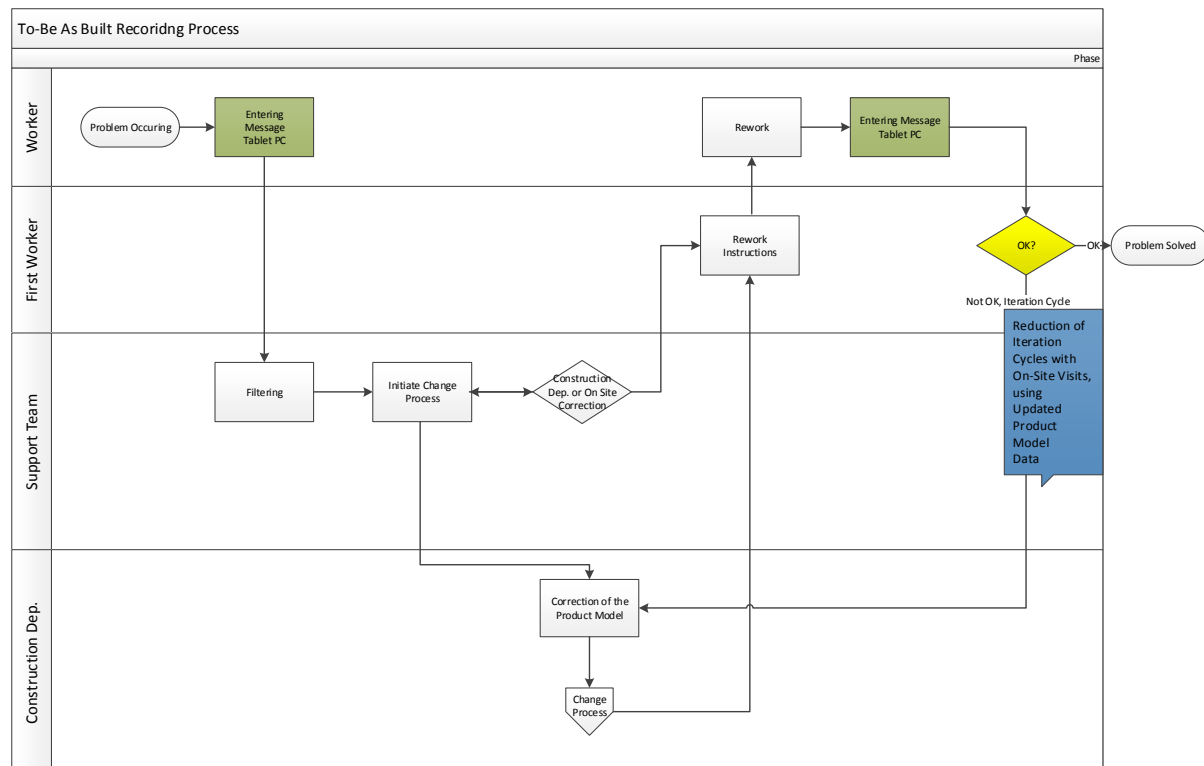


Fig. 3: Simplified swimlane diagram of the to-be-process

3. Realization of a Software Demonstrator, Providing As-Built Recording via an Open and Lightweight Solution (OLS) as a Proof-Of-Concept

To realize the as-built recording software demonstrator via an Open and Lightweight Solution, a given visualization software – Teamcenter Visualization – and its API – PLM Vis Toolkit – was used to program a viewer demonstrator that fulfils the key requirements. According to the field the final software will be used, the demonstrator is being held very simple in its User Interface (UI): Shop floor workers, which are usually not trained on complex CAD systems, should be given the possibility to use it without extensive training. Minimising the amount of user controls, the UI was reduced to a few buttons which can be used for this certain purpose. A low error quote and an easy handling are ensured this way. Being based on JT and PLMXML, an open and lightweight strategy (OLS) is used to ensure both performance and access to the heterogeneous system landscape of the research partner.

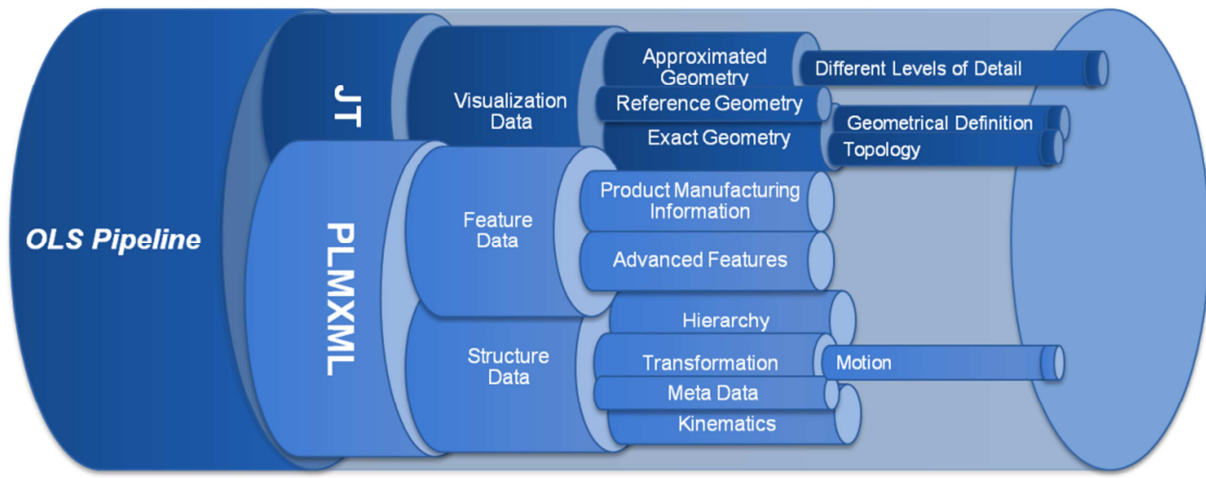


Fig. 4: The OLS Pipeline as in *Eigner et al. (2012)*

A part can be chosen via touch interface or mouse. The built status can be set by the buttons in the top bar. The buttons allow the user to set the built status to “in progress”, “mounted”, “not mounted”, “changed”; also, notes can be attached. A colour coding helps to quickly grasp the status of several parts at once. Red is for not mounted, green is for mounted, yellow for changed, blue for in progress.

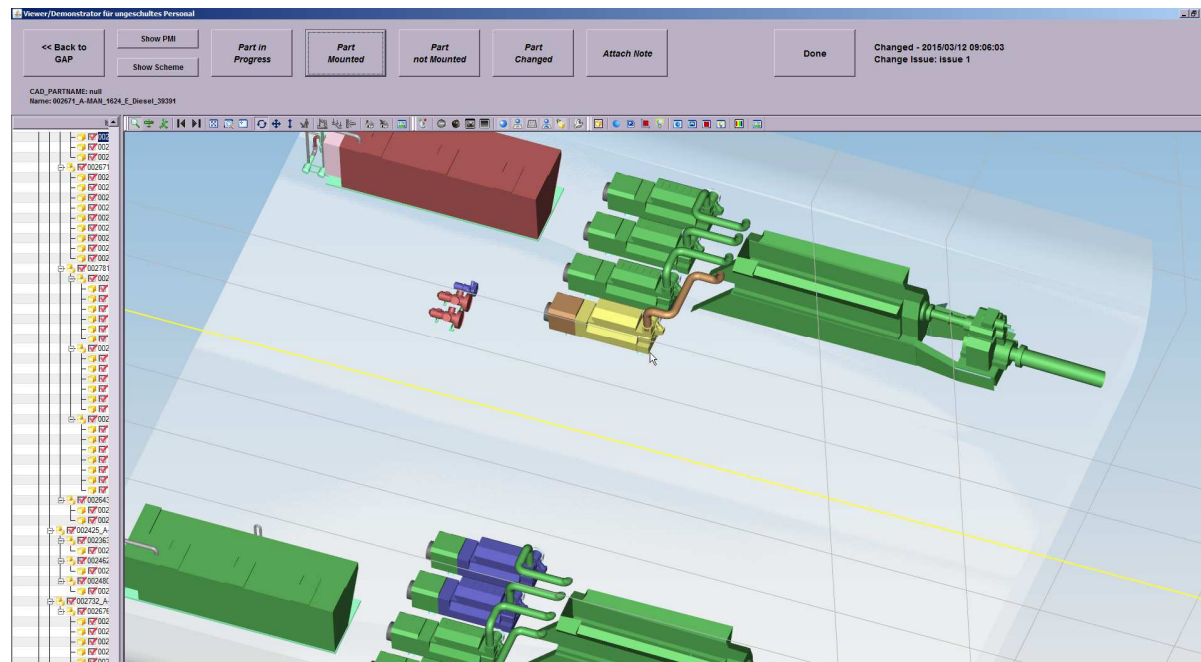


Fig. 5: The software demonstrator

The software was extended also for the handling of piping schemes, which can be represented in JT, too. The build status (and checking) of pipe isometrics plays an important role during the build of a ship or plant. Customer-specific piping databases can also obtain the data from the open format (JT, PLMXML). Also, colouring of the pipe isometrics - depending on the build status - takes place. Setting the build status for pipe segments (instead of the whole pipe) still poses a challenge – this requirement is not yet met.

On the Hardware level, basically any Windows Tablet PC can be used for running the software. It can be run offline, since WiFi is usually not available inside the ship at the shop floor. Data exchanges could for example take place at the end of the work day or during breaks, when a wired connection or WiFi is available.

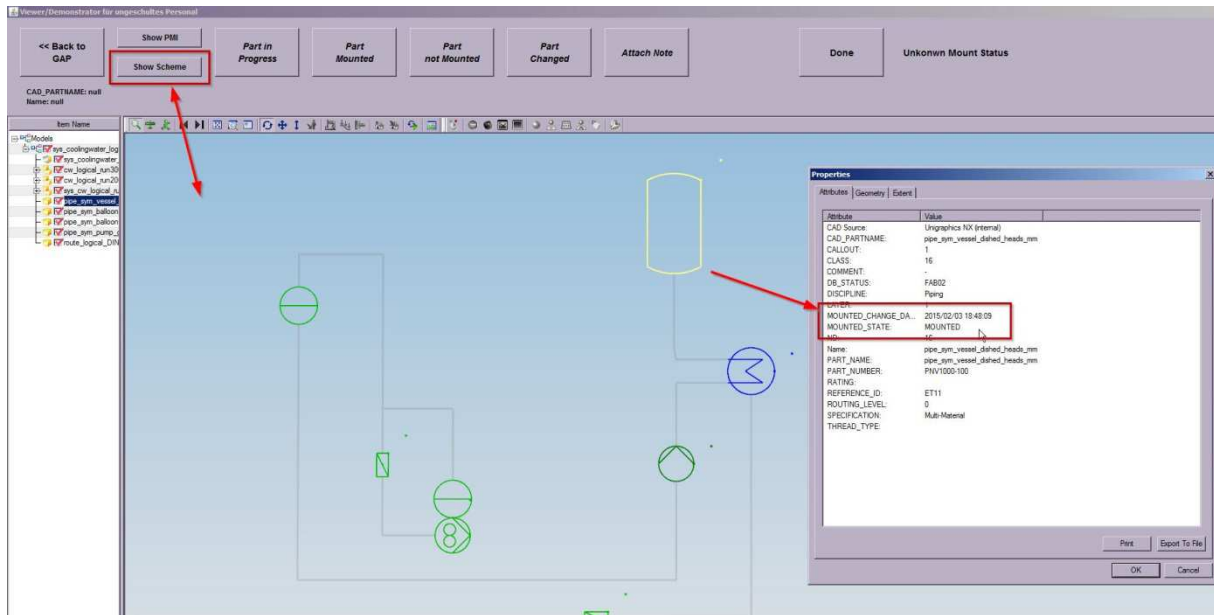


Fig. 6: Recording the as built of piping isometrics, also using JT as an open format

4. Extension of JT as an Upstream Format

By means of the PLM Vis Toolkit, the formerly as a “downstream” container format known JT format was extended for the information upstream. This approach was already published in, *Roth (2012)*. In order to meet the data format requirements, JT was extended by attribute fields for the build status, the user name and the date as well as a note field for extended information, e.g. a note or a link to a photo.

The information is then attached to the JT part. The build status as well as the user name and date are written into newly defined attribute fields. Other applications which are able to read the (open and standardized) JT format can obtain this information for their purposes. The information is attached to the Property Proxy Meta Data Element, which is described in *JT File Format Reference (2011)*.

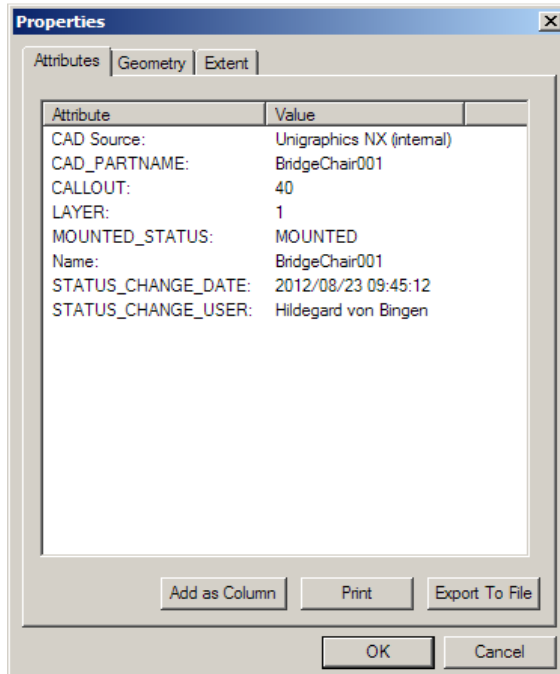


Fig. 7: Extended attributes (MOUNTED_STATUS, STATUS_CHANGE_DATE, STATUS_CHANGE_USER) as in the part properties dialog box, *Roth (2012)*

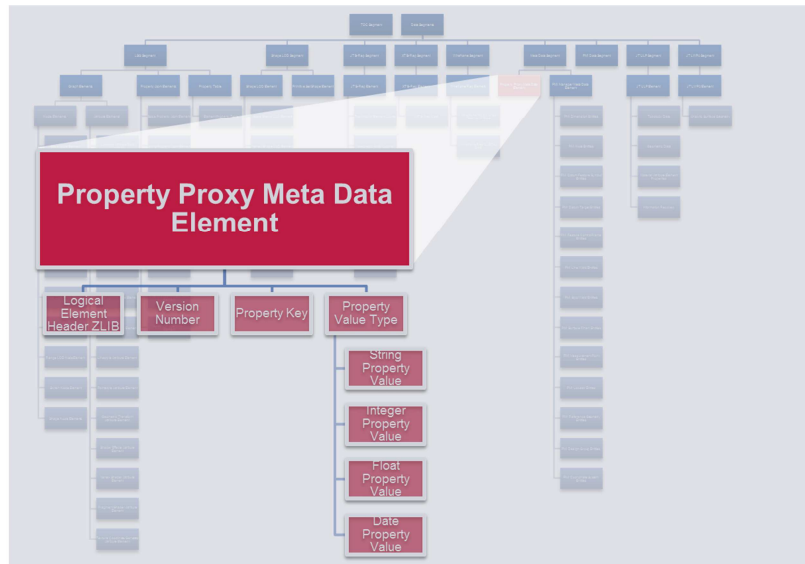


Fig. 8: Structure of the JT file format, the node for the extension of user attributes being highlighted

5. PLM Integration

For the integration of information in the PLM system, workflows for updating the part attribute fields have been designed; those were also taken to initiate approval processes involving the responsible persons in the construction department. Actions on shop floor can lead to serialized parts; to pass the information to the as built application, the approach was to set an *empty* attribute tag for serialization that is recognized as the „okay“ for a part to be serialized by the worker. If this attribute tag is available, the worker can assign a new serialized number. An approval workflow in the construction department will automatically be started and the responsible person gets a notification.

6. Outline of the valuation model for processes, especially regarding data formats

A format benchmark with in the Power-VR research project by Friedewald *et al.* (2011) showed during its setup that the company-specific requirements are mandatory for getting the right results from the benchmark (and the results right). At a closer glance, it was obvious that those came from a process-level - decisions for formats are basically set up by the processes a company has (and to a certain degree vice versa). So during the ARVIDA sub project for as-built recording at Siemens, a process valuation model was asked. As a basis, because of the topicality and closeness to shipbuilding, the process valuation of Hochstein (2014) was chosen. The process valuation model of Hochstein is based on the degree of finalization in a certain time. When a transition of information between two processes takes place and information is lost, Hochstein defined this as the “Design Drop”, picking up an initial idea of Burr (2008). It is the actual amount of information being lost, calculated in a formula including the values FE and FS. FE is defined in Hochstein as an estimated value from 0 to 1. It depends on the necessity of the outcome of a first process to a second process. FS is, according to Hochstein, a value which describes the transition between the system interfaces –from 0 to 1; T_{0B0} is the start time of the “local” process, E is the degree of finalization, P_{recB0} is the “performance” in the recover (rework) phase which follows necessarily the design drop – in order to achieve the same degree of finalization. DD is then the “Design Drop” - being calculated as follows:

$$DD = (E_{1,1} - E_{r,1}) * (1 - (FE_{1 \rightarrow 2} * FS_{1 \rightarrow 2}))$$

The time T_{rB0} to recover (rework) the information was defined by Hochstein as follows:

$$T_{rB0} = T_{0B0} + \left(\frac{T_{1A1} - T_{rA1}}{E_{1A1} - E_{rA1}} * DD \right) * (1 - P_{recB0})$$

6.1. Redefinition of the FS-Value

The difference in the approach of the paper at hand is that FS is not being estimated by a table with verbal descriptions as in Hochstein, but being calculated using the requirements of the processes. The definition needed further extensions in the scope of the ARIVDA sub project to be precise enough for valuations regarding the data format being used. The FS value as a data format valuation incorporates the requirements, their prioritization and the actual fulfilment of requirements by the corresponding formats (see the example in Table I). The result is normalized regarding the maximum possibility of requirements fulfilment and put into comparison to assess the given formats and their abilities. More detailed spoken, requirements per process were taken as the base. They are being prioritized each (values 1..3 for low-medium-high priority). The outcome is a matrix of prioritized requirements corresponding to their respective processes.

Table I: Example table of requirement prioritization per process

Requirement	1	2	3	4
Process 1	Low	Low	--	Low
Process 2	--	--	Low	--
Process 3	High	Low	--	--
Process 4	High	--	Medium	High

$$AP_{ij} = \begin{cases} 1, & \text{if priority is "low"} \\ 2, & \text{if priority is "medium"} \\ 3, & \text{if priority is "high"} \\ 0, & \text{if there is no priority set} \end{cases}$$

This matrix is being multiplied with the format abilities per requirement.

$$AF_{i,n,m} = \begin{cases} 0, & \text{if the requirement is not fulfilled} \\ 1, & \text{if the requirement is fulfilled} \end{cases}$$

The maximum possible value – all requirements fulfilled – is:

$$A_{max,i} = \max_{i \in (1..n_P)} (AP(n, i) \circ AF(i, n, m))$$

The two are set into relation to each other. So, for a given process transition from process 1 to 2, the formula would be:

$$FS_{1 \rightarrow 2} = \begin{cases} \frac{AP(n, 2) * AF(2, n, m)}{A_{max,i}}, & \text{if } A_{max,i} > 0 \\ 1, & \text{if } A_{max,i} = 0 \end{cases}$$

With AP being the prioritized requirement, AF the format ability and FS the outcome per process (in this example: from process 1 to 2).

The results of FS between the current and the to-be processes are shown in Table II. The calculation is based upon the process requirements and corresponding format fulfilments. Processes that are not relevant have been left out. The table shows the significantly higher suitability (higher FS values are better, more prioritized requirements met) of a proper format solution in a more adapted process.

Table II: Comparison of the calculated FS values. Stars (*) mark format transitions, e.g. from oral messages to SAP or native CAD

FS Value / Process ID	Current Process (different formats: oral/Q message/NX native)	To-Be-Process (JT)	To-Be-Process (STEP AP 214)
P1	1	1	1
P2	0,26	0,92	0,82
P3	1*	1	1
P4	0,08	1	1
P5	0,6*	1	1
P6	0,86	0,89	0,75
P7	0,86	1	1
P8	1*	--	--
P9	--	--	--
P10	--	0,9	0,79
P11	0,21	0,93	0,79

Given the actual to-be process from the ARVIDA sub project, the difference between an older format such as STEP AP 214 and JT is not too high. As STEP AP 214 is not lightweight at all, *Friedewald (2011)*, in an industry with extremely large model sizes such as shipbuilding a more “modern” format such as JT can be expected to be more suitable in the practical use, *Friedewald (2011), Eigner (2013)*. It is obvious that this aspect is not yet covered in the valuation model.

Further investigations have to be undertaken to include also FE values and the actual times of each process step. Given the current problem reporting process and the to-be as-built recording process, the comparison of the FS values already shows that the goal to record the as-built will (assuming constant FE values) be achieved faster with a process designed for OLS formats than with the current problem reporting process, which doesn't make use of OLS formats.

7. Conclusion

The given requirements from the process analysis and synthesis led to the idea of using an Open and Lightweight Solution (OLS) as an upstream format. Openness is a key factor to future PLM environments. By realizing a proof-of-concept software demonstrator and a valuation of the as-is compared to the to-be process in an extended process evaluation model, the effectiveness of the approach has been proven. The process valuation model is universal in the context of PLM and data formats.

Further steps have to be taken to put the approach into practice. On a process level, these are for example establishing approval processes and support processes. Questions of an online approval came up during the project. On a software level, practical requirements such as setting the status for segmented pipes or giving the other relevant system views such as cabling or HVAC (Heating, Ventilation, Air Cooling) should be fulfilled. In the valuation model, the FE value and total time has to be calculated. Aspects such as performance are not yet considered.

As an outlook, obtaining an update of the actual production status helps in adapting the time schedule for manufacturing planning as well as taking decisions on the management level. Reducing iteration cycles will significantly reduce costs, and a consolidated product model is also very helpful in MRO processes and retrofit tasks. Put together, this will be the key to a product lifecycle from cradle to grave – which is, as said in the introduction, one of the keys to a successful product.

Acknowledgements

This work was supported by the German Ministry of Education and Research (BMBF) within the project ARVIDA (FKZ 01IM13001U)

References

- BURR, H. (2008), *Informationsmanagement an der Schnittstelle zwischen Entwicklung und Produktionsplanung im Karosserierohbau*, Lehrstuhl für Konstruktionstechnik/CAD, Universität des Saarlandes, Saarbrücken
- EIGNER, M.; GERHARDT, F.; HOCHSTEIN, N.; ROTH, M.; HANDSCHUH, S.; SINDEMANN, S. (2013), *Datenaustausch in der virtuellen Produktentwicklung - Ein Überblick über Formate, Applikationen und Formate*, VPE White Paper Volume 5, Lehrstuhl für Virtuelle Produktentwicklung, Kaiserslautern
- FRIEDEWALD, A.; LÖDDING, H.; VON LUKAS, U.; MESING, B.; ROTH, M.; SCHLEUSENER, S.; TITOV, F. (2011), *Prozessübergreifender Datenaustausch im Schiffbau - Mehr Qualität im Schiffbau Engineering*, Digital Engineering Magazin 8, pp. 34-35
- HOCHSTEIN, N. (2014), *Entwicklung einer Methode zur frühzeitigen Bewertung von CAx-Landschaften am Beispiel des schiffbaulichen Produktentwicklungsprozesses*, Lehrstuhl für Virtuelle Produktentwicklung, Kaiserslautern
- ROTH, M. (2012), *Baustatusprotokollierung in der Einzelfertigung durch die Verwendung einer offenen und neutralen Lösung (OLS-Strategie)*, Go3D Conf., Rostock
- SIEMENS (2010), *JT File Format Reference Version 9.5 Rev. A*, Siemens PLM Software, Plano/Texas
- VETTERMANN, S. (2010), *ProSTEP iViP Standardization Activities*, JT Open International Conf., Barcelona

Real Cost Savings for a Waterjet-driven Patrol Craft Design Using a CAESES-NavCad Coupled Solution

Donald MacPherson, HydroComp, Durham NH/USA, donald.macpherson@hydrocompinc.com
Stefan Harries, FRIENDSHIP SYSTEMS, Potsdam/Germany, harries@friendship-systems.com

Simon Broenstrup, FRIENDSHIP SYSTEMS, Potsdam/Germany

Joseph Dudka, HydroComp, Durham NH/USA

Abstract

Much of the commentary regarding hull form optimization found in industry journals and proceedings focuses on process and methodology rather than outcome. This paper intends to show the real savings in acquisition and life-cycle cost for a waterjet-drive patrol craft that can come from a systems-based optimizing solution that is within reach of even small design offices. Two commercially-available software tools are used as a coupled solution to optimize the hull form for minimum resistance, with follow-on selection of a suitable waterjet model. An optimization process is described herein using FRIENDSHIP SYSTEMS CAESES as hull form modeler and optimizing platform, with HydroComp NavCad Premium responsible for resistance and propulsion prediction. The paper also highlights NavCad's prediction of bare-hull resistance using a novel linear wave-theory code that has been validated for high-speed transom-stern craft, as well as its use of engine and waterjet components for propulsion analysis and selection of an installation of highest propulsion efficiency.

1. Introduction

This story is about a tender for a waterjet-driven patrol boat that was nearing completion of its design, and the speed predictions were coming up short. (The design requirements called for a 26 knot top speed, but projections were indicating barely 23 knots.) The contractor was insisting that the boat be installed with a higher powered engine model – with a resulting increase in capital cost, life-cycle fuel consumption, and weight. The supplier of the main engines, however, felt that the installed power should have been adequate (based on similar installations), and contracted HydroComp for an independent technical review of the Hull-Waterjet-Engine system with the intent of determining how much power would be needed to drive the hull at contract speed. A resistance prediction and propulsion analysis confirmed that the boat would not make the necessary speed with the given hull form installed with the selected engine and waterjet models. However, as the engine builder suspected, the bottleneck was not insufficient engine power. The problem was that neither the hull nor the waterjet were optimized for the target speed and loading condition.

FRIENDSHIP SYSTEMS AG (Potsdam/Germany) and HydroComp, Inc. (Durham NH/USA) have successfully completed an optimized waterjet-driven transom-stern patrol craft design by utilizing the companies' principal software tools as a coupled solution. Geometric hull form modeling and optimization was performed by CAESES® with hydrodynamic analysis conducted in HydroComp NavCad® via its use as an efficient "coupled solver". The resulting design meets the operational objectives without installing a higher powered engine. The following sections describe the procedure and techniques used for this study, which can be employed as a template for anyone using a CAESES-NavCad coupled analysis.

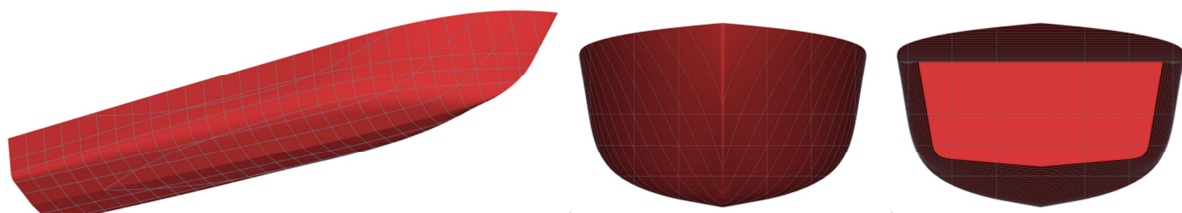


Fig. 1: Hull form of Parent (as imported to CAESES)

Table I gives a summary of principal dimensions of the initial (Parent) patrol boat, Fig. 1, along with bounds for modifications and the final (Proposed) design identified during the optimization. The Parent is a typical round-bilge hull with a immersed transom stern, featuring detached flow in the speed range investigated. The design was studied without appendages. However, the necessary added resistances (e.g., for windage drag) were accounted for within NavCad.

Table I: Principal dimensions and bounds for the optimization

	Parent design	Lower bound	Upper bound	Proposed design
Speed range of interest	Target speed 26 kn	15 kn	30 kn	Achieved 26 kn
LOA	29.00 m	0.96 LOA	1.05 LOA	30.30 m
LWL	27.44 m	0.96 LWL	1.05 LWL	28.62 m
Maximum beam at deck	6.80 m	0.96 B	1.05 B	6.27 m
Maximum B at DWL	5.74 m	0.96 B	1.05 B	5.52 m
Maximum draft T	1.40 m	Fixed to 1.4 m	Fixed to 1.4 m	1.40 m
Transom immersion	0.50 m	0.20 m	1.11 m	0.70 m
Transom's deadrise	5°	1°	9°	3.3°
Displacement \forall	102 m ³	0.98 \forall (constrained)	1.05 \forall (constrained)	106.7 m ³
Center of buoyancy XCB (from transom)	0.503 LWL = 13.8 m	13.65 m (constrained)	14.49 m (constrained)	0.477 LWL = 13.65 m

2. Performance simulation for waterjet-driven transom-stern craft

For details about the system-level connectivity between the two tools, we refer readers to *Harries et al.(2015a)*. That paper introduced the steps to setup and run an optimizing calculation between CAESES and NavCad. In summary:

1. The tools each have clearly defined computational responsibilities. CAESES is the “design manager” of the coupled pair responsible for geometry creation and optimization, with NavCad conducting the hydrodynamic hull form and propulsor analysis.
2. The hull form shape parameters are developed in CAESES, describing the parameters that will be allowed to vary. Optimization parameters are also defined in CAESES.
3. The suitable resistance prediction parameters are set down in a master script. This allows data transfer to be reduced and limited to the geometric variables that have changed.
4. NavCad is launched in silent “server mode” and communication is established between NavCad and CAESES.
5. For each of the variants in the optimization study, CAESES interrogates the variant geometry and packages a script file to be sent to NavCad for analysis. Results are likewise returned in a text file and in diagrams for CAESES to pick up and use in its optimization algorithm and for design assessment.
6. Upon completion, CAESES passes a script call that closes the NavCad Premium server process.

Both CAESES and NavCad are run – and function – simultaneously. Each is launched under compliance of its own end-user licensing. While it is obvious that CAESES should remain running for the duration of a design or analysis study, a dedicated instance of the NavCad application process must also be running and “connected” with calculation authority remaining with CAESES. This insures that calculations are completed and returned properly without interruption.

3. Techniques for successful hull parameterization

Parametric modeling is widely recognized as the most efficient way to change geometry in an automated process. Different to an interactive approach in which, typically, low-level entities like points are modified (e.g., the vertices of a B-spline surface patch), a parametric model changes a larger extent of the geometry in a concerted way. In principle, two types of parametric models are distinguished: a) fully-parametric and b) partially-parametric modeling.

A fully-parametric model builds up geometry from scratch while a partially-parametric model uses an existing parent (or baseline) – for instance from a previous interactive modeling process – and just defines the changes parametrically. There are many potential techniques, all with pros and cons. The reader is referred to *Harries (2014)* for an overview and *Harries et al. (2015b)* for details. Most importantly, a fully-parametric model needs more time to set up but is very powerful, while a partially-parametric model is quicker to build but not quite as “sharp-edged”. CAESES allows using a complete range of parametric modeling techniques, from FFD (Free-form Deformation) to building complex BReps (Boundary representation models), *Harries et al. (2015b)* and UberCloud.

Since a parent existed for the patrol boat and the acceptable time to come up with a parametric model was considered to be in the range of just a few hours, a partially-parametric modeling approach was chosen. From a naval architect’s perspective several changes to the parent were considered to be potentially beneficial:

- Lengthening or shortening the hull (by simple scaling in longitudinal direction)
- Narrowing or widening the hull (by simple scaling in transverse direction)
- Increasing or decreasing the draft at the transom (by means of a surface delta shift)
- Increasing or decreasing the transom’s deadrise angle (by means of a surface delta shift)
- Adjusting the deck contour in transverse direction, thus changing the design waterline (by means of a surface delta shift)

Some of the details of how these parametric modifications were realized within CAESES are discussed in Appendix A. Fig. 2 illustrates the regions where changes take place within the parametric model. It shows the so-called “design velocities” for four representative parameters that belong to the set of free variables chosen for the hydrodynamic optimization.

The color plots in Fig. 2 depict the magnitude of a surface’s normal displacement for very small changes of one parameter at a time. Here, red (the upper two images) means outward displacement while blue (lower two images) relates to inward displacement when incrementing a parameter by a small positive value. For instance, changing the length of the boat as depicted in Fig. 2A affects the bow region the most while the side and bottom regions experience very little modifications. Meanwhile, changing the transom height does not change the bow at all while the transom is pushed upwards (i.e., inward with respect to the parent).

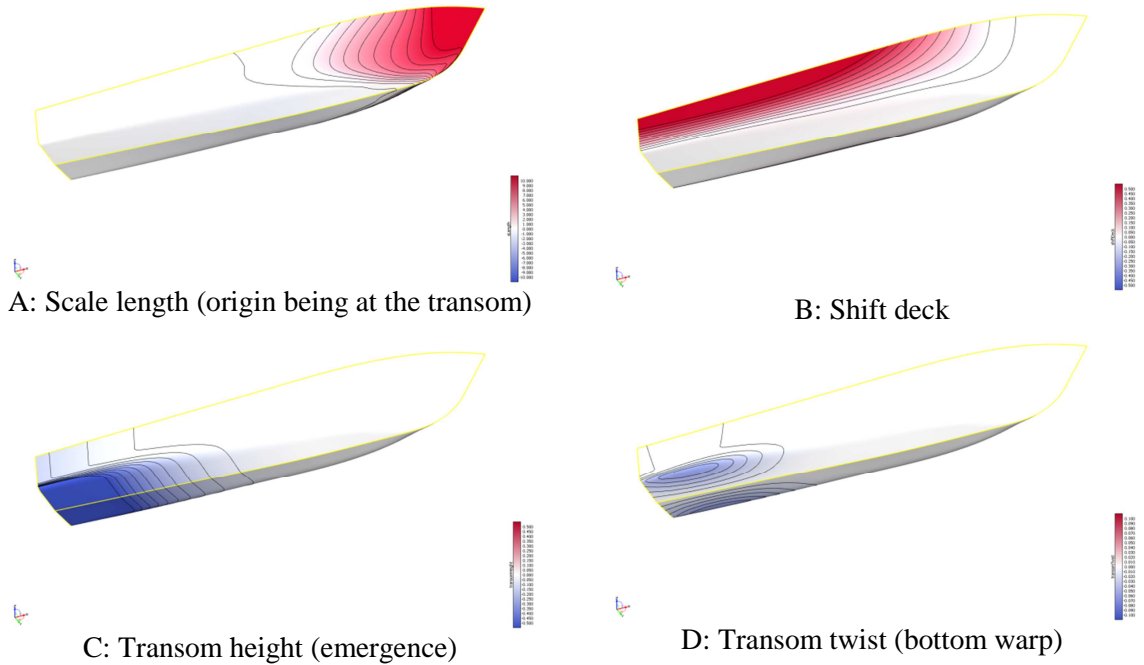


Fig. 2: Design velocities for selected parameters

4. Resistance prediction

The “simulation analysis” for this study starts with the determination of total resistance, including bare-hull, windage, and margins. The entire resistance prediction is conducted by NavCad, with data passed to it from CAESES and results returned for evaluation and optimization decisions. Over 40 parametric prediction methods are available in NavCad for a broad collection of vessel types, as well as a higher-order prediction code that nicely sits between parametric or statistical methods, and panel or even viscous CFD codes. Extremely fast, easy-to-use, and well-behaved, it was this code that was called on for the resistance prediction analysis in this study.

HydroComp has developed a novel implementation of a wave-theory bare-hull resistance prediction that has been deployed in the Premium Edition of NavCad. Inspired by thin-ship wave-making theory, it is a prediction of wave-making drag where the hull geometry is described by the longitudinal distribution of the immersed volume – unlike methods that use longitudinal distributions of the immersed surface (e.g., Michell’s integral waterline cuts, panel codes, CFD). Calculation of viscous drag, including a thorough prediction of form factor and frictional drag coefficients, completes the computation of total bare-hull resistance.

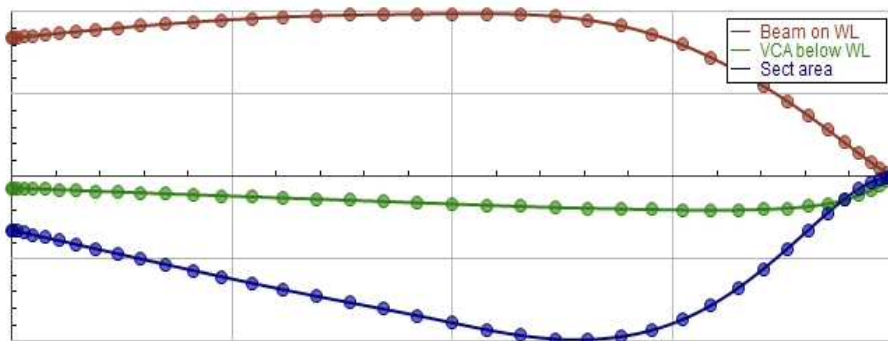


Fig. 3: Distribution of beam, immersion and sectional area

This code is called the “Prismatic Wave Drag” (PWD) method, in consideration of its fundamental use of the sectional area (i.e., “prismatic”) curve. It has proven very capable not only for traditionally slender forms but also for fast transom-stern craft. Its use as the computational foundation of a re-analysis of the Series 64 has shown its capability for craft of this type, *MacPherson* (2015). Fig. 3 shows an example of the distribution data for the Parent hull (that is used by the PWD method).

5. Optimization for minimum resistance

Various approaches can be taken within CAESES to drive formal optimization processes, see *Harries* (2014). For the patrol boat a combination of Design-of-Experiments (DoE) and a deterministic search strategy was selected. Firstly, a Sobol DoE (i.e., a quasi-random exploration of the design space) was undertaken to investigate the design space and to identify favorable parameter combinations. Secondly, several T-Search local optimizations (i.e., a deterministic pattern search) were run to fine-tune the hull form further.

Fig. 4 gives an impression from the assessment of designs within CAESES’s DesignViewer. Input parameters, hydrostatic data and the corresponding hull form are shown along with output data and diagrams from NavCad, allowing the rapid assessment of design candidates. Since the evaluation of any single variant would not take more than a few seconds on a standard notebook computer, several hundreds of variants could be easily investigated within the course of a day.

Fig. 5 depicts the correlation of objectives and free variables in an overview chart within CAESES. The investigation was done by means of a Sobol with 500 variants. While some free variables show little influence on performance (e.g., shiftDeck for the Telfer coefficient at both 22 and 30 kn), other free variables are very important (e.g. transomHeight). (The Telfer coefficient is defined as resistance times LWL divided by displacement times velocity squared.)

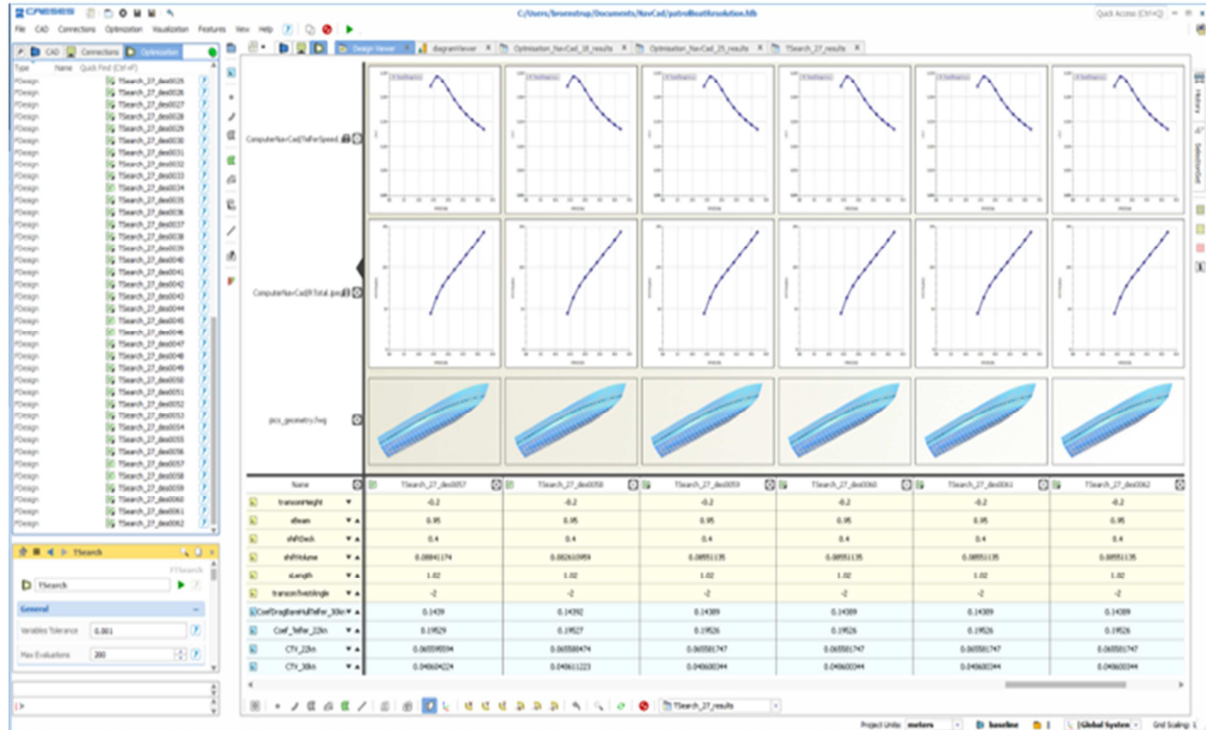


Fig. 4: DesignViewer within CAESES for comparing and assessing variants, showing results from NavCad

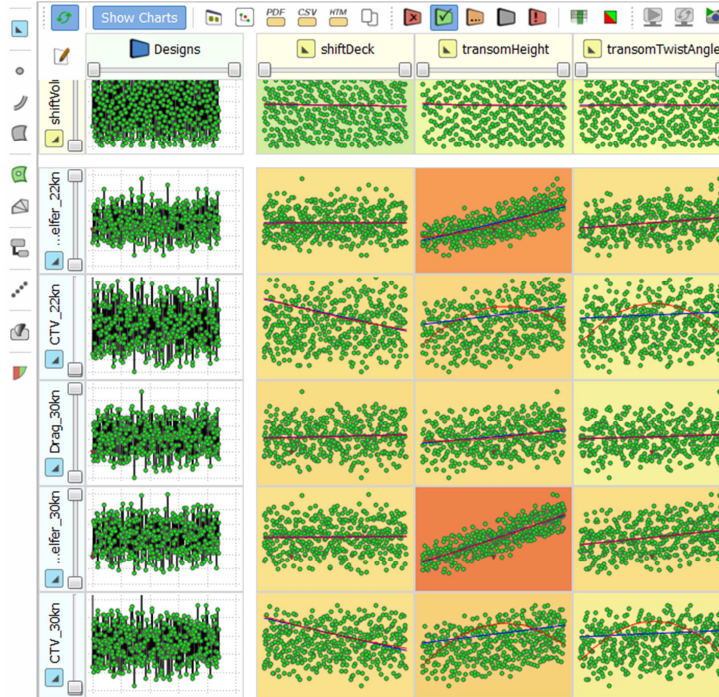


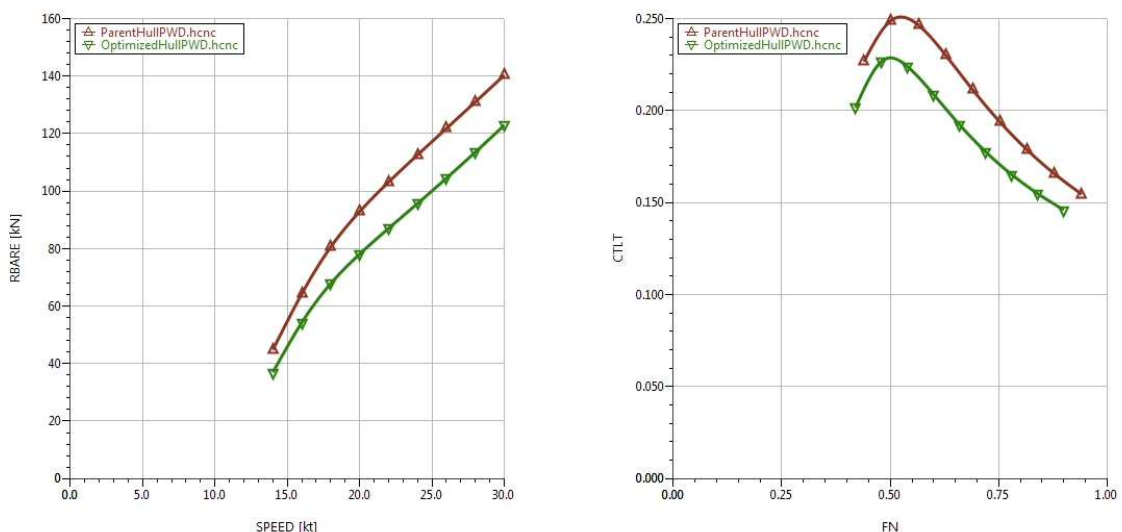
Fig. 5: Correlations between objectives and free variables from a Sobol DoE

5.1 Parent versus optimized hull form

The optimization study recommended new hull geometry (see also Table I) with

- a slightly more slender hull,
- LCB shifted aft,
- greater immersed transom area, and
- a narrower entrance angle.

The resistance improvement is shown in Fig. 6A. The accompanying plot in Fig. 6B represents the hydrodynamic comparison of the total bare-hull's Telfer coefficient versus Froude number. These figures clearly demonstrate the successful – and substantial – reduction in drag with the CAESES optimization running the NavCad PWD analysis.

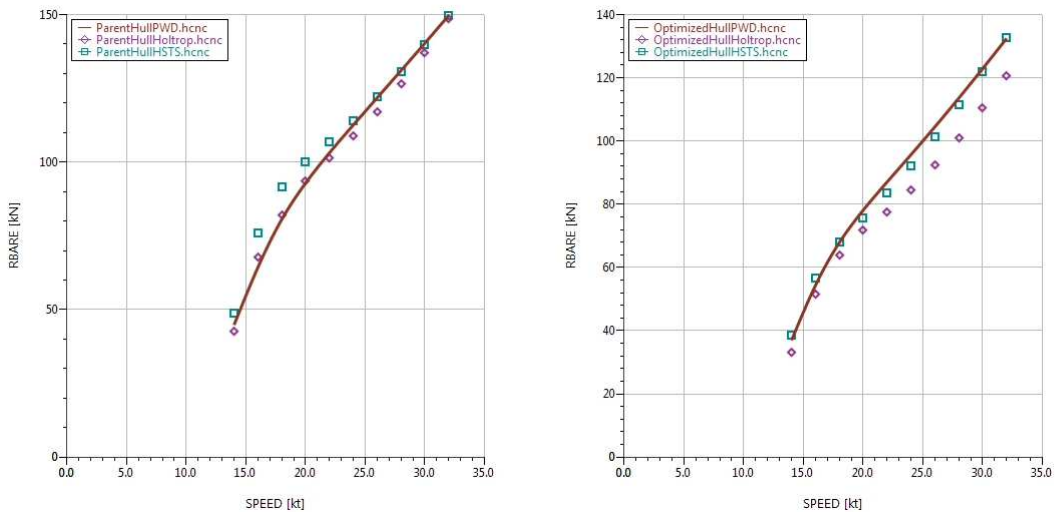


Figs. 6A & 6B: Parent and Proposed comparison of resistance and Telfer coefficient

5.2 Validation

None-the-less, it is still necessary to question the fidelity of the PWD analysis for the Parent and Proposed hull forms. It is completely possible that a mathematical optimization may push the geometry outside the scope of reliable prediction of any method. Therefore, a “confidence check” is recommended using lower order parametric methods. With its library of some 40+ parametric hull resistance methods to call on, NavCad can again be employed not only for the prediction but also to check its reliability.

Using NavCad’s “Method Expert” utility, it was confirmed that two parametric resistance prediction methods were suitable to use as a cross-check of results – the HSTS (highest rated) and Holtrop methods. The Holtrop method was flagged with a user note that it does have a known tendency to underpredict for hulls of substantial immersed transom area. We can see in Figs. 7A and 7B the very good correlation of both magnitude and slope between the distributed volume PWD method and the two parametric methods, giving high confidence in the optimization predictions. (It also shows how the Holtrop method underpredicted drag for the Proposed hull with its nearly 40% greater immersed transom area.)



Figs. 7A & 7B: Resistance of Parent and Proposed hull computed from different NavCad methods

6. Propulsion analysis

Once the resistance prediction was completed for the optimization study of candidate hulls, NavCad was called on to complete a propulsion analysis. Not only was hull drag optimized in the study, but the available analyses in NavCad allowed for selection of a higher efficiency waterjet.

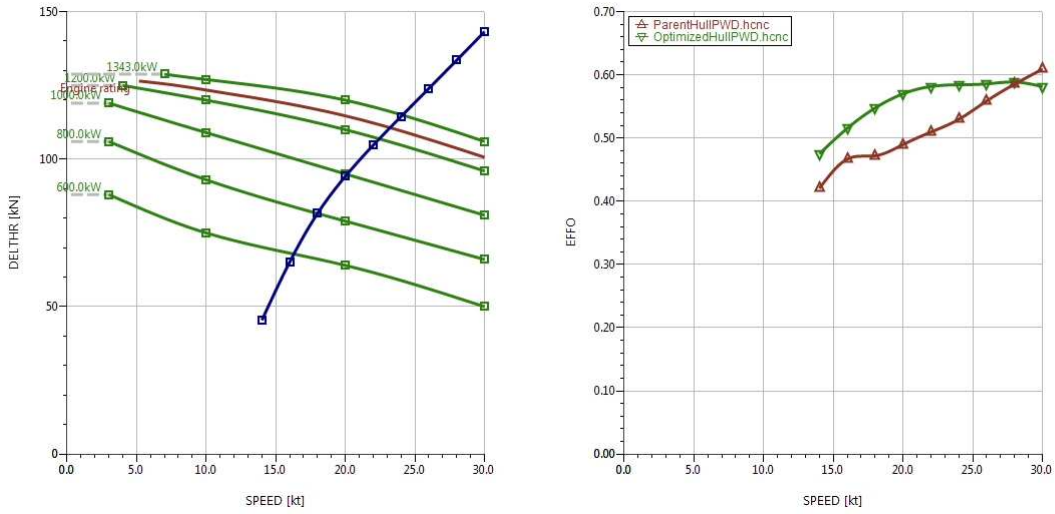
The propulsion analysis was completed exclusively within NavCad, although it could have been conducted using the connectivity with CAESES. A full scripting API supports preparation of propulsion component data, as well as running the propulsion system analysis.

6.1 Methodology of waterjet analysis

Traditional waterjet analysis is a simple graphical lay-over of a waterjet’s thrust curves onto the hull’s required (delivered) thrust curve. If there is sufficient thrust, then the waterjet is deemed acceptable. This was the approach taken by the original designers, but it has one serious deficiency – it does not show the efficiency of the propulsor. NavCad’s analysis employs the same published thrust data, but it exposes the waterjet propulsor efficiency so comparisons can be made between competing product models, *MacPherson (2000)*.

NavCad does not treat waterjets in the same way as propellers, since there are no comparable test frameworks (e.g., KT and KQ curves) for waterjets. In other words, NavCad employs waterjets as a component, whose performance is specified by the manufacturer. (This is similar to how engines are treated, for example. The manufacturers define the specified deliverable power under test conditions – sometimes corrected by naval architects for non-test conditions when deemed appropriate.) The published speed-thrust-power curves are entered as a waterjet component file, along with the impeller power demand data. A surface map is then built from this point cloud data to convert the waterjet thrust map and impeller data to “propeller-equivalent” J-KT-KQ coefficients. This allows a waterjet to be treated in NavCad like any other propulsor.

Still, a traditional waterjet plot can be prepared in NavCad, as shown in Fig. 8A for the Parent design. Intersection of the demand and thrust curves indicates the top speed is approximately 23.0 knots.



Figs. 8A & 8B: Waterjet thrust demand and propulsor efficiency plots

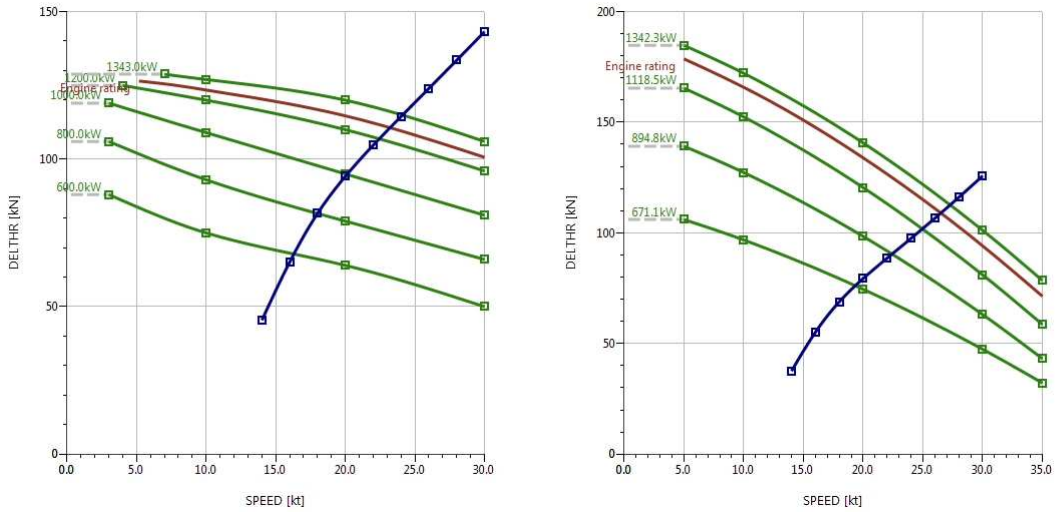
6.2 Waterjet efficiency

As noted, NavCad exposes a waterjet’s propulsor efficiency as part of the analysis. It is important for anyone working on a waterjet-driven craft to understand that waterjets as a component are optimized for a particular speed range. Fig. 8B illustrates the speed-dependency of efficiency for the Parent and Proposed waterjets under consideration in this study.

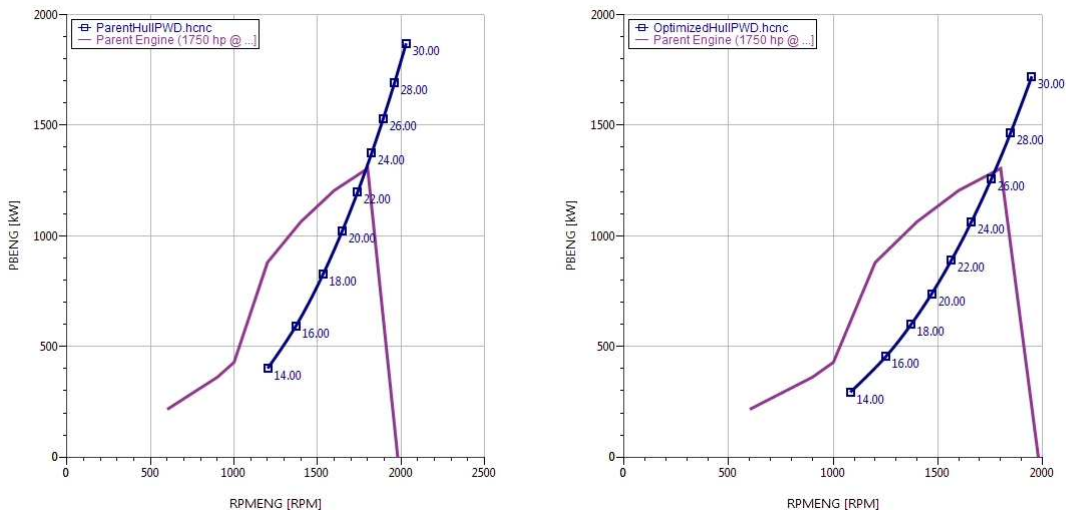
The original (Parent) waterjet model was considered and promoted as a high-efficiency waterjet. This was true, but it was designed for high-speed operation greater than 40 knots. You can see that its efficiency is still increasing at 30 knots. On the other hand, the new (Proposed) waterjet model was designed for 20 to 30 knots. It has lower peak efficiency than the Parent model, but its efficiency is higher in the speed range of interest. It is only by NavCad’s calculation of waterjet propulsor efficiency that a designer can make a rational selection of a waterjet model for highest operational effectiveness and lowest fuel consumption.

6.3 System analysis of Parent and Proposed designs

Successful selection of a waterjet model and its corresponding propulsion system analysis does not end with the thrust curves. A proper match of engine, impeller, and gear ratio are also needed. Engine power curve information is entered in NavCad as a component file from the manufacturer’s published literature. Gear ratio is selected from the available options and matched to an impeller selection. The propulsion system analysis then utilizes all defined parts of the Hull-Propulsor-Engine system to determine equilibrium RPM, power, thrust, efficiency, and fuel consumption. Figs. 9 and 10 show important system performance figures for the Parent (original) and Proposed (optimized) designs.



Figs. 9a & 9b: Waterjet thrust demand for Parent and Proposed hulls



Figs. 10A & 10B: Engine load for Parent and Proposed hulls

7. Conclusions

The CAESES-NavCad optimized hull form with a proper waterjet (selected based on considerations of “speed-dependent” efficiency) increased the operational speed from approximately 23.0 knots to 26.5 knots – meeting the design objectives without installation of a larger engine.

The original Parent hull with its specified high-speed waterjet would indeed have needed an engine of some 10% to 15% more power to meet the design speed. Of course, this directly translates into a comparable increase in fuel consumption – but the increase also would have needed to consider the heavier displacement required for the larger engine, increasing the fuel consumption at design speed even more. Naturally, the initial capital expense would also be greater with a larger engine.

Conservatively, let us assume the engine-only cost of the Parent design to be 100 000 €. The original expectation by the client was to install an engine some 20% larger, which we can scale proportionally to a cost of approximately 120 000 €. So, for the pair of engines needed the client receives a saving of capital expenses of at least 40 000 €, additional savings stemming from a lighter design not yet accounted for.

Operational expenses are even larger. The fuel consumption predicted in the NavCad analyses for a mean cruising speed of 20 knots is 252 l/h per engine for the Parent hull and 185 for the Proposed hull. Given a representative operating demand of 500 hours-per-year for a patrol craft at a cost of marine diesel fuel of ~1.25 €/l – www.globalpetrolprices.com/diesel_prices/Europe – an estimate of the savings of operating cost with the Proposed hull and waterjet will be 84 000 € per year.

8. Outlook

This study was based on a single design point of 26 knots minimum top speed with least resistance and highest waterjet efficiency as optimizing objectives. However, it could also have looked beyond one speed to a multi-mode duty-cycle propulsion analysis. For example, minimum propulsor power was the optimizing objective of an AUV study previously conducted with a CAESES-NavCad solution, *Harries et al. (2015a)*. NavCad's operating modes analysis can deliver weighted results, including a number of Key Performance Indicators (KPIs), to evaluate and compare optimized hulls and propulsion components for a ship's entire mission profile. The hull form optimization function could thus have been extended from the minimization of bare-hull resistance to a comprehensive minimum energy load for the propulsion system across its full duty-profile.

This study clearly demonstrates how a CAESES-NavCad pairing can provide a very cost-effective and time-efficient capability for any naval architectural office. This coupled solution is a powerful instrument for finding improvements in hull form and propulsion components at any stage in a design.

References

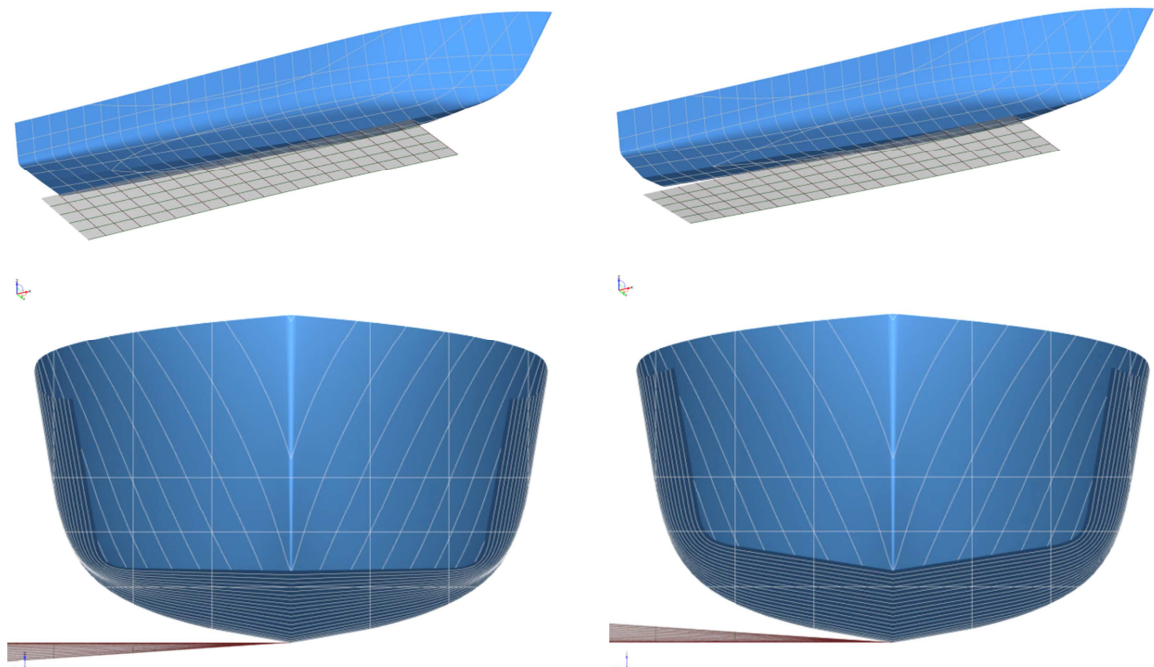
- ABT, C.; HARRIES, S. (2007a), *Hull variation and improvement using the generalised Lackenby method of the FRIENDSHIP-Framework*, The Naval Architect, RINA
- ABT, C.; HARRIES, S. (2007b), *A new approach to integration of CAD and CFD for naval architects*, 6th Conf. Computer and IT Applications in the Maritime Industries (COMPIT), Cortona
- HARRIES, S. (2014), *Practical shape optimization using CFD*, Whitepaper, www.caeses.com
- HARRIES, D.; MACPHERSON, D.; EDMONDS, A. (2015a), *Speed-power optimized AUV design by coupling CAESES and NavCad*, 14th Conf. Computer and IT Applications in the Maritime Industries (COMPIT), Ulrichshusen
- HARRIES, S.; ABT, C.; BRENNER, M. (2015b), *Upfront CAD – Parametric modeling techniques for shape optimization*, Int. Conf. Evolutionary and Deterministic Methods for Design, Optimization and Control with Applications to Industrial and Societal Problems (EUROGEN), Glasgow
- MacPHERSON, D. (2000), *Selection of commercial waterjets: New performance coefficients point the way*, SNAME New England Section, Boston
- MacPHERSON, D. (2015), *A critical re-analysis of the Series 64 performance data*, 13th Int. Conf. Fast Sea Transportation (FAST), Washington, DC.

Appendix A – Hull form parameterization

The Parent geometry was available as a collection of NURBS surfaces and was imported to CAESES via an IGES-file (as shown in Fig. 1). Subsequently, a partially-parametric model was set up, utilizing several of CAESES’ standard “transformations” such as scaling, curve delta shifts and surface delta shifts. Furthermore, an advanced swinging of sections, the so-called Generalized Lackenby, *Abt and Harries (2007)*, was applied in order to capture constraints on displacement and longitudinal center of buoyancy.

CAESES offers an image technology in which a variant is created by assigning a transformation to a source which may be either the baseline shape (any curve, offset, surface, tri-mesh, grid etc.) or any image from a previous parametric modification. In this way transformations can be flexibly combined to define a complex parametric model even from several rather simple modifications.

Fig. A1 may serve to explain one of these simply transformations, namely a surface delta shift. It shows the partially-parametric modification imposed to increase or decrease the twist angle of the transom, introducing a warp in the bottom region of the hull. A ruled surface (shown in grey in Fig. A1 beneath the hull) defines the shift the Parent shall experience into the vertical direction (i.e., the baseline’s surfaces as sources). While the shift is supposed to be its maximum at the transom, it gradually fades out towards the forebody (thereby ensuring curvature continuity in the transition from the modified to the unmodified region). Any point of the original surface under the influence of the surface delta shift receives a $\Delta z(x, y)$ -value according to its original x-y position, shifting it to the new coordinates $(x, y, z+\Delta z)$. As can be readily appreciated from the transom view (lower row of Fig. A1) the deadrise is modified quite substantially, basically flattening out the transom or more strongly pronouncing the flare angle. Furthermore, the shift going to zero towards the maximum section, the changes are confined to the stern (as in “design velocity” in Fig. 2).



A: Hull (blue) along with surface (grey) so as to modify transom area by a twist of -4°

B: Hull (blue) along with surface (grey) so as to modify transom area by a twist of $+4^\circ$

Fig. A1: Surface delta shift for introducing transom twist

The entire parametric model is thus modified by combining a variety of these transformations. Fig. A2 depicts a screen shot of the CAESES DesignViewer with a comparison of variants created by means of five free variables, one of which being the transom twist as discussed in some detail. The DesignViewer allows browsing quickly through parameter sets, constraints, associated shapes and simulation results, Fig. A2.

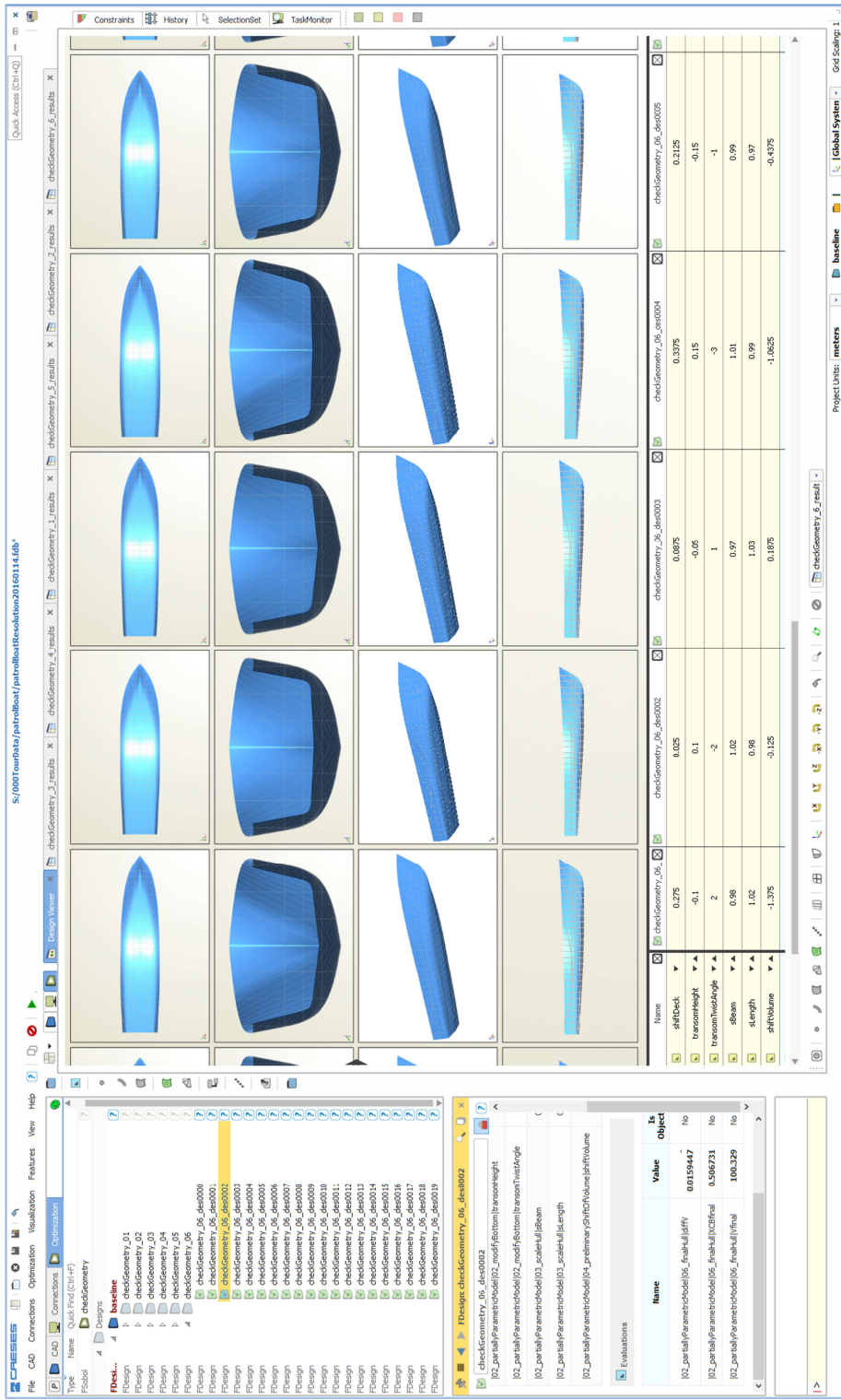


Fig. A2: Different variants realized by a parametric model, shown in CAESES Design-Viewer

Appendix B – Connection between NavCad and CAESES

A number of steps need to be taken to create a “coupled solution” between NavCad and CAESES, see also *Harries et al (2015a)*. Naturally, this effort is only needed when quite a few variants, say a dozen or more hulls, are to be investigated systematically. If a designer is just interested in quickly analyzing two or three variants it may certainly be more practical to independently use CAESES and NavCad one after the other.

```

File.New
File.Open "C:\Users\broenstrup\Documents\NavCad\ParentDesign.hcnc"

Hull.LengthWL 28.6146 m
Hull.BeamWLMax 5.51507 m
Hull.DraftSubmergedMax 1.41017 m
Hull.Displacement 106.715 t
Hull.XBuoyancyFwdTr 13.6489 m
Hull.AngleHalfEntDeg 18.9179
Hull.AreaWaterplane 129.824 m2
Hull.AreaSectAtTr 7.71203 m2
Hull.HullAreaSectMax 14.3036 m2
Hull.HullWettedSurface 158.362 m2
Hull.ImmersionDraftAtTr 0.709451 m
Hull.BeamWLAtTr 4.8061 m

Hull.StationDistribution.Count 38

Hull.StationDistribution.XPosition 0.01 0.767 1.524 2.281 3.038 3.795 4.552 5.310 6.067
6.824 7.581 8.338 9.095 9.852 10.610 11.367 12.124 12.881 13.638 14.395 15.152 15.910
16.667 17.424 18.181 18.938 19.695 20.452 21.210 21.967 22.724 23.481 24.238 24.995 25.752
26.510 27.267 28.024 m

Hull.StationDistribution.BeamWL 4.806 4.866 4.924 4.981 5.036 5.090 5.142 5.192 5.240 5.285
5.328 5.369 5.407 5.440 5.467 5.488 5.502 5.511 5.513 5.512 5.511 5.509 5.496 5.457 5.372
5.211 4.966 4.689 4.388 4.074 3.753 3.424 3.067 2.652 2.164 1.589 0.976 0.413 m

Hull.StationDistribution.AreaSect 2.891 2.985 3.078 3.172 3.265 3.359 3.452 3.544 3.637
3.730 3.823 3.916 4.009 4.103 4.196 4.289 4.383 4.479 4.582 4.698 4.834 4.993 5.154 5.287
5.358 5.328 5.172 4.935 4.638 4.295 3.919 3.507 3.045 2.515 1.894 1.189 0.568 0.133 m2

Hull.StationDistribution.CentroidBelowWL 0.984 0.975 0.966 0.957 0.948 0.939 0.930 0.920
0.910 0.900 0.890 0.880 0.869 0.857 0.845 0.833 0.819 0.804 0.788 0.770 0.750 0.727 0.703
0.679 0.656 0.633 0.614 0.597 0.584 0.574 0.569 0.567 0.568 0.575 0.597 0.637 0.765 1.041
m

SpeedPerformance.Speed 14.00 16.00 18.00 20.00 22.00 24.00 26.00 28.00 30.00 32.00 kt

Analysis.CalculateResistance
Output.Start "C:\Users\broenstrup\Documents\NavCad\patrolBoatResolution\23_TSearch\
TSearch_23_des0032\ComputerNavCad\Output_Values.txt"

SpeedPerformance.AddToOutput Count
SpeedPerformance.AddToOutput Speed
SpeedPerformance.AddToOutput CoefDragBareHullTelfer
SpeedPerformance.AddToOutput CoefDragBareHullWeightRatio
SpeedPerformance.AddToOutput DragTotal
Output.End

Graph.SetAxisXY Speed RTotal
Graph.SaveAsJPEG "C:\Users\broenstrup\Documents\NavCad\patrolBoatResolution\23_TSearch\
TSearch_23_des0032\ComputerNavCad\RTotal.jpeg"

```

Fig. B1: Example script (excerpt) for executing NavCad (data items that are replaced during the optimization are highlighted in yellow)

For the assessment undertaken in NavCad by means of the PWD-method, several parameters and data items need to be provided: for example the length and entrance angle of the design waterline (at rest), maximum beam and, importantly, sectional data such as the number of stations and their longitudinal positions along with each section’s area and immersed centroid, see Fig. B1. In order to gather and provide the input data for NavCad a small feature was written in CAESES that saved all necessary data items (using strings for ease of transfer). The “feature” technique within CAESES enables the

user to package operations into higher-order objects. These “features” can then be carried out, for instance, to compile and write data to tailor-made output files.

In an automated study many hulls are created and evaluated, typically in the range of a few hundred. Hence, NavCad is asked time and again to perform exactly the same type of simulation for every variant about which the optimization strategy requests information. Therefore, in the “coupled solution” NavCad is run in a server mode on the basis of input data fed to NavCad via its API scripting language. CAESES provides the scripts and then triggers a design assessment by NavCad. NavCad then executes the script, compiles results and diagrams and, finally, lets CAESES know that the assessment is completed.

From a practical point of view it is best to run NavCad for the Parent design once manually before any major optimization is undertaken in an automatic mode. (NavCad’s “build script” feature can also be of assistance to prepare an initial script template for the NavCad project.) This helps setting up scripts and the necessary input data as needed. The NavCad script typically contains information about the type of calculation to be performed and what data are to be saved in the output file. For the patrol boat optimization both numerical data such as the resistance at a certain speed and diagrams for post-processing were provided by NavCad, Fig. 4. Fig. B1 gives an excerpt of the corresponding NavCad script.

The integration of NavCad within CAESES is shown in Fig. B2, where the location of the NavCad executable first needs to be specified. Then, CAESES needs to know a) the name and content of the script file, here just “skript.txt”, b) the name and content of the output file, here “Output_values.txt”, and c) the names of the diagrams that NavCad will create, here “Pbeng.jpeg” and “RTotal.jpeg”. During the optimization, CAESES replaces the entries in the script file that change from one variant to the next. Importantly, these are the principal dimensions and the sectional data as shown in Fig. B1, see highlighted data items. Furthermore, CAESES reads and interprets the output file, taking in the results from NavCad for each variant. While doing an optimization, a folder is created for every variant that contains all inputs, outputs, screen-shots, diagrams etc. for possible further processing.

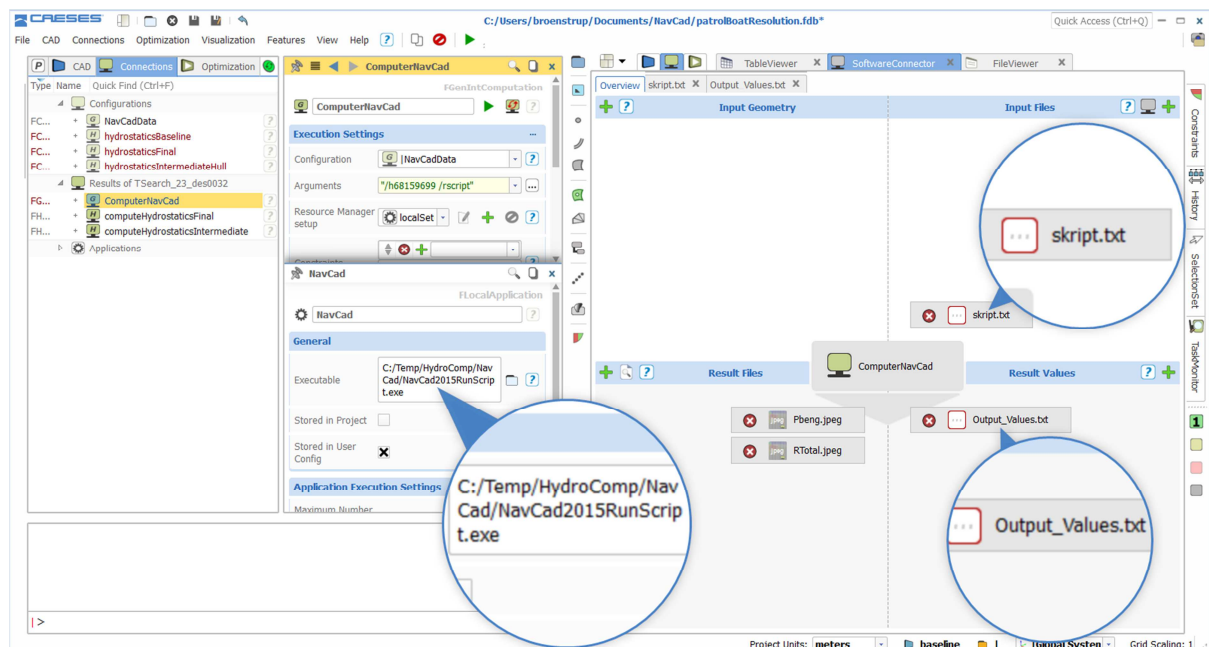


Fig. B2: CAESES SoftwareConnector for integration of NavCad

Cloud Computing for CFD based on Novel Software Containers

Wolfgang Gentzsch, UberCloud Inc. Los Altos/USA, wolfgang.gentzsch@TheUberCloud.com

Aji Purwanto, Numeca, Brussels/Belgium, aji.purwanto@numeca.be

Matthias Reyer, CPU 24/7, Potsdam/Germany, m.reyer@cpu-24-7.com

Abstract

This paper describes a novel software container technology which enables easy software packaging and porting, seamless access and use of workstations, servers, and any cloud, and can scale up to hundreds of parallel cores, dramatically speeding up engineering simulations. As proof of concept we containerized NUMECA's FINE/Marine, FINE/Turbo, and FINE/Open software. A case study shows Glostens simulation and prediction of containership resistance on CPU 24/7 cloud resources.

1. Introduction

The UberCloud Experiment initiative started in July 2012, with a discussion about cloud adoption in technical computing and a list of technical and cloud computing challenges and potential solutions. The major idea of the initiative was to explore these cloud challenges further. Especially small and medium enterprises in digital manufacturing strongly benefit from technical computing in the cloud. By gaining access on demand from their desktop workstations to additional computing resources, their major benefits are: the agility gained by shortening product design cycles through shorter simulation times; the superior quality achieved by simulating more sophisticated geometries and physics and by running many more iterations to look for the best product design; and the cost benefit by only paying for what is really used, increasing a company's innovation and competitiveness.

Tangible benefits like these make technical computing - and more specifically technical computing as a service in the cloud - very attractive. Over the years, many of the challenges have been resolved, like security, privacy, and trust; conservative software licensing models; slow data transfer; uncertain cost & ROI; availability of best suited resources; and lack of standardization, transparency, and cloud expertise, mainly due to novel software container technology described in this paper and applied in this cloud experiment to calculate the barehull resistance of the KRISO containership (KCS) in the cloud.

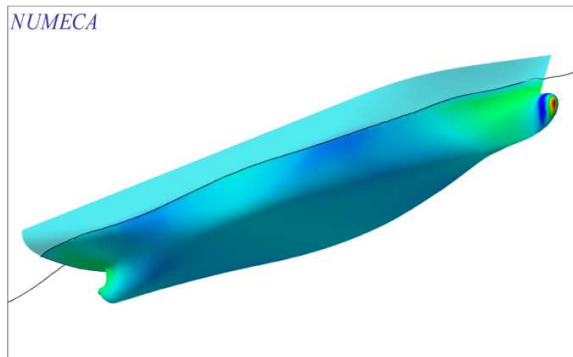


Fig. 1: Calculating the barehull resistance of the KRISO containership (KCS) in the cloud

The KRISO containership is a standard benchmark for computational fluid dynamics in the marine industry. Basic hull form parameters and experimental results are available in published literature. The purpose of this project was to become familiar with the mechanics of running a FINE/Marine simulation in a software container and to assess the performance of the cloud compared to resources currently used by the end-user. The benchmark was analyzed on local hardware, on virtual instances in the cloud, and on the bare-metal cloud solution offered by CPU 24/7 and UberCloud. All simulations were run using version 4 of Numeca's FINE/Marine software.

2. The cloud experiment: Prediction of barehull KRISO containership resistance in the cloud

The cloud experiment team, *Morgan (2016)*, consisted of the industry end user Justin M. Morgan, PE Principal for Ocean Engineering & Analysis at GLOSTEN Inc., the software provider Aji Purwanto, Business Development Director at NUMECA International S.A., the resource provider Richard Metzler, Software Engineer at CPU 24/7 GmbH, and the technology experts Hilal Zitouni Korkut and Fethican Coskuner from UberCloud Inc.

2.1. Engineering use case

In this project, we calculated the barehull resistance of the KRISO containership (KCS) in the cloud. The KRISO containership is a standard benchmark case for computational fluid dynamics in the marine industry. Basic hull form parameters and experimental results are available in published literature, https://www.nmri.go.jp/institutes/fluid_performance_evaluation/cfd_rd/cfdws05/.

2.2. Process and benchmark results

The simulation was set up as a steady-state solution, fixed in trim and sinkage to duplicate the conditions of the experimental data. The half model mesh contains 1.6 million cells. Simulation control variables in FINE/Marine were as follows:

- 300 time steps
- Uniform time step = 5 sub-cycles
- 8 non-linear iterations

The solution converges to a steady-state resistance force within ~150 time steps; however, the simulation was allowed to run to completion on all platforms to provide a performance comparison. The calculated total resistance coefficient for this model is 0.003574, compared to the experimental result of 0.00356 a 0.4% difference. Fig. 2 compares the calculated and measured wave field.

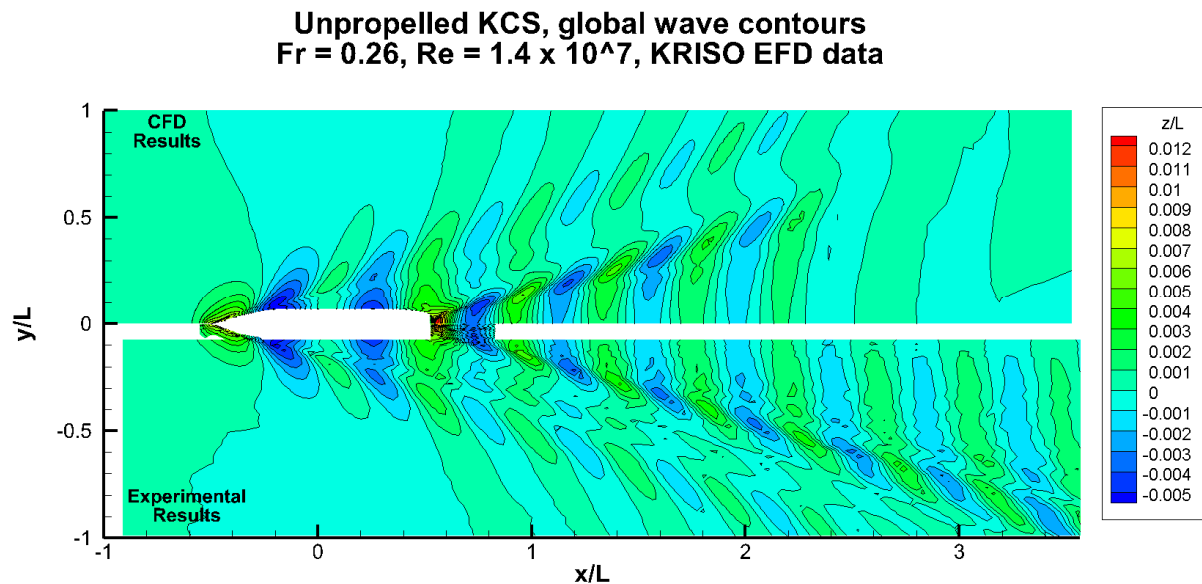


Fig. 2: Comparison of experimental (bottom) and calculated (top) results

The processors offered by CPU 24/7 and available through the UberCloud container provide a significant improvement in performance over local GLOSTEN hardware and over virtual instances available through Amazon Web Services (AWS), Table I. The difference in Table I between software versions v4.2 and v4.1 is only in patches not affecting performance. The AWS compute instance used here is the third generation, c3.8xlarge. A fourth-generation compute instance is available on AWS

with Intel Xeon CPU E5-2666 v3; however, setting up a new virtual instance was considered too costly for this project.

Table I: Performance comparison for different computing resources

Platform	Processor	FINE/Marine	#cores	Time
local	Intel Xeon CPU E5645 @ 2.4 GHz x 2	v4.2	12	6.9 h
CPU 24/7	Intel Xeon CPU E5-2690 v3 @ 2.6 GHz x 24	v4.1	12	3.0 h
CPU 24/7	Intel Xeon CPU E5-2690 v3 @ 2.6 GHz x 24	v4.1	16	2.5 h
CPU 24/7	Intel Xeon CPU E5-2690 v3 @ 2.6 GHz x 24	v4.1	24	1.7 h
AWS	Intel Xeon CPU E5-2680 v2 @ 2.8 GHz x 23	v4.2	16	3.5 h
AWS	Intel Xeon CPU E5-2680 v2 @ 2.8 GHz x 23	v4.2	24	2.9 h

2.3. Conclusions of the cloud experiment

This use case helped us understand the performance benefits offered by UberCloud and CPU 24/7. Glosten considers the UberCloud service to be a viable alternative to a local server upgrade. Additional benefits include the on-demand access and use of the software and hardware resources, a reduction in overhead required to manage virtual instances and to maintain software updates.

No challenges were experienced in downloading project files into the FINE/Marine container, running the simulation, or retrieving data. The remote desktop user interface was responsive without any significant delays. Logging into the system is simple and the Numeca software pre-installed in a software container runs without any user setup.

We showed that the CPU 24/7 HPC bare-metal cloud solution provides performance advantages for Numeca FINE/Marine users who want to obtain higher throughput or analyze larger, more complex models. CPU 24/7 and UberCloud effectively eliminate the need to maintain in-house HPC expertise. The container approach provides immediate access to high-performance clusters and application software without software or hardware setup delays. The browser-based user interface is simple, robust, and responsive.

3. CAE software containers

Server virtualization, a large trend in enterprise IT in the past 10 years, did not really gain a foothold in CAE, especially for highly parallel CAE applications requiring low latency and high-bandwidth inter-process communication. And multi-tenant servers, with virtual machines (VMs) competing among each other for hardware resources such as input/output, memory and network, often slow down CAE application performance.

Because VMs failed to show presence in CAE, the challenges of software distribution, administration and maintenance kept CAE systems locked up in closets, available to only a select few. In fact, the US Council of Competitiveness, *COC (2010)*, estimates that in 2010 only about 5% of all engineers are using high-performance servers for their CAE simulations, the other 95% just use their workstations. In 2013, Docker Linux Containers, [http://en.wikipedia.org/wiki/Docker_\(software\)](http://en.wikipedia.org/wiki/Docker_(software)), saw the light of day. The key practical difference between Docker and VMs is that Docker is a Linux-based system that makes use of a userspace interface for the Linux kernel containment features. Another difference is that rather than being a self-contained system in its own right, a Docker container shares the Linux kernel with the operating system running the host machine. It also shares the kernel with other containers that are running on the host machine. These features make Docker containers extremely lightweight and well-suited for CAE, in principle, *Gentzsch (2016)*.

Containers: Build once, run anywhere

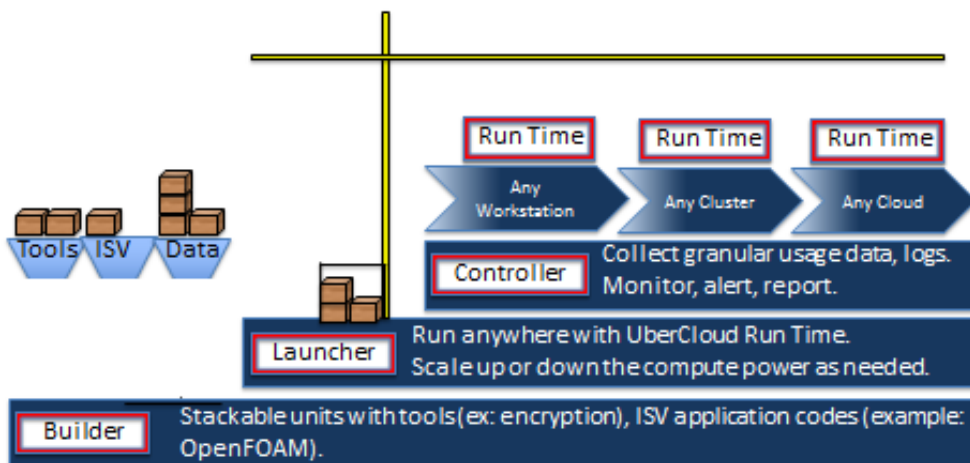


Fig. 3: Software containers to build, launch, control, and run CAE applications in the cloud

Still, it took UberCloud a year to develop (based on micro-service Docker container technology) the macro-service production-ready counterpart for CAE, plus enhancing and testing it with a dozen of CAE applications and with engineering workflows, on about a dozen different single- and multi-node cloud resources, *Gentzsch (2016)*. These high-performance, interactive software containers, whether they are on premise, on public or on private clouds, Fig. 3, bring a number of core benefits to the otherwise traditional HPC (high-performance computing) environments with the goal to make HPC ubiquitous:

- **Packageability:** Bundle applications together with libraries and configuration files.
A container image bundles the needed libraries and tools as well as the application code and the necessary configuration for these components to work together seamlessly. There is no need to install software or tools on the host compute environment, since the ready-to-run container image has all the required components. The challenges regarding library dependencies, version conflicts and configuration challenges disappear, as do the huge replication and duplication efforts in our community when it comes to deploying CAE software.
- **Portability:** Build container images once, deploy them rapidly in various infrastructures.
Having a single container image makes it easy for the workload to be rapidly deployed and moved from host to host, between development and production environments, and to other computing facilities easily. The container allows the end user to select the appropriate environment such as a public cloud, a private cloud or an on-premise server. There is no need to install new components or perform setup steps when using another host.
- **Accessibility:** Bundle tools such as SSH (Secure Shell) into the container for easy access.
The container is setup to provide easy access via tools such as VNC (virtual network computing) for remote desktop sharing. In addition, containers running on computing nodes enable both end users and administrators to have a consistent implementation regardless of the underlying compute environment.
- **Usability:** Provide familiar user interfaces and user tools with the application.
The container has only the required components to run the application. By eliminating other tools and middleware, the work environment is simplified and the usability is improved. The ability to provide a full-featured desktop increases usability (especially for pre- and post-processing steps) and reduces training needs. Further, the CAE containers can be used to-

gether with a resource manager such as Slurm or Grid Engine, increasing the usability even further by eliminating many administration tasks.

In addition, the lightweight nature of the CAE container suggests low performance overhead. Our performance tests with real applications on several multi-host, multi-container systems demonstrate that there is no significant overhead for running high performance workloads as a CAE container.

3.1. Current state of software containers

During the past two years, UberCloud has successfully built CAE containers for software from ANSYS (Fluent, CFX, Icepak, Electromagnetics, Mechanical, LS-DYNA, DesignModeler and Workbench), CD-adapco STAR-CCM+, COMSOL Multiphysics, Flow 3D from Flow Science, NICE DCV, Numeca FINE/Marine, FINE/Turbo, and FINE/Open, OpenFOAM, PSPP, Red Cedar's HEEDS, Scilab, Gromacs and more. These application containers are now running on cloud resources from Advania, Amazon AWS, CPU 24/7, Microsoft Azure, Nephoscale, OzenCloud and others.

Together with recent advances in application software and in high performance hardware technologies, the advent of lightweight pervasive, packageable, portable, scalable, interactive, easy-to-access CAE containers running seamlessly on workstations, servers and any cloud is bringing us ever closer to what Intel calls the democratization of high performance computing.

References

MORGAN, J.M. (2016), *Prediction of barehull KRISO containership resistance in the cloud*, UberCloud Team 181 Case Study, <http://www.theubercloud.com/glosten-inc-uses-numeca-finemarine-in-the-cloud-for-optimizing-containership-hulls/>

COC (2010), *The CoC Studies Make, Reflect, Reveal, and Compete*, Council of Competitiveness, <http://www.compete.org/>

GENTZSCH, W. (2016), *Toward Ubiquitous CAE*, Commentary in Desktop Engineering, January <http://www.deskeng.com/de/toward-ubiquitous-cae/>

Open Architecture Applications: The Key to Best-of-Breed Solutions

Denis Morais, SSI, Victoria/Canada, Denis.Morais@SSI-corporate.com

Mark Waldie, SSI, Victoria/Canada, Mark.Waldie@SSI-corporate.com

Nick Danese, NDAR, Antibes/France, ndar@ndar.com

Abstract

Every process in a shipyard requires data. Despite numerous attempts, there is not now, and realistically never will be a single monolithic software program that is optimal for all tasks. In situations where the value of tight integration is paramount, an application from a single vendor is ideal but in situations where the performance disparity is too great compared to separate best-of-breed applications, external programs are used. This paper shows that the key to making a best-of-breed solution approach work, even in hybrid form, is the ease with which programs can be integrated. This requires software with open architecture.

1. Introduction

Naval architects, marine engineers and shipyard executives are not computer programmers or software engineers; so they should not be expected to be experts in understanding the underlying architecture of how software programs and platforms are designed. That being said, an appreciation of some key concepts can have a direct effect on the future success of businesses in the ship design and construction industries.

The reason is that just about every process involved in shipbuilding requires the use of some kind of computer application. Furthermore, the number of programs used is enormous. All of these programs create and consume data. Then, the data generated is used by other applications as well. Every manager involved in shipbuilding realizes that it is necessary to find a way to somehow tie together these computer programs as well as the associated processes. Everyone would like to avoid the inefficiency and copying errors caused by continually manually retying data from one system into another. Integration is what is desired.

Unfortunately, not all software platforms can easily be integrated with other software platforms. Sometimes integration is so cost-prohibitive that the return on investment is not there. An additional consideration is that a forward-thinking business knows that its requirements will change in the future. It may want to integrate with certain applications today but may need to integrate with different programs a few years from now. Perhaps a business will need to scale up or down. Perhaps it will need to automate what may currently be manual. Perhaps it will need to change programs in order to work with a different contractor or subcontractor. Perhaps it may simply see that there are better programs on the market. In any case, the choice of software should not be a set of handcuffs hindering future business opportunities and efficiency.

In order to address these concerns, it is important to realize that how software is designed plays a key role in determining the ease of integration as well as future flexibility. Only software platforms designed with an underlying open architecture can give businesses what they want and need. This paper will explain why that is so.

2. Why Integration?

Let us first start by trying to get a handle on the scale of the issue involved and why it is important. There are still some in the industry who remember the days when detailed drawings were done by hand. Many other business processes were entirely paper-based as well. But nowadays, even though we still have paper drawings, they are all created on a computer, and just about every other piece of data is created with a computer as well.

We are also subcontracting work all around the world and those naval architects, marine engineers and shipbuilders are using their own computer systems. Getting data from their systems is necessary. More people are using more programs and it is a struggle to unify everything that must be integrated.

Management and certainly those in the IT department would love it if we just had one platform that smoothly ran all software applications, e.g. perhaps it might be ideal if every single application necessary for shipbuilding was a Microsoft or Apple app and it all worked smoothly together. Unfortunately, no single platform, even ones with a broad range of applications, can do everything required and there is no prospect of that ever occurring. Let's look at how we got to our current situation.

3. History of Integrations

This section borrows from *Morais et al. (2013)*.

3.1. Discrete Functional Focus



Fig. 1: Discrete, disconnected applications

The history of the issue begins, as previously noted, at the beginning of the widespread adoption of computers in shipyards, Fig. 1. Vendors set out to build software applications to accomplish specific tasks. These applications had a discrete functional focus and the programmers creating them put little to no thought into how these applications might work with other programs. It did not take long, however, for people to realize that the data needed increasingly came from other computer programs. So it was natural to want to automate the transfer of information.

But that exposed a significant problem because the various programs that people wanted to integrate had incompatible infrastructure and the data structure differed greatly. This forced shipbuilders to use inefficient manual methods and complicated, unintuitive workflows in order to share data between applications. Therefore, several organizations hired programmers to create custom integrations but ran into new difficulties. Custom integrations on a case by case or product by product basis proved to be very costly to implement and maintain. Thus, in frustration, companies looked for a different model.

3.1. Unification

After a period of failed integration attempts, this resulted in a desire to have all software from one vendor in a “monolithic” suite of applications, Fig. 2. We can refer to this as the “unification model” or “unification approach”. Software companies responded to the desire for this model by expanding their product portfolios either through in-house development or via acquisitions. Once monolithic applications of this sort were created, it was thought that the integration problem would be solved. Unfortunately, the problem was not solved, or at least not entirely, and not without significant drawbacks.

It is true, that having an integrated platform made sharing information easier and that there was also the added advantage of having just one system to deal with. But these obvious advantages came with numerous downsides. First of all, implementing these monolithic unified systems was far more complex and costly than often recognized. In fact, the cost of the software was actually relatively minor compared to the implementation costs but the price of the programs was not cheap either. This is because all legacy systems needed to be replaced to gain the interoperability benefits of the new tool.

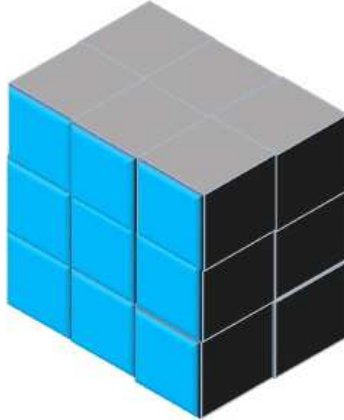


Fig. 2: A single monolithic program that attempts to do every function

Worse still, was the fact that after all the expense, the unification model did not entirely solve the core problem it was designed to fix. This is because even the most comprehensive software packages could not perform all the tasks required so other applications were still needed. As well, there were the numerous cases where inadequacies of the built-in parts of the monolithic system led organizations to use different programs instead. Thus, while unification of all programs sounded great in theory, in practice, it did not work.

3.2. Federation of Platforms: a Hybrid Solution-centric Model

The failure of the unification model has therefore more recently caused organizations to take a more pragmatic approach which could be called a “solution-centric” model, Fig. 3. The solution-centric model is really a hybrid of the application-centric and unification approaches in that it adopts the best of both worlds by analysing areas where tight integration makes sense as compared to areas where suitability for the discrete task is the prime consideration. In essence, tight integration is evaluated simply as another feature. How much benefit can be assigned to that feature is up to an organization to judge while looking at other factors.

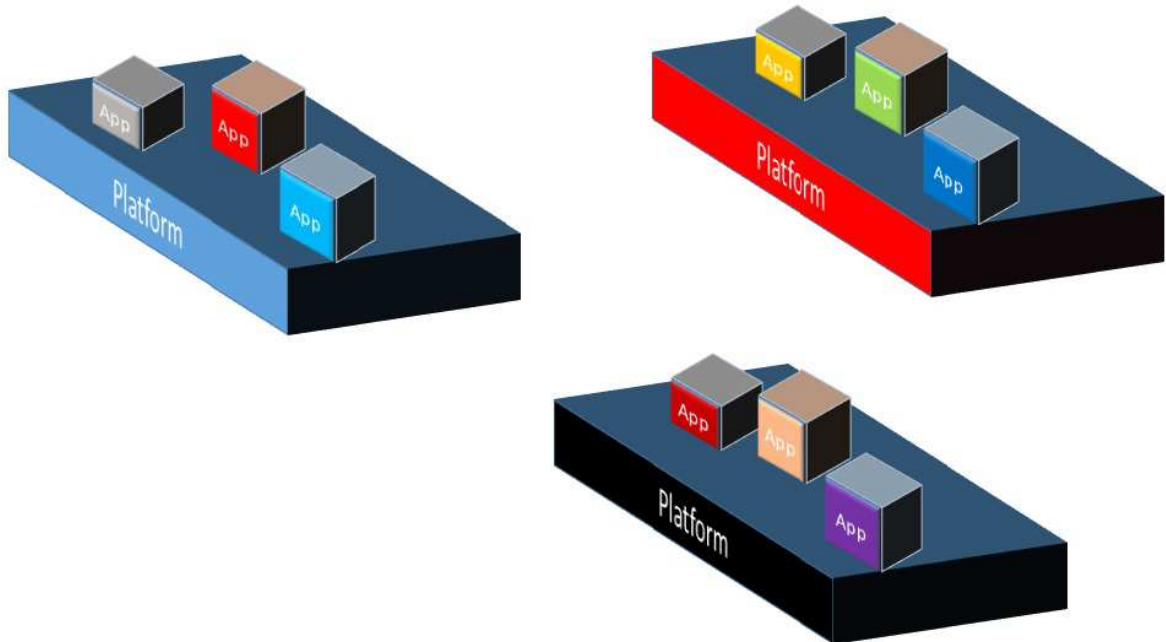


Fig. 3: Applications from different software platforms are used

An example of this solution-centric approach is how many, if not most, shipyards treat the detailing of drawings. Even if an organization owns a monolithic software program which includes a drawing capability, it is generally not used because the AutoCAD program by Autodesk is the industry standard and is typically judged to have superior capabilities in this area. For many companies, this undermines the easy transfer of information but the trade-off is considered to be worthwhile. The same plus/minus calculation is used in other cases when weighing the benefits of adopting potential “best of breed” applications rather than trying to stick with the unified software model.

Another way to describe the current hybrid solution-centric model is to point out that nowadays, companies are using a “federated” approach to implementing software. In political terms, a federation is a group of states that are united but are self-governing within their own spheres. In software terms, different software platforms are united but are individually optimized for certain processes. Note here that we are talking about platforms, not just programs per se.

4. What is a Software Platform?

Fig. 4 shows what we mean by a platform in a software and business context. In carpentry, a platform is something you can build on or place things on or stand on. CIMdata (“The Leader in PLM Education, Research, and Strategic Management Consulting”) gives the following definition:

“Platform: A foundation upon which functional capabilities, data, and processes are enabled and executed.” <http://www.cimdata.com/en/platformization-some-common-definitions>

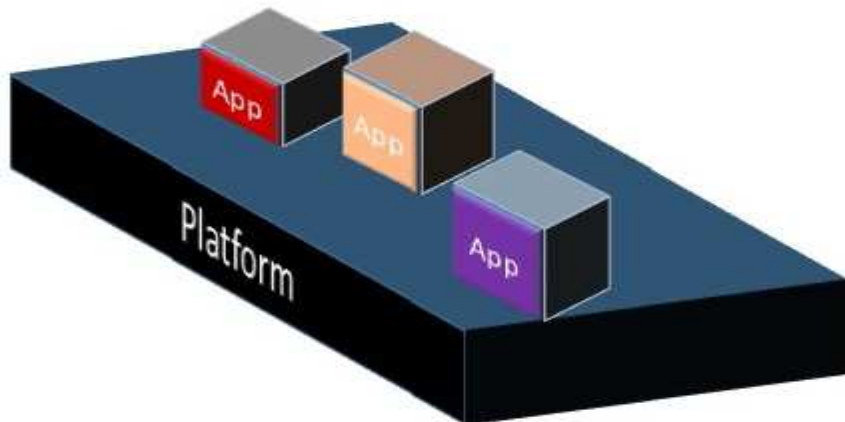


Fig. 4: Applications can be built on top of a software platform

Therefore, using this analogy, a software platform is a major piece of software such as an operating system, a database, or some other significant application upon which various application programs can be designed to run. For example, in the world of mobile phones, there are the iOS and Android platforms that have many apps which run on top of them. Another key point is that platforms allow multiple applications to be built within the same technical framework.

In the shipbuilding industry, we have certain platforms created by various vendors for things such as Enterprise Resource Planning (ERP), Product Lifecycle Management (PLM) and Computer Assisted Design (CAD) amongst others.

Furthermore, as an interesting aside, often platforms can be built on top of other platforms, Fig. 5. A good example of this is the Autodesk / SSI shipbuilding software solution which builds on top of the SQL and AutoCAD platforms, on top of which sits SSI's ShipConstructor Marine Information Model (MIM) plus other tools, on top of which sits ShipConstructor and other applications, on top of which sit other applications connected via what SSI calls the SSI Enterprise-Platform.

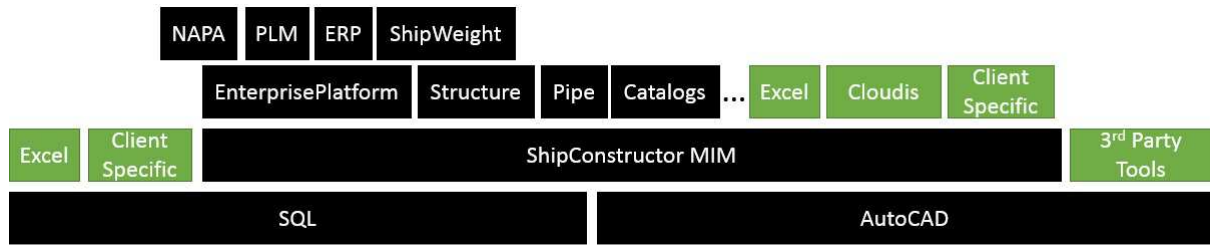


Fig. 5: SSI Shipbuilding Software Solution consists of applications sitting on multiple platforms

5. Best of Breed Solutions

Now that we know what we are talking about when we refer to software platforms, let us get back to the point regarding the need for integration. Shipbuilders want the best application for the job in every situation, that is, the industry desires “best of breed” solutions.

But that brings up an important issue. How are the integrations going to be done? There are better and worse ways to do this, as will be shown below.

6. Levels of Integration

Let us first zoom in to look at integrating an application with a single platform. Note that there are “tighter” or “deeper” methods of integration. The tighter the integration, the more seamless the experience is to the user. In practical terms, that would mean that there are little to no extra steps involved in using different programs. Indeed, it can seem as if you are using the same program if the integration is deep enough.

In technical terms, at the lowest level of integration, there is just a manual exchange of files using industry standards such as IGES or STEP. The problem with merely exchanging files is that not all the information is copied and it requires a manual process to bring in the files. Because of this effort, the information is not “real-time”; it is only as good as the last file exchange so the information can be quite out of date. That is a real problem in the shipbuilding industry where changes occur constantly.

At a deeper level of integration, there is the ability to import / export native application files. This allows more information to be exchanged than using standards. Additionally, because this method collects more information there is less information that needs to be re-entered and therefore less human errors.

However, the best integration is a deep integrated solution where the non-platform application can exchange information without any user intervention. It can access the information it needs, when it needs it from the platform itself. This gives the most accurate and seamless experience to the user.

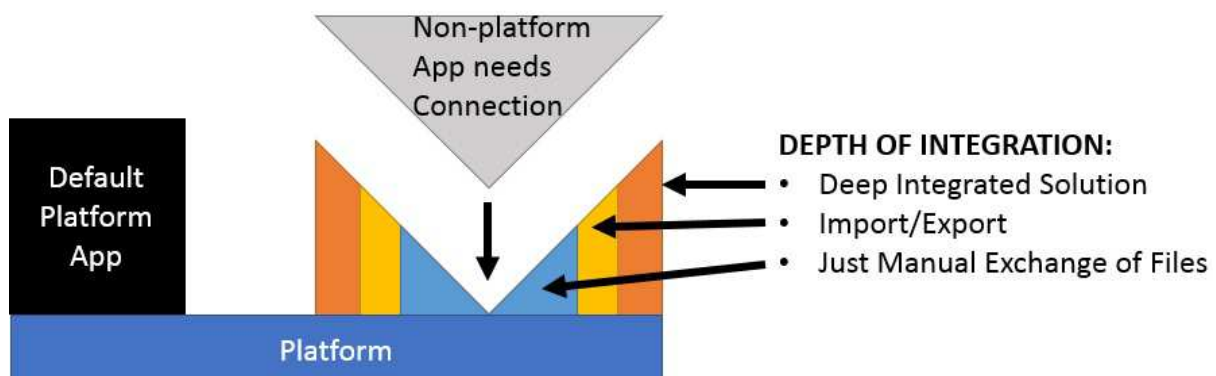


Fig. 6: There are different levels of integration

7. Bad Integration Method: Connecting every application

Now let us zoom out from talking about technical details and get back to a more big picture concept regarding integrations. Remember the original “discrete functional” applications that we talked about earlier in the paper? Here is a good visual of why companies have always had a problem if they try to integrate lots of individual applications. You end up with a maze of complexity, Fig. 7.

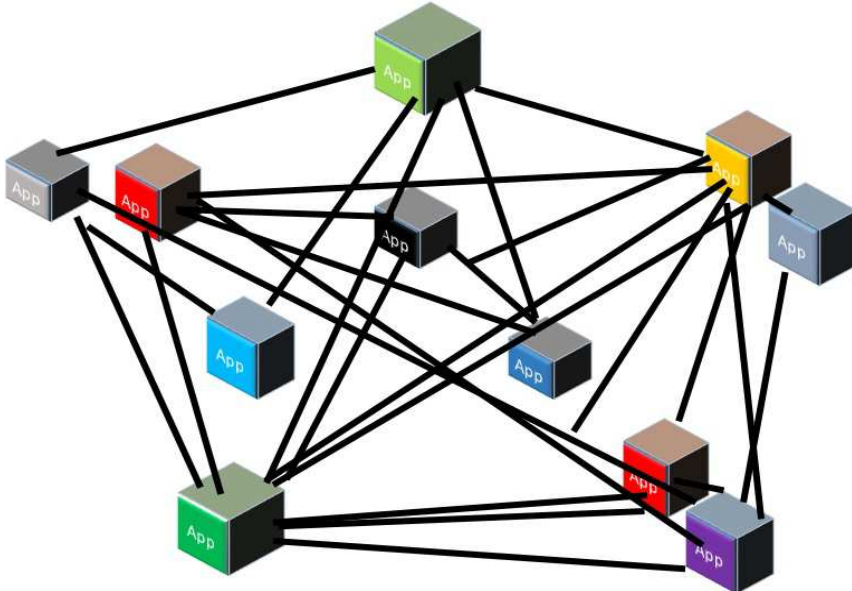


Fig. 7: Connecting individual apps is very complex

It is enormously costly and time consuming to interconnect individual applications from different software platforms. Furthermore, once this rat's nest of complexity has been created, it becomes extremely difficult to undo if a company wishes to swap out different components.

8. Better integration method: Connecting Platforms, not Programs

A much more elegant method would be to connect the software platforms themselves via “bridges”, Fig. 8. Then there would only be a single point of connection between platforms but you could easily get from any app in a platform to any app in another. This integration method is obviously easier to create and costs less than having to link every application. An added advantage is that, if in the future one wanted to change to a different platform, only one connection would need to be replaced.

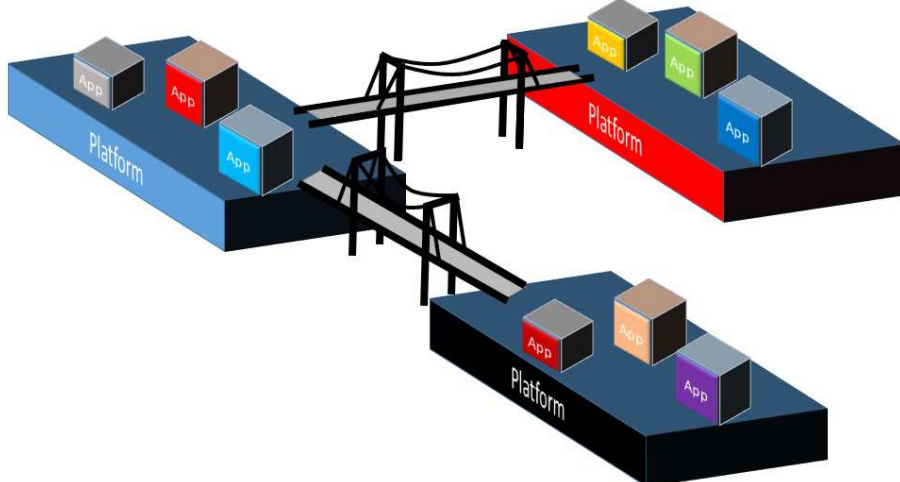


Fig. 8: Integration of Platforms, not Applications via Bridges

In technical terms, when this strategy is used, the applications in each of the platforms leverage the data and processes (workflows) stored in the other platforms (either by linking or sharing information). This reduces errors and leads to deeper and more seamless integration which translates to a better experience for the user. Creating bridges between platforms is the best software integration strategy.

9. Degree of difficulty in bridge construction

But even with a single bridge between platforms, there can be different levels of complexity involved in creating those bridges. Again, this is of critical importance regarding how quickly one could generate a positive ROI on an integration project and how flexible the solution is. Remember, the goal is to be able to make software decisions based on business needs, not based on difficulties related to change.

10. Open Architecture

Discussion of bridge construction complexity leads us to an examination of what makes that difficult or easy. That leads us to the concept of whether or not platforms have an “open architecture.” Open Architecture is a software development concept that is used to refer to how easy it is for one program to get access to the data of another program (hence its ease of integration). Going back to our image of platforms, some are very open so they are easy to build a bridge connection to. Others keep all their applications and data behind big walls so bridges can only be built in a very specific place and a very specific way. (Aside: in the software industry, we call completely enclosed platforms “silos”), Fig. 9.

But note that it is quite popular nowadays for software vendors to say that they are open when, really, they are not very open at all. Fig. 9 shows a true open architecture program with zero walls, another one with several sides walled, and another with much greater walls. It is all a matter a degree. However, these degrees matter enormously to anyone who wants to use a variety of different applications that need to be integrated.

The more difficult things are, the greater the time and effort involved in the integration project. Furthermore, the more difficult things are, the more difficulty (and hence resistance) to change should you need to swap platforms in the future.

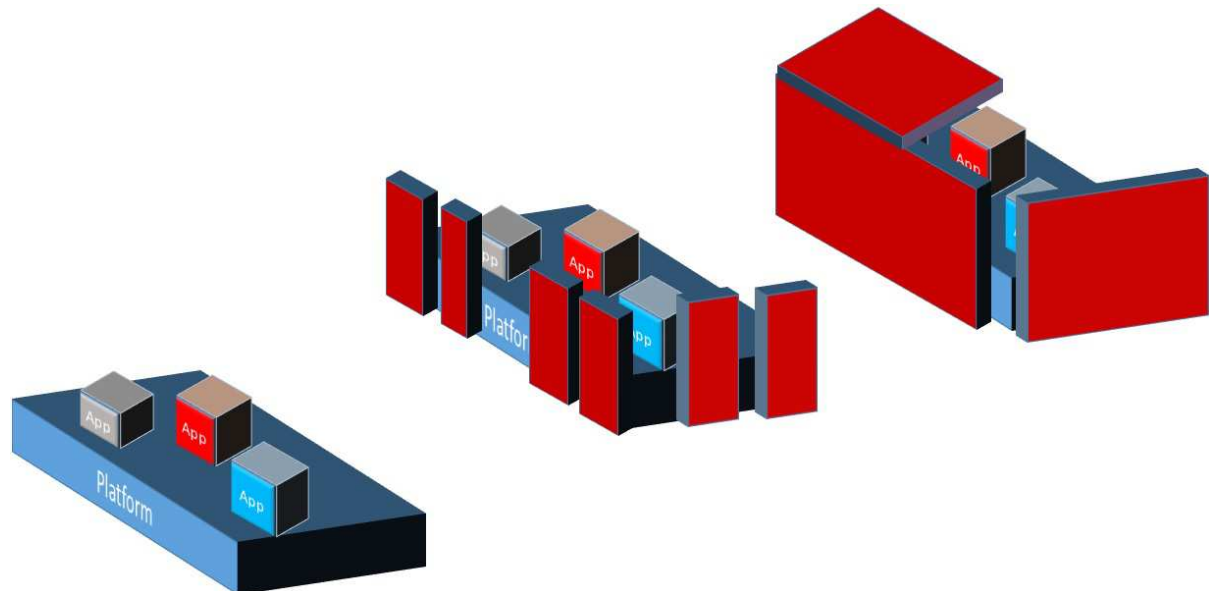


Fig. 9: Degrees of openness affects places where you can build bridges to platforms — Complexity!

11. How to tell if software platforms have an open architecture

No doubt, the above discussion leaves one saying, “Yes, yes, this may be interesting in theory, but how can these points be applied in the real world?” Since naval architects, marine engineers, and shipbuilders are not computer programmers or software engineers, it would be difficult to tell whether or not an entire software platform has an open architecture or not. Therefore, below are some quick tools individuals in the shipbuilding industry can use to make an informed judgment.

11.1. Does it have an API?

The first question you want to find an answer to is whether or not an Application Programming Interface (API) is available for the software platform. Without going into the details, the API should provide controlled access to the underlying data model and to various actions from external applications built on top of it. This is because an API allows developers to add functionality to solve a specific problem for a task and to have those added functionalities maintain a linkage to the underlying application without additional customization.

If there is no API, then an integration project requires modifying the underlying data which will cause issues when the application is updated; the integration will have to be done all over again. In practical terms, if there is no API, it typically means that you will be locked into the old version of software you are using because you will not be able to afford to do all the complex integrations all over again.

Furthermore, even if APIs exist, it should also be noted that how platforms handle APIs can be very different. Some platforms only provide a very small subset of APIs which can limit what can be extended. Also, the APIs can be very convoluted and difficult to use which will increase the difficulty of being able to connect to the platform.

11.2. Does it have Good Developer Community?

Therefore, perhaps the best way to measure the quality of the APIs and the right amount of openness of a platform is to look at the developer community. If there is a healthy developer community creating applications for the platform, then most likely the APIs are easy to use, there is great training material, the vendor provides the right amount of access to internal data/processes and also has many examples. In other words, the vendor has created an ecosystem around development that encourages the growth of new applications as well as the ability to interconnect with other platforms. There is a good supportive structure. This is important because it does not matter what the strategy is of the platform, the technology stack the platform uses or any other criteria. As the saying goes, “the proof is in the pudding.” Lots of developers and lots of programs demonstrate how open a platform is in reality.

12. Why are some platforms not open?

As you ask the questions above, you may find that the answer in a particular case is that a platform is not very open. There are two possible reasons for this:

- a.) It was not designed to be open in the first place and now it is too technically difficult to create an open architecture out of something that was built to be closed.
- b.) It is a deliberate strategy to lock customers into the company’s own ecosystem of products.

Having an open architecture is not just a technology issue, it is a philosophical and cultural issue as well. The desire from customers nowadays is for openness but this has to be embraced by the vendor, from the top management down to the lowest developer. At every stage of an application’s creation, the question has to be asked, “How can the data be shared with other applications?” It cannot be a side

issue. Other applications and platforms needing that data have to be thought of as “first-class citizens”, not second-class afterthoughts. That is the only way that software becomes open and easily integrated with in reality.

13. Practical Implications

The above discussions are not just theoretical. They have real-world consequences, both positive and negative. Let’s look at some practical applications of how an open architecture platform has led to successful integrations.

13.1. Examples from Previous COMPIIT Paper

In 2014 at COMPIIT, we presented several examples of integrations that took advantage of the open architecture framework of SSI’s ShipConstructor software, *Morais et al. (2002)*. These examples included:

- a.) Sharing Data within the Engineering Group: Integrating Autodesk based ShipConstructor with a CAE application called AutoFEM.
- b.) Sharing Data between Engineering and Production Planning: Integrating ShipConstructor with Microsoft Project and Autodesk Navisworks to show animations of the build sequence using the 3D product model geometry.
- c.) Sharing Data between Engineering and Production Machines: Integrating a CNC Profiler with ShipConstructor profile information.

13.2. SSI / Autodesk / BAS ShipWeight

Another example of an integration from a member of SSI’s ShipConstructor Developer Network is the integration of ShipConstructor with the ShipWeight software tool from BAS. ShipWeight is used for weight and cg (center of gravity) estimation and monitoring from early concept design through detailed engineering and construction. The use case for this integration is that ShipWeight can be utilized to create a weight estimation model of an entire vessel in the early stages of design. Then, as detail engineering is done on various blocks in ShipConstructor, the ShipConstructor weights can be fed back into the ShipWeight model. At the end of a project, this information can be leveraged when planning similar ship designs since an organization can reuse and utilize as-built data.

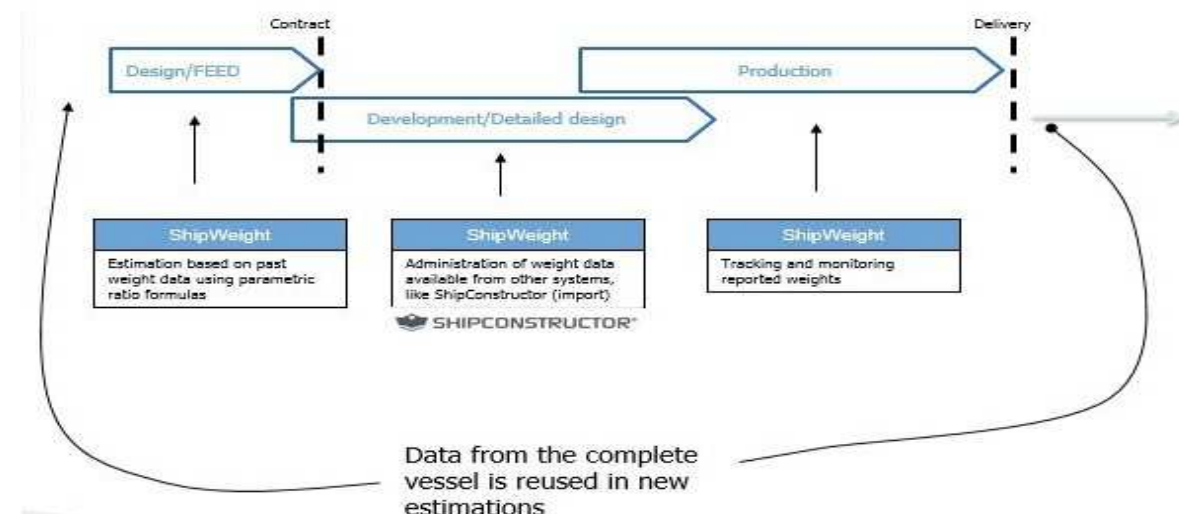


Fig. 10: Integration of ShipConstructor with BAS ShipWeight

13.3. SSI / Autodesk / Microsoft Excel

Another example of a successful integration, this time with a very familiar application (and platform), is the integration between ShipConstructor and Microsoft Excel. Using SSI's EnterprisePlatform tool, virtually any information that a user wants from the ShipConstructor 3D Product Data Model can be automatically queried then loaded into preformatted Excel templates. This allows shipbuilders and designers to easily access, visualize and manipulate detailed Engineering data using the powerful analysis tools of the world's most popular spreadsheet application. Integrating ShipConstructor with Excel has an almost infinite number of practical use cases such as reports on:

- a.) Structural Weight per Unit/Block
- b.) Parts Nested Information
- c.) Quantity of Parts per unit
- d.) Length by System
- e.) Etc.

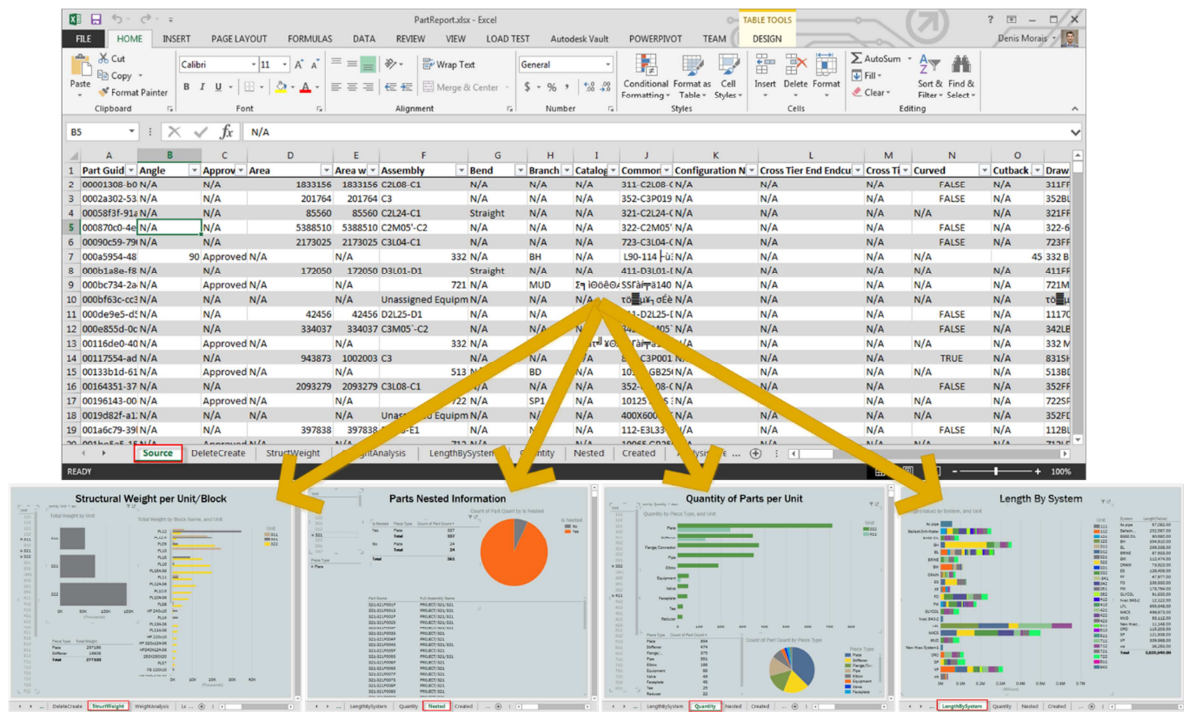


Fig. 11: Integration of ShipConstructor with preformatted Excel Templates

13.4. ShipConstructor / Cloudis

An example of a very deep integration is the integration between SSI's ShipConstructor and the Cloudis CMPIC cable management application. The ShipConstructor to CMPIC interface enables cable-way geometry created in ShipConstructor to be used in CMPIC where the routing, change control and downstream installation of cables are managed. Partnering with Cloudis is an example of how an integrated best of breed solution is advantageous since it enables a user to leverage CMPIC cable management capabilities whilst employing ShipConstructor's modelling and clash detection to create the cable supports, penetrations and cable trays as required. Note that ShipConstructor already had Electrical Modelling capability but CMPIC is used to extend the functionality to provide enhanced capabilities for situations with unique requirements, (e.g. Navy).

The depth of the integration is evidenced by the fact that the interface has been developed at the database level between ShipConstructor's Marine Information Model and CMPIC's Product Model. More importantly, from a user's perspective, the integration is so tight it appears as if CMPIC is simply part of ShipConstructor.

14. ShipConstructor's Open Architecture

The reasons these integrations are possible is entirely due to ShipConstructor's Open Architecture. CAD/CAM developer SSI has created its ShipConstructor software from the ground up to be 100% open. There is not a single piece of information that the ShipConstructor solution holds hostage in a proprietary format. All information can be extracted and leveraged for whatever purpose the user (or another developer) wants.

ShipConstructor supports its open architecture in several ways:

1. At the core of the ShipConstructor Marine Information Model (MIM) is a fully open SQL database. This allows anyone with some industry knowledge of SQL to have full access to all the information contained in the ShipConstructor environment.
2. ShipConstructor provides two API layers. A .NET or C++ datalayer API to make it easy to consume and produce information from/to the SQL database and a .NET or C++ API layer to allow access to geometric data contained in the AutoCAD foundation.
3. By extending the AutoCAD foundation, users are able to use any of the AutoCAD APIs to consume the wealth of information available.

15. Conclusion

This paper has argued that in order to implement best of breed solutions, open architecture software platforms are necessary. An explanation of why this is so has been given along with ways to analyze whether software platforms truly are open. Real-world practical benefits of openness have been highlighted along with the dangers of software platforms that are closed.

The message has been targeted at naval architects, marine engineers and people working in shipyards who are in the process of choosing software solutions. However, it is also a challenge to software vendors as well. Clients will demand the ability to easily integrate and also want flexibility. That will increasingly require software developers to create software platforms that feature an open architecture.

References

CIMData. *Platformization, Some Common Definitions*. <http://www.cimdata.com/en/platformization-some-common-definitions>

MORAIS, D.; WALDIE, M.; LARKINS, D. (2013), *Empowered engineering: availability of engineering data throughout the shipyard*, Int. Conf. on Computer Applications in Shipbuilding (ICCAS), Busan, pp.67-75

MORAIS, D.; WALDIE, M.; LARKINS, D. (2014), *Leveraging engineering information*, 13th Conf. Computer and IT Appl. Maritime Industries, (COMPIT), Redworth, pp.327-337

Augmented Reality Assistance for Outfitting Works in Shipbuilding

Kohei Matsuo, National Maritime Research Institute, Tokyo/Japan, kohhei@nmri.go.jp

Abstract

The paper introduces our recent research activities on a development of the AR application for support of a pipe installation work in a shop floor in shipyards. The application assists a worker by indicating various information on pipe installation through AR technology. Once the worker points a camera with a tablet PC to a marker which is attached on a pipe, the AR system guides the worker which the pipe corresponds to one in the drawing paper, or where the pipe should be installed in the ship by visualizing its 3D image through AR technologies. As workers input their work status naturally through operating the AR application, the application can also monitor and manage outfitting works in shipyards in real-time. The paper explains the AR application itself including its demonstration in a shipyard, but also how we utilize this application in practical shipbuilding facilities. Especially, the paper introduces our new interface with a practical 3D CAD system for pipe design.

1. Introduction

Shipbuilding Enterprises are highly forced to improve their development and production processes regarding time and quality. Digital supported methods are the substantial enabler to achieve improvements in this area. Also Digital Manufacturing is getting to be familiar in a research field and a practical use even in a shipbuilding industry which is characterized as a small batch production, hand working-dependent and to be done under special condition that a ship not fully designated and planned before starting its production.

Although various approaches can be considered to digital manufacturing in the shipyard's shop floor, important approaches could be pointed out for digital manufacturing as follows:

- Advanced utilization of 3D information
This is the approach how to utilize 3D information (e.g., 3D CAD model) as 3D information. 3D information should be qualitatively different from the conventional 2D information, and we should restructure the representation and the handling manner of information according to dimensional expansion of information. Some previous studies introduce examples to apply the 3D CAD model to digital manufacturing in a shipyard, and those are mainly related to a 3D model viewing in the shop floor, a control of NC machines or various robots, and production simulation. Virtual reality technologies are a new way especially for production simulation by feeling in an immersive environment.
- Effective provision of construction information to the shop floor
This is the approach about the concept of a '3D drawing'. It should be a natural desire to see the original 3D image while building a 3D object. Many shipyards are already working with 3D CAD data, including additional information on construction, in the shop floor as worker's reference. Recent mobile devices such as the google glass may change this situation dramatically. In the near future, further NUI (Natural User Interface) devices such as a holography or a haptic device may be became widely used in a shipyard.
- Easy access to ship data even from the shop floor
The concept is not only to refer to construction information but also to make ship data from the shop floor. As recent mobile devices realize easy access to ship data which is usually prepared in a design division, they also help us to create or edit ship data from outside the design division. In the near future, the new manner might be proposed to be designed in front of the real thing in the shop floor rather than in a dedicated design room.

Even though there are several proposals to use 3D model for digital manufacturing, new demands are emerging about a further utilization of 3D CAD models on the shop floor or in a building dock. AR (Augmented Reality) technologies would answer this need. By introducing this technology, there would be expectations not only to watch the 3D view directly on the real object, but also to create new paradigms which change the way to use information around the shipyard. Concepts of a 3D drawing sheet with AR or an interactive information exchange between the shop floor and the design division would be one of example which may cause paradigm change in shipyards. For this reason, we have been interested in this technology and have developed some AR applications for shipbuilding. The paper especially introduces a recent application which supports workers, while they install piping.

2. AR Application for pipe installing work

2.1. Outfitting work in shipbuilding

As there are many kinds of equipment such as pipes, steel structures, electric component and various devices that must be outfitted in a ship, there exists an enormous amount of outfitting works before and after launching the ship in shipyards. Outfitting work is mainly conducted manually by workers, usually referring to two-dimensional paper drawings. As the worker must identify a pipe with its correspondence in the drawing paper to clarify where it must be outfitted, some difficulties exist:

- As there are too many pipes needed to be outfitted, it is difficult to identify those with correspondence in a drawing paper;
- 2D drawings are complicated to understand. It is difficult just to find the objective pipe in the drawing;
- There is no additional information on the drawing except fundamentals such as pipe ID number and location. Workers have to figure out themselves suitable work procedures, such as the order of outfitting etc.;
- Especially for small equipment, there is sometimes only a piping diagram which indicates connection and relationship of pipes and machinery, but no pipe arrangement drawing which explicitly provides locational information.

Fig. 1 is a picture taken in a Japanese shipyard. The worker standing in the centre of the picture is watching the arrangement drawing sheet, trying to find the corresponding pipe in the drawing, while he keeps the objective pipe in his hand.



Fig. 1: Snapshot of a typical scene of outfitting works in shipyard and a typical pipe drawing

At this time, it takes around 10 minutes just to find it in the drawing before its outfitting, and ICT solutions should solve those difficulties. This is our motivation to develop a suitable ICT solution for this, and we focused on AR technologies for this purpose.

2.2. AR Application for pipe installing work

The AR application developed consists of the following functions:

1. Workers can refer to corresponding drawings on the pipe they want to outfit by easy operation (one-touch operation) through a tablet PC or a smart phone from the shop floor, as each pipe and its necessary information are connected beforehand in a design department;
2. The AR application guides the location where to install the pipe;
3. Workers can enter their work status (when to start and finish the installation work) for respective pipes and refer to their work order from the shop floor;
4. Workers can leave notes (e.g. on work status) directly onto the real ship space.

The AR application realizes the above first function by putting a marker on respective pipes. As a marker is related with corresponding information for the pipe, necessary drawings (such as a piping diagram or a pipe arrangement) automatically appear when a worker put his tablet PC or a smart phone to the objective pipe. The objective pipe is highlighted in the pipe arrangement drawing for easy location.

The AR application realizes the above second function by putting a marker on a ship under construction. As positional information with respect to the marker is also prepared and registered beforehand, workers can see a virtual image of the pipe finally installed in the ship through a tablet PC or a smart phone. With the aid of this function, workers can easily understand where a pipe should be installed without referring to drawings; this contributes to better work efficiency. In the future, the application should provide not only virtual images of the pipe finally installed but also interactive work information such as the work procedure.

For the third function of the application, a worker can register his present working status (e.g., start and finish of the pipe installation) from the shop floor for respective pipes with smooth operation with support from the application. As information on the working status can be gathered from all workers on the shop floor, real-time monitoring and management on an outfitting work in the shipyard can be realized even to each small equipment.

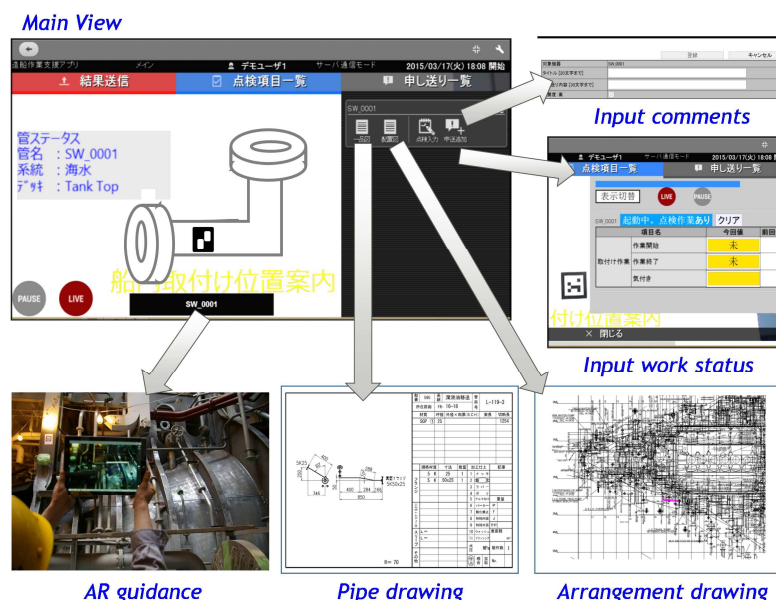


Fig. 2: Concept image of the AR application

Fig. 2 illustrates a conceptual image of those functions of the AR application. The main view of the application is shown at the upper left of the image. This view arises when the application recognizes the objective pipe. Workers can refer to the related drawings and documents of each pipe, leave notes, and register his working status just by touch operation to the display. They can also refer to the summarized working status and schedule of a whole factory. Fig. 3 shows some snapshots when the user of the application is using this AR application in the shipyard.



Fig. 3: Snapshot of the AR application while using in the shipyard

2.3. Practical Use of the AR application

The AR application is almost ready to use in practical shipyards. Beforehand, users must prepare information on pipes in a computer. Although this information can be set by 2D plan, 3D information from 3D CAD systems should be a better way to provide information to the shop floor.

Fig. 4 illustrates a framework of a data interface between a 3D CAD system and the AR application. During the design stage, engineers define pipes (or other equipment) to be installed in a CAD system. Then they convert this information to the AR application. As the data structure is already defined for the AR application, users can generate the information according to the designated manner from various CAD systems.

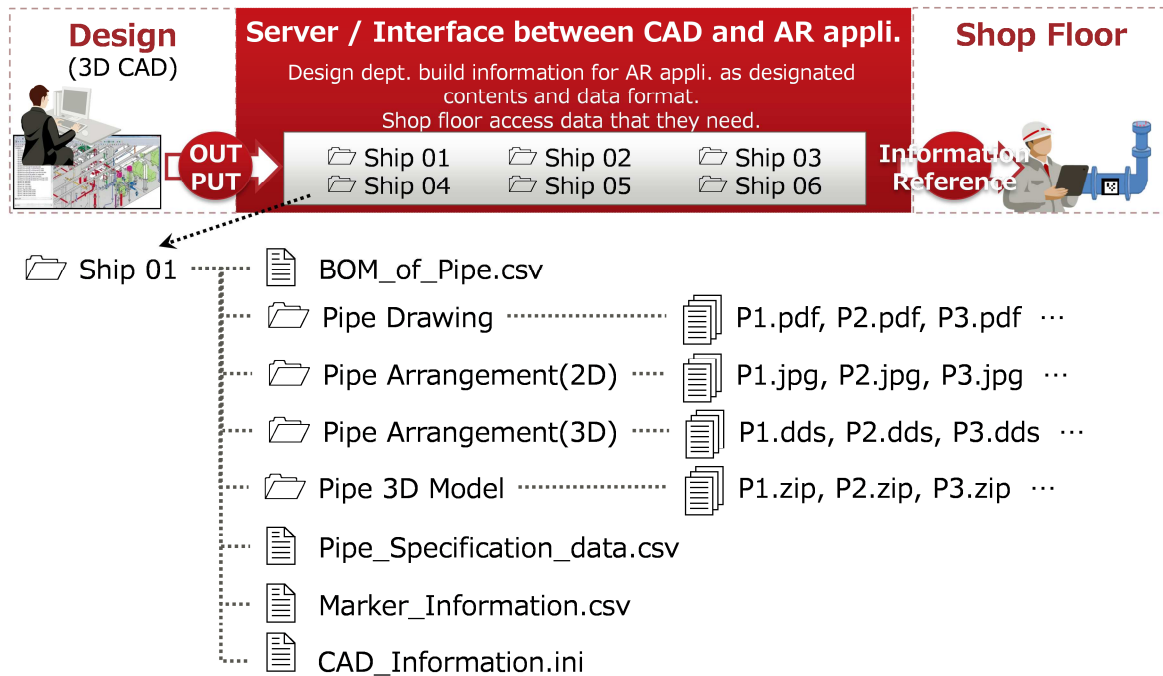


Fig. 4: Framework of data interface between CAD system and the AR application

Fig. 5 illustrates the operational procedure of the AR application on the shop floor. Workers bring a tablet PC or a smart phone; then they start the AR application. The AR function starts after workers have chosen a suitable option (Ship No., worker's name, etc.) from a pull-down menu. For the present system, there are two types of markers needed for identification. A marker for pipe identification is directly attached on the corresponding pipe. Various approaches (such as character recognition etc.) can be substitutable to use a marker. Another marker, for locational identification in a ship, is attached in a designated point of a ship. Once a tablet PC or smart phone is set to the marker on the pipe, an information window displays basic information on the corresponding pipe. Worker can see several drawings on the pipe by touching the icon in the display. Workers also can see the virtual pipe which is installed in a ship through AR technologies. The AR application guides workers where to install pipes but manages their work schedule or work order in real-time.

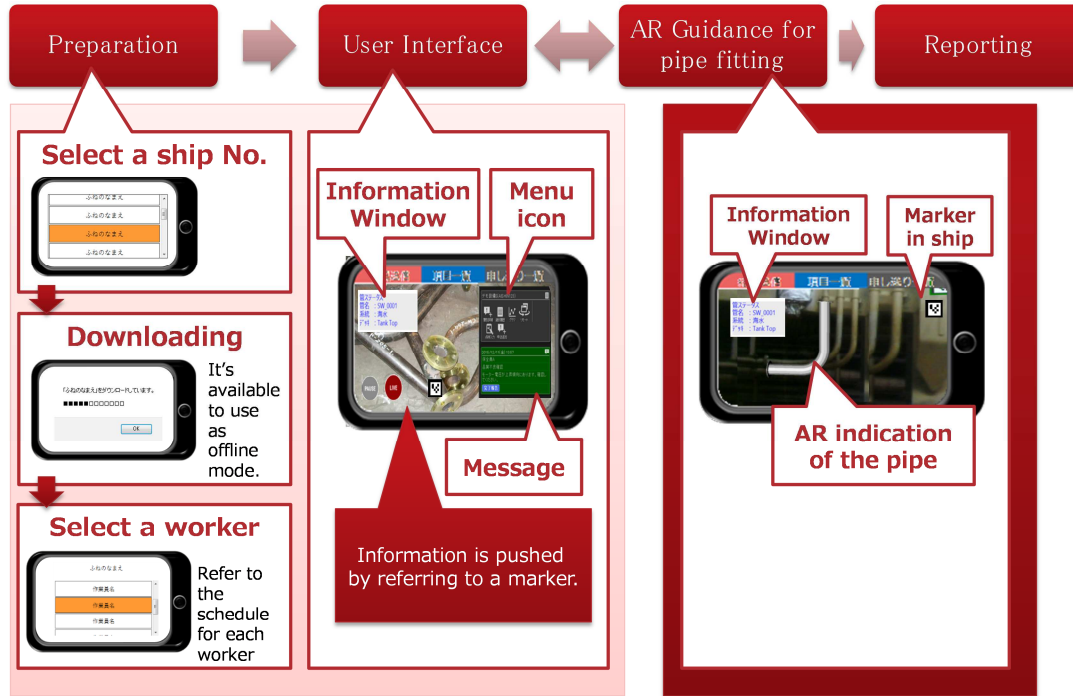


Fig. 5: Operational procedure of the AR application on a shop floor

3. Conclusion

This paper has introduced an AR application to support workers in pipe outfitting in a shipyard. The application was already verified in a shipyard. It can effectively guide workers through the AR indication. We have developed the application for practical introduction to the production line of an actual shipyard. We can expect improvement of the work efficiency, but also effective development of young workers through the AR technology.

The application can collaterally monitor and manage the production line of the shop floor even to every small equipment items. As shipyards usually manage outfitting work by subassembly units which are composed of several equipment items, they do not manage by every single equipment item. This impedes the collection of information from a shop floor and a ship under construction. The AR application we developed can help and guide workers with AR technologies, but the application also collects information on the work status of each worker simultaneously. This procedure does not put extra load on the worker, as his work status is registered by the application. Although the AR application requires additional infrastructure in the shipyard, recent developments on a data interchange system will help the shipyard to use the application without excessive preparation work.

References

- MATSUO, K.; ROTHENBURG, U.; STARK, R. (2013), *Application of AR technologies to sheet metal forming in shipbuilding*, 23rd CIRP Design Conf., Bochum, pp.937-945
- MATSUO, K. (2013), *Demonstration of AR application for sheet metal forming works in shipyard*, Int. Conf. on Computer Applications in Shipbuilding (ICCAS), Busan
- MATSUO, K.; SHIRAISHI, K. (2014), *Introduction of AR applications for shop floor in shipbuilding*, Conf. Computer Applications and Information Technology in the Maritime Industries (COMPIT), Redworth
- MATSUO, K. (2015), *AR application development for pipe installing assistance*, Int. Conf. on Computer Applications in Shipbuilding (ICCAS), Bremen

Ship Power System Modelling for the Control & Optimisation of Multiple Alternative Energy Sources On-Board a Ship

Hans van Vugt, TNO, Delft/Netherlands, hans.vanvugt@tno.nl

Edward Sciberras, Newcastle University, Newcastle-upon-Tyne/UK

Leo de Vries, Ketelbink B.V., Delft/Netherlands, leo.devries@ketelbink.nl

Jonathan Heslop, Newcastle University, Newcastle-upon-Tyne/UK, jonathan.heslop@ncl.ac.uk

Anthony P. Roskilly, Newcastle University, Newcastle-upon-Tyne/UK,
tony.roskilly@newcastle.ac.uk

Abstract

The INOMANS²HIP project aimed to create advanced ship systems models to investigate alternative energy technology installations on-board a Ro/Ro cargo ship. The project developed an energy management system (EMS) and novel human machine interface (HMI) to provide optimized operational set-points and control of installed power systems. This paper will present an overview and results of the advanced modelling, to provide accurate and realistic simulations of the complete ship. It will also discuss the application of Particle Swarm Optimization algorithms (PSO) and Simplex method to optimize on-board energy flow for reduced fuel consumption and, thus, emissions.

1. Introduction

The main question for the marine industry is what the future holds for shipping? With ever more volatile fuel markets and increasing emission legislation on a national, regional and international level, the answer is not as straight forward as it first seems. In this highly competitive and diverse market, new technologies and techniques are being developed and implemented to improve energy efficiency, lower fuel consumption and lower emissions, but one solution is not suitable for all and can come at considerable capital cost to the end users. So, what are the best options for individual ships? Moreover, how can they be integrated and controlled for best operational efficiently? And are the solutions cost effective for the industry?

The cargo ship sector represents around 90% of the gross tonnage of the world's merchant fleet, consisting of around 38000 vessels at the end of 2010, *Marisec* (2011). According to predictions, the world shipping fleet should increase by about 60% by 2020. The container, tanker and bulk carrier sectors will constitute the largest growth as the demand for transporting more resources and goods around the world is likely to double within the same period, *Meech* (2008). Global shipping is estimated to contribute 4.5% to the annual global emissions of carbon dioxide (CO₂), 5-8% of sulphur emissions (SO_X) and up to 30% of nitrogen emissions (NO_X). It is also estimated that greenhouse gas (GHG) emissions from shipping will increase by two to three times of current levels by 2050 as the world shipping fleet grows to meet the increasing global demand for shipping resources and goods, *IMO* (2009).

The INOMANS²HIP project aimed to investigate and develop new concepts for the possible implementation of alternative energy technologies and operational control strategies on-board a cargo ship. The project developed an energy management system (EMS) for the integrated and optimized operational control for a multiple source energy configuration of ship using predetermined set conditions combining traditional power system installations with state-of-the-art alternatives (WHRS power generation, PTO/PTI, PV, battery storage and shore-to-ship power supply) to reduce fuel consumption, operational costs and emissions.

Taking a holistic approach to the energy needs of a ship and using advanced modelling, three ship concepts were investigated based on an existing Ro/Ro cargo ship sailing between a port in the UK and one in the Netherlands. The first two concepts revolved around retrofitting the reference ship with selected alternative energy technologies. The first of these retrofit concepts was cost restricted, imple-

menting only the most cost effective alternative energy technologies with minimal intervention on the original reference ship's design. The second retrofit concept assumed cost was not inhibitive and that minimising emissions was the primary goal, so all alternative energy technologies deemed appropriate were implemented in the original reference ships power network. The final concept considered a new build ship of a similar hull form and operational needs, but implementing the alternative energy technologies in a completely new mixed AC/DC grid distribution network, which is not explored in depth in this paper.

2. Modelling a Ro/Ro Cargo Ship

In the scope of the INOMANS²HIP project, a Ro/Ro cargo ship sailing in the North Sea is chosen with a well-defined operational profile to simulate. The ship has four medium speed engines providing power for propulsion and two smaller auxiliary generators providing the ship's on-board power needs.

The aim of modelling is to present a method of reducing greenhouse gas (GHG) emissions through promoting fuel efficient energy solutions for current operating cargo ships by the optimisation of energy systems on-board and energy balance analyses. To evaluate all the ship concepts in the project a simulation environment was setup to simulate all the global energy systems on-board. The tool simulates these global energy systems, reads various operational profiles and compares the different ship configurations.

To simulate the different ship configurations and compare the different machinery alternatives, the General Energy Systems (GES) object-oriented simulation tool, developed by TNO, was used to perform the analysis. Based on the bond graph method of analysis, GES is a simulation tool using object-oriented design allowing independent domain based energy analysis of complex and multi-faceted power systems. One of its main advantages is normal system descriptions can be used and as a result all the energy flows on-board a ship is visualised. So the main consumers that characterise the operation can be identified and defined within the model. This is necessary for quick new network configuration comparison and optimising energy usage on-board.

2.1. Modelling Environment

The GES simulation environment is a unique open architecture software package developed over twenty years by TNO at the bequest of the Royal Netherlands Navy to facilitate the study the energy flow on-board marine vessels. GES provides a simulation tool allowing analysis of energy flow of complex processes and systems, modelling at a component or sub-system level. GES uses simple connectable building blocks of component models to create whole ship or more complex process systems in a flexible simulation environment, allowing for quick and ease exploration and comparison of different system configurations and energy strategies at an operational level.

Due to the open architecture of GES, many other aspects of the system and components can be included into the model. Aspects such as weight, size, failure rates (MTBF), maintenance times (MTBR), costs, efficiency and fuel consumption can all be included as separate parameters into the simulation. In addition, GES can use excel files to import and export real-time operational data for easy analysis and comparison of different system configurations or designs. Some of the typical applications of the GES program are;

- Analysis of installed integrated and interdependent propulsion and power generation systems
- Determining and comparing the effects of the application of new technology systems or operational strategies on the whole system or individual components
- Enabling rapid system design and analyses
- Optimizing operational performance of installed systems
- Determining the residual capacity of system in case component malfunction
- Cost and environmental impact analyses of entire systems or at a component level

GES's open object-oriented modelling system allows for the easy development of much larger complex systems from basic building blocks at a component and the sub-system level. Libraries of the proposed technology components and sub-system models can be created to allow rapid development and analysis of different arrangements and installations any more complex system, i.e. a complete reference ship as reported in this document.

2.2. The Reference Ship

Using the information and operational data provided by the owner of the reference ship, models of the individual systems were created within the General Energy Systems (GES) simulation environment. These were combined, with additional standard models for ship hull resistance, wind resistance, fuel types etc., to develop a global model of the reference ship. Using the sailing and operational profile of the ship, simulations of a round trip were run and validated in the GES software. The basic reference model of the main propulsion installation is shown in Fig. 1, with an overview of the model curves of the main equipment graphical represented in the GES environment.

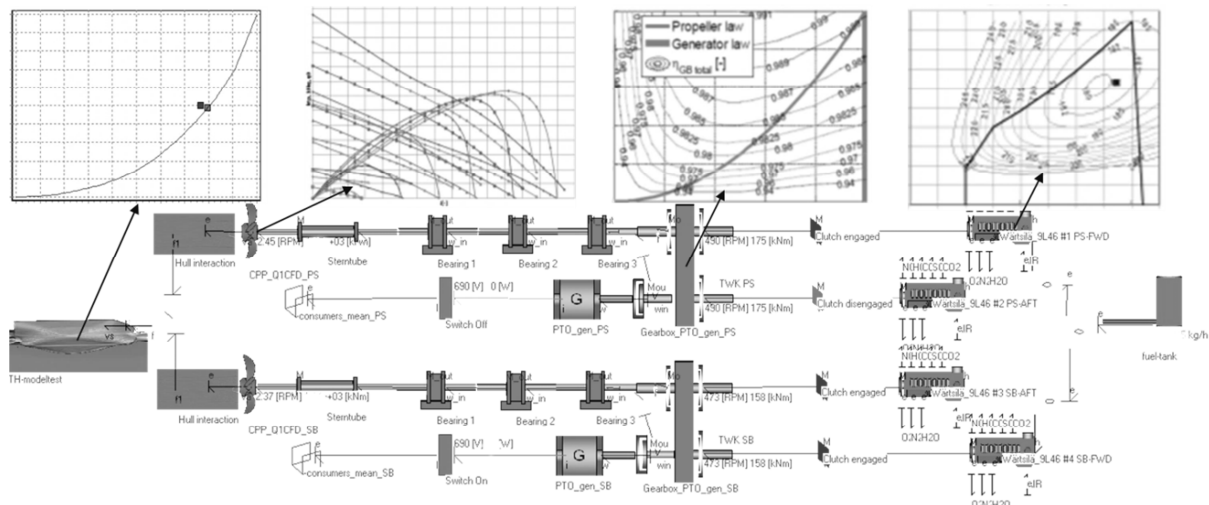


Fig. 1: Basic reference model

2.3. On-board Ship Systems Models

The conventional components of the reference ship are based on those systems installed on a real Cargo vessel, the individual components models being included in the INOMANSHIP GES libraries. this represented conventional components commonly found on-board most classes of cargo ship. The use of these basic conventional modelling blocks are easily adaptable to any configuration of cargo ship within the GES environment. The conventional component models included in the library were:

- Fuel tanks based on the real properties of marine diesel oil (MDO) and heavy fuel oil (HFO).
 - Main and Auxiliary engines based on a combustion model taken into account the operational aspects SFC (g/kWh), NNOx (kg/kg fuel), NHC (kg/kg fuel) and NCO (kg/kg fuel) as function of load (kW) and running speed (rpm).
 - Economizers use the exhaust gases from the engines for heating.
 - Oil – fired Boilers model to provide additional heating needs particularly in port.
 - Electrical power distribution network components
 - Auxiliary systems providing the hotel load
 - Bow thrusters for manoeuvring
 - Control pitch propeller based on a four quadrant Wageningen B propeller
 - Gearboxes subdivided into load dependent, speed dependent and constant loss systems.
 - Rudder models for manoeuvring

In addition to the conventional component models, other influences on the operation of the ship are created to be included in the reference ship's global model. This included the resistance of the ship through the water to correct for speed and power losses, as well as the use of the combinatory curve of the propeller installed on-board the reference ship. Further to the resistance of the ship through the water, wind speed and direction, based on averaged metrological data for the region, were included as an influencing factor speed and operation.

These component models were first combined into sub-systems and systems, such as electrical power generation and propulsion systems, from fuel tank to propeller, finally being combined to create the global ship model of the reference ship.

In addition to the conventional ship component models, component models of novel energy sources being investigated in this project to reduce CO₂ emissions were created and included in the INOMANS²HIP GES library. The technologies are grouped in terms of their proposed nature, i.e. renewable energy systems, electrical machinery energy recovery/efficient systems and alternative distribution networks, energy storage and shore power supply. These will be similarly grouped within the GES libraries shown in Fig. 2. To investigate the influence of these alternative energy systems on the operation of the ship and their potential to aid fuel efficiency, leading to reduced emissions, three new ship configurations were developed and compared to the reference ship.

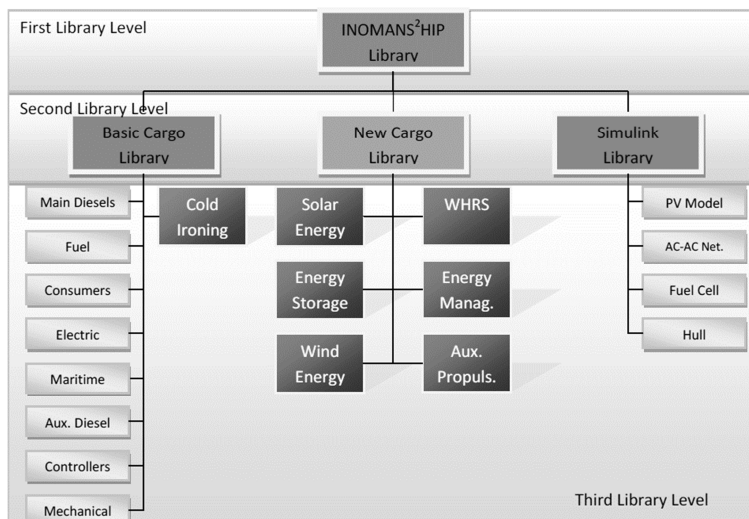


Fig. 2: Overview component library

2.4. Global Ship Models

Using the components and systems models created in the INOMANS²HIP models four global ship models were created in the GES simulation environment.

2.4.1. The Reference Ship Model

The reference ship model created in GES contained all the main systems of the original ship, including four main engines connected in pairs to two CPP for propulsion; two diesel generators for on-board electrical power generation; two oil-fired boilers and two economisers connected to the inside main engines for heating needs of the ship; shaft generators connected to main engines to provide PTO electrical power generation; and two bow thrusters and rubbers for manoeuvring of the ship. Fig. 3 shows the schematic of the reference ship as created in the GES simulation environment. The model is extended with a heating system consisting of economizers and boilers to calculate the fuel consumption in comparing with the real cargo vessel. The spare boiler is not taken into account in the modelling as only one boiler is in operation at any time.

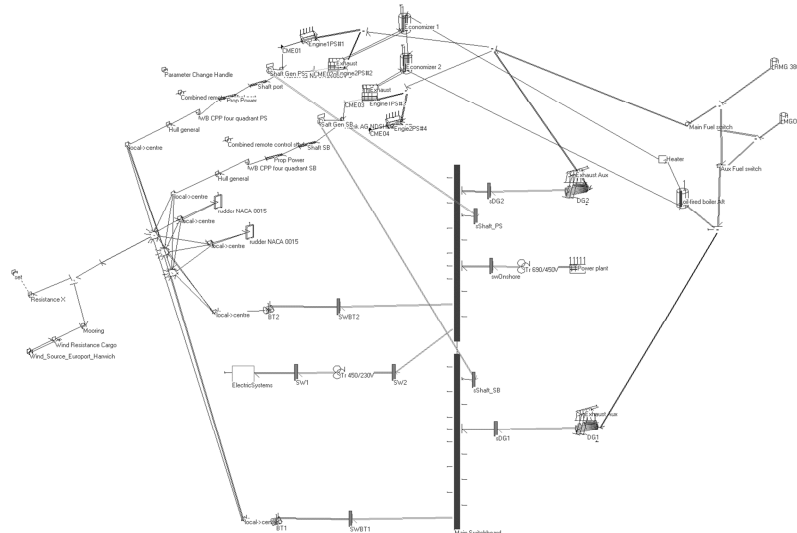


Fig. 3: Reference cargo vessel

2.4.2. The Low Cost Retrofit Concept Model

The low cost retrofit configuration was intended to investigate the implementation of alternative energy sources where cost was an inhibitive factor in the technologies installed. The intention was to investigate a low cost solution with the minimal installation of new systems in order to minimise the initial capital costs while also achieving an observable reduction in fuel consumption and emissions. To this end, the low cost retrofit ship included a shore to ship power supply used during port stays, and two shaft generator/motors being fully implemented on both to be operated as PTO/PTI systems depending on operational needs of the ship. Fig. 4 shows the low cost retrofit ship concept model as created in the GES simulation environment.

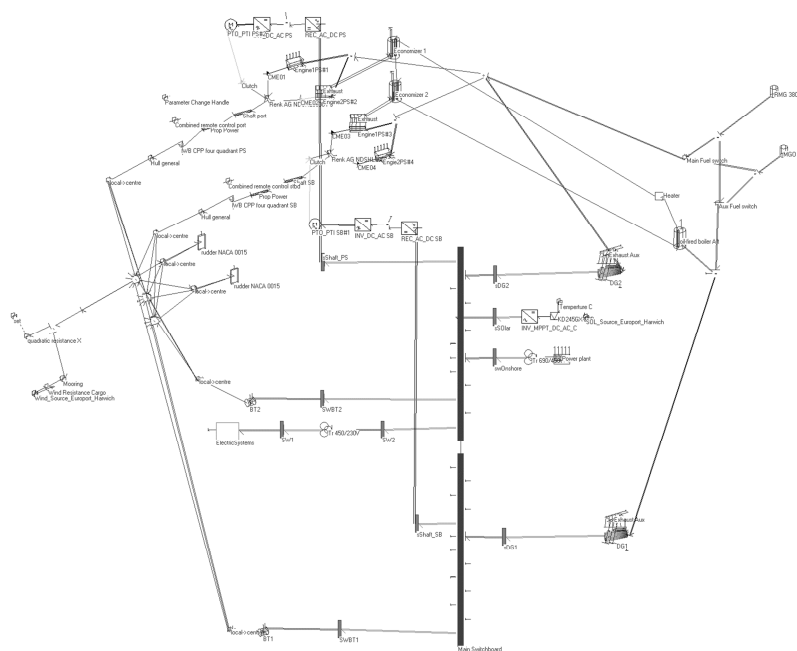


Fig. 4: The low cost retrofit ship concept model

Fig. 4 shows the only changes to the ship was the installation of a shore to ship power supply, allowing the ship to be supplied with power from the shore while it remained in port, and the installation of a bi-directional power control for the shaft generator. This second system enables the shaft generator to be operated as a motor, i.e. a power-take-in (PTI) system. When the main engines

are operated at a higher power than required to propel the ship through the water, the shaft generator runs to supply all or some of the ship's electrical power needs. However, when the ship needs additional power to sail the ship at a required speed or in adverse weather, the shaft generator can be run as a motor to provide extra power without resorting to switching on an additional diesel engine. Both the shore supply and the PTO/PTI systems were modelled in GES.

2.4.3. Low Emissions Retrofit Concept Model

The low emissions retrofit ship configuration considers the scenario where the cost of the installation is no barrier to implementation, but maximising fuel efficiency and emission reduction is. Therefore, a number of alternative energy source technologies were implemented. Fig. 5 shows the line diagram of the low emission retrofit ship concept model created in GES with the most suitable technologies being implemented.

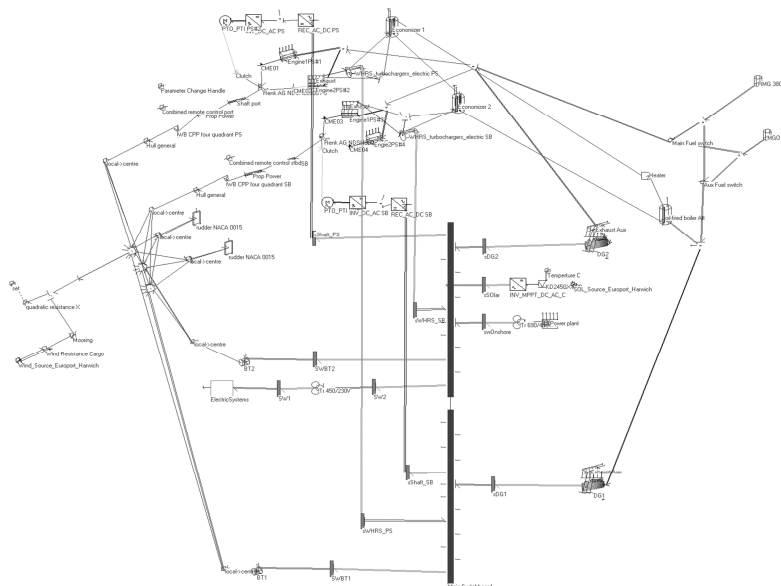


Fig. 5: Low emission retrofit ship concept model

As well as the technologies implemented in the low cost retrofit concept, i.e. shore power supply and bi-directional controller for the shaft generators, the low emission retrofit ship concept included the following technologies.

- Photovoltaic (PV) modules to convert solar energy into electric energy
 - Battery storage for peak shaving to provide additional electrical power for short periods during high or very low power demand to optimise electrical generation.
 - Waste heat recovery (WHR) electrical generation, where energy is recovered from the exhaust gas stream to power a small steam/gas turbine generator for electrical power generation.

The PV system was sized based on available usable space on the reference ship's super structure and decking, as well as available PV technology, power demands of the ship and predicted solar irradiance the ship would experience over a round trip. The model included 20 years of metrological data of solar irradiance of the North Sea and averaged to provide daily irradiance level predictions for the time of the year. In addition to the varying irradiance levels, the model also included effects for angle of incidence and shading. A peak load installation of 208kW was deemed feasible to be implemented on the reference ship in the low emission retrofit model.

A 4MW^{hr} battery system was selected as the energy storage installation and was modelled. A bi-directional power controller was modelled to enable charging and discharging of the battery installation to be simulated. The main role of the battery storage was to provide all the ship's power

for hotel, propulsion (PTI) and thruster loads when leaving port and during slow speed manoeuvres. The intention was to minimise fuel consumption and emission in and around the port area, as the main engines and diesel engines were not required for this period. During normal transit between the ports, the ship would use additional power generated from the main engine PTO, diesel generators, WHR generation and the PV to recharge the batteries, while in port the batteries would be charged using the shore supply.

Main engine exhaust gas energy is the most attractive among the waste heat sources of a ship because of the heat flow and temperature. According to Wartsila, new concept for high-efficiency waste heat recovery (WHR) allows up to 12% of main engine shaft power to be recovered as electrical power for use as additional ship propulsion power and for shipboard services. A simplified linear estimation (SLE) model was originally used to calculate the energy that could be recovered from the main engine exhaust. However, a second method using a full Rankine cycle model was created of the WHR generation system and compared to the SLE. It was found that although the SLE was found to be up to 6% less accurate than full Rankine cycle model, it was deemed acceptable as the Rankine cycle model was deemed too slow for dynamic real-time control simulation.

3. Energy Profiling and Optimisation

A key element in installation of a number of alternative energy sources with conventional power systems is their management. It is possible to have all systems running most of the time, but this will be inefficient. It is, thus, important to optimise the operation of the individual energy sub-systems relative the global needs and goals of the entire system. As part of the INOMANS²HIP project, a major objective was to develop a higher level of control, beyond those currently employed to manage ship systems today. This tertiary level or energy management system (EMS) looked at monitoring the power needs of the ship to provide an optimal energy supply given set operation conditions. In this section, the development and implementation of the EMS and the optimisation algorithms used for the management and control in a multi-source energy system is discussed.

3.1. Operational Profile of the Reference Ship

From information and data provided by the ship owner, it was possible to develop an initial operational sailing and power profile of the reference ship, which was used to develop the models and run simulations based on real operational data. Fig. 6 shows the typical power supplied by the current installed systems need to meet the ship's power demands during a typical round trip sailing from a Dutch port to one in the UK and back again over 24 h.

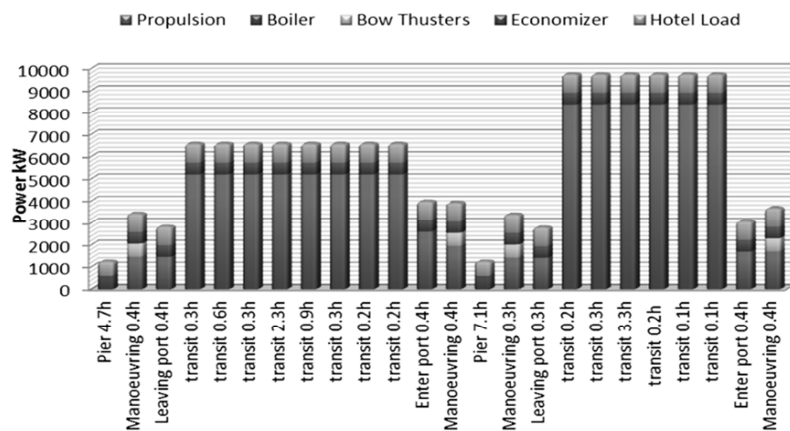


Fig. 6: Operational profile of the reference ship

The reference ship sails easterly at a transit speed of 16 kn and westerly at a speed of 14 kn, either running on 2 or 3 of the main engines depending on the sailing conditions and schedule requirements. While in transit the ship has a hotel demand of 850kWe and in port 650kWe provided by the diesels

generators. In port, one of the oil-fired boilers is on to provide 600kW of heating to the ship. During the sailing the ship relies on the economisers connected to the main engines to provide all of its heating needs. While manoeuvring, the ship required an additional 600kWe of electrical power for the bow thrusters.

3.2. Energy Management Systems (EMS) and Human Machine Interfaces (HMI)

Current industry standards revolve solely around a primary and secondary control loop. However, the INOMANS²HIP proposes a tertiary energy optimization control loop or energy management system (EMS) as shown in Fig. 7.

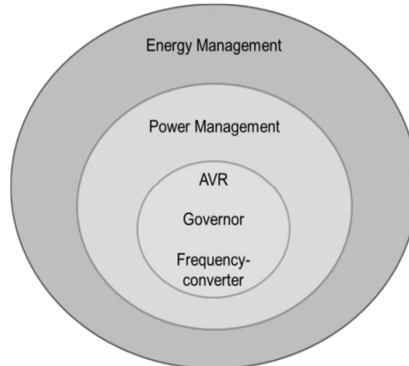


Fig. 7: Proposed cascade control architecture

A vessel purpose is defined by its mission – cargo handling, passenger transport etc. - and this is possible within an operating envelope defined by environmental conditions taken into account during vessel the design process. The on-board machinery systems are designed to cope with the expected environmental operating conditions, with designed allowable margins to cater for ageing as well as unforeseen states. The primary or AVR control loop controls voltage, speed and/or current in order to supply requested power per power source and keeps a more or less constant frequency and voltage. The on-board Power Management System's (PMS) role is to ensure that sufficient power is available at any instance in time to the on-board machinery as required for the vessel's safe operation.

The EMS takes this a step further and provides a higher level of control whose main purpose is minimisation of overall consumption, a concept which is not taken into account by the PMS. The EMS functions as a top-level controller, giving set-points to the PMS. The PMS is in turn responsible for ensuring that sufficient power is available to the machinery systems, with the possibility of overriding the EMS' set-points if necessary. The EMS can be seen therefore as an optional system which however is required in order to fully exploit the benefits of multiple sources and storage systems

As part of the EMS, a novel human machine interface (HMI) was developed to control and monitor the different energy sources and consumers. The HMI provides visual keys for easily observable indicators of the current operational states of all the energy sources and consumers, visualised by the individual icons. Further visual aids indicate the efficiency of current operational mode of individual systems and the global ship's power in reference to optimised set-points determined by the EMS for given operational modes. Three optimised operational set-points criteria could be chosen, either to optimise fuel consumption, minimise emissions or minimise delays. Monitoring individual power levels and alarms, changes in colour, brightness and size of circles around individual systems indicates a problem which needs further investigation by the operator. Detailed real-time operational data and state of operation for individual systems can be accessed by clicking on individual icons or the larger supply and demand circles for an overview. Fig. 8 shows a representation of the HMI developed for the EMS.

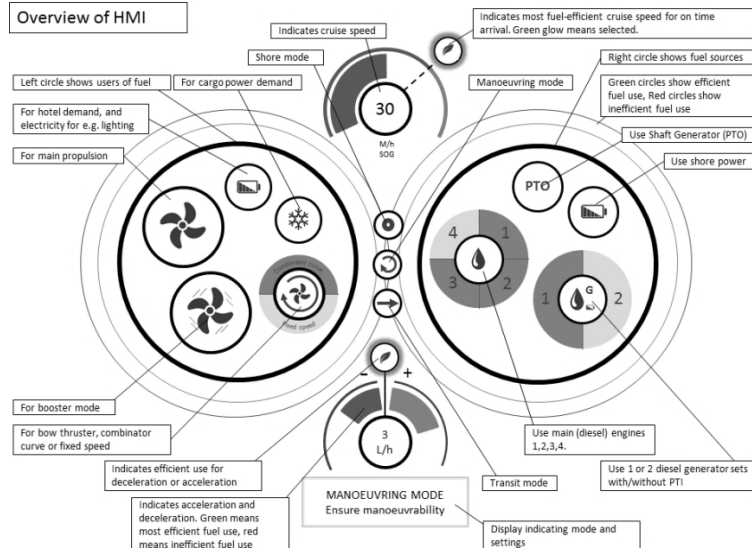


Fig.8: Representation of the EMS control HMI

In addition to the EMS control HMI, the project also developed a propulsion control HMI that allowed real-time interaction with the GES ship models. The propulsion HMI developed by Wärtsilä provides interactive control of the main engines, CPP angle, bow thrusters and rubber. The propulsion HMI developed used the same basic principles of the EMS control HMI, to use simplified visualisation of necessary information, slimming down the traditional displays of current ships. Again, a visualisation of the ship's efficiency and operation modes is used to quickly and easily indicate current operational state, simplifying data transfer and interpretation.

3.3. Energy Optimisation

A key element of the EMS is using it to determine optimised the set-points for the individual energy source, conventional and alternative, to achieve the global goal of minimising fuel consumption. Two methods of optimisation were developed, the Simplex method which is imbedded within the GES simulation environment and Particle Swarm Optimisation (PSO) developed as a standalone algorithm in Matlab.

The previous control loops are considered to be essential for ship operation, whereas the EMS control loop is considered as non-essential. The optimising control loop functions in the domain of minutes, hours, days, months, etc. whereas the primary and power management control loops function in the domain of milliseconds and seconds. For both presented optimising methods, the following generic block scheme applies.

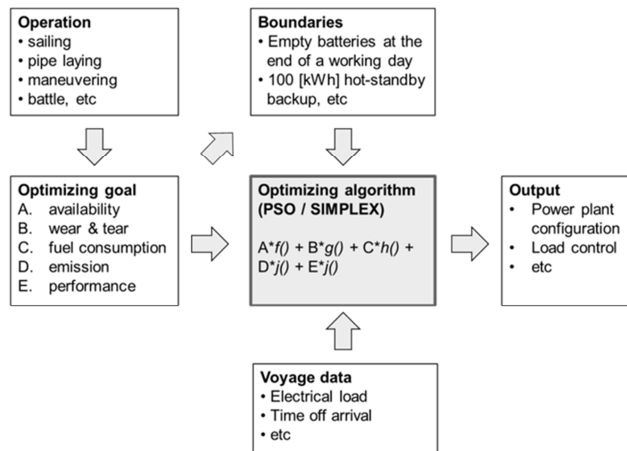


Fig. 9: Optimising algorithm generic block scheme

Operation, e.g. transportation of cargo demands, an optimising goal of fuel saving with boundary conditions, such as time of arrival. Together with actual voyage data, a power plant control output can be determined. The optimising goal will be primarily fuel saving, which implicitly relates to reduction of CO₂ emissions. The two methods used for optimisation were the Simplex method, implemented by TNO in GES, and the PSO method, implemented by UNEW in Matlab/Simulink.

3.3.1. Simplex Method of Optimisation

The Simplex method, which is available within the GES simulation tool and used to optimise the energy exchanges management system. The Simplex method is in practice, a quite robust multidimensional optimisation method. For the INOMANS²HIP project, the results are also compared with the PSO method to check the optimal results of both methods.

The simplex method calculates likelihoods at simplex vertices. For an n-dimensional optimisation method, a geometric shape is set up with n+1 corners. The method moves towards a minimum away from a maximum. Fig. 10 shows a two-dimensional problem with a highest (worst) point x₀ a next highest point x₁ and a lowest optimised point x₂. The idea is to move away from the higher point to the lower point by reflection, reflection and expansion, and contraction or even multiple contraction.

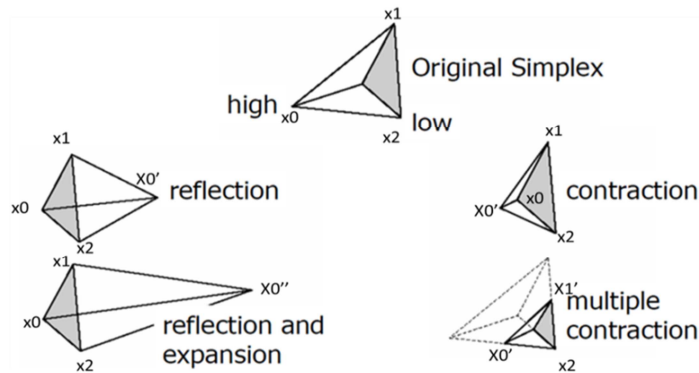


Fig.10: Summary of the Simplex method

In the case of creating an optimisation algorithm for the EMS, for every vertex the total efficiency of one particular operation is calculated, depending on some control parameters (n dimensional) of the vessel. The total efficiency of a vessel for one operation is a nice mineralisation function because the optimum efficiency lies always between 0-100% and is independent of the configuration of the installation and can be used for every system. The total efficiency is defined as:

$$\text{system efficiency} = \frac{\sum_{i=1}^{i=nc} \text{Power consumers}_i}{\sum_{j=1}^{j=nf} \text{Fuel power}_j}$$

The “Power consumers” are for instance: Power ship resistance, Hotel load, Pumps, etc. So all the power consumers that are needed to fulfil an operation. The “Fuel power” is the thermodynamic power of the fuel that is used for the operation. Part load efficiency of the engine is automatically taken into account.

External power deliverables like: Solar panels, offshore power, has a positive influence on the total system efficiency, because they reduce the fuel consumption. Internal power deliverables like: WHRS, Economisers, also have an automatic positive influence on the total system efficiency because they reduce the fuel power.

The algorithm minimized the function:

$$(1 - \text{system efficiency}(p_1, \dots, p_n))$$

Where $p1, \dots, pn$ are the set-points of the equipment for a specific operation.

So to have the lowest fuel consumption of the installation all the equipment do not need to run in the best efficiency point. If equipment is not running in the best efficiency point, parts of the installation can be improved.

The application of the simplex method is a standard tool in GES simulation environment. The optimisation function is the total efficiency of the model that is dependent on the control parameters. The constraints are handled in the GES components, by penalising the fuel consumption of components violating their constraints. This forces the algorithm to move towards a better minimum, which does not violate the constraints parameters. Normally, the parameter variations of the simplex method are continuous. For the power set-points, a switch level is incorporated in the switch components. A threshold level of >0.3 for switch ON is used for this method. Three operational modes are taken into account for the vessel operation: port, transit and manoeuvring. An overview of the control strategy is shown in Fig. 11.

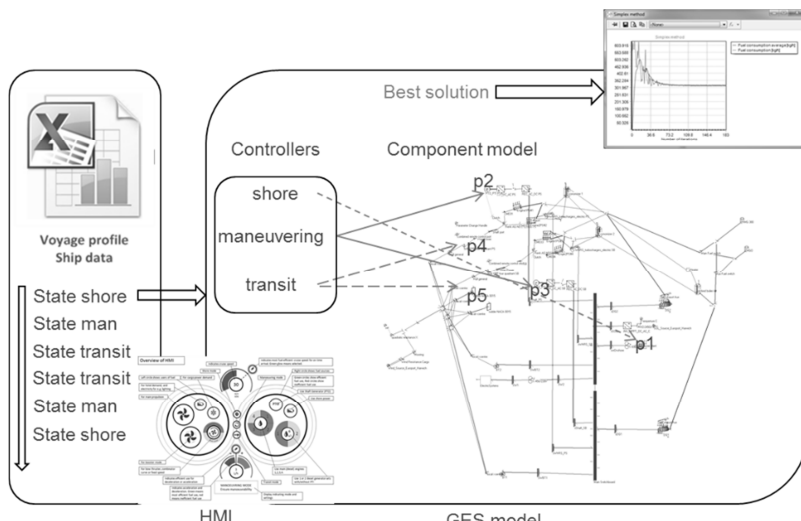


Fig. 11: EMS controller with HMI

In this model, control parameters are defined: $p1, pi, pn$ depending on the configuration. The controller is a module containing specific Simplex controllers for port, transit and manoeuvring modes. Depending on the mode, not all the parameters have to be controlled. For the port mode only $p1$ is controlled and pi, pn are fixed, related to the specific port mode. For Manoeuvring and Transit other parameter combinations are needed. In the component model the total fuel consumption $f(p1, pi, pn)$ as function of the control parameters $p1, pi, pn$ is calculated. The results are optimised by the controller for each the specific operational modes of the ship.

In this method, the user can manually select the controller mode and/or the mode can be selected automatically by the operational profile of the ship at a specific time, which is incorporated in the Excel data of the reference ship. A special Macro in the Excel file is available to enable this concept to run. A call to the simplex method in GES follows the following coding structure, Simplex ($f(), p1, pi, \dots, pn$). The controller module is more complex, because all the parameters and pre-defined variables need to be described.

3.3.2. Particle Swarm Optimisation Algorithm

Swarm intelligence considers the collective interactions and knowledge of a population of members which are individually ‘dumb’ but collectively smart. A swarm of birds (or shoal of fish) operate as a concerted entity, by sharing of each individual’s knowledge such that overall, the whole swarm

benefits. An example of swarm behaviour is illustrated when a flock of birds is searching for food. Once a member of the flock identifies a potential food source, the flock collectively drifts towards this new ‘goal’.

This can be considered as an optimisation function, whereby the location of the food is the optimisation goal. PSO traces its origins to the seminal work in *Kennedy and Eberhart, 1995* by considering the social behaviour of a flock of birds and applying this biologically inspired computer algorithm to optimisation or search problems. In the application of PSO, the term swarm is used to describe the collection of individual agents, who are in turn termed the particles (analogy with flock and birds, or shoal and fish), as illustrated in Fig.12.

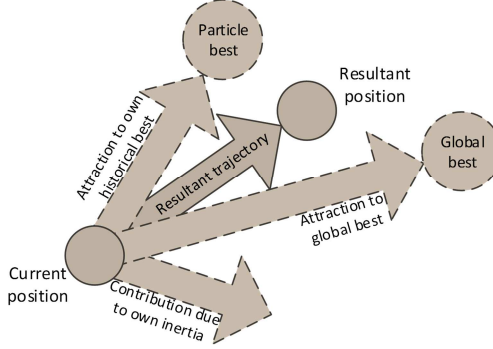


Fig. 12: Representation of PSO

PSO is a black-box search algorithm, where only the variables and in turn the result of the computation are exchanged between the optimisation algorithm and the objective function (GES model). This makes the search algorithm non-system specific and hence permits easy application to different cases. In this work a single-objective PSO algorithm was developed to identify the optimal configuration based on the returned fuel consumption from the GES model. The algorithm is a hybrid PSO, operating on discrete variables (main engines on/off) as well as continuous variables (battery set-points).

Fig. 13 summarizes the application of the PSO algorithm to the on-board energy optimization scheme proposed in INOMANS²HIP. The PSO is the optimization algorithm at the centre, coded in Matlab. The GES models outlined in the previous deliverables are the objective functions, which return the fuel consumption as the fitness value. Constraints are also handled within the GES models, with violations of any constraints passed to Matlab as warning flags. These constraints are operational constraints, especially on the machinery systems. The algorithm then returns the optimal system configuration in terms of power set-points, as well as on/off selection of machinery.

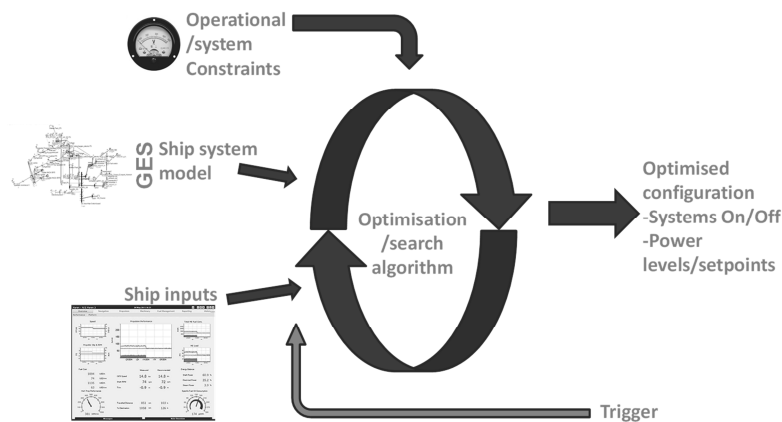


Fig. 13: Overview of generic EMS setup

The algorithm was triggered at predetermined times through the voyage waking as inputs the ship's particular condition at that time, namely speed, auxiliary load, solar irradiance and wind direction and speed. Once the algorithm is completed, the vessel's configuration was updated accordingly. Of course, it was not expected that the actual profile will be fixed in between update periods, but the power control will control the power share between these periods, prior to the energy control updating the configuration for optimal generation.

The basic premise of the optimisation at each step was to minimise the total fuel consumption. However, this does not take into account the wider operational constraints of the vessel's operation. As an example, each engine will return the same fuel consumption value, hence there is no discriminant and due to the stochastic nature of the optimisation, at each optimisation step, the optimal configuration could be one with a different engine selected each time, but which still returns the same fuel consumption. Hence the basic algorithm was modified to include a penalty function, which looks at the previous configuration and calculates the Hamming distance (number of discrete bit changes) to the new particle location. A penalty is then applied to the returned fuel consumption figure, ranging from 0% if the configuration is the same, to a 20% penalty if the total configuration is different. This reinforces the algorithm to preferentially select a configuration, which is similar to the previously operating setup as much as possible, avoiding frequent turning on and off of diesel engines.

With the objective being the reduction of fuel consumption, the provision of power from clean sources other than the diesel engines will be preferred since this will result in reduced fuel usage. By assuming that the batteries are of zero cost, the discharge will be maximised in order to reduce the fuel cost as much as possible. While correct from an optimisation point of view, this does not present a true picture of the cost of battery power. By maximising discharge simply because the state of charge permits it, the potential for prospective (better) savings at a later point of the voyage is lost.

The model was therefore modified to assign a cost to the energy stored as a function of the source used to charge the battery. This takes the form of an accumulator whose value is given by the amount of charge put into the battery together with the amount of fuel used to supply this energy, leading to an equivalent specific fuel consumption (eSFC) figure in g/kWh. The battery is assumed to maintain the constant charge rate for the duration of the waypoint, such that the state of charge at the end of the waypoint can be estimated by linear interpolation.

4. Implementation and Results

The project implemented all the elements developed, i.e. ship models, EMS control HMI, propulsion HMI and optimisation algorithms, into a demonstrator. The demonstrator, a mixture of model simulation and interactive hardware, illustrated to possible operational benefits of developing a multi-source energy strategy on-board the reference ship, as well the realisation of implementing the tertiary EMS control level.

4.1. Results of Simplex Method

In the first stage of optimisation, the Simplex method was used to optimise the original reference ship configuration without the implementation of any alternative energy sources. Optimising the operation of the main and auxiliary engines installations returned about a 2% fuel saving (~33.8 tons/trip). This would be used as a baseline to compare the new concepts of ship being proposed with the alternative energy sources being implemented and optimised using the Simplex method.

The low cost configuration with only PTO/PTI being implemented uses 1.15% less fuel in comparison with the reference vessel (33.43tons/trip). However, if the low cost ship concept with both the PTO/PTI and shore supply being implemented, the fuel consumption when compared to the reference ship is reduced to 32.14 tons/trip, representing a 4.91% saving.

For the low emission concept is the design point of the WHR generation changed to find the best performance. From the energy balance calculation, the best configuration is the low emission configuration with the economisers connected to the main engine exhaust after the WHRS. The difference lies between the 9.1% (30.7tons/trip) and 9.9% (30.35tons/trip), with and without batteries respectively in comparison with the reference cargo vessel.

4.2. Results of PSO Algorithm

Firstly, the PSO algorithm was used to optimise the operation of the conventional reference ship. This produced a similar result as the Simplex method, returning around a 2% fuel saving just by optimising the operation of the conventional power systems.

For the low cost ship concept model the PSO algorithm reduce the fuel consumption of the ship through the implementation of PTO/PTI system and shore power supply by 5.86%. However, if we apply a knowledge of prior events to the PSO, which a deemed a more robust method, the fuel saving is reduced by 1.79tons/trip or 5.31% fuel saving. By applying the PSO method with history to include penalties for results beyond boundary limits, the result is more realistic and robust.

In the case of the low emission ship concept model where battery storage, WHR generation, PV shore supply and PTO/PTI were implemented, the application of the EMS with PSO algorithm produced a 11.11% fuel saving. However, this results represents a basic PSO application without historical information. If historical information is used to influence events then the fuel saving is 11.63%, which represents a fuel consumption reduction of 3.93tons/trip. Fig.14 summarises the results of the simulated voyage using the PSO EMS.

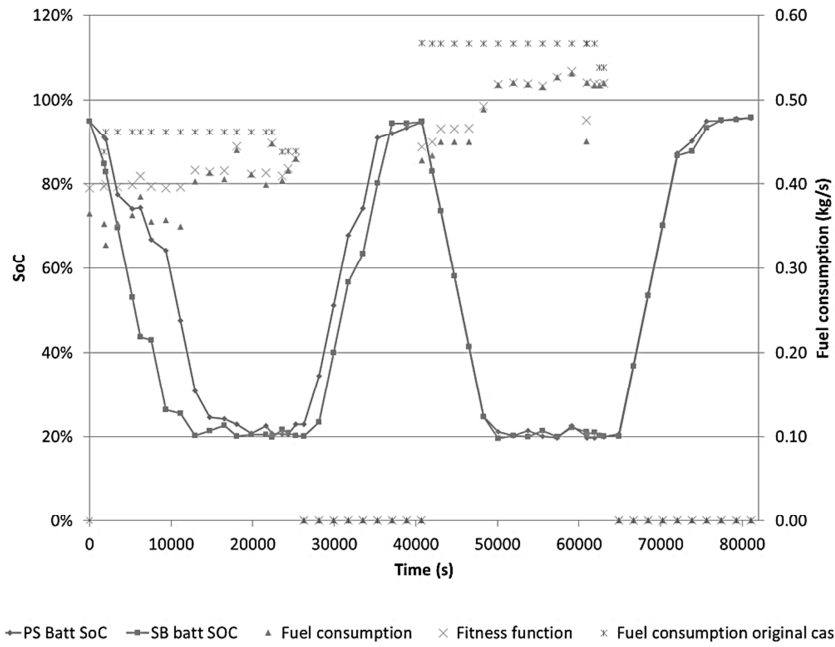


Fig. 14: Resultant profiles for voyage with machinery configuration including battery storage

5. Conclusions

This paper presented an investigation through modelling into the possible benefits for the application of alternative energy sources on-board a cargo ship. Although not all state-of-the-art energy technologies are applicable, significant fuel efficiency can be achieved through the selection of suitable technologies.

Also presented is a method for global optimised control of multi-source energy systems. This tertiary EMS control system with visualised HMI, provides a method for determining the best set-points a

combined multi-source energy network given certain operational conditions and performance requirements, i.e. optimised global fuel consumption or reduced emissions. Two methods of optimised, namely the Simplex method and PSO algorithm, were developed and implemented in the EMS to optimise fuel efficiency within each of the models, i.e. reference ship, low cost concept and low emission concept. The results were compared to determine the best options in terms of fuel consumption and therefore, emissions for future consideration and possible implementation by the marine industry.

Table I shows a summary of results from the INOMANS²HIP investigation into the use and optimised control in the application of alternative energy sources on-board a Ro/Ro cargo ship.

Table I: Summary of Results

Concept	Technologies	Impact
Low Cost without Optimisation	PTO/PTI and shore power supply	2% fuel saving
Low Cost with Simplex Method	PTO/PTI and shore power supply	4.91% fuel saving
Low Cost with PSO	PTO/PTI and shore power supply	5.31% fuel saving
Low Emissions without optimisation	PTO/PTI, shore power supply, PV, WHR generation and battery storage	5% fuel saving
Low Emissions with Simplex method	PTO/PTI, shore power supply, PV, WHR generation and battery storage	9.9% fuel saving
Low Emissions with PSO	PTO/PTI, shore power supply, PV, WHR generation and battery storage	11.63% fuel saving

From the results it is clear that there is a slight variation of the results produced by the Simplex method and PSO algorithms applied. This is thought to be due to their individual preference. The Simplex method is more inclined to prefer optimisation of individual systems rather than the global system, while the PSO algorithm prefers global optimisation at the expense of individual systems. Other influences affecting the result can be generally attributed to the specific application of each optimisation method, with slight variations in defining the boundaries and penalties applied in both cases.

References

- IMO (2009), *Second IMO GHG Study*, International Maritime Organisation, London
- KENNEDY, J.; EBERHART, R. (1995), *Particle swarm optimization*, IEEE Int. Conf. on Neural Network, pp.1942–1948
- MARISEC (2011), *Shipping Facts*, Int. Chamber of Shipping & Int. Shipping Federation (ICS), <http://www.marisec.org/shippingfacts/home/>
- MEECH, R. (2008), *Emissions from ships: Dealing with a new environment*, Environmental Workshop

Parametric Shape Modeler for Hulls and Appendages

Elisa Berrini, Inria / MyCFD, Sophia-Antipolis/France, elisa.berrini@inria.fr

Bernard Mourrain, Inria, Sophia-Antipolis/France, bernard.mourrain@inria.fr

Yann Roux, MyCFD, Sophia-Antipolis/France, yann@mycfd.com

Guillaume Fontaine, K-Epsilon, Sophia-Antipolis/France, guillaume@k-epsilon.com

Eric Jean, Profils, Marseille/France, contact@eric-jean.com

Abstract

This paper describes a parametric shape modeler tool for deforming hulls and appendages, with the purpose of being integrated into an automatic shape optimization loop with a CFD solver. The modeler allows generating shapes by controlling the parameters of a twofold parameterization: geometrical – based on a skeleton approach – and architectural – based on the design practice and effects on the object's performance. The resulting forms are relevant and valid thanks to a smoothing term to ensure shape consistency control. Thanks to this approach, architects can directly use a NURBS CAD model in the modeler tool and will obtain variations of the initial design to improve performance without additional work. The methodology developed can be applied to any shape that can be described by a skeleton, e.g. hulls, foils, bulbous bows, but also wind turbines, airships, etc. The skeleton consists of a set of B-Spline curves composed of a generating curve and section curves. The deformation of the shape is performed by changing explicit parameters of the representation or implicit parameters such as architectural parameters. The new shape is obtained by minimizing a distance function between the current parameters and the target's in combination with a smoothing term to assure shape consistency control. Finally, the 3D surface wrapping the skeleton is rebuilt using surface network technics. This paper presents the general methodology and an example of application to a bulbous bow on a fishing trawler, with RANSE CFD computations to determine the best design.

1. Introduction

Automatic shape optimization is a growing field of study, with applications in various industrial sectors. As the performances of a flow-exposed object can be obtained accurately with CFD (Computational Fluid Dynamics), small changes in design can be captured and analysed. To exploit these performance analysis capabilities, it is important to have a precise and efficient control of the geometry of the objects. The results of the modelling/analysis process rely on two main ingredients. To evaluate with accuracy the hydrodynamic properties of a hull, accurate flow solvers are required. Free surface needs to be captured precisely, as well as turbulent flow phenomena. Reynolds-averaged Navier-Stokes (RANS) solvers, completed with a powerful grid generator, are well adapted to capture accurately the flow around complex objects.

To improve the form of a hull in order to increase its performances, a precise shape consistency control is essential when performing deformations. Naval architects need to use shape quality preserving tools to modify hulls avoiding non-realistic forms.

The coupling of an accurate flow solver and a quality preserving shape modeler is the basis for an efficient automatic shape optimization loop. An optimisation algorithm can optionally complete the loop to determine automatically new shape parameter values according to the CFD results.

We propose a parametric shape modeler tool for deforming objects, with the purpose of being integrated into an automatic shape optimization loop with a CFD solver. Our tool has the ability to generate valid forms from an architectural point of view thanks to an innovative shape consistency control based on architectural parameters. A skeleton composed of a generating curve and a family of section curves represents the object. The generalizable concept of skeleton-based approach allows us to apply our tool to a large selection of shapes e.g. hulls, foils, bulbous bows, propellers, wind turbines, airships, etc.

In this paper we present an application to the bulbous bow of a fishing trawler ship. The aim is to reduce the total drag of the hull thanks to bulb form variations. With the parametric modeler, we create a set of shapes exploring the parameters domain and use RANSE CFD computations to determine the best design.

2. Related work

Optimising the shape of the bulbous bow has been seen as an efficient way to reduce the drag of a hull, and thus the costs of exploitation of the ship, since several years. The coupling of a flow solver to a modeler and an optimisation algorithm is a widely used methodology. Some of the previous work can be seen in *Valdenazzi (2003)*, *Hochkirch (2009)*, *Blanchard (2013)*. Shape deformation for ships is a relatively recent approach. However, deformation techniques have been wildly developed in other application fields, such as 3D animations or movies.

Free Form Deformation (FFD) and morphing are classical methods created for 3D animations purposes, and they have been applied to shape optimization for ships. Morphing generates shapes interpolated from two extremal ones. Such a methodology allows to explore a precise panel of shapes if the architect has a clear idea of the extremal values. FFD consist in enclosing the object within a simpler hull, usually a cube as described by *Sederberg (1986)*, then the object is transformed when the hull is modified. FFD is applied to ship hulls by *Kang (2012)*, *Peri (2013)*. FFD and morphing are usually applied to meshes and not a continuous geometry in a naval context, thus limiting deformation because the meshes can be subject to degeneration. FFD method can be very efficient with a small number of degrees of freedom to control the whole shape of the object. However, in order to perform local deformations, the only way is to increase the number of control points by refining the areas of interest. Moreover, FFD does not take into account any architectural parameters when deforming an object, leading possibly to non-realistic results.

Engineering dedicated CAD software recently provides parametric design features, allowing the user to build parametrized models such as CatiaTM or GrasshopperTM for Rhinoceros 3DTM. When these parameters are modified, the corresponding elements of the object are modified. Thanks to the relationship between elements, the deformation propagates throughout the whole model.

Specific software has been developed during the last decades for ship applications. One of the most widespread is CAESESTM from Friendship Systems, allowing the user to create geometries using advanced parameters that can be modified easily by hand or automatically with a CFD optimization loop as described by *Papanikolaou et al. (2011)*. Similarly, a ship dedicated tool Bataos, used by *Jacquin (2003)*, allows modifying the shape of sections of the hull by multiplying or adding predefined functions to the control points the B-Spline curve describing the section.

The aim of our tool is to be used without any human interaction once an original geometric model is available, independently of the way it is built and of its quality.

3. Parametric modeler

To obtain smoothly deformed shapes, we propose a new modeler tool based on a generic methodology, allowing us to describe a large panel of objects in the same way. We parameterize shape with a generic skeleton concept, completed by specific architectural parameters according to the studied shape.

3.1. Shape parameterization

3.1.1. Geometrical parametrisation

The skeleton consists of a set of B-Spline curves composed of generating curve and section curves. The purpose of the generating curve is to describe the general shape of the object. The sections are

similar to the classic architect's line plan, describing more precisely the outlines of the object around the generating curve. Once the generating curve is identified on the CAD model, sections are computed as intersections between the studied object and a family of planes along the generating curve. A fitting process is used, inspired by *Wang (2000)*, to create the B-Spline curves that approximate the intersection curves.

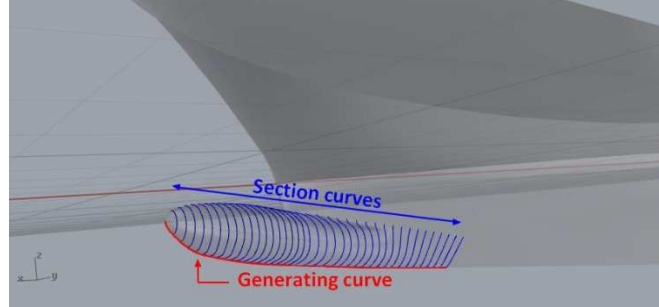


Fig. 1: Skeleton of a bulbous bow

3.1.2. Architectural parameters

We define a set of architectural parameters on the studied object according to the design practice and effects on the object performance. The strategy of our modeler is to control the whole shape through these parameters. Both generating curve and section curves have an independent set of parameters, as illustrated in Fig. 2 and 3. In this example the length, the angle, the height and width are relevant parameters to control the shape of a bulbous bow. Our model allows enriching the parameter set with new kinds of parameters, such as the value of sectional areas included for each section.

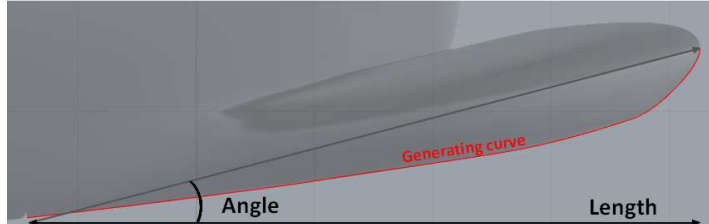


Fig. 2: Generating curve parameters

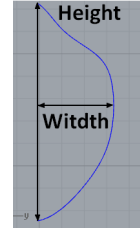


Fig. 3: Section parameters

We introduce an observer function ϕ that computes the set of parameters P on a given geometry G : $\phi: G \rightarrow P$. For the generating curve the parameters are real and finite values whereas sections describe parameters as a function along the generating curve, thus defining ϕ in an infinite dimensional space. In order to reduce the dimension of ϕ we represent the functions of parameters with B-Spline curves with a small number of control points.

3.2. Shape deformation

In our methodology, deforming an object corresponds to finding a new geometry G that matches a given set of architectural parameters P . Referring to the definition of the observer function ϕ , to deform a shape we need to compute $\phi^{-1}: P \rightarrow G$. Starting from the B-Spline description of the object's skeleton, we propose to compute new values of the coordinates of the curve control points c_i until the current parameters matches the target one, for the generating curve and the section curves independently. This problem can be defined as a non-linear constrained optimization problem, the control point coordinates being the solution of a specific minimization system.

The minimisation system is built with four terms:

1. The first term E_{param} measures the distance of the current parameters values to the target ones.

2. The second term E_{shape} is introduced to ensure consistency control by measuring the distance of the current generating or section curve to the original one.
3. The third term allows taking into account specific constraints F for the studied object, usually position or tangency constraints. These constraints are defined for each section and are not necessarily the same for all sections. For a bulbous bow, as we use a half hull, we have to ensure that the section curves end in a plane (here $Y = 0$) and that the tangent at the extremity along the vessel centerline are preserved.
4. The last term controls the overall smoothness of the shape by introducing stiffness between successive control points. It consists in correction terms M_l to control respectively \mathcal{C}^1 and \mathcal{C}^2 properties of control points.

The definition of the problem is well adapted to Sequential Quadratic Programming (SQP). SQP algorithm uses Newton's method to find roots of the gradient. We start with the original curve as the starting point of the algorithm, then we decrease the shape consistency term and the smoothing control term at each iteration and start the SQP again with the last computed curve. The algorithm stops when the value of the objective function reaches a fixed threshold.

3.3. Surface reconstruction

The optimization method outputs deformed sections and generating curves, corresponding to the skeleton of a new shape. To evaluate the shape performances with a CFD solver, we first need to reconstruct the 3D surface wrapping the deformed skeleton. Moreover, building a new surface allows to obtain a cleaned-up model for the meshing tool.

For complex objects, multi-patch surfaces are required. In such cases, a particular attention has to be given to the continuity between them: for our application, patches have to be at least \mathcal{C}^1 . We chose to focus on Surface Network technique, described by *Piegl* (1997), which ensures the continuity between adjacent surfaces by building the curve grids with specific tangency constraints on the boundary. Fig. 4 shows the computed grid.

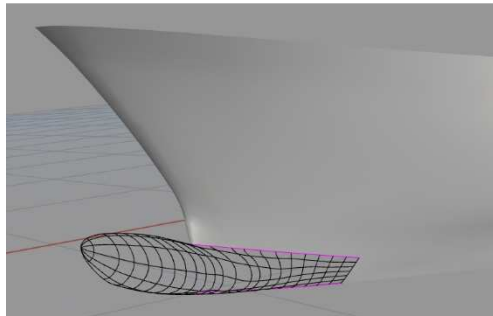


Fig. 4: Skeleton for surface reconstruction

4. Numerical methods

4.1. Mesh generation

To generate non-conformal full hexahedral unstructured meshes on complex arbitrary geometries, we use HEXPRESS™ from Numeca International. In addition, the advanced smoothing capability provides high-quality boundary layers insertion, *Wackers* (2012). The software HEXPRESS™ creates a closed water-tight triangularized volume, embedding the ship hull; then a body-fitted computational grid is built.

One of the meshes used in our simulations is shown in Fig. 5 and 6. The grid generation process requires clean and closed geometries to provide robust meshes. Thanks to the shape consistency

control and the smooth reconstruction of surfaces, the modeler generates shapes which are well-adapted to these requirements and which allows to produce high-quality meshes for computations. During the computation, the automatic mesh refinement has been used. Automatic, adaptive mesh refinement is a technique for optimising the grid in the simulation, by adapting the grid to the flow as it develops during the simulation to increase the precision locally. This is done by locally dividing cells into smaller cells, or if necessary, by merging small cells back into larger cells in order to undo earlier refinement. During the computation, the number of cells increases from 1.9 to approximatively 2.2 million cells, for a half hull mesh. Fig. 5 shows a view of the whole grid, Fig. 6 the mesh refinement around the hull and the free surface at the end of the computation.

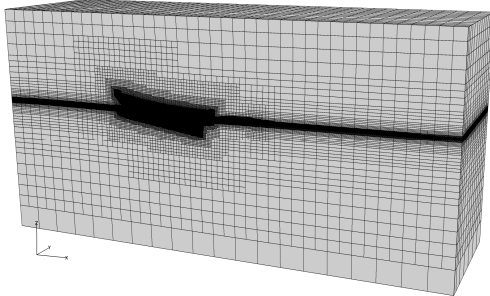


Fig. 5 : General view of the mesh and the computational domain

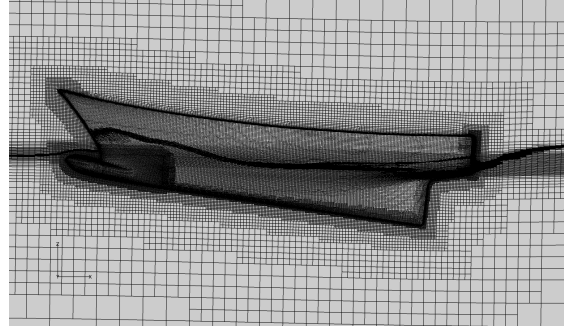


Fig. 6: Mesh around the hull

4.2. Flow solver

ISIS-CFD, available as a part of the FINE™/Marine computing suite, is an incompressible, unsteady Reynolds-averaged Navier-Stokes (RANS) solver. For the turbulent flow, additional transport equations for the modeled variables are discretized and solved. The two-equation $k-\omega$ SST linear eddy-viscosity model of Menter is used for turbulence modeling. The solver is based on the finite volume method to build the spatial discretisation of the transport equations. The unstructured discretisation is face-based, which means that cells with an arbitrary number of arbitrarily shaped faces are accepted. This makes the solver ideal for adaptive grid refinement, as it can perform computations on locally refined grids without any modification.

Free-surface flow is simulated with a multi-phase flow approach: the water surface is captured with a conservation equation for the volume fraction of water, discretised with specific compressive discretisation schemes, *Queutey (2007)*. The vessels dynamic trim and sinkage are resolved during the simulation. Fig. 7 illustrates the surface elevation in one of our test cases.

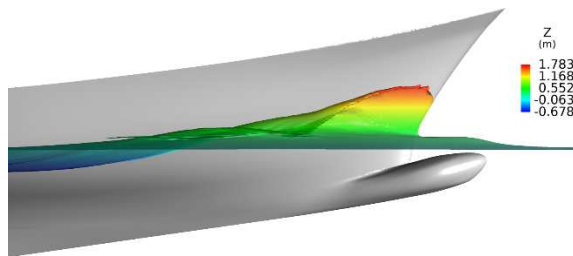


Fig. 7: Free surface elevation

5. Application on bulbous bow deformation

We aim to reduce the total drag of a fishing trawler ship thanks to variations of its bulbous bow shape. Starting from a first geometry of the hull with a bulbous bow, Fig. 8, we generate a set of shape variations with the parametric modeler. Then the total drag of each shape is computed with ISIS-CFD.

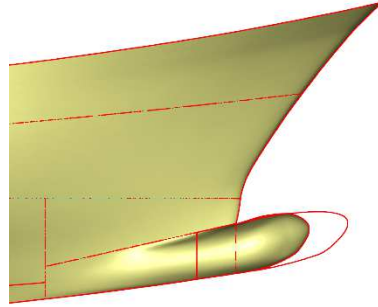


Fig. 8 : Initial hull (yellow) vs. a bulbous bow shape variation (red)

We use this initial set of data to build a Design of Experiments (DOE) on which we will apply a response surface methodology, as explained by *Jones (2011)*, to explore new design possibilities. The DOE can be seen as a database of objective function values, here the total drag of the hull, associated to design parameter values, which are the architectural parameters used in the modeler. The response surface methodology then allows us to compute an estimate value of the objective function for any parameters included in the database bounds. To sample the design parameter values of the database, we use a Latin Hypercube distribution *Iman (1981)*.

We describe the construction of the Latin Hypercube in the following section, then we present the corresponding results computed with ISIS-CFD.

5.1. Deformations of the bulbous bow

We chose three parameters to control the bulb shape: the length and angle of the generating curve (Fig. 2) and the width of the sections (Fig. 3). Deformations are parameterized as percentages of the initial parameters values. We describe the limits of the exploration domain in Table I.

Table I: Limits of parameters domain

	Length	Angle	Width
Initial value	1.61 m	31.52°	0.83 m (value at mid-bow)
Min variation	15% (=1.86m)	-25% (=23.64°)	-20% (=0.66 m)
Max variation	90% (=3.07m)	0% (=31.52°)	20% (=0.99 m)

The initial bulb being quite short, we assumed that shapes with a lower length than 1.86m will not positively influence the drag, likewise we restricted the bulb to not be longer than the extremity of the upper bow. For the angle, we noticed that when the length of the bow is increased, keeping the original value will cause the bulb to pierce the free surface, again this configuration is unwanted. From the bounds described in Table I, intermediary values are computed with a Latin Hypercube method. We illustrate in Fig. 8 the initial hull (yellow) with a one of the variation (red) included in the Latin Hypercube (Length: +42.86% ; Angle: -23.08% ; Width: +0.0%).

5.2. RANS CFD results

The studied trawler ship has a length at waterline of 22.35 m and a displacement of 150 t. Simulations are done at a speed of 13 knots (6.688m/s). Trim and sinkage are solved, while the hull speed is imposed according to a ¼ sinusoidal ramp law. Fluid characteristics are the following:

	ρ (kg/m ³)	μ (Pa.s)
Water	1026.02	0.00122
Air	1.2	$1.819 * 10^{-5}$

We present in Table II the results obtained from the Latin Hypercube distribution. Table II represents the Design of Experiments used for the response surface methodology.

Table II: Drag results for the different bulbous bow shapes

#	Length variation (%)	Angle variation (%)	Width variation (%)	Total Drag (N)	Pressure drag (N)	Viscous drag (N)	% reduction in total drag from original hull
0	0.0000	0.0000	0.0000	73740	63853	9887	0%
1	0.4286	-0.2308	0.0000	71760	61848	9912	2.69%
2	0.8571	0.0000	0.0000	72120	62196	9924	2.20%
3	0.4670	-0.2180	0.084	71428	61451	9977	3.13%
4	0.5069	-0.1821	-0.1786	72441	62508	9933	1.76%
5	0.1944	-0.1026	-0.0467	73015	63186	9829	0.98%
6	0.5349	-0.1252	-0.1364	72479	62490	9989	1.71%
7	0.3807	-0.0861	-0.106	71440	61453	9987	3.12%
8	0.1704	-0.1688	0.164	72603	62701	9902	1.54%
9	0.2693	-0.2262	0.0445	72027	62142	9885	2.32%
10	0.3464	-0.1091	-0.0289	72266	62414	9853	2.00%
11	0.6319	-0.0887	0.1853	71676	61513	10163	2.80%
12	0.6717	-0.1514	-0.1711	72312	62261	10051	1.94%
13	0.2381	-0.1368	0.0324	72037	62200	9837	2.31%
14	0.6777	-0.1411	-0.0069	71634	61588	10046	2.86%
15	0.5870	-0.1981	0.0999	71054	60971	10083	3.64%
16	0.3110	-0.1717	0.1365	71660	61714	9946	2.82%
17	0.4391	-0.2095	-0.0818	72380	62484	9896	1.84%

We illustrate the surface elevation of the best results (#3, #7 and #15) in Fig. 9 to 11.

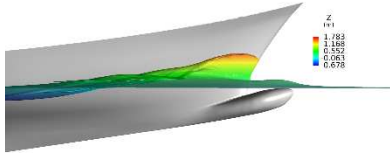


Fig. 9: Free surface elevation for case #3

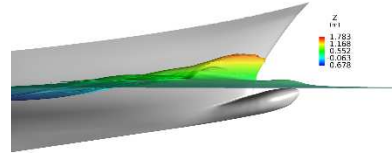


Fig. 10: Free surface elevation for case #7

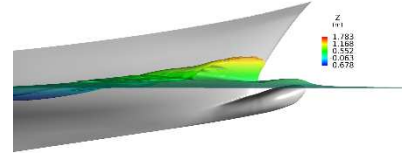


Fig. 11: Free surface elevation for case #15

The response surface can be used as a surrogate model on which we can solve an optimization problem: we can find its minima using a genetic algorithm. Those minima give the parameter values that potentially improve the objective function values, here the total drag of the hull.

We identify one of the minimum though a genetic algorithm corresponding to the following parameters values: Length: +60.3%; Angle: +0%; Width: +9.36%. The response surface predicted a drag of 71019.58 N. We performed a new ISIS-CFD computation with a geometry corresponding to the new parameters values and we obtained a real total drag value of 71553.21 N, representing 2.97 % of drag reduction from the original bulbous bow. To obtain better results, two strategies have to be developed: first the response surface has to be enriched by new values in order to represent more accurately the real distribution of drag according to the parameters. Then more advanced methods to find the point of maximum interest in the response surface can be used. For example, algorithms based on Kriging such as Efficient Global Optimization find minima on a surrogate models by maximizing the probability of improvement of the objective function as shown in *Jones (1998)* and *Duvigneau (2012)*.

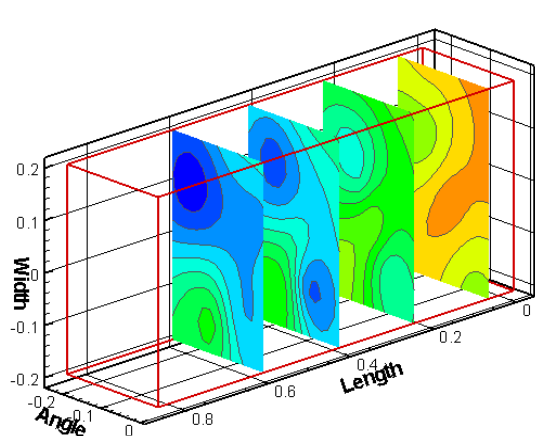


Fig. 12 : Cut planes of the response surface

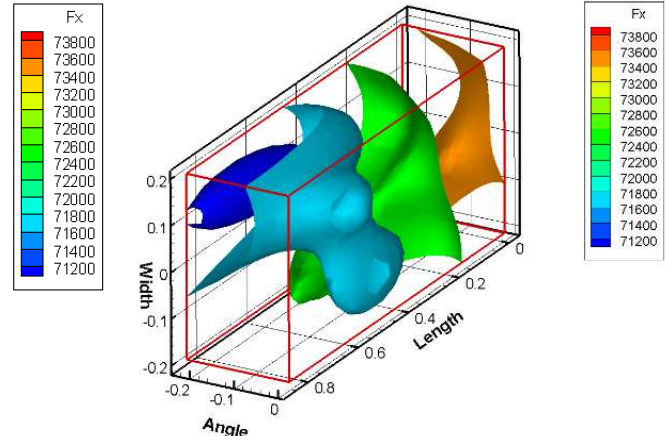


Fig. 13 : Iso values of the total drag F_x in the response surface

Fig. 12 and 13 show the response surface. Fig. 12 represents cutting planes of the design space, showing two main local minima. In Fig. 13, we show iso-values of the total drag F_x . We can identify a region where the objective function is predicted to be smaller than in the other part of the parameter domain.

6. Conclusion and future work

This paper presents a method for smooth shape deformation. The twofold parametrization, geometrical and architectural, demonstrates its capability to generate simulation-suited models with large possible shape domain. The skeleton based approach allows us to use the developed methodology to different kind of objects, e.g. hulls, foils, bulbous bows, propellers, wind turbines, airships, etc.

Further work will focus on the link with CFD solvers. A fully automated optimization loop will be developed. With the integration of an optimization algorithm as Efficient Global Optimization, the process of finding minima on the surrogate model would be significantly improved.

Acknowledgements

The project was achieved with the financial support of ANRT (Association Nationale de la Recherche et de la Technologie).

References

- BLANCHARD, L.; BERRINI, E.; DUVIGNEAU, R.; ROUX, Y.; MOURRAIN, B.; JEAN, E. (2013), *Bulbous bow shape optimization*, 5th Int. Conf. on Computation Methods in Marine Engineering (MARINE), Hamburg, pp. 412-423
- DUVIGNEAU, R.; CHANDRASHEKAR, P. (2012), *Kriging-based optimization applied to flow control*, Int. J. Numerical Methods in Fluids 69/11, pp.1701-1714
- HOCHKIRCH, K; BERTRAM, V. (2009) *Slow steaming bulbous bow optimization for a large containership*, 8th COMPIT, Budapest, pp.390-389
- IMAN, R.L.; HELTON, J.C.; CAMPBELL, J.E. (1981), *An approach to sensitivity analysis of computer models, Part 1. Introduction, input variable selection and preliminary variable assessment*, J. Quality Technology 13/3, pp.174-183

JACQUIN, E.; ALESSANDRINI, B.; BELLEVRE, D.; CORDIER, S. (2003), *Nouvelle méthode de design des carnes de voiliers de compétition*, 9^{ème} Journée de l'hydrodynamique

JONES, D.R.; SCHONLAU, M.; WELCH, W.J. (1998), *Efficient global optimization of expensive black-box functions*, J. Global Optimization 13/4, pp. 455-492

JONES, D.R. (2001), *A Taxonomy of global optimization methods based on response surfaces*, J. Global Optimization 21/4, pp. 345-383

KANG, J.; LEE, B. (2012), *Geometric interpolation and extrapolation for rapid generation of hull forms*, 11th COMPIT, Liege, pp. 202-212

PAPANIKOLAOU, A.; HARRIES, S.; WILKEN, M.; ZARAPHONITIS, G. (2011), *Integrated ship design and multiobjective optimization approach to ship design*, Int. Conf. Computer Applications in Shipbuilding (ICCAS)

PERI, D.; DIEZ, M. (2013), *Robust design optimization of a monohull for wave wash minimization*, 5th Int. Conf. Computation Methods in Marine Engineering (MARINE), Hamburg, pp.89-100

PIEGL, L.; TILLER, W. (1997), *The NURBS Book*, Springer

QUEUTEY, P; VISONNEAU. M. (2007), *An interface capturing method for free-surface hydrodynamic flows*, Computers & Fluids 36/9, pp.1481-1510

SEDERBERG, T.W.; PARRY, S.R (1986), *Free-form deformation of solid geometric models*, SIGGRAPH Computer Graphics 20/4, pp.151-160

VALDENAZZI, F.; HARRIES, S.; JANSON, C.E.; LEER-ANDERSEN, M.; MAISONNEUVE, J.J.; MARZI, J.; RAVEN, H. (2003), *The Fantastic RORO: CFD optimization of the forebody and its experimental verification*, NAV2003

WACKERS, J; DENG, G.B.; LEROYER, A.; QUEUTEY, P.; VISONNEAU, M. (2012), *Adaptive grid refinement algorithm for hydrodynamic flows*, Computers & Fluids 55, pp.85-100

WANG, W.; POTTMANN, H.; LIU, Y. (2006), *Fitting b-spline curves to point clouds by curvature-based squared distance minimization*, ACM Trans. Graph 25/2, pp.214-238

Hybrid Evolutionary Shape Manipulation for Efficient Hull Form Design Optimisation

Joo Hock Ang, Sembcorp Marine Ltd, Singapore, johock.ang@sembmarine.com

Cindy Goh, University of Glasgow, UK, Cindy.Goh@glasgow.ac.uk

Yun Li, University of Glasgow, UK, Yun.Li@glasgow.ac.uk

Abstract

'Eco-friendly shipping' and fuel efficiency are gaining much attention in the maritime industry due to increasingly stringent environmental regulations and volatile fuel prices. The shape of hull affects the overall performance in efficiency and stability of ships. Despite the advantages of simulation-based design, the application of a formal optimisation process in actual ship design work is limited. A hybrid approach which integrates a morphing technique into a multi-objective genetic algorithm to automate and optimise the hull form design is developed. It is envisioned that the proposed hybrid approach will improve the hydrodynamic performance as well as overall efficiency of the design process.

1. Introduction

Faced with volatile fuel prices, low charter rates and new environmental regulations, ships nowadays are expected to be more innovative and energy efficient. In ship design, the shape of the hull is one of the most important design parameters that need to be determined as early as possible. This is due to its impact on the overall performance efficiency and any major changes of the hull form in later design or construction stages will have detrimental effects to the cost and delivery schedule of vessel.

Today, new hull designs are heavily reliant on the designer's experience and often used existing designs as a starting point. Although the use of simulation-based design (SBD) is becoming increasingly prevalent, where new hull designs are modelled and evaluated virtually before final verification through physical model testing, the adoption rate is slow. Possible reasons include the lack of automated shape manipulation and robust optimisation techniques to generate feasible designs, *Ang et al. (2015)*. In the face of an aging workforce and increased costs, more automated and integrated design processes for the ship hull are now a necessity. The next paradigm in smart design and manufacturing, known commonly as Industry 4.0, provides the capabilities and opportunities to bridge this gap where the design of the hull form will become a fully integrated and automated process, *Ang et al. (2016)*. It is crucial for shipyards and design firms to capitalise on these new technological advancements in order to overcome the difficult market conditions.

2. Related works

2.1. Hull form optimisation

Ship design optimisation is an iterative process where multiple design parameters which determine the cost and performance of the vessel are improved to give an optimal solution or a set of optimal solutions. These design parameters can include powering, lines plan (hull form), structure, weight estimate, stability, etc. Due to need to determine the hull form in early design stage and its effect to other design parameters, hull form optimisation is one of the most important topic of research and hence the focus of this paper.

Traditionally, hull form optimisation involves mainly the designer manually modifying the shape of the hull (or hull lines) and evaluating the performance of the new shape using different simulation software. This 'trial and error' approach is extremely time-consuming and optimum designs are not guaranteed. Formal hull form optimisation that integrates the process of geometry modification, optimiser and performance evaluation can help to automate the entire design process. An example of

simulation-based hull form optimisation concept is provided in Fig. 1, which describe the process of automated hull form optimisation using evolutionary algorithm as main optimiser, geometry modification to transform the shape of hull, evaluate the performance using computational fluid dynamic (CFD) techniques and iterates until the conditions are met and provide a range of optimal solutions, *Ang et al.* (2015).

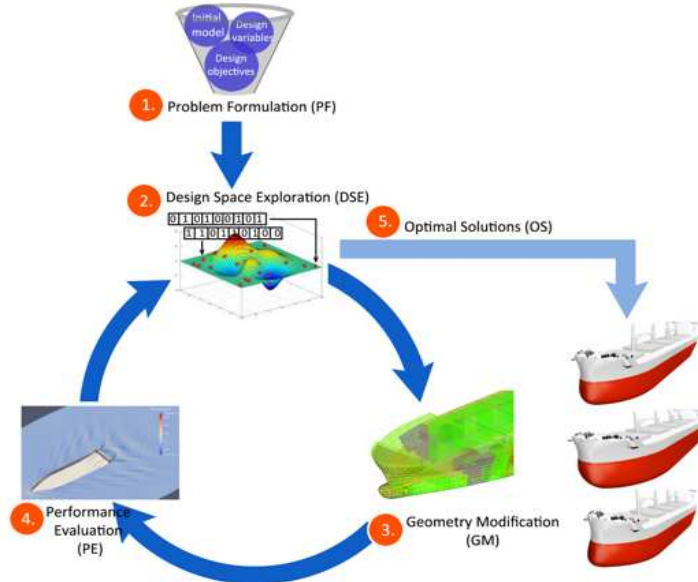


Fig. 1: Simulation-based hull form optimisation concept

2.2. Optimiser

The optimiser plays a key role in the hull form design optimisation process. Here, it can be thought of as parametric optimisation where key design parameters relating the shape of the hull are modified in an iterative loop to produce a set of optimal values at the end of the optimisation process. Key optimisation techniques that were applied to hull form optimisation includes Simplex method of Nelder and Mead, *Jacquin et al.* (2004), *Kostas et al.* (2014), Sequential Quadratic Programming (SQP), *Park and Choi* (2013), evolutionary algorithm such as Genetic Algorithm (GA), *Tahara et al.* (2003), *Baiwei et al.* (2011), *Kim* (2012), and Particle Swarm Optimisation (PSO), *Campana et al.* (2009), *Chun* (2010), *Tahara et al.* (2011), *Chen et al* (2014).

Specifically, Simplex method is a derivative-free local search method which only uses the values of the objective and does not require any derivative information, *Koziel and Yang* (2011). SQP is a gradient based method which possesses a robust and stable scheme to solve local quadratic programming problem through approximation by Taylor expansion around a set of design variable, *Suzuki et al.* (2005). As per *Peri and Tinti* (2012), gradient-based algorithms such as SQP are very efficient for local optimisation however suffer from finding sub-optimal solutions when the design problem is not convex.

Evolutionary algorithms (EAs) are a group of generic population-based meta-heuristic optimisation techniques. EAs are widely applied as they can solve complex problems to come up with a set of globally optimal solutions. However, due to their randomness, they are difficult to formulate and their results cannot be predicted in advance, *Zelinka et al.* (2013). GA, first developed by *Holland* (1975), is a nature-inspired search heuristic method based on Darwinian Theory of natural selection and the ‘survival-of-the-fittest’ principle. Particle swarm optimisation (PSO) is another evolutionary strategy that is applied to solve global optimisation problem. It simulates the social behaviour of swarm of birds or bees which are capable to share information while looking for food.

2.3. Geometry modification

In any hull form optimisation, geometry modification plays an important role in ensuring the hull geometry can be easily manipulated to form new shapes in order for the optimiser to investigate and evaluate. This is no trivial task as every new shape generated must be smooth and a feasible design. There are 2 main approaches in hull form manipulation - direct modification and systematic variation. Direct modification involves the process of changing the hull geometry from model source (Bezier curve, B-splines, etc.). Using control points, hull coordinates or vertices can be adjusted manually through curve (2D) or surface (3D) representations. This method provides flexibility to the designer for local transformation involving specific section of the hull form- bulbous bow, propeller area, etc. However, due to its large number of control points required to represent the shape and largely human dependent, this method is not suited for modifying entire hull form or automated shape transformation. Example of direct modification applied in hull form optimisation includes T-spline, *Kostas (2014)*, cubic B-spline surface, F-spline, etc.

Systematic variation, on the other hand, modifies the hull shape using a function which considers global hull parameters (C_b , C_p , etc.) or a series of local hull representation (NURBS, patches, etc.). Systematic variations are particularly useful for global modification involving entire hull or particular section of the hull (forebody/ afterbody) as well as automatic hull form optimisation with minimum user intervention. Example of systematic variation applied in hull form optimisation includes Karhuen-Loeve expansion (KLE), *Diez et al. (2014)*, *Chen et al. (2014)*, Free-Form Deformation (FFD), *Campana et al. (2013)*, and parametric modification, *Saha and Sarker (2010)*, *Brizzolara and Vernengo (2011)*.

Specifically, FFD provides mapping to change the coordinates of complex a geometry shape by enclosing it within simpler ones, *Peri et al. (2009)*. It is based on scheme of trivariate Bernstein polynomials. While FFD is simple to use and quick to apply in hull form modification, successful application depends greatly on the experience and skill of the designer to control the directions, *Ang et al. (2015)*. Parametric modelling and transformation is another useful method which captures the essence of intended shapes and possible variations. The advantages of this method is that it offers better control on the overall hull shape to be optimised and is faster to apply, *Pérez et al. (2007)*.

2.4. Performance evaluation

Performance evaluation will evaluate each candidate solution produced from the optimiser depending on the objective function. Multi-objective optimisation becomes predominate as compared to single objective. This is especially true for ship design problem. The most important factors that influence the shape of hull include resistance and propulsion, sea-keeping behaviour in seaway, manoeuvring, cargo capacity, etc., *Papanikolaou (2014)*. Consequently, these performance parameters became the key objective functions applied and evaluated in hull form optimisation. For resistance evaluation, Computational fluid dynamic (CFD) had been used extensively in hull form optimisation to simulate the fluid flow around vessel. Prevalent CFD methods used for resistance evaluation include potential flow, *Nowacki (1996)*, and Reynolds Averaged Navier-Stokes Equation (RANSE), *Zha, et al. (2014)*, *Tahara et al. (2006)*, *Perival (2001)*.

Specifically, potential flow is governed by Laplace equation and discretised using body surface and free surface panels, *Nowacki (1996)*. Potential flow model are particularly useful for free surface flows, due to the effects of viscosity are often limited to small boundary layer, *Bertram (2008)*. However, in many hydrodynamic cases, it can only be used as preliminary evaluation due to limitation such as no computation of viscous drag, linear free surface, etc. RANSE are used to solve viscous fluid flows and able to represent complex free surfaces, which enables it to accurately evaluate total resistance, propulsion, appendages and added resistance. Key advantage of RANSE methods are it can capture global and local wave patterns as well as viscous effects at full scale. However, it requires high computational time and quality of result may differ significantly depending on user settings or commercial software used, *Bertram (2008)*. More recently, more complicated

evaluation process was implemented for resistance evaluation which includes Neumann-Michell (NM) theory, *Huang et al.* (2014), *Jeong and Kim* (2013), Unsteady Reynolds-averaged Navier stokes, *Chen et al.* (2014), *Blanchard et al.* (2013), etc. Various numerical methods used for sea-keeping analysis includes strip theory, unified theory, green function method, etc., *Bertram* (2000). Of which, strip theory is one of the main technique used for calculation of wave induced motion of ship.

3. Hybrid evolutionary shape manipulation approach

Considering main issues in existing hull form optimisation with respect to the lack of automated shape manipulation and robust optimisation techniques to generate feasible designs, we proposed a hybrid evolutionary shape manipulation approach, which integrates a Genetic Algorithm (GA) and morphing techniques into a single optimisation platform. By combining the advantages of GA - ability to search for the best global solution(s)- and that of morphing- generate smooth intermittent shapes by combining two or more designs, we can potentially improve the overall efficiency and probability in deriving at the ‘optimum design’. An overview of the proposed concept is provided in Fig. 2.

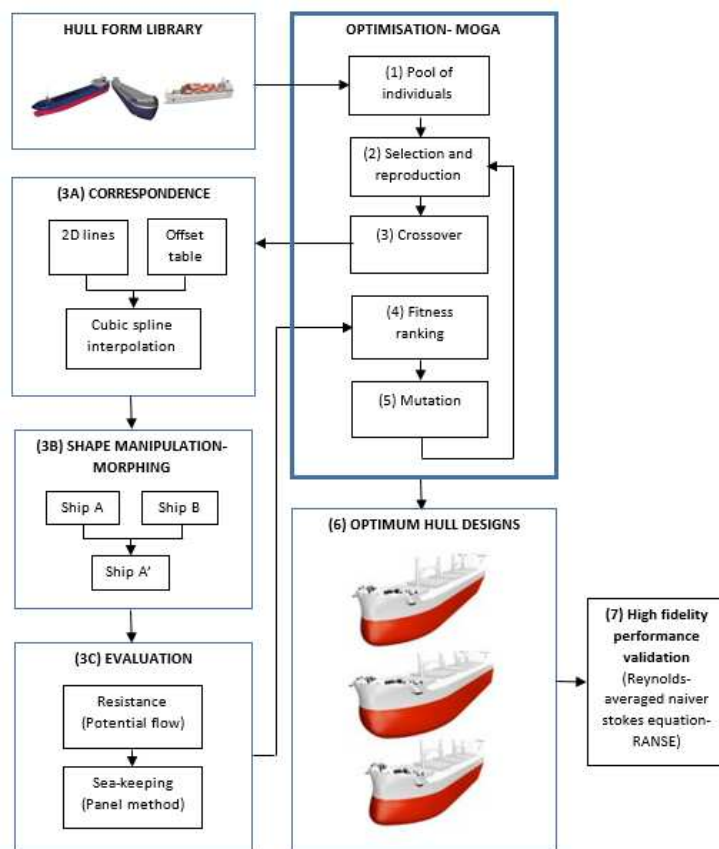


Fig. 2: Hybrid Evolutionary Shape Manipulation Approach

3.1. Hybrid Genetic Algorithm

A GA is a stochastic global search method that mimics the process of natural biological evolution, based on the abstraction of Darwin’s evolution of biological systems. It operates on a population of potential solutions by applying the survival-of-the-fittest principle to produce better approximation to a solution, *Chipperfield et al.* (1994).

Like any real world problems, ship design often requires dealing with multiple conflicting objectives including lower resistance, higher cargo capacity, shorter construction duration and cost to be solved. Hence, it may not be entirely practical to expect any optimisation method to provide one single ‘optimum’ solution to such multi-objective problems. Instead, it may be more useful if an optimiser

can help identify a set of potential (Pareto-optimal) solutions where the user can select the most appropriate and suitable solution according to his needs.

The hybrid multi-objective GA developed in this paper consists of four main components namely: (1) initialisation, (2) selection and reproduction, (3) crossover and (4) mutation. For brevity, the following sections details key mechanisms of the hybrid GA for hull form design optimisation and the reader is referred to *Konak et al. (2006)*, for basic working principles of a GA.

3.1.1. Initialisation

Initialisation is the first step in the GA where the pool of ‘initial solutions’ is populated. In the context of ship design, this can be drawn from existing hull forms from a design library or created from scratch. The approach developed in this paper is based on the former where existing hull forms from a shipyard is used. These hull forms are used as reference or parent designs which will be further improved to meet the new design objectives. The advantage of using existing designs is the assurance of their performances, whilst may not be optimal, are validated to meet basic design objectives and could thus potentially shorten the design cycle.

In the GA terminology, these existing designs (also termed ‘phenotypes’) are first encoded as chromosomes (‘genotypes’). This is a unique way of representing existing designs in the decision variable domain, *Chipperfield (1994)*. For the approach developed in this paper, real-value chromosomes using morphing parameter, which captures the ship’s geometry in 3D (x, y, z- planes) is used. This provides a simple yet direct representation of the ship geometry and helps to reduce the occurrence of infeasible designs (odd shape, unsmooth surface, etc.) generated during later parts of the optimisation process.

3.1.2. Selection and reproduction

In GA, selection is the process of i) determining the number of times (trials) each individual in the population can be chosen for reproduction and ii) conversion of expected number of trials into discrete number of offspring. The most popular selection scheme is the ‘roulette wheel’ mechanism which can probabilistically select individuals based on their performance, *Chipperfield (1994)*.

For proposed hull form application, we can translate fitness value into real value by determining the number of times or frequency a particular hull form will be selected. This is followed by determining the selection probability each hull form will be selected based on its fitness or good attributes as compared to other hull forms in the hull form library, which is also known as sampling. In order to determine the fitness level of each individual, the individual (hull form) pools are first evaluated based on the objective functions such as reduced resistance, improved sea-keeping performance, etc. After which, each individual is assigned with a fitness value and individual that are assessed to be highly ‘fit’ with relate to entire population from the evaluation process are selected for next round of reproduction.

3.1.3. Crossover

Crossover is the most important operator in GA and it combines two chromosomes (parents) to form new chromosome (offsprings). By applying the crossover operator, genes of good chromosome tends to appear more frequently in the population, leading to convergence to overall good solution, *Konak et al. (2006)*. By manipulating the genes of the chromosome, it is assumed certain individual genes code will produce ‘fitter’ individual after recombination. A recombination operator is hereby used to exchange genetic information between a pairs or large group of individuals, *Chipperfield (1994)*. Two-point crossover is most commonly used for reproduction where two points are randomly chosen and design variables are exchanged between the parent variable vectors, *Poloni (2003)*. In our proposed hybrid evolutionary shape manipulation approach, we apply morphing as the main driver within crossover process to i) provide encoding scheme using morphing parameters to our hybrid GA to

manipulate the shape of hull and ii) combine 2 or more existing hull forms (parents) to generate new hull designs (offsprings). The detail process will be further elaborated in the next section.

3.1.3.1 Morphing

Morphing, also known as metamorphosis is a technique that is used widely in the animation industry to generate a sequence of images that smoothly transform a source into a target image. In computer graphic and industrial design, it is also used to compute a continuous transformation from one source shape to another target shape that in. In ship application, morphing was applied by *Tahara (2006)*, *Peri (2009)*, *Kang and Lee (2010)* and *Baiwei et al. (2011)*.

We performed curve morphing based on hull lines data. Since the beginning of shipbuilding and subsequent introduction of computer-aided design, two-dimensional (2D) hull lines remains the most fundamental graphical representation of the ship's hull form. This is the starting point where experienced designers model and modify the hull design prior to hydrodynamic calculations. The advantages of using 2D hull lines are: (i) it is a simple means to represent the entire shape of the hull and (ii) it is relatively easy to modify the hull form by adjusting the lines, *Papanikolaou (2014)*. It also serves as a primary source of hull form data which are used for subsequent plan approval and construction. Fig. 3 shows an example of a typical lines plan of a cargo ship.

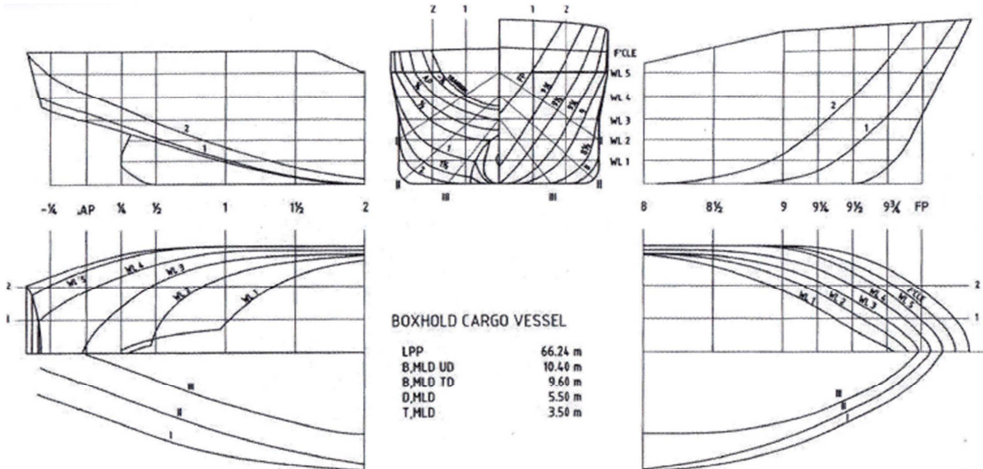


Fig. 3: Ship lines plan of cargo ship, *Friis et al. (2002)*

A) Correspondence

Firstly, before morphing can be performed, we need to first ensure the hull form curve corresponds with each other. This correspondence process is done by creating the same number of points within a section curve for 2 existing (parent) vessels which are to be morphed. In the case where the number of vertices are different for two vessels, one can perform cubic spline interpolation to create same number of points at different interval of the section curve. To give an example, based on data from offset table, section curve at $X=0$ for vessel A consist of 7 points (Y and Z). On the other hand, section curve at $X=0$ for vessel B contain 10 points. In order to morph the section curve at $X=0$ for both vessel A and B, we can create 10 equal points on each curve by cubic spline interpolation, Fig. 4.

Cubic spline interpolation is a piecewise continuous curve which passes through each of the values in a table of points. It can be represented in the following equation:

$$S_i(x) = a_i(x - x_i)^3 + b_i(x - x_i)^2 + c_i(x - x_i) + d_i ; \text{ for } x \in [x_i, x_{i+1}] \quad (1)$$

Where $S(x)$ denotes the spline and $[x_i, y_i]$ represents a table of points for $i = 0, 1, \dots, n$ for function $y = f(x)$

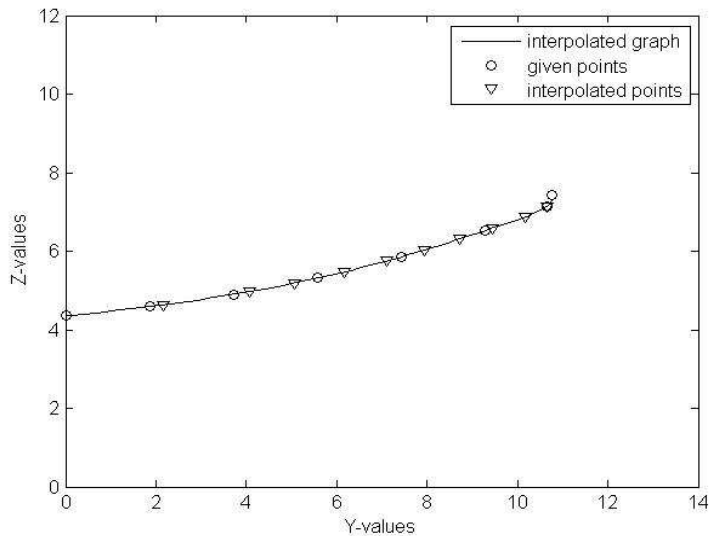


Fig. 4: Correspondence using cubic spline interpolation

B) 2D curve morphing

In this hybrid GA-morphing concept, we apply 2D curve morphing as the systematic shape variation method and apply to crossover function within GA to create new combinations.

I) Linear morphing

Firstly, we apply linear morphing to transform one hull shape to another, which will generate the ‘intermediate’ shapes in between the 2 ‘parents’. Using linear morphing equation:

$$M(t) = (1 - t) \times R_0 + t \times R_1 \quad (2)$$

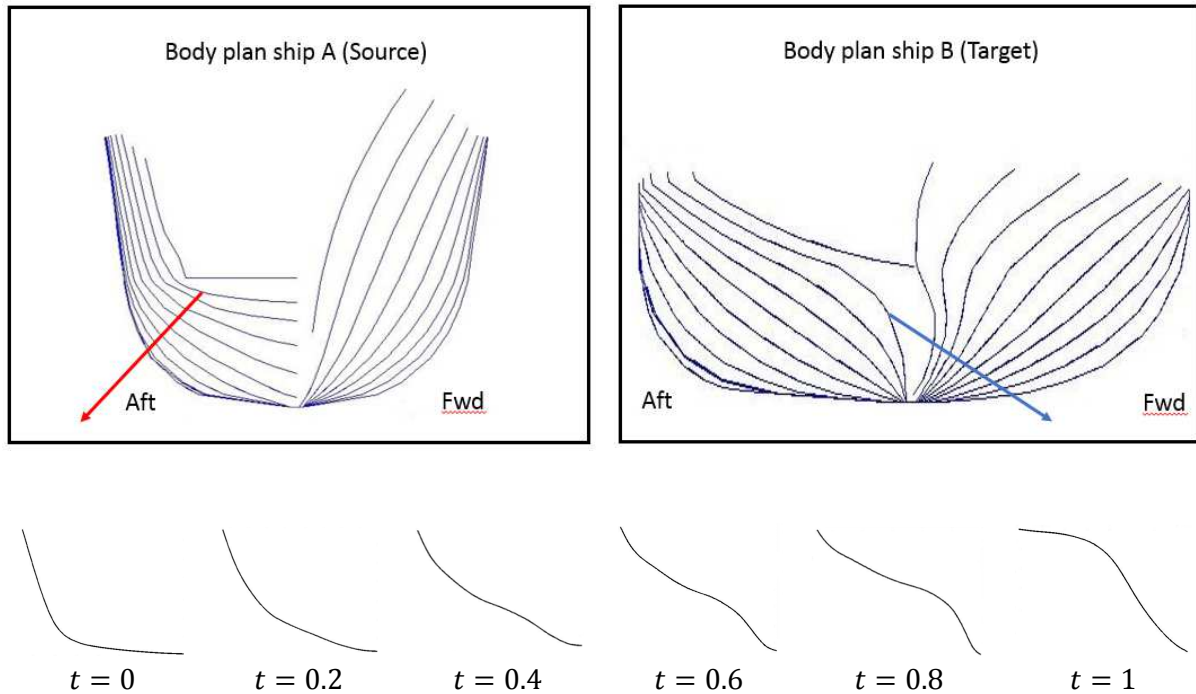


Fig. 5: Linear morphing at station 0.5 from ship A (source) to ship B (target)

Where $M(t)$ is the morphed shape, t is the morphing parameter, R_0 denotes the source shape and R_1 the target shape. From above equation, we can see when $t = 0$, $M(t)$ is also equal to 0 and hence the morphed shape is equivalent to source shape R_0 . Likewise, when $t = 1$, $M(t) = R_1$ which is the target shape.

Using hull lines provided from the body plan of source and target vessel, we can morph and generate n no of intermediate shapes just by changing the morphing parameter(t). As an example, we take one hull lines each from sample ship A (source) and sample ship B (target) at station 0.5 in way of stern of both vessels. By applying the morphing equation with steps of 0.2 ($t = 0, 0.2, \dots, 1$), we are able to generate 4 intermediate curves as illustrated in Fig. 5

By applying constant morphing parameter (t) across all transverse frame or stations, we can effectively morph or create many intermittent forms between the source and target model, which will be further demonstrated in section 4 using actual ship model.

II) Time-varying morphing

In order to create as many variation and possible combination of hull form designs so as to increase the solution space, another method proposed is time-varying morphing where two different sections of hull form can be combined seamlessly using morphing method. This is achieved by setting varying morphing parameter (t) at different transverse curve along the stations or frame lines (x-planes). Using sample ship A and B again as example, we ‘cut’ the body of both vessels at mid-ship (middle body) and combine both of them as illustrated in Fig. 6.

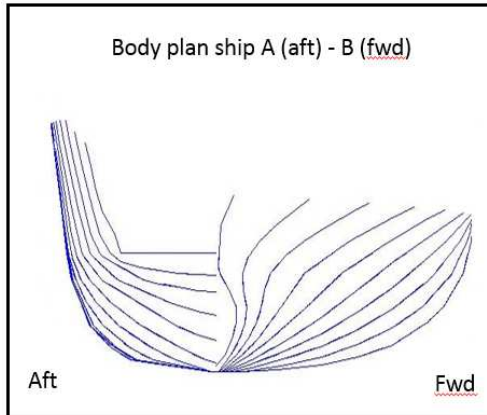


Fig. 6: Combination of ship A aft body and ship B forward body

From the figure above, we can clearly see it will not be a feasible model solely by joining 2 unrelated hull form together as there are a sudden change in way of mid body which results in unsymmetrical forward and aft body. However, by applying a gradual morphing parameter (t) on multiple curves along different stations (X-axis), we can effectively create a smooth transition from aft section of ship A to forward section of ship B. In Fig. 7, we applied morphing to mid body of the vessel by setting morphing parameters (t) of 0.1-0.9 to station 3-7 (highlighted) of the vessel. Note there are no changes to the lines of ship A (source) when $t=0$ and vice versa for ship B (target) when $t=1$.

Using similar concept, we can effectively change the hull shape towards more of ship A or ship B just by varying the morphing parameters at different part of the vessel, as illustrated in Fig. 8a and 8b. Note that there is no changes to the lines (or shape) of aft body of ship A when morphing is applied to forward body of ship B (Fig. 8a) and likewise no changes to forward body of ship B when morphing is applied to aft body of ship A (Fig. 8b).

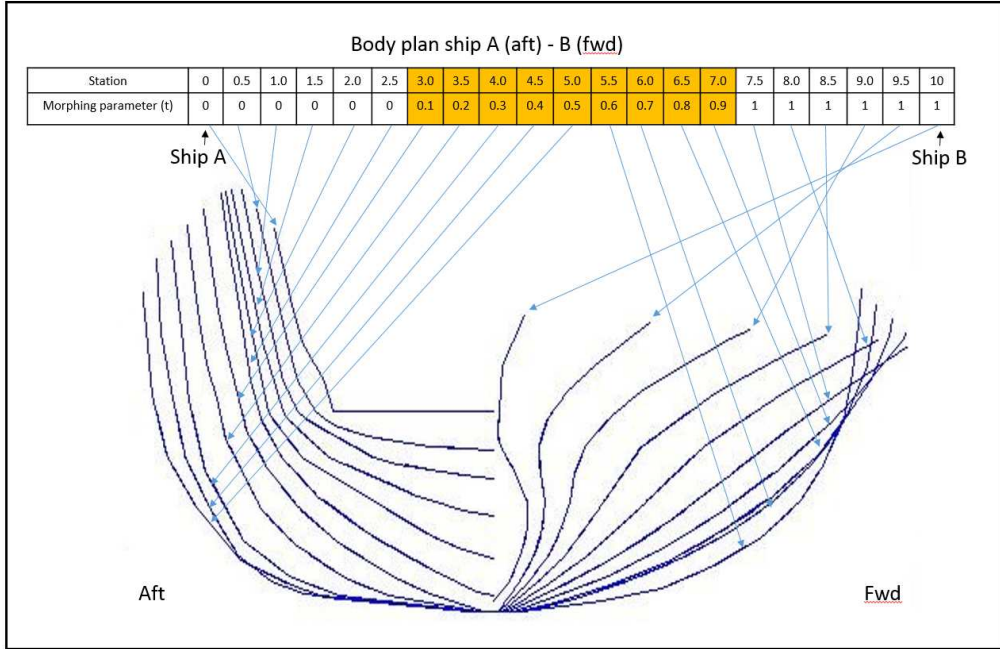


Fig. 7: Morphing applied to mid body of combined ship A (aft) and ship B (forward)

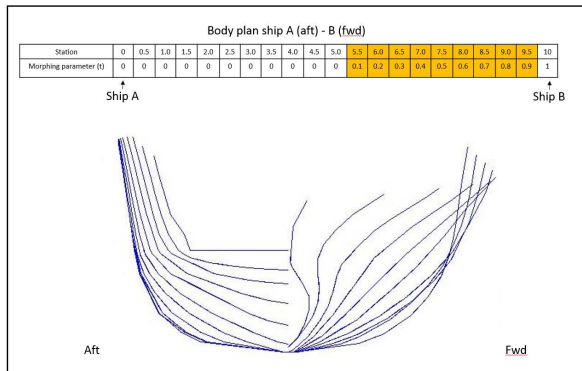


Fig. 8a: Morphing applied to forward body of combined ship A (aft) and ship B (forward)

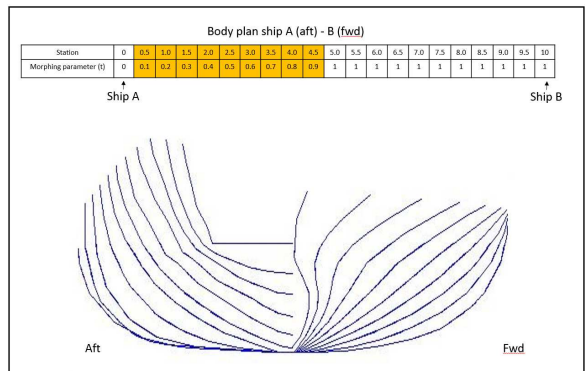


Fig. 8b: Morphing applied to aft body of combined ship A (aft) and ship B (forward)

From above examples, we demonstrated how two different hull bodies can be ‘joined’ smoothly together using cross morphing technique. By varying the morphing parameter (t) at different transverse frame, we can choose which attributes the curve should be transformed, whether it should be more of ship A (toward $t=0$) or ship B (towards $t=1$). This provide great flexibility to change the hull shape effectively at any location of the ship and yet maintain a smooth transition.

III) Multi-target morphing

Using same principle above, we propose another method that can possibly ‘cut’ and join 2 or more vessels at different section such as ship A aft body to ship B mid body to ship C forward body. By changing the source and target model, we can effectively morph the vessel into a combination of more than two vessels, see Fig. 9.

Using earlier example, we include one more sample ship model C (figure 10) and perform multi-morphing and result shown in Fig. 11.

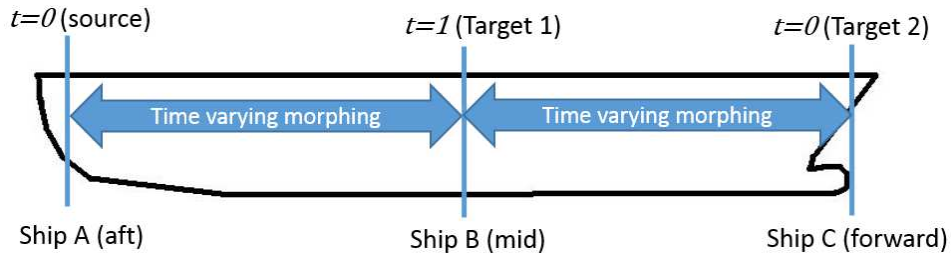


Fig. 9: Combination of ship A aft body and ship B forward body

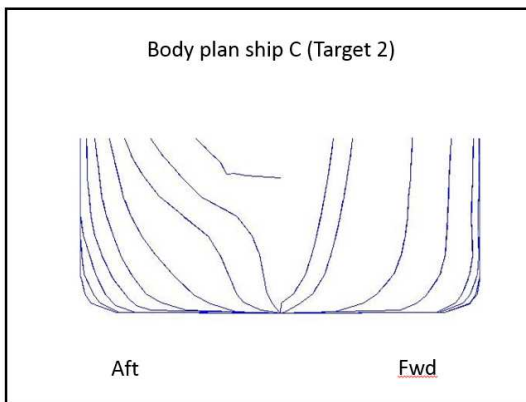


Fig. 10: Sample ship C body plan

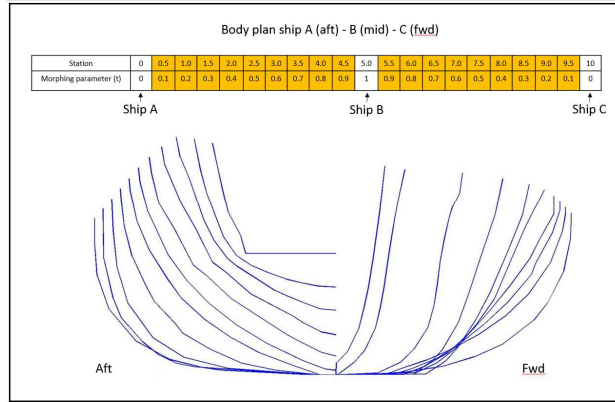


Fig. 11: Combination of ship A aft body, ship B mid body and ship C forward body

On top of morphing 2 or more hull forms together into one hull concept, cross-target morphing can also be applied by mixing different combinations- example instead of joining ship A-B and B-C, we can also join ship A-C and C-B, etc. While time-varying and multi-target morphing may be simple to apply directly for geometrically similar ships, it can also be applied to ships sizes that are vastly different which will be further demonstrated in section 4.

3.1.3.2 Evaluation

After the new hull forms are generated through direct morphing and new hull combinations produced from cross morphing, these designs will form the ‘offspring’ which will be evaluated in the evaluation process to determine the fitness level of individuals before next round of reproduction. As highlighted in earlier section, performance functions that are closely related to shape of hull includes resistance, sea-keeping, manoeuvring, etc. Depending on the objective function set, appropriate evaluation method can be used to analyse the performance of the selected hull forms. In our example, we proposed potential flow for resistance evaluation and panel method for sea-keeping analysis due to its fast calculation although accuracy is somehow compromised as compared to advance RANSE method. This process is not conducted in this study due to time limitation but would be included later as part of author’s ongoing work.

3.1.4. Mutation

Mutation is a process in GA where new genes are created in random to produce a new genetic structure, which helps to introduce new elements into the population. In hull form optimisation, this can be carried out in terms of additional geometry modification where designer can perform local shape transformation (bulbous bow, etc.) using free-form deformation techniques.

3.1.5. Termination

Once all solutions are ranked and termination conditions are met, the iteration will stop and provide the results- identifying the non-dominated solutions or Pareto optimum designs. It is now up to the

designer to choose the final design, which will best meet the customer's requirement. We also propose to include a high fidelity validation process after termination and attainment of a range of Pareto optimum hull designs. This is to ensure the optimum hull form obtained from the optimisation process is truly 'optimal' and it also provides an additional reference for the designer when deciding on the final hull form design.

4. Results and discussions

In order to demonstrate the feasibility of our proposed hybrid evolutionary shape manipulation approach, we will morph two existing vessels; a volume carrier (Very Large Crude Carrier-VLCC) and an offshore vessel (pipe-laying) using the 2D curve morphing. The principle dimensions for both vessels are provided as follows:

Table I: Principle dimensions

	VLCC	Pipe-laying
Length overall (Loa)	327m	182m
Length between perpendiculars (Lpp)	314m	168m
Breadth (B)	58m	46m
Height (H)	31m	23m
Design draft (T)	20m	11m

Firstly, based on offset table and lines plan, the offset data (x,y,z plane) for both vessels were inputted into table format. Correspondence check was then carried out to ensure that both 'parents' have equal number of points. To handle missing data, cubic spline interpolation was used to create additional vertices so as to ensure equal number of vertices before morphing. Fig. 12 shows the isometric view of the two 'parent' vessels and the 'child' obtained at morphing parameter (t) = 0.25, 0.5 and 0.75. It takes less than 2 seconds to compute the morph data for one hull generation.

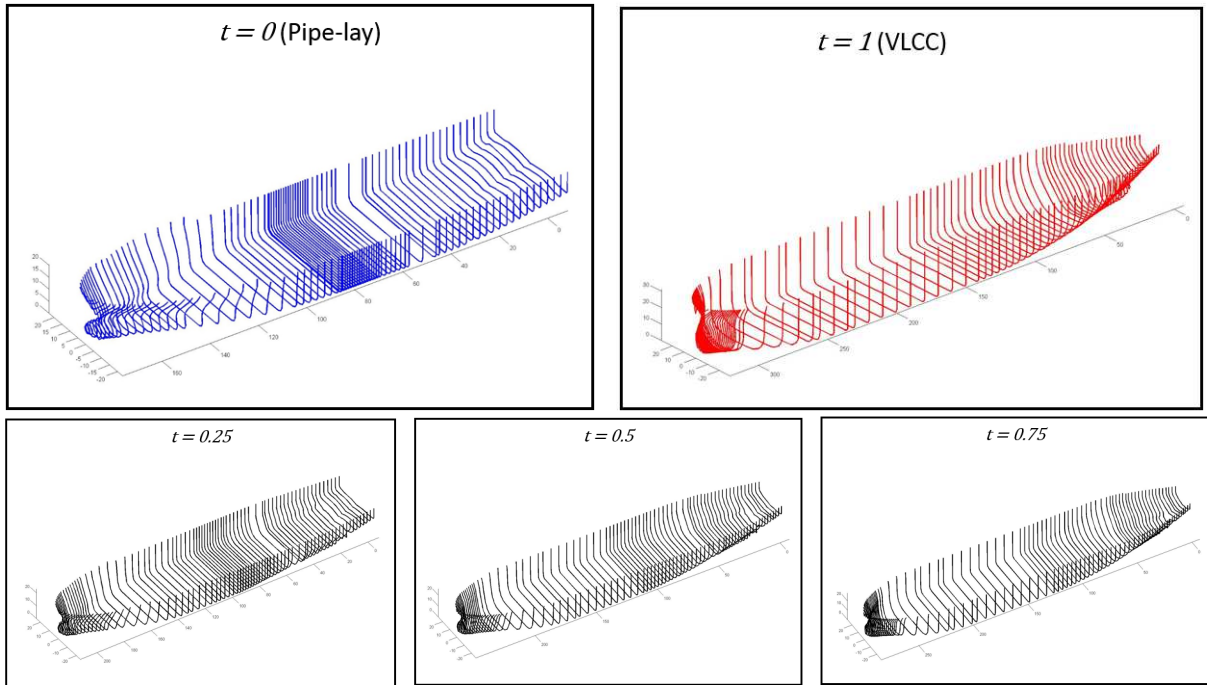


Fig. 12: Isometric view of two parent vessels (Pipe-lay and VLCC) before linear morphing and the child produced at $t = 0.25, 0.5$ and 0.75 .

Once this is completed, the 2D data can then be converted to surfaces using CAD modelling tool such as NAPA as shown in Fig. 13. This will provide better visualisation as well as subsequent preparation for meshing and CFD evaluation.

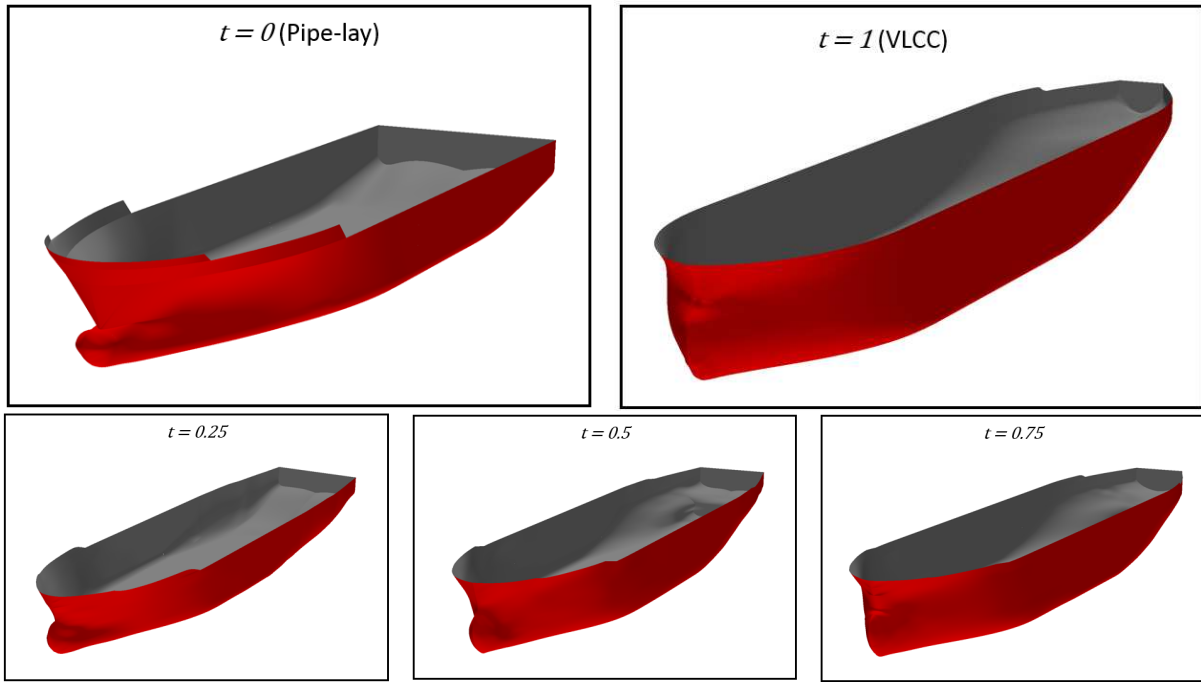


Fig. 13: 3D hull surface generated from 2D curve using NAPA

In order to generate more hull combinations and apply to crossover function within GA, we ‘cut’ both vessels in the mid-ship section and combined them as shown in Fig. 14. It seems impossible to join both vessels properly due to the large differences in size - the VLCC shown in red is almost twice the size of the pipe-lay vessels shown in blue. However, it is possible to overcome this disparity by performing time-varying morphing at the mid body using very small morphing parameter (t) value.

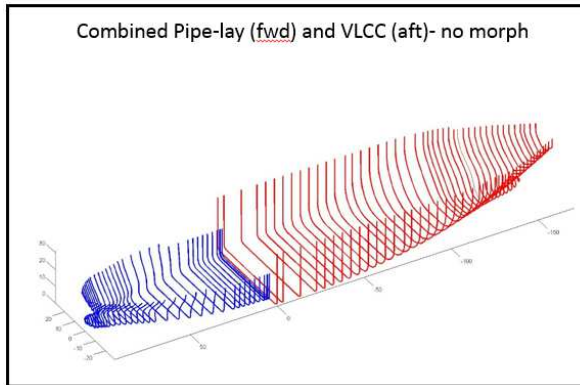


Fig. 14: Combination of pipe-lay forward body and VLCC aft body

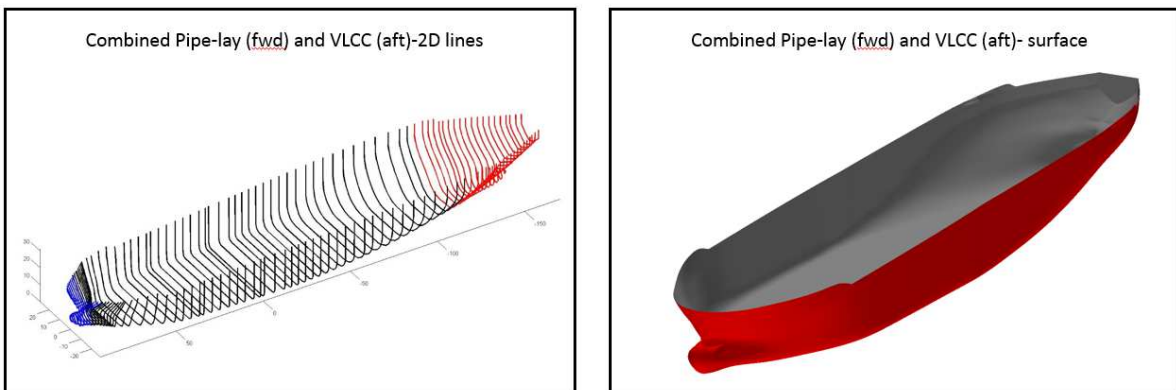


Fig. 15: Isometric view of combined vessel with time-varying morphing

As shown in Fig. 15, when (t) is set at 0.02, the combined vessel at mid body has a smooth ‘blending’ at the cutting site, producing a feasible hull form that is ready for evaluation. It should be noted that for hull forms with vastly different geometries, t needs to be set at smaller intervals while a larger t should be used for geometrically similar ones.

4.1. Discussions and future works

We have presented a new method using 2D curve morphing and applied to hull form manipulation which can effectively transform the shape of hull in 3 ways -i) linear morphing, ii) time varying morphing, iii) multi-morphing. Linear morphing allows the transformation of entire hull form from one ship to another. Time-varying morphing allows gradual transformation of different sections of the ship which depict the ‘joining’ of 2 vessels, whereby allowing partial feature of both ships to be retained. Multi-morphing allows the transformation of 2 or more ships using concept of time-varying morphing which enable changing of the shape hull while retaining particular sections of multiple vessels. The concept put forth in this paper provides a simple, yet promising solution to hull form design optimisation. Through 2D curve morphing, it effectively transforms the shape of a hull and is able to generate a variety of different hull forms. Despite its advantages, several factors need to be considered:

- 1) For completeness, design criteria such as principle dimensions (length, breadth, and height), displacement, and deadweight, etc., constitute part of the design constraints and should also be considered during the optimisation process.
- 2) It should be noted that some design firms or shipyards may not readily possess a large database of existing hull forms. This means that they may not be able to provide a diverse initial population which is an important factor for effective design space exploration. The method should therefore be able to automatically create new hull forms models in CAD software from manual sketches or first principles to populate the initial population.

In summary, advantages of proposed 2D curve morphing technique are as follow:

- 1) Fast generation of intermediate hull forms as well as combination of different vessels.
- 2) Hull shapes generated are based on existing proven designs, thereby ensuring its smoothness and feasibility.
- 3) Hull lines are simple to represent in phenotype space within GA and it provides more flexibility for shape modification as compared to surfaces.
- 4) Allows hull bodies to be ‘cut’ along the length of the hull body and ‘combined’ with another hull body seamlessly.

As demonstrated in this study, morphing technique presents many opportunities and possibilities when applied to hull form optimisation. Some proposed future works include the following:

- 1) To further investigate different morphing methods so as to create more shape variation. In field of metamorphosis, there are many interesting works which looks into the transformation of shapes in pursue of better design performance. Some good example of non-linear morphing includes weighted-average morphing, feature based morphing, etc.
- 2) Automatic conversion from 2D curve to 3D surface and meshing before CFD evaluation
- 3) Couple the proposed hybrid evolutionary shape manipulation approach with performance evaluation to achieve fully automated hull form design tool.

5. Conclusion

Eco-friendly shipping and energy efficiency are two of the most important topics in the shipping industry. This is particularly so in the face of more stringent environmental regulations and volatile fuel prices. The shape of hull affects the overall performance of a vessel and is therefore the area

where the biggest improvements could be reaped. Simulation-based design is proven to be a very efficient tool for hull form optimisation as compared to manual modelling and other simulation based design techniques. Nonetheless, it has not been widely adopted largely due to the lack systematic shape variation and robust optimisation techniques.

In this paper, we developed a hybrid evolutionary shape manipulation approach by combining GA and morphing. The key advantage of this hybrid approach is that it capitalises on both smart optimiser as well as systematic shape variation to develop into a fully automated and efficient hull form optimisation tool. We also presented a novel application of 2D curve morphing method, which can be applied easily to transform the shape of hull by generating many intermediate hull form between 2 or more existing vessels. By combining different sections of the hull body through time-varying and multi-target morphing, we are able to generate many ‘new’ and potential designs when combined with GA. This ensures an effective search for optimal designs. It is envisioned this hybrid evolutionary shape manipulation approach can help to improve the overall design efficiency and hydrodynamic performance of smart vessels in near future.

References

- ANG, J.H.; GOH, C.; LI, Y. (2015), *Key challenges and opportunities in hull form design optimisation for marine and offshore applications*, 21st Int. Conf. on Automation & Computing, University of Strathclyde, Glasgow
- ANG, J.H.; GOH, C.; LI, Y. (2015), *Hull form design optimisation for improved efficiency and hydrodynamic performance of ‘ship-shaped’ offshore vessels*, Int. Conf. on Computer Applications in Shipbuilding (ICCAS), Bremen
- ANG, J.H.; GOH, C.; LI, Y. (2016), *Smart Design for Ships in a Smart Product Through-Life and Industry 4.0 Environment*, IEEE Congress on Evolutionary Computation (CEC)
- BAIWEI, F.; HU, C.P.; LIU, Z.Y.; ZHAN, C.S.; CHANG, H.C. (2011), *Ship resistance performance optimization design based on CAD/CFD*, 3rd Int. Conf. on Advanced Computer Control, Harbin
- BERTRAM, V. (2000), *Practical Ship Hydrodynamics*, Butterworth-Heinemann
- BERTRAM, V. (2008), *Appropriate tools for flow analyses for fast ships*, HIPER, Naples, pp.1-9
- BLANCHARD, L.; BERRINI, E.; DUVIGNEAU, R.; ROUX, Y.; MOURRAIN, B.; JEAN, E. (2013), *Bulbous bow shape optimization*, 5th Int. Conf. Computational Methods in Marine Eng.
- BRIZZOLARA, S.; VERNENGO, G. (2011), *Automatic optimisation computational method for SWATH*, Int. J. Mathematical Models and Methods in Applied Sciences
- CAMPANA, E.F.; LIUZZI, G.; LUCIDI, S.; PERI, D.; PICCIALLI, V.; PINTO, A. (2009), *New global optimization methods for ship design problems*, Optimization and Engineering (OPTE)
- CAMPANA, E.F.; SERANI, A.; DIEZ, M. (2013), *Ship optimization by globally convergent modification of PSO using surrogate based newton method*, Engineering Computations
- CHEN, X.; DIEZ, M.; KANDASAMY, M.; ZHANG, Z.G.; CAMPANA, E.F.; STERN, F. (2014), *High-fidelity global optimization of shape design by dimensionality reduction, metamodels and deterministic particle swarm*, Engineering Optimization
- CHIPPERFIELD, A.; FLEMING, P.; POHLHEIM, H.; FONSECA, C. (1994), *Genetic Algorithm Toolbox User’s Guide V1.2*, University of Sheffield, Dept. Automatic Control and Systems Eng.

CHUN, H.H. (2010), *Hull form parameterization technique with local and global optimization algorithm*, Int. Conf. Marine Technology (MARTEC)

DIEZ, M.; CAMPANA, E.F.; STERN, F. (2014), *Design space dimensionality reduction in shape optimization by Karhunen-Loeve expansion*. Comput. Methods Appl. Mech. Eng.

FRIIS, A.M.; ANDERSON, P.; JENSEN, J.J. (2002), *Ship design (Part 1 & II)*, DTU, Lyngby

HUANG, F.X.; KIM, H.Y; YANG, C. (2014), *A new method for ship bulbous bow generation and modification*, 24th Int. Ocean and Polar Eng. Conf., Busan

HOLLAND, J.H. (1975), *Adaptation in Natural and Artificial Systems*, Univ. of Michigan Press

JACQUIN, E.; DERBANNE, Q.; BELLEVRE, D.; CORDIER, S.; ALESSANDRINI, B.; ROUX, Y. (2004), *Hull form optimisation using free surface RANSE solver*, 25th Symp. Naval Hydrodynamics, St.John's

JEONG, S.K.; KIM, H.Y. (2013), *Development of an Efficient Hull Form Design Exploration Framework*, Hindawi Publishing Corporation, Mathematical Problems in Engineering

KANG, J.Y.; LEE, B.S. (2010), *Computer-Aided Design* 42, pp.970–976

KIM, H. (2012), *Multi-Objective Optimization for Ship Hull Form Design*, George Mason Univ.

KOSTAS, K.V., GINNIS, A.I.; POLITIS, C.G.; KAKLIS, P.D. (2014), *Ship-Hull Shape Optimization with a T-spline based BEM-Isogeometric Solver*, Comput. Methods Appl. Mech. Eng.

KONAK, A.; COIT, D.W.; SMITH, A.E. (2006), *Multi objective optimisation using GA_tutorial*, Reliability Engineering and System Safety

KOZIEL, S.; YANG, X.S. (2011), *Computational Optimization, Methods and Algorithms*, Springer

NOWACKI, H. (1996), *Hydrodynamic design of ship hull shapes by methods of computational fluid dynamics*, Progress in Ind. Math. at ECMI , pp. 232-251

PARK, D.W.; CHOI, H.J. (2013), *Hydrodynamic Hull Form Design Using an Optimization Technique*, Int. J. Ocean System Engineering 3(1), pp.1-9

PAPANIKOLAOU, A. (2014), *Ship design- Methodologies of preliminary design*, Springer

PÉREZ, F.; SUAREZ, J.A.; CLEMENTE, J.A.; SOUTO, A. (2007), *Geometric modelling of bulbous bows with use of non-uniform rational B-spline surfaces*, J. Mar. Sci. Techn. 12, pp.83-94

PERI, D.; CAMPANA, E.F.; KANDASAMY, M.; WAAL, N. de (2009), *Potential flow based optimization of a high speed, foil-assisted, semi-planning catamaran for low wake*, 10th Int. Conf. Fast Sea Transportation (FAST), Athens

PERI, D.; TINTI, F. (2012), *A multistart gradient-based algorithm with surrogate model for global optimization*, Communications in Applied and Industrial Mathematics

POLONI, C.; PEDIRODA, V., (2003), *Genetic algorithm- basics, multi-criteria optimization and constraints handling*, OPTIMISTIC-Optimization in Marine Design, Berlin

PERIVAL, S.; HENDRIX, D; NOBLESSE, F. (2001), *Hydrodynamic optimization of ship hull forms*, Applied Ocean Research 23, pp.337-355

SAHA, G.K.; SARKER, A.K. (2010), *Optimisation of ship hull parameter of inland vessel*, Int. Conf. Marine Technology, Dhaka

SUZUKI, K.; KAI, H.; KASHIWABARA, S. (2005), *Studies on the optimization of stern hull form based on potential flower solver*, J. Mar. Sci. Techn., 10, pp.61-69

TAHARA, Y., SUGIMOTO, S.; MURAYAMA, S.; KATSUI, T.; HIMENO, Y. (2003), *Development of CAD/CFD/optimizer integrated hull form design system*, J. Kansai Soc.

TAHARA, Y.; PERI, D.; CAMPANA, E.F.; STERN, F. (2011), *Single and multiobjective design optimization of fast multihull ship*, J. Mar. Sci. Techn.

TAHARA, Y.; TOHYAMA, S.; KATSUI, T. (2006), *CFD based multiobjective optimization method for ship design*, Int. J. Numerical Methods in Fluids 52, p.28

ZELINKA, I.; SNASEL, V.; ABRAHAM, A. (2013), *Handbook of Optimization- From Classical to Modern Approach*, Springer

ZHA, R.S.; YE, H.X. ; SHEN, Z.R.; WAN, D.C. (2014), *Numerical study of viscous wave making resistance of ship navigation in still water*, J. Marine Sci. Appl. 13, pp.158-166

Autonomous COLREGs Compliant Ship Navigation, Using Bridge Simulators and an Unmanned Vessel

Jesus Mediavilla Varas, Walter Caharija, Renny Smith, Lloyd's Register, Southampton/UK,
jesus.mediavillavaras@lr.org

Zakirul Bhuiyan, Southampton Solent University's Warsash Maritime Academy, Warsash/UK,
zakirul.bhuiyan@solent.ac.uk

Wasif Naeem, Queen's University Belfast, Belfast/UK, w.naeem@qub.ac.uk

Paul Carter, Ian Renton, Atlas Elektronik UK, Winfrith Newburgh/UK,
paul.carter@uk.atlas-elektronik.com

Abstract

This paper presents an approach to COLREGs compliant ship navigation. A system architecture is proposed, which will be implemented and tested on two platforms: networked bridge simulators and at sea trials using an autonomous unmanned surface vessel. Attention is paid to collision avoidance software and its risk mitigation.

1. Introduction

As a result of rapid progress made in hardware (e.g. computer, sensors, and satellite communications) and software (e.g. autonomous navigation) in the last decades, we are witnessing the take-off of autonomous systems in a number of industries, from driverless cars, to flying unmanned aerial vehicles (i.e. drones). Autonomous systems and robotics have been identified as one of the top 8 technologies with disruptive potential, *Willets (2013)*. Despite the maritime industry being traditionally conservative, we are also seeing different types of autonomous system prototypes and operational systems, either underwater, on the surface, crawlers, or in the air. Their applications range from asset inspection, ocean exploration, unmanned mine hunters, etc. Now, the industry is gearing towards smart ships, and commercial and naval autonomous ships are being considered, *Rødseth and Burmeister (2012)*. The GMTT2030 report, <http://www.lr.org/gmtt2030>, discusses the technologies that will make an impact in the future maritime industry. Those include autonomous systems (and hence autonomous ships), and other relevant technologies such as smart ships, sensors, robotics, communications and big data. The drivers for autonomous ships are several, the most important of which are:

- i) Safety - Studies have shown that accidents at sea are greatly caused by human errors, *IMO (2004)*. The continuous reduction in ship manning and increase in automation, especially in navigation tools, puts high demands on the crew, leading to fatigue and then human errors, *Hetherington et al. (2006)*. Human errors and wrong interpretation of the rules are responsible for many of the collision accidents *Mohović et al. (2015)*. Autonomy and autonomous navigation in particular, will contribute to reduce human errors, by offloading the crew from some of their highly demanding tasks and enforcing rules compliance, thus increasing maritime safety.
- ii) Financial - Autonomous ships, with less or no manning, will reduce operational costs. Although investment and shore costs might be higher.
- iii) Social - Autonomous ships will compensate for the scarcity of sufficiently qualified seafarers.

Autonomy is the degree of decision making deferred from the human to the system and is a continuum or spectrum rather than being binary in nature. Autonomy levels range from remotely operated to fully autonomous systems. Note that the terms unmanned and autonomous ships are often interchanged, but they are not the same. An unmanned vessel could be remotely operated, and it's therefore not autonomous; while an autonomous ship could be manned. Autonomous navigation is one important step towards ship autonomy, but there are additional tasks carried out by the crew, e.g. maintenance, cargo-handling.

This paper discusses the work being done in the MAXCMAS (“MAchine eXecutable Collision regulations for Marine Autonomous Systems”) collaborative research project, which aims at developing robust COLREGs (International Regulations for Preventing Collisions at Sea, *IMO* (1972)) compliant machine executable autonomous navigation. COLREGs are the “rules of the road” defined by the International Maritime Organization (IMO) which provides a set of rules to prevent collisions between two or more vessels. The project consortium consists of Rolls Royce (RR) as project lead, Atlas Elektronik UK (Atlas), Southampton Solent University’s Warsash Maritime Academy (WMA), Queen’s University Belfast (QUB) and Lloyd’s Register (LR). The partners bring their technical expertise in a number of relevant areas: RR in systems engineering, vessel and equipment expertise; Atlas in control system integration, simulation and at-sea testing, naval vessel design and unmanned systems design; WMA in high fidelity simulation, seafaring expertise and human factors; QUB in unmanned systems R&D, navigational decision making and machine cooperative behaviour; and LR in risk management, assurance, dissemination and cost-benefit analysis. The project is at an early phase, and only the approach will be discussed here.

2. System architecture and requirements

Fig. 1 shows the system architecture. It combines sensors and data fusion, autonomy software (also known as autonomy executive), a collision avoidance algorithm, and a controller interface, into two platforms:

- i) a networked bridge simulator environment, that will allow testing the system under a number of collisions scenarios, with autonomous, as well as manned vessels of different types, varying weather conditions, including poor visibility;
- ii) the ARCIMS USV mine hunter, where the system will be tested during actual sea trials in a controlled environment. <https://www.atlas-elektronik.com/what-we-do/mine-warfare-systems/arcims/>

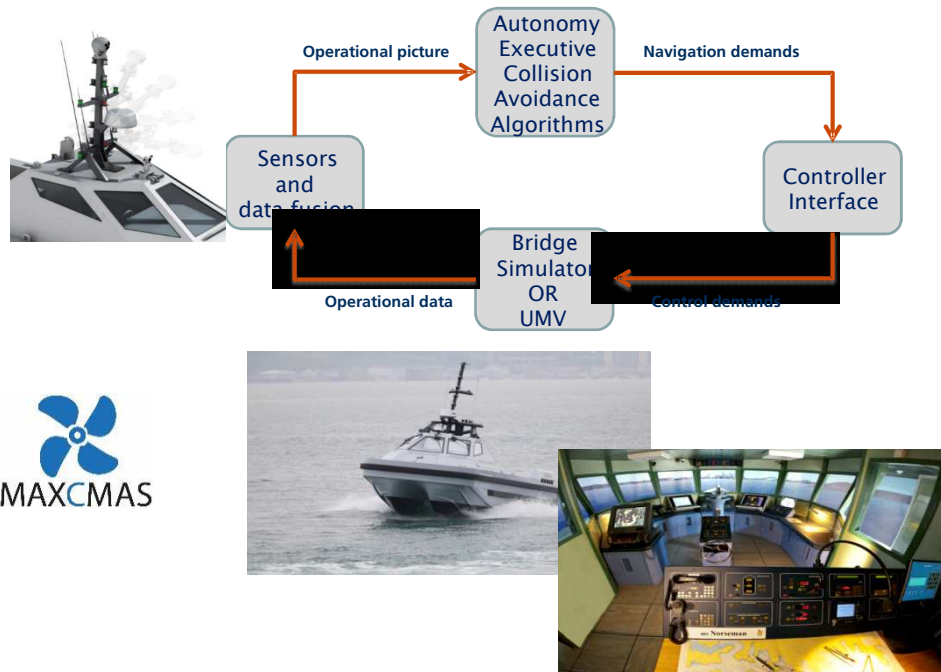


Fig. 1: MAXCMAS system architecture: (top-left) ARCIMS sensors; (bottom-right) Warsash bridge simulator; (bottom-left) ARCIMS USV

Autonomous navigation relies on data obtained from sensors (radar, electro-optic cameras and AIS) about the vessel environment, and data about the own vessel status. The data is combined using data

fusion techniques, giving an operational image. The environmental information, together with the own vessel data (speed, engine status, etc), is passed to the autonomy executive/collision avoidance algorithm, which then translates it into navigational demands (speed, heading). The controller interface translates it into throttle/rudder demands for the vessel (simulated or real).

System requirements have been defined in order to comply with COLREGs and good seamanship practice. A significant challenge is to translate the COLREGs (41 rules and 4 annexes), which were written for human consumption, into requirements for autonomous vessels, in the form of state of the art collision avoidance algorithms and sensors. In total more than one hundred requirements have been derived. For example, Rule 5 states “Every vessel shall at all times maintain a proper look-out by sight and hearing as well as by all available means appropriate in the prevailing circumstances and conditions so as to make a full appraisal of the situation and of the risk of collision”. Compliance with Rule 5 for an autonomous vessel has implications in terms of requirements for the sensors, sensor processing system, picture compilation and collision avoidance. Similarly other requirements are derived by compliance with the other COLREG rules. Additional requirements are imposed on the system, e.g. the collision avoidance system should be scalable from small to large vessels of varying manoeuvring capabilities.

3. Path planning and collision avoidance

Typically a collision avoidance system consists of a risk assessment unit, a decision maker and a path planner. At the start of navigation, a mission is planned consisting of a predefined set of waypoints, based on a known map of an environment. Risk is assessed regularly and/or whenever a target ship is detected in the vicinity by the on-board obstacle detection module, Fig. 2. The mission plan is updated by the path planner should a risk be deemed to exist.

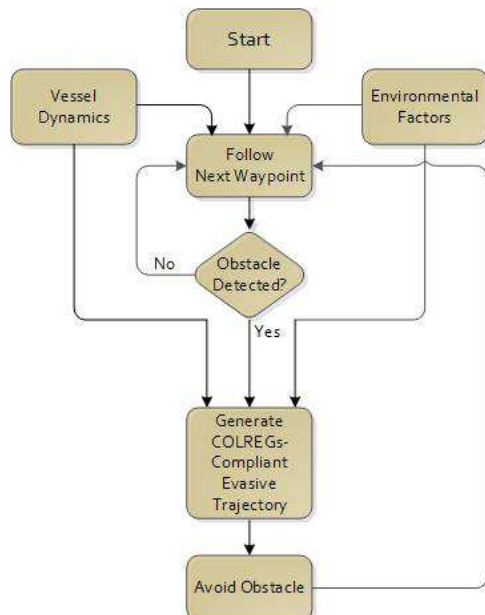


Fig. 2: Flowchart of a generic COLREGs-based path planner

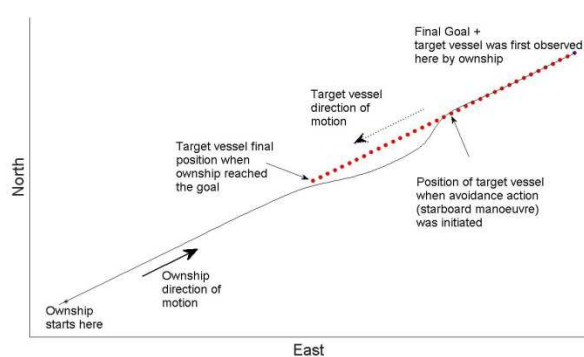


Fig. 3: Own ship trajectory showing successful head-on collision avoidance

The risk assessment primarily works on the principle of estimating the closest point of approach (CPA) which is defined as an estimated point at which the distance between two ships, of which at least one is in motion, will reach its minimum value. It is assumed that vessels will continue their current speed and heading. Assessing risk through estimating the CPA or to be precise TCPA (time to CPA) is a commonly employed method by mariners. For multiple target vessels in low traffic areas, it is usual to consider the risk sequentially meaning that the vessel with the lowest TCPA will be dealt

with first. For an autonomous vessel, however, the challenge is to decide an appropriate course of action once a risk is deemed high or when multiple COLREGs apply.

A software-based decision maker plays a key role in automating a collision avoidance system. The functions of a decision maker include but are not limited to deciding whether a course of action (change of course or speed) is needed; what COLREGs rule (if any) is applicable; and whether multiple COLREGs would apply.

As shown in Fig. 2 a vessel normally follows waypoints from her navigational plan and only deviates from the path when a risk of collision is confirmed. It is important that the evasive path is COLREGs-compliant so that the own-ship behaves in a ‘human-like’ manner which would not cause any confusion or concerns for target ships in the vicinity. A rule-based repairing A* (RR-A*) algorithm was developed earlier, *Campbell et al. (2012)*, to handle the three fundamental COLREGs rules including head-on, crossing and overtaking scenarios. A head-on situation is illustrated in Fig. 3 where an own-ship undertakes a starboard manoeuvre (COLREGs Rule 14) in order to avoid colliding with an on-coming vessel. Note that although the target ship does not adhere to COLREGs by altering course to starboard, the own vessel must follow the collision regulations at all times.

4. Bridge simulator trials

The simulation tests will be performed using a network of six highly immersive bridge simulators at WMA (Warsash Maritime Academy Warsash Maritime Academy), conventionally used for mariner training. These will be employed to demonstrate the human reaction from the crew of a virtual vessel encountering a synthetic autonomous vessel. The autonomous ship mechanism, Fig. 1, will be installed in one of the conventional bridges. This synthetic autonomous vessel may interact with one or more manned bridge simulators, and/or other simulated target ships following predefined routes.

The simulator experiments will be run in a series of sessions, the results of which will allow refining the collision avoidance algorithm and verifying that the system requirements are met (Section 2). A variety of scenarios will be designed ranging from basic level single vessel encounters to more complex level multi-ship situations and these will be included in a simulator protocol to ensure all scenarios are run consistently. With this aim in mind, the MAXCMAS scenarios have been categorised into the following 5 levels:

- i) Basic: Open water exercises involving encounters with one or two target ships.
- ii) Intermediate: Exercises involving multi-ship encounters when approaching a coastline or other navigational hazard from open waters.
- iii) Advanced: Intensive exercises involving the approaches to and passage through areas of heavy traffic with navigational restrictions.
- iv) Good seamanship: Ordinary good practice of seamen with due regard to the application and observance of COLREGs which may be required while navigating a ship.
- v) Breakdown: Navigation during an emergency situation and sensor degradation.

Together with this particular autonomous bridge, there will be test runs by one or two manned bridges. These simulated manned bridges could be combined with either target ships or run in parallel with the autonomous ship so that manned vessel(s) and autonomous vessel encounter the same challenges in similar environmental conditions. The experiments can be potentially progressed up to 5 manned bridges to develop very complex scenarios to comply with the test requirements. However, the real challenge will be the implementation of the safety measures which may be required by good seamanship practice i.e. to avoid any navigational danger during any special circumstances. As it is known a good level of seamanship may be needed for the practical application of the COLREGs and it is normally gained through training and long experience. Seamanship is a huge challenge for developing the machine interpretation algorithms, and feedback from experienced mariners will be obtained by means of questionnaires. A full interaction of weather conditions will be introduced in these scenarios, in different simulated operating areas (Portland Harbour, UK; and San Francisco Bay,

USA) and different own-ship models, with emphasis on understanding their handling. During the scenario trials, every vessel will use common sensors (e.g. gyro, AIS, GPS, radar) and these driving sensors will initially test the algorithms using noise-free sensor information and later the scenarios will be tested with the degraded sensor(s).

The minimum qualifications of personnel on the manned bridges will be navigating officers holding at least the OOW CoC (Officer of Watch Certificate of Competency) in the Level 1 & 2 scenarios and the Chief Mate/Master in Level 2 to 5 scenarios. Potentially both subjective (e.g. performance criteria) as well as objective assessment criteria (e.g. weighted scoring of CPA/TCPA, variables, track parameters) for each scenario will be developed and included in the simulator protocol. The objectives of such a methodology are to empower the structured evaluation of simulator recorded scenario performances against the benchmark criteria/scores.

5. USV sea trials

The sea trials will be done using the 11m ARCIMS USV platform (designed and owned by Atlas Elektronik UK), equipped with the autonomy system described in Fig. 1. Sea tests will be coordinated from the Bincleaves waterfront facility at Portland Harbour, Dorset (UK). The USV sea trials, along with both desktop and Warsash based simulator trials, will serve to verify the system requirements, in a controlled sea environment and three different setups.

- (i) Mixed reality. In “mixed reality” testing, the real vehicle will be used on the water for the first time, but all its collision avoidance targets remain simulated. This will allow the real vehicle dynamics to be tested, and conclusions drawn about how representative of them the software simulation models were. Targets will be added to the system by an operator, and the vehicle will avoid them in open water so that it won’t (at this stage) need to operate in close quarters with any other vessels.
- (ii) Real target with perfect knowledge. The next step is to introduce a real vehicle (or several) as avoidance targets. This will verify that the avoidance still works correctly when the targets move in non-idealized ways (e.g. bobbing back and forth, not following straight lines). Each target boat will be tracked with a GPS receiver and a communications link to the ARCIMS USV, so the avoidance algorithm has “perfect knowledge” of the target position, course and speed.
- (iii) Platform full sense and avoid tests. The final step is to use the sensors on the ARCIMS platform. The sensors will also be independently tested in parallel to ensure they perform as expected and produce reliable, usable track outputs. The USV will then avoid the target boats and static targets using its own sensor capability. A wide variety of real-world scenarios will be demonstrated to ensure the vehicle behaves correctly under the many different circumstances it could encounter.

Tests will be performed against static and moving vessels in overtaking, head-on and crossing encounters in which the autonomous vessel is the give way and stand-on vessel and the encountered vessel acts as expected and otherwise. These scenarios can be tested for multiple moving and static targets in open water and where a coast line bounds the available space to manoeuvre. For the purposes of the MAXCMAS project the bounded scenarios will be limited to the water space at Portland Harbour (where ARCIMS platform testing will occur) and San Francisco Bay (desktop simulations), as in the bridge simulator tests (Section 4).

6. Risk mitigation and software assurance

Collision avoidance performs a safety related function since its ultimate goal is to avoid incidents that may result in loss of life, asset damage and pollution. Successful collision avoidance can be achieved if several safety barriers are put in place encompassing operational as well as technological aspects. This is shown in Fig. 4, where each layer represents one or several elements that may prevent the occurring of a collision scenario and hence mitigate risk. The highest layer highlights the fact that

thorough mission and navigation planning before the commencement of the mission is fundamental since it will identify potential threats such as busy shipping lanes, shallow waters and isolated obstacles in advance. Mid layers such as observers and real time re-planning algorithms, i.e. collision avoidance system, come subsequently, since their role is to continuously analyse the situational awareness picture, identify potential collisions situations and rearrange the route accordingly, while the mission is already underway. The lowest layer is the ultimate collision avoidance measure, one or several very reactive manoeuvres, which have to be identified and executed if the above safety barriers have been breached.

Highest layer: initial mission and navigation planning
Mid layers: real time re-planning (e.g. collision avoidance system)
Lowest layer: very reactive emergency/evasive manoeuvres and procedures (e.g. stop or full ahead)

Fig. 4 Layers or safety barriers for collision avoidance

In the context of autonomous navigation, the mid and lowest layers are done by the system without human intervention, while the highest layer would normally still be done by a person. The scope of the MAXCMAS project is the mid layer. The observers are the sensors, and real time re-planning is done autonomously following the principles of safe navigation described by the COLREGs, as described earlier (Section 3). However, all the appropriate risk mitigation measures categorized in Fig. 4 have to be identified in addition to the real time re-planning (collision avoidance) system to define a complete risk picture and assign, if necessary, any requirements to each identified layer. To this end, the following actions will be taken: system architecture analysis, functional failure analysis (FFA), software assurance and identification of relevant collision scenarios. The analysis of the system architecture includes a high level evaluation of the re-planning algorithm and represents a valuable preparation activity for the FFA session. The scope of the FFA session is to identify and categorize all the relevant functional failure modes of the collision avoidance system and their subsequent consequences on safety aspects. As a result, specific safety requirements are defined and set on parts of the system as well as operational aspects such as sea state limitations or abort mission circumstances. The re-planning algorithm is a key component of the collision avoidance system and hence the safety requirements may result in software quality requirements set upon the re-planning as well as other key software components identified during the FFA. In order to meet these requirements, the collision avoidance software will be developed following best software assurance standards. Even though no specific standards has been chosen, the principles set by standards such as the IEC 61508-3 (process industry), the EN 50128 (railway) and the IEC 62061 (safety of machinery) will be applied. These principles may include, for instance, the V-model for software development. Finally, relevant collision scenarios will be identified, from historical reviews of incidents as well as discussions with experienced seafarers for simulation and testing purposes; and to assess the risk of collision at sea in autonomous ship navigation.

7. Conclusions

This paper has discussed our MAXCMAS approach to COLREGs compliant autonomous navigation. The system will be implemented, tested and validated later in the project, on two platforms: bridge simulators and the ARCIMS USV during sea trials. For this purpose, a number of scenarios will be tested, which will serve to prove that the requirements derived from the COLREGs and good seamanship practice are met. The scenarios will have different levels of complexity, including multi-vessel encounters, areas of heavy traffic and difficult manoeuvrability and emergency situations. Simulation testing has a number of advantages over real tests, allowing us to try many different cases under repeatable environmental conditions, in an inexpensive, fast and realistic way. Further validation will be done with the ARCIMS USV trials in a controlled sea environment, which will be tested in different encounter scenarios and three different setups, i.e. mixed reality, real targets with perfect knowledge, and real targets with limited knowledge from the USV's sensors. Emphasis has been placed on the risk identification and mitigation, including the development of the collision avoidance software following the software assurance best practices.

The project partners aims at commercializing the MAXCMAS technology. A number of applications and markets have been identified:

Unmanned Surface Vehicles

- A0. Its first direct application will be to improve the autonomous navigation capability of the ARCIMS USV. The technology could be applied to the fast growing market of USV in various marine industries, such as defence, offshore, ocean exploration and shipping (e.g. ship inspection with USVs).

Commercial and naval ships

- A1. A short term potential application of this technology would be provide assistance to the officer of the watch (OOW), by giving route recommendations to avoid collision, integrated in either ECDIS or Integrated Navigation System, alongside an obstacle detection warning system.
- A2: A second application of MAXCMAS would be for autonomous navigation under human supervision, like a smart COLREGs compliant track-pilot with collision avoidance capabilities. The OOW would be on stand-by and could intervene when deemed necessary. These two applications would contribute to improving safety of ships by reducing human errors. The drawback is that there would not be operational savings, since the level of manning would still be the same.
- A3: Another potential application, and where the potential economic benefits could be greater, is on unmanned ships, however many challenges remain to be solved.

Rules, standards and certification

- A4. MAXCMAS offers the opportunity to better understand the technologies and the risks and mitigation measures associated with autonomous vessels and autonomous navigation in particular. This will allow developing and improving rules and standards necessary for the certification of USVs and autonomous ships, to guarantee their safe operation.

Unmanned ship navigation poses many challenges: technological, regulatory, social, legal, etc. From a technology view point, unmanned ships will require all crew traditionally performed by the crew, e.g. navigation, maintenance, cargo-handling, berthing, will be done autonomously, for example with the use of robotic systems, <http://www.lr.org/gmtt2030>, or automatically. Stakeholders, such as ship owners, regulators, society, seafarers, will oppose the unmanned ship, if their perceived risk (in terms accidents, jobs losses, and other undesirable consequences) is greater than its potential benefits (e.g. economic savings). The economic argument for unmanned ships, including their risk cost, is being investigated as part of the project.

In the short to medium term, it is expected that small steps in the “autonomy ladder”, and applications like S0-S2, are likely to occur. These will provide smart ships with greater autonomy, making them smarter, while the future of unmanned ships will need further research and convincing.

Acknowledgments

We would like to thank you all the MAXCMAS partners: Atlas Elektronik UK, Southampton Solent University’s Warsash Maritime Academy, Queen’s University Belfast, Rolls Royce, and Lloyd’s Register, for their contributions to the project, and enthusiasm, and especially to Rolls Royce’s Dr. Eshan Rajabally for leading us. This project would have not been possible without the support of Innovate UK, under grant number 50121-378137, which is greatly acknowledged.

References

- CAMPBELL, S.; NAEEM, W. (2012), *A Rule-based Heuristic Method for COLREGs-compliant Collision Avoidance for an Unmanned Surface Vehicle*, 9th IFAC Conf. Manoeuvring and Control of Marine Craft, Arenzano, pp. 386-391
- CAMPBELL, S.; NAEEM, W.; IRWIN, G. (2012), *A Review on Improving the Autonomy of Unmanned Surface Vehicles through Intelligent Collision Avoidance Manoeuvres*, Annual Reviews in Control, pp. 267-283
- HETHERINGTON, C.; FLIN, R.; MEA, K. (2006), *Safety in shipping: The human element*, J. Safety Research 37/4, pp.401-411
- IMO (1972), *International Regulations for Preventing Collisions at Sea*, International Maritime Organization, London
- IMO (2004), *Casualties statistics and investigations - Very serious and serious casualties for the 2001*, International Maritime Organization, London
- MOHOVIĆ, D.; ROBERT, M.; MATE, B. (2015), *Identifying skill gaps in the knowledge and teaching of COLREGs*, 17th Int. Conf. on Transport Science, Portoroz
- RØDSETH, Ø. J.; BURMEISTER, H.C. (2012), *Developments toward the unmanned ship*, Int. Symp. Information on Ships (ISIS), Hamburg
- WILLETS, D. (2013), *Eight great technologies*, Policy Exchange, London
<http://www.policyexchange.org.uk/images/publications/eight%20great%20technologies.pdf>

Guided Underwater Survey Using Semi-Global Visual Odometry

Mohamad Motasem Nawaf, Bilal Hijazi, Djamal Merad, Pierre Drap, Aix Marseille Université, Marseille/France, {Mohamad.Motasem.Nawaf,Bilal.Hijazi,Djamal.Merad,Pierre.Drap}@univ-amu.fr

Abstract

This paper presents a real-time visual odometry method adapted to long autonomy underwater surveys. A fast pose estimation procedure is followed by a semi-global optimization using bundle adjustment. Particularly, we propose a new approach to approximate the uncertainty for each estimated relative pose based on machine learning manifesting on simulated data. Neighboring observations used for the semi-global optimization are established based on a probabilistic distance in the estimated trajectory map. This helps to find the frames with potential overlaps with the current frame while being robust to estimation drifts. Our method is tested on several sorts of sites including a newly discovered shipwreck. The obtained results demonstrate the efficiency in terms of accuracy w.r.t. to local approaches, and the gain in processing time and the used resources w.r.t. global methods.

1. Introduction

In the context of underwater archaeological sites surveys, *Drap* (2012), such as wrecks or remains of artifacts (an example is shown in Fig.1), mobile underwater vehicles are used to scan these sites in order to capture images. These images are then analyzed to obtain several information as well as producing 3D models using photogrammetry techniques, *Drap* (2012), *Bythell et al.* (2001), *Green et al.* (2002). A main problem faced in this scenario is to make sure to cover the full site before ending the mission. The full coverages insures obtaining complete 3D models and reducing the mission cost as no further exploitation is needed. In our work, we propose to guide the survey based on a visual odometry approach *Nistér et al.* (2004). The target hardware is a remotely operated underwater vehicle (ROV) equipped with a stereo camera setup and an embedded computer. Another computer is located at the surface is used to interact with the ROV. Within this configuration, the captured stereo images are used to compute the relative motion that the vehicle undergoes. However, a strong constraint on the adopted method is due to the size and power consumption restrictions of underwater equipment. The embedded computer is responsible for the image acquisition and storage, leaving limited computational resources for the visual odometry computation.

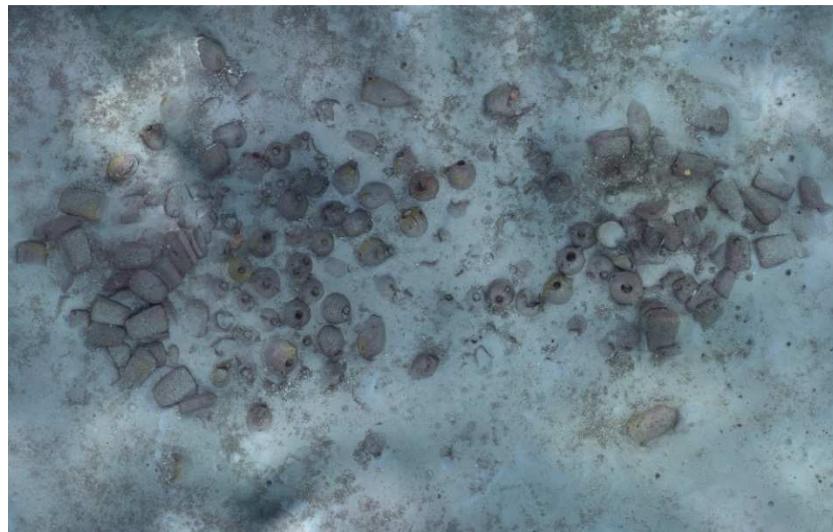


Fig.1: Orthophoto of the newly discovered underwater site, which shows a Phoenician shipwreck named Xlendi located near Malta, *Drap et al.* (2015).

In this context, a traditional approach to compute visual odometry based on image quadruplets (two distant captures of a stereo image pair) suffers from rotation and translation drifts that grows with time *Kitt et al. (2010)*. The same effect applies to the methods based on local Bundle Adjustment (BA) *Mouragnon et al. (2009)*. In contrary, the solutions that are based on using features from the entire image set, such as global BA *Triggs et al. (2000)*, requires more computational recourses which are very limited in our case. Similarly, the simultaneous localization and mapping (SLAM) approaches *Thrun et al. (2005)*, which are known to perform good loop closure, are highly computationally intensive especially when complex particle filters are used *Montemerlo and Thrun (2007)*. So they can only operate in moderately sized environments if real-time processing is needed.

In our solution, we benefit from the fact that the survey is performed in a structured manner, generally, a line by line (S-shape) or spiral scanning. In both cases, the new images are more likely to be captured at the boundaries of the scanned area. Our idea is to maintain a rough coverage map where we keep the information related to the estimated pose. So it is possible to create a sub-region of neighboring observations for the pose being currently estimated. This sub-set can be used in an optimization phase. This will reduce the complexity of the problem, while having the advantages of a global approach by having loop closures, which corrects the drifts in odometry estimations assuming overlaps between current and previous trajectories. This approach is simple to achieve in deterministic environment, or when trajectory measurements are expressed by identity covariance matrix scaled by some factor. In this later case, a simple Euclidean distance is enough to find overlapping frames and construct active regions to be optimized. However, the noise associated to the relative pose estimation is not equal in all directions, which will be shown later. In our work, we propose a solution to model pose estimation noise and maintain probabilistic map, at each point the pose is represented by a Gaussian distribution whose covariance matrix can be of full degrees of freedom (DOF). In this context, any statistical divergence can be used to measure the distances between poses. For instance, we use Bhattacharyya distance for this purpose.

The proposed method consists of three processes; first, a traditional pose estimation for image quadruplets which computes one step of relative motion based on extracted feature points. Second, a map of coverage that represents the scanned areas is updated at each step. Based on this map we can know the closest frames to the current one. Third, a semi-global structure and motion BA is used to reduce the re-projection error and correct the drifts, using only features points from a subset of frames. Moreover, to deal with the limited resources problem, we distribute the computations tasks so that only the feature extraction phase is performed on the embedded computer whereas the surface computer is responsible for the rest of the pipeline.

2. Background

Estimating ego motion of a mobile vehicle is an old problem in computer vision. Two main categories of methods are developed in parallel, namely; simultaneous localization and mapping (SLAM) *Davison (2003)*, and visual odometry *Nistér et al. (2004)*. In the following we highlight the main steps for both approaches as well as hybrid solutions trying to combine their advantages.

SLAM family of methods uses probabilistic model to handle vehicle pose, although this kind of methods is developed to handle motion sensors and map landmarks, they work efficiently with visual information solely. In this case, a map of the environment is built and at the same time it is used to deduce the relative pose, which is represented using probabilistic models. Several solutions to SLAM involve finding an appropriate representation for the observation model and motion model while preserving efficient and consistent computation time. Most methods use additive Gaussian noise to handle the uncertainty which imposes using extended Kalman Filter (EKF) to solve the SLAM problem *Davison (2003)*. In case of using visual features, computation time and used resources grows signifi-

cantly for large environments. A remarkable improvement of SLAM is the FastSLAM approach *Montemerlo and Thrun* (2007) which improves largely the scalability, it uses recursive Monte Carlo sampling to directly represent the non-linear process model, although the state-space dimensions are reduce using Rao-Blackwellisation approach *Blanco et al.* (2008), the method remains not scalable to long autonomy. In the context of long trajectories, several solutions are proposed to handle relative map representations such as *Eade and Drummond* (2008), *Davison et al.* (2007), *Piniés and Tardós* (2007). In particular, by breaking the estimation into smaller mapping regions, called sub-maps, then computing individual solutions for each sub-map. The issues with this kind of approaches arise in sub-mapping creation, overlapping, fusion of sub-maps and map size selection, especially in our context where the S-shape scanning causes very frequent sub-maps switches, which is time consuming. In all reviewed SLAM methods, the measurement noise is modeled by diagonal covariance matrix with equal values that are set empirically for the case of using pure visual information. This modeling leads to produce spherical measurement uncertainty (though estimated pose has an associated full DOF uncertainty) in 3D when using only visual features. This does not approve with practical cases where uncertainty is not spherical. Although there exist several works in literature that studied the uncertainty of 3D reconstructed points based on their distance from the camera and the baseline distance between frames, such as in *Eade and Drummond* (2006) and *Montiel et al.* (2006), the effect of the relative motion parameters on the uncertainty of the pose estimation have not been taken into account. For a complete review for SLAM methods we refer the reader to *Bailey and Durrant-Whyte* (2006).

From another side, visual odometry methods uses structure from motion methodology to estimate the relative motion *Nistér et al.* (2004). Based on multiple view geometry fundamentals *Hartley and Zisserman* (2004), approximate relative pose can be estimated, this is followed by a BA procedure to minimize re-projection errors, which yields in improving the estimated structure. Fast and efficient BA approaches are proposed simultaneously to handle larger number of images *Lourakis and Argyros* (2009). However, in case of long time navigation, the number of images increases dramatically and prevent applying global BA if real time performance is needed. Hence, several local BA approaches have been proposed to handle this problem. In local BA, a sliding window copes with motion and select a fixed number of frames to be considered for BA *Mouragnon et al.* (2009). This approach does not suit S-Type motion since the last n frames to the current frame are not necessarily the closest. Another local approach is the relative BA proposed in *Sibley et al.* (2009). Here, the map is represented as Riemannian manifold based graph with edges representing the potential connections between frames. The method selects the part of the graph where the BA will be applied by forming two regions, an active region that contains the frames with an average re-projection error changes by more than a threshold, and a static region that contains the frames that have common measurements with frames in active region. When performing BA, the static region frames are fixed whereas active region frames are optimized. The main problem with this method is that distances between frames are metric, whereas the uncertainty is not considered when computing inter-frames distances.

3. Semi Global Visual Odometry

The relative visual odometry approach represents a good solution for long term autonomy. This kind of approaches deals with selected region of the map at a time, the aim is to reduce computation time for a new pose. In particular, given a set of stereo frames resulting from camera trajectory. For a new frame at time t , relative pose is estimated w.r.t frame $t - 1$. Moreover, a selection of frames within certain diameter is performed. These frames are assumed to have the largest potential overlap with the current frame. Using these frames, BA is performed to optimize the trajectory. As we have seen earlier, most of proposed methods assume Gaussian noise in all 3D directions with zero covariance, this case is illustrated in Fig. 2 (right). In this context, while searching for nearest frames to be included in the optimization process, the distance d_2 is larger than d_1 both geometrically and statistically. How-

ever, having full covariance representation for the pose, for instance, as shown in Fig. 2 (left), geometrical/Euclidean distance measure is no more appropriate. Since visual odometry approach suffers from drifting. It is worthy to consider a representative uncertainty measure to find close frames. For instance, given accumulated pose estimation errors, the estimation for X_8 follow the Gaussian distribution illustrated in Fig. 2 (right) where we have larger uncertainty perpendicularly aligned with the motion (Section 3.2 show how to obtain this estimation). Here, any divergence measure would estimate d_2 to be smaller than d_1 , which is more realistic.

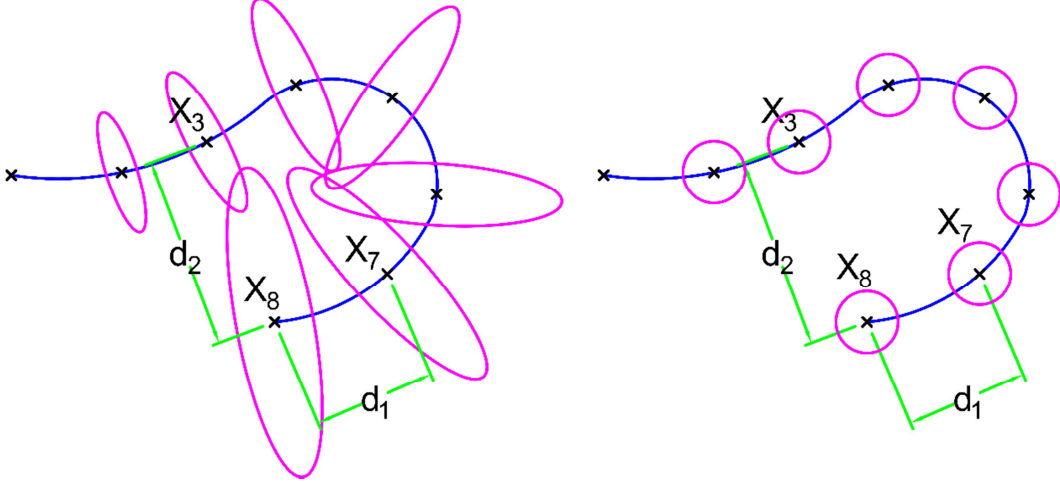


Fig. 2: Example of possible trajectory with uncertainty modelled by full covariance matrix (left), the distance d_2 is statistically estimated to be smaller than d_1 . In contrary, it is the inverse when the noise is modeled with equal variances (right).

In the following, we present our complete visual odometry method, we start by explaining the initial approximate estimation using a traditional approach, then we provide an analysis of pose uncertainty for visual odometry methods. As this cannot be easily formulated, we present a new method which provides such measure based on simulated data using machine learning approach. Our semi-global visual odometry method is then presented, we explain how the environment map is maintained and how the error is propagated along the trajectory. Finally, the selection of the set of local frames and applying BA.

3.1 Initial Relative Pose Estimation

The system relies on stereo cameras already calibrated. So their relative position is known in advance. Both cameras have the same intrinsic parameters matrix K . Given left and right frames at time t (we call them previous frames), our initial visual odometry pipeline consists of three stages; (1) feature points detection and description for every new stereo pair, (2) then feature points matching between two pairs of images; previous left with current left, and previous right with current left, (3) then computing relative motion (up to scale) between the image pairs in step (2), (4) finally we compute correct scale based on the fixed stereo setup.

In details, let $\{f_1 f_2 f_3 f_4\}$ denote the previous left, previous right, current left and current right frames respectively. At a given time, new frame pair is captured (which become current frames f_3, f_4) and we want to compute an initial relative pose estimation with respect to previous frames f_1, f_2 . We consider here the left previous to left current frames $f_1 \rightarrow f_3$ positions to represent the system relative motion. Hence, we start by detecting and describing feature points for f_3 and f_4 , considering the detection and description is already done for f_3 and f_4 in the previous step. At this point, there is a trade-off for choice of the used feature detector and descriptor (for more details we refer to the evalua-

tion study overtaken by *Gauglitz et al. (2011)*). In our implementation, using SIFT features *Lowe (2004)* provides the most accurate trajectory, whereas using SURF *Bay et al. (2006)* we obtain less accurate trajectory while gaining $\sim 40\%$ of computation time. Next, the feature points of f_1 are matched with f_3 , also such of f_2 are matched with f_3 . Using these matches, the corresponding fundamental matrices are computed as F_{13} and F_{23} respectively using RANSAC procedure as described in *Hartley and Zisserman (2004)*. Based on the obtained Fundamental matrices, essential matrices, which embed the rotation and translation parameters, are computed as $E_{13} = K^T F_{13} K$ and $E_{23} = K^T F_{23} K$. Which are in turn decomposed to obtain rotation and translation parameters following the notes in *Nistér (2004)*. Hence, we have $[R_{13}|\bar{t}_{13}]$ and $[R_{23}|\bar{t}_{23}]$, where \bar{t} denote a unit normalized translation vector. This process is illustrated in Fig. 3.

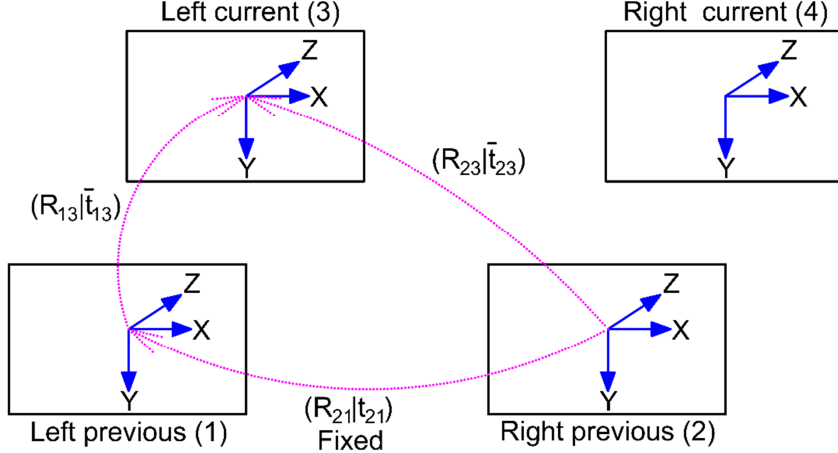


Fig. 3: Image quadruplet, current (left and right) and previous (left and right) frames are used to compute the relative motion using two scaled estimated poses and fixed left-to-right setup.

To recover the scale ambiguity of t_{13} , we benefit from the fixed stereo pair baseline distance t_{21} . Based on the illustrated geometry we can write:

$$s_1 \bar{t}_{23} - s_2 \bar{t}_{13} = t_{21} \quad (1)$$

where s_1 and s_2 are scaling variables, which can be found by solving a linear system of equations. Consequently, we find the final relative pose $t_{13} = s_2 \bar{t}_{13}$, and the overall transformation $[R_{13}|s_2 \bar{t}_{13}]$. This deterministic estimation represents the mean of a probabilistic model to be introduced in the next two subsections.

3.2 Estimated Pose Uncertainty

Like any visual odometry estimation, the estimated trajectory using the method proposed in the previous section is exposed to a computational error, which translates to some uncertainty that grows in time. A global BA may handle this error accumulation, however it is time consuming as explained earlier. From another side, a local BA is a tradeoff for precision and computational time. The selection of n closest frames is done using standard Euclidean distance. Loop closure may occur when overlapping with already visited areas, which in turn enhances the precision. This approach remains valid as soon as the uncertainty is equal in all directions. However, if the uncertainty varies across dimensions, the selection of the closest frames based on Euclidean distance is not trivial. In the following, we are going to prove that it is the case in any visual odometry method. Also, we will provide more formal definition of the uncertainty.

Most visual odometry and 3D reconstruction methods rely on matched feature points to estimate relative motion between two frames. The error of matched features is resulting from accumulating several errors. These errors are due, non-exclusively, to the following reasons; the discretization of 3D points projection to image pixels, image distortion, the camera internal noise, salient points detection and matching. By performing image un-distortion, and constraining the points matching with the fundamental matrix. All the aforementioned errors can be considered to follow a Gaussian distribution; so as their accumulation. This is actually implicitly considered in most computer vision fundamentals *Hartley and Zisserman (2004)*.

Based on the Gaussian error distribution of matched feature points we can prove that the error distribution of the estimated relative pose is not equal among dimensions. Indeed, it can be fitted to a multivariate Gaussian whose covariance matrix has non equal Eigen values as we will see later. Formally, given a number of matched feature points between two frames $m \leftrightarrow m'$. Based on our assumption, each matched point can be represented by a multivariate Gaussian distribution:

$$\mathcal{N}(m, \Sigma) \leftrightarrow \mathcal{N}(m', \Sigma) \quad (2)$$

$$\Sigma = \begin{bmatrix} \sigma^2 & 0 \\ 0 & \sigma^2 \end{bmatrix} \quad (3)$$

The pose estimation procedure relies on the fundamental matrix that satisfies $m'Fm = 0$. Writing $m = [x \ y \ 1]^T$ and $m' = [x' \ y' \ 1]^T$. The fundamental matrix constraint for one matching pair of points can be written as:

$$x'xf_{11} + x'yf_{12} + x'f_{13} + y'xf_{21} + y'yf_{22} + y'f_{23} + xf_{31} + yf_{32} + f_{33} = 0 \quad (4)$$

To show the variance of error distribution of estimated pose, without loss of generality, we consider one example of configuration; identity camera intrinsic matrix $K = \text{diag}(1 \ 1 \ 1)$. Let us now take the case of pure translational motion between the two camera frames, $T = [T_x \ T_y \ T_z]^T$, and $\theta = [\theta_x \ \theta_y \ \theta_z]^T = [0 \ 0 \ 0]$, the fundamental matrix in this case is given as:

$$F = K^{-1} E K^{-1} = K^{-1} [T]_x R K^{-1} = \begin{bmatrix} 0 & -T_z & T_y \\ T_z & 0 & -T_x \\ -T_y & T_x & 0 \end{bmatrix} \quad (5)$$

where $[T]_x$ is the skew-symmetric cross-product matrix of T , and R is the rotation matrix which is the identity in this case. Hence, equation 4 simplifies to:

$$-x'yT_z + x'T_y + y'xT_z - y'T_x - xT_y + yT_x = 0 \quad (6)$$

By using enough matched points (7 points in this case) we can recover the translation vector T by solving a linear system. However, the Gaussian noise whose covariance matrix is expressed by equation 3 will propagate to the variables T_x and T_y , whereas for T_z the error distribution is different due to the product of two variables, where each is a Gaussian distribution. So the covariance is equal to $\Sigma/2$. Moreover, the recovered translation variables are correlated even though the observations are un-correlated. This is due to the usage of least square *Strutz (2010)*. This leads to have the estimated pose follow a Gaussian distribution (proved experimentally in the following) with a full DOF covariance matrix (within the positive semi-definite constraint).

3.3 Pose Uncertainty Modelling

Pose uncertainty is difficult to estimate straightforward. This is due to the complexity of the pose estimation procedure and the number of variables. In particular, noise propagation through two consecu-

tive SVDs (used for Fundamental matrix computation and Essential matrix decomposition). Instead, inspired by the unscented Kalman filter approach proposed in *Wan and Van Der Merwe (2000)*, we proceed similarly by simulating noisy input and try to characterize the output error distribution in this case. This process is illustrated in Fig 4. In our work, we propose to learn the error distribution based on finite pose samples. This is done using a Neural Network approach which fits well to our problem as it produces soft output.

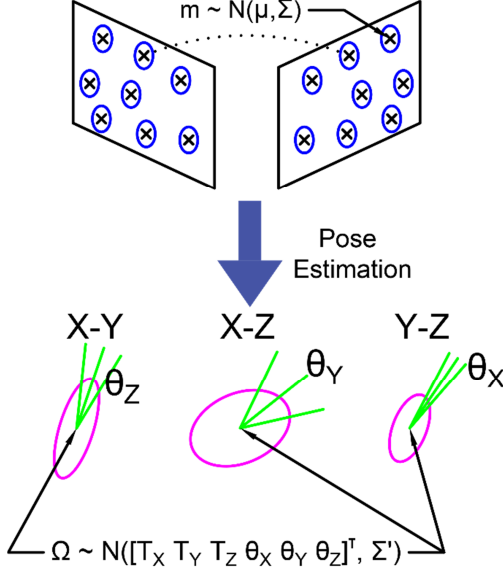


Fig 4: Illustration of error propagation through the pose estimation procedure. Estimated pose uncertainty is shown for each of the 6 DOF. Full covariance matrix can result from diagonal error distribution of matched 2D feature points

There are two factors that play a role in the estimated pose uncertainty. First, the motion $\Omega = [T \theta]^T$ between the two frames expressed by a translation T and a rotation θ , which is explained in the previous section. Second, the 3D location of the matched feature points. Although their location is not computed explicitly in our method, their distance from the camera affects the computation precision.

In particular, the further the points are from the camera the less precise is the estimated pose. This is due to the fact that close points yield larger 2D projection disparity which is more accurate to estimate after the discretization. For instance, in pure translation motion, if all the matched points are within the blind zone of the vision system (yield zero-pixels disparity after discretization), the estimated motion would be equal to zero. In the contrary, it will be more accurate when points are closer. Both mentioned factors are correlated to some point. For instance, given some points in 3D ($n > 7$), the estimated pose precision is a function of their depth, but also to the baseline distance. Hence, considering one factor is sufficient. In our work, we consider the motion as a base to predict the uncertainty.

Formally, given a motion vector $\Omega_j = [T_j \theta_j]^T$, ideally, we want to find the covariance matrix that express the associated error distribution. Being a positive semi-definitive (PSD), such $n \times n$ covariance matrix has unique $(n^2 + n)/2$ entries, where $n = 6$ in our case, this yields 21 DOF in which 6 are the variances. However, learning this number of parameters freely violates the PSD constraint. Whereas finding the nearest PSD in this case distorts largely the diagonal elements (being much fewer). At the same time, we found experimentally that the covariance between T and θ variables is relatively small compared to such of inter T and inter θ . Thus, we propose to consider two covariance matrices Σ_T and Σ_θ . So in total we have 12 parameters to learn, in which 6 are the variances.

For the aim of learning Σ_T and Σ_θ , we have created a simulation of the pose estimation procedure. For a fixed well distributed 3D points $\{X_i \in \mathbf{R}^3 : i = 1..8\}$, we simulate two cameras with known relative

rotation and translation. The points are projected according to both cameras to 2D image points, let us say $\{x_i \in \mathbf{R}^2\}$ and $\{x'_i \in \mathbf{R}^2\}$. These points are disturbed with random Gaussian noise as given by the equations 2 and 3. Next, the 3D relative pose is estimated based on the disturbed points. Let $\tilde{\Omega}_j = [\tilde{T}_j \ \tilde{\theta}_j]^\top$ be the estimated relative motion. Repeating the same procedure (with the same motion Ω_j) produce a motion cloud around the real one. Now, we compute the covariance matrices Σ_T and Σ_θ of the resulting motion cloud in order to obtain the uncertainty associated to the given motion Ω_j . (We increase the number of simulation runs until the output mean is close enough to the input real motion Ω_j , in our case we run the simulation 10000 times for each pose.) Further, we repeat this procedure for a wide range of motion values. (In the performed simulation, we use the range [0-1] with 0.25 step size for each of the 6 dimensions, these values are in radians in case of rotation. This raises up to 15625 test case.) Now, having the output covariance matrices (two for each motion vector Ω_j), we proceed to build a system which learns the established correspondences (motion \leftrightarrow uncertainty). So that in case of new motion we will be able to estimate the uncertainty. This soft output is offered by Neural Networks by nature, which is the reason we adopt this learning method. In our experiments, we found that a simple Neural with single hidden layer *Bishop (1995)* was sufficient to fit well the data. The input layer has six nodes that correspond to motion vector. The output layer has 12 nodes which corresponds to the unique entries in Σ_T and Σ_θ , hence, we form our output vector as:

$$O = [\Sigma_T^{11} \ \Sigma_T^{22} \ \Sigma_T^{33} \ \Sigma_T^{12} \ \Sigma_T^{13} \ \Sigma_T^{23} \ \Sigma_\theta^{11} \ \Sigma_\theta^{22} \ \Sigma_\theta^{33} \ \Sigma_\theta^{12} \ \Sigma_\theta^{13} \ \Sigma_\theta^{23}]^\top \quad (7)$$

where Σ_{ij}^{ij} is the element of row i and column j of the covariance matrix Σ .

In the learning phase, we use a gradient-descent based approach Levenberg-Marquardt backpropagation which is described in *Hagan et al. (1996)*. Further, by using the mean-squared error as a cost function we could achieve around 3% error rate. The obtained parameters are rearranged in symmetric matrices. In practice, the obtained matrix is not necessarily PSD, although this is rare to happen in case of small variances. We proceed to find the closest PSD as $Q\Lambda_+ Q^{-1}$, where Q is the eigenvector matrix of the estimated covariance, and Λ_+ the diagonal matrix of Eigenvalues in which negative values are set to zero.

After determining the error distribution arising with a new pose, it has to be compounded with propagated error from the previous pose. Similar to SLAM approach, we propose to use a “Kalman filter” like gain which allows controllable error fusion and propagation. Given an accumulated previous pose estimation defined by $\{\Omega^p, \Sigma_T^p, \Sigma_\theta^p\}$ and a current one $\{\Omega^c, \Sigma_T^c, \Sigma_\theta^c\}$, the updated current pose is calculated as:

$$\Omega^u = \Omega^c \quad (8)$$

$$\Sigma_T^u = \left(I - \Sigma_T^p (\Sigma_T^p + \Sigma_T^c)^{-1} \right) \Sigma_T^p \quad (9)$$

$$\Sigma_\theta^u = \left(I - \Sigma_\theta^p (\Sigma_\theta^p + \Sigma_\theta^c)^{-1} \right) \Sigma_\theta^p \quad (10)$$

3.4 Semi-Global Visual Odometry

After initiating the visual odometry, the relative pose estimation at each frame is maintained within a table which contains all pose related information (18 parameters per pose, in which 6 for the position, and 12 for two covariance matrices). At any time, it is possible to get the observations in the neighborhood of the current pose being estimated in order find potential overlaps to consider while performing BA. Since we are dealing with statistical representations of the observations, a divergence measure has to be considered. Here, we choose Bhattacharyya distance (Modified metric version can

also be used *Comaniciu et al. (2003)*) for being reliable and relevant to our problem. In our case, the distance between two observations $\{\Omega^1, \Sigma_T^1, \Sigma_\theta^1\}$ and $\{\Omega^2, \Sigma_T^2, \Sigma_\theta^2\}$ is given as:

$$D = \frac{1}{8} (\Omega^1 - \Omega^2)^T \Sigma^{-1} (\Omega^1 - \Omega^2) + \frac{1}{2} \ln \left(\frac{\det \Sigma}{\sqrt{\det \Sigma_1 + \det \Sigma_2}} \right) \quad (11)$$

where

$$\begin{aligned} \Sigma_{\cdot} &= \begin{pmatrix} \Sigma_T & \mathbf{0} \\ \mathbf{0} & \Sigma_\theta \end{pmatrix} \\ \Sigma &= \frac{\Sigma_1 + \Sigma_2}{2} \end{aligned} \quad (12)$$

where both matrices are 6×6 PSD.

Having selected the set of frames F in the neighborhood of the current pose statistically, we perform BA as follows; First, we divide F into two subsets similar to *Sibley et al. (2009)*, the first subset F_d contains the current and previous frames in time, whereas the other sub-set F_s contains the remaining frames, mostly resulting from overlapping with an already scanned area. Second, BA is performed on both subsets, however, although F_s parameters are included in the optimization, they are masked as static so they are not optimized in contrary to F_d . This strategy is necessary in order to keep past trajectories consistent.

4. Evaluation

The proposed method is desired to represent a trade-off between precision and computation time, the maximum precision being the case of global BA, whereas the fastest computation time is pure visual odometry. Moreover, a performance improvement is expected w.r.t local method due to better selecting neighboring observations. Therefore, we analyze the performance of our method from two points of view; computation time and precision.

4.1 Computation time

Most visual odometry and SLAM approaches share more or less the same initial pose estimation, which compromise feature extraction, description, matching and relative motion estimation. Modern methods including ours can process 3-10 stereo pair/sec using an average machine. (Using two parallel threads which utilize two cores of intel I7-4790 CPU @ 3.6 GHz with stable RAM memory usage $\sim 1\text{GB}$. Brute-Force based feature points matching implemented with OpenCL which uses Nvidia Quadro K2200 GPU.)

This time can be reduced at the cost of lower precision by either using faster less accurate methods, for instance there is 40% of gain by passing from SIFT to SURF, or simply by reducing the image size which showed to decrease linearly the computation time. This time aspect is not of our interest here, where we emphasize on the optimization phase, which corresponds to BA in visual odometry approaches, and to prediction-update in SLAM methods. For computational complexity of SLAM approaches we refer to the study of *Bailey and Durrant-Whyte (2006)*, whereas we provide an analysis of computation time for BA based methods.

We run our experiments using the speed optimized BA toolbox proposed in *Lourakis and Argyros (2009)*. We compute the time needed for BA as a function of the number of frames. The results are shown in Fig. 5. We can see that the computation time is not linear in the number of frames. This analysis can be useful to choose the number of frames to consider in BA in local methods such as ours. For instance, having 15 frames needs 0.2 s which is fair to be integrated within a 3 frames/s visual odometry method. We note that since we use neural networks for learning, maintaining the uncertainty has neglected computation time.

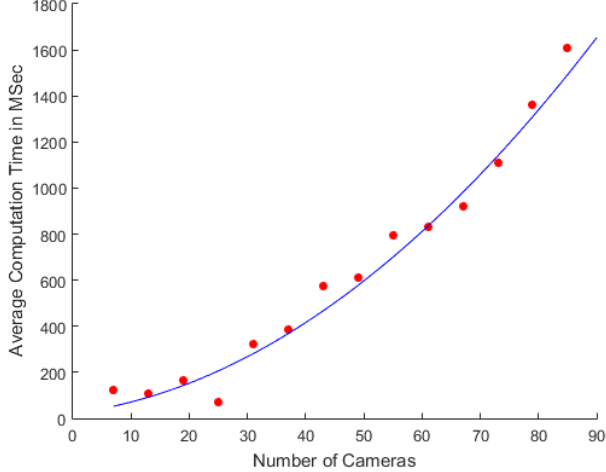


Fig. 5: Analysis of computation time as a function of the number of frames used in BA

4.2 Simulation Using Orthophoto

Our work falls within a preliminary preparation for a real mission. All the experiments are tested within a simulated environment which uses images from previously reconstructed orthophoto *Drap et al.* (2015), which is illustrated in Fig. 6. The area covered is approximately $60m^2$ with very high resolution ~ 330 megapixels. The advantage of using simulated environment is that we can define precisely the trajectory, and then, after running the visual odometry method we can evaluate the performance and tune different components. Especially, with the lack of real sequences provided with odometry ground truth. Hence, we created a dataset of images based on simulating stereo camera motion as shown in Fig. 6, which shows an S-shape type scanning scaled in one direction. The reason is to test the visual odometry method in two cases; when there is an overlap with previously scanned area and another case when there is not. Our method is more adapted to the first case scenario.

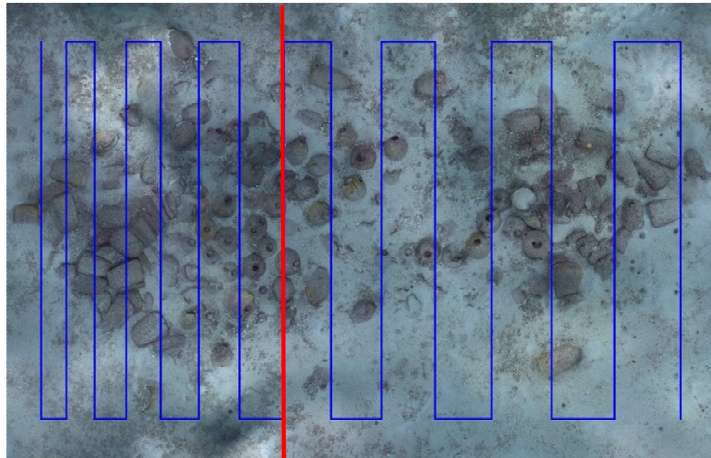


Fig. 6: Simulation scenario with modified S-shape scanning profile which covers two situations; neighboring observations. Red border divides the map in overlapping/non overlapping path.

First we test our method on the created data set, as expected, the estimated trajectory is very satisfactory and very close to the ground truth, see Fig. 7. Following a standard evaluation method *Geiger et al.* (2012), we obtain an average translation error of 2.44 % and average rotation error 0.011 [deg/m]. This average is 1.45% in the trajectory to the left of the red line illustrated in Fig. 6, which can be interpreted by the previously mentioned arguments.

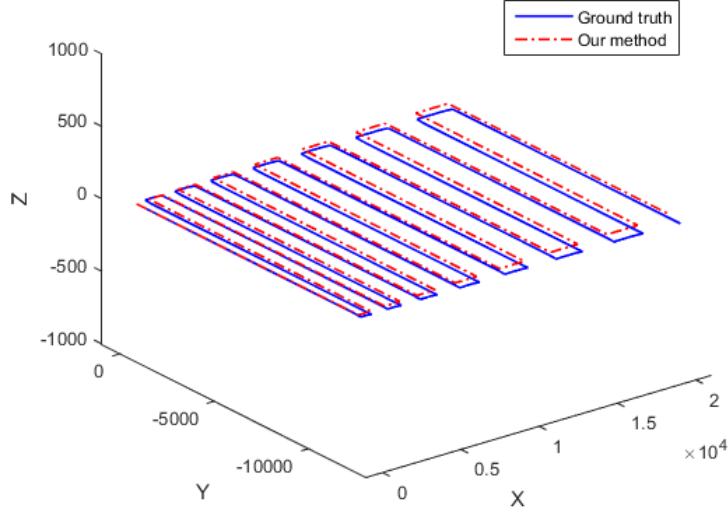


Fig. 7: Estimated 3D trajectory using our method compared to ground truth

In a second step, we estimate the odometry using three more methods; first using global BA, then without using BA, in addition to our method. The obtained trajectories are shown in Fig. 8. Indeed, this method suffers from a constant drift. The corresponding translation error is 6.8% while the rotation error 0.08 [deg/m]. From another side, the method that uses global BA performs best in this context. The translation error is 1.2% while the rotation error 0.009 [deg/m]. Hence, our method comes as trade-off compared to both.

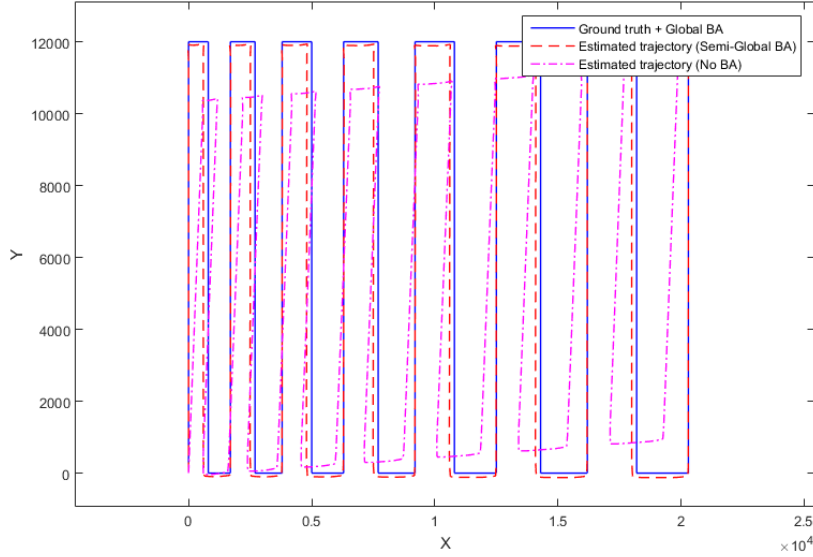


Fig. 8: Comparison between several cases of visual odometry in terms of using BA. Note that the trajectory produced by the method without BA is scaled by ~ 1.8 for visualization purpose.

5. Conclusions and Perspectives

Having the bundle adjustment performed only on neighboring observations to the current frame improves largely the computation time and leads to obtain constant processing time in long autonomies. The proposed method is adapted to the case when the camera moves in a structured manner so that there are overlaps between current trajectory and previously visited areas. This can be a very useful in underwater surveys to give indications about the covered area. The proposed method is also a step

forward of local optimization methods because of using more efficient statistical distance which takes into account the uncertainty of relative pose estimation.

Our work falls within a preliminary preparation for a real underwater mission. Although most of the constraints have been met, few issues remains to be solved. In particular, the aspects related to memory management. Each time a new pose is estimated, the images are freed as they are not needed further, on the other side, their feature descriptors are kept in memory for possibly future overlap, as they are needed to perform BA. Our perspective is to bring a smart solution based on the created map in order to decide whether an observation will be useful in the future or not. For instance, this can be done based on analyzing scanned patches and keeping only observations at the borders.

Acknowledgements

This work has been partially supported by both a public grant overseen by the French National Research Agency (ANR) as part of the program “Contenus numériques et interactions (CONTINT) 2013” (reference: ANR-13-CORD-0014), project: GROPLAN (Ontology and Photogrammetry; Generalizing Surveys in Underwater and Nautical Archaeology) (<http://www.groplan.eu>), and by the French Armaments Procurement Agency (DGA), project: DGA RAPID LORI (LOcalisation et Reconnaissance d’objets Immergés).

References

- BAILEY, T.; DURRANT-WHYTE, H. (2006). *Simultaneous localization and mapping (SLAM): Part II*, IEEE Robotics & Automation Magazine 13, pp.108-117
- BAY, H.; TUYTELAARS, T.; VAN GOOL, L. (2006). *Surf: Speeded up robust features*, European Conf. on Computer Vision, pp.404-417
- BISHOP, C. M. (1995). *Neural networks for pattern recognition*, Oxford University Press
- BLANCO, J.L.; FERNANDEZ-MADRIGAL, J.A.; GONZÁLEZ, J. (2008). *A novel measure of uncertainty for mobile robot slam with rao—blackwellized particle filters*, Int. J. Robotics Research 27, pp.73-89
- BYTHELL, J.; PAN, P.; LEE, J. (2001). *Three-dimensional morphometric measurements of reef corals using underwater photogrammetry techniques*, Coral Reefs 20, pp.193-199
- COMANICIU, D.; RAMESH, V.; MEER, P. (2003). *Kernel-Based Object Tracking*, IEEE Trans. Pattern Anal. Mach. Intell. 25, pp.564-575
- DAVISON, A.J. (2003), *Real-Time Simultaneous Localisation and Mapping with a Single Camera*. 9th IEEE Int. Conf. Computer Vision - Volume 2, IEEE Computer Society
- DAVISON, A. J.; REID, I. D.; MOLTON, N. D.; STASSE, O. (2007), *MonoSLAM: Real-time single camera SLAM*, Pattern Analysis and Machine Intelligence, IEEE Trans. 29, pp.1052-1067
- DRAP, P. (2012), *Underwater photogrammetry for archaeology*, INTECH Open Access Publisher
- DRAP, P.; MERAD, D.; HIJAZI, B.; GAOUA, L.; NAWAF, M.; SACCONI, M.; CHEMISKY, B.; SEINTURIER, J.; SOURISSEAU, J.-C.; GAMBIN, T.; CASTRO, F. (2015), *Underwater Photogrammetry and Object Modeling: A Case Study of Xlendi Wreck in Malta*, Sensors 15, pp.29802

EADE, E.; DRUMMOND, T. (2006). *Scalable Monocular SLAM*, IEEE Conf. Computer Vision and Pattern Recognition, pp.469-476

EADE, E.; DRUMMOND, T. (2008), *Unified Loop Closing and Recovery for Real Time Monocular SLAM*, BMVC, Citeseer, pp.136

GAUGLITZ, S.; HÖLLERER, T.; TURK, M. (2011). *Evaluation of Interest Point Detectors and Feature Descriptors for Visual Tracking*, Int. J. Computer Vision 94, pp.335-360

GEIGER, A.; LENZ, P.; URTASUN, R. (2012), *Are we ready for Autonomous Driving? The KITTI Vision Benchmark Suite*, IEEE Conf. Computer Vision and Pattern Recognition, Providence, pp.3354-3361

GREEN, J.; MATTHEWS, S.; TURANLI, T. (2002). *Underwater archaeological surveying using PhotoModeler, VirtualMapper: different applications for different problems*, Int. J. Nautical Archaeology 31, pp.283-292

HAGAN, M.T.; DEMUTH, H.B.; BEALE, M.H.; DE JESÚS, O. (1996), *Neural network design*, PWS Publ., Boston

HARTLEY, R. I.; ZISSEMAN, A. (2004), *Multiple View Geometry in Computer Vision*, Cambridge University Press

KITT, B.; GEIGER, A.; LATEGAHN, H. (2010), *Visual odometry based on stereo image sequences with ransac-based outlier rejection scheme*, IEEE Intelligent Vehicles Symp. (IV), pp.486-492

LOURAKIS, M.I.; ARGYROS, A.A. (2009), *SBA: A software package for generic sparse bundle adjustment*, ACM Trans. Mathematical Software 36, pp.2

LOWE, D.G. (2004). *Distinctive image features from scale-invariant keypoints*, Int. J. Computer Vision 60, pp.91-110

MONTEMERLO, M.; THRUN, S. (2007), *FastSLAM 2.0*, FastSLAM: A scalable method for the simultaneous localization and mapping problem in robotics, Springer, pp.63-90

MONTIEL, J.; CIVERA, J.; DAVISON, A.J. (2006). *Unified inverse depth parametrization for monocular SLAM*, Analysis 9, pp.1

MOURAGNON, E.; LHUILLIER, M.; DHOME, M.; DEKEYSER, F.; SAYD, P. (2009). *Generic and real-time structure from motion using local bundle adjustment*, Image and Vision Computing 27, pp.1178-1193

NISTÉR, D. (2004), *An efficient solution to the five-point relative pose problem*, Pattern Analysis and Machine Intelligence, IEEE Trans. 26, pp.756-770

NISTÉR, D.; NARODITSKY, O.; BERGEN, J. (2004), *Visual odometry*, IEEE Conf. Computer Vision and Pattern Recognition, pp.I-652-I-659

PINIÉS, P.; TARDÓS, J.D. (2007), *Scalable SLAM building conditionally independent local maps*. IEEE Conf. Intelligent Robots and Systems, pp.3466-3471

SIBLEY, D.; MEI, C.; REID, I.; NEWMAN, P. (2009), *Adaptive relative bundle adjustment*. Robotics: Science and Systems, pp.33

STRUTZ, T. (2010), *Data fitting and uncertainty: A practical introduction to weighted least squares and beyond*, Vieweg & Teubner

THRUN, S.; BURGARD, W.; FOX, D. (2005), *Probabilistic robotics*, MIT Press

TRIGGS, B.; MCLAUCHLAN, P.; HARTLEY, R. ;FITZGIBBON, A. (2000), *Bundle adjustment: a modern synthesis*, Vision algorithms: Theory and Practice, pp.153-177

WAN, E. A.; VAN DER MERWE, R. (2000). *The unscented Kalman filter for nonlinear estimation*. IEEE Adaptive Systems for Signal Processing, Communications, and Control Symp., Lake Louise, pp.153-158

Engineering Requirements for a Maritime Digital Infrastructure

- A Sea Traffic Management Perspective

Anders Dalén, Viktoria Swedish ICT, Gothenburg/Sweden, anders.dalen@viktoria.se

Sandra Haraldsson, Viktoria Swedish ICT, Gothenburg/Sweden, sandra.haraldsson@viktoria.se

Mikael Lind, Viktoria Swedish ICT, Gothenburg/Sweden, mikael.lind@viktoria.se

Niklas Mellegård, Viktoria Swedish ICT, Gothenburg/Sweden, niklas.mellegard@viktoria.se

Ulf Siwe, Sjöfartsverket, Stockholm/Sweden, ulf.siwe@sjofartsverket.se

Almir Zerem, Viktoria Swedish ICT, Gothenburg/Sweden, almir.zerem@viktoria.se

Abstract

The path from concept to prototypical implementation is an iterative refinement process where vision meets reality. This paper details this complex process to technically specify a maritime digital infrastructure for Sea Traffic Management and beyond. To define this comprehensive support and structure its development, the method of requirement engineering is employed. This involved: (1) requirement elicitation, (2) modeling and analysis, (3) facilitating communication and (4) describing hypotheses and key requirement agreement. In closing, the paper discusses the resulting technical specification, lessons learnt and the need for a governance body to maintain and develop the specification.

1. Introduction

The idea of Sea Traffic Management (STM) was born in 2008, but it had yet to find its current form and even its name. The original idea was to exchange routes between ships in the same vicinity, in order to build a common situational awareness which would increase the safety. In the EU co-financed MONALISA project 2010-2013, technical tests were performed transferring route information over the AIS network. Having the route information available in the AIS network also means that it can be made available to shore actors and this opens up for many new service possibilities. Discussions with the leading European program for developing air traffic management, SESAR, inspired a more holistic approach and STM was coined as a concept.

To enable the STM concept and future services we need standards and a common infrastructure. Today the use of real-time data for shipping management is fragmented, uncoordinated, and not very efficient. As stated by *Lind et al. (2014)*, an interoperability infrastructure needs to be established to facilitate the exchange of real-time data. In the MONALISA 2.0 project a maritime service infrastructure was defined, *Lind et al. (2015)*.

This article takes the requirements engineering perspective on the hitherto development. The main challenges, lessons learnt and processes to develop a digital infrastructure that support the maritime ecosystem will be highlighted. A brief background to the STM project will be given in the next section. This is followed by the main analysis where requirement elicitation, modelling, communication and agreement activities are explained. Here one of the central STM concepts called PortCDM is used as an example to tie theory to practice. The article ends with a discussion on primary success principles, lessons learnt and a conclusion.

2. Sea Traffic Management

The MONLISA projects invented and defined the STM Concept. The current STM Validation Project will run full-scale test-beds in the Mediterranean and in Northern Europe. 300 ships will have test equipment on board, 13 ports will establish PortCDM, and 5 service centres will assist the ships. Route information will be exchanged using the MONALISA 2.0-developed RTZ-format a part of the IEC-standard since 2015, and other information formats will be tested which after validation will be proposed as new standards. All information exchange in the test beds will be compatible with the Maritime Cloud-infrastructure, currently under development in the EffienSea2-project.

In the subsequent EU funded project MONALISA 2.0 2013-2105, the STM concept was defined in detail. The analysis used many aspects, e.g. legal, commercial, operational, to build a target concept and the road map to reach it. The main components of STM are, *Siwe et al. (2015)*:

- Strategic Voyage Management (SVM) has the goal to optimise a company's initial planning phase of a voyage. This is done by providing services based on a current awareness of all influencing factors relating to the undertaking and success of the planned voyage. SVM enables the process at the earliest possible planning horizon prior to voyage commencement. The planning horizon can be years, months, weeks or only hours.
- Dynamic Voyage Management (DVM) helps in optimising the ongoing voyage. It is important to have the latest information from all involved actors at hand. By using real-time information, the Voyage Plan becomes dynamic, changing along the way due to new facts and input from STM services and tools. The safety enhancing vessel-to-vessel tool that assist bridge personnel in finding the out intentions of other vessels based on Route Exchange is complemented by optimisation, cross-checking and navigational assistance services involving actors outside the vessels.
- Flow Management (FM) – Whilst Voyage Management concerns optimising everything regarding one single vessel, FM is optimisation based on many vessels in an area, preferably all. FM aims at increasing the safety of the sea traffic flow, during all planning and executing phases, while taking to account other factors. Optimising traffic is achieved by coordination, not control, always leaving the final decision to the Master.
- Port Collaborative Decision Making (PortCDM) – PortCDM enables digital collaboration among key actors involved in a port call and the port and its surroundings. The digital collaboration is established by an information sharing platform for involved actors to share intentions and actual occurrences, in real-time, for key events to enable a common situational awareness. PortCDM addresses four collaboration arenas, port-internal coordination, voyage synchronization, port-to-port collaboration and hinterland integration. One driver for Port CDM is to enable increased predictability to enable just-in-time operations, optimal berth productivity, shorter turnaround times and higher capacity utilization.

3. Analysis

Time spent understanding the solution and its underlying problem will pay dividends in the end. For example, *Hofmann and Lehner (2001)* found that teams who spend considerable effort on requirement engineering in general (28% of the time) and balanced time on elicitation, modelling and validation (11%, 10% and 7%), were more successful than projects who spent less time on these tasks.

3.1. Elicitation

As the name suggests, elicitation goes further than the capturing of statements. A thorough analysis that consist of user interactions with prototypical implementations and models. Traditional elicitation techniques usually begin by capturing statements, constraints and insights through interviews, questionnaires and literature reviews. Workshops, both open ended and focused, complement the traditional approaches by involving several participants to develop the statements and questions further. A procedure called “zooming” propose that increasingly sophisticated and expensive methods are used increasingly as well defined topics of inquiry become clear, *Goguen and Linde (1993)*. The elicitation process can also involve stakeholders in the elicitation and is recognized to both increase the understanding and improve the prioritization in the requirement engineering process, *Hofmann and Lehner (2001)*. Moreover, including end users as developers has further improved the value of the resulting product. Therefore, this kind of “user innovation lends itself to be a promising dimensions of the requirement process”, *Jiao (2006)*, p.180. Similarly, the elicitation method of including users in requirement engineering as prescribed in human-centered design (ISO 9241-210) is widely used in information systems development and its application is currently spreading to transport sector development, *König (2012), Katrina (2015)*.

In STM the development process followed the notion of user innovation and was largely driven by stakeholders that would ultimately use the solutions. During the MONALISA 2.0 project (2013-2015) maritime experts and ICT system developers worked closely together to understand and develop conceptual solutions. The complex issue that sea traffic management focuses on, which span ecosystems of participants (e.g. shipping lines, charterers, ship operators, cargo handlers, port support, industry organisations and authorities), meant that several affected stakeholders had to be integrated in the elicitation process.

A “zoom” approach was adopted naturally as many, less polarizing, decisions for solutions were taken by the conceptual teams. For more complex issues, for example how the notion of the “freedom of the seas” should be threatened, it was raised in forums with international expertise. Due to the wide scope of the solutions of STM, including both voyage and port processes from berth-to-berth, it was difficult to attract representatives for all the perspectives. A notable omission, in the MONALISA 2.0 project, was representatives from shipping lines. As they are a central stakeholder in the maritime transport chain there is a risk of suboptimal ecosystem solutions as a result. As representation is voluntary and each project partner need to evaluate their own incentives it is still an open question how these gaps can be covered.

The fundamental constraints from this human-centered elicitation process within the voyage and port ecosystems that shaped the requirements were that:

- Freedom of the seas (mare liberum) shall not be compromised
- Ownership and control of access reside with creator of the data
- A unique identifier is needed to provide structure and traceability among the disparate systems
- All fundamental practices within STM shall be based on open and standardized technologies and information models

3.2. Modelling

3.2.1 Ecosystem model as domain model

The maritime industry is conceived as a self-organized ecosystem. Traditionally, the focus has been separated between the navigation ensuring efficient routes going from one geographical point to another as one practice, and the profession of port operations as another. As explained in Section 2 on STM, the overall goal with the project is to enable interaction between port operations and navigational processes from a berth-to-berth perspective. Comparing with other transport sectors a single actor being responsible for the whole berth-to-berth voyage is not possible due to the distributed nature of sea transports. The solution, provided via STM, instead need to enable each actor to share information to authorized parties creating foundations for better resource planning and situational awareness both within each practice and between the practices. Efficiency, safety, and environmental sustainability in sea transports builds upon that involved actors share intentions and actuals, for example when a certain waypoint is planned to be and has been reached. Three typical use cases would be:

- Sharing routes, using the route exchange format (rtz), between different vessels informing each other of intended routes
- Sharing information about timestamps among involved actors, using the port call message format (pcm)
- Enabling just-in-time arrivals by the vessel sharing intended arrival time and the port sharing information about when it is ready to realize the purpose of call

To enable digital collaboration within and between the practices there would be a need to elaborate on the format and principles for sharing data between different actors operating in the practices. As indicated in Fig. 1, the scope taken by STM is the berth-to-berth voyage, initiated and concluded by port operations, realizing the purpose of call at the port of origin and the port of destination as part of the

voyage. Furthermore, the necessary digital collaboration enabled by secure information sharing is needed within and between each practice for the purpose of overcoming the complexity of realizing efficient, safe, and environmentally sustainable voyages berth-to-berth.

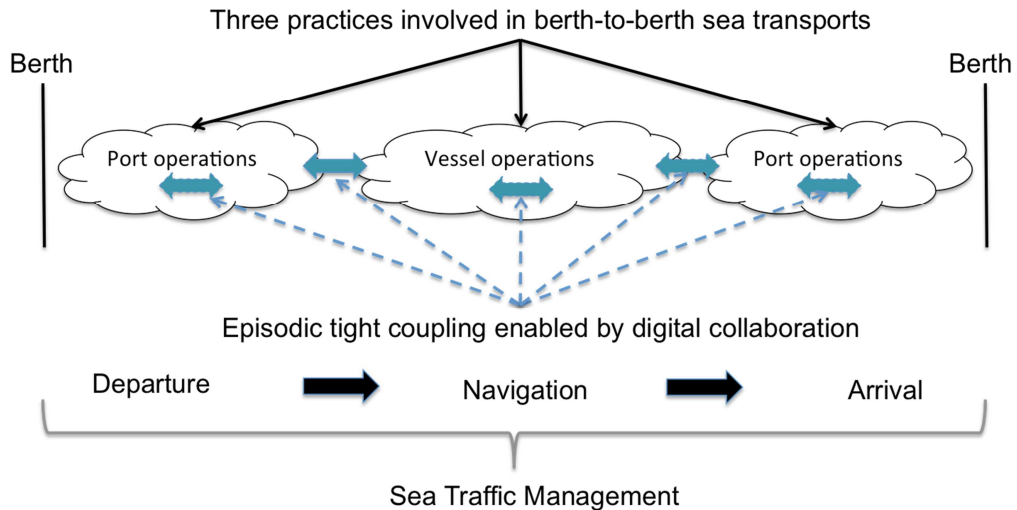


Fig. 1: Operative scope of STM, from berth to berth

STM does thus require the engagement of many actors. Important enablers are an increased degree of connectivity, increased possibilities of digital collaboration, seamless interoperability between systems and highly distributed coordination (i.e. each actor taking responsibility for its actions acting on behalf of the ecosystem) in sea transports. This is enabled by episodic tight couplings. The temporary nature of this interaction presents an opportunity to move away from a traditional approach to traffic management with a central governance unit. STM will involve and engage multiple actors on multiple levels and will require new procedures for information sharing in a distributed manner within each stakeholder's action scope. Adopting such a modern approach to traffic management, as proposed by STM, enables and requires that each involved actor is engaged as a traffic management co-producer and adopt common principles of authentication, access management, and messaging. This does however require that each stakeholder have good enough incentives for such engagement.

3.2.2 Data model

Based on this view on sea transports as self-organized ecosystems a necessity is to agree upon standards for such digital collaboration. Different message formats need to rely on data models capturing the (digital) service interaction patterns. In the development of the port call message format as an enabler for the service interaction within port operations and between port operations and navigation a data model was developed capturing the structure of the messaging format. At the core, the port call message standard enables involved actors to share timestamps, Fig. 2.

PortCall is the central object in the data model. A PortCall encapsulates the data related to one Vessel's visit to one Port as part of one inbound Voyage and one (optional) outbound voyage. The Vessel, Port and Voyage entities are assumed to be part of and defined in the sea traffic management (STM) information domain (indicated in the model by the <<STM>> stereotype). While the PortCall entity may not be part of the STM information domain, it shall have a unique STM identifier allowing port call data to be interchanged outside of the port. This is crucial as the progress in the port call, as part of an outbound voyage, will directly affect the planning of the port call on the inbound side of that voyage – this is especially important with short-sea shipping.

Port call data are encapsulated in a number of abstractions. The top level abstraction is the ProcessStep, which represents overarching port call phases currently envisioned to be: Arrival, Port visit and Departure.

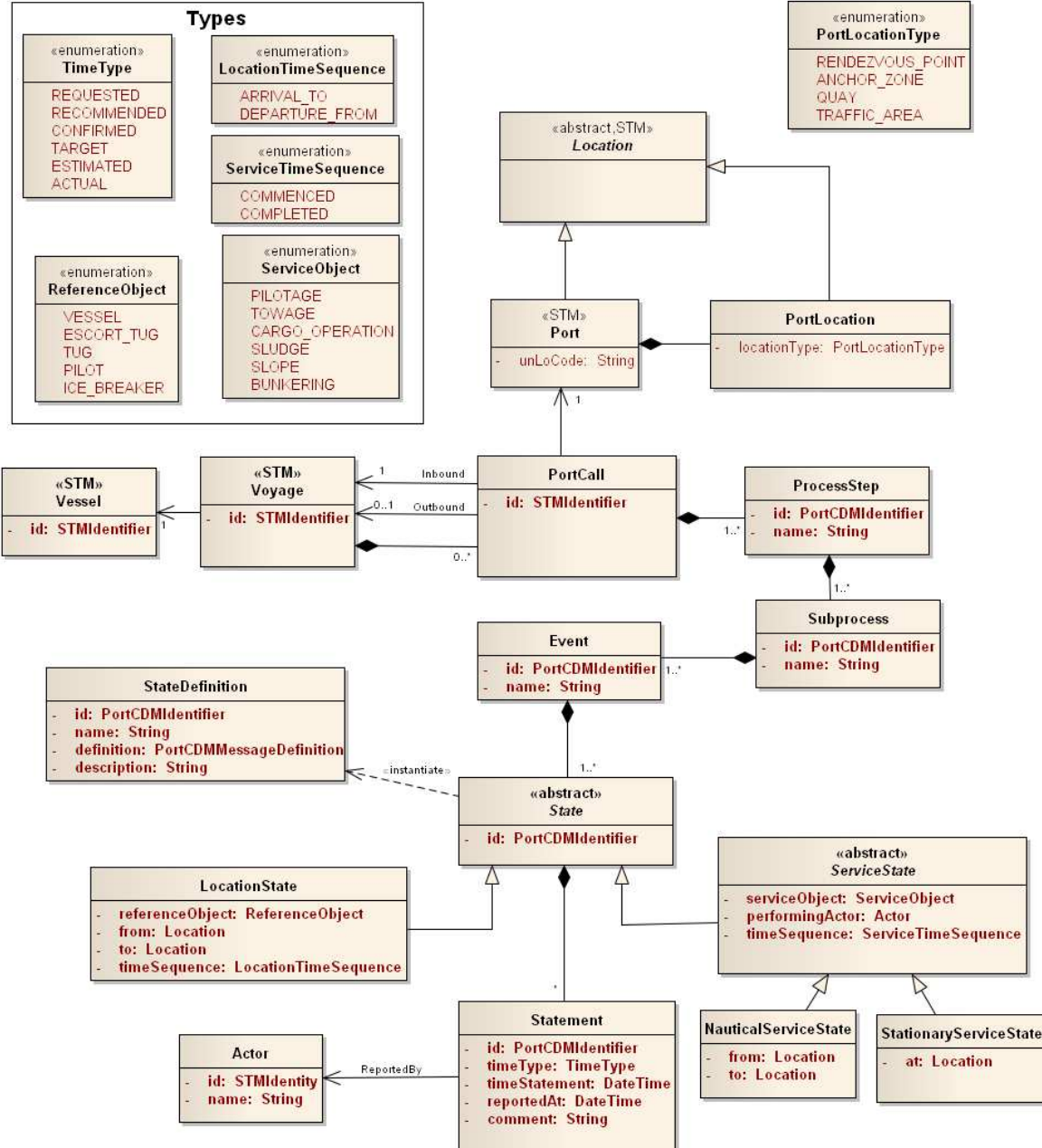


Fig. 2: Data model encapsulating port call related data. Note that only a subset of attributes has been included in the model

A ProcessStep is further subdivided into SubProcess entities, where a SubProcess represents a set of related operations. An example of a SubProcess instance is a shifting operation, i.e. taking a vessel from an anchoring zone to berth, or between quays.

A SubProcess entity is subdivided into Event instances, where an Event represents a small and coherent unit of work. Examples of typical events are pilotage, towage, cargo operations, berth arrival, berth departure, port arrival, and port departure.

An Event, in turn, comprises State instances. A State represents a progress (i.e. state) of a specific operation. The progress of an operation is chosen carefully such that it carries important properties for synchronizing and evaluating overall port call progress, and for planning future operations. Typical examples of State instances are: vessel arrival to traffic area (i.e. to the port), cargo operations completed, and towage commences. As can be seen in the model, concrete instances of a State can be ei-

ther a LocationState or a ServiceState, where a LocationState represents a reference object departure from or arrival to a location and a ServiceState represents the progress of a service. The abstract ServiceState is specialized by the two classes NauticalServiceState or StationaryServiceState depending on whether the service concerns movement (e.g. towage) or is performed in a specified location (e.g cargo operations).

A State may contain any number of Statement instances. Statement, together with LocationState and ServiceState, dictates content and structure of the Port Call Message format. A Statement represents a reported data point, and corresponds directly to exactly one message in the Port Call Messaging format. A Statement comprises, a stated time (timeStatement) and a specification of the meaning of that time (controlled by the type TimeType). For instance, providing a time for the State ‘vessel arrival to traffic area’ with the TimeType ESTIMATED would mean an estimate for the vessel to arrive to the port at the stated time. In addition, a Statement comprise statement meta-data (which Actor reported the data, and at which time) as well as a free text comment.

In addition to the information model described above, the StateDefinition entity represents a valid PortCDM state. While combining elements of the Port Call Message format may produce any number of possible States, only a subset of these is considered valid within PortCDM. It is envisioned that a standardized State Catalogue defines the set of valid PortCDM states in terms of StateDefinition instances. A StateDefinition shall comprise at least an identifier, a name/description together with the Port Call Message (PCM) format elements that define it. Example StateDefinition instances include:

ID:	ARRIVAL_VESSEL_TA
Name:	Vessel’s arrival to port traffic area
PCM definition:	Type: LocationState, ReferenceObject=VESSEL, TimeSequence=ARRIVAL, Location=Port
ID:	COP_Commenced
Name:	Cargo operations start
PCM definition:	Type: StationaryServiceState, ServiceObject=CARGO_OPERATION, TimeSequence=COMMENCED

One experience from developing and applying this data model as a foundation for the messages to be shared between different actors involved in berth-to-berth sea transports clearly revealed that different vocabulary was used within the different practices. For example ECDIS-suppliers used the planned time of arrival (PTA), actual time of arrival, and estimated time of arrival (ETA) as the timestamps within the navigational practice. Within the practice of port operations the PTA timestamp was however dismissed giving rise to the need for a timestamp that could express the underlying meaning of planned time. The agreement was to use targeted time of arrival (TTA) as timestamp to enable episodic tight coupling between the different practices.

3.2.3 Behavioral model and action affordances

New principles of sharing data enable new actions to be pursued by involved actors. Taking for example the ports point of view, the port could be regarded as a multi-organizational phenomenon, *Haraldson and Lind (2011)*, in which the different port actors collaborate for the purpose of optimizing the port call, and as a transportation hub in relation to vessels making a port call, Fig. 3. This would enable the vessel to consume services offered by the port as one (compound) actor at the same time as the port actors could acknowledge each other’s contribution to the optimized port call giving rise to a high degree of predictability.

PortCDM, as one of the concepts of STM, provides images for situational awareness based on provided timestamps from involved actors related to port calls. Such situational awareness is today established by each involved actor based on the sources they have at hand where these actors take the responsibility of coordinating other actors.

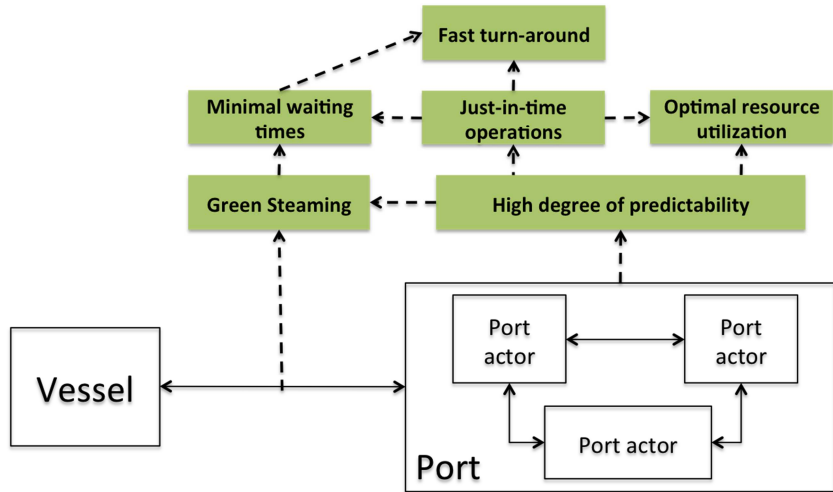


Fig. 3: Desired effects from enhanced collaboration related to port calls

PortCDM, as one of the concepts of STM, provides images for situational awareness based on provided timestamps from involved actors related to port calls. Such situational awareness is today established by each involved actor based on the sources they have at hand where these actors take the responsibility of coordinating other actors.

Within today's practice there is however a risk for sub-optimized coordination not taking all different sources into account. A solution building on sharing timestamps in real time where everyone share, and have the same information simultaneously, has proven to create positive effects on the coordination ability of the port as a multi-organizational actor. PortCDM provides a basis for enhanced quality of planning performed by each involved actor in the port call.

A common maritime service infrastructure with accessible information services does also give rise to the possibilities for new information and application service providers to contribute with its services to the ecosystem. The characteristics this maritime infrastructure builds upon principles of nomination, identity management, and a common service registry providing possibilities to expose and discover services. As for today, there are high entry barriers for new service providers to distribute competitive services. A service ecosystem is enabled by standardized message formats, common principles of authentication and common principles of access management in an overarching architecture, which allows different providers to offer access to their information services. This architecture is further outlined in Section 3.3.

2.2.4 Non-functional Model

Key factors to success with PortCDM include data quality, data security and data interchange automation. Data interchange automation is essential, as port organizations typically already manage their work in dedicated and often bespoke IT-systems. Therefore, PortCDM aims to enable data interchange between these systems and more – the key design principle is “not another system”.

One strategy to accomplish this, while ensuring data quality, is to strictly define what type of data that can be shared in STM (e.g. on the PortCDM platform), and strictly defining formats in which the data are interchanged. More specifically, PortCDM defines the precise data elements that are key to facilitate port call collaboration and improved operation synchronization. These data element are represented as important operation state changes. The data format is defined with extensibility in mind to allow additional data elements to be identified in the future. As the data shared by maritime stakeholders may reveal trade secrets, data security and fine-grained access control is important. In STM, each data point is assigned a unique identifier, allowing the data provider to specify on data point level who shall be granted access. The non-functional modelling, thus, emphasizes the need for combined state-of-the-art data security mechanisms and fine-grained and secure access control in its implementation.

3.3. Communication

3.3.1. Requirement Abstraction Model

A software requirements specification is to a large extent a tool for communication (IEEE 830), often between a large and diverse set of stakeholders. For a software requirements specification to be useful it shall (IEEE 29148):

- Enable an agreed understanding between stakeholders (e.g., acquirers, users, customers, operators, suppliers)
- Be validated against real-world needs, can be implemented
- Provide a basis of verifying designs and accepting solutions

In addition, a requirements specification can serve as basis for estimating costs and schedules, and facilitate the transfer of the software product to new users and platforms (IEEE 830). In that capacity, a requirements specification concerns many of stakeholders and for a variety of reasons, and may have a significant impact on the success of the development and deployment of a software product.

Producing an adequate requirements specification is a notoriously difficult task; requirement shall be specified unambiguously, be testable, be chosen such that they cover all important aspects of the system under specification while omitting what is trivial or obvious, and be understandable by all concerned stakeholders. To accomplish this, the use of proven and rigorous methods is essential.

In the STM project this became all too evident when strategic managers and domain experts from each of the four STM components (SVM, DVM, FM and PortCDM) collaborated with IT experts to define the requirement on the IT infrastructure necessary to enable the implementation of the components. While there was no shortage of requirements, the elicitation process was not straightforward. Often highly detailed requirements were mixed with high-level goals, and discussions often resulted in misunderstanding and confusion. Further challenges presented when trying to assess if the specification was complete enough, and whether the requirements were consistent. It became increasingly clear that the requirements elicitation process needed a guiding method.

A prominent example of such a structure is the Requirement Abstraction Model (RAM), *Gorschek and Wohlin (2006)*, which has the goal of ensuring consistency and traceability among requirements in order to increase the overall quality of requirement specifications. The RAM defines a number of abstraction levels to which each requirement is classified and checklists are provided to ensure that the requirements are assigned their proper abstraction level. *Gorschek and Wohlin (2006)* suggest, but do not limit their model to, four abstraction levels:

- Product: Product level requirements have a goal-like nature, very high-level descriptions of the desired functional and qualitative properties of the product;
- Feature: Feature-level requirements describe the features that fulfil the product level goals;
- Function: Function level requirements define which functions should be provided by the system in order to provide the features;
- Component: Component level requirements describe how something should be solved, i.e. bordering to design information.

The RAM ensures traceability between requirements through all levels of abstraction by enforcing that, with the exception of the product level, no requirement may exist without a link to the more abstract requirement. The rationale is that no requirement may exist unless there is a clear and unambiguous reason for its existence motivated by higher-level requirements, and conversely, high-level requirements should be traceable to the lower-level requirements that satisfy them.

In the RAM, the relevant aspects of the entire system shall be specified at each level of abstraction,

providing the means to verify completeness and correctness of the specification at multiple abstraction levels, thus providing a full system specification for various types of stakeholders. Furthermore, the traceability between abstraction levels provide the means to verify that the more detailed requirements necessary to realize a more abstract requirement has been identified, thus providing the means to verify completeness of the specification.

3.3.2 Architecture

To specify and develop a common digital infrastructure and an architectural framework which allows meaningful, efficient and flexible use of it is always a task of great complexity. Such endeavour demands both in-depth knowledge of the operational context and wide technical competence to evaluate, choose, configure, if needed also develop, integrate, deploy and operate the most suitable technical components. To find an appropriate, stable and sustainable model for governance and maintenance of such platform is often quite a challenge itself, especially if the platform crosses the organisational boundaries.

The maritime ecosystem is a global, complex, diverse and from the digitalization perspective in general relatively immature environment. It is governed by combination of the international, regional and national legislations and influenced by very old and strong traditions. It is a meeting point for vast number of different professions, private interest as well as governmental bodies, in many cases also autonomous actors competing with each other. Extensive manual paper work and physical or semi-digital information exchange are very frequent phenomena.

In this context, thinking in the terms of a common infrastructure and architecture is overwhelming. Comprehending the sheer scope of the task and the issue of finding a pragmatic methodology to deal with it is one of the most obvious pitfalls for this kind of initiatives. Still it is tempting to try to figure out one-size-fits-all solutions and aim for the full improvement potential at once. It would almost certainly lead to dead-ends, intractable goals and demands. One example is cyber security, an issue which certainly must not be underestimated. However, it might not be necessary to implement the highest possible level of information protection with all its complexity everywhere, especially considering that the information currently flows completely unprotected.

It does not mean at all that long-term visions and overall architecture pointing the direction and holding it all together should be omitted. On the contrary, these aspects are absolutely necessary to be envisioned and described, especially in a distributed and agile environment. Instead of exclusively trying to enforce a heavy hierarchical top-down architectural approach an emerging, highly iterative strategy with minimum of infrastructural investments and operational changes should be embraced. With this approach, immediate win-win situations and lowering the barriers to entry for potential users, which is regarded as one of the single most important success factors, becomes a central process. Each concrete milestone in every developing iteration has to be prioritized, related to and categorized under the overall infrastructural and architectural goals.

End-to-end use-cases are useful to engage stakeholders and elicit their preferences. However, to be effective, avoid misunderstandings and enable a constructive dialog on the use-cases, a basic language, including both vocabulary and grammar, needs to be developed. In practice, this means developing various information nomenclatures, expressive and simple enough to be easily adopted and immediately used by many, but still generic and scalable to allow adaptations and enhancements for future yet unforeseen needs. Already established standards are highly recommended to be considered and referred to, but not necessarily to be imposed as the only alternative, especially as they often are extremely complex and require a lot of specialist competence. Other parameters, for example adoption rates, should also be consulted when making these decisions. On a technical level, open source frameworks and supplier and technology agnostic standards should whenever possible be the first choice. To establish easily accessible open source libraries of reusable technical components and to make it easy and convenient for third party developers to join the community is of great importance for adoption and dissemination of the common digital infrastructure.

In STM the requirement engineering is organized in layers to fit the iterative infrastructural and architectural approach. On the conceptual level, attention has to be paid to the overall requirements such as an absolute minimum of centralized infrastructure to provide authentication, data owner authorization and service management. On the opposite level of abstraction, the technical solutions have to cope with specifics and limitations of the operational context, e.g. limited access to broadband in communication involving vessels away from the shore, huge variety of proprietary IT legacy, different level of IT maturity and access to IT competence.

3.3.3 Hypotheses

In MONALISA 2.0 one important basis for the elicitation of requirements on the maritime digital infrastructure was the emergence of the enabling STM concepts. During MONALISA 2.0 these concepts were validated. PortCDM was validated by a hypothesis-driven approach where formulated hypotheses were verified/falsified by the use of a combination of different data derived from real-life tests, analytics, and actor conceptions. Fig. 4 shows the principles for this approach to validate the PortCDM concept.

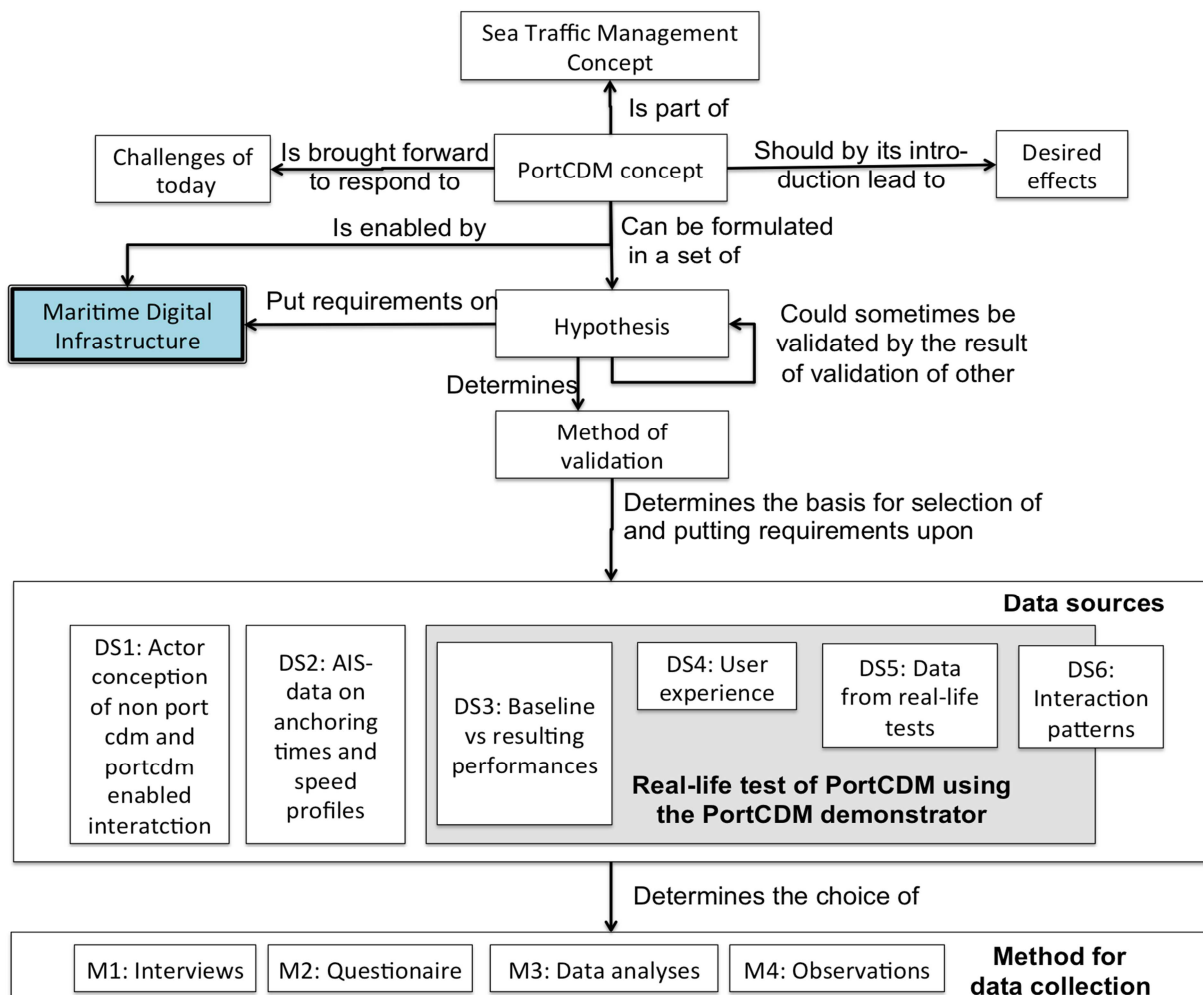


Fig. 4: Principles for validation of the PortCDM concept, *Haraldson et al. (2015)*

As indicated in the figure the maritime digital infrastructure has a core role in the realization of the PortCDM concept. Based on the requirements elicited in the sections above and the proposed architecture, a set of hypotheses has been formulated. The hypotheses originate from the objectives identified for the maritime digital infrastructure founded in today's challenges and leading to desired effects. The following hypotheses related to the maritime digital infrastructure are proposed to be validated in the STM validation project:

- Agreed principles of authentication and access management leads to lower entry barriers for potential information providers
- Provision of standardized solutions for authentication and access management leads to lower entry barriers for potential information providers
- Provision of standardized message formats leads to lower entry barriers for potential information
- Common service registry leads to enhanced collaboration among involved actors
- Common service registry as a source for service discoverability leads to a variety of services to use for operational performance.
- Common principles for service interaction facilitates episodic tight coupling within and between the different practices

3.4. Agreement

The ultimate aim with the communication activities, described in Section 3.3, is to establish a common understanding and come to an agreement based on the shared insight. The final agreement step is, however, more elusive and complex to reach than it first might seem. Conflicting goals and different biases affect the potential to reach a common agreement, *Nuseibeh and Easterbrook (2000)*. Awareness and an effort to detect differences and inconsistencies in perspectives is essential, Pohl (1994), but commonly underestimated, *Boehm et al. (1998)*.

Much research has gone into smooth the transition between understanding and agreeing on requirements. Particular effort is spent understanding each stakeholder's main benefit from the implementation. Prioritizing the major win-win cases ensures an appropriate focus of the solution and helps sustain the agreement, *Boehm et al. (1998)*. The ecosystem of stakeholders in the STM project provides a multitude of viewpoints. However, with the range and maturity of current information and communications technology several scenarios and concepts could be defined that allows for a gradual shift towards disseminating more information. This eliminated the need to agree on the full STM vision and instead lay the foundation for concurrent negotiations and development.

Naturally, developers need to understand the requirement specification to prototype according to it, *Hull et al. (2010)*. However, a conscious effort to balance negotiations and development can spare time from being wasted at either end. For example, *Boehm et al. (1998)* noticed less inconsistencies and less redundant documentation when requirement negotiations and development happened concurrently. The first draft of requirements is commonly lack direct applicability without testing and editing, *Lamsweerde (2000)*. Agreement on requirements and their implementation in the development has also been facilitated by an interaction between conceptual discussions and technical implementation in the STM project. By inviting users to participate in use-case scenarios and user interface reviews, invaluable feedback was collected that benefited both the conceptual and technical development.

There is also a risk with tight interaction between negotiations and development when it is not pursued equally over the whole project. If the scope of the technical development only reflects a subsection of the overall goal the result might be inconsistent with the larger vision. More specifically, in MONALISA 2.0, the methodology of concurrent prototyping was only pursued by some teams, which made their solution more rigid than other, more conceptual, parts. Rather than reaching a more solid agreement throughout the project, this methodological discrepancy in some cases provided support for the overall development while in other it dictated directions that might not be suitable for the holistic goal. In fact, it became clear in the STM Validation project that some assumptions had been too narrow in scope, and subsequently had to be redesigned. This is not an argument against concurrent development. On the whole, the tangible outcome of the development efforts contributed greatly to the constructive conflict, which is part of any agreement process, *Easterbrook (1994)*.

4. Discussion

Casting the past and ongoing processes of developing a technical specification to enable sea traffic management in the engineering requirement mold highlights some important aspects of the MONALISA 2.0 and the STM Validation projects and future directions. The resulting technical specification draft that guides the first implementation leverages the lessons learnt. For example, due to concerns about trust a highly distributed implementation is pursued with a limited number of central components. Furthermore, in this distributed environment, the priority of data ownership, security and control provide another challenge.

On a project level, the bottom-up approach where assumptions are tested in smaller batches is spreading. Although this is natural as requirements mature, the immediacy with which this is happening is fueled by the positive experience that is evident throughout the project's requirement engineering efforts. The implementation will, thus, progressively grow and encompass more sophisticated service offerings. Obviously the ambition of STM is not limited to validating certain requirements but also to lay the foundations for future growth. This perspective is important at the start as "early stages of the system development life cycle are crucial to the successful development and subsequent deployment and ongoing evolution of the system," *Yu (1997)*, p.226.

4.1. Development Support

Fundamental for all the technical specification is the requirement to use open and widely adopted standards where available. Allowing third party actors to participate and add new features is necessary to drive innovation.

The need to supporting development, however, goes beyond well defined standards. It also encompasses creating forums where new stakeholder connections can be made. The approach taken in MONALISA 2.0 for validation of the PortCDM concept as an STM concept is used for the validation of the same concept in the ongoing STM validation project. In these efforts a LivingLab approach and a technical artifact put into use are two main sources for continuous validation formulated hypotheses. A process from adopting a living lab approach eliciting explicit requirements on the technical solution including supporting maritime digital infrastructure and establishing trust among the parties. The Living Lab approach enables a user-centric iterative development process between business representatives from key roles in the port community and concept and technical developers. Business representatives, as potential users, are co-produces enabling a high degree of acceptance for the end-product.

Due to the continuous dialogue and close relationship that evolves among involved actors, such approach allows developers to get instant feedback based on suggestions and/or proposed changes and design decisions. The technical implementation would inform about challenges to overcome adopting the technical architecture as proposed in this paper. The technical architecture will be use in the 13 ports with STM compliant services. These will be run in different trials where focus periods of use of the technical artifact will identify further requirements. In order to support the implementation of PortCDM in the 13 ports a developer zone as a virtual living lab will support operational business development teams and technical development teams at respective port.

4.2. Governance

As no maritime organisational body can represent the whole ecosystem, the STM Validation project will also evaluate appropriate forms for this kind of organisation. A federated approach using representatives from key stakeholders is a likely compromise. Governance will assume several roles to maintain, monitor and evolve the maritime digital infrastructure, as further described here below. Maintenance tasks would include keeping the code base up to date and continuously work to stabilize the core features. It would also include maintaining the service registry to ensure that information there is current and functional.

The monitoring aspect has two main goals. First, to ensure that security constraints (e.g. authentication, encryption and access control) are used appropriately. This could entail automated reporting and testing. The second goal is to evaluate usage patterns and needs to prioritise the development efforts. For example, an analysis of the main barriers of entry and how to remove them is key to allow more data sources.

Even though the goal of STM is unlikely to change (to improve the safety, efficiency and environmental impact of the maritime industry by securely sharing information), the requirements that support this development today will change over time, *Lamsweerde* (2001). New standards and a continued technical development will place new demands and expectations on a maritime digital infrastructure. To this end, STM promotes modularized development and service oriented architecture that enables standalone parts to be modified without affecting the overall system.

5. Conclusion

Eliciting requirements on digital infrastructure in self-organizing ecosystems to provide the right means to glue different actors to each other is a complex task. In this paper we have used a long-term endeavour of developing a concept of Sea Traffic Management (STM) concept and its supporting infrastructure. Most likely there will not be a single digital infrastructure but several separate instances will be established for the purpose of supporting STM. Therefore there is an obvious need to join forces with contemporary initiatives that also elicit requirements and test solutions for a maritime digital infrastructure. To summarize the requirements put upon the maritime digital infrastructure are:

- Access to information is enabled by information as a service and is controlled by the information owner
- Principles of authentication and access management must be enabled at the client side
- Connectivity is supported by common registries for identities and services enabling providers of services to expose their services and for consumers to consume services
- Service realization is, after connectivity has been established between service provider and service consumer, is done peer-to-peer
- Trust is given to the maritime digital infrastructure by federative governance

This paper presents an analysis of how a maritime digital infrastructure for Sea Traffic Management has been elicited. The process starts out by exploring the characteristics of the ecosystem that the infrastructure is intended to support, which results in a representative model. This elicitation analysis pointed at the necessity to facilitate and support secure processes of episodic tight couplings by digital collaboration in the maritime domain. The collaborative aspect then leads to the central theme of this article, namely the need to define standardized message formats to ensure that actors “speak” the same language.

Similarly, prototyping assumptions in their specific context have also proven to be a successful method to provide useful solutions throughout the requirement engineering processes. A holistic view is important to understand the interactions between stakeholders and interconnections in their data, however, building the maritime digital infrastructure for STM top-down has proven difficult. Hypotheses are necessary to prioritize and test the prototyping efforts. Furthermore, a contextual validation of the maritime digital infrastructure is ensured by testing these hypotheses in the context of one of the Sea Traffic Management concepts.

Empirical grounding of the analysis has been made by relating to the emergence of architecture and a technical artifact for the validation of the PortCDM concept as one of the sub concepts of Sea Traffic Management. Further research would be to first take the identified hypotheses and verify / falsify them and secondly to match the design principles of the maritime digital infrastructure with contemporary initiatives having elicited similar requirements in the same domain.

References

- BOEHM, B.; EGYED, A.; KWAN, J.; PORT, D.; SHAH, A.; MADACHY, R. (1998), *Using the WinWin Spiral Model: A Case Study*, Computer 31/7, pp.33-44
- EASTERBROOK, S. (1994), *Resolving requirements conflicts with computer-supported negotiation*, Requirements Engineering: Social and Technical Issues, Academic Press Professional, pp.41-65
- GOGUEN, J.A. ; LINDE, C. (1993), *Techniques for requirements elicitation*, IEEE Int. Symp. Requirements Eng.
- GORSCHEK, T.; WOHLIN, C. (2006), *Requirements abstraction model*, Requirements Eng. 11/1, pp.79-101
- HARALDSON, S. ; LIND, M. ; MELLEGÅRD, N. ; KARLSSON, M. ; FERRÚS CLARI, G. ; DEEHAN, S.; McBRIDE, J. (2015), *PortCDM Validation Report*, D2.7.1. MONALISA 2.0. <http://monalisaproject.eu/wp-content/uploads/ML2-D2.7.1-PortCDM-Validation.pdf>
- HARALDSON, S.; LIND, M. (2011), *Value Chains in Value Networks: A Multi-Organizational Business Process Definition*, Australian Conf. Information Systems, Australia
- HOFMANN, H.F.; LEHNER, F. (2001), *Requirements engineering as a success factor in software projects*, IEEE Software 18/4, pp.58-66
- HULL, E.; JACKSON, K.; DICK, J. (2010), *Requirements Engineering*, Springer
- JIAO, J. (2006), *Customer Requirement Management in Product Development: A Review of Research Issues*, Concurrent Eng.: Research and Applications 14/3, pp.173-185
- LIND, M.; BRÖDJE, A.; WATSON, R.; HARALDSON, S.; HOLMBERG, P.; HÄGG, M. (2014), *Digital infrastructures for enabling sea traffic management*, ISIS, Hamburg
- LIND, M.; JENSEN, J.; HARALDSON, S.; WATSON, R.; SETTERBERG, P.; HOLMBERG, P.E. (2015), *Service and communication infrastructure for sea traffic management*, COMPIT, Ulrichshusen
- MONALISA (2015), *PortCDM Validation Report*, MONALISA 2.0 – D2.7.1
- NUSEIBEH, B.; EASTERBROOK, S. (2000), *Requirements Engineering: A Roadmap*, Conf. The Future of Software Engineering (ICSE), pp.35-46
- POHL, K. (1994), *The Three Dimensions of Requirements Engineering: A Framework and Its Applications*, Information Systems 19/3, pp.243-258
- SIWE, U.; LIND, M.; HÄGG, M.; DALÉN, A.; BRÖDJE, A.; WATSON, R.; HOLMBERG, P.E. (2015), *Sea Traffic Management – Concepts and Components*, COMPIT, Ulrichshusen
- LAMSWEERDE, A.v. (2001), *Goal-oriented requirements engineering: A guided tour*, 5th IEEE Int. Symp. Requirements Engineering
- LAMSWEERDE, A.v. (2000), *Requirements Engineering in the Year 00*, 22nd Int. Conf. Software Eng. (ICSE)
- YU, E.S.K. (1997), *Towards modelling and reasoning support for early-phase requirements engineering*, 3rd IEEE Int. Symp. Requirements Eng., pp.226-235

Vessel Monitoring Based on Sensors Data Collection

Andrea Coraddu, DAMEN Shipyard, Singapore, andrea.coraddu@damen.com
Toine Cleophas, DAMEN Shipyard, Gorinchem/NL, toine.cleophas@damen.com
Sandor Ivancsics, DAMEN Shipyard, Gorinchem/NL, sandor.ivancsics@damen.com
Luca Oneto, University of Genoa, Genova/Italy, luca.oneto@unige.it

Abstract

The main purpose of this work is to build data driven models for identifying operational profile of vessels based on historical sensor data acquisitions. The proposed approach utilize the advantage of the new generation of automation systems which allows gathering a large amount of data from on-board machinery. A data driven modelling of the operational profiles of the vessels could provide a tool both for diagnose and predict the state for improving the performance and the efficiency of the vessel, and for improving design solutions. The developed model has been tested and validated on a real DAMEN vessel where on-board sensors data acquisitions are available from the automation systems.

1. Introduction

In the upcoming years the role of data logging, data analysis and remote monitoring will significantly increase. Two main aspects of remote monitoring can be analysed: remote services and analysis of operational profiles. One of these aspects is the data logging and monitoring the condition of the ship in order to provide remote assistance and condition based maintenance, all gathered under the name of remote services. A completely different aspect of data logging and remote monitoring is the analysis of the data to advise the operators on their best utilization of their ship. On the long term this feedback from the operator should lead to designs that are more similar to the actual operation by the customer. In other words, this is the discrepancy between the intended use by the designer and the actual user experience by the operator. Ship design is typically performed optimising the system (hull form, propellers, engine, gearbox, etc.) for a technical specification requirement starting from a-priori operational profile. However, usually a vessel operates in her design conditions for a small proportion of her lifetime, *Greitsch et al. (2009)*. Usually operational profiles are in practice estimated based on experience, not based on measured data. Until now a limited verification of design considerations compared with real data on ship's equipment has been performed. Realistic operating profiles can be obtained by means of detailed information about the use of the vessel digitally available from different sources: (i) data stored on board of vessels; (ii) Automatic Identification System (AIS); (iii) data available through the internet such as vessel tracking GPS. The operational profile of a ship can be defined as the combination of a speed and operational modes distribution. Understanding the current trends of operations, allows for improved design options to be considered; such as the right determination of vessel parameters and characteristics (e.g. design speed, design draft, etcetera) and equipment selection and sizing to reflect the expected future operation (including routes) for the ship. Moreover shipbuilding optimization could be further improved by taking account of more than the design points, relating to the learned operational profiles, *Banks et al. (2013)*. The information age brings along an explosion of big data from multiple sensors which monitor every aspect of a ship, *Coraddu et al. (2015a,b)* could play an important role in operational use of ships in order to improve ship design as shown in Fig. 1.

Recent trends in the area suggest that in the following years the exponential data growth will continue, *Mills et al. (2012)*, and that there is a strong need to find efficient solutions to deal with aspects such as data storage, real-time processing, information extraction and abstract model generation. Big data analytics focuses on collecting, examining and processing large multi-modal and multi-source datasets in order to discover patterns, correlations and extract information from data, *Zhai et al. (2014)*. This is usually accomplished through the use of supervised and unsupervised machine learning algorithms that learn from the available data. However, these are usually highly computationally

expensive, either in the training or prediction phases (e.g. Support Vector Machines-SVM and k -Nearest Neighbors-KNN, respectively), to the point of becoming intractable using serial algorithm implementations as they are not able to handle current data volumes, *Wu et al. (2014)*. Alternatively, parallel approaches have been proposed in order to boost processing speeds, *You et al. (2014)*, but this clearly requires technologies that support distributed computations. Several technologies are currently available that are capable of exploiting multiple levels of parallelism (e.g. multi-core, many-core, GPU, cluster, etc.), *Cao et al. (2006)*, *Zaharia et al. (2012)*, *Olukotun (2014)*. Their trade-off aspects such as performance, cost, failure management, data recovery, maintenance and usability in order to provide solutions adapted to every application.

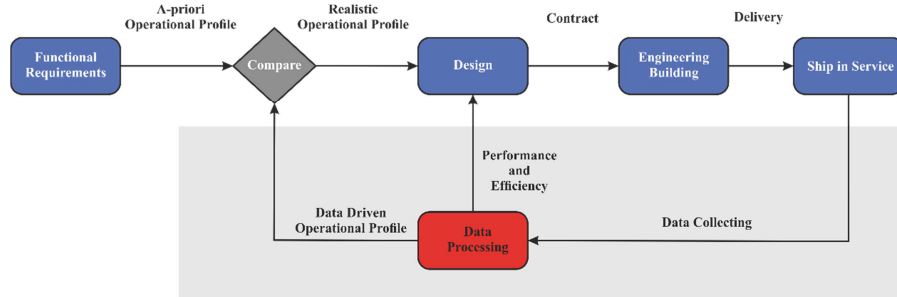


Fig. 1: Design improvement

2. Problem Description

2.1. Ship description

We propose Machine Learning techniques based on kernel methods to create realistic operating profiles and improving design solutions. To show the effectiveness of the proposed method, it is here tested on Damen Hybrid Azimuth Stern Drive Tug 2810, Fig. 2, Table I.

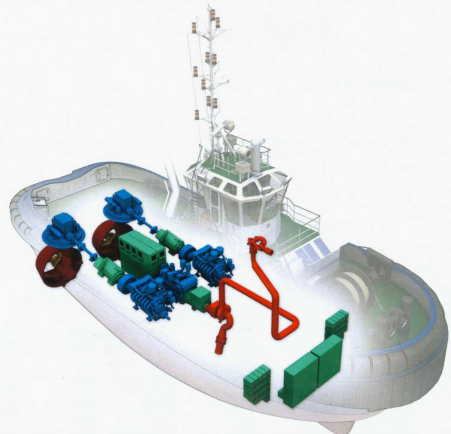


Fig. 2: Ship propulsion system layout

Table I: Main features of the case study

Length O.A.	28.76 m	Battery packs	2 x 120 kWh
Beam O.A.	10.43 m	Main electrical engines (ABB M3LP450)	1000 kW
Depth	4.38 m		1500 rpm
Draught AFT	5.15 m		440 V
Displacement	604 t		60 Hz
Diesel power	3680 kW	Azimuth thrusters (Rolls Royce US 205)	1500 kW
Prop. diameter	2400 mm		1500 rpm
Prop. genset (MTU 12V 2000 M41B)	800 kVA 440 V 60 Hz		18 t 51 t 2200 mm

The hybrid propulsion system consists of two diesel engines and two electric engines connected in tandem with two steerable rudder propeller units with fixed pitch propellers in nozzles. Two battery packs are installed and can be used to drive the electric engines at limited load.

Table II: Operational mode

Operational Profile	Symbol	Operational Profile	Symbol
Harbour	OP1	Towing	OP4
Free Sailing	OP2	Hybrid Control Unit (HCU) Override	OP5
Stand-by	OP3	Fire fighting	OP6

2.1. Data logging system

The ship under study is provided with a data logging system installed by Alewijnse which is used by the company both for on board monitoring and for land based performance control. The installed data logging system is designed to enable continuous access to data both on board and ashore through an interactive web based solution and to provide an efficient information flow. This goal is achieved by collecting data from systems and sensors on board, distributing them in the right format to fleet management offices and/or suppliers support systems. Issues related to the measurement of speed through water (LOG speed) are well known and such measurements are often partly unreliable as a consequence of the fact that the flow through the measurement device can be easily disturbed by its interaction with the hull or by other environmental conditions. On the other hand measurements of speed over ground (GPS speed), although more reliable, do not include the influence of currents, which can be as strong as 2–3 kn depending on time and location and therefore influence ship power demand for propulsion. Fig. 3 shows the dataTaker DT80LM intelligent data logger system. This system is a low-powered logging platform with an integrated cellular modem, making it perfect for remote applications. The rugged design and wide operating temperature range of the DT80LM provides reliable operation in virtually any environment. Logged data can then be easily extracted also via a USB memory stick, or downloaded using the web interface into files ready for import into spreadsheets. Table III summarises the available measurements from the continuous monitoring system.

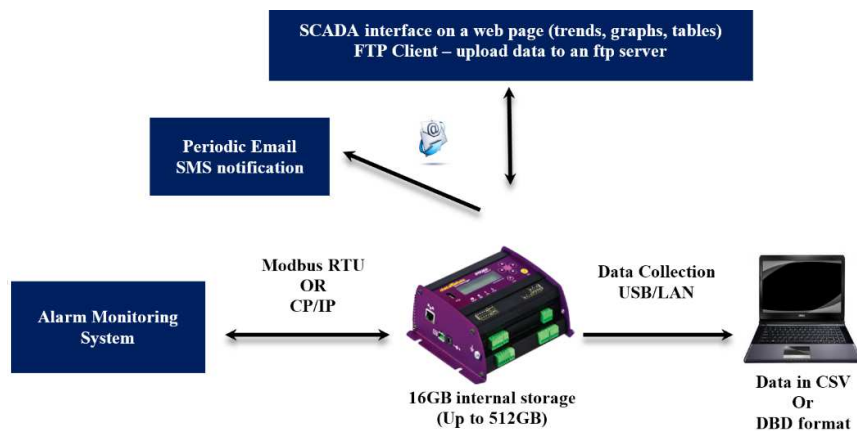


Fig. 3: On-board data log system - DataTaker DT80LM

Table III: Values available from the monitoring system

System	Variable name	Unit
Vessel General info	Latitude Position	[deg; min]
	Longitude Position	[deg; min]
	Heading Position	
	Vessel Speed	[m/s]
Shaft line info	Shaft Torque	[kNm]
	Shaft power	[kW]
	Shaft rpm	[rpm]

Diesel Engine	Port side Load	[kNm]
	Port side Speed	[rpm]
	Port side Fuel Consumption	
	Starboard side Load	[kNm]
	Starboard side Fuel Consumption	[kg/mins]
	Starboard side Speed	[rpm]
Electric Motor info ABB electric propulsion motor/generator. 440 volts, 60 HZ AC, and has a power output of 230kW at 900 rpm	Starboard side Speed	[rpm]
	Starboard side Power	[kW]
	Starboard side Speed	[rpm]
	Starboard side Power	[kW]
Auxiliary info MTU 12V2000 diesel engine Rated 695 kW at 1800 rpm to drive a generator	Auxiliary Generator Engine Speed	[rpm]
	Auxiliary Generator Fuel Consumption	[kg/mins]
	Auxiliary Generator Engine Load	[kW]
Azimuthing propulsion units Rolls-Royce US 205 FP	Port side Steering Angle	[deg]
	Starboard side Steering Angle	[deg]
Battery	Port side Battery Power	[kW]
	Port side Battery State of char	[%]
	Starboard Battery Power	[kW]
	Starboard Battery State of char	[%]
	Port side Clutch Response	[s]
	Starboard Clutch Response	[s]
	Towing line force	[N]
	Outstanding wire length	[m]

3. Data Analytics

In order to check the actual operational condition of a ship we need models that must deliver accuracy and reliability. Two main approaches exists for the derivation of such models. The first approach is based on traditional Naval Architecture and Marine Engineering principles and relies on mechanistic modelling of the physical phenomena involved in the determination of the operational condition. The second approach instead, infers the desired model directly from the measured data through a statistical data analysis. This second approach relies on the new generation of automation systems which allow gathering a large amount of data from on-board machinery. The classical models are able to describe the behaviour of the ship resistance, propeller characteristics and engine performances based on governing physical laws and taking into account their mutual interactions, *Lewis (1988)*. The higher the detail in the modelling of the physical equations which describe the different phenomena, the higher the expected accuracy of the results and the computational time required for the simulation. These models are generally rather tolerant to extrapolation and do not require extensive amount of operational measurements; on the other hand, when employing models that are computationally fast enough to be used for online optimisation, the expected accuracy in the prediction of operational variables is relatively low. In addition, the construction of the model is a process that requires competence in the field, and availability of technical details which are often not easy to get access to. Examples of the use for the optimisation of ship trim are, *Lee et al. (2014)*, who employed advanced CFD methods, and *Moustafa et al. (2015)* who employed simpler empirical models (*Holtrop-Mennen*) for the estimation of possible gains from trim optimisation. Data driven models, *Vapnik (1998)*, instead, build upon statistical inference procedures based on the historical data collection. The advantage of these methods is that there is no need of any a-priory knowledge of the underline physical system. Furthermore, thanks to the nature of these approaches, it is possible to exploit even data from sensors that could contain some kind of hidden information that cannot be easily extracted with a parametric approach. These approaches can produce black-box (non-parametric) models that are not supported by any physical interpretation, *Shawe-Taylor and Cristianini (2004)*, or they can also pro-

vide white-box (rule-based) models that can provide a data-driven explanation of the phenomena with if-then-else rules, *Safavian and Landgrebe* (1991) at the expenses of a lower accuracy respect to the black-box ones. Obviously these methods require a certain amount of historical data in order to produce reliable models, *Petersen et al.* (2012), *Coraddu et al.* (2015b). In particular there are two main family of data driven methods: the supervised and the unsupervised learning methods. Supervised learning is task of inferring a function from labeled training data, *Vapnik* (1998). The training data consist of a set of training examples. In supervised learning, each example is a pair consisting of an input object (typically a vector) and a desired output value. A supervised learning algorithm analyses the training data and produces an inferred function, which can be used for mapping new examples. An optimal scenario will allow for the algorithm to correctly determine the class labels for unseen instances. This requires the learning algorithm to generalise from the training data to unseen situations. Since in this work we will focus on the problem of identify the operational conditions we will deal with classification problems which is a particular case of the more general supervised learning problem.

More formally in the conventional classification framework, *Vapnik* (1998), *Shawe-Taylor and Cristianini* (2004) a set of data $\mathcal{L}_n = \{(\mathbf{x}_1, y_1), \dots, (\mathbf{x}_n, y_n)\}$, with $\mathbf{x}_i \in \mathcal{X} \in \mathbb{R}^d$ and $y_i \in \mathbf{Y} \in \{1, \dots, c\}$, are available from the automation system. The goal of the authors is to identify the unknown model $\mathfrak{S}: \mathcal{X} \rightarrow \mathcal{Y}$ though a model $\mathfrak{M}: \mathcal{X} \rightarrow \mathcal{Y}$.

The accuracy of the model \mathfrak{M} in representing the unknown system \mathfrak{S} is evaluated with reference to a loss function which counts the number of misclassified samples. In particular, given a series data $\mathcal{T}_m = \{(\mathbf{x}_1, y_1), \dots, (\mathbf{x}_m, y_m)\}$, our model will predict a series of outputs $\{\hat{y}_1, \dots, \hat{y}_m\}$ given the inputs $\{\mathbf{x}_1, \dots, \mathbf{x}_m\}$. Based on these outputs it is possible to compute the percentage of misclassified samples (PMS) as follows:

$$\text{PMS} = \frac{1}{n} \sum_{i=1}^n [y_i \neq \hat{y}_i], \quad (1)$$

where the Iverson bracket notation is exploited.

Unsupervised learning is the task of inferring a function to describe hidden structure from unlabelled data. Since the examples given to the learner are unlabelled, there is no error or reward signal to evaluate a potential solution, *Hastie et al.* (2009). This distinguishes unsupervised learning from supervised learning. Unsupervised learning is closely related to the problem of density estimation in statistics, *Bishop* (1995). However unsupervised learning also encompasses many other techniques that seek to summarise and explain key features of the data. One of the most important Unsupervised learning problem is the Clustering one, *Jain* (2010). Clustering is the task of grouping a set of objects in such a way that objects in the same group (called a cluster) are more similar (in some sense or another) to each other than to those in other groups (clusters). It is a main task of exploratory data mining, and a common technique for statistical data analysis, used in many fields, *Duran and Odell* (2013). Clusters can be achieved by various algorithms that differ significantly in their notion of what constitutes a cluster and how to efficiently find them. Popular notions of clusters include groups with small distances among the cluster members, dense areas of the data space, intervals or particular statistical distributions. Clustering can therefore be formulated as a multi-objective optimisation problem. The appropriate clustering algorithm and parameter settings (including values such as the distance function to use, a density threshold or the number of expected clusters) depend on the individual data set and intended use of the results. Cluster analysis as such is not an automatic task, but an iterative process of knowledge discovery or interactive multi-objective optimization that involves trial and failure. It will often be necessary to modify data pre-processing and model parameters until the result achieves the desired properties.

More formally in the conventional clustering framework, *Hastie et al.* (2009), a set of unlabelled data $\mathcal{U}_n = \{\mathbf{x}_1, \dots, \mathbf{x}_n\}$ with $\mathbf{x}_i \in \mathcal{X} \in \mathbb{R}^d$ are available from the automation system. The goal of the au-

thors is to identify group of data than can be considered similar in some sense, in particular if clusters of measurements belongs to the same operational profile.

3.1. Support Vector Machines

One of the state of the art algorithm in the classification framework is the Support Vector Machines (SVMs), *Vapnik (1998)*, *Oneto et al. (2016)*, *Fernandez-Delgado et al. (2014)*. SVMs deal just with binary classification problems $\mathcal{Y} = \{\pm 1\}$. The SVM classifier is defined as:

$$f(\mathbf{x}) = \mathbf{w} \cdot \phi(\mathbf{x}) + b \quad (2)$$

where the weights $\mathbf{w} \in \mathbb{R}^D$ and the bias $b \in \mathbb{R}$ are found by solving the following primal convex constrained quadratic programming (CCQP) problem, *Cortes and Vapnik (1995)*:

$$\begin{aligned} \min_{\mathbf{w}, b, \xi} \quad & \frac{1}{2} \|\mathbf{w}\|^2 + C \sum_{i=1}^n \xi_i \\ \text{s.t.} \quad & y_i (\mathbf{w} \cdot \phi(\mathbf{x}_i) + b) \geq 1 - \xi_i \\ & \xi_i \geq 0, \quad i \in \{1, \dots, n\} \end{aligned} \quad (3)$$

The above problem is also known as the Tikhonov formulation of the SVM, because it can be seen as a regularised ill-posed problem. By introducing n Lagrange multipliers $\alpha_1, \dots, \alpha_n$, it is possible to write the problem of Eq. (3) in its dual form, for which efficient solvers have been developed throughout the years, *Cortes and Vapnik (1995)*, *Shawe-Taylor and Sun (2011)*:

$$\begin{aligned} \min_{\alpha} \quad & \frac{1}{2} \sum_{i=1}^n \sum_{j=1}^n \alpha_i \alpha_j y_i y_j K(\mathbf{x}_i, \mathbf{x}_j) - \sum_{i=1}^n \alpha_i \\ \text{s.t.} \quad & 0 \leq \alpha_i \leq C \\ & \sum_{i=1}^n y_i \alpha_i = 0 \end{aligned} \quad (4)$$

where $K(\mathbf{x}_i, \mathbf{x}_j) = \phi(\mathbf{x}_i) \cdot \phi(\mathbf{x}_j)$ is a suitable kernel function, *Shawe-Taylor and Cristianini (2004)*. After solving the Problem (4), the Lagrange multipliers can be used to define the SVM classifier in its dual form:

$$f(\mathbf{x}) = \sum_{i=1}^n y_i \alpha_i K(\mathbf{x}_i, \mathbf{x}) + b \quad (5)$$

The hyperparameter C in the kernel in Problem (4) is tuned during the model selection, *Anguita et al. (2012)*, and defines the generalisation ability of the learned model. In this paper authors will use the Gaussian Kernel for its good generalisation properties, *Keerthi and Lin (2003)*, *Oneto et al. (2015)*:

$$K(\mathbf{x}_i, \mathbf{x}_j) = e^{-\gamma \|\mathbf{x}_i - \mathbf{x}_j\|^2} \quad (6)$$

This kernel require to set another hyperparameter γ which balances the non-linearity of the final model, *Keerthi and Lin (2003)*. Then, any model selection technique can be applied to choose the tuple $(C; \gamma)$ which is characterised by the best generalisation performance. Several methods exist for this purpose: out-of-sample methods, like the well-known k -Fold Cross Validation (KCV), *Kohavi (1995)* approach, represent the state-of-the art model selection approaches when targeting several applications, *Anguita et al. (2012)*.

In KCV, the original dataset \mathcal{D}_n is split into k independent subsets (namely, the folds), each one consisting of n/k samples: $(k-1)$ parts are used, in turn, as a training set, and the remaining fold is exploited as a validation set. Note, in fact, that the error performed by the trained model on the validation set can be reliably used for estimating the generalisation error, because this fold has not

been used for training the model, *Guyon et al. (2010)*, *Anguita et al. (2009)*, *Kohavi (1995)*, *Dietterich (1998)*. The procedure is iterated k times. It is worth underlining that k itself could be considered as a hyperparameter, *Anguita et al. (2012)*: however, in practice, $k = 3; 5; 10$ or 20 represent feasible choices in the largest part of applications, *Anguita et al. (2012)*.

The KCV procedures for SVM is presented in Algorithms 1. Given a training set \mathcal{D}_n , a fixed number of folds k , and a grid of values to be explored for the hyperparameters C and γ the original dataset is split into k folds, as a first step: let $\mathcal{S} = \{1, \dots, n\}$ be the set of indexes of the samples in \mathcal{D}_n ; then, k sets of indexes $\mathcal{S}^{(t)}$, $t \in \{1, \dots, k\}$, are created. These subsets are such that:

$$\bigcup_{t=1}^k \mathcal{S}^{(t)} = \mathcal{S} \quad \bigcap_{t=1}^k \mathcal{S}^{(t)} = \emptyset. \quad (7)$$

Ideally, the range where to search for the hyperparameters should be $C, \gamma \in [0, +\infty)$, and the search grid should have infinite resolution. Obviously, both the coarseness of the grid and the size of the searching space severely influence the quality of the solution and the amount of computation time needed by the learning procedure. Nevertheless, some practical suggestions can be retrieved in literature, which help finding good trade-offs between performance and computational time, *Bergstra and Bengio (2012)*. The best error for the KCV procedure is initialised to $L_{\text{KCV}}^* = +\infty$.

Then, for every possible set of values in the grid for the hyperparameters tuple $(C; \gamma)$; a KCV stage is run. At the t -th KCV step, the patterns in the validation set are indexed by $\mathcal{S}^{(t)}$, while the training set consists of the remaining samples, whose indexes are $(\mathcal{S} \setminus \mathcal{S}^{(t)})$.

A model is then trained on the training set and its performance is verified on the validation patterns by computing the empirical error

$$\hat{L}_{n/k}^{(t)}(f^{(t)}) = \frac{1}{n/k} \sum_{i \in \mathcal{S}^{(t)}} [f^{(t)}(\mathbf{x}_i) \neq y_i]. \quad (8)$$

After the k KCV steps are over, the estimated generalization error for the hyperparameters tuple can be computed by averaging the t empirical errors on the validation sets:

$$L_{\text{KCV}} = \frac{1}{k} \sum_{t=1}^k \hat{L}_{n/k}^{(t)}(h). \quad (9)$$

If the obtained error is lower than the best L_{KCV}^* reported so far, the hyperparameters tuple is saved as potential best configuration for the learning procedure. As a final issue the authors want to point out that, in order to select the best hyperparameters tuple, k models are created at every KCV step. Once the best tuple is found, the final model is trained on the whole set \mathcal{D}_n by running the learning procedure where hyperparameters are set to the identified best values. In order to extend the SVM to the multiclass setting the All versus All (AVA) method will we adopted.

AVA consists in building $c(c - 1)/2$ training sets $\mathcal{L}^{u,v}$, each one containing data only from two different classes, u and v . These sets are used for training $c(c - 1)/2$ different biclass SVMs and the resulting models are saved for the feedforward phase. When a new pattern x has to be classified, it is applied in input to all the biclass SVMs and the multiclass label is then found. In the case of conflicts among different classes, a Winner-Take-All (WTA) arbiter is used for assigning the pattern to the final label: the class corresponding to the highest $f(x)$ value is considered as the final \hat{y} by of the datum. The AVA technique is usually characterized by a good performance in terms of error rate, since the granularity in classifying every class versus all the others helps reaching a high accuracy.

Algorithm 1 The k -Fold Cross Validation (KCV) model selection procedure for SVM.

Require: X, k , a grid for every hyperparameter involved $\mathcal{G}_{C,\gamma}$

```
1:  $L_{\text{KCV}}^* = +\infty$ 
2:  $(C^*, \gamma^*) = (-\infty, -\infty)$ 
3:  $\mathcal{S}^{(t)} = \text{split}(\mathcal{S})$ ,  $t = 1, \dots, k$ 
4: for all  $(C, \gamma) \in \mathcal{G}_{C,\gamma}$  do
5:    $L_{\text{KCV}} = 0$ 
6:   for  $t = 1 \rightarrow k$  do
7:     Train  $f^{(t)}$  with SVM Problem (4) on the set of data indexed by  $(\mathcal{S} \setminus \mathcal{S}^{(t)})$  and with the hyperparameters  $(\lambda, \gamma)$ 
8:     Compute  $\hat{L}_{n/k}^{(t)}(h^{(t)})$  according to Eq. (8)
9:   end for
10:  Compute  $L_{\text{KCV}}$  according to Eq. (9)
11:  if  $L_{\text{KCV}} < L_{\text{KCV}}^*$  then
12:     $L_{\text{KCV}}^* = L_{\text{KCV}}$ 
13:     $(\lambda^*, \gamma^*) = (\lambda, \gamma)$ 
14:  end if
15: end for
16: Train  $f^*$  with SVM Problem (4) by using the whole set  $\mathcal{D}_n$  and the tuple  $(\lambda^*, \gamma^*)$ 
17: return  $h^*$ 
```

3.1. Spectral Clustering

There are many types of clustering, *Hastie et al. (2009)*. Hierarchical algorithms find successive clusters using previously established clusters. These algorithms usually are either agglomerative ('bottom-up') or divisive ('top-down'). Agglomerative algorithms begin with each element as a separate cluster and merge them into successively larger clusters. Divisive algorithms begin with the whole set and proceed to divide it into successively smaller clusters. Partitional algorithms typically determine all clusters at once, but can also be used as divisive algorithms in the hierarchical clustering. Density based clustering algorithms are devised to discover arbitrary-shaped clusters. In this approach, a cluster is regarded as a region in which the density of data objects exceeds a threshold. Subspace clustering methods look for clusters that can only be seen in a particular projection (subspace, manifold) of the data.

These methods thus can ignore irrelevant attributes. The general problem is also known as Correlation clustering while the special case of axis-parallel subspaces is also known as Two-way clustering, coclustering or biclustering: in these methods not only the objects are clustered but also the features of the objects, i.e., if the data is represented in a data matrix, the rows and columns are clustered simultaneously. They usually do not however work with arbitrary feature combinations as in general subspace methods. But this special case deserves attention due to its applications in bioinformatics. Many clustering algorithms require the specification of the number of clusters to produce in the input data set, prior to execution of the algorithm.

An important step in most clustering is to select a distance measure, which will determine how the similarity of two elements is calculated. This will influence the shape of the clusters, as some elements may be close to one another according to one distance and farther away according to another. For example, in a 2-dimensional space, the distance between the point $(1; 0)$ and the origin $(0; 0)$ is always 1 according to the usual norms, but the distance between the point $(1; 1)$ and the origin can be $2, \sqrt{2}$ or 1 if you take respectively the 1-norm, 2-norm or infinity-norm distance.

Common distance functions are the Euclidean distance (2-norm), the Manhattan distance (1-norm), the maximum norm (infinity norm), the Mahalanobis distance, the angle between two vectors can be used as a distance measure when clustering high dimensional data, the Hamming distance measures the minimum number of substitutions required to change one member into another. Another important distinction is whether the clustering uses symmetric or asymmetric distances. Many of the distance functions listed above have the property that distances are symmetric (the distance from object A to B is the same as the distance from B to A). In many other cases, this property cannot hold any more. One of the most useful clustering technique is the k -means algorithm (Lloyd 1982) which assigns each point to the cluster whose center (also called centroid) is nearest. The main advantages of this

algorithm are its simplicity and speed which allows it to run on large datasets. Its disadvantage is that it does not yield the same result with each run, since the resulting clusters depend on the initial random assignments (the k-means++ algorithm addresses this problem by seeking to choose better starting clusters, *Arthur and Vassilvitskii (2007)*). It minimises intra-cluster variance, but does not ensure that the result has a global minimum of variance. Another disadvantage is the requirement for the concept of a mean to be definable which is not always the case.

For such datasets the k -medoids variants is appropriate, *Park and Jun (2009)*. An alternative, using a different criterion for which points are best assigned to which centre is k -medians clustering. A promising alternative that has recently emerged in a number of fields is to use spectral methods for clustering, *Zelnik-Manor and Perona (2004)*, *Ng et al. (2001)*, *Weiss (1999)*. Here one uses the top eigenvectors of a matrix derived from the distance between points. Such algorithms have been successfully used in many applications including computer vision and machine learning. But despite the empirical success different authors still disagree on exactly which eigenvectors to use and how to derive a cluster from them. Also the analysis of these algorithms has tended to focus on simplified algorithms that only use one eigenvector at the time.

Here the authors report a work that is built upon, *Weiss (1999)*, *Meilpa and Shi (2001)*, who analysed algorithms that uses the k eigenvectors simultaneously and give condition in which algorithm can be expected to do well. The Spectral Clustering algorithms is reported in Algorithm 2 and clusters the data \mathcal{U}_n in k cluster, the parameter σ controls how rapidly the affinity A_{ij} falls off with the distance between \mathbf{x}_i and \mathbf{x}_j .

Algorithm 2 Spectral Clustering.

Require: \mathcal{U}_n , σ and number of clusters k

1: Form the affinity matrix $A \in \mathbb{R}^{n \times n}$ defined by

$$A_{ij} = \exp(-\|\mathbf{x}_i - \mathbf{x}_j\|^2/2\sigma^2) \quad \text{if } i \neq j, \quad A_{ij} = 0 \quad \text{if } i == j \quad (10)$$

2: Define D to be the diagonal matrix whose (i,i)-element is the sum of the A 's i-th rows and construct the matrix $L = D^{-1/2}AD^{-1/2}$

3: Find the k ($\mathbf{x}_1, \dots, \mathbf{x}_k$) largest eigenvector of L (chosen to be orthogonal in case of repeated eigenvalues) and form the matrix $X = [\mathbf{x}_1, \dots, \mathbf{x}_k] \in \mathbb{R}^{n \times k}$ by stacking the eigenvector in columns

4: Form the matrix Y from X by renormalizing each of X 's row to have unit length

$$Y_{i,j} = X_{i,j} / \sqrt{\sum_j X_{ij}^2} \quad (11)$$

5: Treating each row of Y as a point in \mathbb{R}^k , cluster them with k -means or any other algorithm

6: Finally assign the original point s_i to the cluster j if and only if row i of the matrix Y was assigned to cluster j

4. Experimental Results

The first one, $\mathcal{D}_{n_{\text{train}}}$, consisting of n_{train} samples, which is used for the training phase, thus including model selection and creation. Note that during the unsupervised learning phase the labels are not taken into account. The second one, $\mathcal{D}_{n_{\text{test}}} \subseteq \mathcal{D}_n \setminus \mathcal{D}_{n_{\text{train}}}$, consisting of $n_{\text{test}} = n - n_{\text{train}}$. The feedforward phase of the model f^* , trained on $\mathcal{D}_{n_{\text{train}}}$, is run on these samples analogously to an application setting of the regressor. As the target outputs are available for $\mathcal{D}_{n_{\text{test}}}$, it is always possible to compute the PMS that f^* would obtain in the application scenario. Table IV shows the percentage of time in which the ship is in each Operational. The table shows the complexity of the task since there are Operational Profile which are common for the ship (e.g. OP1 and OP4) while others are really unusual (e.g. OP3 and OP6).

Table IV: Dataset description with operational profiles (OP) and percentage of time

Harbour	OP1	69.01%	Towing	OP4	21.21%
Free Sailing	OP2	8.17%	HCU Override	OP5	0.59%
Stand-by	OP3	0.21%	Fire fighting	OP6	0.39%

For this reason, instead of using the simple PMS for measuring the accuracy of the model we exploit the average percentage of misclassified samples per class (APMSPC) where

$$\text{APMSPC} = \frac{1}{c} \sum_{i=1}^c \frac{1}{n_i} \sum_{j=1}^{n_i} [y_j \neq \hat{y}_j] \quad (12)$$

where n_i is the number of samples belonging to the class $i \in \{1, \dots, c\}$.

By adopting the supervised learning approach on our data, exploiting the Multiclass SVM for different values of n_{train} , it is possible to obtain the confusion matrixes of Table V. Note that in the proposed cases all the experiments are repeated 30 times in order to obtain statistical relevant results. By exploiting, instead, the unsupervised learning approach the confusion matrixes of Table VI were obtained. By changing n_{train} the graph of Fig. 4 and 5 have been obtained, which represents the trend of the APMSPC for the supervised learning and unsupervised learning approach respectively.

Table V: Confusion matrixes using Supported Vector Machines (errors are in percentage)

$n_{\text{test}} = 10^4$						
\hat{y} y \	OP1	OP2	OP3	OP4	OP5	OP6
OP1	99.92 \pm 0.97	0.01 \pm 0.43	0.00 \pm 0.21	0.04 \pm 0.46	0.03 \pm 0.32	0.00 \pm 0.36
OP2	1.95 \pm 0.14	95.82 \pm 0.78	0.05 \pm 0.24	2.05 \pm 0.29	0.13 \pm 0.01	0.00 \pm 0.31
OP3	14.20 \pm 0.26	35.50 \pm 0.52	36.69 \pm 0.36	11.24 \pm 0.32	2.37 \pm 0.18	0.00 \pm 0.31
OP4	0.47 \pm 0.15	0.32 \pm 0.16	0.00 \pm 0.24	99.11 \pm 0.78	0.00 \pm 0.11	0.10 \pm 0.18
OP5	9.69 \pm 0.12	1.36 \pm 0.38	0.00 \pm 0.08	1.53 \pm 0.34	87.41 \pm 0.47	0.00 \pm 0.20
OP6	67.86 \pm 0.72	4.59 \pm 0.39	0.00 \pm 0.22	20.92 \pm 0.50	0.00 \pm 0.26	6.63 \pm 0.34
$n_{\text{test}} = 10^5$						
\hat{y} y \	OP1	OP2	OP3	OP4	OP5	OP6
OP1	99.93 \pm 0.82	0.02 \pm 0.35	0.01 \pm 0.00	0.04 \pm 0.44	0.00 \pm 0.20	0.00 \pm 0.11
OP2	2.03 \pm 0.37	96.65 \pm 0.75	0.11 \pm 0.46	1.20 \pm 0.15	0.00 \pm 0.39	0.01 \pm 0.15
OP3	7.49 \pm 0.44	3.74 \pm 0.34	85.03 \pm 0.62	3.74 \pm 0.35	0.00 \pm 0.42	0.00 \pm 0.08
OP4	0.43 \pm 0.06	0.12 \pm 0.07	0.05 \pm 0.20	99.25 \pm 0.65	0.00 \pm 0.39	0.16 \pm 0.11
OP5	3.29 \pm 0.46	0.16 \pm 0.08	0.00 \pm 0.07	0.00 \pm 0.44	96.54 \pm 0.60	0.00 \pm 0.31
OP6	70.11 \pm 0.61	0.26 \pm 0.31	0.00 \pm 0.09	4.23 \pm 0.38	0.53 \pm 0.22	24.87 \pm 0.31
$n_{\text{test}} = 10^6$						
\hat{y} y \	OP1	OP2	OP3	OP4	OP5	OP6
OP1	99.95 \pm 0.74	0.01 \pm 0.17	0.01 \pm 0.31	0.02 \pm 0.47	0.00 \pm 0.11	0.01 \pm 0.01
OP2	1.57 \pm 0.26	97.49 \pm 0.87	0.05 \pm 0.05	0.89 \pm 0.34	0.00 \pm 0.44	0.00 \pm 0.02
OP3	7.65 \pm 0.41	5.46 \pm 0.43	86.89 \pm 0.63	0.00 \pm 0.39	0.00 \pm 0.45	0.00 \pm 0.37
OP4	0.32 \pm 0.39	0.11 \pm 0.14	0.00 \pm 0.40	99.42 \pm 0.60	0.00 \pm 0.03	0.15 \pm 0.19
OP5	0.88 \pm 0.01	0.00 \pm 0.33	0.00 \pm 0.18	0.00 \pm 0.42	99.12 \pm 0.73	0.00 \pm 0.26
OP6	56.48 \pm 0.60	0.24 \pm 0.11	0.24 \pm 0.29	4.65 \pm 0.32	0.00 \pm 0.26	38.39 \pm 0.25

In the unsupervised learning approach the error is measured directly on the training set since no label are provided to the algorithms, *Ng et al. (2001)*. From the results reported it is possible to note that the supervised approach works fine in most of the situation with an accuracy which is very high. The only issue regards the Fire Fighting Mode which is not identifiable in an effective way. This compromises the final accuracy.

This result can be due to the small amount of on-board sensors and this support the current and future trend in the naval design where more and more ships are planned to be more and more sensorized. Also the unsupervised approach (again except for the Fire Fighting) is very effective and this is an important achievement since we are able to cluster the data without the supervisor which tell us what are the different operational profiles.

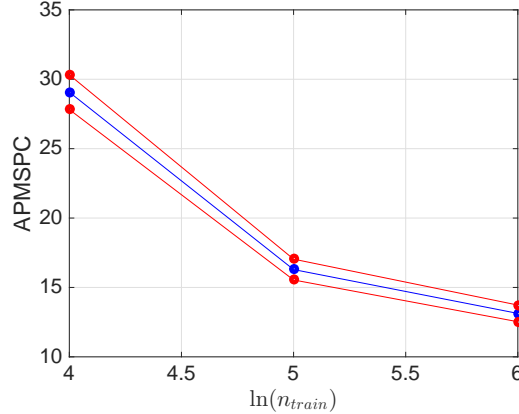


Fig. 4: APMSPC by varying n_{train} – Supported Vector Machines

Table VI: Confusion matrixes using Spectral Clustering (errors are in percentage)

$n_{test} = 10^4$						
\hat{y} y \	OP1	OP2	OP3	OP4	OP5	OP6
OP1	99.73±0.73	0.02±0.18	0.00±0.08	0.02±0.10	0.00±0.44	0.22±0.13
OP2	2.88±0.33	95.34±0.63	0.00±0.10	1.48±0.21	0.00±0.17	0.29±0.43
OP3	34.91±0.47	50.00±0.40	9.43±0.16	5.66±0.20	0.00±0.26	0.00±0.29
OP4	1.43±0.46	0.48±0.03	0.00±0.17	97.65±0.55	0.00±0.02	0.44±0.01
OP5	86.69±0.69	3.85±0.19	0.00±0.09	8.76±0.14	0.70±0.39	0.00±0.13
OP6	63.47±0.55	6.74±0.25	0.00±0.09	12.18±0.19	0.00±0.32	17.62±0.25
$n_{test} = 10^5$						
\hat{y} y \	OP1	OP2	OP3	OP4	OP5	OP6
OP1	99.92±0.97	0.01±0.43	0.00±0.21	0.04±0.46	0.03±0.32	0.00±0.36
OP2	1.95±0.14	95.82±0.78	0.05±0.24	2.05±0.29	0.13±0.01	0.00±0.31
OP3	14.20±0.26	35.50±0.52	36.69±0.36	11.24±0.32	2.37±0.18	0.00±0.31
OP4	0.47±0.15	0.32±0.16	0.00±0.24	99.11±0.78	0.00±0.11	0.10±0.18
OP5	9.69±0.12	1.36±0.38	0.00±0.08	1.53±0.34	87.41±0.47	0.00±0.20
OP6	67.86±0.72	4.59±0.39	0.00±0.22	20.92±0.50	0.00±0.26	6.63±0.34
$n_{test} = 10^6$						
\hat{y} y \	OP1	OP2	OP3	OP4	OP5	OP6
OP1	99.93±0.82	0.02±0.35	0.01±0.00	0.04±0.44	0.00±0.20	0.00±0.11
OP2	2.03±0.37	96.65±0.75	0.11±0.46	1.20±0.15	0.00±0.39	0.01±0.15
OP3	7.49±0.44	3.74±0.34	85.03±0.62	3.74±0.35	0.00±0.42	0.00±0.08
OP4	0.43±0.06	0.12±0.07	0.05±0.20	99.25±0.65	0.00±0.39	0.16±0.11
OP5	3.29±0.46	0.16±0.08	0.00±0.07	0.00±0.44	96.54±0.60	0.00±0.31
OP6	70.11±0.61	0.26±0.31	0.00±0.09	20.92±0.50	0.53±0.22	24.87±0.31

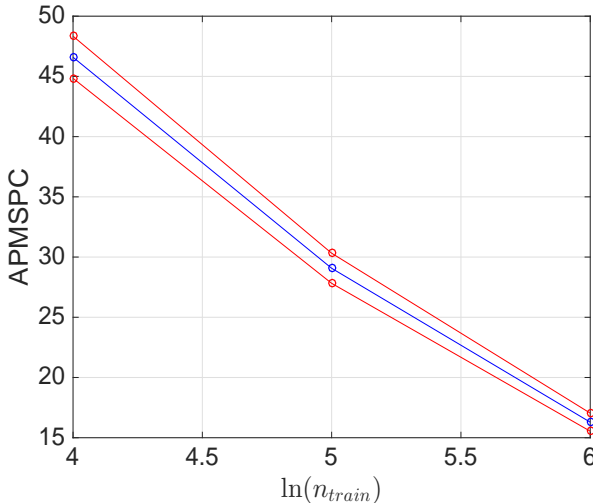


Fig. 5: APMSPC by varying n_{train} - Spectral Clustering

4. Conclusion

We have shown how data driven models be applied to create realistic operating profiles in order to assess and compare different design solutions for the next generation of DAMEN vessels. The proposed methodologies have been tested on real world historical data collected from a real vessel during one and half year of on board sensors data acquisitions. Thanks to the high accuracy of the developed models, the authors have been able to propose an effective tool which exploits the prediction of the operational profile for the implementation of design optimization. From Tables V and VI it can be observed that for some operational profiles the effectiveness of the machine algorithm is reduced.

This can be explained taking into account that for such cases, i.e. OP3 and OP6) few samples are available and the data acquisition system has not been designed for the purposes of this analysis. For this reason some important parameters are missing which could alter significantly alter the prediction. Moreover the operator has the freedom to modify the preselected mode characteristics switching on and off equipment (e.g.: hydraulic pump while not in towing), beside that there can be a discrepancy the selected operational mode and the actual operation. Both effects lead to some errors in the prediction of the state. With this in mind for the next generation of vessels' acquisition system more sensoring would be implemented and expert logics would be included in the automation. As future works it will be interesting to understand if the error over the clustering is due to an incorrect detection of the operational profile by the clustering algorithm or is due to a mistake of the supervisor.

References

- ANGUITA, D.; RIDELLA, S.; STERPI, D. (2009), *K-fold cross validation for error rate estimate in support vector machines*, Int. Conf. on Data Mining
- ANGUITA, D.; GHELARDONI, L.; GHIO, A.; ONETO, L.; RIDELLA, S. (2012), *The k in k-fold cross validation*, European Symp. Artificial Neural Networks
- ANGUITA, D.; GHIO, A.; ONETO, L.; RIDELLA, S. (2012), *In-sample and out-of-sample model selection and error estimation for support vector machines*, IEEE Trans. Neural Networks and Learning Systems 23(9), pp.1390-1406
- ARTHUR, D.; VASSILVITSKII, S. (2007), *k-means++: The advantages of careful seeding*, ACM-SIAM Symp. Discrete Algorithms
- BANKS, C.; TURAN, O.; INCECIK, A.; THEOTOKATOS, G.; IZKAN, S.; SHEWELL, C.; TIAN,

X. (2013), *Understanding ship operating profiles with an aim to improve energy efficient ship operations*, Low Carbon Shipping Conf.

BERGSTRA, J.; BENGIO, Y. (2012), *Random search for hyperparameter optimization*, J. Machine Learning Research 13(1), pp.281-305

BISHOP, C.M. (1995), *Neural networks for pattern recognition*, Oxford Univ. Press

CAO, L.J.; KEERTHI, S.S.; ONG, C.J.; ZHANG, J.Q., PERIYATHAMBY, U.; FU, X.J.; LEE, H.P. (2006), *Parallel sequential minimal optimization for the training of support vector machines*, IEEE Trans. Neural Networks 17(4), pp.1039-1049

CORADDU, A.; ONETO, L.; BALDI, F.; ANGUITA, D. (2015a), *A ship efficiency forecast based on sensors data collection: Improving numerical models through data analytics*, IEEE Oceans, Genova

CORADDU, A.; ONETO, L.; GHIO, A.; SAVIO, S.; ANGUITA, D.; FIGARI, M. (2015b), *Machine learning approaches for improving condition-based maintenance of naval propulsion plants*, J. Eng. for the Maritime Environment

CORTES, C.; VAPNIK, V.N. (1995), *Support-vector networks*, Machine learning 20(3), pp.273–297

DIETTERICH, T.G. (1998), *Approximate statistical tests for comparing supervised classification learning algorithms*, Neural computation 10(7), pp.1895–1923

DURAN, B.S.; ODELL, P.L. (2013), *Cluster analysis: a survey*, Springer Science & Business Media

FERNANDEZ-DELGADO, M.; CERNADAS, E.; BARRO, S.; AMORIM, D. (2014), *Do we need hundreds of classifiers to solve real world classification problems?*, J. Machine Learning Research 15(1), pp.3133-3181

GREITSCH, L.; ELJARDT, G.; KRUEGER, S. (2009), *Operating conditions aligned ship design and evaluation*, 1st Int. Symp. Marine Propulsors

GUYON, I.; SAFFARI, A.; DROR, G.; CAWLEY, G. (2010), *Model selection: Beyond the Bayesian/frequentist divide*, J. Machine Learning Research 11, pp.61-87

HASTIE, T.; TIBSHIRANI, R.; FRIEDMAN, J. (2009), *Unsupervised Learning*, Springer

JAIN, A.K. (2010), *Data clustering: 50 years beyond k-means*, Pattern Recognition Letters 31(8), pp.651-666

KEERTHI, S.S.; LIN, C.J. (2003), *Asymptotic behaviors of support vector machines with Gaussian kernel*, Neural computation 15(7), pp.1667-1689

KOHAVI, R. (1995), *A study of cross-validation and bootstrap for accuracy estimation and model selection*, Int. Joint Conf. Artificial Intelligence

LEE, J.; YOO, S.; CHOI, S.; KIM, H.; HONG, C.; SEO, J. (2014), *Development and application of trim optimization and parametric study using an evaluation system (solution) based on the RANS for improvement of EEOI*, Int. Conf. Ocean, Offshore and Arctic Engineering

LEWIS, E.V. (1988), *Principles of Naval Architecture*, SNAME

LLOYD, S.P. (1982), *Least squares quantization in pcm*, IEEE Trans. Information Theory 28(2), pp.129-137

MEILPA, M.; SHI, J. (2001), *Learning segmentation by random walks*, Neural Information Processing Systems

MILLS, S.; LUCAS, S.; IRAKLIOTIS, L.; RAPPA, M.; CARLSON, T.; PERLOWITZ, B. (2012), *Demystifying big data: a practical guide to transforming the business of government*, Tech. Rep. <http://www.ibm.com/software/data/demystifying-bigdata>

MOUSTAFA, M.M.; YEHIA, W.; HUSSEIN, A.W. (2015), *Energy efficient operation of bulk carriers by trim optimization*, Int. Conf. Ships and Shipping Research

NG, A.; JORDAN, M.; WEISS, Y. (2001), *On spectral clustering: Analysis and an algorithm*, Neural Information Processing Systems

OLUKOTUN, K. (2014), *Beyond parallel programming with domain specific languages*, Symp. Principles and Practice of Parallel Programming

ONETO, L.; GHIO, A.; RIDELLA, S.; ANGUITA, D. (2015), *Support vector machines and strictly positive definite kernel: The regularization hyperparameter is more important than the kernel hyperparameters*, IEEE Int. Joint Conf. Neural Networks (IJCNN)

ONETO, L.; RIDELLA, S.; ANGUITA, D. (2016), *Tikhonov, Ivanov and Morozov regularization for support vector machine learning*, Machine Learning

PARK, H.S.; JUN, C.H. (2009), *A simple and fast algorithm for k-medoids clustering*, Expert Systems with Applications 36(2), pp.3336–3341

PETERSEN, J.P.; JACOBSEN, D.J.; WINTHER, O. (2012), *Statistical modelling for ship propulsion efficiency*, J. Marine Science and Technology 17(1), pp.30-39

SAFAVIAN, S.R.; LANDGREBE, D. (1991), *A survey of decision tree classifier methodology*, IEEE Trans. Systems, Man, and Cybernetics 21(3), pp.660-674

SHawe-Taylor, J.; Cristianini, N. (2004), *Kernel methods for pattern analysis*, Cambridge Univ. Press

SHawe-Taylor, J.; Sun, S. (2011), *A review of optimization methodologies in support vector machines*, Neurocomputing 74(17), pp.3609-3618

Vapnik, V. (1998), *Statistical Learning Theory*, Wiley

Weiss, Y. (1999), *Segmentation using eigenvectors: a unifying view*, IEEE Conf. Computer Vision

WU, X.; ZHU, X.; WU, G.Q.; DING, W. (2014), *Data mining with big data*, IEEE Trans. Knowledge and Data Engineering 26(1), pp.97-107

You, Y.; Song, S.L.; Fu, H.; Marquez, A.; Dehnavi, M.M.; Barker, K.; Cameron, K.W.; Randles, A.P.; Yang, G. (2014), *Mic-svm: Designing a highly efficient support vector machine for advanced modern multi-core and many-core architectures*, IEEE Int. Parallel and Distributed Processing Symp.

Zaharia, M.; Chowdhury, M.; Das, T.; Dave, A.; Ma, J.; McCauley, M.; Franklin, M.J.; Shenker, S.; Stoica, I. (2012), *Resilient distributed datasets: A fault-tolerant abstraction for in memory cluster computing*, USENIX Conf. Networked Systems Design and Implementation

ZELNIK-MANOR, L.; PERONA, P. (2004), *Self-tuning spectral clustering*, Advances in Neural Information Processing Systems

ZHAI, Y.; ONG, Y.; TSANG, I. (2014), *The emerging big dimensionality*, IEEE Computational Intelligence Magazine 9(3), pp.14-26

Port ETA Prediction based on AIS Data

Thomas Mestl, DNV GL, Høvik/Norway, thomas.mestl@dnvgl.com
Kay Dausendschön, DNV GL, Hamburg/Germany, kay.dausendschoen@dnvgl.com

Abstract

This paper presents three methodologies for port ETA prediction based on AIS data and a quantitative assessment of their application. The first two, ETA-for-Liners and ETA-for-Tramps, are valid for vessels in port. ETA-for-Liners can be used to predict n-ports ahead (and ETA), assuming the future operations of the vessel can be predicted based on its history. ETA-for-Tramps can be used to predict the next ports together their probabilities and their ETAs. This method is based on the behavior of similar vessels that were in the same (current) port as the vessel in question. The third method applies to ships at sea. It uses the latest position of the ship (based on its AIS signal) and compares its progress to historic voyages (AIS traces). Being able to obtain an ETA could help numerous stakeholders in the logistics chain who can benefit from a reliable prediction of a vessel's estimated time of arrival in port (ETA).

1. Introduction

Knowing the arrival time of a vessel at a specific port is of interest to many stakeholders ranging from port authorities, port operators, bunker providers, ship operators, etc. We distinguish between short-term and long-term ETA (= Estimated Time of Arrival) prediction. Short term is in the range of hours to days, whereas long term is from weeks to months ahead. The ETA problem consists actually of two problems: what is the next port and what is the ETA for this port.

2. ETA prediction

2.1. Sources of ETA information

From an outsider perspective, not only the ETA is unknown but also what port the vessel is heading to. No single source supplies all the required ETA information for all ships. Instead, ETA information from various sources may be merged for more reliable and complete insight:

- Notification to port authorities – An EU directive requires notifying local port authorities 24 h prior to arrival. Some ports make this information public, e.g. Honk Kong, Montreal or Dubai.
- Piloting – Public information about ordered pilots offer ETAs usually in the range of hours but sometimes also weeks ahead.
- DNV GL Navigator/Port Clearance – For historical data as data is transferred only at arrival in port.
- Port schedules from port operators – Mainly for cruise vessels which have a rather stable schedule.
- Vessel schedules from operators – Many ship operators publish their schedules, especially for containerships. Given arrival times are generally “planned”, not “actual”.
- Departure/Arrival search engines – Several search engines on the internet give presumably planned, not actual arrival times, e.g. www.landscape.com/, www.jocsailings.com
- AIS messages – AIS messages contain free-text fields <Destination port> and <ETA>. These are filled in manually. The rule rather than the exception is that these fields are either not filled in at all, filled in wrongly, e.g. “Haburg” (instead of Hamburg) or “going home”, not updated or the previous destination port is still contained. Our own research has shown that e.g. for the port of Hamburg only 4% of the ships filled in the destination correctly.
- AIS provider – Vesseltracker claims that “based on arbitrary positions on the globe we calculate distances, journey times and ETA”. Marine Traffic offers an interactive, map-based

service providing ETAs and offers even an alert service. However, there is no public information on how these providers determine their ETA predictions.

- DNV GL's in-house AIS-based insight system - DNV GL has built a large data base with global AIS data for all vessels with AIS transponder starting since 2012. Data samples are spaced 6-10 minutes apart. The system identifies presence in ports, and in some cases even terminals, automatically. The system has been used for a variety of applications supporting ship operators in improving their competitiveness, as described e.g. in Dausendschön (2015).

2.2. Sailing patterns and effect on ETA prediction

We might distinguish between two extremes: one where the future is totally predictable when knowing the history of the vessel, and one where the future of a vessel cannot be predicted based on its history.

- Recurring patterns – Liners (e.g. containerships) serve a fixed route over a foreseeable time. They feature recurring port patterns, Fig. 1. In this case, vessel voyage histories can be used to predict future destination ports and their ETAs. However, occasionally ports might be jumped and served by sister vessels.
- Erratic patterns - Tramps (e.g. bulk carriers) have no recurring patterns. Predicting the next port (and ETA) based on the vessel's history is usually not possible; a different approach is needed.



Fig. 1: Example of liner port pattern (source: Maersk)

3. ETA prediction algorithms for ships in port

3.1. ETA for liner shipping

Here we assume that the history of a vessel (port sequences and times) suffices to predict its future. The next port is determined by looking for chain of previous ports that uniquely determines the next port. The algorithm does not work if the current port has never been visited before. The ETA for the predicted next port is based on the typical sailing time for the vessel between the current port and the next port plus typical port stay time in the current port. The “typical” time is taken as the median rather than the mean of the historically recorded times. If the next port cannot be determined uniquely the algorithm gives probabilities for possible next ports along with their ETAs.

3.2. ETA for tramp shipping

Here we assume that historic information from similar vessels in the same port can be used. This approach results in much larger uncertainties. It depends on the number of similar vessels which are in a similar situation, and especially on the definition of “similar”. If we look only at vessels of same type and size, operating in the same market segment (same cargo, comparable size of operating company, etc.) we might end up with a too small data set. If interpreted “similar” too widely we end up comparing apples with pears as a tanker may have different destination ports from a bulk carrier. Even for the right balance between too strict and too loose, the inherent uncertainty may still be too high to provide actionable information.

Filtering criteria for “similar” ships include:

- Ship type (e.g. bulk carrier)
- Time period since current time (e.g. within last 6 months)
- Calling at same terminals / berths (indicative of cargo type, e.g. coal)
- ...

Generally, anything that constrains the variability in vessels improves predictability of next ports and the corresponding ETAs. Ship operator / owner characteristics may give some additional insight.

4. ETA for ships on voyage

The methodology presented here relies heavily on information from the voyage database. As the voyage database only contains finished sailings, it is by design not up-to-date! Once a vessel has left port and starts its voyage to the next port, at some point it will become apparent what will be the next destination port, Fig. 2. Then the next port and ETA prediction can be updated. Actually, we could either update the list and probabilities of the next ports as given by the ETA for Liners/Tramps, or we could discard this information and predict potential next ports based on the historic traces (either of the vessel in question or of a selection of vessels) that are found in the vicinity of the current position. The latter approach would result list of probable next ports and correspondingly lower probabilities for each port.

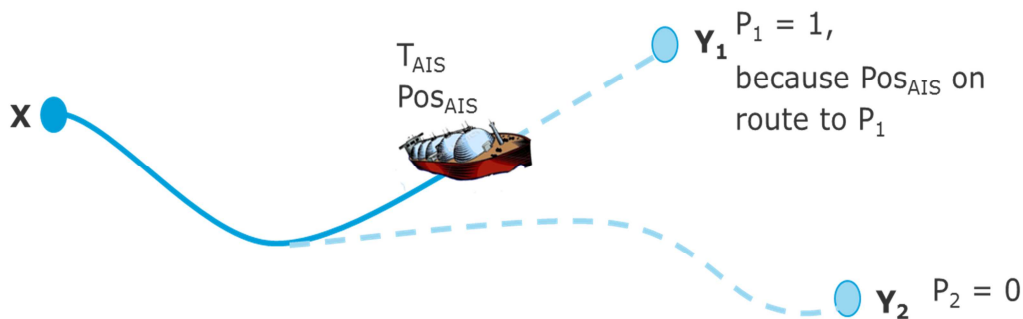


Fig. 2: While in Port X, the ETA algorithm may suggest two potential next ports Y_1 and Y_2 with probabilities P_1 and P_2 . Once the vessel has sailed for a time T_{AIS} and reached position Pos_{AIS} it is apparent that the vessel is on a route to port Y_1 . This means the probability of going to port Y_1 has changed to $P_1=1$, the ETA should be recomputed based on current position Pos_{AIS} .

As ships often sail on common sailing routes, this information can be used to update the list of next possible ports (and their probabilities). If a vessel is on a specific route leading to a set of possible next ports we can immediately exclude ports that will not be reached from that route, Fig. 1. So when a vessel passes a route branching point/area the next-port list can be updated. In general, the longer the vessel is on its way the more branching points will be passed and the more reliable the prediction will become.

Natural constrictions in the shipping geography, Fig. 3, often make it impossible to separate different sailing routes before the constrictions have been passed. E.g., from Las Palmas the next possible ports may be Rotterdam, Hamburg or Copenhagen. The English Channel bundles all the sailing routes to these ports such that only after passing the Channel it will become apparent where the ship will go. Other such natural constrictions include the Strait of Gibraltar, Strait of Malacca, Singapore Strait, Cape of Good Hope, Suez Canal, Panama Canal, etc.

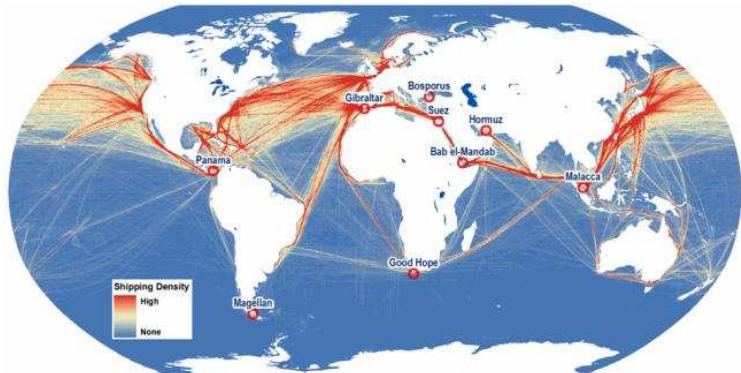


Fig. 3: Natural constrictions in sailing patterns (source: www.revistamilitar.pt)

For updating the potential next ports based on the current ship's position, the general sailing route network with its branching points/areas can be used, Fig. 4. Sailing routes can be extracted from global AIS data. They can be tailored to ship size, ship type, selected time period or even season.

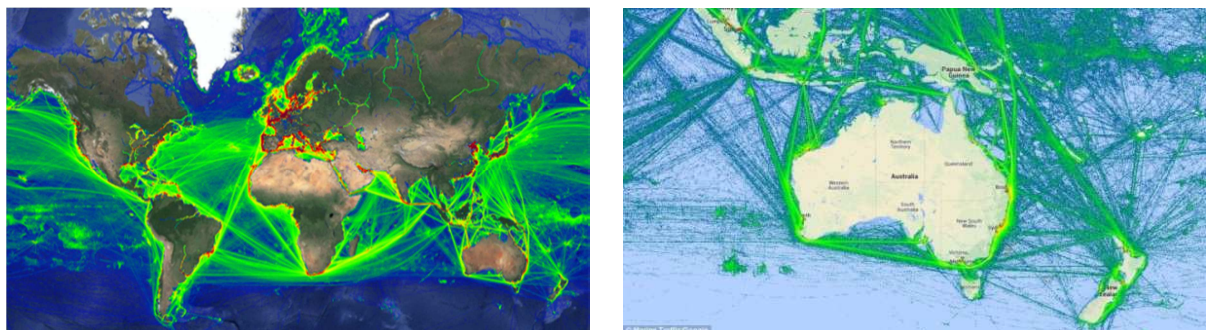


Fig. 4: General sailing routes derived from AIS samples

The algorithm for updating next port(s) is based on historic AIS traces. Our approach works even if very few historic traces are available. It provides a probability whether the vessel in question is on route R_1 to Port P_1 or on route R_2 to P_2 (or general R_i). The question whether being on route R_1 or R_2 is to a large degree answered if we know the proximity of current position and heading of the vessel to R_i . A vessel may be heading towards P_2 even if it is on the route to P_1 as two routes may cross. So in some cases, additional information must be processed to come to the correct prediction.

What if the vessel is heading towards a port which was not predicted by the ETA algorithm or if no historic AIS traces are available for that vessel? Every time new AIS arrival data appear, the next port, probability and corresponding ETA are computed and the corresponding entries in the sailing table are updated.

Then the probabilities for next ports are computed based on historic traces of the vessel. If a vessel is on known routes/towards known ports the list of next ports, their probabilities and ETAs can be updated in the in sailing table. If probabilities for all known routes are zero the vessel is heading towards an 'unknown' port. Then we could extract AIS traces near the current location for all similar ships and derive potential routes. For these routes potential next ports and associated probabilities and ETAs are again derived. Taking in additional information (e.g. available terminals or port histories for sister vessels) allows reducing the potential port list.

The voyage data base cannot be used to update the ETA. In order to update the ETA one has to extract from the large AIS data base all historic sailings of considered and similar vessels between ports X→Y, Fig. 5. The updated ETA is the typical the remaining sailing time for all the ships being close to the considered location, i.e. $\text{ETA}_j = \text{T}_{\text{end } j} - \text{T}_{\text{AIS } j}$

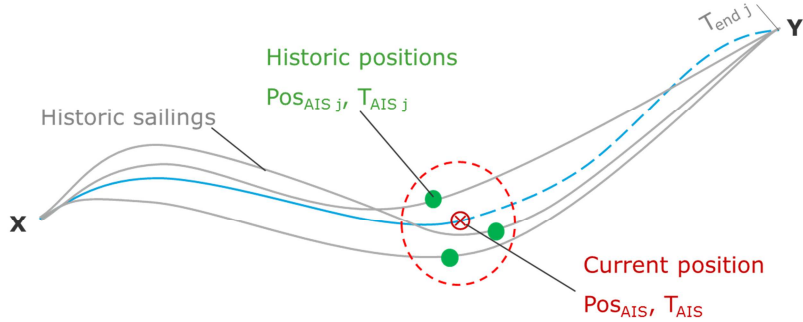


Fig. 5: Case where general sailing routes approach is not applicable

5. Validation

5.1. Validation of ETA-for-Liners

As a test set, 136 container vessels were chosen representing collectively some 25000 port transitions. We used the last 10% of their known port transitions to benchmark the algorithm. Fig. 6 gives an overview of the number of port transitions for each vessel in the test set. About 10 vessels had very few port transitions (i.e. short port histories) which made it difficult to predict the next port correctly. In this validation all vessels are assumed to be in port, i.e. no vessel is under sailing.

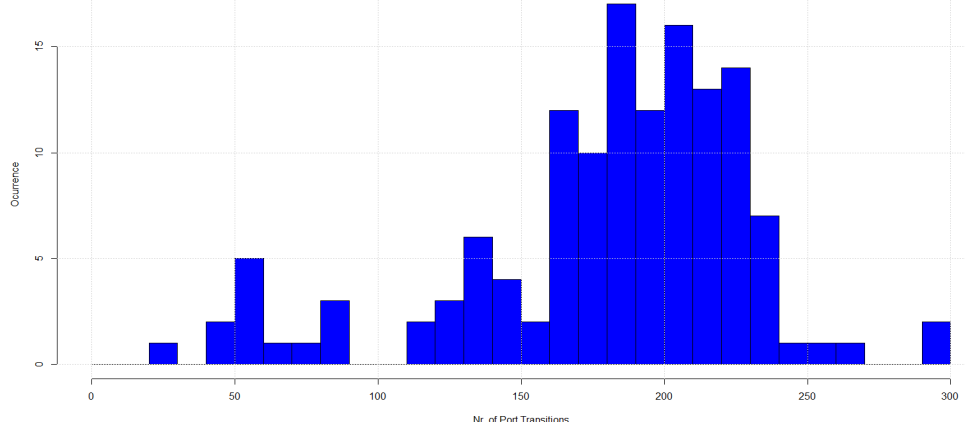


Fig. 6: Histogram of number of port transitions for the test set of containerships

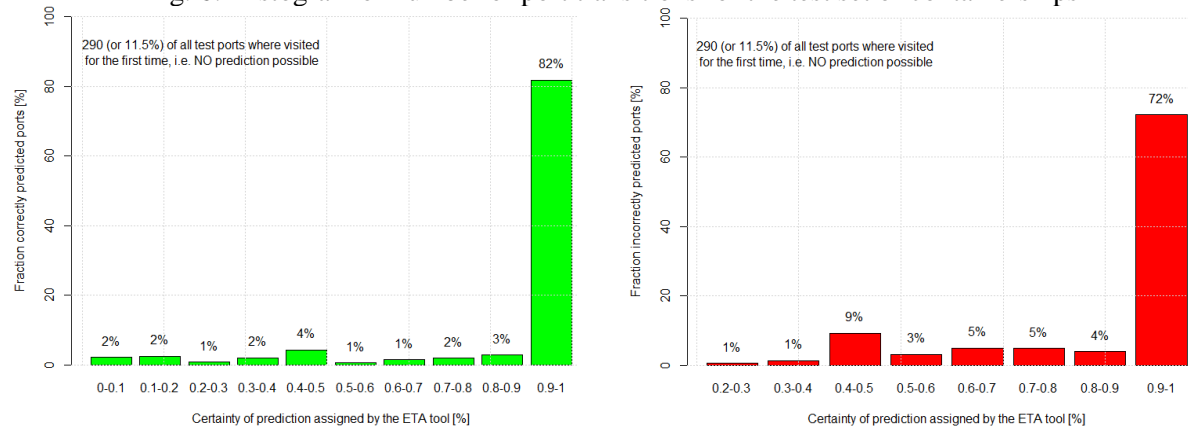


Fig. 7: Certainty of prediction assigned by the ETA tool for correct predictions (left) and false positives (right)

The test shows that 2/3 of the next ports could be identified correctly. Of the next ports that were where identified incorrectly ~1/3 were visited for the first time and the history of the vessels could therefore not be used to predict the next port at all. Fig. 7 shows how certain the algorithm is in its prediction of the next port. For 82% of the successfully predicted ports, the ETA algorithm indicated to be certain with probability of >90%, Fig. 7 (left). In cases when the algorithm was wrong about the next port (false positives) the certainty assigned to it was significantly lower, Fig. 7 (right).

Fig. 8 shows the error of ETA estimation, i.e. difference between calculated ETA and actual arrival time. For 64%, the error was less than ± 12 h, for 91% less than ± 1.5 days. The typical (median) error was 8 h. This can be considered as a good result considering the median sailing time of vessels.

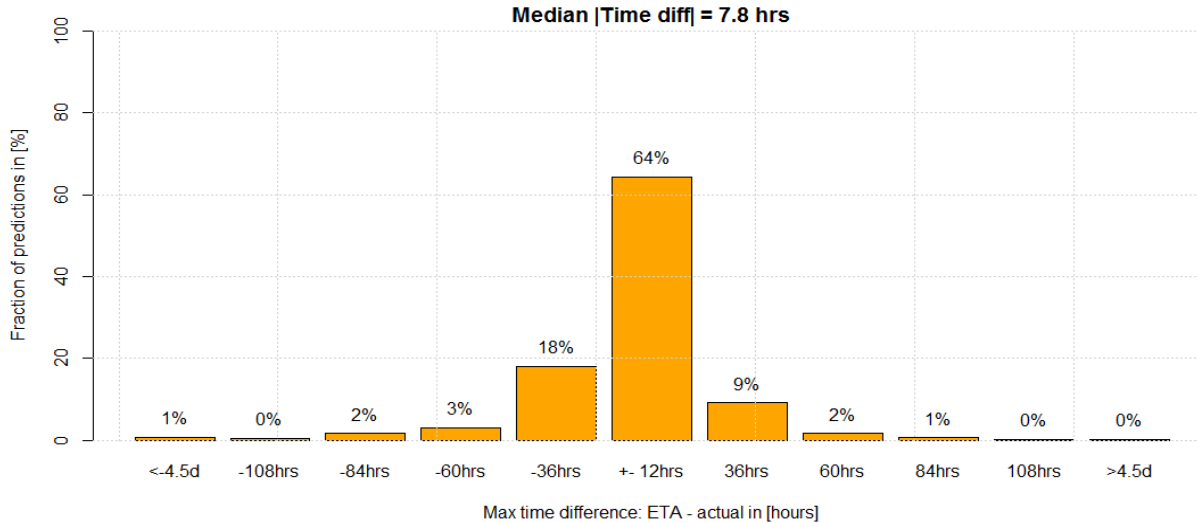


Fig. 8: Error in the ETA for next ports that were identified correctly

Note that this next port and ETA prediction methodology depends entirely on the assumption that the history of the vessel alone indicates its future behavior. If, due to macro-economic changes, the ship owner/charterer changes the routes of their vessel then the ETA methodology will perform poorly. On the other hand, the tool could be used to detect alterations/trends in route patterns and therefore changes in the macro economy with changes in trading patterns.

5.2. Comparing ETA-for-Liners with ETA-for-Tramps

In order to compare our two approaches (ETA-for-Liners and ETA-for-Tramps) we establish a baseline given by using the vessels history to predict its next ports, i.e. using ETA-for-Liners on Tramps.

The test set contained 345 bulk carriers that visited dry-bulk terminals in Hamburg port since in 2015. As before, 10% of the last port visits were used to test the algorithm. The correct next port prediction rate was only 10%. (Note that we consider a prediction to be successful if the correct port is contained in the list of predicted ports even if not with highest probability.) Almost 60% of all next ports in the test sets were visited for the first time (in the chosen time period) which confirms that the history of tramps are ill suited for predicting future ports.

In order to get an indication of the success rate of ETA-for-Tramps, preferably a large number of bulk ports should be chosen and the corresponding largest probability of the next port should be computed. The resulting distribution of largest probabilities would provide an estimate of the next port prediction accuracy of the ETA-for-Tramps. Unfortunately, this task is very time consuming, in the range of hours for one port. We therefore restricted our validation to the study of some selected ports, 5 in Europe (DEHAM, DEBRE, GBHUL, RUMMK, ITRAN), 2 in South America (BRARB, ARBUE) and 1 in the US (USNNS), Table I.

Table I: Maximum probability of predicting the next port correctly based on ETA-for-Trumps

Port	# vessels	Max. correct probability for next port prediction
DEHAM	345	7.8%
ITRAN	282	8.0%
USORF	214	6.6%
RUMMK	194	5.7%
USNNS	147	18.4%
BRARB	143	7.6%
DEBRE	111	18.6%
GBHUL	29	10.2%
ARBUE	28	20.0%
MEDIAN	166	11 %

In general, the more vessels are in a port the more difficult it gets to predict the next port correctly (28 vessels give 20% probability whereas 345 vessels give 7.8%). The average correct next-port prediction probability is near 11%. This is more or less in the area as for the ETA-for-Liner method.

5.3. Deep dive for a tramp example

This case study provides more details with respect to correct next-port predictions of both approaches. We look the Hamburg example from the previous section, applying successive constraints:

- Constraint 1 - Dry cargo only: 345 bulk carriers visited dry-bulk berths in Hamburg port in 2015. For Hamburg, there are 127 possible next ports with a probability of correct prediction of only 0.3 - 7.8%. If we base our prediction on the vessel history (ETA-for-Liners), we can correctly predict the next ports for 5.5% of the ships, which is only slightly less than the ETA-for-Tramps approach. (As before, correct means that the actual next port is contained in the next-port list suggested by the algorithm, not necessarily having the highest probability).
- Constraint 2 – in addition requiring Chemicals berths: Based on these constraints the ETA-for-Tramps approach resulted in a higher probability of 2.4% - 14.3% for predicting the correct next port. In comparison, if we base our prediction on the history of the vessels (ETA-for-Liners), we are correct for 5% of the involved ships, which is less than half of that for the ETA-for-Tramps approach.
- Constraint 3 – in addition requiring self-discharging bulk: Constraining even further, the ETA-for-Tramps approach resulted in a probability of 12.5% - 25% for predicting the next port correctly. Using the ETA-for-Liners approach, we are correct in 20% of the next ports, which is only slightly less than the ETA-for-Tramps approach.

6. Conclusions

If data about many port visits are available and for vessels with non-recurring port sequence pattern, , the prediction rate of the ETA-for-Tramp method seems to be in the same range as the ETA-for-Liners approach, i.e. 10-11% correct prediction of the next port. By introducing constraints (i.e. additional knowledge) the ETA-for-Tramps method provides a significantly better prediction rate than using the history of the vessel. This is plausible as filtering out vessels that are not similar should provide a more usable data set and hence better prediction. However, using too many/too stringent constraints will result in a single data set – that of the vessel in question. Which method gives the best prediction depends on the nature of the vessel, i.e. whether it shows more a Tramp-like (erratic) or a Liner-like (regular) behavior. In practice, we suggest to apply both methods as we often don't know whether the vessel in question behaves regularly or irregularly. In economic challenging times, ship owners may jump on available offerings and a vessel may then behave as a Tramp, whereas in better times the charterer may want to assure he has a vessel and books it more in advance. The same vessel will then show a more regular, predictable pattern.

References

DAUSENDSCHÖN, K. (2015), *Big Data – Business Insight Building on AIS Data*, 14th Conf. Computer and IT Applications in the Maritime Industries (COMPIT), Ulrichshusen

Applications of Network Science in Ship Design

Rachel J. Pawling, UCL, London/UK, r.pawling@ucl.ac.uk
Alexander S. Piperakis, UCL, London/UK, a.piperakis@ucl.ac.uk
David J. Andrews, UCL, London/UK, d.andrews@ucl.ac.uk

Abstract

Ship design has historically adopted numerical approaches from other domains to solve the many decision making, design and engineering problems encountered in the design process and one such development is the application of network science. Networks are most suited to problems that can be described in terms of connections between entities, and both past and current university level research has seen their application to a range of problems, primarily in the early, formative stages of ship design. Areas of application include the analysis of database and model structures and as an alternative to conventional computationally intensive modelling techniques.

1. Introduction

The UCL Design Research Centre (DRC) is part of the Marine Research Group (MRG) in the Department of Mechanical Engineering at UCL. Its main research focus is on computer aided ship design methods, particularly in the early stages of design. This research encompasses process and tools, particularly the development and implementation of the Design Building Block approach, an architectural approach to preliminary ship design, *Andrews and Pawling (2006)*. The wide range of DRC research has been described in several papers, including ones on risk-based approaches to fire safety, *Pawling et al. (2012)*, human factors, *Andrews et al. (2008)*, *Piperakis et al. (2015)*, survivability, *Piperakis and Andrews (2014)*, machinery integration, *Fitzgerald et al. (2015)* and submarine concept exploration, *Collins et al. (2015)*.

Since 2011, the UCL DRC has been part of a joint research project, funded by the US Navy Office of Naval Research, bringing together several universities to develop new approaches to early stage ship design. The first project, which ran from 2011 to 2015, involved University College London (UCL), Delft University of Technology (TU Delft) and the University of Michigan (UofM) and focussed on methods of generating general arrangements in preliminary design. The collaborative aspect of this project was presented in *Pawling et al. (2013,2015)*. A second ONR funded collaborative project began in 2015, introducing Virginia Tech and M.I.T. to the group and focusing the development on methods of assessing survivability and systems design, in early stage design.

Of interest to several members of this partnership is the application of network science to ship design. This paper gives a brief introduction to networks and various methods of analysing them. The various aspects of ship design to which they have been applied are described, ranging from education to the assessment of layouts and systems and the representation of ship design tools and processes. The paper then outlines ongoing and future developments in the application of these approaches including some of the network-oriented approaches recently investigated at UCL.

2. Computers and Numerical Approaches in Ship Design

Computers have found application in all stages of ship design, from the earliest stages of concept to the detailed structural and systems design. They have been used in three main ways; analysis, modelling and synthesis. The first applications were in the field of analysis, initially using the computer to perform the same calculations previously done by hand, only more rapidly. Modern analyses, however, make use of a wide range of mathematical techniques that originated outside of naval architecture (the mathematics of which was previously primarily geometry). These approaches include genetic algorithms, artificial neural networks, and the techniques of computational fluid dynamics (CFD) and finite element analysis (FEA). The second area of application, modelling,

became significant once computer storage was large enough to avoid significant simplifications in the models. Modern tools allow the storage of the complete production description of the ship, down to the level of individual pipe sections. Computer aided ship synthesis tools have undergone a similar transformation to analysis tools. Early synthesis tools were a method of rapidly and reliably carrying out traditional calculations. Applications of exogenous technologies to this aspect of ship design have included; the development of interactive computer graphics, permitting an architecturally centered approach, *Andrews* (1984), *Andrews and Pawling* (2006), genetic algorithms and optimization techniques for concept exploration, *Burger and Horner* (2011), risk-based approaches, *Vassalos et al.* (2006), and approaches to decision-making under uncertainty adopted from the financial sector, *Knight et al.* (2015). An example of such a mathematical approach that is seen to have applications to design synthesis, most significantly in the formative initial stages, is network science.

3. Networks

3.1. What is a Network?

A network is, in the broadest sense, a collection of points, usually called vertices or nodes, joined by lines, usually referred to as edges or arcs, *Newman* (2010). The edges can have no direction or be uni- or bi-directional. Such a network can be represented in a matrix, Fig. 1.

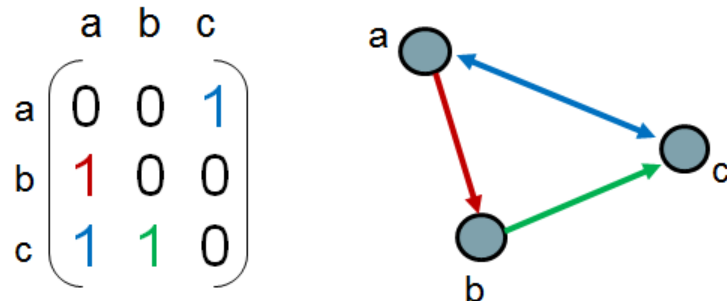
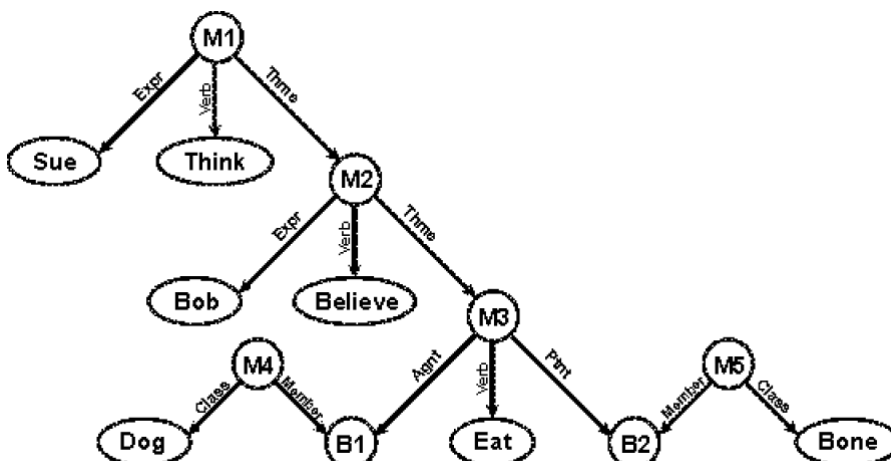


Fig. 1: Matrix representation of a directed network of three nodes (after *Collins et al.* (2015))

Additional information can be attached to both nodes and edges. They can be assigned numerical weights, or textual data and these can be stored in additional matrices. Some of the earliest applications of networks were to the understanding and visualisation of knowledge, in a Semantic Network. Fig. 2 gives an example of such a semantic network for a simple English sentence. Such semantic networks can be used to define the behavior of AI, *Sowa* (1992).



“Sue thinks that Bob believes that a dog is eating a bone”

Fig. 2: A semantic network representing a simple sentence, *Sowa* (1992)

Networks have application to problems that can be characterised by interconnected entities. These entities may be discrete objects, such as the physical components of a system or they may be the constituent parts of some more readily recognised object. Alternatively the entities may be more abstract concepts, such as fragments of design knowledge. The connections (edges) between the entities (nodes) can themselves have numerical and textual properties, so further increasing the depth of modelling and analysis possible.

3.2. Analysing Networks

Several metrics and analysis methods have been proposed for the analysis of networks. *Newman (2010)* and *Mrvor (2016)* provide a comprehensive description of these quantitative methods, and this section will only summarise those metrics which used for the analysis of various networks presented in the ongoing UCL research. Most network metrics do not provide useful information per node, but rather have to be used in the context of the variation of the metric across all the nodes in the network. There is some similarity to statistical analysis, in that the size and characteristics of the sample (e.g. the number of edges in the network) will help determine the most appropriate metric.

- Centrality measures are the most common metrics used in the analysis of networks. These can be categorised into three groups; degree, closeness and betweenness. Degree centrality is a measure of the number of direct connections a node has. Closeness centrality is a measure of how close a node is to all other nodes in a network, thus incorporating indirect connections. Betweenness centrality estimates the extent to which a node lies in the shortest (i.e. geodesic) path between pairs of nodes in a network. Proximity prestige is a similar metric, used in weakly connected directed networks, that considers the ranking of nodes close to each node.
- Degree refers to the direction of the edges, with in-degree being the number of edges point at the node, and out-degree being the number pointing from that node to others. It is possible to incorporate the weighting of edges into this metric.
- Communities are clusters of nodes which there are more arcs inside the cluster than among clusters. Detecting these through numerical metrics allows emergent properties in the structure of the network to be determined without recourse to visualisation and observation, which can be difficult for large networks.
- Geodesic paths are defined as the shortest path between a pair of nodes in a network. The network diameter is the length of the longest geodesic path in a network. Both parameters are applicable to directed or undirected, weighted or unweighted networks.

3.3. Applications of Network Science to Ship Design

Networks were first applied to ship design by *MacCallum (1982)*, where they were used to explore relationships between and influence of various parameters in early stage ship design models. The development of a range of methods and software tools for the modelling and analysis of networks has led to a recent renewal in interest. Networks have been proposed as an alternative to the various methods proposed for generating general arrangements in early-stage ship design.

Automated methods such as the Intelligent Ship Arrangements ISA developed by the University of Michigan (*Daniels et al. 2006*) and the TU Delft Packing approach, *van Oers (2011)* are used to generate a large number of arrangements in response to technical requirements. These research institutions are investigating various aspects of the use of networks in ship design, either as an alternative or adjunct to, automated approaches *Killaars et al. (2015)*. The network based method proposed by *Gillespie (2012)* applies network analysis methods to the databases of spatial relationships used in the automated tools. Community detection was used to identify configurational solutions implicit in the relationship database, which can be used to determine drivers on the arrangements, *Gillespie et al. (2013)*. Essentially, such analysis aims to understand arrangements without generating them. The community detection approach was also used by *Rigterink et al. (2014)*, with the addition of networks representing distributed systems, such as the electrical and firefighting systems. This

latter work introduces an aspect of vulnerability analysis, in that the ability of the systems to survive damage can potentially be evaluated.

Design processes, including the organizational aspects, can be represented as networks (the commonly used flowchart representation of processes could be regarded as a network, for instance). *Parker and Singer (2013,2015)* applied several network metrics to various ship design models and processes, furthering MacCallum's investigation of the influence of different variables. This work also used the concept of knowledge domains in ship design, to integrate the analysis of the numerical models with some understanding of the social and knowledge aspects of the design process. *Shields et al. (2015)* continued this work, examining the process of iteration to a design solution – a fundamental feature of ship design processes. The use of networks to capture the origin of design knowledge and identify where model structures may be based on assumptions, general practice or first-principles has also been described by *Collins et al. (2015)*, with particular reference to the incorporation of novel technologies into the generally conservative field of submarine design.

Some of these applications of network science to ship design have sought to investigate problems that are, essentially, already defined as networks – specifically the investigation of numerical models, where all links are pre-defined. Others, such as the investigation of databases to determine design drivers, have taken a set of relationship defined in at a detail level and used network modelling to “join them up” to examine the results at the whole-ship level. The latter research, and in particular the work on distributed systems, uses the networks as a type of abstraction of the potential designs, allowing them to be investigated in a less computationally demanding way than, for instance, developing large numbers of possible arrangements.

4. UCL Applications of Networks to Ship Design

4.1. Database of Layout Knowledge

Networks have potential for capturing, storing and applying design knowledge, and the UCL DRC has investigated this application to the topic of general arrangements, as was reported by *Pawling et al. (2015)*. There is perceived to be a need to improve the rigour with which general arrangements design is approached, particularly in the areas of education (where it is not taught with the same clarity as other aspects such as hydrodynamics) and the capture of institutional and individual knowledge.

A prototype database has been developed using the NodeXL tool, <http://research.microsoft.com/en-us/projects/nodexl/>, to explore the use of networks in storing design knowledge and applying it in concept design and teaching activities. The relationships are developed in a pairwise approach (DBB1 has a relationship with DBB2 of a specified type and importance). The advantage of this pairwise approach is that the database can be built up in an ad-hoc manner, thus supporting a wide range of knowledge elucidation techniques and the structure derived later through the network tools. *DeNucci (2012)* developed method of elucidating designer knowledge, by presenting arrangements generated through the packing approach. The UCL approach is not a sophisticated; instead a list of spaces and possible relationships are presented, and the designer must define the combinations by hand.

Nodes can represent individual spaces, type of spaces (e.g. “accommodation”), major features (such as the damage control deck) and broad arrangement locations and practices (e.g. “forward” and “split”). The edges are assigned multiple text tags (from defined lists) to store the nature of and justification for the relationship, along with the functional group. There are thus multiple ways of viewing the resulting network. The importance of understanding relationships when generating general arrangements has been discussed by *Andrews (1984)* and *Dicks (2000)*, both featuring tabular methods of storing relationships between entities in the design and different visualisation techniques. Fig. 3 shows the arrangement networks produced in this study. Three levels of relationship were defined; 1) desirable but tradeable during design; 2) key relationships that should be met 3) key relationships that must be met.

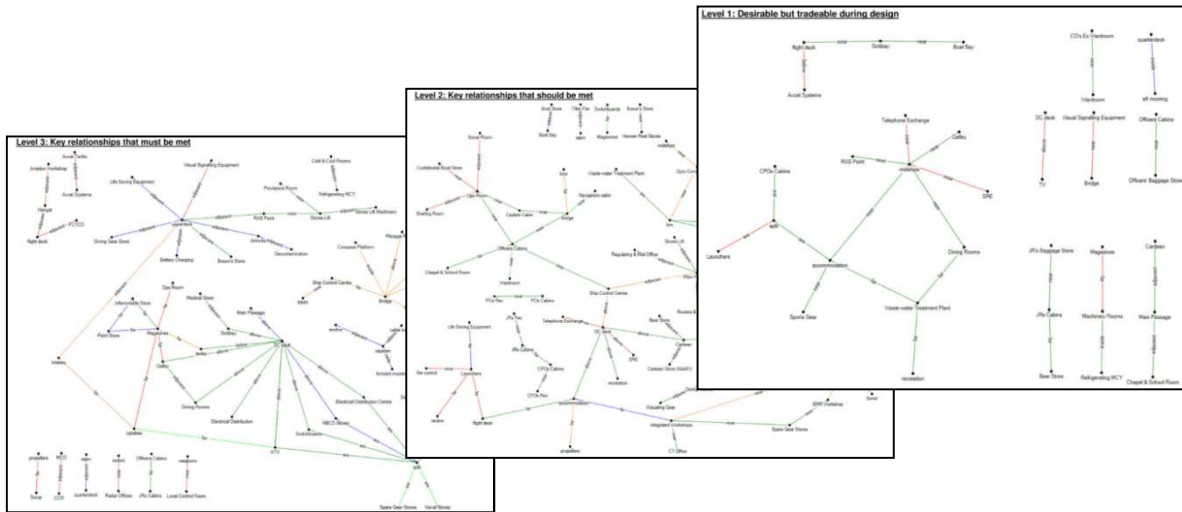


Fig. 3: UCL prototype database of layout knowledge

The ability to retrieve such information and apply it in the context of a new design can provide guidance for future ships of a similar type (such as the different naval types: naval combatants, submarines, aircraft carriers, amphibious warfare vessels) where knowledge may have been lost due to staff turnover, long intervals between designs, etc. The key benefit of such a database is that it helps make rules and guidance explicit and clear, so allowing them to be examined on a rational basis. The prototype database has been connected to the developmental UCL layout toolset (*Pawling et al. 2015*), allowing the comparison of proposed arrangements with the stored knowledge.

It is also possible to apply network metrics to explore implicit or emergent relationships in the knowledge database, and perhaps determine some aspects of “style” in the design approach embodied within it. The prototype database was populated by a single designer with some experience of warship concept design, and Fig. 4 shows the result of a betweenness centrality analysis of the network. This metric evaluates how many paths between nodes pass through each node (i.e. how connected each node is to all others in the network). The importance placed on survivability in warship design can be seen by the high ranking of the damage control (DC) deck and the need to duplicate and split systems. The significance of the upperdeck arrangement in surface warship design is also reflected here.

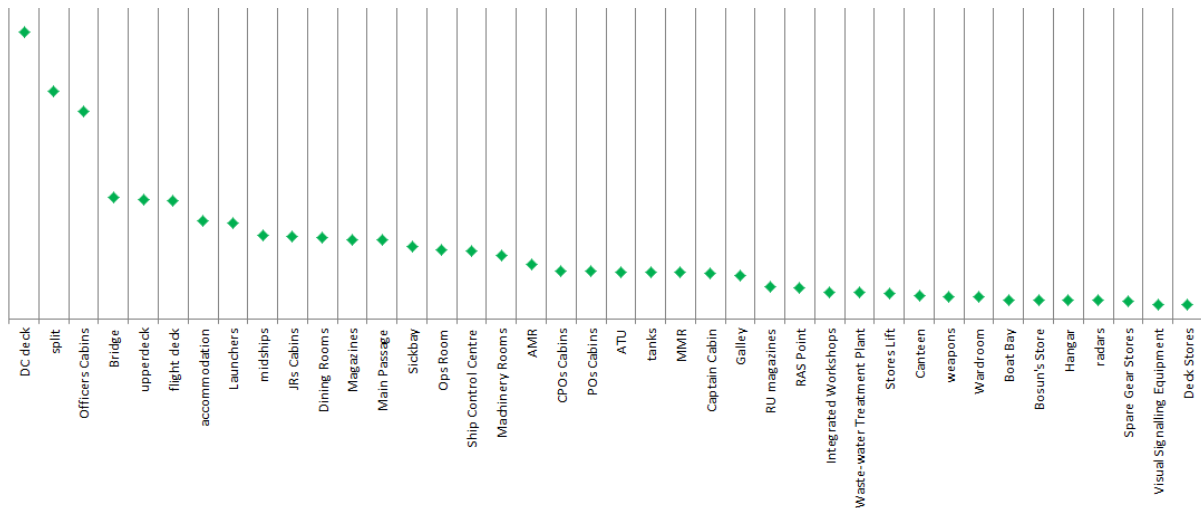


Fig. 4: The betweenness centrality of the 40 highest ranked nodes, *Pawling et al. (2015)*

4.2. Analysis of Naval Architectural Processes

Another potentially useful application of network science is the visualisation and analysis of processes. Recent work on the analysis of the structure and implicit behaviour of engineering models has been described by *Parker and Singer (2013,2015)*. By applying network science metrics to representations of the design processes, insight can be gained into the importance of different tasks and variables (represented as nodes). This can provide understanding of otherwise hidden procedural drivers, allow the identification of leading indicators of programme performance etc. Within the UCL context, gaining an understanding of the implicit structures within existing procedures used in teaching post-graduate students could allow improvement of teaching practice and better alignment of tools and data with the methods.

4.2.1. Investigating Influence in the UCL Ship Design Procedure

UCL has developed a directed temporal network representing the functions employed in the UCL monohull sizing procedure, as described in *UCL (2010a,b)*. This procedure is used by MSc and PhD students at the Department of Mechanical Engineering of UCL, the former as part of the annual ship design exercise, part of the Naval Architecture and Marine Engineering MSc programmes in UCL. Fig. 5 provides a simplified overview of the procedure, showing the main objectives and analyses performed at each stage.

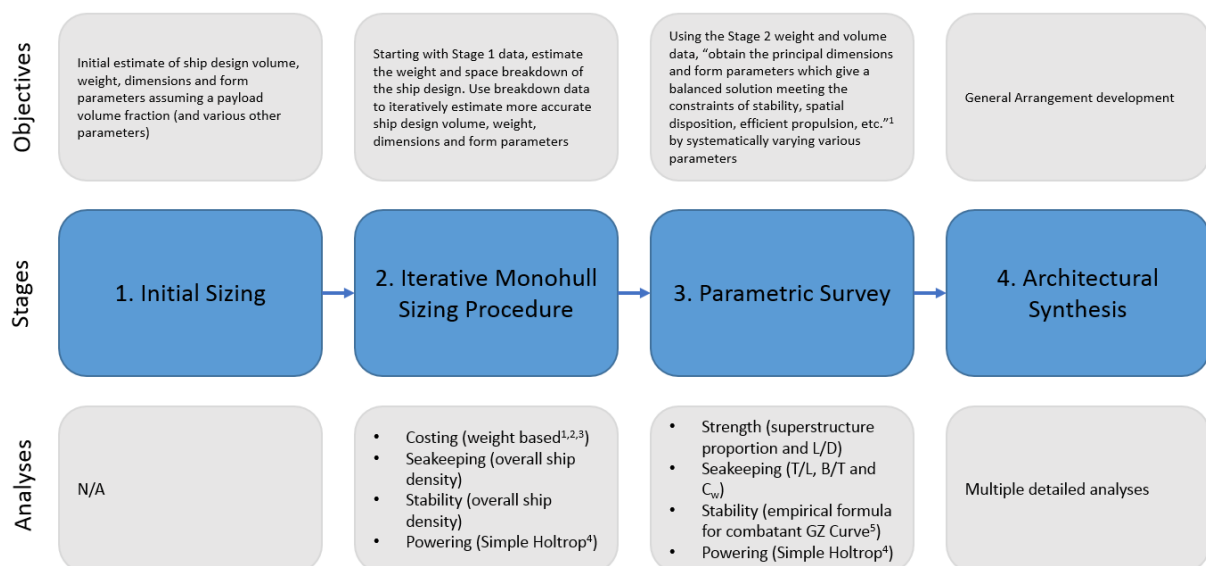


Fig. 5: Generalised and simplified form of the UCL monohull sizing procedure

The architectural synthesis stage is not included in the network analysis, as it does not use a clearly defined procedure within the context of the UCL MSc SDE procedure (but has been investigated in more detail by the UCL DRC (*Andrews and Pawling, 2008*). The application of network analysis to general arrangements is a separate challenge, as described in the previous section. Fig. 6 shows the entire temporal network and the three individual stages as visualised in the Pajek network visualisation and analysis software (*Mrvář, 2016*). (Each stage is translated into a time-step in the temporal network). Due to the very large size of the network model (containing 473 unique nodes and 973 arcs in total), node labels have been omitted for clarity.

In Fig. 6, the significant majority of the nodes represent individual variables used in the functions employed in the sizing procedure. The arcs connecting the nodes represent the connection between the variables and the flow of data both within and between the functions. As in the work of *Parker and Singer (2013,2015)*, the main output variables of the sizing procedure are grouped into disciplines (10 in this case). Table 1 lists the disciplines and the main output variables that belong to each discipline.

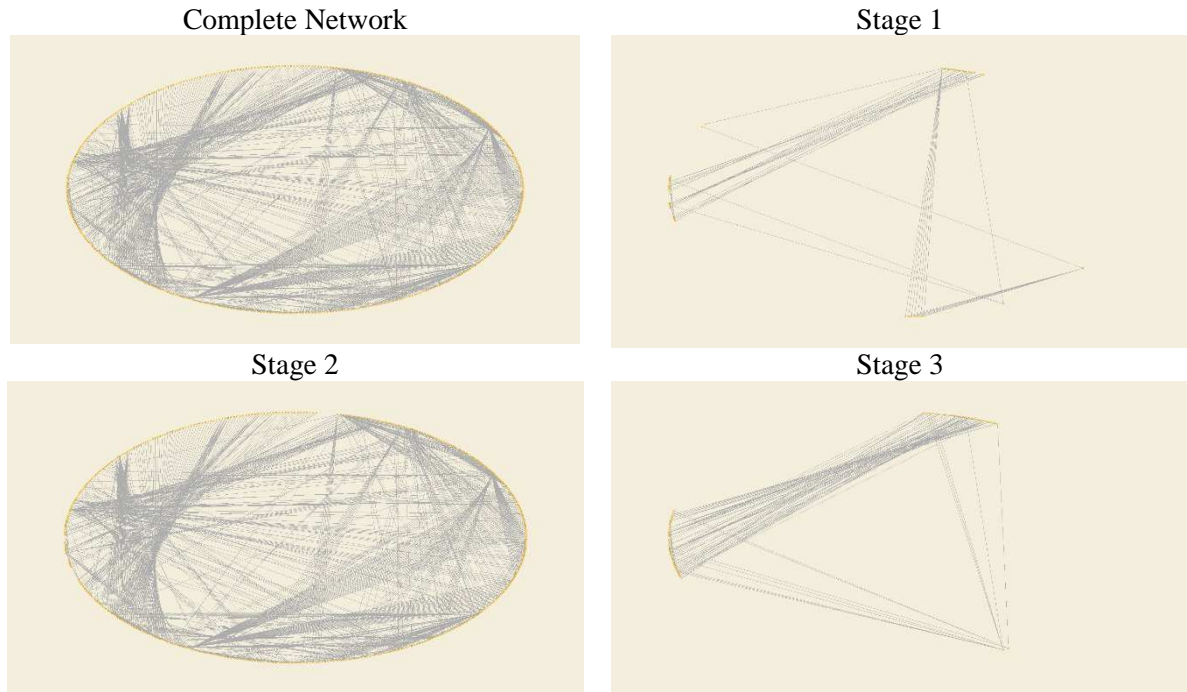


Fig. 6: UCL monohull sizing procedure network model

Table 1: Main output variables and disciplines of the UCL monohull sizing procedure network model

Discipline	Main output variables
VOLUMES	Volume, Group 1 volume - Hull, Group 2 volume - Personnel, Group 3 volume - Ship Systems, Group 4 volume - Propulsion, Group 5 volume - Electrics, Group 6 volume - Payload, Group 7 volume - Variable, Total required internal volume, Superstructure volume, Main hull volume
WEIGHTS	Displacement, Group 1 weight - Hull, Group 2 weight - Personnel, Group 3 weight - Ship Systems, Group 4 weight - Propulsion, Group 5 weight - Electrics, Group 6 weight - Payload, Group 7 weight - Variable, Lightship weight, Deep weight
DIMENSIONS	Length WL, After cut-up, Draught, Beam WL, Beam OA, Transom beam, Freeboard, Bow depth, Depth, Length OA, Deck height, Double bottom height
HULLFORM SHAPE	C_m , C_w , C_p , C_b
POWERING	Shaft power
STABILITY	Overall ship density, GZ
SEAKEEPING	Overall ship density, Draught:length WL ratio, Beam WL:draught ratio, C_w
COSTING	Unit procurement cost, Through life cost, Whole life cost
CONFIGURATION	Number of internal decks
STRENGTH	Length WL:depth ratio, Superstructure proportion

Table 2 summarises the types of nodes at each stage. Some variables are used in more than one stage.

Table 2: Types of nodes at each stage in the design process

	Stage `1	Stage 2	Stage 3	Totals
No of variable nodes	37	435	55	527
No of discipline nodes	4	8	9	21
No of other nodes	2	11	0	13
				561

Network metrics can be applied to these networks. The authors are all familiar with the UCL SDE and these metrics can be compared to their experiences of the process (both subjective and objective-based i.e. what does the designer think is important at each stage). Table 3 lists the five most influencing and five most influenced nodes of stage 1, Fig. 6, of the UCL monohull sizing procedure. As a possible single metric for the measure of influence, the in proximity prestige subtracted from the out proximity prestige. This metric compares the network proximity of the node to those nodes that have an input to it, and those that it provides input to.

Table 3: Proximity prestige of stage 1 nodes

Node	Proximity prestige (out – in)
Most Influencing	
Circular M	0.13
C_b	0.11
Outline requirement/staff target	0.11
Specified equipment (payload)	0.10
Beam WL:draught ratio	0.10
Most Influenced	
Depth	-0.09
WEIGHTS	-0.10
Bow depth	-0.10
VOLUMES	-0.11
DIMENSIONS	-0.26

The third and fourth most influential nodes in the network representation of stage 1 of the sizing procedure do not represent numerical variables, but rather major decisions regarding the role of the vessel. The initial sizing of a monohull at this stage is heavily dependent upon the requirement and the way it is interpreted and met. The remaining three of the five most influential nodes in Table 3 are all independent variables, therefore having a node in degree and betweenness centrality of zero; i.e. they only influence other variables, and are themselves not influenced. In the UCL design procedure these variables are selected (usually based on historical values) to generate the initial estimate of the hullform. What was surprising was the lower influence of the “Payload Volume Fraction” and “Payload Volume” variables (ranked 8th and 9th by this metric) as they are the focus of much designer attention in the early stages of the process, as shown in Fig. 6. Discipline nodes in the network model are the only nodes with a zero out degree, and this is reflected in their being the most influenced. The main objective for the designer in Stage 1 of the process is to estimate the overall dimensions of the vessel and this is reflected in the highly influenced discipline of DIMENSIONS. Potential limitations of the procedures may be identified by noting which disciplines are not involved at each stage, or which disciplines are ranked as being least influenced (i.e. not being given much attention). Tables 4 and 5 present similar results for stages 2 and 3 of the UCL monohull sizing procedure.

Table 4: Proximity prestige of stage 2 nodes

Node	Proximity prestige (out – in)
Most Influencing	
Specified equipment	0.13
Specified equipment (payload)	0.12
Outline requirement/staff target	0.10
Operational profile	0.10
Speed	0.09
Most Influenced	
Through life cost	-0.16
Whole life cost	-0.16
Unit procurement cost	-0.16
WEIGHTS	-0.16
COSTING	-0.18

The four most influential nodes in the network representation of stage 2 of the sizing procedure do not represent variables, but rather the major role decisions that were also influential in Stage 1. This indicates that the sizing of a monohull is most heavily dependent upon the requirement and the associated high level decisions, rather than the detailed design choices. This can be contrasted with a desire amongst designers to fix such requirements and develop detailed design solutions – given their significance, it may be more appropriate to hold the requirements themselves open as long as possible. As this is the design stage where it is possible to make costing estimates, it is unsurprising that COSTING is the most influenced discipline (as it is a major output), and costing variables are the most influenced. It should be noted, however, that if DIMENSIONS and VOLUMES were combined into a single GEOMETRY discipline, then they would have a proximity prestige of -0.20, therefore, being the most influenced discipline at this stage.

Table 5: Proximity prestige of stage 3 nodes

Node	Proximity prestige (out – in)
Most Influencing	
C _b	0.22
C _w	0.17
C _p	0.16
Angle of flare	0.16
Superstructure proportion	0.15
Most Influenced	
SZ	-0.13
Total resistance	-0.16
Wave resistance	-0.20
Viscous resistance	-0.22
DIMENSIONS	-0.27

The main objective of the parametric survey (i.e. Stage 3 in Fig. 6) is to obtain more accurate values for the principal dimensions and form parameters. The survey consists of two stages. In the first stage (major parametric survey) two parameters are varied; the superstructure proportion and the number of internal decks, *UCL* (2010a). These variables are ranked fifth (Table 4) and sixth in the list of most influencing nodes. In the second stage (minor parametric survey) the hullform parameters are varied, and the significance of these is captured as they are the top three most influencing nodes in Table 5.

An additional finding of this network analysis is that the ‘CONFIGURATION’ discipline is only explicitly incorporated in one of the three monohull sizing stages and has very few connections to other nodes. This highlights a weakness of the UCL monohull sizing procedure as the design configuration is a major driver of the ship size, performance and nature of technical solutions adopted. This tends to add support to the calls from the third author for a more holistic architecturally centered approach to early stage design, *Andrews* (2003).

4.2.2. Community Detection Methods

Other properties may be detected by applying community detection methods to the sizing network. Communities in this case are clusters of nodes which there are more arcs inside the cluster than among clusters. Fig. 7 depicts the four communities distinguished in stage 1 of the monohull sizing procedure (taking only nodes which represent variables into account) by applying the Louvain method incorporated in Pajek. It should be noted that this figure has been edited to move the nodes closer together (in the horizontal), as the default display in Pajek would not read well in print. The communities, however, are as determined by the software.

Communities of related and more strongly connected variables according the UCL procedure are clearly visible and may be broadly categorised as (from top to bottom in Fig. 7):

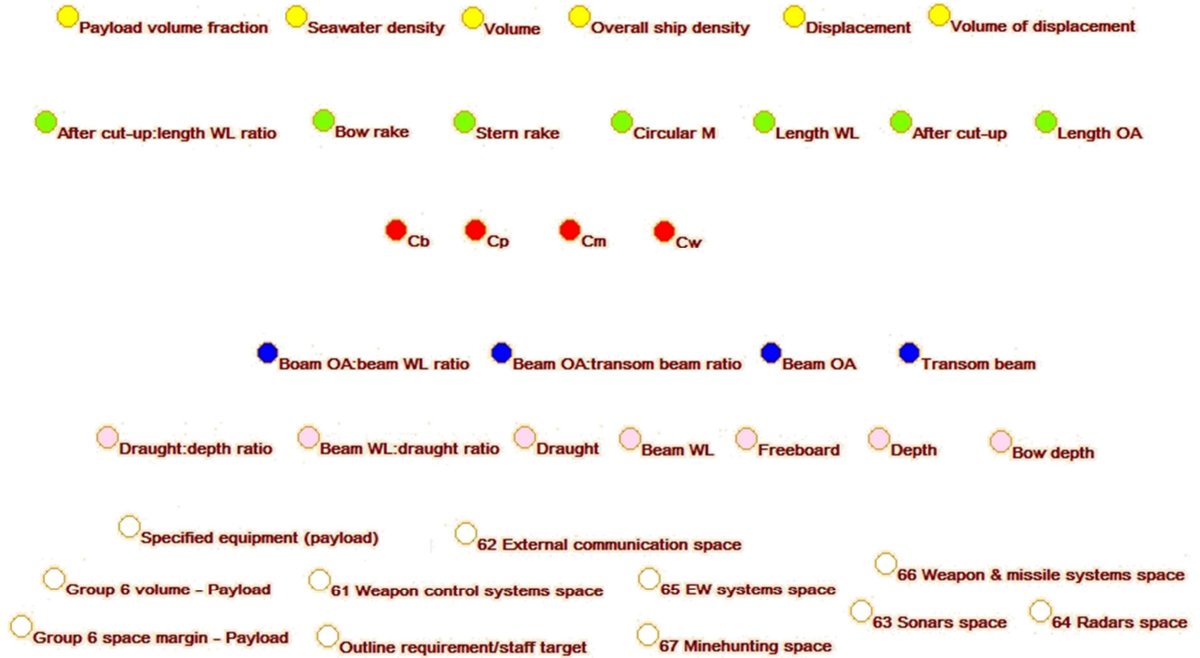


Fig. 7: Communities of stage 1 nodes

- Overall volume and weight (yellow);
- Major and minor length parameters (green);
- Hullform parameters (red);
- Beam (blue);
- Draught and depth (pink);
- FIGHT / payload volume and area (white).

This community detection analysis indicates that the initial sizing method is segregated into a smaller number of key characteristics of the ship, mostly the overall dimensions.

The work described above has illustrated the potential for the use of network models to analyse and gain insight of behaviour and structures within ship design processes and models. However, as with all analysis methods, there are limitations that must be considered:

- Although it is easy to detect most influencing and influenced nodes, the metrics used do not allow the evaluation of the impact of the connections, only that they exist. This has been noted by *Parker and Singer (2013)*.
- The choice of network metrics may influence the results. For example, had the analysis examined only the “out” connections, then the discipline of RESISTANCE would have been lower ranked than some of its constituent variables.
- Decisions were required on the part of the researcher generating the network models, to determine how to represent the existing procedure as a network. This was most significant in the assignment of disciplines, and different decisions may generate different results. The use of disciplines, although requiring some human interpretation, was itself introduced to overcome the difficulty of some disciplines having more variables purely due to having a more clearly explained method, with more sub-steps included.

4.3. Analysis of General Arrangements

The most recent, and on-going UCL investigation into the use of networks in ship design is in the area of warship vulnerability to enemy weapons. UCL has developed an early stage analysis tool, the

Rapid Vulnerability Assessment Model (RVAM), *Edwards (2015)* which uses the layout, structural definition and systems location to determine the vulnerability of the proposed design. The objective of this research is to determine if network modelling, which can be carried out very rapidly, can be used as either a proxy or an alternative for the more detailed analysis. This work is still at an early stage, and can be summarised as a comparative exercise; network representations of the arrangement are being developed, various metrics applied, and these are being compared against the results from RVAM to determine if the two network modelling generates information of use to the designer. Fig. 8 illustrates the complexity of the networks being generated. This network combines several types of information used in vulnerability analysis; the size of each space (size of the nodes); failure criteria for the structure under blast loading (edge weighting); systems locations and connections (directed edges shown by arrows).

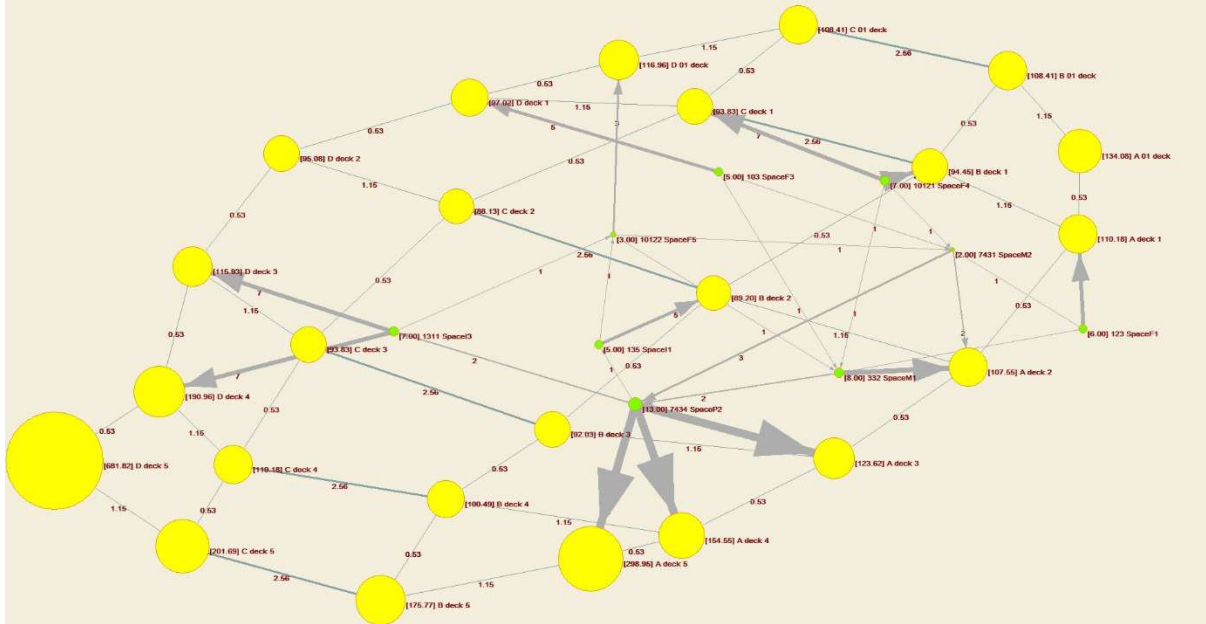


Fig. 8: Network representation of internal blast data including modelled systems

5. Summary

Ship design has historically adopted numerical approaches from other domains to solve the many decision making, design and engineering problems encountered in the design process. A numerical technique that has been recently applied to some aspects of early stage ship design is network modelling and analysis. Networks are collections of nodes connected by edges and can be enriched with numerical and textual data. Thus, they are most suitable for ship design problems that are, or can be abstracted as, a set of interconnections between objects. Recent work has seen network science used to; investigate implicit structures and drivers in design databases, evaluate existing numerical sizing models in the context of the design organization to understand relative influences, and as a method of analyzing layout drivers and even performance without the need to generate detailed representations of systems.

UCL is investigating the application of network science to ship and submarine design, and this paper has summarized the ongoing work on application to surface ships. Three main development areas are of interest; capturing, investigating and re-using designer knowledge regarding general arrangements; exploring the structure of the existing UCL MSc ship design methods; developing an alternative numerical approach to evaluating the vulnerability of warships to damage, suitable for application to the earliest stages of the design definition.

6. Future Work

The UCL work described in this paper is still at an early stage, with several areas for future development. The arrangements relationship database is currently only populated with a single designer's input, and the addition of datasets from other individuals will allow the investigation of the use of network metrics over a larger sample. Additional work is required on developing the tools to apply this database to new designs, to allow evaluation of their arrangement performance.

The use of this database and toolset in the UCL MSc SDE is also under development, to improve the teaching of general arrangements. The design exercise contains several numerical synthesis models for different ship configurations and hull types and it may be useful to conduct a network analysis on those, to compare with the monohull model.

The main area for further research is in the application of network models to existing engineering analyses. Through MSc and PhD projects, UCL has a range of analytical tools for examining aspects of survivability, systems design and energy flows (such as heat flow). These types of problems are seen to have conceptual characteristics suitable for application to network modelling.

Acknowledgments

Funding for the collaborative study in the Preliminary Ship Design General Arrangements NICOP project and its successor was provided by Ms. Kelly Cooper from the US Navy Office of Naval Research and is gratefully acknowledged.

References

- ANDREWS, D.J. (1984), *Synthesis in Ship Design*, PhD Thesis, University College London
- ANDREWS, D.J. (2003), *A creative approach to ship architecture*, Int. J. Maritime Engineering, Vol.145/3
- ANDREWS, D.J.; CASAROSA, L.; PAWLING, R.; GALEA, E.; DEERE, S.; LAWRENCE, S. (2008), *Integrating personnel movement simulation into preliminary ship design*, IJME 150/A1
- ANDREWS, D.J.; PAWLING, R., (2008), *A case study in preliminary ship design*, Int. J. Maritime Engineering 150/A3
- BURGER, D.; HORNER, D. (2011), *The use of Paramarine and modeFRONTIER for ship design space exploration*, 10th COMPIIT, Berlin
- MacCALLUM, K.J. (1982), *Understanding relationships in marine systems design*, IMSDC, London
- COLLINS, L.E.; ANDREWS, D.; PAWLING, R. (2015), *A New Design Approach for the Incorporation of Radical Technologies: Rim Drive for Large Submarines*, 12th Int. Marine Design Conf., Tokyo
- DANIELS, A.S.; TAHMASBI, F.; SINGER, D.J. (2009), *Intelligent Ship Arrangement (ISA): Methodology - Improvements and Capability Enhancements*, IMDC, Trondheim
- DeNUCCI, T.W. (2012), *Capturing Design - Improving Conceptual Ship Design Through the Capture of Design Rationale*, PhD Thesis, Delft University of Technology
- DICKS, C.A. (2000), *Preliminary Design of Conventional and Unconventional Surface Ships Using a Building Block Approach*, PhD Thesis, University College London

EDWARDS, G.W.B. (2015), *Rapid Vulnerability Assessment Model*, MSc Thesis, University College London

FITZGERALD, M.D., PAWLING, R.J., GROOM, J., ANDREWS, D.J. (2015), *A Holistic Approach to Machinery Choice in Early Stage Ship Design*, 12th Int. Marine Design Conf., Tokyo, JP, May 2015.

GILLESPIE, J. (2012), *A Network Science Approach to Understanding and Generating Ship Arrangements in Early-Stage Design*, PhD thesis, University of Michigan

GILLESPIE, J.W.; DANIELS, A.S.; SINGER, D.J. (2013), *Generating functional complex-based ship arrangements using network partitioning and community preferences*, Ocean Eng. 72, pp.107–115

KILLAARS, T.; VAN BRUINESSEN, T.M.; HOPMAN, J.J. (2015), *Network science in ship design*, 12th Int. Marine Design Conf., Tokyo

KNIGHT, J.T.; STRICKLAND, J.; KRING, D. (2015), *Valuing a retractable aft lifting body for improved human factors using real options analysis*, 12th Int. Marine Design Conf., Tokyo

MRVAR, A. (2016), *Pajek: analysis and visualization of large networks*, <http://mrvar.fdv.uni-lj.si/pajek/>

NEWMAN, M.E.J. (2010), *Networks: An Introduction*, Oxford University Press

PARKER, M.C.; SINGER, D.J. (2013), *The impact of design tools: Looking for insights with a network theoretic approach*, 12th Int. Conf. on Computer and IT Applications in the Maritime Industries, Cortona, pp.96-109

PARKER, M.C.; SINGER, D.J. (2015), *Comprehension of design synthesis utilizing network theory*, 12th Int. Marine Design Conf., Tokyo

PAWLING, R.J.; GRANDISON, A.; LOHRMANN, P.; MERMIRIS, G.; PEREIRA DIAS, C. (2012), *Methods and tools for risk-based approach to fire safety in ship design*, Ship Technology Research 59(3), pp.38-49

PAWLING, R.; PIPERAKIS, A.; ANDREWS, D. (2015), *Developing architecturally oriented concept ship design tools for research and education*, 12th Int. Marine Design Conf., Tokyo

PAWLING, R.; ANDREWS, D.; PIKS, R.; SINGER, D.; DUCHATEAU, E.; HOPMANN, H. (2013), *An integrated approach to style definition in early stage design*, 12th COMPIT, Cortona

PAWLING, R.; MORANDI, R.; ANDREWS, D.; SHIELDS, C.; SINGER, D.; DUCHATEAU, E.; HOPMANN, H. (2014), *Manifestation of style and its use in the design process*, 13th Int. Conf. on Computer Applications and Information Technology in the Maritime Industries (COMPIT), Redworth

PIPERAKIS, A.S.; ANDREWS, D.J. (2014), *A comprehensive approach to survivability assessment in naval ship concept design*, Int. J. Maritime Engineering 156/A4, pp.333-352

PIPERAKIS, A.; PAWLING, R.J.; ANDREWS, D.J. (2015), *The integration of human factors into preliminary risk-based ship design*, Int. Conf. on Computer Applications in Shipbuilding (ICCAS), Bremen

RIGTERINK, D.; PIKS, R.; SINGER, D.J. (2014), *The use of network theory to model disparate ship design information*, Int. J. Naval Architecture and Ocean Engineering 6/2, pp.484-495

SHIELDS, C.P.F.; BREFORT, D.C.; PARKER, M.C.; SINGER D.J. (2015), *Adaptation of path influence methodology for network study of iteration in marine design*, 12th Int. Marine Design Conf., Tokyo

SOWA, J.F. (1992), Semantic Networks, <http://www.jfsowa.com/pubs/semnet.htm>

UCL (2010a), *Ship Design Procedure*, MSc Naval Architecture Course, University College London

UCL (2010b), *Ship Design Data Book*, MSc Naval Architecture Course, University College London

VAN OERS, B.J. (2011), *A Packing Approach for the Early Stage Design of Service Vessels*, PhD Thesis, Delft University of Technology

VASSALOS, D.; GUARIN, L.; KONOVESSIS, D. (2006), *Risk-based ship design implementation – Riding the learning curve*, 9th Int. Marine Design Conf. (IMDC), Ann Arbor

The Internet of Things for Smarter, Safer, Connected Ships

Mary Etienne, Dell, Saint Denis/France, Mary_Etienne@dell.com
Anthony Sayers, Dell, Dubai/UAE, Anthony_Sayers@dell.com

Abstract

A lot of sensors, devices, and equipment systems on Ships have always collected data. The difference now is that advances in technology, and in particular connectivity as well as cloud and big data, will put ship intelligence at the forefront of the next major transition for the shipping industry. From ship design, to supply chain to support services and environmental solutions, analytics are allowing vessel owners to connect data sources and analyze data that previously resided in separate silos. Operational Technology (the bespoke systems that manage the ship) is now able to converge with Information Technology, specifically big data and analytics. This convergence is providing valuable business insights and helping maritime customers reduce costs and improve vessel efficiency and safety. This paper presents different approaches to managing data, and gives an overview of Internet of Things (IoT) developments in other industries that could easily be applied to the maritime industry. It describes many of Dell's technologies that will be part of the intelligent ships of tomorrow.

1. Introduction

The Internet of Things (IoT) has captured the attention of organizations because of the profound insights that it can provide. In the past, computers—and, therefore, the Internet—were almost wholly dependent on human beings to input information. However, sensor technology has enabled computers to observe, identify and understand the world—without the limitations of human-entered data. And so at its core, the concept of the Internet of Things, first coined in 1999 by Kevin Ashton of Proctor & Gamble, is simple: it is about connecting devices over the internet, allowing them talk to us, applications, and to each other.

We live in an increasingly connected world. Today, there are about 8 billion connected devices. This is predicted to rise to 26 billion by 2020. From monitoring diesel engines for marine power generation applications to tracking the navigation path of ships at sea, sensors coupled with analytics and data visualization tools can help companies get much more out of their physical assets – improving the performance of machines, extending their lives, and learning how they could be redesigned to do even more. Many companies are already starting to challenge existing business models to create smart, innovative ways of providing new services, managing assets and developing new products.

A recent McKinsey report estimates the potential economic impact – including consumer surplus – of as much as \$11.1 trillion per year in 2025 for IoT applications in nine settings, namely: home, office, factories, worksites, retail, cities, vehicles and the outdoors. Our conclusion: the potential for the maritime industry is hugely significant as ships belong to all of these categories. .

2. Managing Data: Different Approaches

The next logical question is what data can be collected, what data should be collected, how long should the data be retained, and what data should be analyzed and where? There are many different approaches to managing IoT data based on your business objectives and the technical challenges. Organizations are using centralized cloud and data center environments in certain situations to support IoT based analytics. This centralized data integration approach is especially important in analyzing disparate data sources and when real time and speed are not priorities. However, there are other situations where IoT data needs to be analyzed in near real time in order to ensure rapid execution and effect change. For example, real-time analysis of sensor data on a manufacturing system can detect too much moisture or too high a temperature. This situation will require immediate action to prevent

failure. Achieving this type of rapid response creates a new set of requirements in areas such as storage, security, data management and bandwidth. Without an infrastructure that supports this type of real-time action, many companies are not realizing the full potential of IoT data.

One of the ways organizations are beginning to gain more insight and value from IoT data is by architecting for analytics at the “edges” of their environments. This architecture requires that analytics be embedded both directly within endpoints such as sensors, controllers, equipment, and machines, and in nearby aggregation locations such as on the ship’s deck, in its engine control rooms, in data closets and ceilings. Collecting and analyzing data close to the endpoints means that action can take place locally in real or near-real time. In this way, only meaningful information needs to be backhauled to the datacenter or cloud for storage, benchmarking or advanced statistical analysis.

3. Managing and Executing Analytics on Sensor Data from a Centralized Location

There are many complexities involved in gaining the type of insights that businesses increasingly require from their IoT data. To be successful, organizations need to have the right foundation in place. These organizations need to make it a priority to evaluate the potential challenges of executing analytics on IoT data from a centralized environment. Some of the challenges are caused by the nature of the data itself and the physical environment where the data resides. Other challenges are related to how to protect highly sensitive data.

In addition, companies need to be mindful of issues related to latency, and the overall complexity of the environment. The challenges are based on four imperatives:

- IoT infrastructure is highly fragmented
An IoT environment is typically comprised of a myriad of sensors and devices communicating over non-standard protocols that are difficult to integrate and manage. This is especially the case in commercial and industrial environments where organizations need to integrate legacy equipment. Additionally, wireless mesh sensors are often capable of running for years on a single battery by requiring small amounts of power and not connecting directly to the Internet.
- Latency and inconsistent connectivity can be inhibitors
IoT solutions often require rapid data insights and control responses. Typically, you cannot achieve the required speed if latency is introduced from sending data and application calls between remote devices and centralized systems. For example, there are many use cases where inconsistent wide area connectivity can make centralized analytics impractical. Depending on the use case, a large organization could have hundreds to millions of sensors constantly going on and offline.
- Data movement and storage can be costly
Billions of devices, sensors and networks are connected to the Internet and create and receive data around the clock. This generates tremendous amounts of data that must be transferred to a location for storage and analysis. As the number of devices expands and the volume of data increases, the costs of data transport and data storage can quickly become prohibitive.
- Connecting infrastructure and devices can introduce security risks
Security is paramount to any data-driven solution. Traditionally, IoT solutions have been designed to be closed-loop networks that have no exposure to the Internet. While isolation is certainly a way to avoid risk, it also prevents the system from taking advantage of the value of external data feeds and tapping into even more powerful remote processing to supplement local analytics capabilities. In addition, many connected devices that collect and transfer data to a centralized repository lack the capability to deploy sophisticated security controls and safeguards. Further, if every single IoT device were linked across the Internet to a centralized cloud, it would expose an incredibly large attack surface for hackers to gain access to critical data and applications. Even more troubling, this centralized approach can potentially send malicious control commands back to the devices. One effective solution is to consolidate mul-

multiple sensor connections into a secure aggregation point behind a firewall. Centralizing data behind the firewall helps reduce the overall attack surface.

4. Managing and Executing Analytics on Sensor Data Using Edge Computing

A new generation of devices – the intelligent edge gateway – is providing enterprises with the option of performing critical data analytics close to endpoints at the edge of the network. In addition to unifying fragmented sensor data, an intelligent edge gateway has the processing capacity to perform additional analytics in real or near-real time to make data-driven decisions as close to the data generation as possible. Performing analytics on the gateways helps reduce network bandwidth cost because only meaningful information needs to be sent to the next tier, whether it is another gateway, the datacenter, or cloud. In contrast, analytics in the datacenter or cloud is often focused on larger data sets and performed in batches. Distributed IoT architectures that include intelligent gateways help balance the overall system and reduce the big data burden on the datacenter and cloud.

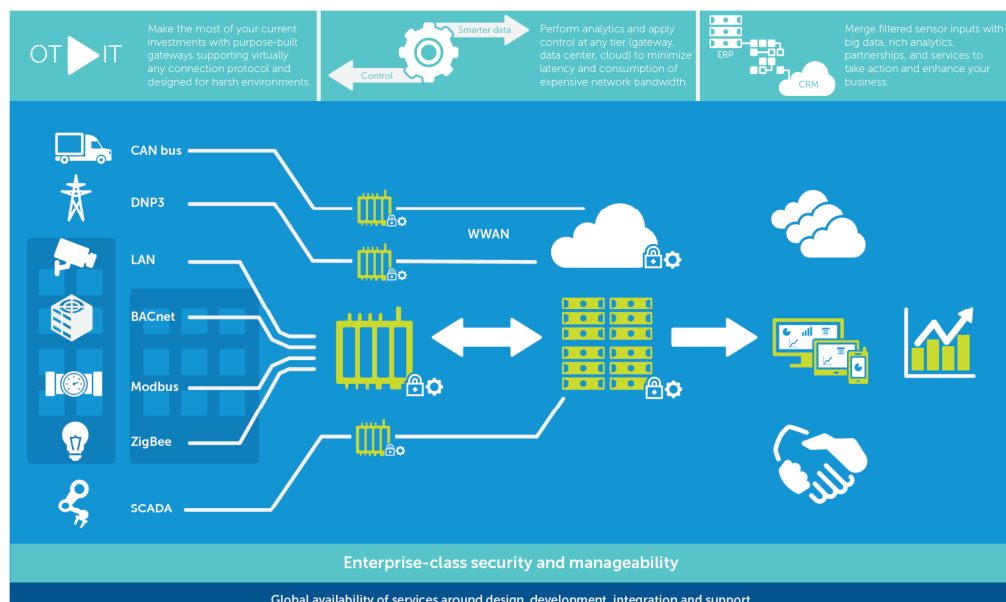


Fig. 1: Using Intelligent Edge Gateways to Solve Industry Specific Challenges

As Fig. 1 shows, an IoT analytic system can be broken up into four key elements:

- Data sources
The system can consist of a variety of endpoints that gather and transmit data. The data sources can be discrete endpoints such as sensors, machines, energy producers, medical devices or even security cameras. In addition, the data sources can be entities that aggregate many endpoints, for example a building, factory, or vehicle. The data coming from these endpoints is often transmitted in a variety of protocols including DNP3, LAN, ZigBee and SCADA.
- Edge aggregation and analytics
Depending on the use case, the data sources may be set up to feed data directly into an edge aggregation and analytics device or directly to the cloud. In the case of an intelligent gateway, some data can be processed with local analytic software in real or near-real time to generate data-driven actions and insights. Additionally, data may simply be passed through to the next tier such as another gateway, datacenter or cloud. In the framework presented in Fig. 1, several gateways have been deployed. Some of the gateways have a single endpoint feeding it data while one of the gateways has several endpoints streaming data to it in a variety of protocols. Consider an intelligent gateway inside of a ship's HVAC unit that collects hundreds of data points a second. The organization's central monitoring station may require only a few key points be sent every day. Meanwhile, the gateway can be used to analyze every piece of col-

lected data in real time in order to optimize performance or sense an impending failure. The gateway can then trigger events to alert repair crews or safely shut itself down. Once in the centralized system, the subset of data from the HVAC unit can be used for batch analytics and longer-term energy efficiency planning. Transferring only the most important information greatly reduces the amount of data sent across the network while still providing insights and business value to the end user.

- **Storage and analytics**

Sensor data sent to the datacenter or cloud can be stored and further analyzed for benchmarking, predictive analytics, and other long-term planning. In Fig. 1 some of the data is transmitted from the gateways to the cloud via a wireless wide area network while other gateways transmit data to a datacenter. Data scientists can run advanced analytic algorithms against the data to gain new insights and fine-tune the analytics performed on the edge device.

- **Data insights**

The final element in an IoT system is the ability for customers and employees to gain insight from the data. To gain deeper contextual insight, IoT data can be blended with internal and third-party data sources. For example, IoT data can be integrated with CRM or ERP system data, as well as social media or weather data. In addition, organizations can provide rich analytic-based applications for customers to view and interact with their data.

5. The Benefits of Bringing Analytics to the Edge

Intelligent, purpose-built gateways are valuable tools to offset many of the cost and performance issues associated with running all analytics in a centralized location. For system integrators and OEMs, these gateways provide a flexible platform to develop analytics solutions that make big data more manageable, increase efficiency, maintain operations, and improve scalability. In this section we highlight some of the reasons why organizations are considering intelligent gateways as part of a distributed IoT architecture.

- Better efficiency and ‘less-big’ data

Intelligent gateways can help organizations filter data close to the point of inception through real or near-real time analytics such as stream or Complex Event Processing (CEP). Only the most meaningful and pre-processed data and events are sent to a centralized data-hub. The ability to filter out noncritical data and only transfer the most important data to centralized data centers is a key capability of gateways and reduces the consumption of network bandwidth. The pre-filtering of data is especially critical in use cases such as smart city, fleet and remote applications where cellular is a common communication choice.

- Self-sufficiency

Intelligent gateways are capable of bi-directional data flow in terms of aggregating new sensor data and pushing back control to connected actuators and equipment. With local intelligence, an edge gateway can execute either pre-programmed or dynamic control instructions based on analytics, autonomously from the backend. The ability to store data locally avoids the potentially catastrophic problems caused if an Internet connection is lost.

- Improved security

The processing power of an intelligent gateway can help secure IoT solution because the gateway has the processing capacity to encrypt data from less capable connected devices and sensors. The increased processing power allows the gateway to run local stream analytics that can search for behavioral anomalies. Security measures can be built into the gateway solution to ensure that only trustworthy devices are allowed to connect. Gateways also aggregate data streams from otherwise cloud-connected devices, thus reducing the overall attack surface between the enterprise firewall and the cloud for hackers to exploit.

- Highly adaptable to vertical use cases and industries

Compared to legacy controllers and appliance-like routers, intelligent gateways can run modern operating systems and are designed to be highly extensible through new applications. The gateway’s operating system and flexibility allows partners and customers to develop and de-

ploy purpose-built applications that meet specific industry and use-case requirements. Examples of edge analytics solutions that have been implemented or are currently underway include energy management within buildings, predictive maintenance for industrial equipment, video analytics for quality control, tracking for critical shipments using wireless mesh sensors and intelligence within vehicles for reducing fuel consumption and breakdowns.

- Leverages existing assets

Even if existing assets and systems were not originally designed to connect to the Internet and share data, data can still be collected from these previously untapped resources by attaching intelligent gateways.



Fig 2: The Dell Edge Gateway 5000 can be mounted on the wall and operate in extreme temperatures

6. IoT Implementations in Other Industries

Intelligent edge gateways provide a robust development platform for partners and customers to create industry and use-case-specific analytical solutions. Here are just some examples from other industries where there is a corresponding or similar application potential for maritime.

6.1. Mines and Datacenters

ELM Energy is a solution provider that monitors and manages power to critical work sites such as mines and datacenters. One of ELM Energy's clients is a mining company that operates an off-the-grid mine. The mine has a number of electrical sources, including solar, battery and generator. The challenge for the mine was that it needed a way to manage the power sources in real time so that the most efficient source could be utilized while at the same time never losing power. The need for real-time analytics and the fact that the mine is located in an off-the-grid location made an on-site solution mandatory.

ELM Energy deployed its software solution called FieldSight that runs on a Dell intelligent gateway. The solution monitors the mine's energy requirements and the output from energy sources and then changes the energy source as needed in real time. For example, as solar power decreases the organization needs the system to be able to monitor and either pull energy from battery storage or increase generator output. In addition to performing local analytics on the gateway, the gateway transfers pre-processed data to a cloud-hosted version of its FieldSight software. Once the data is transferred to the cloud, further benchmarking and advanced analytics can take place. In addition, the maintenance of the gateway can be performed remotely.

This is especially important for ELM Energy because the company often works with clients that have isolated sites. With its solution, customers are able to run reports, perform further analytics, and view the data via ELM's Software as a Service (SaaS) application. By implementing Dell's intelligent edge gateway in its IoT strategy, ELM Energy is able to make automated, real-time energy decisions on client sites while at the same time, transfer the most meaningful data to its cloud for even deeper analytics.

6.2. Facilities Management

Dell is currently working with a customer to develop a bespoke solution for a large facilities management customer, responsible for 2,000 buildings. In this instance, the customer has to proactively send an engineer to the boiler room in each facility every two to three weeks to check for leaks and monitor carbon monoxide levels. As you can imagine, the cost overhead is considerable, particularly as most visits do not discover any problem. Of course, there is also the potential that an incident may go undetected for some weeks in between visits.

As part of a proof of concept, the customer has installed a Dell Gateway with 3G card and connected sensors in a number of the boiler rooms. The sensors message information back to the Gateway, which in turn communicates in real-time to the control center. Motion sensors on the door detect unauthorized access; others monitor carbon monoxide, humidity and temperature levels while another device detects any leakages. The net result? Engineers are only called out when required, leading to huge efficiencies and cost savings. It is not difficult to imagine similar benefits being replicated on board the ship.

Looking specifically at the transport/vehicle market, according to McKinsey, Air China is installing a system that will download performance data from aircraft to ground-based systems in real time. The goal is to improve maintenance effectiveness, reduce downtime and the cost of routine maintenance, and lengthen the useful life of equipment. McKinsey estimates that condition-based maintenance in airplanes could reduce maintenance spending by 10 to 40 percent for air carriers by shifting from rules-based maintenance routines to predictive maintenance based on actual need, which is made possible by connected sensors and real-time monitoring. The new maintenance regime could also reduce delays due to mechanical issues by 25 percent and cut the instances in which equipment must be replaced by 3 to 5 percent. Again, this scenario has the potential to be applied to the maritime industry.

7. Specific Challenges & Opportunities within the Maritime Industry

It is important to recognize that a ship is not just a floating city made of steel. The number one priority has always to be the safety of the people onboard. Vessels also require a great deal of ongoing maintenance, for example excess vibrations can cause a ship to be removed from service.

The crew needs to be on high alert, prepared for mechanical mishaps, fires, open-sea rescues, and extreme weather of all kinds. From an IoT infrastructure perspective, one cannot always assume access to “a cloud” when navigating on the high seas. The conveniences of unlimited bandwidth and “always on” connectivity to the computers and devices industry takes for granted shore-side is not a given. As Fig. 3 illustrates, siloes of connected systems that exist in isolation do not make a ship smarter; systems have to inter-connect and scale not only within the ship but also to the terminal, shore, and HQ office.

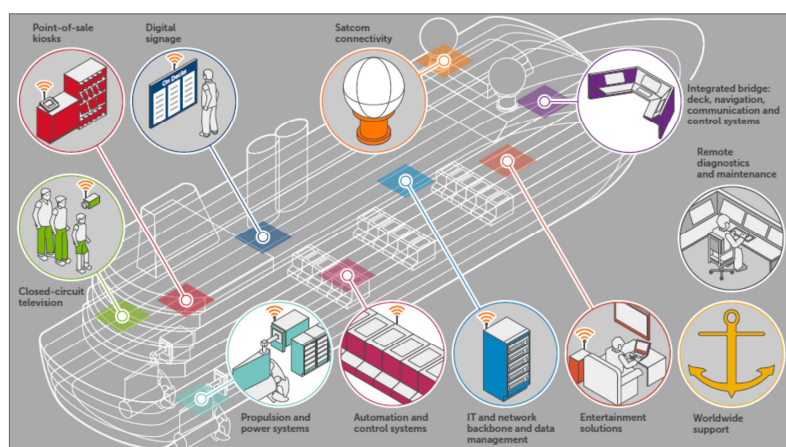


Fig 3: The Connected Ship

Dell believes that the Internet of Things has transformative potential for the maritime industry. Businesses that adopt IoT systems can improve operations and gather greater insights for data-driven decision-making. As the graphic below illustrates, we believe that the biggest opportunities are through connected devices, smart asset management and remote monitoring. Areas with the highest potential include:

- Intelligent data analytics and virtual reality for remote maintenance service via the Internet or to dispatch replacement parts before a failure occurs.
- Alarm monitoring and remote asset management in the control room
- ECDIS systems to provide routing based on traffic, port, safety information and weather conditions
- Energy distribution and usage in engine rooms and HVAC systems for improved energy management
- People-counting analytics to enable rescue teams to be deployed quickly in an emergency
- Purchasing and operational software to be linked to backend databases to manage operational logistics for all job roles onboard like a change in port of call
- Video surveillance and security systems, point of sales and card reader technology for onboard purchases, entertainment systems for passengers, email and telephone service for crew wellness.

When we discuss with shipping leaders ways to capitalize on the Internet of Things, their five key focus areas are: energy efficiency (route optimization, speed control; predictive maintenance through collection and analysis of data from onboard systems; emission control and reporting; crew welfare and ship to shore links with ports and terminal authorities on documentation and reporting.

Additionally, experts say that connected navigation has the potential to generate significant savings across different modes of transportation and sectors of the economy. McKinsey estimate that raising average ship speeds using IoT technology could reduce transportation costs by 11 to 13 percent, which could have an economic impact of \$4.5 billion to \$9.3 billion per year in 2025.

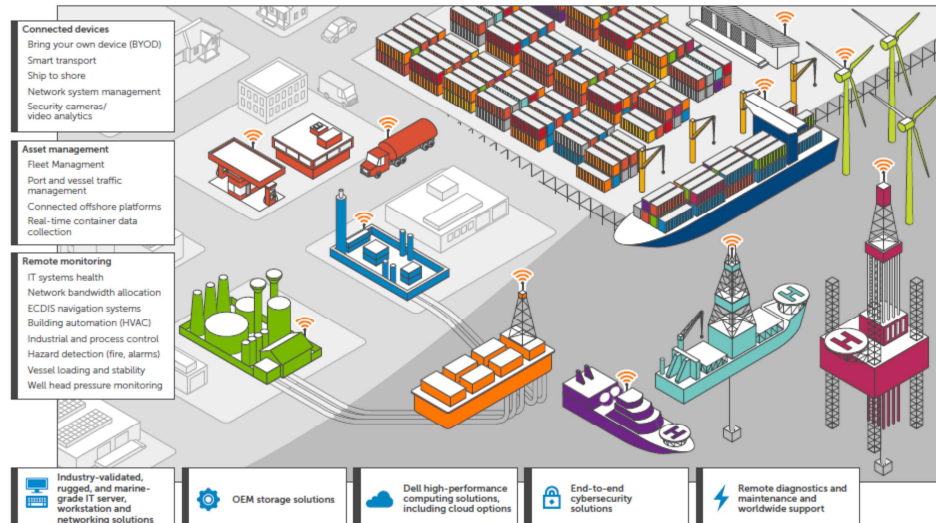


Fig 4: The potential of the Internet of Things onboard ships

8. Conclusion

The need for more analytics, control and greater insight on IoT systems cannot be met by just connecting more sensors, endpoints and other devices to the Internet. It is imperative to take a holistic approach to creating an environment that provides a scalable, predictable, secure, and manageable solution. This engineered approach to IoT allows customers to be able to control costs by leveraging the most effective way to manage data movement, compute and storage. By creating a platform that

supports change and growth, IoT environments can become a way to protect company assets and enable new business opportunities.

As enterprises increase their investments in the Internet of Things, intelligent gateways can play a significant role in keeping the balance between expansion and security. Intelligent gateways enable organizations to securely connect and process data at the place where it makes the most sense. Many of these IoT gateways must operate in harsh conditions where traditional devices such as PCs, routers and servers would be ineffective. Pushing analytics to the edge of the network with intelligent gateways for IoT data is also helping organizations make real-time decisions close to the data and reduce data storage and transfer challenges by focusing on the most meaningful data.

Dell believes that these innovations present a true advantage and are game-changers for the marine equipment supply chain: helping customers to integrate operations, reduce production costs, improve safety, and effectively manage changes in technology to meet global distribution and service needs. Processing power combined with the Internet of Things and data analytics onboard vessels will revolutionize the maritime industry, making it easier for shipping, ship management, transportation, and logistics companies to transport goods from point A to point B.

It is important to point out that even today where organizations are capturing data; it is mostly used for anomaly detection and control, not optimization and prediction, which provides the greatest value. According to the McKinsey report, only 1 percent of data from an oil rig with 30,000 sensors is examined. The net conclusion is that a great deal of additional value – even from organizations currently leveraging the Internet of things - remains to be captured.

The key take-away is that businesses that fail to invest in capabilities, culture and processes as well as new technologies are likely to fall behind competitors that do.

References

KIRSCH, D. (2015), *The Value of Bringing Analytics to the Edge*, Hurwitz & Associates
http://i.dell.com/sites/doccontent/shared-content/data-sheets/en/Documents/Value_of_Analytics_at_the_Edge_Final.pdf

NN (2015), *The Internet of Things: Mapping the Value Beyond the Hype*, McKinsey Global Institute: June 2015, pages 8, 82 and 97

Big Data in Shipping - Challenges and Opportunities

Ørnulf Jan Rødseth, MARINTEK, Trondheim/Norway, OrnulfJan.Rodseth@marintek.sintef.no
Lokukaluge Prasad Perera, MARINTEK, Trondheim/Norway, Prasad.Perera@marintek.sintef.no
Brage Mo, MARINTEK, Trondheim/Norway, Brage.Mo@marintek.sintef.no

Abstract

Big Data is getting popular in shipping where large amounts of information is collected to better understand and improve logistics, emissions, energy consumption and maintenance. Constraints to the use of big data include cost and quality of on-board sensors and data acquisition systems, satellite communication, data ownership and technical obstacles to effective collection and use of big data. New protocol standards may simplify the process of collecting and organizing the data, including in the e-navigation domain. This paper gives an overview of some of these issues and possible solutions.

1. Introduction

Shipping is currently on its way into its fourth technical revolution, sometimes called Shipping 4.0 or cyber-shipping. The first revolution was the transition from sail to steam around 1800, then from steam to diesel engines around 1910 and the third came with the introduction of automation and computerized systems around 1970. The current revolution is about digital data in all aspects of shipping operations and can be compared to what is called Industry 4.0 in the land industry, *Hermann et al. (2015)*. Shipping 4.0 includes extensive use of new technology like Cyber-Physical Systems (CPS), Internet of Things (IoT) and the Internet of Services (IoS). This technology provides more intelligent on-board equipment with embedded computers that provide a plethora of new data and information as well as new shore services to use the data.

It is not obvious that this is really “big data”. Big data is often being defined as being high volume, high speed and/or high variety so that “conventional” data processing techniques are insufficient for efficiently using the data in analytics, decision-making or control, *De Mauro (2015)*. In terms of processing power and computer capacity one can hardly say that this is the case in shipping today. While large sets of data from ships may be awkward or impossible to handle in some simple tools, it does not really pose big data challenges to today’s computer systems. However, the volume and the complexity of the information will require new methods and tools to enable the users to understand the information properly and, in that sense, can be said to be a form of a big data problem.

While the fourth shipping revolution provides a vast number of new possibilities for more advanced on-line control and off-line analytics, there are also a number of other problems than the sheer size of the data sets. This paper explains some of the issues that have emerged in our work on big data and gives some suggestions as to how they can be solved.

2. Increase in availability of data

Several trends contribute to the availability of more data about ship and ship systems, i.e. navigation and automation systems. All of these trends are connected to Shipping 4.0, but materialises in quite different ways and with very different impact on how easy it is to use the data. This section will give an overview of some of the main data sources used today.

2.1 Bridge data network, mandatory and special purpose instrumentation

The ship bridge equipment is normally interconnected with digital interfaces from the IEC 61162 family of standards, *IEC (2007-2015)*. This makes it relatively easy to get access to measurements from the navigation sensors and equipment. A steady but slow increase in carriage requirements from IMO and flag states increases the available data from the bridge.

In addition, some special ships will require special instrumentation relevant for their operations. This may include wave radars, oil spill detectors, high accuracy inertial navigation sensors etc. These may or may not be accessible via standard interfaces.

The voyage data recorder (VDR) is sometimes used as a collection point for such data, but one should be aware of limitations in the number of data points the VDR collects and how often the data is registered.

2.2 Conventional automation

Automation systems on most ships collect large amounts of data, but of variable quality. Even on a relatively old bulk ship the number of input/output points may be several hundreds. On modern and more complex ships the number of data points can be several tens of thousands.

There are two main problems with this type of data: The first is to get access, as the data is normally only available within closed and vendor-specific systems. The second is the quality of the data. As the data is used in closed loop control or in alarm limit supervision, sensors may not be particularly accurate. For older automation systems, it may also be a problem that sensors are defect or disconnected. The automation system rarely provide quality attributes on the data so the user will need to check if the measurement are sensible and if values are stuck or fluctuates too much.

Sometimes, modern integrated bridge systems are equipped with both navigation and automation systems integrated into a single platform. This can more easily facilitate new cyber-physical systems. These systems also can collect significant amounts of data and that may introduce the same types of problems as discussed in this paper.

2.3 New cyber-physical systems

Modern ships make use of more advanced equipment with built-in sensors and control systems. This includes engines and power generation, winches with torque-control, advanced dynamic position systems, new navigational sensor systems and so on. The systems have computers and sensors for condition monitoring, closed loop control or for detecting alarm conditions. This type of integration of physical systems with computer control is one of the main characteristics of Industry 4.0: Cyber-Physical Systems (CPS).

The problems of using data from these systems are similar to that of automation: Difficulty of access and suitability for use outside the system for which they are intended. For CPS, general quality may be less of an issue as most data points are used in active control or monitoring of the equipment and errors in sensors will be detected rapidly.

2.4 Ship performance monitoring

Later years, particularly when the oil prices were high, saw a substantial increase in ship instrumentation for performance monitoring and optimization. This typically included shaft torque meters, fuel mass-flow meters, improved environmental sensors, trim measurements etc. This instrumentation was fitted explicitly to provide data for improved ship performance and one can expect that both access to and quality of data is good, dependent on how and by whom the instruments were fitted. In some cases, instruments and services may be provided by third parties and this may reduce access to the information.

2.5 Ship reporting

Ships are sending a number of operational and administrative reports to shore. This includes various mandatory port and port state reports, noon at sea reports, technical maintenance reports etc. Many of these can be very valuable as input in data analysis as they represent operational decisions by the

crew. These reports are normally generated from manual input and this makes them susceptible to data entry errors. Some reports also have impact on the economic performance of the ship so figures may be tweaked to avoid penalties or additional costs.

This again means that one needs to be careful about quality control and verification of data in such reports. On the other hand, these reports also represent the crew's opinion of the state of affairs and general operational outlook, which may be used to quality control and verify other automatically acquired data as well as to complement more technical measurements.

2.6 External ship monitoring – AIS and VTS

Another growing source of ship data is external monitoring. Most coastal states operate automatic identification system (AIS) base station networks along their coast. This will monitor ship traffic within range of the VHF radios on the base stations. Low Earth Orbit satellite AIS receivers are used to extend detection beyond the range of the coastal stations. AIS receivers can provide very valuable data on ship movements. Under way, ships will send AIS data quite frequently, normally minimum each 10 seconds. Data that is transmitted is position, speed, course, true heading and rate of turn. Less frequent messages will transmit ship static data, draught and other voyage related information.

In addition to coast state authorities, there are also several private providers of AIS data, either using shore stations or satellite. Thus, access to AIS-data is normally not a problem, but quality and prices may vary. In most cases one will get "filtered" data so that one also needs to consider any implications on data quality from the filtering. Filtering is normally some form of decimation of data in high density reporting areas or interpolation in areas without registrations.

In addition to AIS, coastal states also operate vessel traffic services (VTS) that monitor ship traffic with radar and CCTV systems in certain areas. In some cases, they may also use synthetic aperture radar or other forms of satellite sensors to improve local situation awareness. Neither of these data is normally available to the public.

2.7 Weather data

Forecasted and historic weather data is available for free or for payment, dependent on the level of detail one requires. The free information is relatively low resolution, but can give good high-level information about environmental effects on the ship. The data is less useful close to the coast or in areas where weather phenomena are influenced by smaller scale geographic features, e.g. close to islands or within narrow ocean currents.

2.8 Port call data

Port and ship agents are collecting valuable information on ship movements close to and in ports. This is mostly operational data that can give very accurate information on port delays, time taken for loading and discharge etc. The data is often made available to the ship and ship owner as a statement of facts or a port log. The data tends to be accurate as it is often used as basis for calculating port fees, performance claims and other commercially important data.

3. Obstacles to efficient collection of ship data on board

The previous section gave an overview of commonly used data sources on or off the ship and some of the problems encountered when trying to access and use the data. Table I summarises the main problems and links them to the data sources in question. The following sub-sections will give more details about each of the acquisition problems.

Table I: Common data acquisition problems

Problem area	Type of data acquisition			4. Performance	5. Reporting	6. Monitoring	7. Weather	8. Port data
	1. Bridge	2. Automation	3. CPS					
Context dependent data quality	X	X	X					
Safety and security considerations	X	X	X					
Complex phenomena are difficult to measure	X			X			X	
Non-automated data entry create errors					X	X		X
Commercial issues may induce wilful errors in reports					X			X
Bad quality instrumentation, no quality attribute on data			X					
Proprietary and costly interfaces to data		X	X					
Ownership of derived data				X	X			
Lack of standards		X	X	X				
Artefacts in AIS base station and satellite reception						X		
Cyber attacks	X				X	X		

3.1 Context dependent data quality

The specific acquisition context of sensor data is more or less a problem for all measurements that are taken from one system and used in another. One example is different sensors of similar types, where they are located and how they relate to each other: As an example, the ship normally has a number of position sensors, each with its own local position reference and individual quality attributes that may not be known outside the bridge system. Using raw position data from the navigation system can cause accuracy or consistency problems.

A similar problem occurs in sensors used in closed loop control or as alarm limit sensors. Basic sensor properties such as linearity, offsets, accuracy and stability will always be adapted to the task at hand and the fitting of a specific sensor is a trade-off between cost, robustness and fitness for purpose. For control and alarm applications, sensor artefacts can be adjusted in the control and monitoring software and the absolute quality of the measurement may be of lower importance. Unless the adjustment factors are known to external systems, use of these measurements outside their systems rapidly becomes problematic. Unfortunately, the context problem is not easy to solve and will require very complex attribute lists for any measurement that shall be used outside its original context. In practical terms, this may be too complicated to implement in a standardised way, *Rødseth (2016)*.

3.2 Safety and security

Connections to the bridge or other data networks that provide safety or security related functions may be a safety or security hazard. Any physical connection into networks or systems can be a vector for error propagation or hostile attacks. Thus, such connections are often not allowed by flag state or class authorities. On bridge networks, there have been developments in safer Ethernet networks and firewall technology for connecting to external networks *IEC (2015), Rødseth and Lee (2015)*.

For automation networks there may also be possibilities for using safe connections via firewalls and gateways. Unfortunately, standards for this have not yet been developed so this type of solutions can become expensive (see sec. 3.9).

3.3 Measuring complex external phenomena

Complex phenomena such as environmental impact on the ship performance are difficult to measure accurately and care must be taken when such data is used in calculations. Speed through water, wind speed, waves and other similar data vary significantly around the ship and it is generally difficult or impossible to estimate overall impact just from one measurement point, which is normally what one has on most ships.

In addition, the fact that the sensors are mounted on or outside the hull contributes to errors. They are susceptible to damage, coating by foreign matter or general degradation that make the measured values less reliable.

3.4 Non-automated data entry create errors

Experience shows that manual entry of data into report forms, computer systems or AIS transceivers is an important source of errors. For AIS, this will manifest itself particularly in voyage destination, ship draught and sailing mode, but it also sometimes shows up as illegal or wrong ship identity.

For AIS there are also issues related to the transmission of navigational data such as rate of turn and true heading that should be got from sensors external to the AIS. Many AIS transmitters are not connected to such sensors and send non-valid data or data derived internally from the position.

It is difficult to avoid this problem. One obvious solution is to use automated data entry, but this is often too costly if it requires physical connections to other systems. Extensive validity check is probably the most relevant solution in the short term. However, automated ship reporting is a prioritized solution in the e-navigation strategic implementation plan, *IMO (2014)*, so one may expect some developments in this area in the coming years.

3.5 Commercial considerations may induce wilful errors in reports

Some reports from the ship to shore have commercial implications, e.g. for owner or charterer. This may be bunkering, fuel consumption and speed reports including reports on contractual performance, exceptions related to bad weather or ship safety issues. Traditionally, this has rendered some reports less reliable as the operator has had direct economic interests in reporting misleading data.

Today, the possibilities of tampering with such data is much lower as it is fairly straight forward to do consistency checks via AIS satellite, weather data or other generally available information. However, the problem does to some degree persist and needs to be taken into consideration when commercially sensitive data is used in analysis.

3.6 Low quality instrumentation – no quality attributes

Sensor data on older ships and sensor data that are rarely used operationally can sometimes be of dubious quality. This can be because the sensor has failed, it has been disconnected, painted over or from any number of other problems. This is a relatively common problem with data from the automation and alarm systems.

Most automation systems will not perform quality checks on the data or provide any other quality attributes to the measurements. When data is exported out of the system, it will be difficult to assess whether the data can be relied on or not.

Today, this problem needs to be handled by careful data quality checks in the systems that use the data. There is work under way to look at new interface standards (sec. 3.9) that may introduce improved quality attributes for automation data.

3.7 Proprietary and costly interfaces to data

Most parties accept that the ship owner is the owner of any data measured or otherwise produced on-board. However, as long as these data are not readily available via standard interfaces, the owner or operator is likely to pay a high price for getting access to them. It will normally require retrofitting of special hardware and software that together with the required service personnel can be expensive.

This is less of a problem for systems that use established interface standards, such as the bridge data network. Unfortunately, standards are missing for many ship systems and in particular for interfacing to automation systems. This may change with recent standards initiatives (sec. 3.9).

It is particularly difficult to avoid these costs for older ships that are being retrofitted, but it should be kept in mind for new-builds where new interface technology and costs are easier to negotiate with the yards.

3.8 Ownership of special or derived data

Some systems may be delivered with special restrictions on the use of data internal to the system. In some cases, condition based maintenance and general monitoring is provided as a service to the ship owner where the owner does not at all have access or ownership to the underlying data. Similar third party services are sometimes also used for various ship or fleet monitoring or optimization functions. This may also imply restrictions on ownership of the data.

Even if the ship-generated measurements are accessible to the ship owner, there may also be derived and intermediate data that is not. These may be the results of various calculations and analysis performed on the ship or on shore.

If third party services are used for monitoring of ship or fleet, one should consider how ownership of collected and derived data could be ensured. This is not as clear-cut as for general on-board data, but will be something that can be negotiated with the service provider.

3.9 Lack of interface standards

The lack of open interface standards is an important problem for many types of data acquisition although most pronounced for interfaces to automation and embedded control systems. Bridge and navigational systems have some established standards that are suitable for open interfacing (sec. 2.1) and some types of ship reporting is using standard formats, *Rødseth (2016)*. Lack of interface standards means that all data acquisition interfaces will need to be built to purpose and that the configuration of the interface most likely will be different for all implementations, even on almost identical ships (sec. 3.7). This is costly, time consuming and error prone. Arguably, one can say that this is one of the fundamental obstacles to more efficient data analytics on ships. There is work underway to develop interface standards for automation systems. *ISO (2015a, 2015b)* has proposed two new standards to cover respectively digital interfaces and data tagging for shipboard use. It remains to be seen when these standards will be finished and accepted in the market.

3.10 Artefacts in AIS base stations and satellite reception

Data acquisition from AIS shore systems is limited to when the ship is within range of a base station. Reception will also be hindered by radio shadows. When reception is possible, the ship's transmission rate is highly variable and dependent on ship speed and manoeuvres.



Fig. 1: North Europe view of AISSat1 and AISSat2 orbits over a 24-hour period

Satellite reception is limited by the orbits and radio equipment of the satellite. Norway currently operates two satellites in polar orbits (see Fig. 1). These give around eight minutes observation windows approximately each 45 minutes north of 75° , but this rapidly decreases to about one window each two hours around the south part of Norway. At Equator, one will get two observations per day, one for each of the satellites. The satellites are also subject to a number of radio-technical and atmospheric disturbances that further decreases probability of observations, *Rødseth et al.* (2015). This is particularly a problem near areas with high ship traffic density due to cross-talk between ships. Fig. 2 shows a plot of satellite observations of a ship operating around 80° North over a period from January 2014 to November 2014. The y-axis shows time between observations in hours. The high peaks (long observation drop-outs) are typically during port calls while the reduction in time between observations from July 2014 is due to the start of the testing of the second AIS satellite, AISSat2, *Rødseth et al.* 2015. In the period up to June 2014, only AISSat1 was operational.

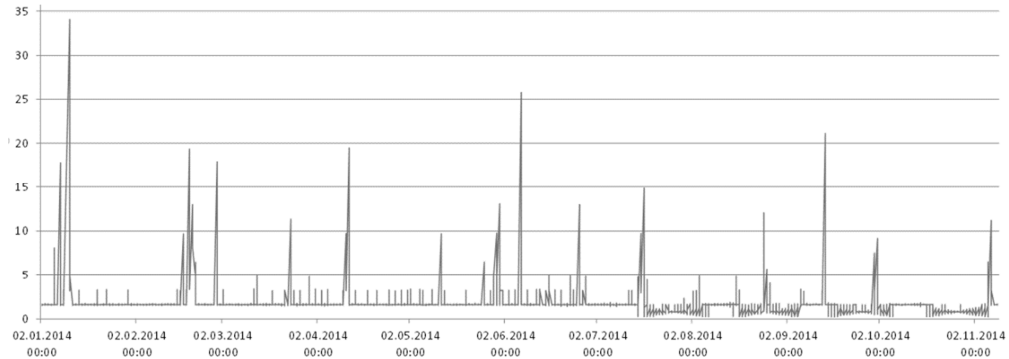


Fig. 2: Hours between AIS observations

The irregular reception pattern means that data may have to be carefully interpolated and filtered to avoid sampling artefacts in calculations that are dependent on regular time series. One also needs to consider the sources of AIS data before assumptions on acquisition frequency, probability or data quality can be made.

3.11 Cyber-security challenges

Cyber security is not considered a major factor in general data acquisition on-board, but one should be aware that certain data could be jammed or spoofed from cyber-attacks. Examples have shown that even GPS position signals can be spoofed. All data that relies on wireless transmissions from other ships or shore are susceptible to spoofing or jamming. As examples, this applies to AIS or radar targets acquired by the ship and sent to shore. It will also apply to AIS signals data collected by shore or satellite systems.

All reports sent from the ship to shore (or vice versa) can also be intercepted and tampered with. Any application of ship data needs to consider if this problem is serious enough to include in the analysis of errors sources, *Rødseth and Lee (2015)*.

4. Maritime big data management and applications

As the previous sections have shown, there are many sources of data on the ship, potentially high volumes of data and correspondingly many possibilities for errors. Data management on the ship and on shore has to be performed along three axes as shown in Fig. 3.

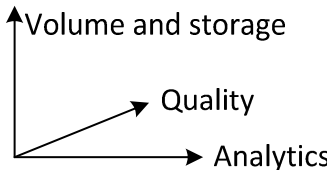


Fig. 3: Three dimensions of big data management

Volume and storage management manages large volumes of data in a structured collection on board and/or on shore. Volume management will also have to consider the cost and capability of moving large sets of data between ship and shore. The science of examining these data with the purpose of drawing meanings can be categorised as data analytics. Quality control of the data needs to be considered by either or as a separate activity and is critical for the correctness of the analysis results.

4.1 Volume and storage management

Sensors and data acquisition systems collect large quantities of ship performance and operational data. Some systems, in particular bridge and performance monitoring can be equipped with several sensors that often collect similar types of parameters. The same is the case for AIS observations where different base stations can receive simultaneous data from the same ship. Many sensors, including AIS, also collect data with a time resolution that is often much higher than required for ship performance analysis.

Generally, measured data can be functionally or temporally redundant in many situations and those situations should be identified during the volume and storage management process. Most data sets can normally be reduced to a much smaller data set by removing redundancy. This significantly improves the data handling and communication process, *Perera and Mo (2016)*. However, extensive knowledge about the structure of the data sets and the intended analysis is required to avoid removing important data.

There are also ways to reduce the amount of data using statistical methods that remove some of the data details but focuses on keeping the main components and the variation in the data, e.g. principal components analysis, PCA. Data processing of this kind may both reduce the size of data sets and filter out noise.

Virtually all methods that reduce the volume of the data will also remove information, typically about phenomena that is not related to the principal interest of investigation or main statistical trends in the data. Removing data items that have been registered by different sensors can, as an example, remove information about the relative reliability of each sensor.

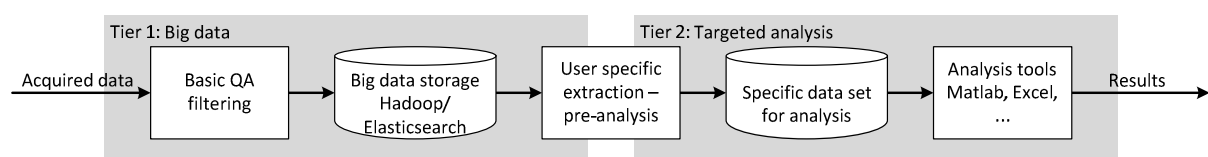


Fig.4: Proposed system for ship performance data

Data management needs to consider how data is stored and structured, particularly where one has to handle large data sets efficiently. In light of the conflict between having consistent and easy to manage data set and not losing details in the data sets that may be of use later, we are currently looking into a two-tier storage system as illustrated in Fig. 4. The lowest tier will use big data technology to store as much data as possible, after initial bad data removal and careful data reduction. The second tier will use specific extraction, structures and tools for the analytic problem at hand.

4.2 Ship-shore communication

The digital connectivity of ships is increasing, in particular for advanced and well-managed ships. Land based mobile communication systems is also more accessible to ships at a relatively low costs and high capacities. However, high sea satellite communication is in many cases a limiting factor for transfer of data between ship and shore.



Fig.5: Ship density in the world (B.S. Halpern, from T. Hengl; D. Groll / Wikimedia Commons)

Operators of telecommunication satellites will point their beams to areas where there are customers, and many areas of the deep seas are not prime locations for high throughput services (see Fig. 5). This means that for most ships, there will be limitations in maximum available bandwidth and costs of transmissions, at least in certain areas. This also means that the data management system needs to consider how the available communication capacity can be used to best possible effect.

This process can be integrated with analytical processes, e.g. to develop hierarchical performance indicators where higher level indicators give an overview of status while it is still possible to drill down into more details if and when that is required. This principle is used in technical condition and safety indexes, Rødseth *et al.* (2007), and in the Shipping KPI system, Rialland *et al.* (2014). This principle can save processing and transmission costs and time as only selected data elements needs to be handled at a given abstraction level and time.

Perera and Mo (2016) have also discussed possibilities for using principal component analysis for data compression. Here, a volume saving of 30% at an information loss of about 6% has been demonstrated. This will come in addition to any conventional data compression technique used in such system.

For all data reduction approaches one should also consider to keep a more complete record of measurements on-board for later off-line analysis. Much of the value of the big data approach is that one can use novel and deep investigations on large data sets collected over time to investigate phenomena that was not even thought about at the time of data collection. To do this successfully, one will have to be careful about how data is filtered.

4.3 Data quality

Several data quality issues were discussed in sec. 3 and one can identify four main groups of quality problems that can occur individually or in combination:

1. Unreliable data: The data input is completely or partly faulty and there is no clear or consistent relationship between data value and the observed phenomenon.
2. Context specific artefacts: The input value needs additional and possibly unavailable information to be interpreted correctly, e.g., the exact location of the sensor on the ship.
3. Temporal artefacts: The data input frequency creates problems due to too high, too low or too irregular sampling frequency. This is also related to the Nyquist–Shannon sampling theorem.
4. Non-proportional data: The input data is not proportional to the phenomenon observed. This may be due to problems with linearity, offsets, hysteresis, saturation, etc.

Each of these classes of problems can use many specific and diverse methods to filter out errors and correct for artefacts. However, a common situation is that the actual cause of data degradation is not known and one may have to use general statistical methods to try to detect measurement artefacts.

As discussed in *Perera and Mo (2016)*, systematic data reduction can be used for quality enhancements. Reducing redundancy in measurements will be an opportunity to detect and remove data that is outside expected values or areas. This could be based on mathematical models of the physical system, empirical or statistical methods or on various forms of machine intelligence. In all situations, the quality and level of details of the methods will determine what information is removed and lost. Lost information may or may not be acceptable for general data acquisition. Even directly faulty data can contain information, e.g. on sensor reliability. However, data that is outside expected ranges should always be flagged as such so that it is not used in analysis without proper precaution. Data analytics in itself, when having access to data that has redundancy in the systems states they observe, can also be used for sensor fault detection.

Quality management can also be performed independently of analytics and volume management. Sensor system knowledge, outlier detection, trending and statistical methods can be used to identify and possibly remove suspicious data elements.

4.4 Data analytics

Information is sometimes defined as data that answers a question about the world. There are two main ways to convert data to information as illustrated in Fig. 6. One can use knowledge about the world to formulate the question that the data provides the answer to (model based) or one can use various forms of discovery methods, e.g. based on statistics, correlation techniques or "machine intelligence" (MI), to discover new and unknown relationships in the world. Much of the ICT-oriented research on big data focus on the latter while much of what is currently going on in the shipping sector make use of the model based information extraction.

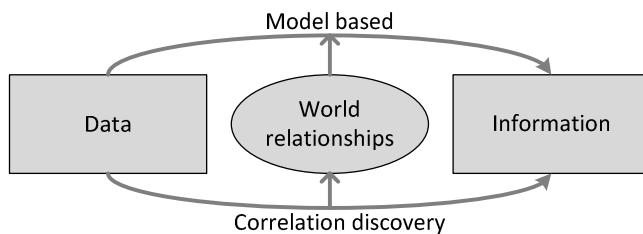


Fig.6: Model or discovery based data transformation

Model based extraction has strengths in having more possibilities for systematic analysis of data, including scientific hypothesis testing. The drawback is that the model or hypothesis must exist before the model can be used. Discovery based methods has the potential of finding new models and relationships, but with the danger that the model is not in fact valid, but only occurs as a random or otherwise correlated relationship between data.

In our case, initial studies on data analytics has been based on various empirical ship performance and navigation models. However, these conventional mathematical models often fail to handle large-scale data sets due to system-model uncertainties, sensor noise and fault conditions and complex parameter interactions. In some situations, these models cannot be adapted to predict actual ship navigation

situations that are described by large data sets. Machine intelligence (MI) and statistical analysis are often used in such situations to overcome these data handling challenges. MI and statistical analysis can therefore be the more attractive approach in big data handling.

MI techniques have been used for data classification and regression analysis in various research and industrial applications. This can also be used under big data applications in shipping. Statistical techniques are often used to determine the relationships among the parameters in big data sets, e.g. through principal component analysis. These methods can be combined so that the parameter relationships among the classified data sets are investigated by statistics and the regression tools are used on these relationships to extract conclusions.

5. Operational time scale of big data applications

The new big data applications can be used in many different time scales from on-line decision support tools to long-term fleet statistics analysis. One can also have loops within this framework where results of long-term analysis is used to update control parameters in on-line decision support. We will not go into details on these issues in this paper, but only highlight some of the possibilities.

5.1 On-line ship decision support

Examples of more or less real-time applications are trim optimization, heavy weather decision support, engine optimization systems and so on. These will typically analyse immediate or short-term historical data to give decision support on current optimization possibilities, related to fuel consumption, ship movements or other ship parameters.

5.2 Ship performance optimization

Other applications will analyse data over longer periods to determine more general optimization possibilities. In addition to best practice operational guidance, this can also include technical condition monitoring and maintenance planning. One example of such a service is technical condition monitoring which uses monthly controlled measurements to assess the technical condition of ship machinery, *Rødseth et al. (2007)*.

5.3 Fleet optimization

Even larger data sets can be used to compare performance between similar ships over longer periods. This can typically be used to determine statistical operational constraints for certain routes or more general best practice suggestions over the fleet. Other possibilities are analysis of technical performance of various technical and operational procedures, such as maintenance strategies, voyage optimization, hull coating performance etc. The Shipping KPI project is one example of such a service, *Rialland et al. (2014)*.

5.4 Predictive analysis

Other interesting possibilities that opens up in a big data perspective is to use historical data to determine characteristics of new ships or new operational principles. Virtual prototyping and simulation of new ship designs in known and historically verified operational conditions is one interesting application of this, *Fathi et al. (2013)*.

6. Conclusions

Big data processing for ships and shipping can tap a number of so far underused data sources and have a great promise in establishing more efficient technical solutions and operational regimes for ships and shipping. On the other hand, there are a number of error sources that can disturb the analytical processes and lead to erroneous conclusions. Therefore, various online and offline tools and

techniques need to be developed to overcome such situations. This is particularly important for systems that operate on-line and that may be implanted as a part of modern integrated bridge systems. Systems using data collected over longer periods have more possibilities for filtering out bad data points through use of larger sets of historical data and using averaging over longer time periods to remove spurious bad points. However, even for online and real-time data handling there are new methods emerging that may promise better identification of sensor and acquisition fault situations. The quality of the data sets can be improved and instantaneous vessel performance can be observed at a much higher level of detail and with fewer errors.

Offline data handling may require additional data management tools to save, search and recall the required data sets, where the overall vessel and fleet performance in detail can be analysed. Therefore, the development of both data management and analytics will play an important role in the field of big data in shipping.

Connectivity between ship and shore is still a factor for some ships, but this is getting less of a problem as communication technology develops and prices of bandwidth decreases. Even with limitations in connectivity, there are many promising applications for big data applications in ship and fleet analysis.

A major cost-increasing factor for big data applications on ships is the lack of technical standards for interfacing to the different data sources. This means that ad hoc and costly interface solutions have to be developed for each ship. In addition, it will also be costly to configure databases, create system models and link the different measurements to the relevant phenomena. Work is under way in this area, but this work need more support from owners, yards, system manufacturers and scientists.

Another main factor for successful application of big data applications in the maritime field is to have a good understanding of the possibilities and limitations of the different data sources and the technologies that are available to handle the different problems.

References

- DE MAURO, A.; GRECO, M.; GRIMALDI, M. (2015), *What is big data? A consensual definition and a review of key research topic*, AIP Conf. Proc. 1644, pp.97–104.
- FATHI, D.E.; GRIMSTAD, A.; JOHNSEN, T.A.; NOWAK, M.P.; STÅLHANE, M. (2013), *Integrated decision support approach for ship design*, IEEE Oceans, Bergen
- HERMANN, M.; PENTEK, T.; OTTO, B. (2015), *Design principles for Industrie 4.0 scenarios: a literature review*, Report, TU Dortmund
- IEC (2007-2015), *Maritime navigation and radiocommunication equipment and systems - Digital interfaces*, (Part 1 and 2: Serial line, Part 450 Ethernet; Part 460 Safety and security), IEC 61162
- IEC (2015), *Maritime navigation and radiocommunication equipment and systems - Digital interfaces - Part 460: Multiple talkers and multiple listeners - Ethernet interconnection - Safety and security*, IEC 61162-460
- IMO (2014), Sub-committee on Navigation, Communications and Search and Rescue, Report to the Maritime Safety Committee. NCSR 1/28, Annex 7: *Draft e-Navigation Strategy Implementation Plan*
- ISO (2015a), ISO/NP 19847 *Shipboard data servers to share field data on the sea*, ISO/TC 8 / SC 6N 359
- ISO (2015b), ISO/NP 19848 *Standard data for shipboard machinery and equipment of ship*, ISO/TC 8 / SC 6N 360

PERERA L.P.; MO, B. (2016). *Data compression of ship performance and navigation information under deep learning*, 35th Int. Conf. Ocean, Offshore and Arctic Engineering (OMAE 2016), Busan

RIALLAND, A.; NESHEIM, D.A.; NORBECK, J.A.; RØDSETH, Ø.J. (2014), *Performance-based ship management contracts using the Shipping KPI standard*, WMU J. Maritime Affairs 13(2), pp.191-206

RØDSETH, Ø.J.; STEINBACH, C.; MO, B (2007), *The use of technical condition indices in ship maintenance planning and the monitoring of the ship's safety condition*, Int. Symp. Maritime, Safety, Security and Environmental Protection, pp. 20-21.

RØDSETH, Ø.J.; KVAMSTAD-LERVOLD, B.; HO, T.D. (2015), *In-situ performance analysis of satellite communication in the high north*, IEEE Oceans, Genova

RØDSETH, Ø.J.; LEE, K. (2015). *Secure communication for e-navigation and remote control of unmanned ships*, 14th Conf. Computer and IT Applications in the Maritime Industries (COMPIT), Ulrichshusen

RØDSETH, Ø.J. (2016), *Integrating IEC and ISO information models into the S-100 Common Maritime Data Structure*, E-navigation Underway International, Copenhagen

Design Optimization using Fluid-Structure Interaction and Kinematics Analyses

George Korbetis, Serafim Chatzimoisiadis, Dimitrios Drougas,
BETA CAE Systems S.A., Thessaloniki/Greece, ansa@beta-cae.com

Abstract

This paper describes an analysis approach for maritime fluid-structure interaction (FSI) problems. CFD and FEA algorithms are combined to analyse the vessel's behaviour. Several iterations are needed to achieve convergence. The interpolation of the dynamic loads from the CFD to the FEA is of key importance. However the use of an FSI algorithm can yield accurate results much faster, making design optimization a realistic and cost-effective approach. The case study concerns a free-fall lifeboat, using an FSI solver. A kinematic solver calculates the initial conditions of the FSI analysis for different initial positions of the vessel.

1. Introduction

Lifeboats are found in oil platforms (offshore structures with drilling equipment that extract oil and natural gas) and large transport vessels. They are fully enclosed vessels designed specifically for the fast evacuation of the vessel. Such lifeboats can carry from 18 up to 70 persons and provide a safe and rapid transport of people to safety. The lifeboat is launched from a specifically designed tilted platform on which it slides and then free falls to the seawater.

Lifeboats, as all other boats, follow design specifications and standards (DNV) in order to be used in service. Two of the most important factors in the safety specifications of free fall lifeboats are the "Motion pattern", DNV (2010), and the Combined Acceleration Ratio (CAR) Index values.

The lifeboat should follow a specific trajectory from its initial position, into the water and to re-emerge moving away from it starting point, structurally safe and keeping the passengers unharmed. At the time the lifeboat surfaces, "the minimum distance between the lifeboat and the host facility should be no less than 40m" DNV (2010). Passengers should experience accelerations (negative, during entry) that will not surpass the specified values during free fall.

Mørch et al. (2008) used computational fluid dynamics method coupled with the rigid body of such a lifeboat, to investigate the effects of the shape of the vessel, the waves, and wind on the behaviour of the lifeboat during its entry in the water. Using a CFD solver, overlapping grids and local refinement they evaluated the accelerations that the lifeboat undergoes in several conditions.

In this paper, an optimization study was performed to simulate the free-fall process for various positions of the lifeboat, regarding height, initial trim, and list angle of the launch platform. An embedded kinematic solver calculated and applied the initial conditions for each starting position of the lifeboat. The investigated result was the motion pattern of the vessel, to assess whether there is sufficient distance between the lifeboat and the host structure after surfacing, and also the CAR index values at specific points in the lifeboat to minimize the accelerations of the human body.

The use of the FSI algorithm (LS-DYNA) helps for faster and more accurate simulations of free fall lifeboats. It drastically reduces the development and testing time of such products, since experimental testing is reduced. Along with the FSI algorithm, the ALE (Arbitrary Langragian Eulerian) method was used since it has shown decent results in comparison with experimental results and other methods, Tokura (2015). Also, the ALE method has demonstrated an acceptable behaviour for fluid structure interactions between shell structures and ALE solid domains, Wang and Chen (2007).

2. Robust analysis description

Unpredictable weather conditions can be a major factor in the safe evacuation of offshore platforms or large transport vessels. Wind, waves, water level, tides, and also ice, snow, salinity and temperature can have a great influence in the free fall evacuation process. DNV standards provide information regarding the long term probability distribution of such loads focusing on wave height (H_s) and peak period (T_p). Along with these parameters, any possible damage to the structure and the load or cargo of the large offshore structure that is constantly changing makes the free-fall evacuation a multi variable problem.

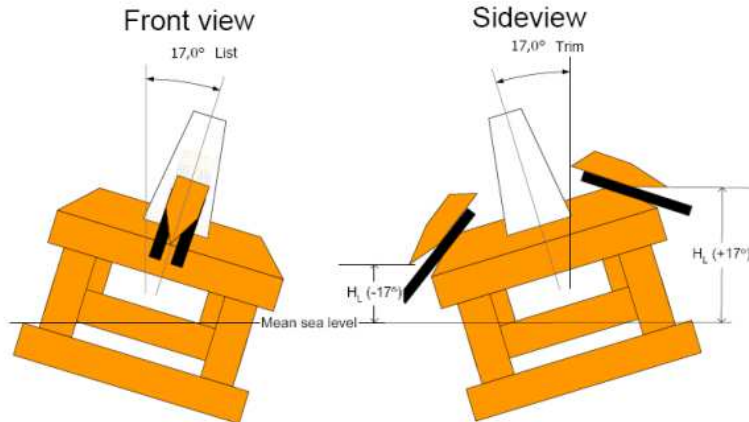


Fig. 1: Front and side view of possible launching positions (damaged structure)

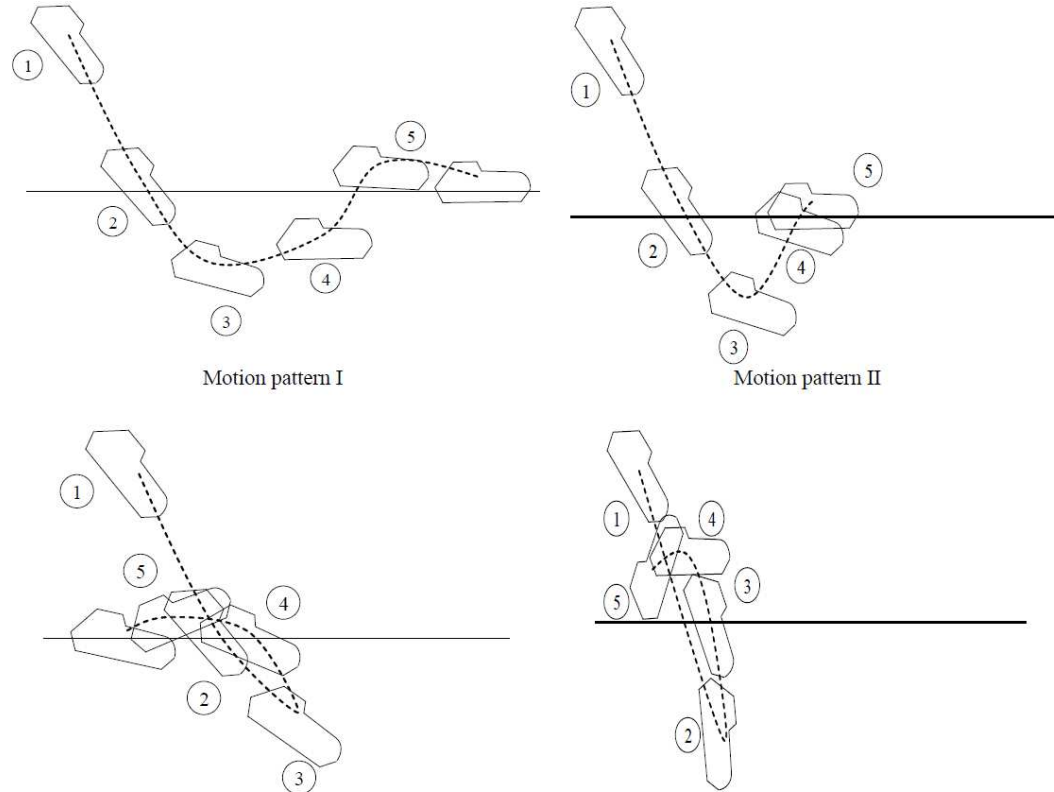


Fig. 2: Motion patterns for a free fall lifeboat

In this early stage of this work, wind and wave parameters were not taken into account. However the substitute no collision requirement (minimum 40m distance) was set as a design constraint. To analyse the robustness of this design, three parameters were investigated. The height of the lifeboat

from the sea level, the list angle of the launch platform, and also the trim angle of the platform, Fig. 1. These three parameters have a great impact on the motion pattern, Fig. 2, of the vessel that consequently affects the acceleration the passengers undergo during the entry to the sea (and the distance from the accident).

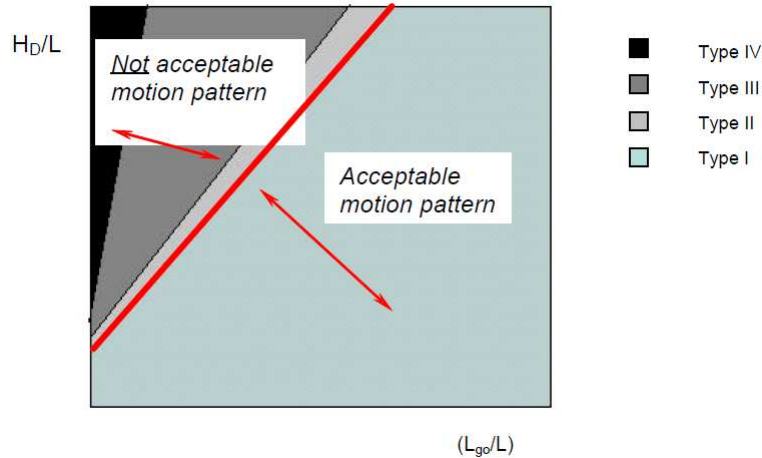


Fig. 3: Relationship between launching parameters drop height H_D , sliding distance L_{go} , length of lifeboat L and resulting motion patterns I, II, III, IV

Only specific motion patterns are acceptable by offshore standards, related to drop height, sliding distance and the length of the vessel, Fig. 3. The relative launching parameters are presented in detail in Fig. 4.

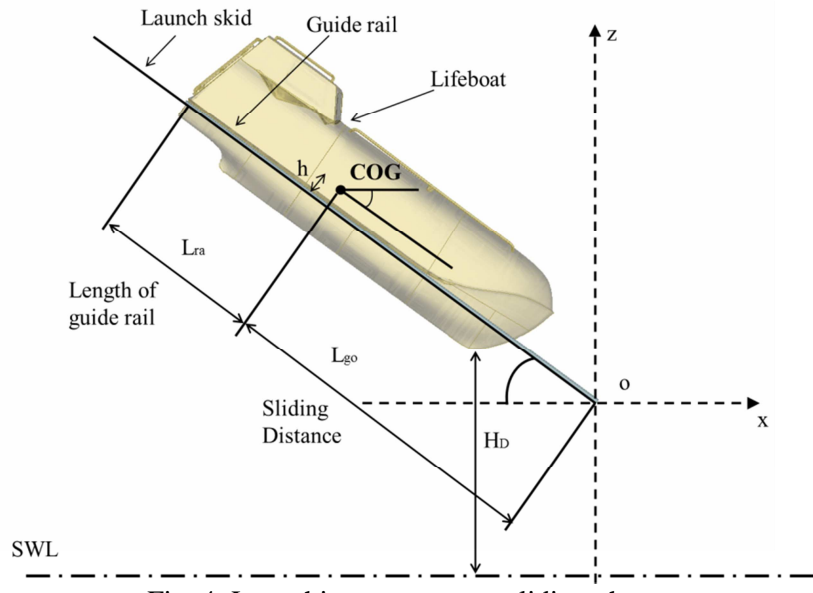


Fig. 4: Launching parameters, sliding phase

where:
 H_D : drop height
 L_{go} : sliding distance
 L : lifeboat length

The investigation focused on identifying the range of values for these parameters that result in a safe evacuation, concerning motion pattern and the CAR index values. The CAR index is calculated using Eq.(1) and according to the DNV, it should be below 1.

$$CAR = \max \sqrt{\left(\frac{a_x}{18g}\right)^2 + \left(\frac{a_y}{7g}\right)^2 + \left(\frac{a_z}{7g}\right)^2} \quad (1)$$

a_x , a_y and a_z are accelerations measured at the local coordinate system of the lifeboat seats, Fig. 5.

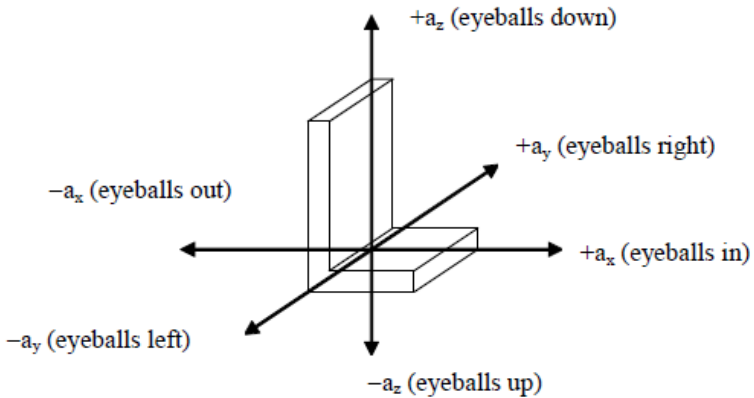


Fig. 5: Seat local coordinate system for measuring accelerations

Two values of CAR are used,

CAR_1 : for out-of-seat acceleration calculated from positive a_x , a_y , a_z values and

CAR_2 : for in-to-seat acceleration calculated from negative a_x , a_y , a_z values.

For CAR_2 the normal CAR equation is used. In this study, the calculation for the CAR_2 (Eq.(1)) was used as in-to-seat accelerations are the most significant for the passengers safety. CAR_1 have not been taken into account as they should generally be minimized and preferably eliminated with using specifically designed harness and seats. CAR_1 and CAR_2 values should be below 1. DNV (2010).

$$CAR_1 = \max \sqrt{\left(\frac{a_x}{9g}\right)^2 + \left(\frac{a_y}{7g}\right)^2 + \left(\frac{a_z}{7g}\right)^2} \quad (2)$$

3. Pre-processing

The Lifeboat model, Fig. 6, was a fully closed vessel with a length of 10.5m and width 3.4m. It weighs 9517kg and its maximum capacity is 30 persons. All pre-processing actions, including meshing, property and material definition, and preparation for solution with LS-DYNA, was performed with the ANSA pre-processor. The materials used for this model is GRP (Glass Reinforced Plastic) for the main body and steel for several features of the model including handrails, door, hinges and window outlines. The defined materials were rigid type (MAT20 MAT_RIGID).

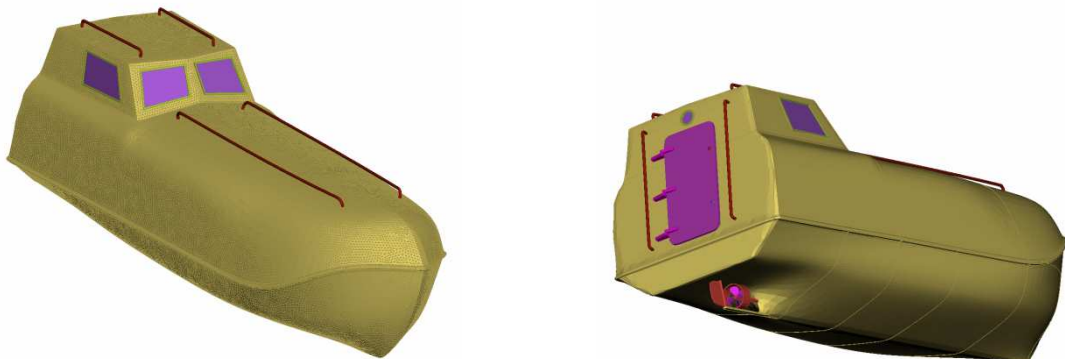


Fig. 6: Free fall lifeboat

The extra weight of the engine, ancillary equipment and passengers, as shown in Table 1, was distributed as ELEMENT_MASS LS-DYNA keywords on the nodes of the vessel using a special tool of ANSA for mass balance which ensures the mass distribution according to the desired COG for the entire model, Fig. 7.

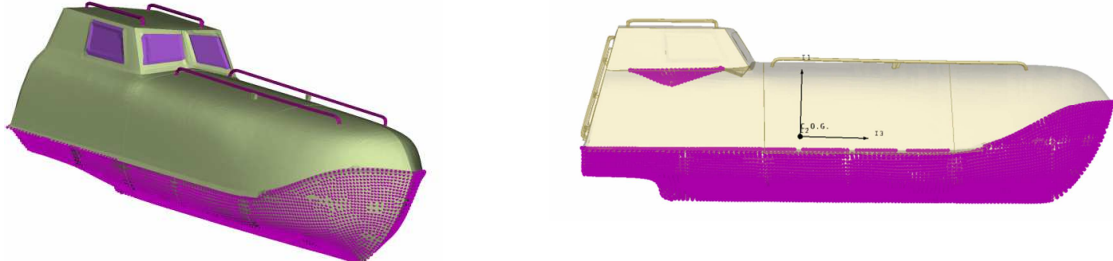


Fig. 7: Added weight

Table 1: Added weight

Passengers	3000 kg
Powertrain	500 kg
Ancillary equipment	250 kg

The ALE (Arbitrary Lagrangian Eulerian) method was used, in order to simulate the air and water domain surrounding the lifeboat. Two domains of solid HEXA elements were defined, simulating air and seawater. The HEXABOCK tool of ANSA was used in order to create the two domains and also to give the ability of re-meshing during the testing period, Fig. 8.

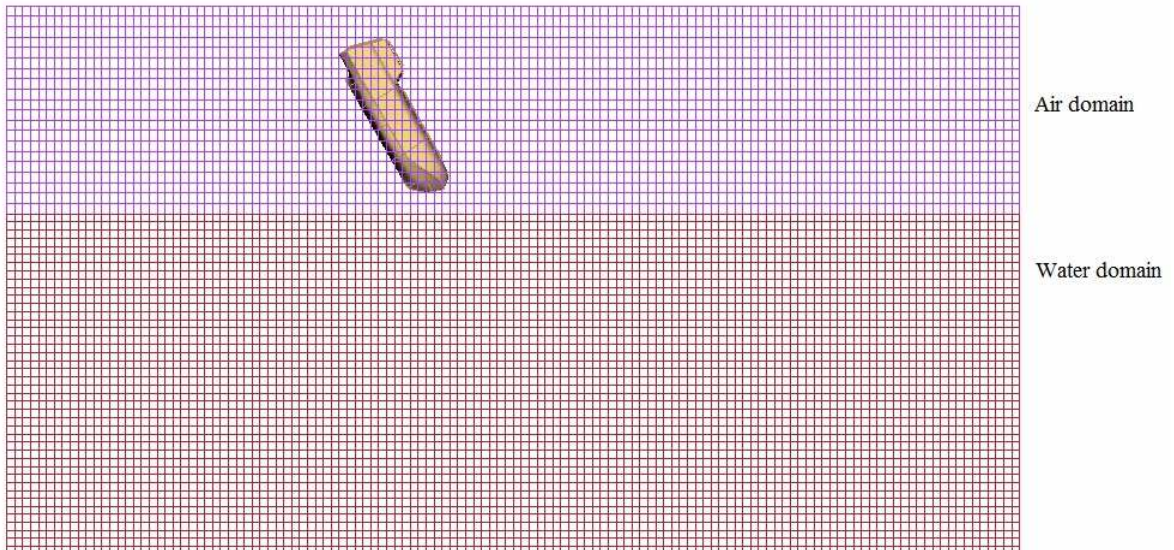


Fig.8: ALE element Air and Water domains

For both these entities SECTION_SOLID properties were created, with ELFORM option EQ:11, for one point ALE – Multimaterial element. EOS (Equation of state) cards were created for both air and water and two ALE multi material groups were created respectively (ALE_MULTI-MATERIAL_GROUP). The INITIAL_HYDROSTATIC_ALE keyword was also used in order to also take into account the Hydrostatic pressure. Also, the distinction between Langragian and Eulerian entities was done with the CONSTRAINED_LANGRAGE_IN_SOLID entity. Details regarding the model characteristics are shown in Tables 2 to 4.

Table 2: Seawater Equation of State (Gruneisen) settings

C	1520
S1	1.97
S2=S3	0
Gama	0.35

Table 3: Air Equation of State (Linear Polynomial) settings

C4	0.401
C5	0.401
E0	253312.5
V0	1

Table 4: Finite Element Model Details

Shell elements	40636
Mass elements	21724
HEXA elements	222208
Total weight	13tn

3.1 Kinematics

A built in Kinematics Tool of the ANSA pre-processor was used in order to simulate the free fall of the lifeboat. To simulate the slide of the vessel on its launch platform, kinematic contacts were defined for the lifeboat model side rails and the launch platform edges, Fig. 9 and the Kinematic solver calculated the trajectory of the lifeboat due to gravity.

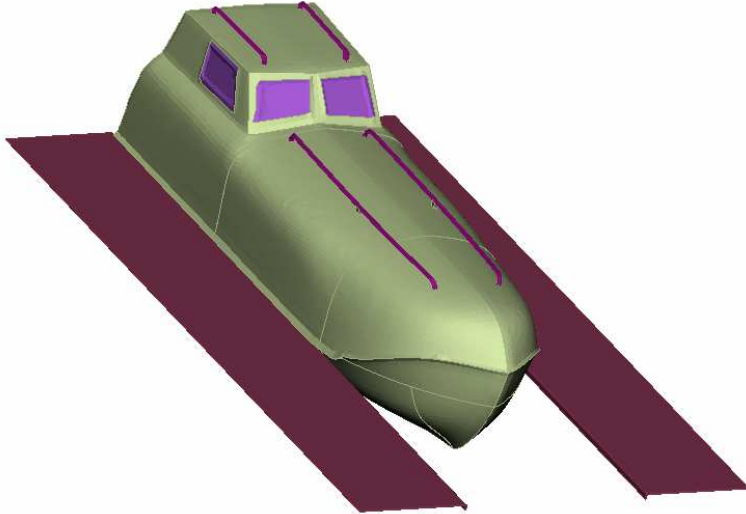


Fig. 9: Lifeboat on slide structure

Using the kinematic simulator tool, it was possible to simulate the sliding of the boat on the ramp, - taking friction also into account- and to calculate the free fall of the lifeboat from the tip of the ramp up until a defined distance above the sea level, Fig. 10.

At that point the model was stopped by a sensor entity that measures the distance from a specified point and stops the kinematic solver. The velocity components on that position were automatically calculated, converted and were applied on the model as initial conditions (INITIAL_VELOCITY _GENERATION), Fig. 11.

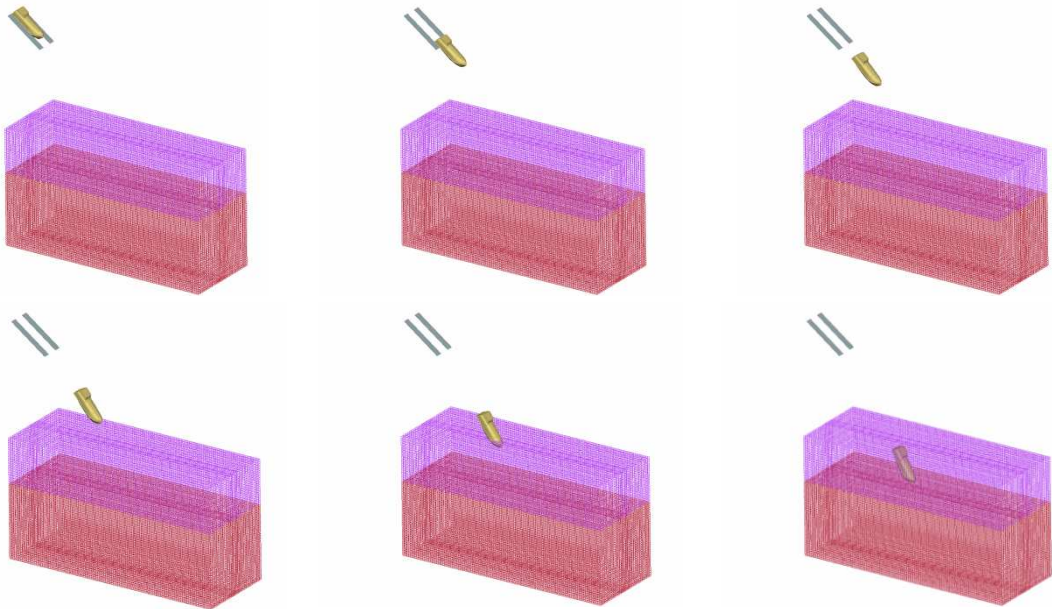


Fig. 10: Kinematic calculation of slide and free fall

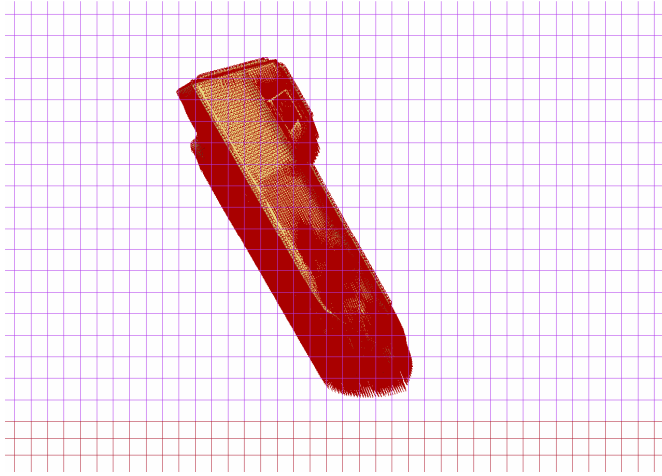


Fig. 11: Initial Velocity

3.2 Robustness Parameters

This study of robust design focused on the identification of the parameters that govern the motion pattern of the lifeboat as it enters, submerges and emerges from the water. The starting position of the life boat varies due to weather, loading conditions or a possible damage on the offshore platform (or transport vessel). To simulate the various positions and to make sure that the lifeboat will always evacuate the passengers safely, three dimension parameters were defined in order to change the physics of the free fall process.

The first parameter controlled the angle of the launch platform in relation to the sea level (trim angle). The second parameter controlled the height of the model (lifeboat and platform) in relation to the sea level and the third parameter controlled the list angle of the structure, Fig. 12.

Most of the service time of the offshore structures, the position of the lifeboat regarding height, trim and list angles is almost fixed or varies close to its nominal position. In this case the nominal values and the Standard deviation are listed in Table 5.

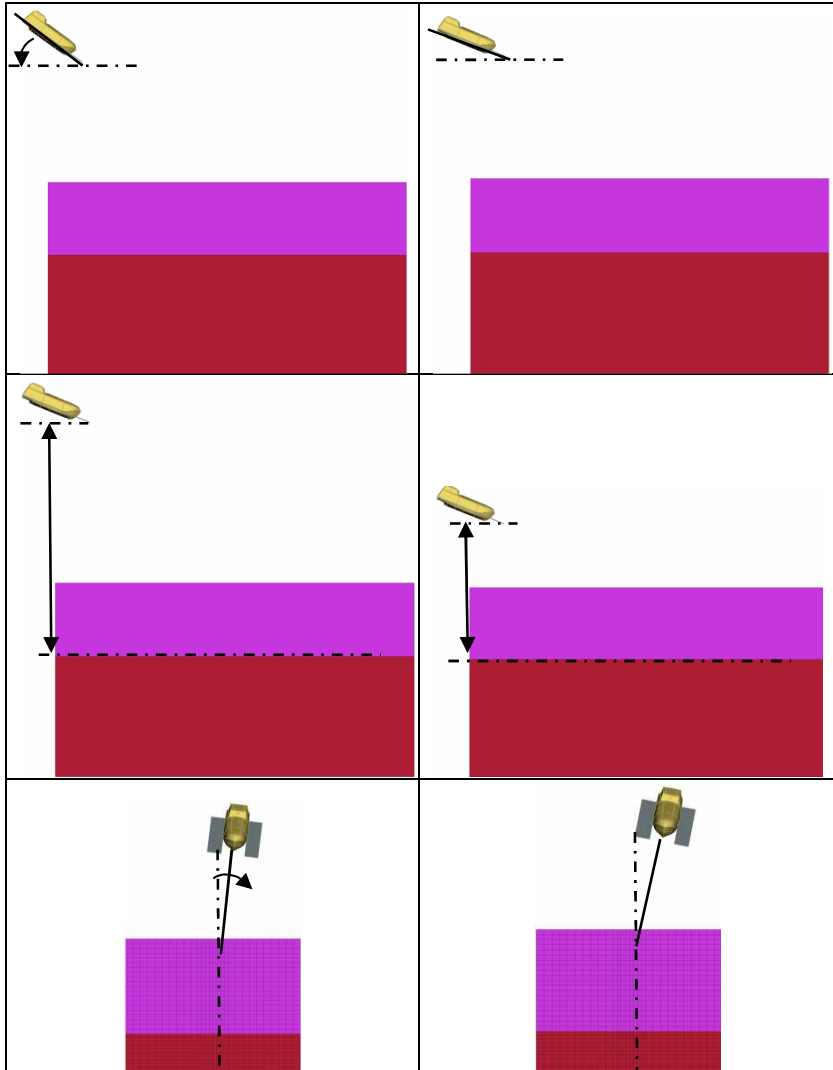


Fig. 12: Robustness parameters a) Trim angle, b) Drop height, c) List angle

Table 5: Mean values and σ of Robustness input parameters

Parameter	Mean value	σ
Height	36m	1.5
Trim angle	0° (35° launch platform to sea-level)	1.2
List angle	0°	1

These parameters however were not defined by deterministic values but as distribution of values since there is a statistical probability that affects which value appeared (distribution method: Normal). Following the Robust design optimization concept the target was to find an optimum solution for the lifeboat hull that is affected as less as possible from the stochastic parameters variation.

3.3 Shape optimization Parameters

Morphing parameters were also introduced that controlled the shape of the lifeboat. Using the special entities of ANSA pre-processor, the Morphing Boxes, one parameter changed the shape of the “nose” of the vessel. Changing the shape of the nose altered the entry behaviour of the lifeboat, Fig. 13. A second morphing parameter was introduced to control the shape of the rear part of the keel of the vessel, Fig. 14. Both morphing parameters were added to examine the relation between the shape of the boat and the accelerations produced during the entry. The shape of both areas, front and rear, significantly affect the negative accelerations produced during the entry of the lifeboat to the water.

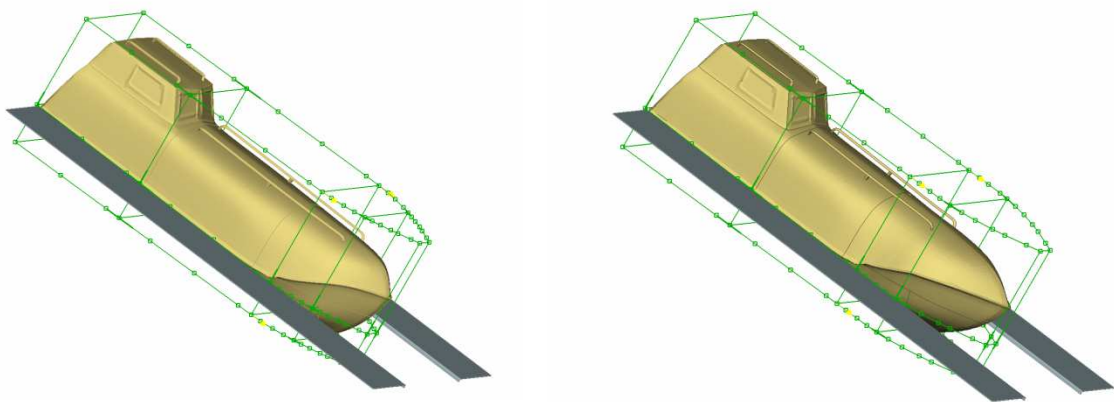


Fig. 13: Nose shape parameter

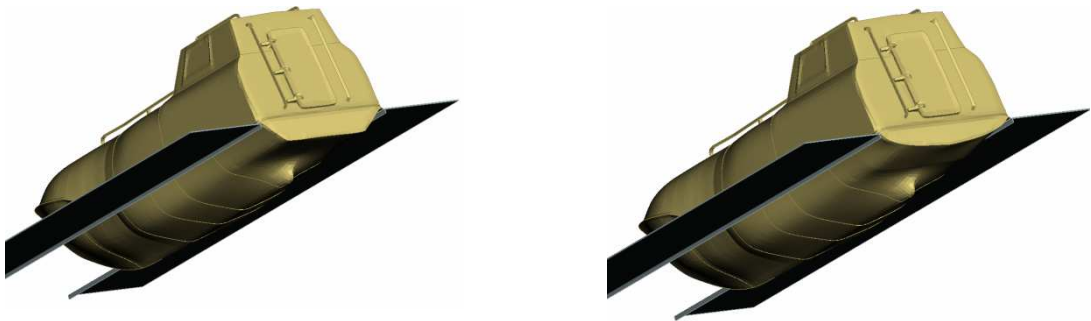


Fig. 14: Rear shape parameter

These shape parameters were set up in order to minimize these accelerations, making sure the maximum CAR (Combined Acceleration Ratio) index values are below the limits set by the DNV standards.

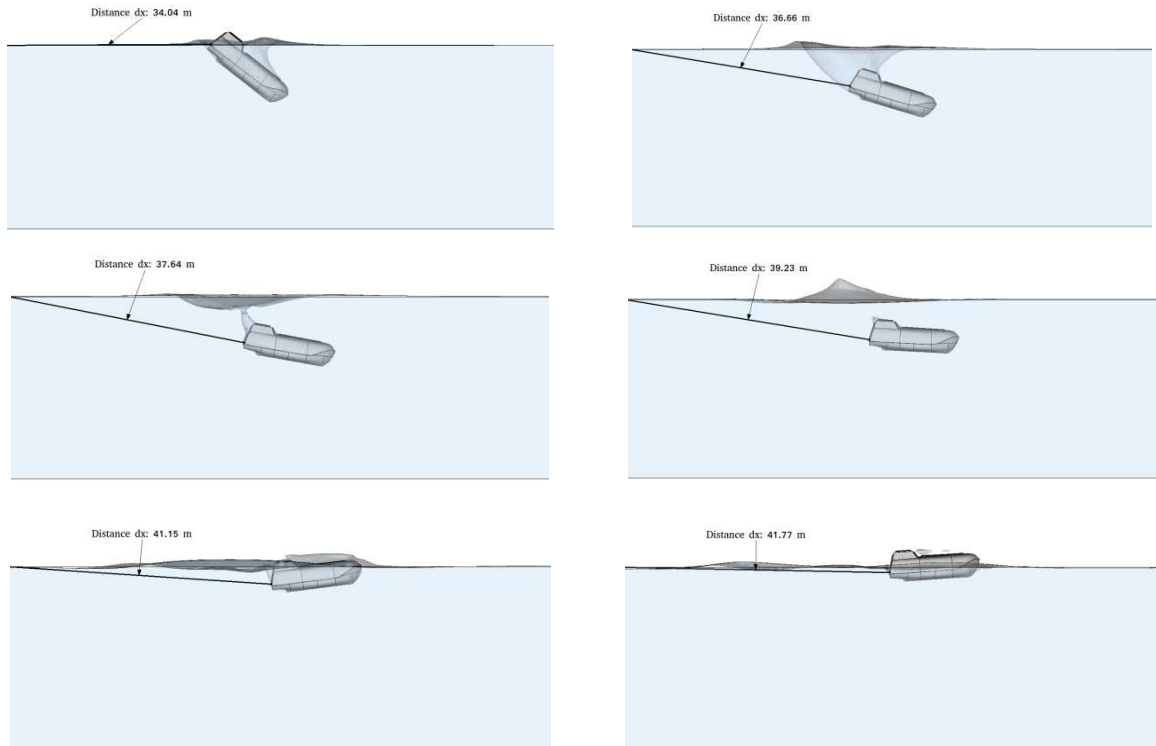


Fig. 15: Motion pattern and dx distance

4. Post processing

Using the Optimization tools of the μ ETA post-processor experiments that resulted in acceptable motion patterns were identified by means of time and distance from the starting position. For each experiment, the distance was measured at the time the COG of the lifeboat surfaced, in order to identify whether the motion pattern was acceptable. Nodal accelerations were also measured at strategically selected history nodes simulating the positions of the passenger seats.

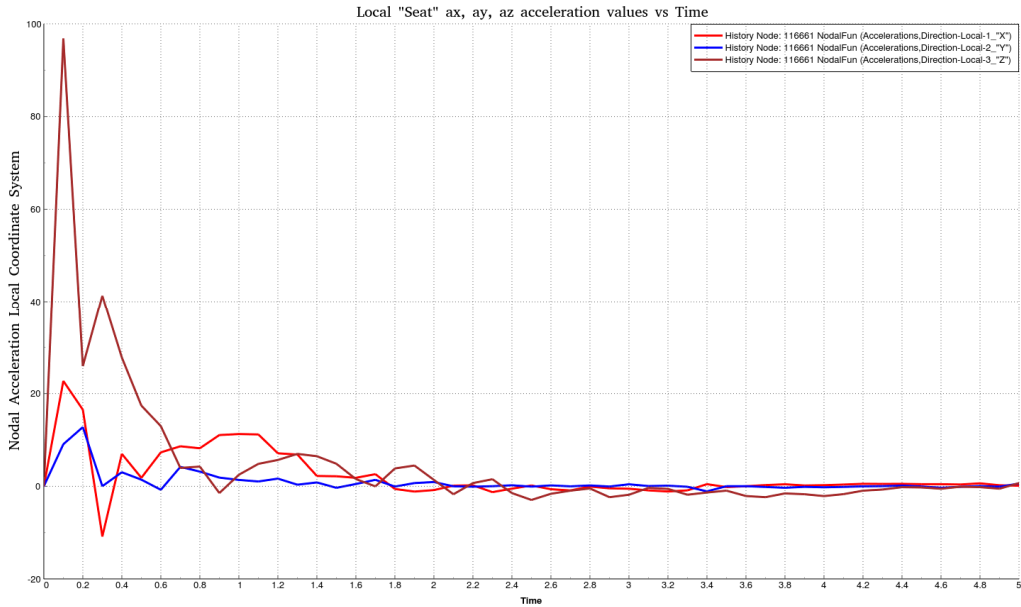


Fig. 16: Local XYZ accelerations vs Time

The results for the acceleration of each history node were calculated for the “moving” local coordinate system of the seats. The maximum values for each a_x , a_y and a_z curves were identified and were used in the calculation for the CAR index value using Equation 1. These values were captured as responses and used for constraint and objective entities in the setup of the optimization process.

5. Robust Optimization

The modeFRONTIER optimizer has been used in this problem which is able to couple with the ANSA pre-processor. The optimizer gives different values for the three stochastic parameters resulting in a new initial position of the lifeboat. The model’s shape is updated using morphing functionality by updating the discrete values for the two shape parameters.

In order to feedback and update the Kinematic solver of this movement, the kinematic entities were also included in the morphing actions. This way, the kinematic solver ran for every different set of Height/Trim/List configuration, resulting in different initial conditions per experiment. A workflow has been created in modeFRONTIER in order to manage the Robust Optimization process. Nodes for ANSA, mETA and a shell node for the LS-DYNA Solver were defined and five input parameters were automatically created in the workflow, Fig. 17.

The algorithm selected for this Robust Optimization case was the SIMPLEX. This algorithm provides fast conversion, is able to take into account discrete variables and constraints and does not require a large number of DoE initial experiments. The fact that we had a single objective also supported the selection of the SIMPLEX algorithm that led to a smaller number of total designs.

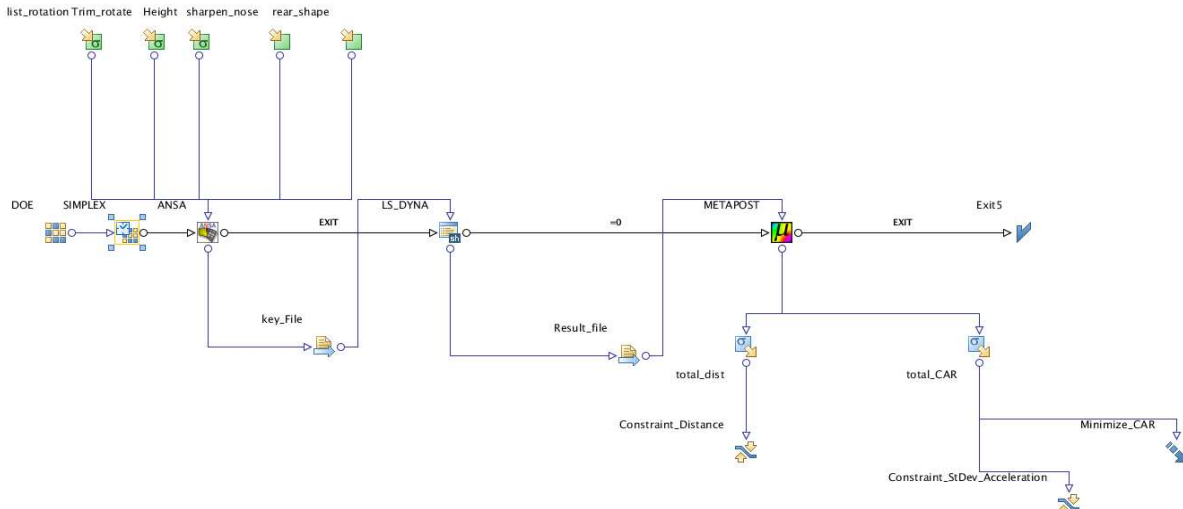


Fig. 17: Optimization Workflow in modeFRONTIER

Distribution and Standard deviation (Multi Objective Robust Design Optimization) properties were assigned to the three input variables that concerned the initial position of the lifeboat. Also the Normal distribution method was selected in order to model the uncertainties of these three input parameters (Trim_rotation, List_Rotation, Height), Fig. 17. Minimum and Maximum possible values were automatically input from ANSA while a value for the Standard deviation was manually added for these three variables.

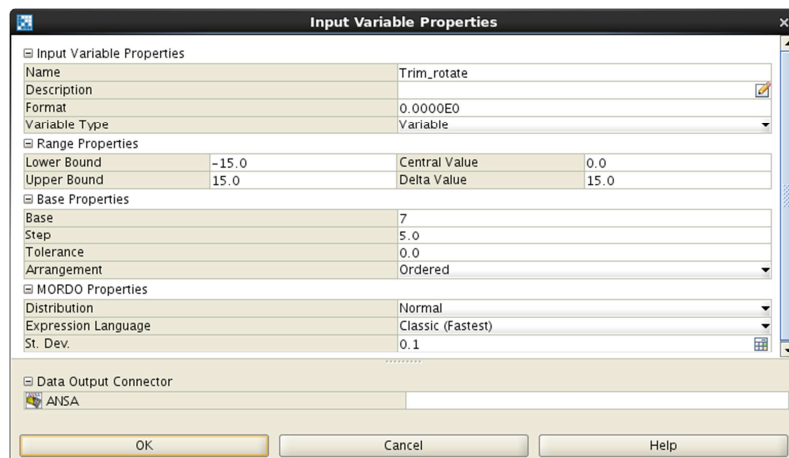


Fig. 18: Robust design input variable settings

Responses from the postprocessor, regarding motion pattern/distance and the CAR (Combined Acceleration Ration) values for the occupants were defined and assigned as Constraint and Objective respectively.

As per DNV standards, at the time the COG of the lifeboat surfaces after the entry face, measuring the distance covered, provides us with an indication whether the motion pattern was acceptable and the minimum distance between lifeboat and host structure is larger than 40 meters. The 99.97% of the distribution of the Distance dx from the source structure was constrained to a minimum value.

The 99.97% of the CAR index distribution was also defined as a constraint to be less than 1 and the Objective was the minimization of the 99.97% of the CAR distribution, thus minimizing the accelerations on the human body.

Table 6: Robust Optimization Constraints and Objective

Constraints	
99.97% Distance from source	Greater than 40 m
99.97% CAR	Less than 1
Objective	
Minimizew CAR	

6. Results

The results focused on the accelerations developed during the entry of the lifeboat in the water. The acceleration values were calculated in the form of CAR (Combined Acceleration Ratio) index. The target was to prove the robustness of the design of the freefall configuration while minimizing the CAR index, thus minimizing the accelerations the passengers feel during the entry face. The preliminary results have shown some grouping of the designs in a scatter chart of CAR vs Total Distance from the host structure, Fig. 19. This is consistent with a robust design for the suggested optimization case and the dispersion is within acceptable range.

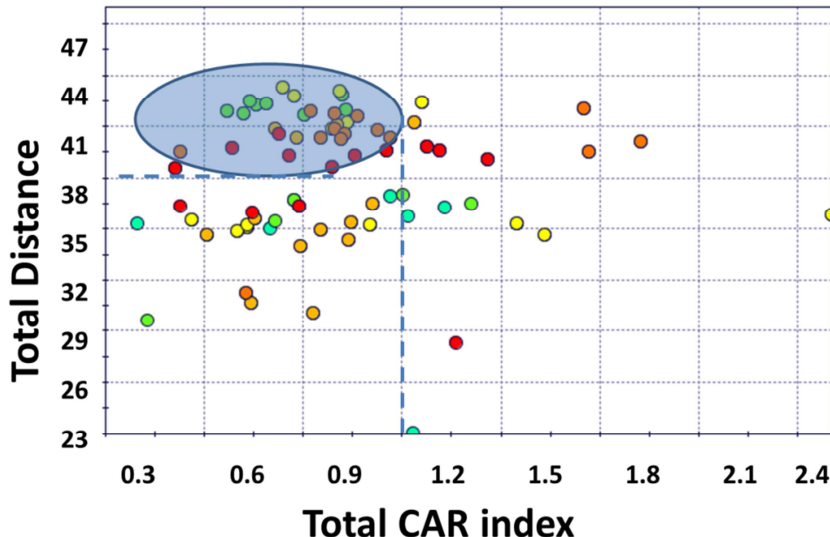


Fig. 19: CAR index vs Total Distance Scatter chart

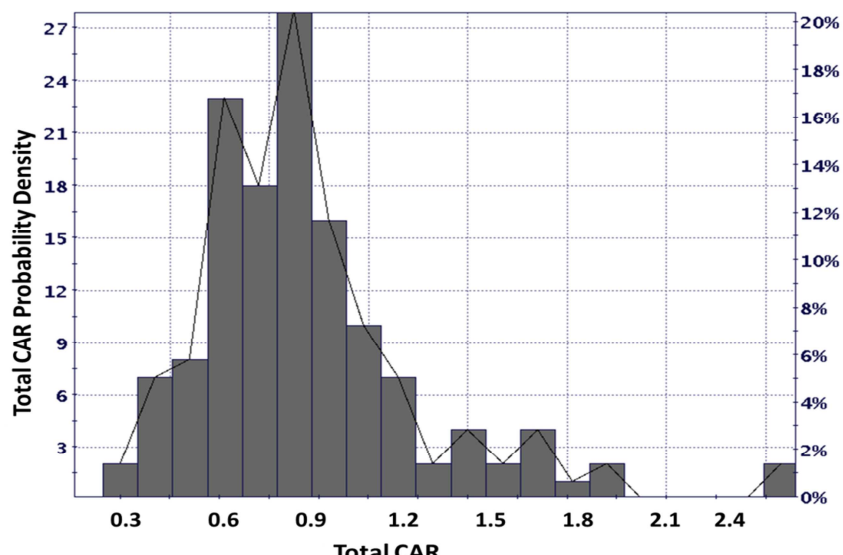


Fig. 20: Probability Density Function

The standard deviation regarding CAR index is within an acceptable range while the 99.97% of CAR index values was less than 1 that was one of the constraints of the optimization problem, Fig. 20. Also the results show that there was a small gradual minimization of the 99.97% of the CAR index values, which suggests that the robust analysis coupled with the shape optimization of nose and rear shape of the life boat managed to decrease the acceleration values that the passengers undergo when the lifeboat enters the seawater.

7. Future work

Due to the complexity and the great amount of parameters that affect the launch of the lifeboat, more work is required in order to have a complete overview of the process. The major external parameters that greatly affect all stages of the process, the wind and waves are going to be investigated and added to the robustness analysis. Stochastic design variables will be created controlling the various wind speed and wave height that are possible in the lifetime of an offshore structure. Furthermore utilizing the occupant safety tools included in ANSA, (dummy and seat positioning, seat belt tool) we will get much more accurate and detailed results regarding the accelerations on the human body and possible impact injuries of the occupant.

References

- DNV (2010), *Design of Free Fall Lifeboats*, 1st Offshore Standard DNV-OSO-E406
- MØRCH, H.J.; ENGER, S.; PERIC, M.; SCHRECK, E. (2008), *Simulation of lifeboat launching under storm conditions*, 6th Int. Conf. CFD in Oil & Gas, Metallurgical and Process Industries SINTEF/NTNU, Trondheim
- WANG, J.; CHEN, H. (2007) *Fluid structure interaction for immersed bodies*, 6th European LS-DYNA User's Conf., pp.4.3-4.8
- TOKURA, S. (2015), *Validation of Fluid Analysis Capabilities in LS-DYNA Based on Experimental Result*, 10th European LS-DYNA Conf., Würzburg
- LS-DYNA (2006), *Keyword User's Manual Version 971*, Livermore Software Technology Corp., Livermore
- modeFRONTIER (2014), *User Manual modeFRONTIERTM 2014*, Esteco SpA 2014

Maritime Asset Visualisation

David Thomson, AVEVA, Hamburg/Germany, david.thomson@aveva.com
Andrew Gordon, AVEVA, Hamburg/Germany, andrew.gordon@aveva.com

Abstract

In order to efficiently manage the operations, maintenance and safety of large and complex assets in remote locations, the operators of these assets need efficient access to reliable information. This information is often buried within reams of documents, drawings, databases, photos and CAD data. Organising this data and documents in such a way that the user can intuitively locate, discover and view the relevant information is now a significant challenge for Owner-Operators in the plant, offshore and marine industries. This paper looks at current best practice, using AVEVA's Asset Visualisation tools to provide a view of the entire Digital Asset from 'as-designed' to 'as-operated' by enabling the capture, validation and in-context viewing of information throughout the life cycle of the asset.

1. Introduction

Maritime assets created and operated by our customers include platforms for offshore oil and gas drilling and processing, power generation, and accommodation. They also include ships and floating vessels of all types including above and underwater military vessels, passenger vessels, cargo ships, and special-purpose vessels. In all of these cases, there is an increasing need to master more complicated engineering, construction and asset management challenges than ever before.

As oil and gas resources become harder to locate and exploit, the designers and operators of offshore platforms must take into account that harsher conditions in even more remote operations will involve even greater technical challenges and may restrict movement of personnel and equipment. Increasing concern over accidents and environmental hazards mean that regulatory and corporate controls are continually tightened. At the same time technological advances and the higher price of oil and gas have created conditions in which it is profitable for existing offshore assets to continue producing for longer than initially anticipated (UK Health and Safety Executive).

Many types of ships are larger than ever before while the size of the operating crew stays the same. Often the ship has become just a floating platform for complex processing systems for oil production, seawater desalination or power generation. Automation systems have taken over responsibility for many key systems on board by continually monitoring performance and operating conditions.

So when a fault occurs or major maintenance is required it is essential that the necessary information can be easily retrieved and relied upon. The information required to safely and efficiently operate a platform or a vessel may have grown exponentially but unfortunately existing methods to store, maintain and retrieve it has not kept pace with this growth.

In general, the information that will be required for safe and efficient operation of a vessel or platform will include both construction information and operating information. Construction information relates to the original design of the structure and systems; representing the as-built condition, as well as any subsequent changes resulting from repairs and refits. Operating information will include the maintenance history and the historical and actual values of operating parameters. Both onshore and offshore users should be able to locate and identify any of this information quickly and intuitively.

2. Limitations of digital information

Documented information can be easily stored digitally in the Adobe PDF standard, making it easier to transfer across different hardware and operating systems, but at the same time preserving the look and feel of the original document. However, information contained in these PDFs cannot easily be

searched, cross-referenced or linked to other relevant information. This is a serious limitation, as a single pdf can contain a great many individual items of information (consider a parts list, for example.)

Moreover, there are many other sources of context-rich information which could also be of use by owner-operators.

- Photographs showing as-built or as-is status, or used to highlight problems or document progress.
- Laser scan point clouds capturing as-is status with an extremely high degree of accuracy.
- BubbleViews™ combining laser point clouds and photographic information to provide realistic images for review.
- Engineering databases and spreadsheets containing information regarding systems, components etc.
- 3D geometry models describing the layout of the asset, to be used for familiarisation and training.

One of the main problems is how to integrate and link the information from this disparity of sources. Each requires the appropriate viewing tool and some means of association to other data sources with relevant information. Furthermore there must be some qualification of the validity of the information.

At AVEVA we have defined a concept known as the Digital Asset. The digital asset needs to contain the information needed to design, build, operate and maintain the physical asset across its lifecycle. The marine equivalent, the Digital Ship, is now beginning to exist but it is not yet a sufficiently mature asset to be easily used and reliable or comprehensive enough to support efficient operations.

3. Asset Visualisation

The term ‘visualisation’ is typically associated with a realistic representation of physical objects through the use of photographs, drawings or 3D models. However, in the age of ‘big data’ and complex engineering assets, visualisation of abstract data has become an important business capability.

Visualisation can turn data into information and help to provide a better understanding of it. Understanding enables prompt and effective decisions and actions, and enhances collaboration and the reuse of information. Visualisation of data is achieved in many ways, ranging from a simple form or datasheet to view a set of attributes related to an engineering object, through to interactive 3D models and dashboards combining diagrams, drawings and charts.

In order to visualise a complete set of data associated with an engineering asset, it must be possible to capture all data and documents regardless of their source formats or authoring systems. The data must then be classified and organised according to the business processes that will consume it; for example, a product, work or information breakdown structure.

The AVEVA NET Gateways provide the interfaces to these information sources. Their job is to extract the project information from within the published data and documents, to validate that information against defined project data standards and to create web-viewable renditions of the documents and drawings.

There are over 30 standard Gateways available covering all the major 2D and 3D engineering design systems – including PDMS, MicroStation, SmartPlant, PDS and AutoCAD – as well as document management systems and general document and data file formats. There are also a number of service Gateways that can be used to integrate information from bespoke or in-house systems.

The information extracted by the Gateways is stored within the AVEVA NET Workhub which serves as a managed repository for the validated project data. The Workhub does more than just store the information however; it also automatically builds and maintains relationships between the engineering objects, their data and the documents that reference them. This makes it easy to report on data consistency across the various information sources.

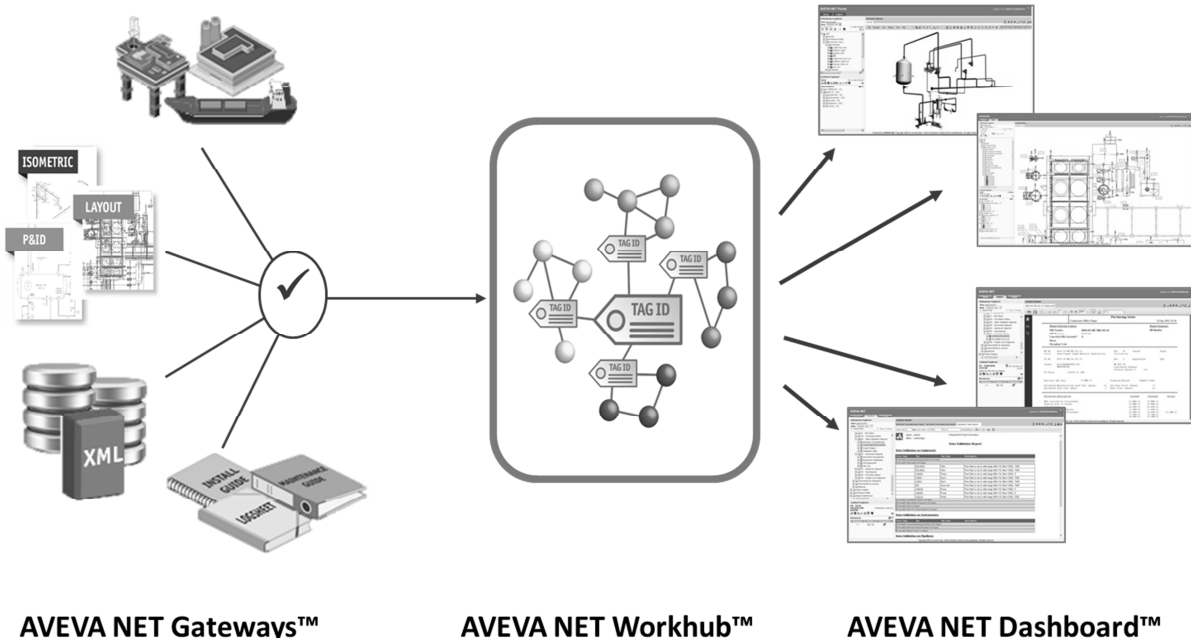


Fig. 1: Information flow within AVEVA software eco-system

The discrete data objects so captured must then be automatically associated with any other existing data, according to their logical relationships. For example, a pump referenced in a diagram is associated with the same pump in the 3D model, photographs of the pump in position, as well as the pump in the datasets captured from the purchasing, maintenance, document management systems, etc.

The information so created is then made available to users in a neutral format, independent of the original source application and therefore without requiring any special viewers. Through the use of logical relationships, the information is contextualised so that it can be more easily understood and effectively used.

In the context of an operating asset or vessel we call this Asset Visualisation. AVEVA'S Asset Visualisation solution turns data from multiple information sources and systems into ‘actionable information’ improving operational safety, asset information integrity and reducing risk. A true information portal for operations; Asset Visualisation provides a rapid, contextualised and easy to use view of the entire digital asset, providing access to the right information, in the right place, at the right time.

Over the last few years, we have successfully implemented this solution for a variety of customers across the world. Whilst these solutions all use the same set of products, each one has been quite unique and tailored to meet the customer’s specific requirements across various data sources like documents, drawings, 3D models, registers, laser scans and operations databases.

Our current strategy is to provide Asset Visualisation in a web browser interface, making it easily accessible to non-specialists via a variety of web-enabled devices. However, as new and enhanced devices continually emerge, we envisage an evolution in the way information is made accessible in real-world scenarios. For example, it may become desirable to exploit Immersive Reality technologies to put contextualised information access literally on the spot in an engine room or machinery space.

4. Deploying Asset Visualisation

Typically, new marine technology gains general adoption progressively, being deployed only on new vessels while older vessels reach their end of life and are removed from the global fleet. Asset Visualisation is likely to follow the same path, as the economic benefits for existing vessels with limited remaining service lives may not be sufficiently compelling for retrospective deployment. However, there are always exceptions; for example, naval vessels are particularly complex and frequently life-extended with major refits and upgraded equipment. In such circumstances, Asset Visualisation can be deployed – and deliver benefits – in a progressive manner similar to that used on large onshore or offshore assets.

For newbuildings, best practice is to compile the Digital Ship from the earliest stages of design, with more and more data being captured as the project advances. In onshore and offshore capital engineering industries this practice has reached a high level of sophistication, with Digital Asset data being transferred progressively from contractor to client so that the new physical asset's operations systems are fully populated before commissioning and start-up. The savings can be considerable and the new asset begins its operating life already supported by its Digital Asset counterpart.

Establishing Digital Assets for existing assets requires a different approach that can be applied equally successfully in the maritime industry. It follows a logical sequence of steps, as described below:

4.1. Step 1 Capture existing information

- Whether paper or digital, available drawings and engineering documents will provide an overview of all critical systems and safety features, so the first logical step is to digitise all drawings and documents.
- These should then be linked to each other according to system logic. For example, the fire extinguishing schematic diagram should be connected to other safety-related material, or the main engine oil system diagram connected to the oil heating system diagram and the vendor documents for the pumping equipment. Often this ‘linking’ is initially achieved by good document naming.

Drawings thus become the entry point into most of the ship’s information. For example, the operator can open the General Arrangement plan, zoom into the engine room area, click on this zone and see a list of all of related drawings and documents, open the lube oil flow diagram and click on a pump to find its technical documents.

This in itself would greatly facilitate the finding of information on board many vessels, providing an intuitive way to navigate information via the familiar medium of drawings. However, limitations would remain; technical data would remain locked up in documents and thus not be searchable.

4.2. Step 2 Index data and classify objects

The next step is to collect and validate data about key systems and equipment on the vessel. Normally, this information is held either in the Computerised Maintenance Management System (CMMS) or an Asset Management system. Associating this with objects that are classified according to an enterprise information standard will provide an additional layer of richness, enabling technical searches and reporting across relationships between data, objects and documents. Once classified correctly, objects themselves can be an effective way to navigate the Digital Ship, enabling the user to browse through tree-like data structures to items of interest.

4.3. Step 3 Enhance information with 3D models and other rich media

If 3D model data is available, for example after a refit, it makes sense to bring this into the mix. The shipyard or design agents will have created a 3D model with sufficient detail to enable the identifica-

tion of all major items. If contractually required, this model can be stripped of any proprietary intellectual property (for example, the precise hull surface form, or internal details of equipment) before being handed over to the vessel's operator or owner.

- Since the 3D model effectively describes the location and spatial arrangement of items on the vessel it can quickly become the basis for additional processes in vessel operation. For example, it can be used for training and simulation, or for the condition monitoring of key items.
- A sufficiently complete and detailed 3D model provides the most intuitive way to navigate the vessel's information, as we can most directly relate to a model that reflects our everyday surroundings.
- The model can also be an effective tool for personnel who provide technical support from an onshore location.

4.4. Step 4 Enhance information with laser point cloud and immersive imaging

In many cases a 3D design model will not be available or, even if it is, its resemblance to the in-service vessel can neither be guaranteed nor verified. As a result, there is an increasing use of 3D data capture devices, particularly in preparation for major refits and conversions.

Different data capture methods may be used, depending on the required accuracy and use case, but 3D laser scanning is generally the preferred choice.

- Static scanners are the most accurate but cannot reach all areas. Complete surveys can be built up by 'stitching together' overlapping scans from different viewpoints onto a common coordinate system. Inaccessible views may be filled in by the use of hand-held or drone-carried scanners; these are generally of lower accuracy but their data can be registered into static scans.
- The recent availability of spherical or 360-degree video provides a very quick way to capture the as-operated vessel. It suffers from similar limitations to fixed laser scans and does not generate 3D point cloud data that could be integrated with laser data. However, it could in theory be hotspotted and linked to documents and data.

Laser scans create point clouds which traditionally have needed specialised tools to view the data. However, current state of the art now enables overlapping photo-realistic scans (BubbleViews™) to be navigable in the same way as a native 3D CAD model is. The result (HyperBubble™) is a highly realistic virtual ship that can be made intelligent by linking individual objects to underlying Digital Ship information. It is an ideal tool for the non-specialist user seeking information quickly.

5. Conclusions

Asset visualisation can mean much more than simply representing an asset in a realistic way. By capturing data from multiple sources and linking this information, a detailed and navigable representation of the model can be created, allowing users to easily identify objects or systems of interest and access the information required.

Efficient Use of Virtual and Mixed Reality in Conceptual Design of Maritime Work Places

Kjetil Nordby, Oslo School of Architecture and Design, Oslo/Norway, kjetil.nordby.aho.no

Stian Børresen, state.space, Bergen/Norway, stian@statespace.no

Etienne Gernez, Oslo School of Architecture and Design, Oslo/Norway, etienne@opensailing.net

Abstract

We present a system that enables real time scanning of human avatars for use in virtual reality supported design processes. The system uses off-the-shelf 3D sensors to generate high-density 3D meshes and high resolution textures of human beings in real-time. Designers can insert real time avatars in virtual scenes using a game engine. Informal preliminary tests of the system, in context of ship bridge design, suggest that the system is capable of enabling effective human-to-human communication in virtual reality supported participatory design.

1. Supporting participatory design processes

Immersive virtual reality (VR) technologies enabled by head mounted displays (HMD) are gradually becoming a viable tool in maritime design. Human-to-human communication is an important part of such processes. Rich and natural communication among participants have been difficult to achieve with current technologies since HMD-based systems mainly offer single user experiences. To meet such a challenge we present a system enabling human-to-human communication in VR, Fig. 1.



Fig. 1: Screen capture from the HMD supported VR system showing a designer presenting a ship bridge concept to a user (user in 1st person view)

When designing for maritime workplaces, such as ship bridges, there is a need to understand new design proposals according to maritime operational contexts. To make sure the designed systems are adapted to people's needs, companies employ participatory design processes where users and professional designers collaborate in forming the new workplace, *Sanders and Stappers (2008)*. Such processes take advantage of mariners' knowledge to improve usability and increase innovation in maritime design.

To engage mariners in the design process, it is necessary to use tools to mediate the future context. For instance in ship bridge design, designers may use a wide variety of digital and analogue tools to visualise the design proposal and to enable a discussion of design options, *Bligård et al. (2014)*. *Österman et al. (2016)* compared the use of scale models, 1-1 models, 2D drawings and CAD drawings for use in collaborate ship bridge design. Their work show that, although user preferred 1-1 models, each medium has strengths that designers may use at different stages in a design process. Their work underlines the importance of the moderator role in facilitating discussions among users and designers in participatory design, for example using visualisation tools.

Real-time 3D renderings are now at a point where we can achieve comprehensive real time visualizations of future products to support participatory design. This is well known in the maritime industry where the use if ship simulators is common, *Kristiansen and Nordby (2013)*, and VR has been researched for many years, e.g. *Zini et al. (2000)*, *Venter and Juricic (2014)*. Also, research from other fields show that virtual worlds can effectively support collaborative conceptual design in architectural design, interior design and user interface design, *Koutsabasis et al. (2012)*. *Hjelseth et al. (2015)* explored the use of game engines for collaborate maritime design. He used 3D models as tools helping contextualise the design discussions between the designer and the expert user. His work emphasises how technologies can support communication in user collaborative design processes.

Immersive VR are not as widely used in maritime design as in other comparable fields such as automotive or aviation. However, the barriers for adopting new technologies in maritime design are lowering, and it is likely that immersive virtual reality can become a viable tool also in design processes for the maritime industry, *Morais et al. (2011)*.

2. Communication in immersive virtual reality

VR concern a series of technologies that together allow people to immerse themselves in a virtual, computer-generated world. Recent commercial systems such as HTC Vive, htcvive.com/us, and Oculus Rift, www.oculus.com/en-us/rift/, include spatial tracking that transfer user's motion in real space to the virtual space. Users can interact in the virtual world using a wide variety of tools such as optical tracking of body or specialised physical equipment. Recent VR technologies are now at an affordable level and offer a quality of immersion that may lead people to achieve presence; the feeling of being physically situated in a virtual space as opposed to the physical world, *Slater and Wilbur (1997)*. Such presence is important in allowing users to focus on the design proposals at hand in the virtual environment and not the technologies communicating the virtual environment. Maintaining such presence is a problem when communicating with users in a single user immersive VR scenario. Since the user is alone in the VR environment, the feeling of presence may dissolve when the user becomes aware of voices emerging from outside the virtual environment. We have regularly experienced this break in our VR lab.

We can meet the communication problem by introducing human representations (avatars) in the virtual space to support communication. Realistic avatars (visual and behavioural realism) improve social co-presence in a virtual world, *Kang and Watt (2013)*. Such avatars are usually built manually in CAD software or created with 3D scanners. The avatars are then rigged with a skeleton system, making it possible to animate them.

Even though predefined avatars can convey human presence in VR, they are seldom able to transfer believable body and facial motion. This is a problem since with high model fidelity, users also expect high behavioural fidelity. Avatars that are close, but fail to, achieve users' expectations of visual and behavioural realism may lead to low acceptance of the avatar. This phenomenon is often referred to as the uncanny valley, *Mori and Kageki (2012)*. The VR industry is very aware of this problem and recently chief scientist at Oculus, Michael Abrash, wrote: "Perhaps the most important problem yet to be solved is figuring out how to represent real people convincingly in VR, in all their uniqueness." <https://www.oculus.com/en-us/blog/welcome-to-the-virtual-age/>.

Scanning of human bodies using low cost 3D scanners such as the Kinect, *Zhang (2012)*, can be used to create realistic avatar models, *Tong et al. (2012)*. Although such models have high visual fidelity, they lack in behavioural fidelity. New developments in real time scanning meet this challenge by capturing the 3D mesh and the surface texture, combining them and transferring them to a virtual environment in real-time. This technique results in a mixed reality setup where high visual fidelity is traded for high behavioural fidelity. There are some examples of such technologies in research, *Suma et al. (2011)*, <http://doc-ok.org/?p=965>, however we know of no tools offering this functionality to designers. We suggest it is useful to investigate such tools to be able to develop knowledge of how we may efficiently adapt virtual reality technologies to participatory design processes.

3. Prototype system

Our proposed system is developed by the Oslo School of Architecture and Design and state.space Ltd. The system comprises a room-scale VR setup, Fig. 2, realised through the HTC Vive developer edition VR system, which allows free movement in a 5x5m physical space. The HTC Vive system captures the user's motion in real time and transfers it to the Unity 5 game engine, which renders the environment on the HMD, thus generating an illusion of 1:1 motion in a virtual world.



Fig. 2: HTC Vive developer version. Top right: one of two sensors enabling full room tracking

Our system takes advantage of low cost 3D scanning equipment (Kinect 2.0) to detect people standing in front of the sensor and translate the depth and image data into a high poly, fully textured, 3D avatar rendered and animated in real time in Unity 5. Transforming the raw data delivered by the Kinect sensor to a 3D mesh in Unity is done in several steps repeated 30 times per second. As the capture rate of the sensor is limited to this frequency, it is vital to decouple the scanning process and rendering loop of the game engine, which has to run at 90 Hz to provide a comfortable VR experience. First, the RGB pixels from the color camera are converted to a texture map and applied to the material used by the game objects in unity. The depth values are then separated into pixels belonging to any scanned human, and those that are part of the background. The depth values are mapped into x, y, and z coordinates in the coordinate system used by Unity, and after triangulation, the meshes are rendered to the scene. The system is able to scan up to six people simultaneously, and separates the people from the background by utilizing the human detection capabilities that are part of the Kinect SDK.

Our system has two representations in Unity 5. The first is the representation of the Kinect scanner in the virtual scene, Fig. 3a. The second appears as an avatar in the scene, when someone enters the physical scanning areas and is detected as human (by the Kinect software). The human entering the

real scene appears in the virtual scene relative to the virtual 3D scanner object, Fig. 3b. After the users have spawned in the 3D world, they can be treated as independent objects, Fig. 3b, making it possible to transform and move them freely and independently from each other. This allows populating a virtual scene with up to six independently positioned real-time avatars. The scanned person facilitating the design session has access to a screen where he or she can see what the VR users are looking at through the HMD, Fig. 4. This gives scanned users the ability to control how they appear and allows them to control their motion in virtual space. The scan area spans a 5 m radius, making it possible for the avatar to walk around in a large fan shaped area inside the virtual model, Fig. 5c.



Fig. 4: We have placed the Kinect scanning the facilitator right over a screen that shows the viewport as seen from the point of view of the VR user.

4. Using the system in design

We have been using the system continuously since December 2015 as part of a master student project oriented towards design of a ship bridge console for a Wind Farm Support Vessel. During the project, the two master students have produced several iterations of the ship bridge consoles and used virtual reality to involve users and other designers in the design process. The VR model allows users to explore the design proposals in relation to a maritime operation staged in Unity 5.

4.1 Setup

When setting up the scene it is important to carefully plan where to place the VR user and the facilitator in the VR scene to support the design session. Due to the limitation in the scanning system and the areas available for free motion, we found it best to place the nearest spot the avatar appear slightly inside the area where the VR user can move freely, Fig. 5a. This limits the effect of lack of geometry on the side and behind the avatar, Fig. 6. In doing so the real-time avatar can only enter a small part of the user's motion space. However, it can move in a very large area outside user space, Fig. 5c. VR user and facilitator avatars can meet up close at the borders of each other's motion space, Fig. 5f. In setting up the system in such way, the facilitator could walk up to the ship bridge console, reach over it and even point to specific buttons, Fig. 1. Note how the avatar stands accurately behind the console

while the hand pointing on the console is in front of the console. This is possible since the avatar is fully realised in 3D space. The avatar can also direct user's attention to outside features for the scenario accurately by pointing in 3D space, Fig. 7.

A key feature of the system is the ability to simulate eye contact between the VR user and the real-time avatar. To facilitate such eye contact we placed the screen supporting the facilitator just below the Kinect sensor, Fig. 4. Although ideal eye contact is achieved by looking right into the sensor, we achieve a very convincing eye contact effect by looking at the screen right below the sensor. The effect of eye contact is best when the VR user are close to the virtual representation of the Kinect scanner, Fig. 5b, since at this point the scan area is fully aligned with the virtual scan area.

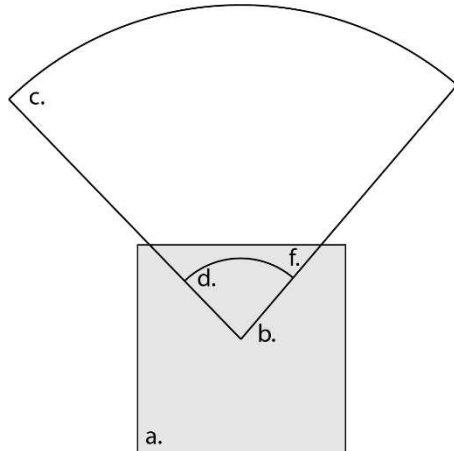


Fig. 5: Top down view of proposed virtual setup of the system. a. Physical space 5x5 m for the user to move physically. b. Virtual placement of the Kinect sensor. c. 8 m radius motion space for scanned facilitator. d. Area where facilitator cannot move due to closeness to sensor. f. Area where facilitator and VR user may meet.

4.2 Technical limitations of the real time avatar system

The experienced quality of the system is dependent on several technical limitations and missing features in our test system. The most prominent limitations we met are:

1. The image sensor captures 1920x1080 pixels at 30 frames per second (30 Hz). The human figure covers only a small number of such an area making the final texture quality on the avatar much lower.
2. The sensor offers a depth map on 512x424 pixels at 30 Hz, which are translated into a mesh that can be displayed in the game engine. Similarly as with the texture, the resolution actually used on the human model is significantly less than the offered height map.
3. The depth image has a secondary weakness in the inherent noise in the captured depth data. This translates to small vibrations on the avatar surface that appears when moving up close to the model. While it is possible to use filters to minimize this problem, such filtering can however present additional challenges. It is computationally expensive, making it more challenging to keep the main rendering loop running at a steady 90 Hz. This is important since maintaining a high and steady frame rate is vital to minimize the risk of "Simulator-Sickness" when using VR. More computational steps also mean an increased latency between the movement of the real person and their virtual representation in VR, making the synchronization of the real and virtual world more challenging. Finally, we have experienced that filtering the captured raw data too aggressively can create a sense of unrealism in the final rendered mesh. The smoothed human model starts to look more like a 3D avatar, thus falling back into the "uncanny valley" we are trying to avoid. More experimentation is needed to define where the "sweet spot" of filtering is to be set for applications of this kind.
4. Since a camera carries out the human scanning from a single point, the 3D capture is less effective when the scanned person is moving close to the camera. In addition, there will appear

geometry “shadows” (occlusion) on the avatar if for instance hands are stretched out in front of the body. Also, the single point capture lead to an incomplete model that deteriorate as the viewer moves to a position where the model can be seen from the side, Fig. 6. We try to limit this problem by positioning the avatar strategically in the scene, Fig. 5.

5. The version of the system used did not allow for streaming of scanned avatars over the network. This limits the ability to use the system as a communication medium across distances. Also, the lack of streaming abilities forces us to both scan the model and render the VR scene on the same machine, placing some strain on how we physically arrange the scanning and VR equipment according to each other.
6. The version we used did not support playing back captured audio at the correct position in the virtual world. Due to this the scanning sessions needed to be carefully orchestrated, to avoid mismatch between where a person is seen in VR space and the direction where his or hers voice appear to come from. We regularly experience breakdown in immersion when we tested the system with bad alignment of virtual space and the facilitators’ voice position. We will include audio in future version to avoid this problem.



Fig. 6: Real time avatar seen from the side. Screen grab from HMD.

4.3 Experiences from using the system in design

The setup process of the system is very simple, and there is little need for technical skill to use the system given basic knowledge of Unity 5. When the virtual scenes are up and running and the Kinect sensor connected, there is no further need to interact with the scanner system. Anybody can enter the virtual scene simply by walking into the scan area in front of the Kinect. In practice, this was a great benefit, since it allowed several facilitators to jump in and out of the VR scene simply by moving in and out of the scanner field. We could also have several people present in the virtual world simultaneously to communicate with the VR user. The simplicity in setup and intuitive use made the threshold for using the scanner in design very low. Because of this, the scanner was always on whenever we used the VR system, both when involving users and whenever the designers were using the system themselves.

In using the system, we found that the real-time avatar allowed VR users to gain a better immersion in the virtual scene. When we had people entering VR without the avatar, they often took off the HMD

to be able to talk to the designers directly. This effect was much less prominent when users had a human avatar present to talk to in the VR space.

Eye movement is important in enabling social communication through avatars. Such eye movement was accurately transferred through the system despite the low resolution of the animated texture. In addition, the system simulated convincing eye contact whenever the VR user and the real time scanned avatar were properly aligned, Fig. 1. With avatar and user close to each other, the experience demanded the VR user positioned close to the virtual representation of the Kinect Scanner, Fig. 5c. However, this was less important if the avatar and user were moving further away from each other. We believe it is likely that this contact support user immersion in VR space. However, further tests are necessary to be able to confirm this.



Fig. 7: Screen capture from the HMD showing the real-time scanned avatar

During tests we found that the use of body language was important in three ways. First, it served well in supporting natural conversation with the VR user adding considerable behaviour fidelity to the avatar. Second, it was useful in directing attention towards different areas of the VR model such as design details on the console as well as activities going on outside the ships bridge, Figs. 1 and 6. Third, it offered a sense of scale to the VR scene in addition to the VR users own body. This is important for people reading of the virtual model, *Österman et al. (2016)*. The facilitator could take up positions in relation to the workplace such at the seating position to show the relations between a human body, such as reach, and the design.

The asymmetrical communication setup was experienced as an important limitation in the system. While the VR users are fully immersed, the facilitator can only see the virtual world through the screen, Fig. 4. In addition, seeing oneself through the point of view of another person makes it necessary to have some training in controlling the appearance of oneself. We can improve this experience by adding several view angles to the facilitators screen such as view from above, view from avatar's perspective, perspective view of avatar as well as view from VR user. Even so, the facilitator experience will not be as immersive as the VR users, making it harder for the facilitator to engage effortlessly in discussions with the VR user.

The system we have developed does not have the same model fidelity as state-of-the-art avatars that usually have more detailed geometry, are complete models and have very detailed textures. However, the state-of-the-art avatars that are accessible for use in design usually have severe limitations in their

ability to convey behavioural fidelity, such as detailed body and facial motions. Therefore, most avatars in use in design today fall well within the uncanny valley problem. Our system managed in most instances to avoid the uncanny valley effect. Even though the model fidelity was lacking compared to traditional avatars, the behavioural fidelity seems to compensate. Some users commented on the rough edges of the model, yet most users did not appear to be distracted by the avatar quality. We found that users generally accepted the real-time avatars as acceptable for communication. We think this acceptance is due to the system's ability to convey human behaviour fully situated in the 3D space.

5. Conclusion

To be able to use VR efficiently in participatory design processes we suggest there is a need to facilitate good human-to-human communication in virtual space. We have presented a system that supports such communication through real-time scanned 3D avatars. Our current experience from using the system makes us believe that real time avatar are useful in many aspects of participatory design. It may support formal tests, ideation processes and design evaluation. The ease of use of the system makes it possible to add human presence to a VR process with minimum efforts, thus making it a powerful tool for supporting human collaboration in VR space. For design, it allows us to make VR experiences more natural and as such, it supports the efficient communication necessary for efficient design collaboration.

Acknowledgements

Thanks to Hans Martin Erlandsen and Petrit H. Gerxhaliu for contributing the images, testing the system as well sharing their insights in using the VR system. Also, thanks to Ulstein Power and Control for supporting the work.

References

- BLIGÅRD, L.O.; ÖSTERMAN, C.; BERLIN, C. (2014), *Using 2D and 3D models as tools during a workplace design process—a question of how and when*, 11th Symp. Human Factors in Organizational Design and Management (ODAM), Copenhagen, pp. 799-804
- HJELSETH, S.; MORRISON, A.; NORDBY, K. (2015), *Design and computer simulated user scenarios: Exploring real-time 3D game engines and simulation in the maritime sector*, Int. J. Design 9(3), pp.63-75
- KOUTSABASIS, P.; VOSINAKIS, S.; MALISOVA, K.; PAPAROUNAS, N. (2012), *On the value of virtual worlds for collaborative design*, Design Studies 33(4), pp.357-390
- KRISTIANSEN, H.; NORDBY, K. (2013), *Towards a design simulator for offshore ship bridges*, ECMS, pp.212-218
- MORAIS, D.; WALDIE, M.; LARKINS, D. (2011), *Driving the adoption of cutting edge technology in shipbuilding*, 10th Conf. Computers and IT Applications in the Maritime Industries (COMPIT), Berlin, pp.490-502
- MORI, M.; MacDORMAN, K.F.; KAGEKI, N. (2012), *The uncanny valley [from the field]*, Robotics & Automation Magazine 19(2), pp.98-100
- ÖSTERMAN, C.; BERLIN, C.; BLIGÅRD, L.O. (2016), *Involving users in a ship bridge re-design process using scenarios and mock-up models*, Int. J. Industrial Ergonomics 53, pp.236-244
- SANDERS, E.; STAPPERS, P.J. (2008), *Co-creation and the new landscapes of design*, CoDesign 4(1), pp.5-18

SLATER, M.; WILBUR, S. (1997), *A framework for immersive virtual environments (FIVE): Speculations on the role of presence in virtual environments*, Presence: Teleoperators and virtual environments 6(6), pp.603-616

SUMA, E. A.; KRUM, D. M.; BOLAS, M. (2011), *Sharing space in mixed and virtual reality environments using a low-cost depth sensor*, IEEE Int. Symp. VR Innovation (ISVRI), pp. 349-350

TONG, J.; ZHOU, J.; LIU, L.; PAN, Z.; YAN, H. (2012), *Scanning 3d full human bodies using kinects*, IEEE Trans. Visualization and Computer Graphics 18(4), pp.643-650

ZHANG, Z. (2012), *Microsoft kinect sensor and its effect*, MultiMedia 19(2), pp.4-10

ZINI, A.; ROCCA, A; RAFFA, M.; COSTA, R. (2000), *The integration of virtual prototyping in ship design*, 1st Conf. Computers and IT Applications in the Maritime Industries (COMPIT), Potsdam, pp.490-502

Enhanced Voyage Support System based on Detailed Weather and Performance Monitoring

Hideo Orihara, Japan Marine United Corporation, Tsu/Japan, orihara-hideo@jmuc.co.jp
Hisafumi Yoshida, Japan Marine United Corporation, Tsu/Japan, yoshida-hisafumi@jmuc.co.jp
Ichiro Amaya, Japan Marine United Corporation, Tsu/Japan, amaya-ichiro@jmuc.co.jp

Abstract

In this paper, voyage support system enhanced by implementing detailed weather and performance monitoring is described. The new system is an enhanced version of “Sea-Navi” voyage support system which is an integrated on-board monitoring and optimum routing system. In the present development, on-board monitoring function is enhanced by implementing a suit of wave monitoring and ship’s motion sensors and a new performance analysis function. For wave monitoring, a wave field sensor analysing radar backscattered power and a Doppler-type wave height meter are introduced. Wave field sensor provides directional wave energy spectrum. For motion monitoring, a vertical gyro and accelerometers are implemented to measure ship’s global motions and local accelerations. Use of measured directional wave energy spectrum enables detailed full-scale performance analysis and improved optimum routing. In performance analysis, weather disturbances can be evaluated using measure wind and wave data, and its effects on ship’s performance can be rigorously identified with respect to each weather factor. Availability of the present system is examined by the optimum routing calculations conducted by using the modified performance data.

1. Introduction

In recent years, the new international rules established by International Maritime Organization (IMO) have stimulated significant efforts for the reduction of Green-house Gases (GHG) emissions from ocean-going ships in maritime community. Among the IMO rules for GHG emission reduction, Ship Energy Efficiency management Plan (SEEMP), *IMO* (2012), has large impact on the operation of ocean-going ships. SEEMP is defined as an operational measure that establishes a mechanism to improve the energy efficiency. The SEEMP also provides an approach for shipping companies to manage ship and fleet efficiency performance over time in service. The SEEMP urges the ship owner and operator at each stage of the plan to consider new practice for optimising the performance of a ship. In SEEMP, ship performance monitoring and weather routing are recommended as measures effective for enhancing the performance of a ship in service.

Under these circumstances, optimum routing (or weather routing) which optimizes voyage route in terms of minimum fuel-consumption based on weather and ocean current forecast has been employed widely for reducing GHG emissions and fuel consumptions in shipping. While this type of approach have long been employed as an effective measure to achieve safe operation, their potential as a mean for improving voyage economy has also recognized in their capability of reducing fuel consumption through voyage optimization. Acquisition of accurate weather data is also beneficial for conducting high-fidelity assessment of ship’s responses under actual sea weather conditions and enhancing ship’s operational safety.

To cope with these environments, Japan Marine United Corporation (JMU) has developed voyage support system called “Sea-Navi” for reducing GHG emissions and fuel consumptions of ocean-going ships, *Orihara and Yoshida. (2010)*, *Orihara et al. (2014)*, *Orihara and Yoshida (2015)*. “Sea-Navi” can optimize voyage route under actual operating conditions by taking account of relevant weather parameters, including wind, waves and ocean currents. In the present work, “Sea-Navi” is developed for the enhanced safety in ship operation by implementing a suit of wave monitoring and ship motion sensors and improved route optimizing algorithms.

A description of enhanced “Sea-Navi” system is given in the next section with emphasis on the

features implemented in the present work. Then the effectiveness of enhanced “Sea-Navi” system is examined by conducting route optimizing simulations for winter trans-pacific voyage cases, where enhanced “Sea-Navi” system’s effectiveness in enhancing fuel efficiency and operation safety is examined. Brief conclusions are presented in the final section.

2. Voyage support system “Sea-Navi”

Voyage support system “Sea-Navi” consists of the following two sub-systems:

- 1) Optimum routing system

Optimum route for safe, economic and ecological (least GHG emission) voyage is provided by use of vessel-specific characteristics of hull and machinery, weather and ocean current forecast data.

- 2) On-board monitoring system

Monitoring is made of actual state of weather encountered, hull responses, installed machinery conditions. Monitored data are transmitted to the shore-based system’s server via satellite communication. With these monitored data, system’s users can conduct voyage performance analysis that confirms exact relationship between actual encountered weather and the vessel’s performance.

2.1. Optimum routing system

Sea-Navi optimum routing system calculates an optimum route for the specific voyage case using both vessel-specific performance characteristics and latest weather and ocean-current forecast available on-board ship. Ship’s actual operating condition is properly considered in optimum-routing calculation. Various route types can be selected in optimum routing calculation while satisfying safety constraints by setting the limits of safety criteria in terms of ship responses (roll angle, pitch angle, vertical acceleration, bow slamming green water on deck, propeller racing, etc.) as well as encountered weather conditions. Thus, optimum routes are determined so that it does not pass the regions where either ships responses or encountered weather conditions exceed the specified safety limit values. In addition, user-specified arbitrary routes can be evaluated along with the optimum routes. For the details of optimum routing system other than the features incorporated in the present work, *Orihara and Yoshida (2010,2015)*.

In the present development, optimum routing algorithm has been improved so that the safety of voyage is enhanced by reducing ship’s motions and unfavourable responses in heavy weathers.

Firstly, types of safety criteria for route optimization are extended to include lateral and longitudinal accelerations at the specified locations on a ship. This is intended to take into account the lateral and longitudinal loading to reduce mainly cargo damage and cargo lashing requirements as well and to improve human comfort. Since rolling motion is significant in terms of magnitude among 6 degrees of freedoms of ship’ rigid-body motion, its attenuation is important for safety in operation.

Secondly, ship’s motion prediction procedure is modified so that rolling motion calculations can be executed based on actual metacentric height (GM). In the previous version of “Sea-Navi”, GM values has been explicitly defined for the specified standard displacement cases as part of the pre-set vessel-specific performance model, that is GM value is uniquely set for each displacement cases. Although this approach of GM value treatment is generally valid for the case of tankers and bulk carriers most of whose operations are conducted at standard displacement cases (e.g. full-loaded and ballast conditions) with small variation in GM values for respective condition, this approach cannot be applied similarly to the cases of container and ro-ro ships whose loading conditions (displacement and GM values) vary significantly depending on the voyage cargo conditions. In addition to the variation in GM, GM values for these ship types are smaller than tankers and bulk carriers, this feature results in large variations in roll natural period and roll motion responses in waves.

To cope with the GM variation during ship operations, vessel-specific performance model is modified such that ship motion response characteristic data are established as function of GM and displacement values. For each displacement case, GM range anticipated in actual operations is specified. Then, ship motion responses are evaluated for the entire range of anticipated GM values and stored in the vessel-specific performance data. In optimum routing calculations, ship's performance characteristic data corresponding to the actual GM value is automatically selected and used for performance predictions.

Since ship's rolling motion has smaller effect on ship's added resistance and thus required propulsive power and fuel consumption in waves in contrast to the longitudinal modes of ship motions (heave and pitch), optimized fuel-efficient route can occasionally result in large rolling motion and be unfavourable in terms of ship and cargo safety. With the present modification in the roll motion treatment, "Sea-Navi" route optimizing capability can be improved for roll-sensitive container and ro-ro ships.

2.2. On-board monitoring system

Configuration of enhanced "Sea-Navi" monitoring system is shown in Fig. 1. These basic features are same as those of the previous version (*Orihara and Yoshida (2010)*). Monitoring system primarily consists of a suite of sensors and a system's PC to acquire, analyse and display data. Most of hull-related data (ship's speed, course, heading wind, rudder angle etc.) are obtained from Voyage Data Recorder (VDR) as a LAN output data. Machinery-related data (fuel-oil flow rate, fuel-oil temperature, shaft power etc.) are obtained from an engine-room data logger.

In the present development, ship motions and encountered wave monitoring function have been upgraded. For the ship motion monitoring, accelerations are added for measuring lateral and longitudinal accelerations to monitor local horizontal loading due to ship motions. Monitored accelerations are used for the validation of the performance prediction procedures in optimum routing calculations.

For the encountered wave monitoring, Wave Monitoring Radar System (WMRS) and Doppler Wave Height Meter (DWHM) both developed and manufactured by Japan Radio Co. Ltd. (*Hirayama et al. (2015)*) are implemented. WMRS uses radar image from on-board X-band navigational radar to determine directional wave spectral properties. WMRS analyse intensity of sea clutter appeared in the radar image to determine the length and direction of wave components comprising encountered directional irregular waves. Radar image data are produced once a revolution of the radar antenna scanner. Directional wave spectra obtained from radar image data analysis are averaged over the duration about 2 minutes with 50 image data. Magnitude of the directional wave spectrum data is modulated so that the integral of wave energy spectrum corresponds to the square of the encountered wave height. This modulation is conducted using the modulation transfer function that defines the relationship between radar sea clutter intensity (radar signal/noise ratio) and wave height. The transfer function is calibrated specifically for each on-board installation case to account for the influences of the installed radar equipment layout on radar signal sea clutter characteristics. Fig.2 an shows example of directional wave spectra obtained from WMRS. As can be seen in the left case in Fig. 2, multi-directional wave characteristics (i.e. wind waves from port stern quartering direction and swells from head direction) is clearly seen in the analysed wave spectrum. WMRS incorporated in the present upgrade is improved type employed in the past "Sea-Navi" trail (*Orihara and Yoshida (2015)*) which can conduct the wave measurement over wide range of wave signal range settings (less than 12 NM setting). Thus wave measurement can be made continuously by sharing with navigation X-band radar instead of installing additional X-band radar for the wave measurement purpose.

DWHM is installed to measure the encountered wave height and to supplement the WMRS wave measurement. DWHM consists of K-band Doppler module, DPS digital signal processor and Micro Electro Mechanical Systems (MEMS) motion sensor. DWHM measure the distance from the sensor to wave surface and calculate instantaneous wave height by correcting the effect of the ship motion using acceleration and angular displacements obtained from the MEMS sensor. Measured data are merged as a time-history data of 20-min duration. Then, statistical analysis is conducted for obtaining wave parameters (e.g. significant wave height, mean encountered period).

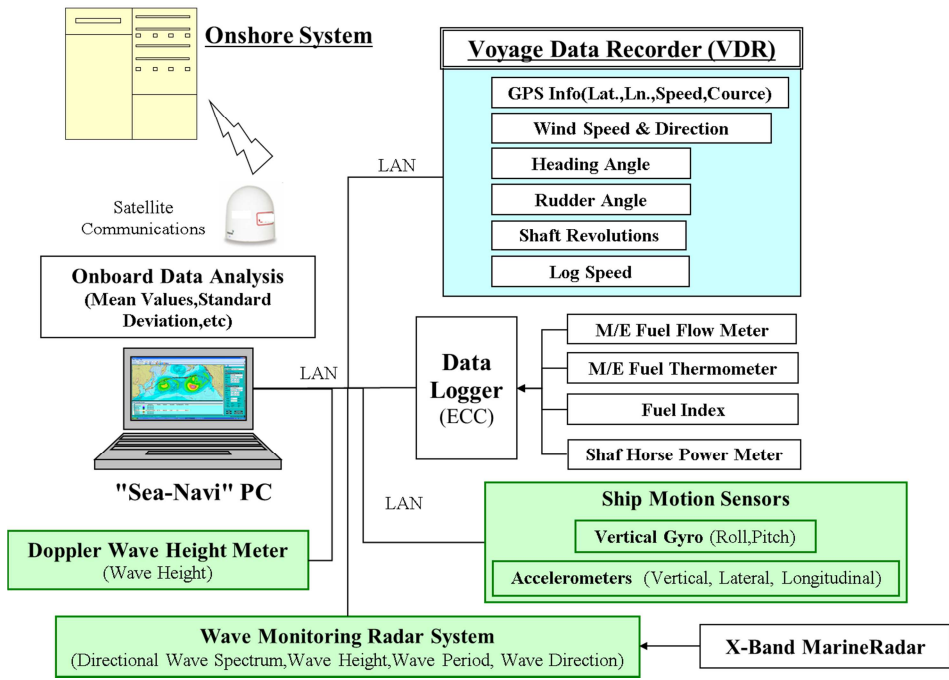


Fig. 1: Configuration of "Sea-Navi" on-board monitoring system

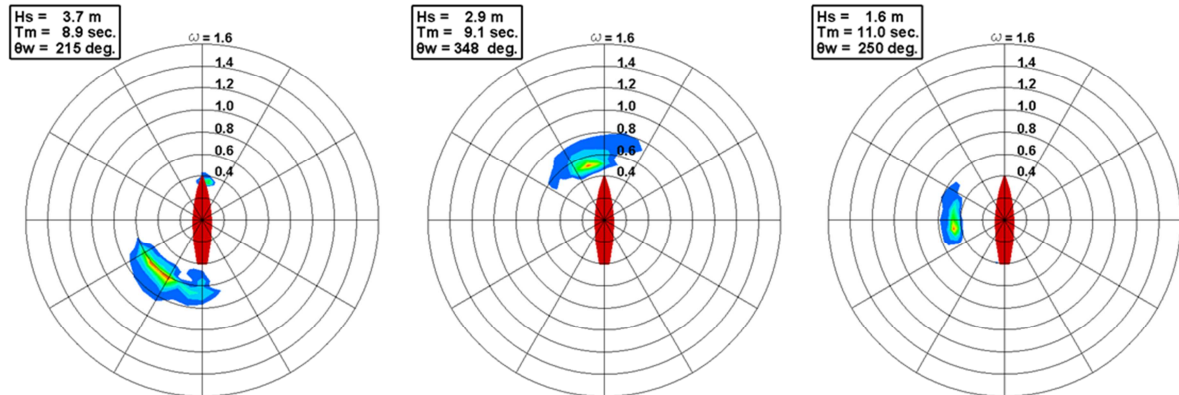


Fig. 2: Directional wave spectra obtained from WMRS

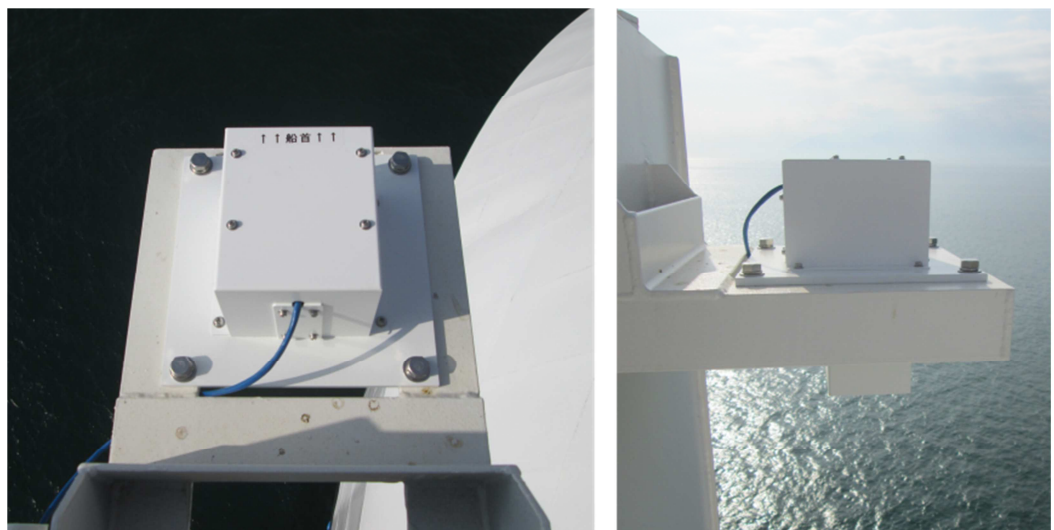


Fig. 3: Doppler wave height meter mounted at the side of the ship

2.3. Ship's performance prediction procedure

To accurately estimate ship's hydrodynamic performance and main engine's fuel consumption in service, "Sea-Navi" employs vessel-specific performance model which is derived from the results of theoretical calculations, model tests, sea trial and main-engine shop tests.

For the prediction of ship motions, strip-method calculation results are usually used with empirical corrections. Strip method calculation is conducted for an entire range of anticipated service speeds and at all wave headings, then 6-degree-of-freedom motion response amplitude operators (RAOs) are obtained. Fig. 4 shows an example of calculated RAOs for heave, pitch and roll motions in a polar plot form for a pure car truck carrier hull form. Magnitudes of normalized motion amplitudes are depicted in colour-contour form. Fig. 5 shows a comparison of the calculated motion amplitude (part of Fig. 4) with model test results in quartering waves ($\theta_w = 60^\circ$; $\theta_w = 0^\circ$: head waves, $\theta_w = 180^\circ$: following waves), where the model test was conducted in the JMU Seakeeping and Manoeuvring Tank ($L \times B \times D = 70\text{m} \times 30\text{m} \times 3\text{m}$). As shown in Fig. 5, strip-method results agree well with the model test results. According to our experience in model tests in waves, similar degree of agreements in ship motions are usually obtained for most of large merchant ship types including tankers, bulk carriers, container carriers and car carriers. Ship motions in an actual seaway, that is short-crested waves, estimated using Pierson-Moskowitz type wave energy spectrum with direction spreading function. Accuracy of "Sea-Navi" ship motion predictions have verified by comparing with the full-scale data for the container ship, *Orihara and Yoshida (2010)*, and the large hulk carrier, *Orihara and Yoshida (2015)*.

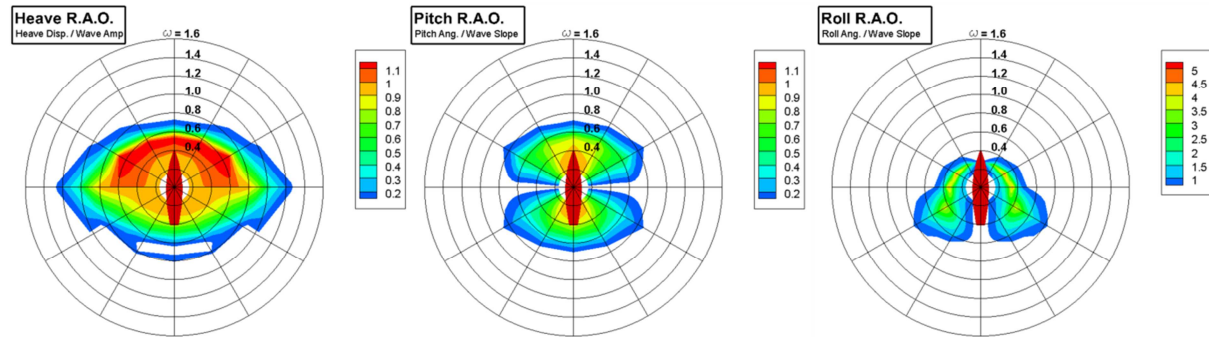


Fig.4: Example of ship motion response amplitude operators employed in "Sea-Navi".

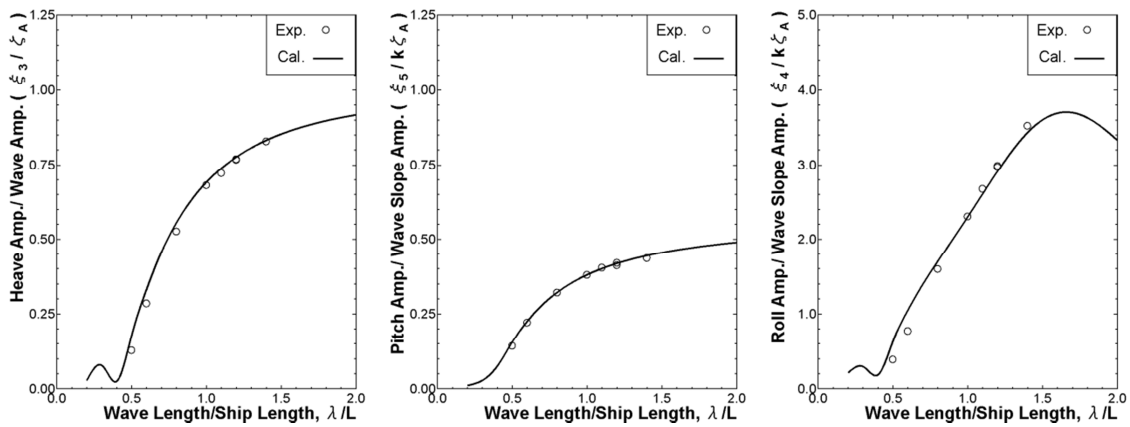


Fig.5: Comparison of ship motion response amplitudes in quartering waves ($\theta_w=60^\circ$)

3. Optimum Routing Simulations with Constraints in Ship Motion Responses

To examine the availability of the enhanced version of "Sea-Navi" in the treatment of ship motion safety criteria in optimum routing, touting simulations are conducted and the effects of them on fuel efficiency is examined.

3.1. Condition of simulation

North-Pacific westbound winter voyage case (U.S. west coast to Japan) is simulated for a pure car track carrier (PCTC). Following 3 route cases are examined:

- 1) G-C Route: Simulation on the great circle route
- 2) OPT1 Route: Simulation on least F.O.C. route for the same conditions as the G-C route simulation (points of departure and arrival, time of departure and arrival), with no constraint condition in ship motion.
- 3) OPT2 Route: Simulation on least F.O.C. route for the same conditions as the G-C route simulation (points of departure and arrival, time of departure and arrival), with constraint condition in ship motion (roll significant angle $\leq 4^\circ$, lateral acceleration at the side of the hull $\leq 0.1g$).

So-called “now-cast” weather and ocean current forecast data is used in the simulations. Details of forecast data are described in *Orihara and Yoshida (2010)*. Constant-revolution engine operation mode is selected. This means that engine revolution is fixed at the specified value during the entire voyage for each route cases. Since the voyage time is set the same for all the route cases, engine revolution set values differ among the route cases to account for the effects of route distance and encountered weather disturbances.

3.2. Results and discussions

Fig. 6 shows the snapshot of weather condition during the routing simulation. Surface pressure and significant wave height are shown in contour map and colour contour map, respectively. Wind speed and direction are depicted as arrow marks. As seen in the colour contour maps, weather conditions are rough and higher wave area (> 4 m) resulting from strong winds covers large portion of the north pacific.

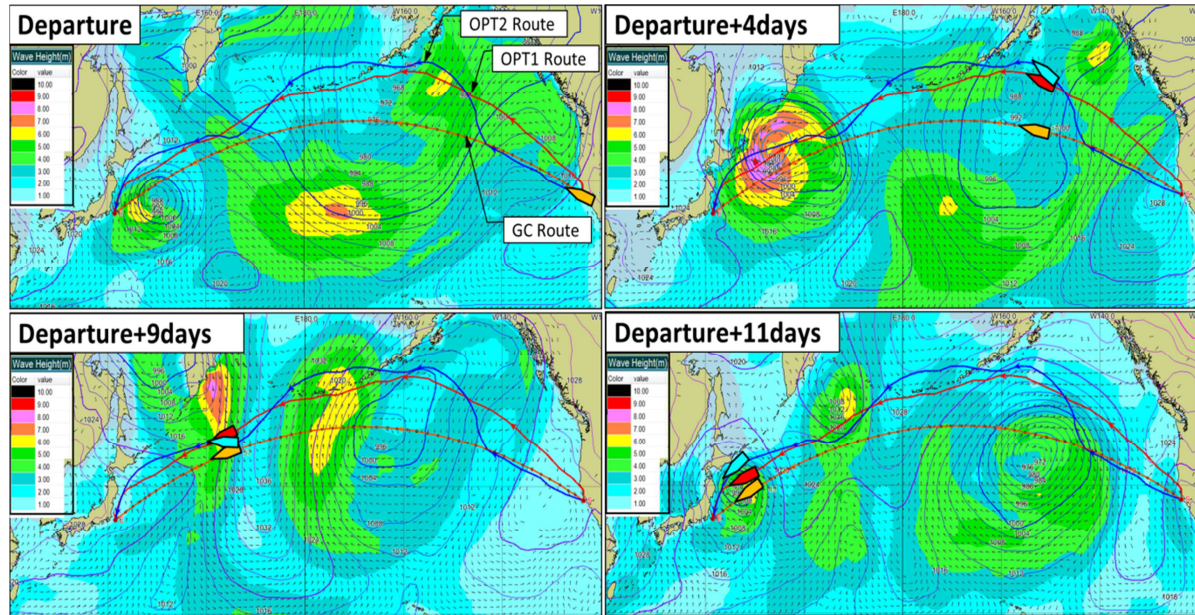


Fig. 6: Weather conditions during the optimum routing simulation

Encountered wave conditions along the simulated routes are shown in Fig. 7. While encountered significant wave height is similar among all the routes, wave directions differ noticeably. As seen in the roll response characteristics shown in Fig. 4, roll motion responses changes significantly with relative wave direction. Thus, change in ship's heading can contribute efficiently to reduce roll responses.

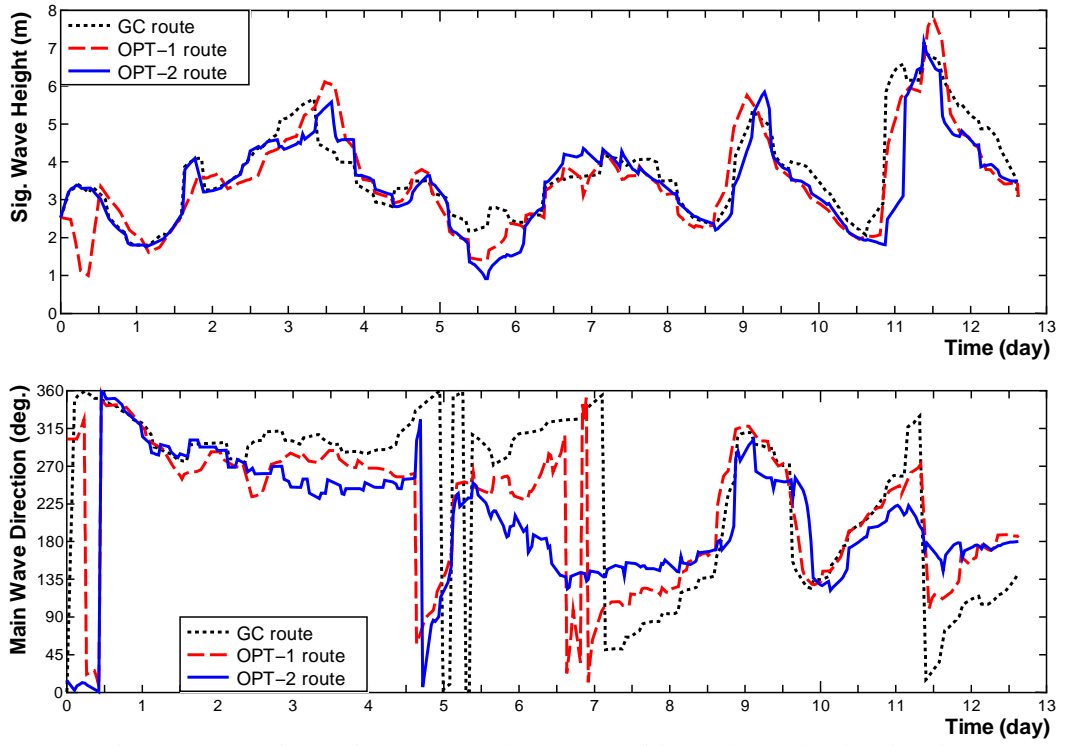


Fig. 7: Comparison of encountered wave conditions along the simulated routes.

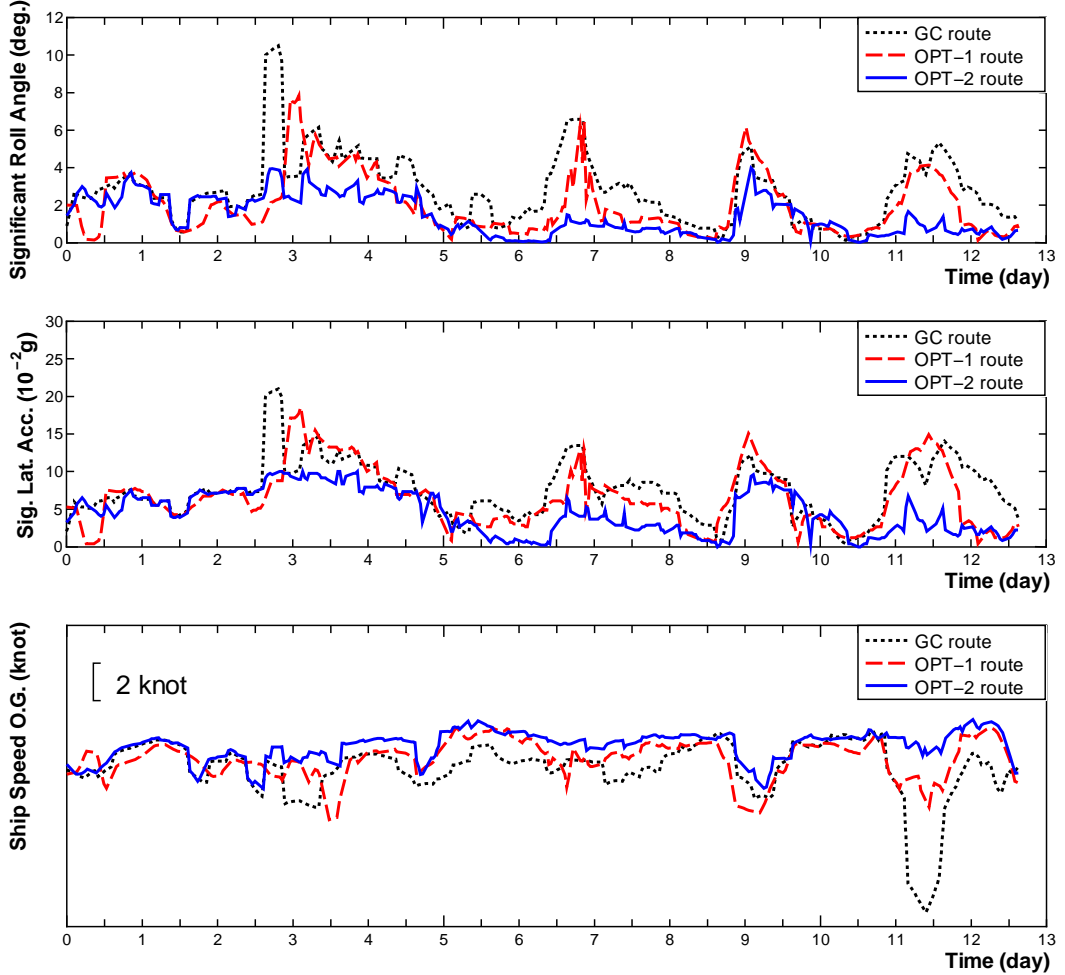


Fig. 8: Comparison of ship responses along the simulated routes.

Fig. 8 compares ship motion response time histories among the simulated routes in terms of significant roll angle, significant lateral acceleration at the side of the ship and ship speed over ground. Although magnitudes roll angles and lateral accelerations are similar between G-C and OPT1 routes, these responses for OPT2 route are reduced by around 50% at the peak relative to G-C route case. Since the roll angle and lateral acceleration is responsible for most of lateral loadings acting on on-board cargo, the suppressed motion responses for OPT2 route case can be beneficial in reducing cargo damage and human comfort in a seaway.

In terms of ship speed variations, it is noted that higher speed is maintained along the OPT2 route with small speed reduction (less than 2 knots) compared to the other routes.

Table I: Comparison of calculated route efficiency

Route Type	Distance (%)	Power Sea Margin (%)	F.O.C. (%)
G-C	100.0	43.6	100.0
OPT1	103.7	26.2	88.9
OPT2	108.5	17.1	94.7

Table I list the calculated route efficiency for the present voyage simulation case. Route distance and main engine fuel oil consumption (F.O.C.) are listed in percentage value of the G-C route value. Also listed is average power sea margin which is evaluated as the power increase from the still water condition (no wind/wave condition). As usual in the optimum routing in rough weather conditions, route distance of least FOC optimum routes are increased appreciably from G-C (minimum distance) route. In the present case, route distance is increased by 3.7% and 8.5% for OPT1 and OPT2 routes, respectively. Distance difference between OPT1 and OPT2 routes seems to be due to the effect of imposed ship motion constraint conditions which, as mentioned earlier, tend to change ship heading frequently and results in longer route.

In terms of F.O.C., reductions from the G-C route case are 11.1% and 5.3 % for OPT1 and OPT2 routes case respectively. When comparing the F.O.C. values for OPT1 and OPT2 route cases, it is noted that F.O.C. for OPT2 route is increased by 5.8% although average power sea margin is reduced by 9.1%. This can be explained by the difference in route distance. Since the routing simulations are conducted on the fixed voyage time basis, route average speed is proportional to the distance of the route. F.O.C. is approximately proportional to the propulsive power which proportional to the cube of ship speed. Then, reduction in power sea margin is cancelled by the increase in route distance. In the present case, OPT2 route's F.O.C. increase due to distance increase is estimated to about 15% based on the above-mentioned cubic relationship between distance and F.O.C. By deducing the power sea margin of 9.1% from this estimated value, we have an estimate of 5.9% F.O.C. increase from OPT1 case. This agrees well with the actual F.O.C. increase of 5.8% mentioned above and confirms the validity of the reasoning concerning F.O.C. variations for optimized routes.

From the simulated results, it is shown that the treatment of ship motion constraint conditions introduced in the present study works satisfactory for improving safety in operation. Optimized route with ship motion constraints achieve improvement in both fuel efficiency and ship motion responses compared to the reference G-C route. But, since the application of ship motion constraint in route optimization results in F.O.C. increase, the setting of its limit values need to be determined on the trade-off between fuel efficiency and operational safety.

4. Future Work

Newly developed enhanced version of "Sea-Navi" has installed and operated on the PCTC recently delivered by JMU. On-board trial of the enhanced version is planned for the duration of 2 years. During the on-board trial, newly incorporated functions will be validated. For wave monitoring function, wave data obtained from the on-board sensors (WMRS, DWHM) will be examined in terms

of the capability of wave measurement. For ship motion monitoring function, prediction capability is thoroughly examined through the comparison with on-board monitored data. Ship speed/power performance prediction procedure will also be verified using monitored wave data. For optimum routing function, optimum routing capability is evaluated under realistic operational conditions including the setting of ship motion safety criteria.

In addition to the examination of enhanced “Sea-Navi” system, monitored detailed encountered weather and ship performance data will be utilized in the full-scale performance analysis for the verification of performance in service.

5. Conclusions

Enhanced version of “Sea-Navi” voyage support system is developed by incorporating detailed weather and performance monitoring is described. In the present development, on-board monitoring function is enhanced by implementing a suit of wave monitoring and ship’s motion sensors and a new performance analysis function. The features of the newly introduced functions are described in detail.

The effectiveness of the enhanced “Sea-Navi” system in improved safety in operation is examined by the optimum routing simulation for winter north pacific voyage case. It is shown that by introducing the ship motion constraint in optimum routing both fuel efficiency and operational safety can be improved compared to the reference route case.

Enhanced “Sea-Navi” system will be further examined in the on-board trial currently conducted on the pure car truck carrier. Ship motion prediction capability will be thoroughly verified with the comparison of full-scale measured based on the actual weather condition data obtained from on-board wave sensors. Optimum routing capability is evaluated under realistic operational conditions including the setting of ship motion safety criteria.

Acknowledgment

We would like to thank Japan Radio Co Ltd. for their help in the implementation of their on-board wave monitoring sensors in “Sea-Navi” system.

References

- HART, P.E. (1968), *A Formal Basis for the Heuristic Determination of Minimum Cost Paths*, IEEE Trans. Systems Science and Cybernetics 4/2, pp.100-107
- HIRAYAMA, K.; BABA, M.; ISEKI, T. (2015), *Wave monitoring on board*, Marine Dynamics Symp., Japan Society of Naval Architects and Ocean Engineers, Tokyo, pp.229-246 (in Japanese)
- IMO (2012), *Guideline for the Development of a Ship Energy Efficiency Management Plan (SEEMP)*, MEPC.213 (63) Annex 9.
- ORIHARA, H.; YOSHIDA, H. (2010), *Development of voyage sup-port system “Sea-Navi” for lower fuel consumption and CO₂ emissions*, Int. Symp. Ship Design and Operation for Environmental Sustainability, London, pp.73-80
- ORIHARA, H.; YOSHIDA, H.; HIROTA, K.; YAMASAKI, K.; SAITO, Y. (2014), *Verification of full-scale performance of eco-friendly bulk carriers under actual operating conditions by on-board performance monitoring*, 2nd Int. Conf. Maritime Technology and Engineering, Lisbon, pp.755-763
- ORIHARA, H.; YOSHIDA, H. (2015), *Verification of Energy Saving Capability of Optimum Routing by Full-Scale Trial navigation*, 14th Conf. Computer and IT Application in the Maritime Industries, Ulrichshusen, pp.343-354

A Web Based Real-Time 3D Simulator for Ship Design

Virtual Prototype and Motion Prediction

Olivia Chaves, UNIFEI, Itabira/Brazil, oliviachaves@poli.ufrj.br
Henrique Gaspar, NTNU, Ålesund/Norway, henrique.gaspar@ntnu.no

Abstract

This paper proposes an open-source application capable to run real-time ship motion simulations in a web browser, in any device of any operational system with HTML5 compatibility. This becomes possible by implementing closed-form expressions for wave-induced motion in JavaScript code, assisted by THREE.js and WebGL libraries to handle 3D graphics. Furthermore, this approach offers support for parametric 3D models and fast collaborative virtual prototype development. The breakthrough advantage consists in adapting the simulation tool requirements to user's common platform (modern web browser), instead of forcing the user to comply with the tool requirements (operational system, installs, updates, commercial software or file format).

1. Introduction – Virtual Simulation for the Web Environment

Virtual simulators have been used in maritime applications for decades, where experience-based design has progressively integrated simulation and virtual tools to assist the design process. Nowadays, industry relies in such tools to predict system response, assist operation, and assess design options. Analysis regarding stability, hydrodynamics and structure, together with 3D modelling, are examples of the most common virtual applications in ship design – Compit proceedings are full of such examples.

Currently, mainly commercial software programs are used to perform simulations. The benefits they provide are undoubtedly. However, most of them are restricted to a specific operating system (e.g. Windows), and codes are usually black boxes, preventing collaborative development and constraining its applicability and usability. Moreover, when it comes to 3D modeling software, each of them typically has its own proprietary file extension format, often causing compatibility issues, and imposing obstacles for sharing.

With respect to ship motion, several non-commercial programs have been developed to simulate vessel's response in waves, using diverse approaches. *Bertram (2014)* provides a compilation on this subject. Two factors could have contributed to the wide application of self-projects: the ship motion theory is accessible, and if kept to a basic level, the ruling equations do not require sophisticated solvers. Such projects would be recommended for the conceptual design, where fast and low-cost solutions are desired, and precise results are not essential. However, such projects may become outdated, due to the programming language they are written in, and possibly discontinued.

As the internet is essential for everyday life, it is very unlikely that a language specially developed for web will fade away soon, especially with big players in the market (e.g. Google) supporting common and open standards such as HTML5, www.w3.org/TR/html5/, and JavaScript. Actually, the tendency points to a fast and constant development based on current technology, without discontinuation. Recently, open-source web applications have been growing and computational capacity has been expanding towards web efficiency. Whereas hardware suppliers constantly and rapidly release new processors optimized for web performance, software suppliers often release new versions with improvements on features rather than on programming, not necessarily updating their code to meet new processor's routines.

Given these circumstances, software installed in the client machine will normally be more costly for computer capacity than any application running inside a web browser, doing the same as the software. In a recent benchmark, for instance, it was analyzed that MatLab can take up to 800x more time to a simple parse integer operation when compared to modern script languages, <http://julialang.org/>. More-

over, even commercial software developers are adapting to web trends, creating online versions of their products (e.g. Microsoft Office, AutoCAD and Adobe Photoshop).

In this context, we propose a web-based open-source ship motion simulator, focusing in collaborative development. The idea is to give continuity to the work, instead of rebuilding new versions of old achievements, because they are now unassessed due to the disuse of software programs, programming languages, or emulators. Besides, developing for web means developing for any device or operating system (OS), increasing the application reach and eliminating the need of client-side software.

The present simulator is based on *Jensen et al. (2004)*, who proposed closed-form expressions to estimate wave-induced motion for mono-hull vessels. These expressions require only vessel main dimensions and basic hull form coefficients, being especially relevant for conceptual design, where little information about the hull form is available. The approach allows the designer to vary those parameters, and quickly assess their influence on the wave-induced motion. Jensen's expressions were implemented in JavaScript code, and transposed to time domain. In this way, parametric real-time simulations are provided by the application, together with a 3D visualization of vessel's motion in regular waves.

2. Open-source tools overview

2.1. Open-source technology

Open source is a development methodology (or philosophy) that stands up for a transparent and collaborative platform, where monetary profit is secondary. It is based on free access to the software code, allowing users to not only see, but also modify it. In short, it can be summarized by the following facts:

- Continuous improvement; anyone can contribute or fix the code without having to wait for the next version release.
- Room for customization; issues can be better addressed due to customized solutions.
- Company independence; the software improvement or continuation may depend on the users, rather than exclusively on the owner company.
- Free support online; there are many user's communities online ready to assist each other.
- Total cost; comparing to commercial software, it is cheaper due to collaborative development and lack of investments in marketing, security, testing, etc.
- Flexibility; the code can be modified to best adapt to user's needs.

Although anyone can adapt the source code, its ownership/license may remain with the original developer (if desired), regardless anyone's contribution to the software. Famous examples of open-source software are Linux operating systems (e.g. Ubuntu, Gentoo) and the Mozilla Firefox browser. An overview of the license terms for maritime engineering is discussed by *Bertram et al. (2006)*. All tools and resources used to develop the Ship Motion Simulator are either free or open source, and a brief overview about them will be given in the following topics.

2.2. JavaScript

According to Mozilla Developers Network (MDN), <https://developer.mozilla.org/>, JavaScript (JS) is a lightweight, interpreted, programming language with first-class functions. It is best known as the scripting language for the Web. It is a prototype-based, multi-paradigm, dynamic scripting language, supporting object-oriented, imperative, and functional programming styles. Practically, JavaScript is responsible for adding interactivity to webpages. As the most used programming language nowadays, it will stay relevant as long as people use the Internet. JavaScript is compatible to diverse OS and devices. If there is a web browser the code can be executed. It has the analytical capacity of any other programming language, plus it can run real-time simulations. There is no need to compile or wait for the results, and a text editor (e.g. Notepad) suffices to write code. Compared to the old times, where each

mobile OS had its own programming language (e.g. Objective-C for iOS; Java for Android; C# for Microsoft), JavaScript presents a great evolution in standardizing. Additionally, it runs in the client machine, which performance may be either enhanced or constrained by the client's hardware; it does not require constant connection to the net.

2.3. WebGL

WebGL (Web Graphics Library) is a cross-browser JavaScript library/API, which is used by THREE.js as a rendering complement. It allows interactive advanced graphics to be rendered within a web browser and optimizes the hardware use. WebGL demands less from hardware because it "shares" the rendering work. Some features that needed to be handled by the hardware can now be handled by the language, resulting in a lower hardware requests. In addition, WebGL does not use plug-ins and there is no need for installs or updates, which is another significant advantage compared to the decaying Adobe Flash. WebGL has been used in applications from gaming to science. For example, NASA released their interactive educative tool 'Experience Curiosity', Fig. 1, which simulates the Curiosity Rover's adventure in Mars. Neuroscientists have developed a real-time visual exploration of the connectome data including FreeSurfer structural reconstruction, tractography, and network data all within the browser, Fig. 2, *Ginsburg et al. (2011)*, all WebGL based.

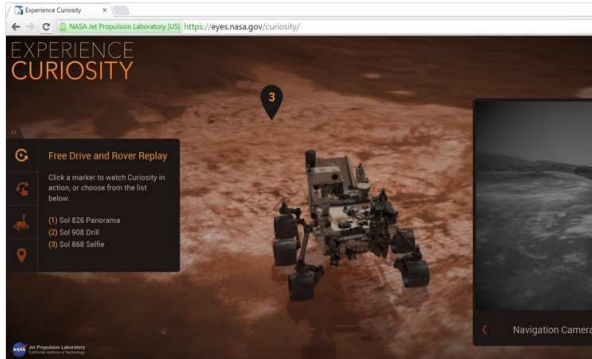


Fig. 1: Experience Curiosity

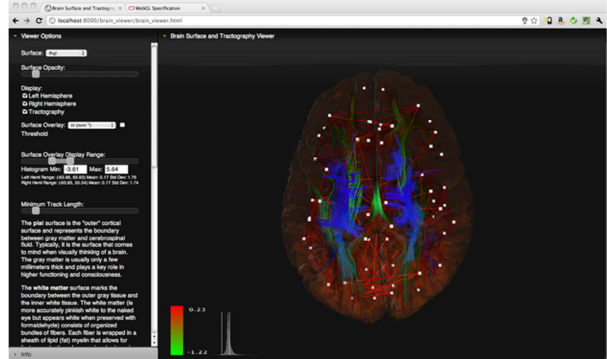


Fig. 2: Connectome visualization

2.4. THREE.js

THREE.js is another cross-browser JavaScript library/API, threejs.org. It is used to create and display animated 3D computer graphics on a browser. THREE.js allows GPU-accelerated 3D animations to be created as part of a website using JavaScript language. Significant advantages of THREE.js are the possibility to add and remove objects from a scene at run-time, communication with OpenGL (through WebGL), several compatibility solutions, collaborative development, and free support online. Moreover, the THREE.js library has innumerable features such as (currently) three camera options, six control types, thirteen material variations, four texture types, nineteen loader options, debugging, etc. This set of features allows building 3D animations just like in any dedicated software.

2.5. STL (STereoLithography)

STL is a three-dimensional representation of a surface geometry. Although lacking some modern features and criticized for its heavy file size, it is an open-standard file format accepted by almost every CAD program in the market today. Especially used for 3D rapid prototyping and 3D printing, this format carries information exclusively about the object's geometry, describing its surfaces through triangles, without any other object property such as color or texture. Thus, despite its simplicity, this format can be used to transport the hull geometry into the Simulator, not requiring any specific software to generate it.

2.6. Collada (COLLAborative Design Activity)

Collada (COLLAborative Design Activity) is a file format used to transport 3D assets. It is capable to carry more information about the 3D environment (including geometry, materials, shaders, effects, lights, or even physics and animations). Compared to STL, Collada is preferred as it can confer material properties to the model and offers support for exchanging advanced 3D graphics assets between applications. However, more sophisticated software is required to generate such file, and in this case, there are much fewer free programs supporting Collada than STL. Yet, Blender is an example of free, open-source software that supports Collada, www.blender.org/, Fig. 3.

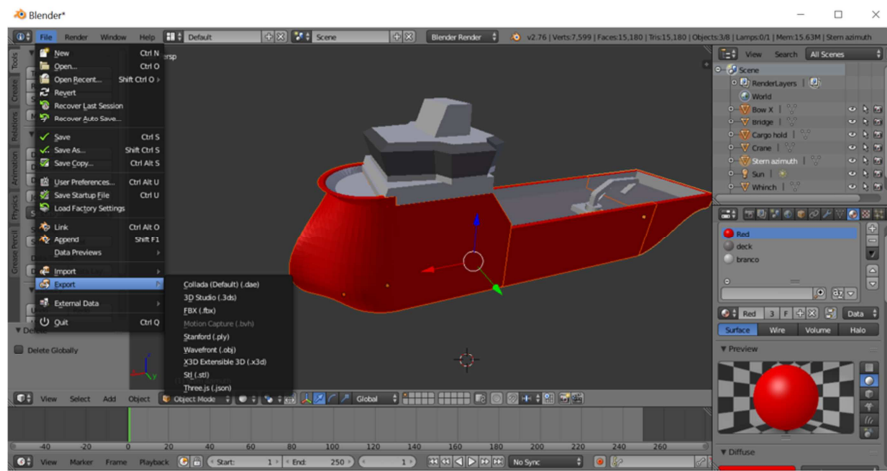


Fig. 3: Blender interface and exporting formats, such as Collada and .STL files

3. Virtual Prototype and the Web

Virtual prototyping, *Chaves et al. (2015)*, is extensively used by industry, but has not crossed the internet's barrier regarding the ship design sector. Currently available JavaScript APIs (e.g. THREE.js and WebGL) generate favorable conditions to bring prototyping to the web or even to a web-based virtual reality environment. Although there are not many examples yet, the internet is evolving to embrace productivity tools (e.g. Office and Photoshop), and engineering applications (e.g. Hull Lines Generator, www.shiplab.hials.org/app/shiplines/, 3D Configurator, www.shiplab.hials.org/app/3dconfigurator/, and Ship Motion Application, www.shiplab.hials.org/app/shipmotion/).

Software engineering is completely focused on the end user, which fundamentally should provide solutions that people wants to see. *Pressman (2005)* establishes a comparison between software and web applications, demystifying their difference and distance: Web pages are user interfaces, HTML programming is programming, and browser-deployed applications are software systems that can benefit from basic software engineering principles.

Web is today the most optimized and used GUI (Graphical User Interface) worldwide. Based on Event-driven Programming, a Web GUI provides interactivity by “watching” for events. Events include user’s actions such as mouse click, scrolling, hover over, key press, etc. This type of GUI is ready to accept user’s input at any time, rather than accepting inputs only when asked, Fig. 4.

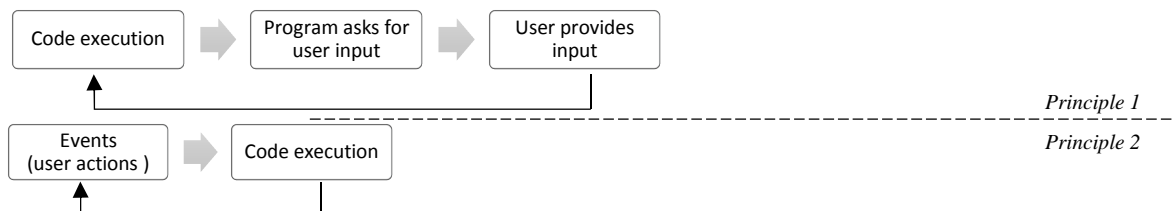


Fig. 4: GUI action principles

Both the amount of interactivity and the focus on usability make the web appealing and contribute to attracting more and more adepts. User-friendly characteristics are even more enhanced on mobiles, increasing the potential to use it as a tool. According to *Hoos et al. (2015)*, mobile apps provide a huge potential for increased flexibility and efficiency due to their ‘anywhere and anytime’ characteristics.

User-friendly comes with simplicity. Therefore, making extensive trials or complex procedures to become user-friendly might be a challenge when it comes to adapting engineering tools to the web frame. However, precise analyses and optimized results are not necessary in the early design phase. Design concepts are full of considerations and assumptions, creating simplified models to be further developed. So, we believe that the potential to apply web-based engineering tools are in solving these early simple problems, in order to save time, money and avoid mistakes.

For ship design, web tools allow an intuitive, multi-platform application, which can be used in mobiles, computers, tablets, or any device supporting HTML5. The presented simulator allows assessing design options by varying vessel’s main dimensions and verifying resulting ship motion. It also includes a vessel’s 3D visualization (representation), making room for virtual prototyping, *Chaves et al. (2015)*.

4. Methodology

4.1 Code structure

Considering today’s trends, recognizing JavaScript potential and WebGL capabilities to handle 3D advanced graphics, THREE.js was chosen to develop a web-based simulator, Fig. 5. The 3D environment is composed by four basic elements: camera, light, scene, and render. In order to allow the user to navigate the camera, orbit controls were implemented. Then two core objects, the vessel and the ocean, were included in the scene and their motion encoded. Finally, a console (GUI) was added so that the user can input both wave and hull form parameters.

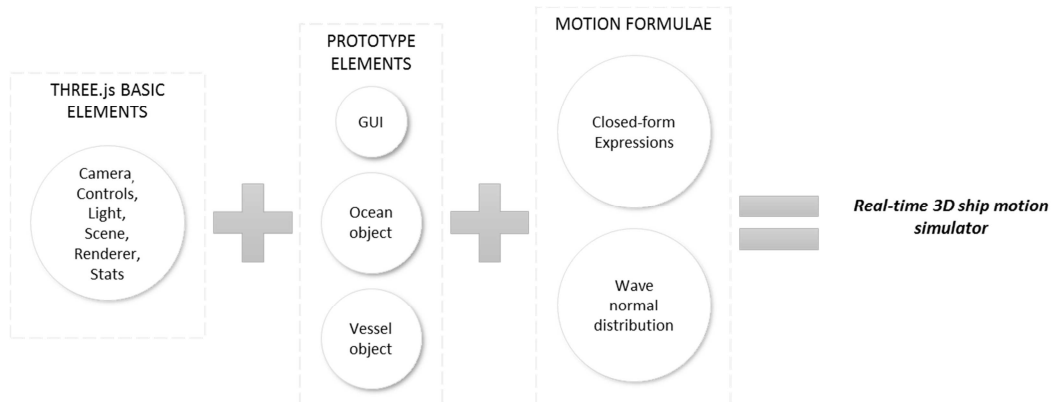


Fig. 5: Ship Motion Simulator main components

The vessel 3D model was designed outside the web application, and included (imported) into the scene exclusively for visualization purposes. As modeling a hull is not simple, and becomes even more difficult without using a dedicated CAD software, the following procedures are suggested to create a Collada file.

- (1) Using a hull modeling dedicated CAD software to generate the hull 3D geometry;
- (2) Exporting the 3D geometry in a standard format such as .stl, .obj, .igs;
- (3) Importing to a software that supports 3D advanced assets, and is capable of exporting Collada (e.g. Blender, Rhinoceros);
- (4) Adding material, texture, shaders, effects, ambient light, and/or any other asset to the hull geometry, in order to confer reality to the hull representation;
- (5) Exporting the final scene as Collada file.

Collada was the file format chosen to transport advanced 3D assets from the modelling software to the web application. Simpler file formats such as STL and OBJ could also be used, and the procedure above would stop at number (2), but the visualization realism would be considerably decreased.

The vessel motion amplitude is calculated by closed-form expressions given in *Jensen et al. (2004)*, based on hull form parameters (L , B , T , C_B , C_P , C_{WP} etc.). This method provides a rational and efficient procedure to predict the wave-induced motions with sufficient engineering accuracy in conceptual design. *Bertram (2014)* discusses that this method, together with many others for seakeeping analysis, works well if used within its designed scope. Apparently, both *Jensen et al. (2004)* and *Bertram (2014)* agree that this method provides acceptable results, but remind us that reality is more complex. For instance, roll motions are dominated by nonlinear viscous damping, which are much more difficult to calculate.

In *Jensen's et al. (2004)* method, the ship is represented by a homogeneously loaded box-shaped barge with the beam modified so that the total mass of the ship equals the buoyancy. The method considers the vessel in regular waves and deep waters. Pitch and heave are always considered with 90° phase angle between them, disregarding coupling between them. The closed-form expressions' results were verified against model tests and strip theory calculations.

For the real-time Simulator, the motion amplitude is transposed to the time domain:

$$\eta_j(t) = |\eta_j| \times \sin(\omega \times t + \theta_j) \quad j = 3, 4, 5. \quad (1)$$

Where η_j is the closed-form expressions output for a given frequency;

ω is the wave period set by the user;

t is the time;

θ_j is the phase angle;

$j = 3, 4$ and 5 indexes refer to heave, roll and pitch, respectively.

The ocean 3D object is constructed entirely by THREE.js features. It is basically a plan geometry, Fig. 6, in which a texture is applied, Fig. 7.

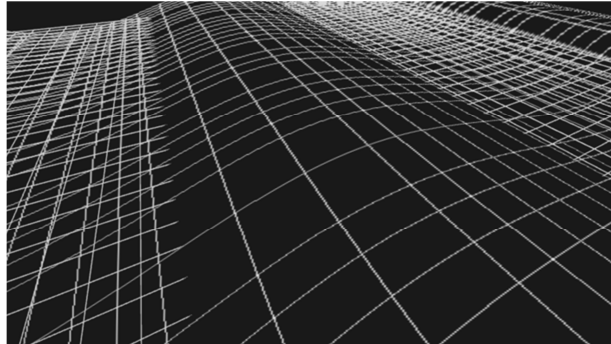


Fig. 6: Ocean dynamic geometry



Fig. 7: Ocean geometry + texture + sky

The geometry is divided in several sub-segments, and set to dynamic. The waves are generated by a normal distribution function that updates the height of each vertex, forming waves in the plan. The normal distribution complies with the wave elevation equation for regular waves.

$$\zeta(x, t) = \zeta_a \times \sin(\omega \times t - k \times \vec{x})^0 \quad (2)$$

Where ζ_a is the wave amplitude set by the user;

x is assumed zero.

The console, Fig. 10, allows the user to define wave characteristics, scale vessel's main dimensions, and input hull form coefficients. At the moment these are changed, the application updates all the calculation and visualization instantaneously. Although the backside calculation is based on wave fre-

quency, this parameter is inverted in the GUI. For practical reasons and usability concerns, wave period is the parameter that the user specifies.

4.2 Simulator workflow

The Simulator workflow can be explained as any other input-process-output system, Fig. 8. It runs in two synchronized parallel routines that use the same input parameters. Each step is explained as follows.

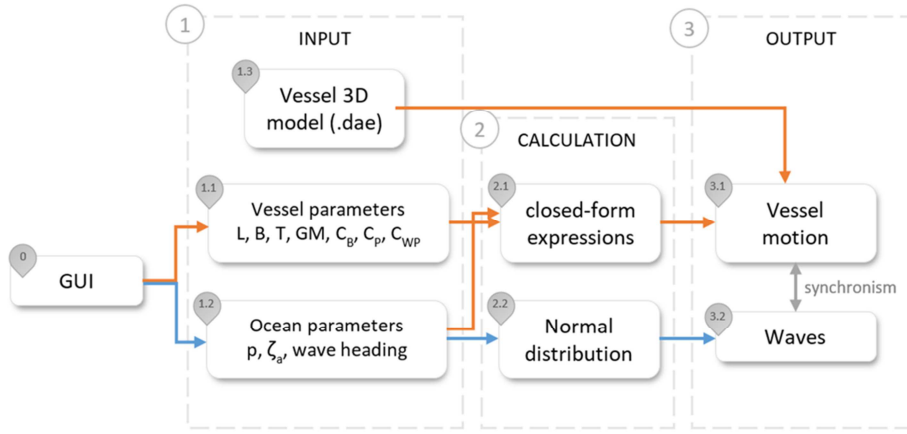


Fig. 8: Ship Motion Simulator workflow

The GUI centralizes all inputs the user can manage. It provides interactivity and instantaneously response. As a matter of organization, the GUI inputs are divided into vessel and ocean parameters:

- Input 1.1 - Parameters related to the hull form, exclusively used for the vessel motion calculation. They are length, beam, draught, metacentric height, block coefficient, prismatic length ratio, and waterplane area coefficient.
- Input 1.2 - Parameters related to the sea state, used for calculating vessel motions and wave generation. They are wave period, amplitude and heading.
- Calculation 2.1 - The closed-form expressions calculate the wave-induced motion for the parameters given in the GUI and return the motion amplitudes (heave, pitch and roll) separately. This function is called every rendered time step as the application runs; so every change in the GUI will automatically update the amplitudes.
- Calculation 2.2 - The normal distribution generates regular waves as a sinusoid. The same parameters used in Calculation 2.1 are used here. There is no collision or physics engines calculating the interaction between the ocean and the vessel; they are rather ruled by two distinct synchronized set of equations. The ocean is simply a representation of the waves coming in the vessel, which are considered inside the closed-form expressions.
- Output 3.1 - The vessel motion is given by Eq.(1) and updated every render loop. This formula returns motion amplitudes for each time step, and assigns it to the vessel's 3D model (Input 1.3), making the model to move.
- Output 3.2 - The waves' formation is given by Eq.(2), which is updated in the same time step as Eq.(1). This formula applied to the ocean geometry generates the waves.

5. Web Based Real-Time 3D Simulator - Virtual Prototype and Motion Prediction

The application interface is very clean and focuses on the 3D environment. All features are meant to be straightforward and user-friendly. There is no need to ‘learn the software’, as it will be intuitively unveiled within few minutes of use.

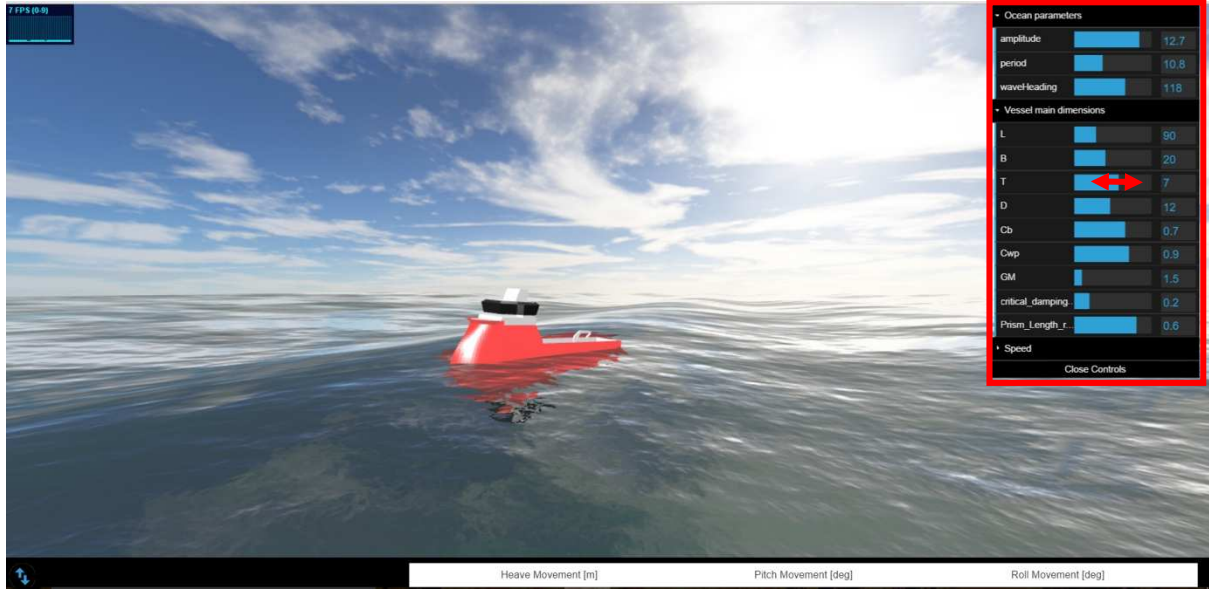


Fig. 9: Ship Motion Simulator: GUI

The GUI stays at the right-hand side, Fig. 9, and allows the user to vary each parameter value either by dragging and dropping the blue bars or typing a number. For better precision, it is advised to type the desired value. There is a retractable tab at the bottom side of the application, which contains the closed-form expressions output, the movements' amplitude, and the wave length corresponding to the given wave period, Fig. 10. The wave length λ is calculated under the assumption of deep water as:

$$\lambda = \frac{2\pi g}{\omega^2} \quad (3)$$

g is the gravity acceleration, ω the wave circular frequency.

Also, down the page, there are graphs of the three uncoupled motions of the vessel, Fig. 11. The same formulas responsible for updating vessel's position and rotation also feed the graphs. In this way, they display the vessel motion in real-time, along with the 3D model.

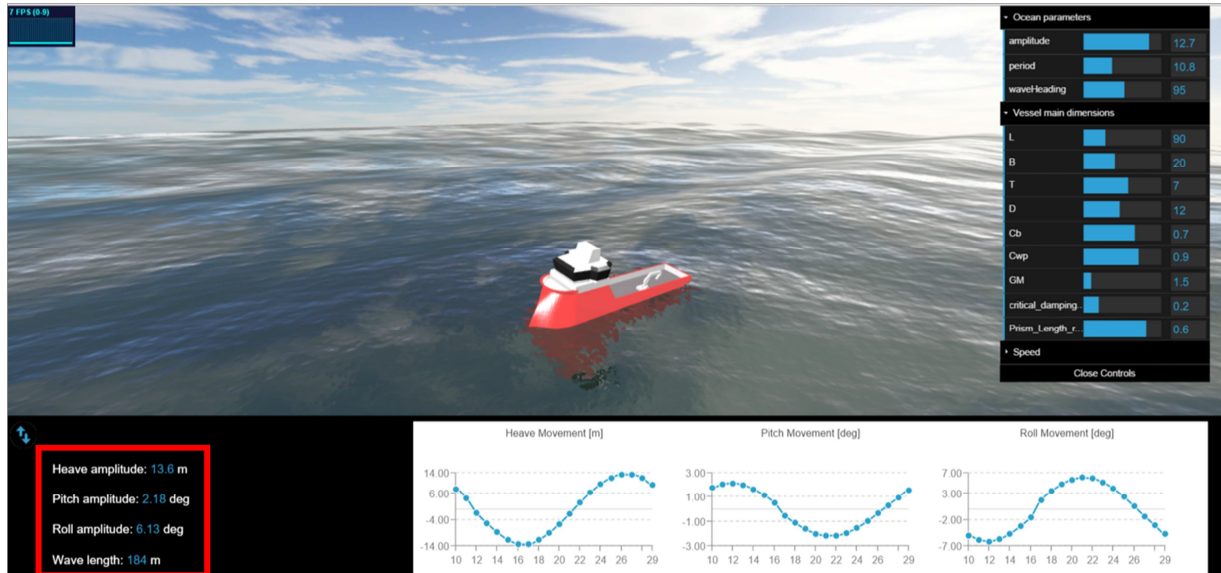


Fig. 10: Ship Motion Simulator: Amplitudes

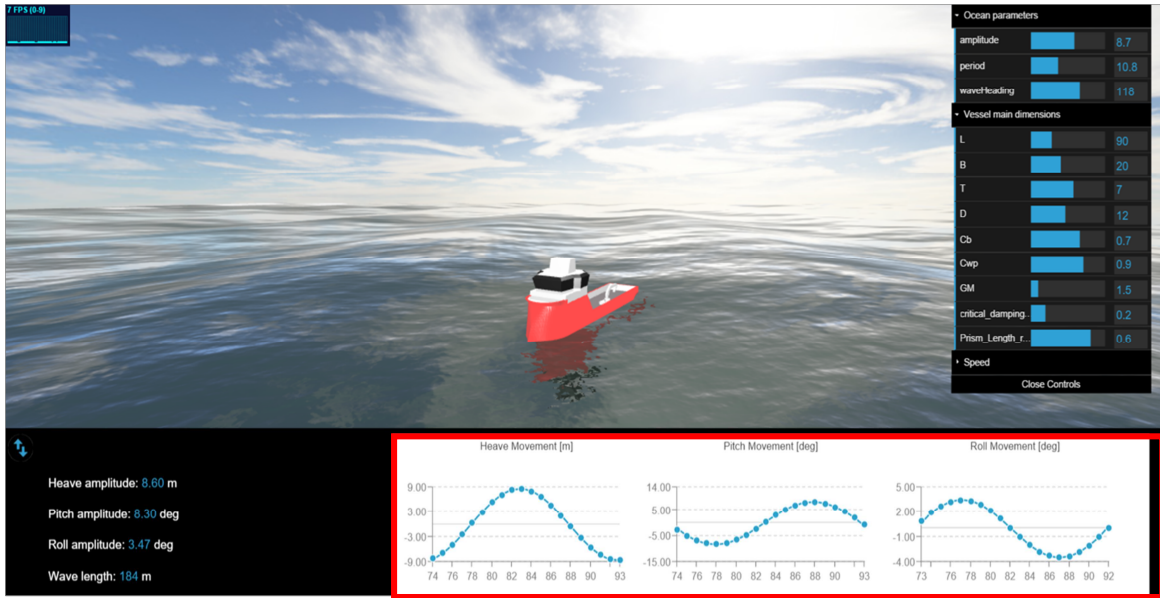


Fig. 11: Ship Motion Simulator: Real-time graphs

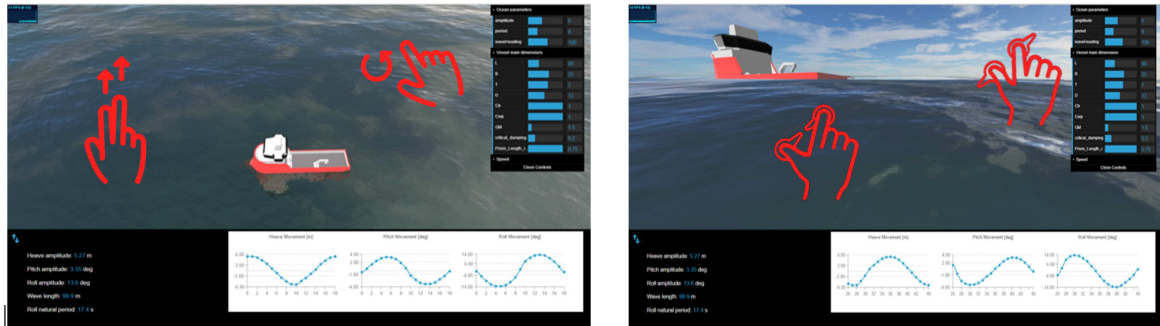


Fig.12: Ship Motion Simulator: Controls

It is also possible to navigate through the 3D environment. On mouse-controlled devices, the right button drags and drop the scene, the left button rotates it, and the scrolling button zooms in and out. On touchscreen devices, the controls are even more intuitive, since it follows the same scheme as in any other application: pinch to zoom in and out, twist fingers to rotate, and slide your finger to drag, Fig. 12.

6. Concluding remarks and extension of the work

There is no doubt that the current level of web-based technology allows the creation of simple and customized web-based tools that facilitate the engineer's and the designer's work. Mainly in early design stages, those tools provide enough support to go on with the project, saving time and money. Using open and free resources, it is possible to create applications to improve working practices.

If these applications are made open it favors fast and collaborative development. Open-source codes allow any user to add contributions, thus accelerating improvements. However, cooperation has its limits. While we can find many cooperative examples among academic developers, industry seems to make much less use of such boost. Most companies (or even scholars) are not willing to share their proprietary knowledge and assets. In doing so, they renounce all the benefits a cooperative undertaking could bring, balancing between profitability and obsolescence.

Our experience is that JavaScript has proved its versatility and potential when applied to maritime engineering toolbox. Diverse free libraries are available to implement brand new capabilities, or improve the existing ones without the need of hard coding. With the development of advanced solvers, more complex formulations can be implemented, and the computational capacity hardly will be a constraint.

Visualizing the system's response in a 3D web environment is certainly an enhancement when compared to the traditional 2D graphs, which often are not obvious to interpret even for experts. For the client side, companies can explain or document their results much more intuitively. 3D is appealing and understandable by anyone.

Considering JavaScript's expected durability, no work is likely to be lost or outdated, favoring developments continuity. New features are in process to be implemented in the presented application, such as first person camera view and motion. Further work could point towards a platform multi-user, where the same virtual environment would support two simulations at the same time, commanded by two users in different machines, possibly interacting with each other.

Acknowledgments

The Simulator's source code benefited from Juliano Monte-Mor's (UNIFEI, Brazil) and Elias Hasle's (NTNU, Norway) expertise in programming. They significantly contributed to improve the code and fix bugs, providing fundamental assistance. We also benefited from Lars Ivar's (NTNU, Norway) work, experience in developing WebGL engineering tools, and assistance, helping on the project's kick off. This research is connected to the Ship Design and Operations Lab at NTNU in Ålesund, which is partly supported by the EMIS Project, in cooperation with Ulstein International AS (Norway) and the Research Council of Norway.

References

- BERTRAM, V.; VEELO, B.; SÖDING, H.; GRAF, K. (2006), *Development of a freely available strip method for seakeeping*, 6th Conf. Computer and IT Applications to the Maritime Industries (COMPIT), Oestgeest, pp.356-368
- BERTRAM, V. (2014), *Computational methods for seakeeping and added resistance in waves*, 13th Conf. Computer and IT Applications to the Maritime Industries (COMPIT), Redworth, pp.8-16
- CHAVES, O.; NICKELSEN, M.; GASPAR, H.M. (2015), *Enhancing virtual prototype in ship design using modular techniques*, 29th Eur. Conf. Modelling and Simulation (ECMS), Varna
- GINSBURG, D.; GERHARD, S.; CALLE, J.E.; PIENAAR, R. (2011), *Realtime visualization of the connectome in the browser using Webgl*, 4th INCF Congress of Neuroinformatics, Boston
- HOOS, E.; GRÖGER, C.; MITSCHANG, B. (2015), *Mobile apps in engineering: a process-driven analysis of business potentials and technical challenges*, CIRP 33, pp.17-22
- JENSEN, J.J.; MANSOUR, A.E.; OLSEN, A.S. (2004), *Estimation of ship motions using closed-form expressions*, Ocean Engineering 31/1, pp.61-85
- PRESSMAN, R. (2005), *Software engineering: A Practitioner's Approach*, McGraw-Hill

Big Data and (Inland) Shipping: A Sensible Contribution to a Strong Future

Arno Bons, MARIN, Wageningen/The Netherlands, a.bons@marin.nl
Meeuwis van Wirdum, MARIN, Wageningen/The Netherlands, m.v.wirdum@marin.nl

Abstract

Inland shipping is constantly being challenged to improve both economic and environmental performance. From a hydrodynamic and operational perspective a large improvement potential remains merely unused. This paper describes how CoVadem introduces a big data solution that will add significant value to the inland shipping industry. Cooperatively sourced big data from a growing pool of over 50 vessels all over Europe (over 55.000.000 measured values a day) is used to provide effective key performance indicators (KPI's) to judge actual performance and cater for the necessary metrics to analyze, interpret and decide upon improvement measures. With the right technical and organizational implementation a revolutionary basis is introduced that allows for effective, continuous and holistic improvement.

1. Introduction

Whatever the level of expertise of the entrepreneur and his organization may be, one of the main prerequisites for effective business optimization is the availability of reliable metrics. The availability of actual and relevant metrics allows for the definition of effective Key Performance Indicators (KPI's), that in turn will serve effective decision making and allow for the analysis of effective optimization measures.

Where other businesses often benefit from higher economies of scale, challenges for Inland Water Transport (IWT) are rising when it comes to the upkeep of their traditional competitive advantage in terms of both business efficiency, fuel economy and – more and more important – environmental performance. In recent years, in other transport modes a significant increase in the availability of (big) data, continuously being harvested from a wide variety of sources proves to be capable of generating new forms of insight, often with a high actuality and at relatively low costs. Although a significant amount of relevant signals are available on individual ships, they tend to be stand alone, not logged, and not combined. IWT has long been lagging behind in respect of the application of these modern day information developments.

Turning their backlog into a benefit, the CoVadem consortium (www.covadem.com) has taken the initiative to arrange for a trusted and reliable organization model right from the start. This model incorporates the relevant experience in other sectors and allows for a supervised, trusted introduction of a long term focus business model of relevant new information. At the same time CoVadem initiates a parallel and joint stakeholder research program to further develop value adding applications of these data for the future.

With the generation and provision of both actual and forecasted navigable water depths along the EU IWT network, CoVadem not only aims to add significant value to IWT infrastructure users, the skippers. CoVadem also generates promising new possibilities for river bed monitoring, dredging management and knowledge validation and development. Shortly following the generation of actual water depths is the introduction of innovative performance monitoring.

For the first time in history of inland shipping, fuel consumption is being monitored against relevant other parameters such as under keel clearance, cargo load and other indicators on a continuous, straight through processed basis. This is extremely relevant as this generates a unique insight in the operational profiles of inland vessels without the introduction of administrative burden. Thus, CoVadem will allow for real time voyage optimization, new and updated understanding of vessel-

cargo-river-voyage interactions (allowing for improved future vessel and logistics development) as well as new, updated and improved understanding of river hydrology, water management etc, allowing for improved water safety.

CoVadem thus unleashes the potential of collaborative big data deployment for the generation of a wide range of metrics and KPI's, allowing today's entrepreneurial experts to effectively improve efficiency, societal benefits and environmental performance. CoVadem combines the available bits of information and turns them in hands on improvement potential. CoVadem aims to become the biggest preferred and widely accepted measurement network for IWT vessels and infrastructure, without having own sensors installed onboard.

This paper reviews the relevance of performance monitoring in relation to environmental values such as water depths, itineraries and cargo load specifications. Furthermore, it elaborates the unique organisational approach CoVadem is working on, as this is a key feature in the quest to establish a self supporting business plan that at the same time maintains high levels of confidentiality, security, objectivity and neutrality within a trusted environment.

2. Real time and future water depth information

2.1. Big data and inland shipping

The basis of the CoVadem system is the generation of a real time water depth chart, based on the individual echo sounder data of participating ships. With this basis, the generation and provision of both actual and forecasted navigable water depths along the EU IWT network comes within reach. Currently over 50 inland ships are participating in the CoVadem network. These ships navigate the European inland waterways, continuously sharing water depth information. The echo-sounder, loading gauges and GPS already present onboard an inland ship are linked to one another via the CoVadem Box, a universal multiplexing device developed by CoVadem. Each second, this device gathers raw measurement data from these sensors and forwards them to a server onshore, Fig. 1. These data need to be processed in order to create valuable information for CoVadem based calculations. Two main post processing steps are mentioned in the next chapter. All post processing of raw data is carried out on servers onshore. Therefore, the CoVadem Box onboard does not need large computer processing power, which reduces the hardware costs.

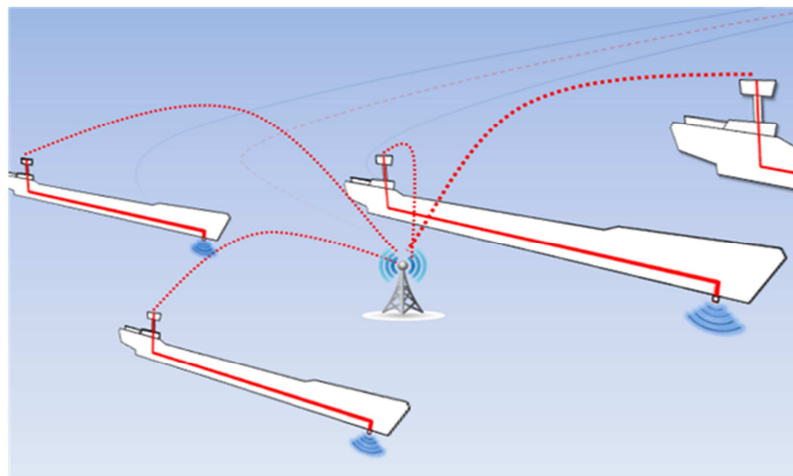


Fig. 1: CoVadem creates Big Data by a network of participating inland vessels

With permission of all the participating ships, anonymous measurement data of individual ships is aggregated and redistributed to the benefit of all participants. CoVadem creates profiles of the European waterways for individual ships, Fig. 2. For more detailed information about the generation of a real time water depths chart by using collaborative measurement data, *Bons et al. (2015)*.

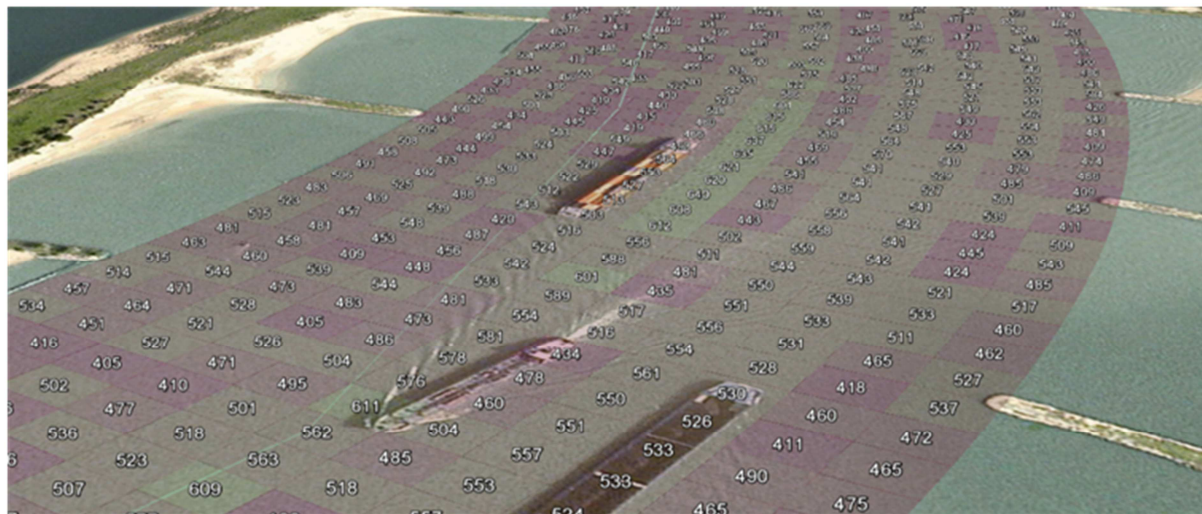


Fig. 2: Real time CoVadem water depths (in cm) presented on Google Earth

2.2 Hydrodynamic and hydrological prediction models

The hydrodynamic and hydrological prediction models of the Dutch knowledge institutes MARIN and Deltares, respectively, play an important part in the post processing of the raw measurement data gathered from sensors of the participating ships. The function of both prediction models are briefly described below.

The MARIN developed hydrodynamic prediction model, called Virtual Ship, accounts for the continuous calculation of dynamic influences. Aiming at a real time insight in local water depths, the measured under keel clearance by the echo sounder, has to be corrected for initial draught and for squat. Squat is the reduction of under keel clearance resulting from dynamic hull sinkage and trim, which occurs when a ship moves through the water, especially in confined water. The virtual ship is a based on Ankudinov predictions, *Ankudinov et al. (1996)*, verified by systematic CFD calculations at MARIN. More details about the virtual ship can be read in *BONS et al. (2015)*.

A key component of CoVadem is the FEWS-Waterways model of Deltares, which is an operational real time hydrological forecasting model. The operational system computes actual and predicts future water depths and flow velocities in width and length of the waterway. These data are usefull by themselves, but are also input for extra CoVadem based applications such as the calculation of the optimal track in the river and the maximum amount of cargo that can be transported. In addition, the optimal speed during the entire voyage will be calculated and continuously updated in relation to the desired ETA (Expected Time of Arrival), for which fuel consumption and emissions are minimal. Since the calculation of future predictions needs the real time situation as input, the more ships collect and share their data with each other, the more detailed and accurate the actual navigation depth chart becomes, and the more accurate the future predictions become. More detailed information about the FEWS-Waterways module can be read in *Mark et al. (2014)*.

2.3. The benefits: more cargo, less fuel, less emissions

The use of inland waterways can be optimized if real time water depths and clearance below bridges are available continuously and throughout the main network. Within CoVadem, a principle is developed for collaborative data collection by inland ships. Based on the gathered data, individual ships gain access to real time river depth information. Skippers are enabled to optimize cargo volumes in accordance with actual fairway conditions. Furthermore, fuel consumption can be reduced by supporting energy efficient ship operation by the implementation of hydrodynamic modelling.

The provision of real time and future water depth information can be used to provide vessel specific

information allowing maximized cargo capacity and avoidance of grounding and collisions with objects, like bridges, for each specific trip. Depending on the route and actual water levels, IWT vessels often cannot be fully loaded. Measures need to be taken in order to pass the critical sections on the route. During high water levels on the other hand, the air clearance under bridges becomes important.

In general, CoVadem integrates cooperatively sourced depth soundings in order to provide the best possible voyage information and planning in terms of economy, environment and efficiency. In the future, the system will be expanded to incorporate predictions as well. The basic functionalities and applications of the CoVadem data aims at:

- Generation of real time local water depth information based on cooperative depth measurements;
- Determination of maximum allowable loading condition for specific voyages based on real time and future water depth predictions;
- Determination of the optimal track in terms of minimum fuel consumption, incorporating the vessel and route specific hydrodynamic interactions;
- Supporting skippers on optimal engine settings during the voyage in relation to the desired ETA, for which fuel consumption and emissions are minimal.

Based on real time water depth information, services are being developed that support energy efficient ship operation. One of the services is the Virtual Ship module developed by MARIN which optimizes total fuel consumption for a given route. Furthermore, the Virtual Ships advises skippers on optimal rpm during the voyage. More details about the virtual ship can be read in *Bons et al. (2015)*.

3. Performance monitoring

Since 2015, CoVadem has added fuel consumption monitoring to some of the participating vessels. By doing so, CoVadem is further enhancing the principle of collaborative data acquisition for improved performance of IWT and incorporates automated performance administration.

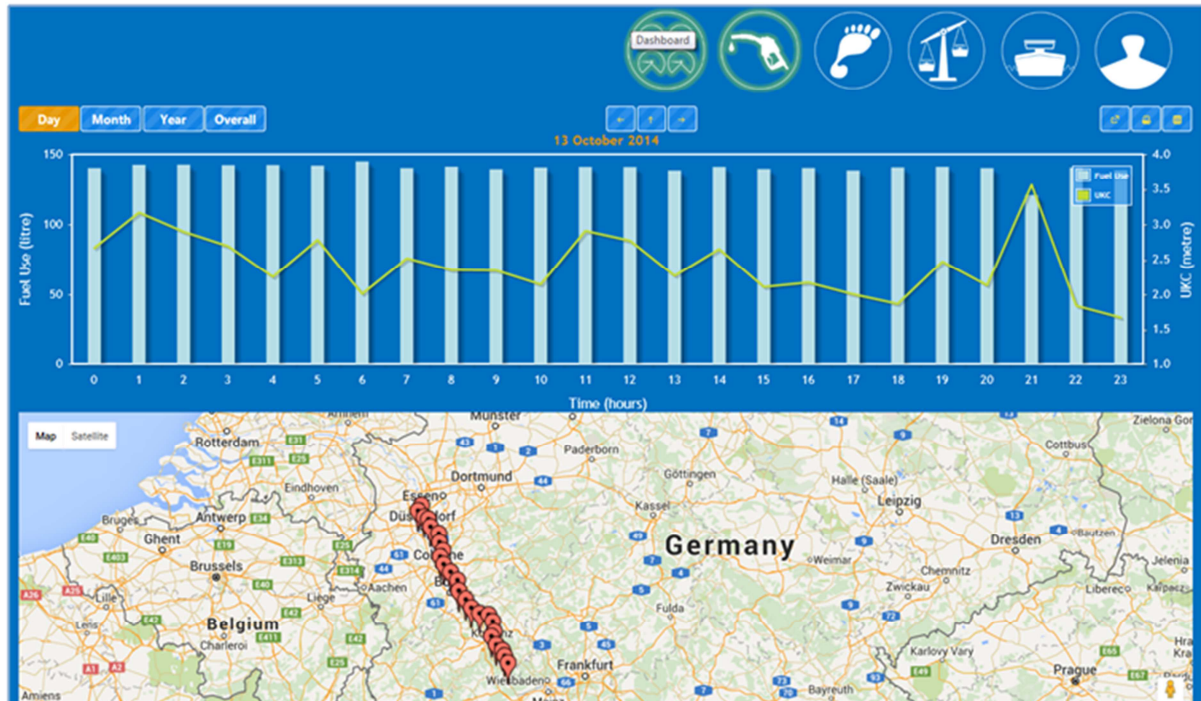


Fig. 3: Performance web application

A performance web application is developed that can be used on almost any smart phone, tablet or computer. Performance data can be shown for a period of minutes, days, months or years. For the selected time period, the location of the vessel is shown on a map. The CoVadem performance web application displays the fuel consumption related to the under keel clearance in a way that can easily be understood by vessel operators. Consequently CoVadem has developed a working concept that relates ship performance to the river condition, Fig. 3. Furthermore, an energy and emission dashboard for onboard use is created. The cumulative values are displayed for sailed distance, tons of cargo transported, fuel consumption and emission CO₂. In addition, the averages are given for sailing speed, under keel clearance, ton fuel consumption, fuel consumption per ton kilometres and emissions of CO₂.

Finally, ship owners can compare their own performance with the anonymous rest of the CoVadem fleet. Of course there is much to discuss about comparing the performance of vessels, since it is impossible to find identical ships sailing with identical loading conditions in exactly the same weather and fairway conditions. Nevertheless, the goal of the performance application is to benchmark with an anonymous selection of “comparable” vessels. In general, CoVadem aims at enabling ‘high performance’ vessel owners to objectively share their performance with third parties in order to increase environmental awareness amongst their contractors and strengthen their market position. Encouraging people to invest in sustainable solutions by means of independent performance indicators is a proven concept. For example, since January 2008, all residential property offered for sale in the Netherlands must have an ‘energy label’. By means of a rating, the label provides an indication of the home’s energy efficiency. The rationale is that homes with a good energy rating will be more attractive to potential buyers or tenants than those which are less efficient. This will encourage owners to invest in energy-saving measures. By the introduction of working benchmarking principles and on the basis of transparent performance data CoVadem is expected to have a large impact on the way IWT is dealing with performance in general.

4. Added value for each stakeholder

Big data and (inland) shipping: a sensible contribution to a strong future. Cooperatively sourced big data from CoVadem not only aims to add significant value to IWT infrastructure users; the skippers, but for the complete IWT sector. Potential benefits for each stakeholder are described below.

4.1. Fleet / Vessel operators

More cargo, less fuel and fewer emissions. Skippers are enabled to optimize cargo volumes in accordance with actual fairway conditions. Furthermore, fuel consumption can be reduced by supporting energy efficient ship operation, which result in reducing individual carbon footprint, lower emissions per ton kilometre and more reliable ETA’s. Some benefits:

- Skippers continuously have access to real time and future (water depth) information to get the most out of their vessels, voyages and cargo, without losing transport productivity.
- Skippers have access to a set of information to optimize voyage planning and increase the reliability of their service, which can be implemented in existing products and services of third parties, like navigation systems, voyage planners and performance monitoring systems.
- A system is developed that provides skippers with insight in their ship performance related to the actual fairway condition. A reliable, objective and independent body in the ‘golden triangle’ of public bodies, industry and knowledge institutes supervises the use of their data, as outlined in the next chapter.

4.2. Inland ship owners

In addition to the benefits of skipper, the ship owner will have full access to data of his fleet, which enables him to carry out adequate performance analyses.

4.3. Transport and logistics

The added value for logistics chain partners is to strengthen the role of inland navigation in the logistics sector. By sharing the performance information of the participating vessels, environmental gains, energy efficiency gains and more reliable ETA's can be achieved.

4.4. Emission monitoring

Currently, emission level conformity is based on the availability of a valid engine type approval. In reality, however, studies have shown that real life emissions of type approved engines are not necessarily lower than those of engines with older type approvals or engines with no type approval at all. This is particularly relevant in case of the application of retrofit emission reduction techniques.

Nowadays, the Dutch Authority responsible for the enforcement of emission level conformity in IWT is studying the feasibility of a new approach based on real time on board measurements, and the requirements to set for the relevant measurements.

By providing a trusted, secure and accepted network for on board data, CoVadem facilitates the vessel operator to share relevant data with, in this case, the authorities while remaining in control over their data: they determine whether or not and which data they want to share. In this way the network is not threatening the users. If the vessel owner actually wants to share particular information with a defined set of others is actually up to bilateral agreement between the vessel owner and the party in question. For example: as the engine of vessel X has no valid type approval for area Y, the vessel owner will be forced to install a new engine in order to still be able to operate in that area. If in fact the emission levels of his existing engine prove to be according to the enforced admission level, sharing his data with the authorities might save him the cost of an engine replacement. CoVadem will in that case serve as a neutral base for his performance data and leaves the vessel owner in control.

A second development worthy to mention here is the fact that not only officials are interested in measured data, but also market stakeholders gain an increased interest in metrics concerning transport mode performance as to serve their Corporate Social Responsibilities Goals and client base with reliable and transparent metrics concerning (emission, CO₂) performance. Being able to serve clients with transparent data might eventually turn into a prerequisite to obtaining the best orders and thus become of substantial business value.

4.5. Waterway Management Authorities

Real time water depth information in combination with hydrological prediction models, like FEWS-Waterways model of Deltares, enables proactive instead of reactive waterway management. Nowadays, waterway authorities use survey vessels equipped with multibeam echo sounders to acquire water depth information; to determine water depths, obstructions, and dangers to navigation. In the Netherlands, these surveys are executed two times a year. Most of the time, critical points on the river are removed just in time, which requires continuous availability of dredging equipment. Due to the network of vessels sailing continuously over the rivers, a new data source comes available, which enables better understanding of the development of river bathymetry. Finally, the employability of dredging equipment can be improved, which result in lower waterway maintenance costs.

4.6. Knowledge institutes

Real world measurement data is valuable for the development of new or improved services. This new source of big data consisting of real time measurements can be used for:

- Validation of existing tools like the hydrodynamic and hydrological prediction tools of MARIN and Deltares respectively;
- Improvement of existing hydrodynamic and hydrological prediction tools and models;

- Better understanding of river bathymetry developments by using real time and predicted data. Furthermore, this gives better insight in the impact of measures taken on the waterway.

4.7. Design and engineering

Instead of using the traditional spiral design methodology based on a single design point, naval architects can accomplish concept design point studies based on operational aspects. These studies can be checked by means of this new source of measurement data of CoVadem, which gives better insight in the real operational profiles of inland vessels.

4.8. Society

In general, using collaborative data will improve the performance of inland shipping, which will be cleaner and more energy efficient shipping.

5. Technical and organizational implementation

Currently, over 50 vessels participating the CoVadem network. The organization is in a transitional stage from research project to a financial self sufficient-system with 250 vessels. First of all to have a better coverage of (water depth) information of the waterways all over Europe in the coming years. This financial self sufficient-system is also necessary because more and more customers of CoVadem data are expected, taking into account the potential stakeholders as mentioned in the previous chapter. Scaling up to 250 vessels requires a reliable, scalable, fast and secure database service. Furthermore, supervision of the CoVadem data by an independent organization is required in order to obtain acceptance by the IWT.

5.1. Technical implementation of database service

In 2013, CoVadem started with storage of measurement data and computing services on local databases at Autena Marine and MARIN. For research purposes, this technical implementation was sufficient for the prove of concept that collaborative measurement data can be used to improve the performance of inland shipping. The concept has shown that a real time water depth chart can be generated by using collaborative measurement data. With this information the ship operator is capable to optimize his voyage in terms of cargo, reliability and fuel economy, see *Bons et al. (2015)*.

At the moment, cooperatively sourced big data is obtained from a growing pool of over 50 vessels. Subsequently, there are about 15 to 20 tracks on the CoVadem pilot section of the river Waal per day. In total CoVadem receives over 55.000.000 measured values a day, which has to be processed and stored. Note, this is only the beginning of big data and inland shipping. Serious plans are being made to scale up the network to 250 participating vessels in the coming years. Due to a growing network of participating vessels and a growing number of projects using CoVadem data, the ICT infrastructure had to change to provide a reliable 24/7 data service to IWT.

Therefore a production database service is set up with a bigger scalable storage capacity, which delivers a fast and consistent input/output operations performance. At the end of 2015 the local CoVadem databases are moved to an Amazon relational database service in the cloud, which makes it easy to set up, operate, and scale a relational database. It makes use of a highly reliable infrastructure with the possibility to scale database's computing and storage resources often without any downtime. Furthermore, the cloud service provides security policies to prevent unauthorised use and access by third parties. The layout of the current ICT-infrastructure is shown in Fig. 4.

Each individual ship forwards real time measurement data to the raw measurement database with an upload frequency of 1 Hz. The most important measurement parameters are: local time, under keel clearance, initial draught and GPS position. In addition, fuel consumption is monitored on board of

some of the participating vessels since 2015. Besides measurement parameters, some main particulars and the positions of the sensors of the ship are required. These parameters have to be defined once by the installer of the CoVadem Box onboard. This is done via a ship configuration web page and the data is stored in a separate ship database.

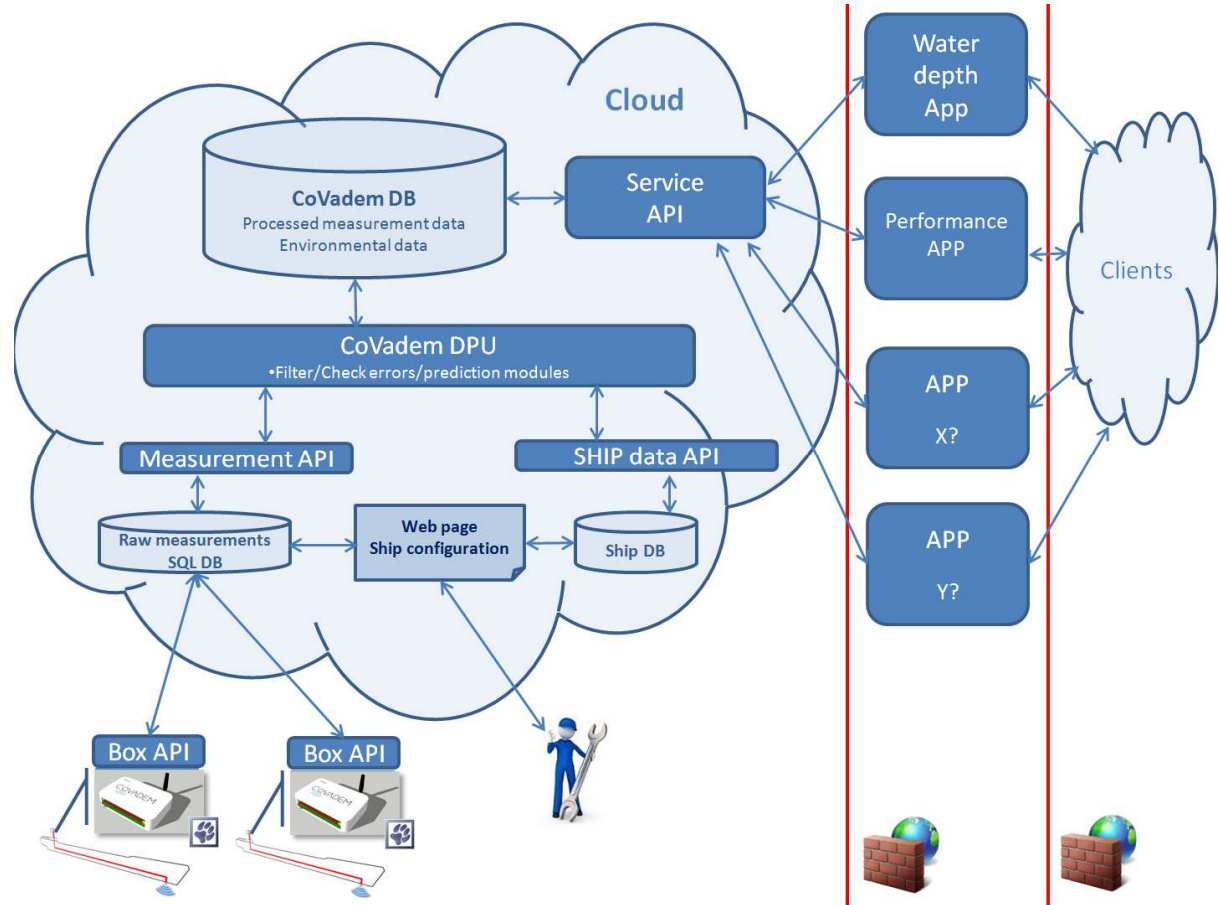


Fig. 4: ICT infrastructure CoVadem database service

The measurement data is filtered and processed by the data processing unit. One of the processing steps is adding a column of calculated water depths. Since we are interested in the local water depth, the measured under keel clearance has to be corrected for initial draught and for squat, which is briefly explained in chapter 2.2. The data processing unit manages the CoVadem databases and polls the measurement database. By means of the service application programming interface (service API) data can be made available to CoVadem based applications. For security and maintenance reasons it is very important that CoVadem based applications does not have permission for direct access to the CoVadem cloud database. By introducing a service API an extra security layer is created to protect CoVadem information securely against unauthorised use and access.

A detailed description of the ICT infrastructure can be read in *Molenmaker (2014)*, containing the description of the file formats of data to be exchanged between the different computational modules of CoVadem, the technical description of the interfaces and several use cases.

5.2. Organizational implementation

Since CoVadem is in a transitional stage from a research project to a financial self sustaining system with >250 vessels, it is very important to set up an independent organization that is accepted by both the IWT sector and other stakeholders needed to cater for financial self sustainability. This is relevant for IWT in particular, where, considering the long lasting discussions on the confidentiality of AIS signals, the privacy must be treated with utmost attention.

Rapid developments in other market segments have by now resulted in a vast amount of experiences concerning the collection, enrichment, management and distribution of big data and the organisational approaches around it. Here, IWT can turn its typical backlog in this field of expertise into an advantage.

This means that the CoVadem organization, management and control should be set up in such a way that it can be guaranteed that measured data cannot be traced back to an individual participating vessel or ship owner without the acceptance of the ship owner, to keep all participating vessels onboard the project. Finally, the end user, skipper or ship owner, should determine whether or not and which (anonymous) individual measurement data they want to share with applications and/or parties. The CoVadem organization will be set up from a point of view that an independent, secure and reliable governance is guaranteed. The practical operational data management and market implementation will be done by a separate company and will be supervised by an independent supervisory body in the 'golden triangle' of public bodies, industry and knowledge institutes, which is required in order to obtain and maintain acceptance by the IWT stakeholders. This independent supervisory body will be a foundation that controls authorised use and access of maritime inland data, Fig. 5.

To scale up the network to 250 vessels, costs are involved to purchase, install and maintain hardware on each vessel. Other costs are involved to scale up and maintain the ICT infrastructure and to set up an organization as described above. Since this big data initiative for inland shipping is a cross-sectoral cooperation, it should be financed by the Dutch top sectors Water (Delta, Maritime) and Logistics, by crowd funding from IWT companies/organizations and financial support from public bodies, Fig. 5.

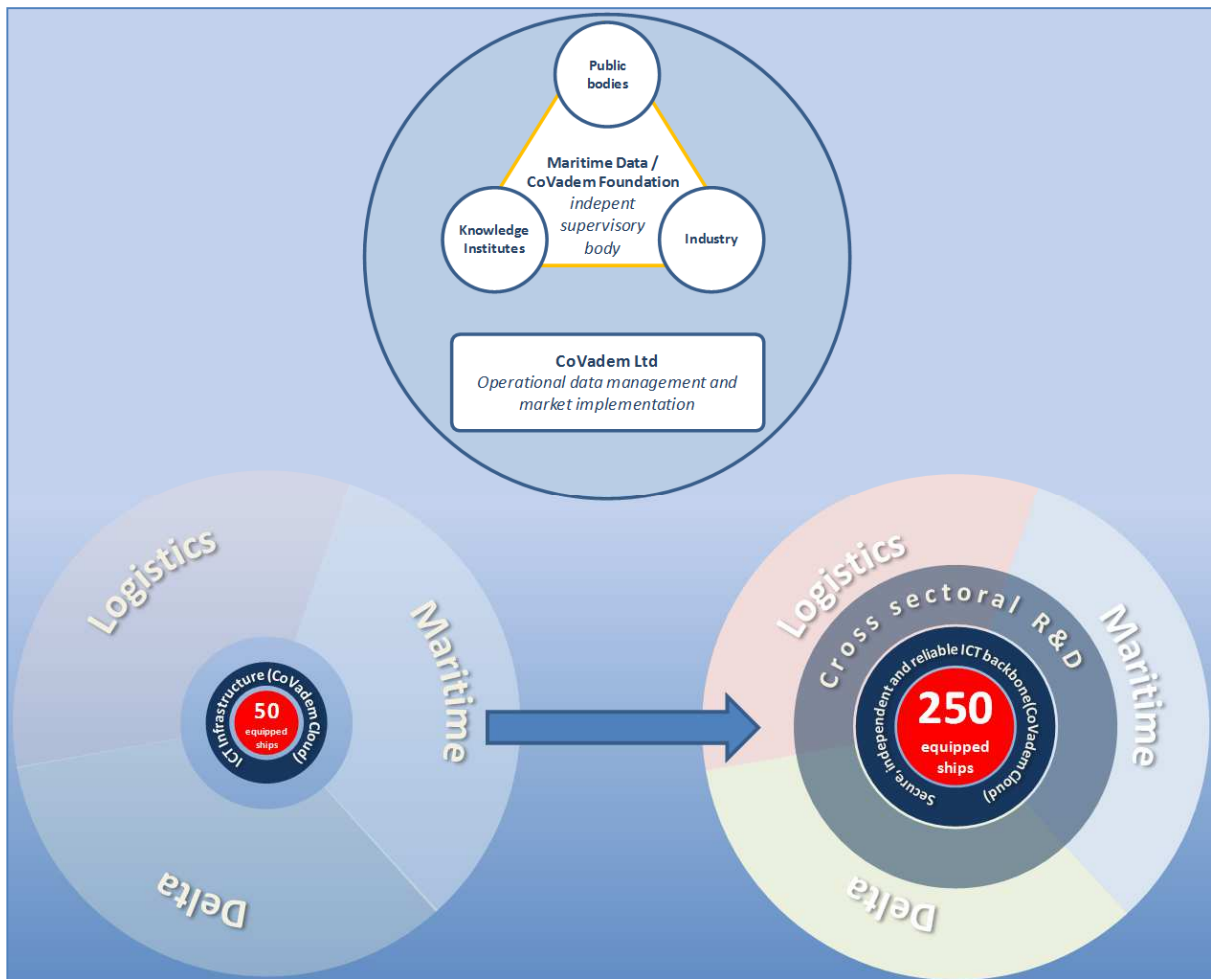


Fig. 5: Implementation of CoVadem organization

6. Conclusions

The CoVadem consortium has successfully introduced a big data solution that will add significant value to the inland shipping industry. At the moment, cooperatively sourced big data from a growing pool of over 50 vessels all over Europe to provide effective key performance indicators to judge actual performance and to analyze necessary metrics, interpret and decide upon improvement measures.

By using these data, the individual ships gain access to actual and future river depth information. With this information, the ship operator is capable to optimize his voyage in terms of cargo, reliability and fuel economy. The first added value for ship owners is the provision of the maximum allowable loading condition for a given route, in such a way that critical points on the route can be passed. Secondly, a web performance application is developed which gives skippers insight in their ship performance related to the actual fairway conditions.

CoVadem currently prepares to scale up to a growing, financially self sustaining network of 250 vessels. First of all, to have a better coverage of (water depth) information of the main waterway corridors all over Western Europe in the coming years. This ambition requires a reliable, scalable, fast and secure database service. Such an ICT infrastructure is realized, which is ready for the future. Furthermore, supervision by an independent organization that controls authorised use and access of collaborative data is required in order to get accepted by the IWT community.

This paper shows that big data for inland shipping not only aims to add significant value to IWT infrastructure users but also to ship owners, waterway authorities, transport and logistics chain partners, knowledge institutes, design and engineering companies, public bodies and the society.

Acknowledgement

The work presented in this paper is a result of research projects funded by the European Commission (FP7 EU project MoVeIT!) and Rijkswaterstaat (Dutch projects IDVV and CoVadem). The authors would like to thank the members of the projects CoVadem and MoVeIT! for their contributions and the close cooperation.

References

- ANKUDINOV, V.; DAGGET, L.; HUVAL, C.; HEWLETT, C. (1996), *Squat predictions for maneuvering applications*, Int. Conf. Marine Simulation and Ship Maneuverability (MARSIM), Rotterdam
- BONS, A; MARK, C.F.v.d.; WIRDUM.v.d.M (2015), *Collaborative data for improved performance of inland shipping*, 14th COMPIT 2015, Ulrichshusen
- MARK, C.F.v.d.; DHONDIA, J.; VERHEIJ, H. (2014); *FEWS-Waterways: Tool for sharing data between inland stakeholders*, Deltas, 34th PIANC World Cong., San Francisco
- MOLENMAKER, K. (2014), *EconomyPlanner Design Overview*, MARIN, Wageningen

On Ways to Collect and Utilize Data from Ship Operation in Naval Architecture

Jan Furustam, NAPA Group, Helsinki/Finland, jan.furustam@napa.fi

Abstract

Ashore, IoT is bringing more intelligence to everyday life resulting in smart homes and appliances that adapt to the operational environment. The same applies for ships - performance monitoring is driving increased sensor installations onboard ships offering virtually endless opportunities to learn about the way the ship is operated, what kind of weather conditions it is operating in and how the ship performs in various conditions. This offers completely new opportunities for improving ship designs to better suit the needs of operation. The paper will present a framework for data collection and analysis along with a practical example on how to utilize the results in improving a ship design. The operation of a cargo vessel is analyzed in terms of fuel oil consumption and the hull form is optimized to minimize the fuel consumption considering actual weather conditions and operational profiles that the ship has been operated in.

1. Introduction

The lifetime of the ship is long, the weather conditions which she will encounter vary, the operational profile changes. At the same time, the naval architect is serving the owner with new designs that are to be even better than the ones before – and more importantly, better than the competitor's designs. The physics of the ships behaviour is well covered in naval architecture as such but the way that the ships are operated in real life is basically restricted to the data obtained during sea trial. Typically, the ship is optimized for one design point, namely design draft and service speed. In practice, however, is the vessel often operated in quite different ways compared to what it has been designed for.

Table 1: Recorded drafts (1 h aggregation) and speeds of a container ship during 264 days at sea. Design point was never reached.

		Time Sailed [h]												
		Speed [kn]												
Draft [m]	12.0	0	0	0	0	0	0	0	0	0	0	0	0	0
	6.0	0	0	0	0	0	0	0	0	0	0	0	0	0
	6.5	0	0	0	0	0	0	0	0	0	0	0	0	0
	7.0	0	0	0	0	0	0	0	0	0	0	0	0	0
	7.5	0	0	0	0	0	0	0	0	0	0	0	0	0
	8.0	0	0	0	0	0	0	0	0	0	0	0	0	0
	8.5	0	1	0	0	0	0	0	0	0	0	0	0	0
	9.0	0	0	7	0	3	0	0	0	0	0	0	0	0
	9.5	1	1	5	1	0	0	0	0	0	0	0	0	0
	10.0	3	4	3	0	0	0	5	1	0	0	0	0	0
	10.5	6	3	11	21	29	2	14	25	0	0	0	0	0
	11.0	13	7	23	14	9	1	28	62	64	10	4	0	0
	11.5	19	17	35	38	92	14	149	86	40	35	37	16	0
	12.0	7	11	9	70	100	32	74	184	205	70	5	1	0
	12.5	12	28	228	118	366	85	141	242	168	40	0	0	0
	13.0	7	23	85	60	60	99	444	525	189	46	2	0	0
	13.5	8	29	106	73	74	11	299	442	242	131	40	0	0
	14.0	0	4	4	4	1	1	49	27	66	1	0	0	0
	14.5	0	2	2	1	1	4	12	7	2	0	0	0	0

The question arises whether the traditional design point is the way to go in the future and whether the ship should be optimized for the conditions that she most likely will encounter in real operation? If the hypothesis is that the vessel should be optimized for something else than design draft and service

speed, the next question is how to get the reliable and especially enough information about how the ship is operated.

During the past decade, fleet performance monitoring is an emerging activity which has been gaining foothold among environment conscious ship owners and operators. Today it is becoming standard to install rather extensive sensors and monitoring systems onboard – which are mainly designed to serve the operator of the vessel. But why could not the naval architect also take advantage of the valuable information that is available? In use together with the 3D product model of the ship, the information can be used for gaining important insight on how to design ship in order to make her more efficient in the future from the viewpoint of:

- The Environment (Emissions)
- Economy (Fuel bill)
- Safety (Stability, Longitudinal Strength, Motions/Seakeeping)

The ship operator uses a performance monitoring system for obtaining results that assist in optimizing the operations of the vessel. The ClassNK-NAPA GREEN solution does the following in the beginning of the value chain:

- Collecting data onboard the vessel
- Pre-processing the data (aggregations, transformations, basic statistical analysis, etc.)
- Automatically sending the data ashore
- Statistical processing (machine learning)
- Hosting of data and access to reports for the end-user

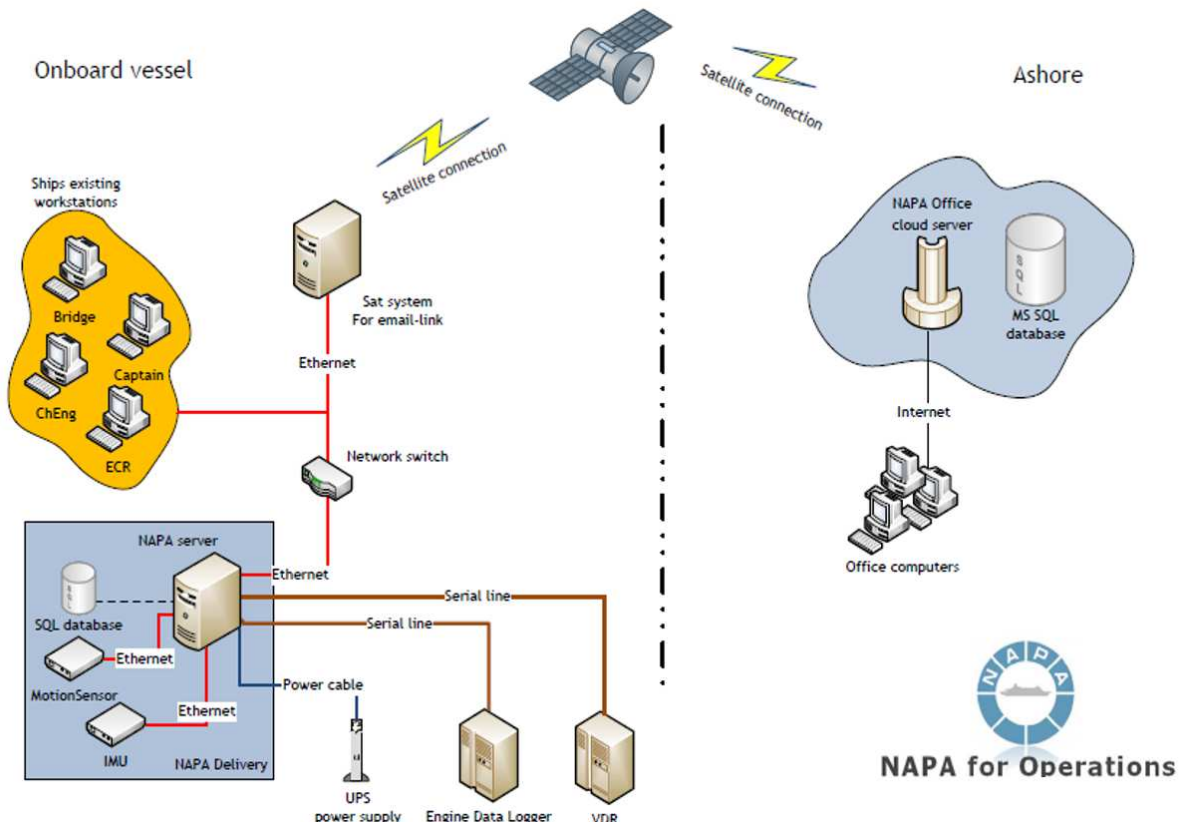


Fig. 1: Schematics of a performance monitoring system

The results of the analysed can, among other, be used for

- Improving the operation of the ship for saving fuel and safety
 - Optimal trim
 - Optimal route
- Follow-up on the development of the performance (e.g. hull fouling) which further assist on planning hull / propeller cleaning and docking.
- Detection of problems
- ...

An important part of the ship performance monitoring system with fleet performance optimization is the analysis of weather conditions and computation of optimal routes. In addition, the measurements of the encountered weather conditions and their effects on the vessel behaviour can be collected and stored for further analysis. For the naval architect, this means that completely new information (compared to the past) is available for improving designs. These new paradigms and methods in design of the hull form is discussed below for the case study on a bulk carrier, which is equipped with the ClassNK-NAPA GREEN solution.

2. Case Study: Optimizing the bulbous bow of a bulk carrier

Considering a slow cargo ship, if the hull form of the vessel is optimized for calm sea conditions, then the design may be driven by minimizing the viscous resistance as this will sum up as the largest portion of the total resistance. If this aspect is solely considered, it can be speculated that the design of the forebody will be driven towards the blunt and full direction in order to minimize the wetted surface to volume ratio and thus minimize the viscous resistance while keeping the wave resistance reasonably low.

The hypothesis of the case study are that the forebody of the vessel should be something else than the blunt and full if we

- Consider actual encountered weather conditions and put emphasis on the added resistance in waves
- Consider an actual operational profile and optimize the vessel for more than one combination of draft, trim and speed.

The example case is a bulk carrier delivered in late 2012 by Sanoyas Shipbuilding Corporation, Fig. 2 and Table 2. The vessel is equipped with an installation of the ClassNK-NAPA GREEN solution and has been logging data since the maiden voyage.



Fig. 2: The vessel used for data collection

Table 2: Principal particulars

Length Over All	229 m
Breadth	32.24 m
Depth	20.2 m
Summer Draft	14.62 m
DWT	83,027 t
GT	43,656 t
Service Speed	14.5 kn
Main Engine	MAN B&W 6S60MC-C8

The hull form used in the optimization was based on the Japan Bulk Carrier developed by NMRI and SRC. The hull form was transformed to match the main dimensions and hydrostatics of the reference vessel. The hull form of the original vessel was not used due to confidentiality reasons.

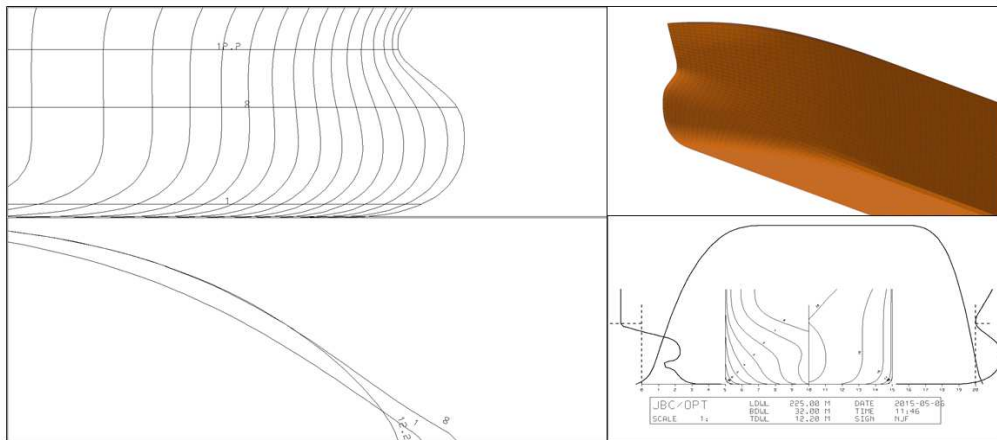


Fig. 3: The Japan Bulk Carrier hull form

3. Operational Conditions

The vessel is operated as bulk carriers normally are:

- Light/Heavy ballast
 - Design draft
 - Heavy load draft

While the design draft is 12.2 m, histograms from operation reveal that the vessel is operated typically in 4 loading conditions ranging from heavy ballast condition to full laden condition. For each draft and trim, Table 3 lists typical speeds. Table 4 lists the weather conditions that the vessel was operated in during the measurement period.

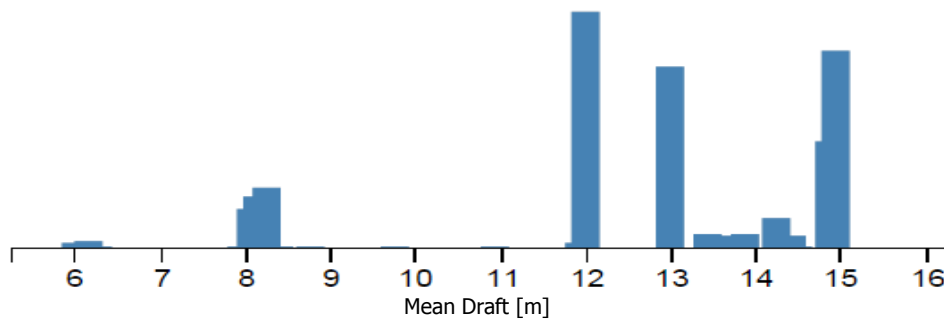


Fig. 4: Histogram of encountered drafts

Table 3: Typical loading conditions with corresponding speed

DRAFT	Trim	Speed
8.1 m	2.7 m (aft)	12.5 kn
12 m	0.6 m (aft)	11.9 kn
13 m	0.3 m (aft)	10.5 kn
14.8 m	1.4 m (aft)	12.5 kn

Table 4: Encountered weather conditions

H _{1/3}	Occurrence	%	T _Z	V _{wi}
0.5	86,100	64 %	2.8	7.9
1	24,649	18 %	4.2	10.4
1.5	11,468	9 %	5.2	11.7
2	5,229	4 %	5.8	13.9
2.5	3,026	2 %	6.4	15.3
3	2,234	2 %	6.9	16.1
3.5	1,053	1 %	7.5	15.4
4	524	0 %	8.3	16.2
4.5	282	0 %	9.5	21.8

H_{1/3} Significant wave height

Occurrence Number of measure point which satisfy the given wave height, zero crossing period and wind speed

T_Z Zero crossing period

V_{wi} Wind speed

An approximation of the wave period was applied by fitting a third-degree polynomial as a function of wave height using the collected wave data.

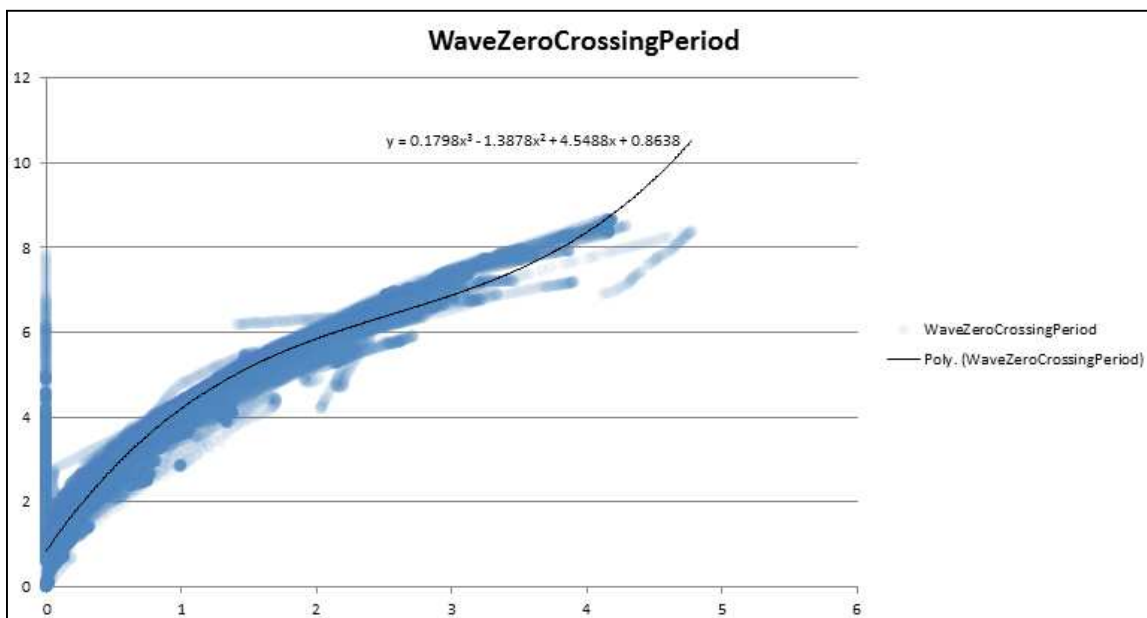


Fig. 5: Approximation of wave period

Combining the probability that a given weather condition occurs with the probability that a given load condition occurs gave a set of design conditions that were used in the optimization.

Table 5: Design conditions for optimization

V _s [kn]	T _A	T _F	H _{1/3}	T _z	V _{WI}
12.44	6.65	9.35	0.5	2.8	7.9
12.44	6.65	9.35	1	4.2	10.4
12.44	6.65	9.35	1.5	5.2	11.7
12.44	6.65	9.35	2	5.8	13.9
12.44	6.65	9.35	2.5	6.4	15.3
12.44	6.65	9.35	3	6.9	16.1
12.44	6.65	9.35	3.5	7.5	15.4
12.44	6.65	9.35	4	8.3	16.2
12.44	6.65	9.35	4.5	9.5	21.8
11.9	11.7	12.3	0.5	2.8	7.9
11.9	11.7	12.3	1	4.2	10.4
11.9	11.7	12.3	1.5	5.2	11.7
11.9	11.7	12.3	2	5.8	13.9
11.9	11.7	12.3	2.5	6.4	15.3
11.9	11.7	12.3	3	6.9	16.1
11.9	11.7	12.3	3.5	7.5	15.4
11.9	11.7	12.3	4	8.3	16.2
11.9	11.7	12.3	4.5	9.5	21.8

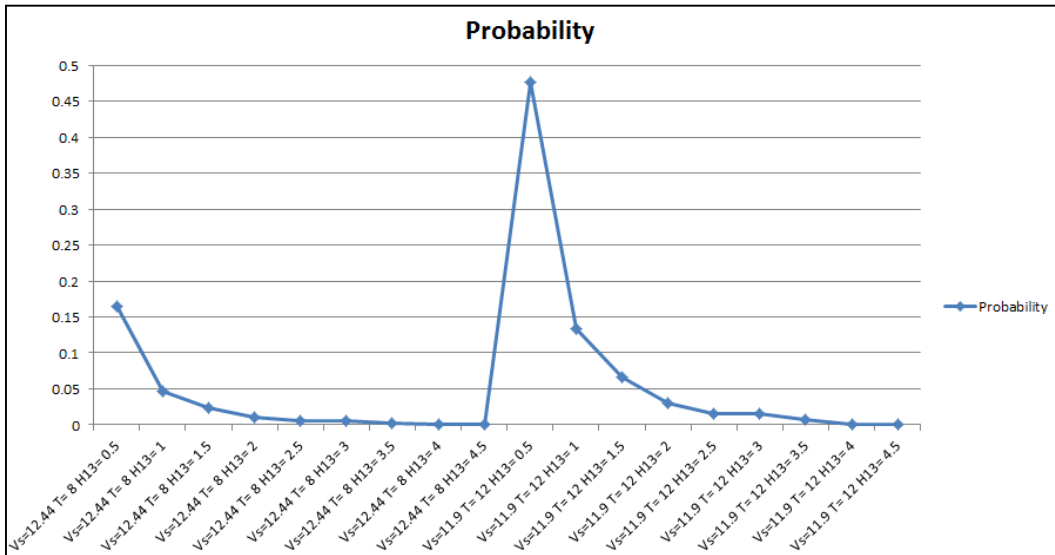


Fig. 6: Probability of encountering a given design condition

4. Optimization process

The optimization procedure was built up using the geometry model, hydrodynamics and the optimization framework built in the NAPA system. Fig. 7 shows the optimization loop. The vessel's bow shape was varied by Free Form Deformation (FFD) of the facet surface used for CFD and seakeeping calculations. The variations ranged from a very blunt bow to a long, sharp and slender bulbous bow.

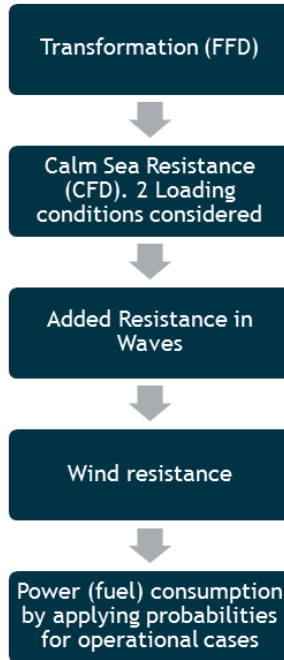


Fig. 7: Optimization process

The variations of the forebody can be seen in Fig. 8 consisting of sections taken at the centreline of each hull form.

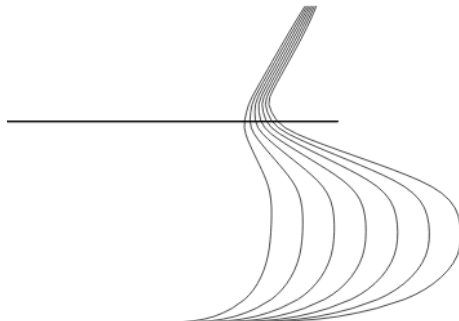


Fig. 8: Variation of the bulbous bow

Calm-water resistance was calculated by the RANS solver integrated into NAPA. The solver is based on the FLOWPACK code developed by Prof. Yusuke Tahara working at Osaka Prefecture University at the time of development (currently National Maritime Research Institute). Added resistance in waves was calculated by using the Seakeeping subsystem in NAPA. The used method is a combination of strip theory and a solution based on the reflection off a cylindrical wall to ensure coverage of the whole wave length regime. Wind resistance was calculated based on the projected transverse wind area. The objective of the optimization was to find a forebody for the vessel that would perform better in the conditions that the reference vessel has been operated in. An approximation of the yearly fuel oil consumption was done by using the following formula:

$$FOC = P_e \cdot SFOC \cdot 365 \cdot 24 \cdot R_{oper}$$

Where:
 P_e effective power
 V_s service speed
 $SFOC$ specific fuel oil consumption, 250 g/kWh assumed
 R_{oper} operation rate of vessel, 0.9 assumed

The goodness of the design was evaluated by the sum of fuel oil consumption for each design condition weighted by the probability of occurrence according to:

$$FOC_{tot} = \sum_{i=1}^n p_i \cdot FOC_i$$

Where: p_i probability of occurrence

For the proof-of-concept of the methodology, a few assumptions were applied to keep things as simple as possible:

- Added resistance in waves was computed by the strip theory, which only allows head waves for R_{aw}
- A major factor in the overall performance of a vessel is the decrease of hull performance due to e.g. hull fouling. This effect was disregarded, and a clean hull was assumed in calculations.
- A common panel model was applied to all loading conditions. For more accurate results, dedicated panel models would be useful to take into account the floating position.

5. Results and Conclusions

The obtained results show that a slender bulb is more favourable for the reference vessel's operational profile. The study shows that the longest bulb variant is around 7 percentage units more effective than the original hull form and about 13 percentage units more effective than the shortest bulbous bow. Applying this to the reference vessel's operational profile, the savings potential in fuel costs amounts to ~ 1,000 tons per year.

Table 6: Results of optimization

BLEND	PE_Laden	PE_Ballast	TFOC	AVRRW	PE	Laden	PE	Ballast	AVRRW	TFOC %
					%	%	%	%	%	
-1	3660.63	3101.58	14784720	27496.8	6.11 %	6.12 %	14.07 %	14.07 %	6.31 %	
-0.5	3547.66	3000.05	14308664	25726	2.84 %	2.65 %	6.72 %	6.72 %	2.89 %	
0	3449.78	2922.71	13907281	24106	0.00 %	0.00 %	0.00 %	0.00 %	0.00 %	
0.5	3359.99	2861.97	13552265	22663.7	-2.60 %	-2.08 %	-5.98 %	-5.98 %	-2.55 %	
1	3286.01	2812.43	13259296	21366.8	-4.75 %	-3.77 %	-11.36 %	-11.36 %	-4.66 %	
1.5	3233.99	2774.54	13088228	21988.4	-6.26 %	-5.07 %	-15.77 %	-15.77 %	-5.89 %	
2	3199.7	2743.22	12893969	19241.5	-7.25 %	-6.14 %	-20.18 %	-20.18 %	-7.29 %	

BLEND	Blending factor for Free Form Deformation
Pe Laden [kW]	Effective power, laden condition
Pe Ballast [kW]	Effective power, ballast condition
AVRRW [kN]	Added resistance in waves
TFOC [ton]	Approximated yearly fuel oil consumption for the given operational profile

Acknowledgements

This paper is based on work done by Sanoyas Shipbuilding Corporation and NAPA. The author would sincerely like to thank Dr. Kenta Koike and Mr. Ryo Yoshida for their extremely valuable contribution which is completely essential for the existence of this paper.

References

FURUSTAM, J.; KUUTTI, I; KOIKE, K; YOSHIDA, Y (2015), *Designing ships for service with the help of performance monitoring*, Int. Conf. Computer Applications in Shipbuilding, Bremen

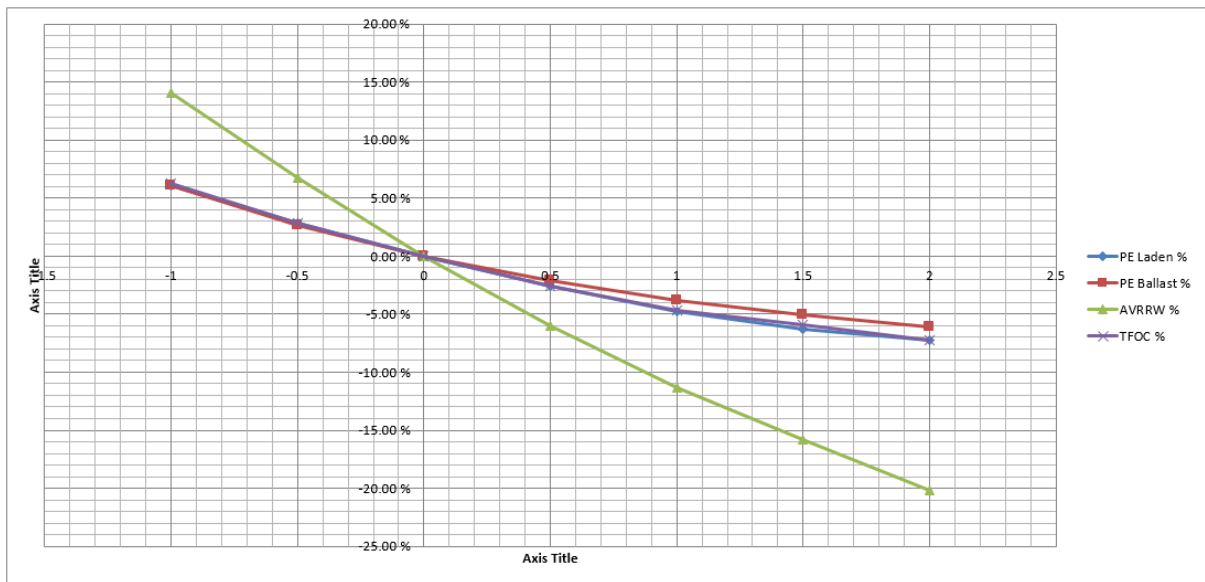


Fig. 9: Graph of optimization results

Project Helm: Insights from AIS, Fouling Control and Big Data

Richard Ramsden, AkzoNobel, Gateshead/UK, richard.ramsden@akzonobel.com

Pete Lelliott, South Coast GIS, Arundel/UK, peteelliott@gmail.com

Jeremy Thomason, Ecoteknica, Newcastle/UK, jeremy@eco-teknica.com

Duncan Van Roermund, Tessella, Den Haag/The Netherlands, duncan.vanroermund@tessella.com

Abstract

Predicting fouling on an underwater hull is a vital part of optimising the efficiency of a maritime vessel. Predictions are also complex given the factors which affect biofouling e.g. vessel operation, environmental, biological and coating characteristics. This is a Big Problem requiring a Big Data solution. Mashing together multiple data streams for relevant vessel attributes, positional data, environmental data and fouling coating performance factor generated a dataset of over 3.5 Billion records. This vast data repository is being exploited via multivariate analysis, utilising over 1,500 variables with the aim of providing state-of-the-art predictive fouling modelling capabilities and visualisations.

1. Introduction

In the shipping industry, the potential accumulation of biofouling represents a huge risk factor affecting vessel performance; biofouling growth on a ship's hull can cause operating fuel costs to rapidly spiral to uneconomical levels. It has been known for many years that large increases in power are required when a vessel is heavily fouled, compared to the vessel in an unfouled state, NN (1952). More recently Schultz (2007) has quantified the effect of different types and extents of biofouling on the powering requirement of particular hullforms. Schultz's work has been viewed as an integral stepping stone towards the development of enhanced tools to characterise the impact of fouling control coating choice on vessel operational efficiency, Kidd *et al.* (2016).

The risk of a vessel fouling depends on a host of intertwining vessel, biological and environmental factors, some of which are illustrated in Fig. 1. In order to understand fouling risk we need to also consider the underlying fouling challenge. "Fouling challenge" can be defined as the inherent level of accumulation and growth of fouling that would occur on an unprotected surface at any particular geographical marine location at any particular time point. For a vessel, the overall fouling risk can therefore be determined by aggregating the individual fouling challenge metrics at each point in time, taking into consideration the vessel's operational profile (speed, activity, etc.).

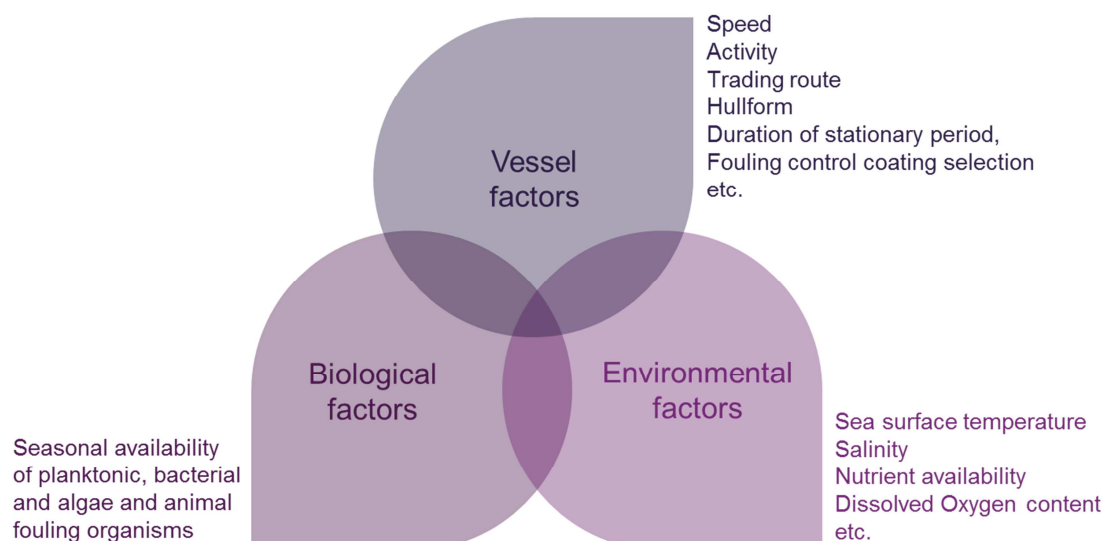


Fig. 1: Selected high-level factors affecting fouling risk

Conventionally, a fouling control coating system will be applied to the vessel to control this risk. In order to fully understand the risk of biofouling posed to commercial shipping, knowledge of both the inherent local biofouling challenge and the operational profile of the vessel's voyage are therefore required, as well as knowledge of the efficacy of any fouling control system that are employed. Better understanding of the biofouling risk would permit the specification of fouling control coatings which are more tailored to particular vessel operational characteristics, ensuring minimal biofouling growth and improved vessel performance.

The approach presented here to tackle this highly complex technical challenge, as undertaken by the Helm project, *Ramsden (2015)*, is to build on current best-in-class modelling, *Thomason (2010)*, by using a vastly increased database of those factors affecting fouling settlement and growth. By pulling together multiple data sources which describe these factors, an unprecedented opportunity is afforded to conduct multi-variate modelling to advance the understanding and prediction of fouling in the dynamic marine environment.

The objective of this paper is to describe the progress and process employed in the Helm project to develop next generation fouling challenge and risk models and associated data exploration tools. The process of data aggregation, cleansing, modelling and visualisation can be demonstrated by a flow chart, as shown in Fig. 2.

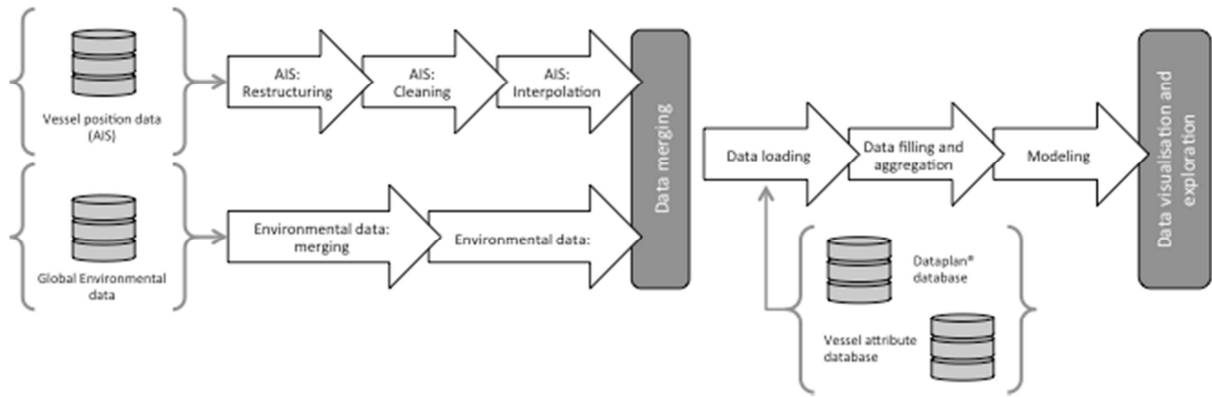


Fig. 2: Process followed by the Helm project from data aggregation to modeling and visualisation

The ultimate aim of this process (and the project) is to allow greater understanding of the factors which affect fouling settlement and growth to allow for more targeted development and bespoke specification of fouling control coatings for fouling prevention.

2. Data sourcing

This study is restricted to data between Jan 2009 and December 2013. This 5 year period has a large amount of available, processed data, which can be readily obtained from a number of commercial sources.

The transmission of Automatic Identification System (AIS) data from marine vessel for the purpose of collision avoidance was introduced into IMO law in 2007. Vessels carrying passengers or over 300 metres long must report their positions at regular intervals, typically between 6 s and 1 minute. This reporting is done by VHF radio waves and as such is readily available commercially both in local and global formats. Frequency of data delivery from such commercial vendors can be tailored; however considerations should be paid to the volume of data delivered at higher relative frequencies of reporting.

The main global environmental datasets incorporated into Helm were: sea surface temperature, salinity, pH, chlorophyll, silicate, phosphate, nitrate content and dissolved oxygen content. The series of environmental data products used in this work are commercially available from multiple suppliers,

and are delivered in fully interpolated gridded raster maps, with associated conversion methodologies. The resolution of these data sets varies from 300 s to 3600 s, however the resolution is such that interpolations can be carried out.

Vessel attributes such as length, beam, underwater area, etc. were sourced commercially also. There are multiple free sources of such data, and large scale batch data download are provided by the major marine class societies.

Crucial input variables for fouling control application and inspection were obtained from the AkzoNobel proprietary coating application and inspection archive Dataplan®, *Thomason (2010)*. Dataplan® contains records of all coatings applied by AkzoNobel International Paint since 1974 (>250,000 records) and their performance. The performance of the fouling control coating applied to a vessel can be considered as the target variable. This performance is calculated as an index of the fouling based on percentage cover of different types of fouling organism ('fouling control index'). Other variables from this database can be used as predictor variables, such as size of vessel, vessel type, underwater cleaning events etc.

3. Data handling, processing and modelling

The first major technical task was to prepare the larger datasets for use by modelling software (SPSS modeller). This involved cleaning and validation of vessel positions from raw records and subsequent merging of environmental data for each validated location. Finally, the data was stored in an initial PostGIS database for further quality control and exporting.

A major challenge was to process the large datasets at scale and within the time frame of the project. For ease of data handling and agility it was decided to process on local production workstations. After early experimentation using common proprietary GIS software it became apparent that using open source software options and distributed computing we could design workflows smartly and at speed. Python Celery is a popular interface for distributing processes across networks using task queues (<http://www.celeryproject.org/>), it supports several message brokers, notably RabbitMQ and this was adopted to manage the system.

3.1 Restructuring AIS data

In order to clean the AIS data, it was first necessary to transform raw files from time domain to vessel domain. The input data was delivered in several formats and several encodings so it was necessary to establish a lookup table to help with the automatic field assignment to a common structure. Establishing this lookup table took considerable time since the contents of each input file required primary inspection to determine formatting.

This interim vessel data was stored as simple CSV files in order to avoid the extra overhead that a database would introduce. A workflow was developed in order to:

- Split files into subsets of n records and push onto the queue,
- Assign a worker daemon to take next subset of records from the queue (typically 250,000 records) and carry out the basic data validation:
 - Removing commonly suspicious data records, for example records with erroneous formatting,
 - Removing records outside of the specified time period,
 - Removing records with a greater frequency of reporting than every 15 minutes
 - Removing records with no corresponding Dataplan application and inspection data,
- For remaining data, sort by IMO vessel number and each grouping given a unique write to queue assignment.

This processing led to a deselection of about 60% of the original data records. The resulting records were grouped by IMO vessel number and saved to network disk space. This approach worked well for the processing of the data, but had major problems with such a heavy disk write, especially direct to the local network. Saving to local disk proved more suitable, but again had a limited capacity for disk write. The solution was to split the ~24,000 vessels into 4 distinct write queues that would write to 4 separate 1TB SSD drives. Once this part of the workflow was complete, the data was copied back to the network in order to amalgamate the data back together.

3.2 AIS processing, cleaning and interpolation

With the distributed system now firmly established and with the data now grouped by vessel for the entire study period the next phase of work was a more rigorous cleaning process before any merging with the environmental data. Several supplemental datasets were introduced into the process to provide some way of data validation.

A key element in the cleaning process was to determine if an apparent vessel position was on land (i.e. erroneous) and this required a GIS dataset that represented the global network of waterways at an appropriate scale for the data. Performing a vector-based spatial query of this nature for every location is a very process-expensive operation. To overcome this, an approach to query a binarised raster representation of the data was adopted. The major trade-off of this approach is that the data becomes far more generalised. Since the grid cell size was 5 minutes this risked rejecting many records close to the land/sea interface. The solution was to rephrase the question, “Is the vessel on land?” to “Is the vessel definitely not near water?” by buffering the waterways dataset by 5 minutes before the rasterization process. Early results showed that no single vector data source could reliably account for all the waterways, so multiple datasets were merged as a pragmatic solution.

To further aid in the validation of the datasets a database of vessel specifications was utilised. This data was exported to a JSON file for easy serialising to Python. The vessel attribute database contained 14,000 vessels that were matched to the IMO vessel numbers from Dataplan and vessel positioning sources. Developing cleaning workflows to deal with these particular datasets was based on the author’s experience of cleaning GPS data within the hydrographic field. The main perceived risk of employing this methodology in the current work is that speed outlier detection and filtering is not explicit.

For the remaining records in the dataset, an interpolation was performed to increase the resolution of the system for fouling modelling. The Pandas analysis library (<http://pandas.pydata.org/>) was used to perform this interpolation, which included forcing NULL values (for interpolation) for suspect data. An initial validation was performed and where interpolated positions intersected the waterways dataset, then the entire segment of interpolation was rejected as crossing land. This validation is relatively crude: if one interpolated point intersects land then the entire segment is rejected. More advanced transit analysis could be added to this part of the process, i.e. with higher temporal resolution, but would require significantly more processing and analysis resource because of the size of the enhanced dataset.

3.3 Environmental data merging and data loading

Each remaining record (‘good’ and ‘good–interpolated’) was overlaid with multiple environmental datasets including sea surface temperature, pH, salinity and chlorophyll. The spatial resolution of these additional datasets ranged from 300 s to 3600 s, and was delivered in a number of different formats. A JSON catalogue for each environmental raster dataset was generated that would allow a fast indexing system to identify the correct raster for any point in time point over the study period. A generic GDAL function was used to query the environmental raster that took a listing of XY positions and returned a list of equivalent raster values for each position on a 0-255 scale. Each of these values would then be transformed into a true environmental value, using supplier provided conversion algorithms. This data processing accounted for about 78% of the total processing time. The major

time limitation to this processing was the requirement for additional data filling. Filling rules were established to interpolate across missing values and to graft small scale localised data into the database.

Post-merging, the entire per vessel dataset was pushed onto a database writer queue. A local PostGIS database server was provisioned and 4 separate writer queues helped spread the work effort loading the data. All indexing was undertaken after all data had been loaded to avoid any decrease in database write performance. In total, 4 machines utilising 50 cores were used as process workers and 4 PostGIS database writers. The system took 9 man-months to build, but only 2.5 days for the initial run. Further details of processing, including total number of records, are shown in Fig. 3.

Machine	Workers	Vessels	Records	Days Cleaning	Days Interpolating	Days calculating state	Days Merging	PostGIS Upload
1	12	6,198	878,999,250	1	0.55	1.86	13.69	0.65
2	18	6,199	881,007,584	0.93	0.46	1.82	12.08	0.62
3	12	6,198	873,374,896	1.12	0.57	2.32	17.85	0.75
4	8	6,139	869,503,847	1.02	0.54	2.05	15.81	0.72
Totals	50	24,734	3,502,885,577			76.41 days		

Fig. 3: Breakdown of processing speeds and record numbers per machine (synchronously)

3.4 Data filling and cleaning

The cleaned and interpolated AIS CSV dataset was uploaded into a DB2 SQL database and manipulated and modelled through an IBM Modeler V17 frontend. An advantage of using this setup is that processes created in Modeler are translated into SQL and pushed back to run in the database reducing considerably time consuming input/output operations. Despite this some of the process runs took over 240 h.

Initial data audits revealed that only ~50% of the records had complete information, i.e. not every variable was filled, and this was considered likely to have a detrimental impact on subsequent modelling. The main reasons for the incomplete data were:

1. Patchy data collection by satellites, particularly for the chlorophyll data which is impacted not only by cloud cover but also by attenuation of sensor sensitivity towards the poles due to the earth's tilt, *Blondeau-Patissier (2014)*,
2. Mismatch between spatial coverage of the datasets near the coasts.

Thus a hierarchy of rules was created to permit the interpolation of missing data, and a set of rules was independently specified for each variable. The rules included nearest neighbour analysis, fills based on relevant values found in the literature or by using local or regional models. For example, missing chlorophyll values were filled with nearest neighbour values if the nearest neighbour was <50 nautical miles distance. For other variables the distance was greater or smaller depending on the overall spatial variability of the data. Most remaining values were filled using localised historical datasets and other missing values were filled with the median values for the NOAA defined large marine eco-regions, *Mahon (2010)*. The final rulebook contained 68 rules and the post-interpolation dataset approached 100% saturation.

AkzoNobel's Dataplan® dataset contains a unique code that is linked to application of a coating and gives access to the key application data such as date and geographic location. It is also linked to the inspection data, which not only includes the target variable, i.e. the fouling control index, but also the mechanical condition of the coating at inspection. The interaction variables were aggregated within the bounds of the application and inspection dates for specific coating on a specific ship. Within our time frame of January 2009 through to December 2013 there were vessels in the dataset with left-censored events (no application date but an inspection date) and also right-censored events

(application date but inspection date). For the modelling data, only non-censored vessel/event tracks were analysed but for future predictions, left-censored data could be utilised.

As the various coating technologies have different mechanisms of action, *Finnie and Williams (2010)*, and therefore generally provide different levels of fouling control (antifouling performance) it was decided to partition the modelling using the fouling control coating type, on the assumption that the model for each coating would require different predictor variables.

The resulting dataset was further cleaned to remove vessels which had any track steps >1000 nm, which approximated to 3 days steaming for a typical ocean going vessel. Vessels that had voyaged in ice were removed, as were vessels that had been subject to an underwater clean prior to inspection. The final two filters were to exclude vessels which had had been subject to catastrophic coating failure due to application errors and vessels which had been inspected outside the bounds of the expected in-service life of the applied coating scheme. At present, this analysis has only been performed on vessels which voyage mainly (>90% of time) in the marine environment as this obviously represents by far the largest commercial sector.

3.5 Data aggregation and modelling

A classic Cross-Industry Standard Process for Data Mining (CRISP DM) approach, *Kurgan and Musilek (2006)*, was used to model the data. The difficulty in deciding a priori the relative importance of variables guided towards this approach. This CRISP-DM method, unlike standard statistical modelling is not about testing hypotheses, but focuses on deriving insight and predictive analytical models from the data using automated data mining processes.

An initial appraisal led us to consider aggregating the data into a large set of variables to capture the interactions of the various environmental factors experienced by a vessel while voyaging. This was done in order to generate suitable predictor variables. For example the interaction between vessel speed and the mean, maximum, minimum and variance in each of the environmental factors was captured by one set of variables in the suite. In view of the high number of predictor variables, the selected modelling method used in project Helm was Kass' Chi-squared Automatic Interaction Detection (CHAID) algorithm, *Kaas (1980)*, *Antipov and Pokryshevskya (2010)*. Predictor variable importance was calculated and a supervised step-down approach was used to build a parsimonious set of variables useful to predict with sufficient accuracy without over fitting the performance of each of the coating types. The suite of ~1500 predictors were by this process reduced to 97 that could between them be used to predict a series of fouling ratings that subsequently determine the fouling control index.

Prior to modelling each variable was automatically cleaned: nominal variables with >100 categories and categorical variables with one category with >95% of the data were excluded and continuous variables had their outliers removed and were subject to Box-Cox transformations to achieve normality. The target variable was also Box-Cox transformed. The dataset as well as being split by coating was randomly partitioned into training and testing partitions with 50% of the records in each.

The criteria for the CHAID model were: the maximum number of branches was set to 5 and the method used initially up to 10 models in the ensemble (boosting) to increase accuracy; the minimum number of records in a parent branch was limited to 2%, and 1% in a child branch; significance level of merging and splitting was 0.05, Bonferroni adjustment of significance was used; the set limit for convergence was 100 iterations; and over-fit prevention was set to 30%.

Examination of the accuracy versus ensemble size enabled a reduction in the number of models in the ensemble to 3. The predictive power of each variable was examined and this led to reduction in the number of variables to 97. This is still a considerable number but was consistent with the initial assumption that each coating type required different predictor variables. Each model had accuracy of >95% against the testing partition.

The final step was then to use the model to predict the fouling control index for each of the non- and right-censored vessel tracks in the database. Thus for each suitable vessel in the database we ended up with predictions for the fouling control index at 15 minute resolution.

4. Database performance, back-end considerations and data visualisation

Dealing with billions of records means a scalable solution is necessary. To manage the required increase of available capacity and performance a cloud-hosted database was employed. One advantage of the composition of the underlying data used in this study is that the number of entries per vessel is relatively limited. One record per fifteen minutes, for five years, amounts to around 175,000 rows per vessel. When creating visualisations for a single vessel, only a manageable subset of all records is needed. Limiting the amount of data that is transferred can highly improve the response time of the system.

Carrying out calculations on multiple records on the database side again minimises transfer of data. For example, aggregating the data per month would reduce those 175,000 records per vessel to only 60. All of this aggregated data can be precomputed and cached which removed the need of having to calculate values on-the-fly and reduces the computational power required to interrogate the database, execute the models, and generate visualisations.

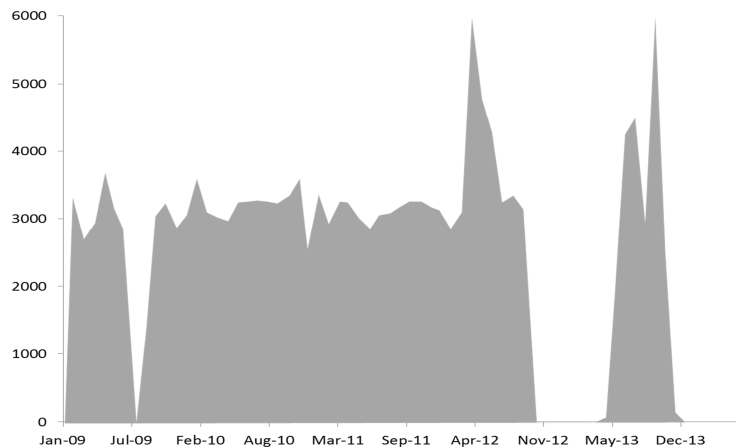


Fig. 4: Example of entries over time, grouped by month for a particular IMO vessel number

As with all Big Data projects, data management is key. Given the nature of the AIS data, records can be missing, garbled or even spoofed, and a large proportion of time has been spent mitigating against erroneous results. A particular goal has been to rapidly and easily identify anomalies in the data, so they can be filled, corrected or removed. A useful visualisation here is to plot the number of entries over time for each vessel, grouped by month, as shown in Fig. 4. Clearly visible is a large data gap from October 2012 and May 2013 for this vessel, which was subsequently filled via the processes described above.

Given the large volume of available data, it would be infeasible to process all of this at the same time. A number of use-cases were therefore developed. For example, one use-case focusses on individual vessels, allowing the user to investigate the historical location of a single vessel and associated conditions, with the ultimate goal of identifying areas of spatial and temporal high fouling-risk, as well as vessel-specific risks.

One obvious simple visualisation tool is a map depicting the vessel's historic trading route. An overview of the environmental and operational conditions associated with a vessel at each point in time can accompany the map to provide further insight. Fig. 5 shows a typical example map for a vessel, alongside associated temperature distribution and monthly averages. These allow the identification of common values and trends over time.

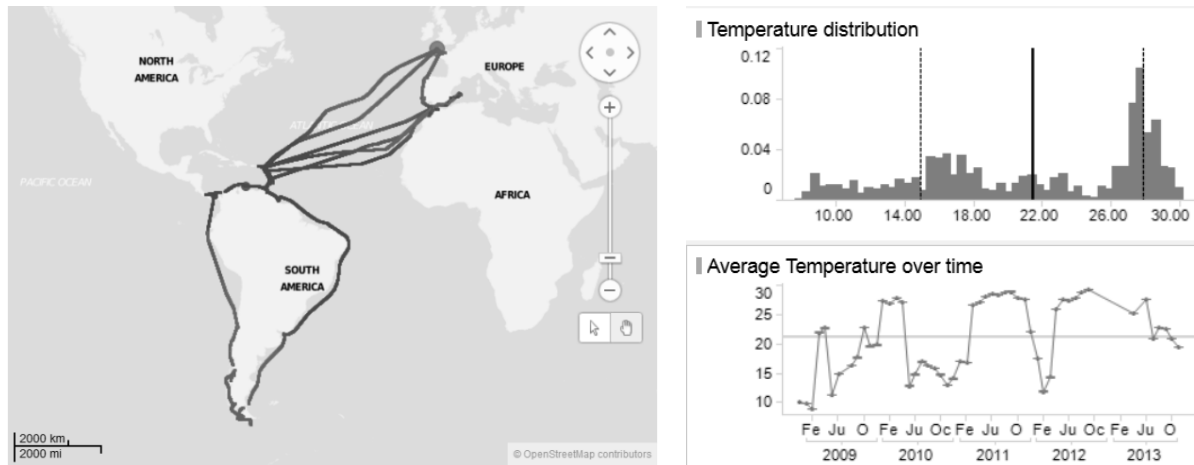


Fig. 5: Map visualisation and corresponding temperature data

It is apparent that this particular vessel made a number of transatlantic trips from the Caribbean to Northern and Southern Europe, as well as circumnavigating South America. However, while this simple map illustrates the vessel's route, it does not clearly indicate the amount of time the vessel spent in any particular region and therefore gives limited information on how the fouling challenge experienced by this vessel varied over its in-service period.

A more useful tool to visualise this aspect is a tree map, as shown in Fig. 6. In this example, each block represents a region, where the size of the block indicates the time spent there by the vessel. In this example it is now obvious that the vessel has spent particularly significant periods of time in the Caribbean and the Celtic-Biscay shelf, reflecting the fact that this particular vessel has had extensive static periods in these locations. This information is not clear from the simple route map alone. The examples above are clearly relatively simple cases which have been chosen to illustrate the general utility of the approach. More sophisticated use-cases are currently under development which will make better use of the extreme underlying complexity of the data.



Fig. 6: Tree map of entries per region, blocks sized by cumulative time

5. Conclusion

The ability to effectively control fouling is of critical importance to ship owners and operators but the accurate prediction of fouling risk is a highly complex problem. Large strides have been taken through the work of the Helm project to understand and model these risks. Multiple data sources for relevant vessel attributes, positional data, environmental data and fouling coating performance factors are being leveraged using Big Data techniques. Errors in these source datasets have been identified, solutions generated and a large list of rules, hierarchies and data standards has been developed. The

approaches used reflect the current state-of-the-art and have the potential to blueprint future generations of data analysis and modelling using datasets of the type described herein.

This work is still at a relatively early stage and so full exploitation of the insight gained from modelling and visualising this data will only become apparent over the next few years. However the ultimate aim of this work is to generate improved prediction models for fouling risk which will allow for more targeted development and bespoke specification of fouling control coatings. Obvious future stepping stones towards this goal therefore include a program of validation and this will form the basis of future work to ensure the accuracy and reliability of the model predictions.

Acknowledgement

This work was partly funded under the Innovate UK competition ‘Data Exploration – Creating New Insight and Value’ (<https://www.gov.uk/government/organisations/innovate-uk>). The Project Helm overview (number 101930) can be viewed here: <http://gtr.rcuk.ac.uk/projects?ref=101930>.

References

- ANTIROV, E.; POKRYSHEVSKAYA, E. (2010), *Applying CHAID for logistic regression diagnostics and classification accuracy improvement*, J. Targeting, Measurement and Analysis for Marketing pp.109-117
- BLONDEAU-PATISSION, D.; GOWER, J.F.R.; DEKKER, A.G.; PHINN, S.R.; BRANDO, V.E. (2014), *A review of ocean color remote sensing methods and statistical techniques for the detection, mapping and analysis of phytoplankton blooms in coastal and open oceans*, Progress in Oceanography, pp.123-144
- FINNIE, A.A.; WILLIAMS, D.N. (2010), *Paint and coatings technology for the control of marine fouling*, Biofouling, Wiley-Blackwell
- KAAS, G.V. (1980), *An exploratory technique for investigating large quantities of categorical data*, Applied Statistics, pp.119-127
- KIDD, B.; FINNIE, A.A.; CHEN, H.L (2016), *Predicting the impact of fouling control coatings on ship powering requirements and operational efficiency*, 1st Hull Performance & Insight Conference (HullPIC), Pavone, pp.298-311
- KURGAN, L.; MUSILEK, P. (2006), *A survey of knowledge discovery and data mining process models*, The Knowledge Engineering Review, pp.1-24
- MAHON, R.; FANNING, L.; McCONNELL, P.; POLLNAC, R. (2010), *Governance characteristics of large marine ecosystems*, Marine Policy, pp.919-927
- NN (1952), *Marine Fouling and its prevention*, Woods Hole Oceanographic Institute
- RAMSDEN, R. (2015), *Project Helm: Predicting marine fouling with vessel tracking and Big Data*, AIS SUMMIT, Hamburg <http://www.aissummit.com/>
- SCHULTZ, M. (2007), *Effects of coating roughness and biofouling on ship resistance and powering*, Biofouling, pp.331-341
- THOMASON, J.C. (2010), *Fouling on shipping: data-mining the world’s largest antifouling archive*, Biofouling, Wiley-Blackwell

Digital Twins for Design, Testing and Verification Throughout a Vessel's Life Cycle

Kristine Bruun Ludvigsen, DNV GL, Trondheim/Norway, kristine.bruun.ludvigsen@dnvgl.com

Levi Kristian Jamt, DNV GL, Trondheim/Norway, levi.jamt@dnvgl.com

Nicolai Husteli, DNV GL, Trondheim/Norway, nicolai.husteli@dnvgl.com

Øyvind Smogeli, DNV GL, Trondheim/Norway, oyvind.smogeli@dnvgl.com

Abstract

This paper presents a digital twin simulation platform, “Nauticus Twinity”, with the vision of providing a more efficient verification scheme for the maritime industry. A digital twin of a vessel consists of a number of simulation models that are continuously updated to mirror its real-life twin. A key feature of the simulation platform is the open architecture allowing integration and co-simulation of models developed by DNV GL and our partners. The platform facilitates new tools for design, classification, verification, commissioning, condition monitoring, and decision-making throughout a vessel's life cycle. The paper focuses on co-simulation and use of digital twins for the new build phase, and includes an example of how Nauticus Twinity can improve the commissioning and the verification process for complex integrated systems.

1. Introduction

Digitalization has become a key aspect of making the maritime and offshore industries more efficient and fit for future operations. Increased use of advanced tools for designing and evaluating system performance, safety and structural integrity are generating a range of digital models of a vessel and its equipment. In the operational phase, cheaper sensors and increased connectivity together with increasing data storage and computational power are enablers for new ways of managing a vessel's safety and performance, *Knutsen et al. (2014), Låg (2015)*.

As the total amount of data generated on a vessel increases, so does the potential to fully utilize these data to achieve greater insight into the vessel's status, and even make predictions. Combining live ship data with models generated during the design phase of a vessel, provide the basis for digital twins applicable for smarter asset management, *Manno et al. (2015), Låg et al. (2015)*.

In the maritime industry, there are initiatives emerging that focus on building digital models based on sensor data for monitoring, analytics and prognostics of assets. One example is GE Marine's SeaStream Insight, *Kellner (2015)*. Also other manufacturers that supply the maritime industry with systems, components and associated control system software are developing infrastructure and services to perform this type of life cycle asset management through continuously harvesting data from their products, *Løvoll and Kadal (2014)*.

Modern vessels include systems and components that are highly interconnected. In addition, these are being produced and installed by a range of different manufacturers. Assuring the total safety and operational performance of today's vessels is a challenge, and requires efficient methods for assessing system-integration for the vessel as a whole. Many of these systems are in fact cyber-physical systems (<http://cyberphysicalsystems.org/>) and dependent on control system software that is critical for safe and efficient operation of the vessels. Possible ways to test, verify and validate such software are discussed in *Smogeli (2015)*.

The challenge is then to develop a concept leveraging on the different levels of system specific services already provided by manufacturers, where safety and performance of complex integrated systems can be managed from the early stages of a vessel new build project and throughout the vessel's life-cycle. Nauticus Twinity is the first prototype of such a service, introducing digital twins for vessels in the form of a multidisciplinary model-based tool.

2. The Digital Twin

To exploit the potential of digitalization of manufacturing and asset management processes, multiple industries are embracing the concept of the ‘digital twin’. The digital twin concept was first introduced by Michael Grieves at the University of Michigan in 2003, *Grieves (2014)*. A digital twin is a model of a physical asset, implemented for example as a mathematical model, information model or a visual model. It could be a model of anything: an engine, a building, a thruster and so on. What makes a digital twin different from generic models is that they are specific to their physical counterparts. The digital twin follows its corresponding real life twin through its life cycle, through collecting sensor measurements, simulation model updates and software upgrades. Any change on the physical asset must also be reflected in the digital twin model.

When developing digital twin technology for the maritime industry, one should adopt best practices from manufacturing processes in the defense, aerospace and automotive industries, e.g. *Glaessgen and Stargel (2012)*, *Ríos et al. (2015)*. Following these practices, the digital twin models will be constructed prior to and in parallel with the actual building of a vessel, enabling virtual manufacturing and commissioning, integration testing and analysis already before the keel is laid. During the operational phase, the digital twin becomes a system for integration, processing and analysis of the operational data. Ideally, the digital twin will provide decision support and predictions for a ship owner or for subsystem manufacturers. Made possible using model-based simulation in combination with sensor measurements from the real vessel, without the need for physical inspections.

Models building up a digital twin of an asset may be of many different forms, *Manno et al. (2015)*. In essence, the digital twin should be able to take advantage of all digital information available for an asset: system and data information model, 3D visualization models, mathematical models, dependability models, condition and performance indicators and data analytics.

An increasing number of systems and processes on board a modern vessel are dependent on computers and networks for monitoring and control. Feedback loops from system measurements are included in the computations and affect the controllers. As these systems exploit the benefits of increased connectivity and low-cost sensors, the complexity level is rising and new methods for design, testing and verification are required. Such systems have become known as “cyber-physical systems”, *Bahereti and Gill (2011)*, *Lee (2014)*.

The introduction of the digital twin concept for verification and asset management will support the maritime and offshore industries in fully taking advantage of the explosive adoption of cyber-physical systems.

3. CyberSea

In DNV GL Marine Cybernetics services (previous Marine Cybernetics AS), we have over the past decade developed an advanced time-domain simulator technology platform called CyberSea. The technology was originally developed for delivering hardware-in-the-loop (HIL) testing as a service for marine and offshore control systems, *Smogeli (2015)*. CyberSea is used to create simulators that consists of models for sensors, actuators, mechanical components, networks, and environmental loads to simulate the real plant and environment that the control systems are communicating with. Fig. 1 illustrates the normal operation where the physical asset with sensors and actuators are connected to the control system, Fig. 2 how the HIL simulator is replacing the real asset making the control system control a digital twin of the asset.

In this paper, we refer to simulation models as models of a dynamic systems described by differential, algebraic and discrete-time equations. Our library of simulation models are primarily modelled in well-known simulation tools such as Matlab/Simulink. Through an automated workflow these models are transformed to native code, wrapped as modules and loaded into the CyberSea platform. There are several simulators built on the CyberSea platform to simulate the various plants under control.

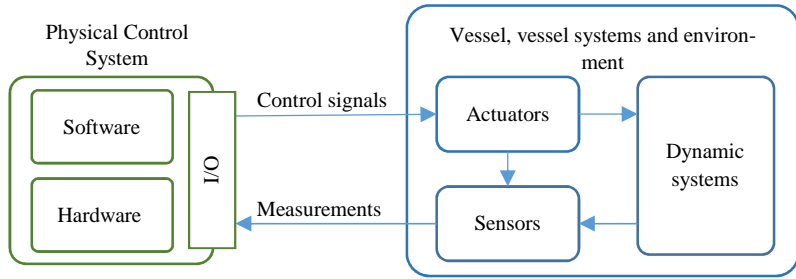


Fig. 1: Normal operation

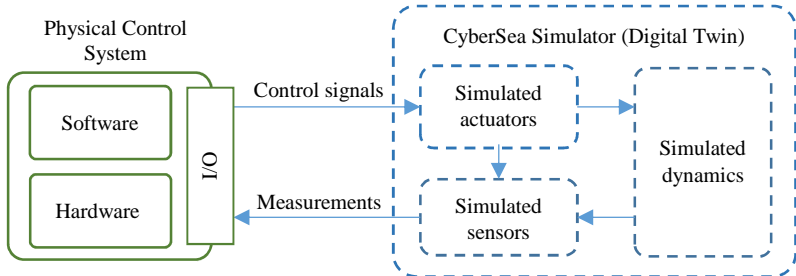


Fig. 2: HIL setup

The simulators can interface dynamic positioning (DP) systems, power management systems, blow out preventers, drilling systems, crane systems and more. For DP testing we use an advanced vessel simulator. It consists of simulation models for generators, thrusters, rudders, power distribution, position reference systems and sensors in addition to vessel motion and environmental loads for wind, waves and current. For HIL testing, our vessel simulator is a digital twin of the real vessel the control system is controlling.

3.1. Co-simulation

CyberSea have certain characteristics that makes it suitable for efficient modelling of digital twins. The applications created on this platform is built with a modular architectural approach. It consists of simulation models with loose couplings and well-defined communication interfaces. Furthermore, the simulations are performed taking a co-simulation approach, which means that there is no centralized equation solver. Instead, each model has its own solver and the CyberSea simulation core engine orchestrates the communication between the models. The core engine is the master that implements what is often referred to as a master algorithm, *Cremona et al. (2016)*. It involves reading the outputs and setting the inputs of the simulation models in addition to stepping model time.

An obvious advantage of co-simulation is the flexibility of interchanging parts of the simulated system, an advantage that enables cooperation. A known challenge is handling coupled stiff systems. For a centralized equation solver this is easier to manage. Setting the integration step size for all models to accommodate for the fastest dynamics in the system will avoid numerical instability for the stiff systems. Using variable step equation solvers is also an option. For co-simulation, our approach is to leverage on the modularity and introduce simulation groups. The simulation models are put in groups that are stepped at different rates. The stiff systems are modelled in the same module accommodated with a stiff solver and put in a simulation group with a sufficiently short step size. This way all models are stepped at a sufficiently high rate, optimizing the computational effort.

3.2. Software-in-the-loop

When testing a physical control system in a HIL setup as shown in Fig. 2, the control system is a black-box controlling its asset under control in real time. Fig. 3 illustrates testing of control system

software in a software-in-the-loop (SIL) setup. Virtualizing the control system HW gives you control of system time and there will be no real-time requirements. Depending on computational power available and model complexity, the simulations can be done several magnitudes faster. Alternatively, the simulations can be done slower than real time for debugging or investigating fast dynamics.

Physical components, e.g. a thruster, must be modelled to be part of a simulated environment as the simulated actuators depicted in Fig. 3. In contrast, the thruster control software is by nature already a virtual entity that may run, unmodified, on hardware emulators in a SIL setup. This is an important feature that from a software testing point of view must be exploited.

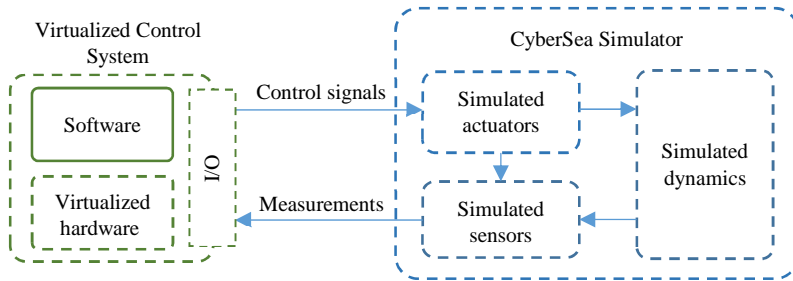


Fig. 3: SIL setup

4. Open platform using Functional Mock-up Interface

As the CyberSea architecture already follows the co-simulation principles, the platform is well suited for collaboration and inclusion of external models. For efficient collaboration, a standardized interface for co-simulation is needed. The Functional Mock-up Interface (FMI) was initiated by the automotive industry with the goal of improving exchange of simulation models between suppliers and original equipment manufacturers. FMI is a tool independent standard, and an increasing number of simulation tools are supporting FMI for model-exchange and FMI for co-simulation. The FMI development activities are today managed as a Modelica Association Project and is a continuation of the results from MODELISAR, an ITEA 2 project (<http://www.eurekanetwork.org/content/itea-2-modelisar/>).

4.1. Model exchange vs co-simulation

The FMI for Model Exchange enables models from one simulation tool to be exported as a Functional Mock-up Unit (FMU) to be used in other simulation environments (<https://www.fmi-standard.org/>). In this case, the FMU is a passive component, meaning that the equations provided by the FMU must be solved by an external solver managed by the simulation tool importing the model. In the case of using FMI for co-simulation on the other hand, each FMU has its own built in individual solver. The intention is to provide a standard for coupling of simulation models exported by different tools in a co-simulation environment. The FMUs are simulated as slaves, managed and synchronized by a master algorithm like CyberSea.

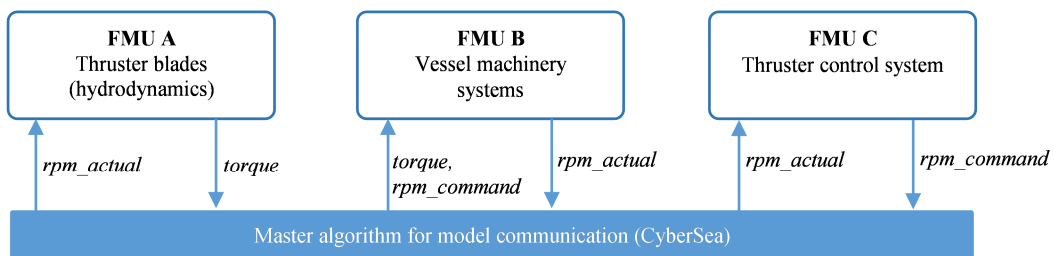


Fig. 4: FMI for co-simulation example

Let us take an example. Fig. 4 illustrates how three models are co-simulated with CyberSea as the master. The hydrodynamic forces acting on the rotating propeller blades are simulated in model A. It

takes the shaft speed as input and produces torque as output. Model B undertakes the ship machinery systems from the prime movers via electrical or mechanical transmission of energy to the propeller shaft. It takes torque and commanded shaft speed as input and produces the actual shaft speed. The commanded shaft speed are produced by the thruster control system (model C), based on the actual speed. This example will be revisited and further elaborated in section 5.

The FMI standard opens for co-simulations across platforms and frameworks, an ability that we wanted to exploit with CyberSea. By enhancing CyberSea with FMI support, we have further opened the simulation platform by reducing the effort for collaborative simulations. Depending on what system or artefact to be modelled, the appropriate tool supporting FMI can be chosen. Which again enables digital twins to be created more efficiently as proprietary models from designers and equipment manufacturers can be run on the same platform. A common open platform for system modelling and simulation will facilitate a more agile development of a new build by bringing experts together in a continuous process starting at an early stage of the project.

A library of DNV GL reference models are available and can be utilized to model parts of the plant in combination with models provided by the designers and manufacturers. When contributing to build the digital twin by providing simulation models of their system, manufacturers can explore how their system interacts with the complete vessel. The yard will have a preview of the real commissioning and can gain early insight into potential conflicts, resulting in fewer errors and less need for on board modifications.

5. Nauticus Twinity for integration testing of thruster control software

The concept named Nauticus Twinity is the result of an innovation project initiated to demonstrate the digital twin concept and map its potential in future verification and advisory services. The objective was to create a setup for easy instantiation of digital twins for time-domain vessel simulations by combining existing technologies within DNV GL and develop necessary user interfaces. Testing of control system software and their effect on overall vessel functions, safety and performance became the main target for the first applications of Nauticus Twinity. Integration testing of a thruster control system will demonstrate the new platform.

To carry out missions for the more complex vessels depending on dynamic positioning (DP), the thruster control software handles safety critical features in all operating conditions. A local thruster control system must be designed and tuned to interact with several other control systems on board, that being local motor and engine controllers and common control systems such as the DP system or power management system (PMS). The digital twin for such a case study had to include dynamic simulation and interactions between machinery systems, power distribution systems, propulsion systems, navigation systems, control systems and hydrodynamic and environmental loads. Fig. 5 presents the setup of Nauticus Twinity as used in this demo case, and each feature is elaborated further below.

5.1. Co-simulation: CyberSea and COSSMOS

CyberSea is developed primarily for HIL testing of control systems. The functionality currently available reflects this purpose. To gain insight into overall performance of a thruster control system, the integrated effects on the total machinery system and fuel consumption should be included. CyberSea does not have models detailed enough for accurate simulations of fuel performance, thus other tools were sought to cover these aspects. Machinery and propulsion systems require complex cross-domain simulation models, thus we wanted an efficient way to include process models for machinery with high level of fidelity. Such models must accurately simulate scenarios where fuel consumption, thermodynamic and electrical properties in the machinery can be analysed. A modelling framework developed to cover these aspects, DNV GL COSSMOS (COmplex Ship Systems MOdelling and Simulation), *Kakalis et al. (2014)*, was chosen. Models from CyberSea and COSSMOS was co-simulated as illustrated in Fig. 5. The two simulators ran with different solvers and exchanged data at time steps controlled by CyberSea.

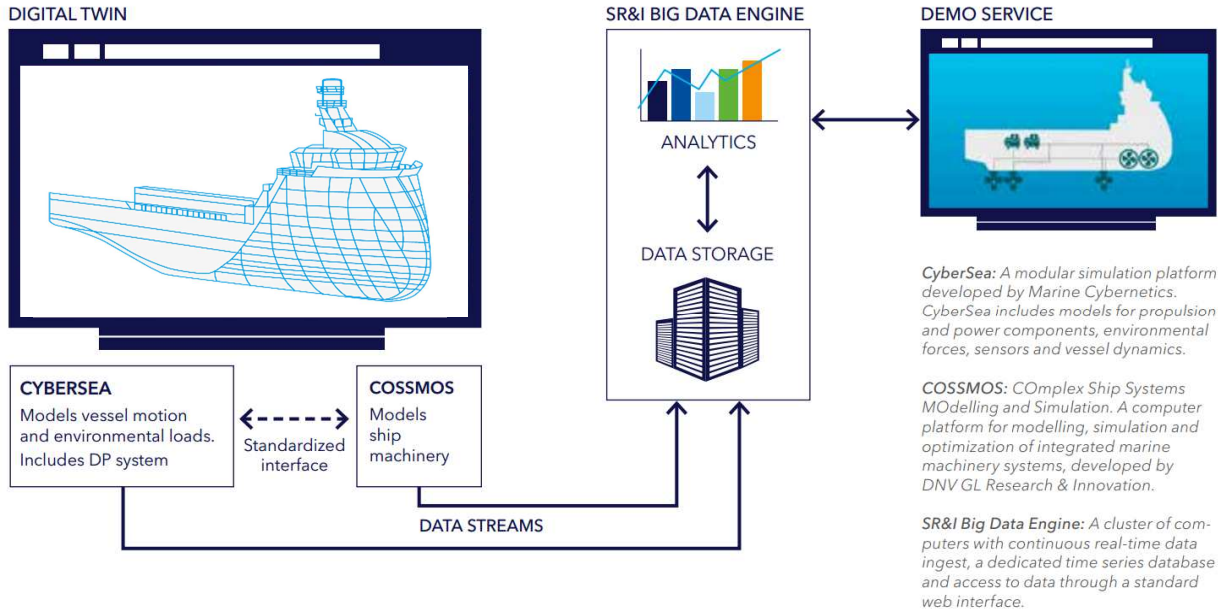


Fig. 5: Nauticus Twinity demo

5.2. Data infrastructure and analytics

An important aspect of the digital twin concept is to follow the real asset also during the operational phase. Nauticus Twinity therefore includes an infrastructure to manage simulation data as well as operational data from vessels. The analytical toolset and web application framework currently used in other pilot projects investigating data streams from real vessels in operation as presented in *Låg et al. (2015)* was adapted. Data generated from the co-simulation is fed into an on premise big data cluster for storage and analytics as illustrated in Fig. 5. The data stream is pushed into the persistence layer using Apache Kafka (<http://kafka.apache.org/>). The persistence layer is the OpenTSDB time series database (<http://opentsdb.net/>) running on the scalable Apache Hadoop (<http://hadoop.apache.org/>) and HBase (<http://hbase.apache.org/>) platform. The Hadoop platform supports a wide set of data analytics tools both for historical data using batch analysis and for in-stream-analyses of data flowing into the persistence layer.

To enable testing and condition monitoring of integrated system functionality for vessels throughout the whole life cycle, a structured way of linking the vessel's functions and components, potential failure modes and generated sensor data is essential. The Nauticus Twinity platform adapts the ship data model introduced in *Låg et al. (2015)* for this purpose. The data model is described in Web Ontology Language (<https://www.w3.org/TR/owl-features/>), and allows reasoning and queries on the data model. The model is based on DNV GL's product model for vessel documentation as presented in *Vindøy (2008)*, linking functions and grouping components subject to classification.

For the purpose of the Nauticus Twinity prototype, the end user gets access to the system through an interactive web application providing:

- graphical representation of systems status
- real-time simulation data of any signal
- data analytics and aggregated data of signals
- weather indicators

See Figs. 6 to 8 for screen shots of the web application. The example elaborated below shows how data streams from this co-simulation setup can be analysed to extract valuable information about the system.

5.3. Demo: Verifying software update with Nauticus Twinity

Case: A thruster manufacturer has made updates to his control system software for a specific vessel delivery. Nauticus Twinity is used to verify that the update does not cause conflicts with the existing system design.

1. The manufacturer accesses his web portal for the vessel in question. Here he finds a virtual test environment where a simulation model of the actual thruster together with emulated control system hardware are integrated in an overall vessel simulator, Fig. 6. He uploads his updated software to the emulated control system hardware.

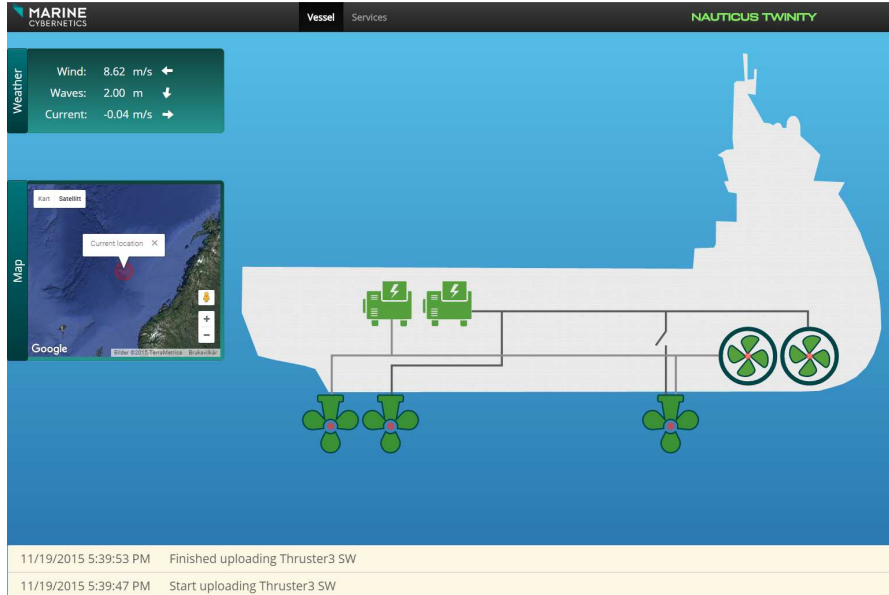


Fig.6: Web interface for Nauticus Twinity

2. Before accepted by the test system, the simulator runs a pre-defined set of functional tests and failure-scenarios and verifies how the control system handles these scenarios. The test setup includes control software and component models from a range of suppliers, enabling integration testing that can minimise the number of issues detected during future on-board tests.
3. When the model is accepted, he can access the relevant thruster and trend parameters of interest during the simulations as shown in Fig. 7. The data streams are continuously analysed to check for failures or deviations from expected behaviour. Fig. 8 shows analytics of signals after such a deviation is detected, an event named “azimuth inconsistent movement”. Drilling into the data detects a small increase in low frequent azimuth oscillations and fuel consumption after the update.



Fig.7: Trending simulation variables

Fig.8: Analytics after event alarm

4. An optimal performance of a thruster in all operating modes of a vessel requires tuning of a range of parameters in the control systems (propulsion control, DP and PMS). To find the cause of the event, the manufacturer is now able to debug his product's behaviour in an integrated environment with other suppliers in terms of both functionality and performance in order to remove the issue at the design stage.

The demo shows how Nauticus Twinity provides a collaboration platform that prepares the integrated systems for real commissioning through early insight into potential conflicts. This will result in reducing the number of integration errors and less need for onboard modifications.

As several vendors connect and upload their parts of the digital twin, the platform facilitates an agile approach for virtual commissioning of the control system software and the components they interface. We will again point out that in such arrangement it will be the exact same control system software running in the digital twin as will be used for the real vessel. An agile virtual commissioning process to build the digital twin will enable valuable insight, earlier retirement of risks, and reduced time to field that in turn will reduce the probability of delays when commissioning the real vessel. It enables early system testing and integration, which obviously is a great advantage compared to a “big-bang” integration on site.

6. Digital twins for independent verification of control system software

The current prototype of Nauticus Twinity is based on simulation models developed by DNV GL. The open architecture will allow stakeholders to interact directly with this simulation platform through FMI using their own proprietary models, as described in section 4, without compromising their intellectual property rights. This enables the use of dynamic system models supplied by involved manufacturers and designers for independent verification of control system software and the corresponding cyber-physical systems.

By enhancing traditional system documentation with simulation models on the digital twin platform, significant value can be added also to the class verification and approval process. System simulations can move the process from an approval regime showing compliance with prescriptive rules based on analogue drawings, specifications and functional descriptions of systems and components, towards verification of functional requirements through model-based approval.

An example of adding value to the approval process is the ability to study consequences of a failure on the digital twin model. The digital twin can enable a different approach to the traditional DP Failure Mode and Effect Analysis (FMEA) trials that aim to prove the worst case single failure in the DP system and its consequences. A number of the tests could be done virtually, and the remaining could potentially be run without the presence of a surveyor as sensor data from the trials can be run on the digital twin model platform proving a successful test. Test results will be stored in a database and used for benchmarking throughout the life cycle of the vessel.

Such a model-based approval regime demands for efficient quality-assurance and validation of the simulation models in the digital twin. This could for example be done through quality assurance of product simulation models in connection with type approval and technology qualification, with an additional small project-specific validation during case-by-case certification.

An important benefit of doing verification and approval of control system software in a virtual environment is the possibility of test automation. An engine for running scripted tests is already in place for the CyberSea technology. A broad set of automatic regression tests that covers most functionality of a control system software will act as a safety net for any change or update done to this control system. The procedure for updating the control system software should be to thoroughly test any altered functionality and the set of automatic tests will then detect possible side effects.

The possible benefits of including Nauticus Twinity in the verification process will be to:

- Give manufacturers and yards a tool for early prototyping and integration testing
- Facilitate good engineering processes for all stakeholders
- Enable demonstration of integrated effects of system failures
- Provide early feedback on system design with respect to applicable rules for classification
- Improve quality and efficiency of the type approval and certification processes for cyber-physical systems
- Introduce more flexibility in system design through facilitating the use of functional based rules
- Provide access to the platform for pre-commissioning of systems and verification of updates; enabling continuous system improvements
- Enable proper software change management in operation, including testing on the digital twin
- Result in models qualified for condition monitoring; allowing classification societies to replace periodical surveys with condition and event based inspections
- Enable live troubleshooting, incident investigations and similar

7. Concluding remarks

In this paper it is shown how the prototype of a digital twin platform can be implemented by combining existing technologies within DNV GL. Services based on digital twins can be prototyped today, enabling vessel owners to leverage on the increased digitalization and connectivity offered for maritime systems.

Key properties of the Nauticus Twinity concept are:

- Through combining simulation models and sensor data on an open platform it facilitates the design and verification of cyber-physical systems.
- Facilitates optimal design and early integration of systems from multiple manufacturers.
- No separate instrumentation or data transmission infrastructure from DNV GL on the vessel required – the platform can exploit whatever data streams that are made available from the vessel.
- Ability to perform diagnostics and prognostics of integrated systems through model-based simulation.
- Improved documentation and overview of total system functionality.

Combining existing technology through implementation of FMI enables a platform for collaborative simulation and integration of complex systems. For the current prototype, the simulation models should be included as FMUs at the same server as the CyberSea simulator is running. In near future we see the possibilities for distributed co-simulations, meaning that stakeholders can run their simulation models on their own computers and connect to a standardized network bus for collaborative simulations.

The success of a further development of Nauticus Twinity for the maritime market is believed to depend on taking a stepwise approach in developing the service, and securing an open architecture allowing all stakeholders to benefit from the service in terms of a more efficient design and approval process.

References

BAHETI, R.; GILL, H. (2011), *Cyber-physical Systems*, Book section from: The Impact of Control Technology, by T. Samad and A.M. Annaswamy (eds.), Available at www.ieeccc.org

CREMONA, F.; LOHSTROH, M.; TRIPAKIS, S.; BROOKS, C.; LEE, E. A. (2016), *FIDE – An FMI Integrated Development Environment*”, SAC’16, April 4-8, 2016, Pisa, Italy. ISBN 978-1-4503-3739-7/16/04.

GLAESSGEN, E. H.; STARGEL, D.S, (2012), *The Digital Twin Paradigm for Future NASA and U.S. Air Force Vehicles*, 53rd AIAA/ASME/ASCE/AHS/ASC Structures, Structural Dynamics and Materials Conference, 23 - 26 April 2012, Honolulu, Hawaii.

GRIEVES, M. (2014), *Digital Twin: Manufacturing Excellence through Virtual Factory Replication*, Whitepaper, Apriso www.apriso.com, Accessed: March 2016, Available from: http://www.apriso.com/library/Whitepaper_Dr_Grieves_DigitalTwin_ManufacturingExcellence.php

KAKALIS, N.M.P.; DIMOPOULOS, G.; STEFANATOS, I. (2014), *A novel framework for dynamic modelling of integrated machinery systems*, Conf. Computer and IT Applications in the Maritime Industries (COMPIT), Redworth, pp. 137-149

KELLNER, T. (July 2015), *If Ships Could Fly: Big Data Dawn on the High Seas*, GE reports, Retrieved from <http://www.gereports.com>

KNUTSEN, K.E.; VARTDAL: B. J.; MANNO, G. (2014), *Beyond condition monitoring in the maritime industry*, DNV GL Position Paper 6-2014

LEE, E.A. (2015), *The Past, Present and Future of Cyber-Physical Systems: A Focus on Models*, Sensors, 2015, 15, 4837-4869; doi:10.3390/s150304837

LØVOLL, G; KADAL J. (2014), *Big Data – the new data reality and industry impact*, DNV GL Position Paper 4-2014

LÅG, S.; KNUTSEN, K.E.; MANNO, G.; LØVOLL, G. (2015), *Implementing a Scalable Condition Monitoring System for Ships*, Conf. Computer and IT Applications in the Maritime Industries (COMPIT), Ulrichshusen, pp. 529-543

LÅG, S. (2015), *Ship connectivity*, DNV GL Position Paper 4-2015

MANNO, G. et al. (2015), *MODAM: Model based Data Driven Asset Management*, DNV GL, ABB Marine and BW Gas - Project Plan

RÍOS, J.; HERNÁNDEZ, J.C.; OLIVA, M.; MAS F. (2015), *Product Avatar as Digital Counterpart of a Physical Individual Product: Literature Review and Implications in an Aircraft*, Transdisciplinary Lifecycle Analysis of Systems, R. Curran et al. (Eds.), doi:10.3233/978-1-61499-544-9-657

SMOGELI, Ø. (2015), *Managing DP System Software - A Life-cycle Perspective*, 10th IFAC Conference on Manoeuvring and Control of Marine Craft (MCMC'2015), Copenhagen, IFAC-PapersOnLine 12/2015; 48(16):324-334

VINDØY, V. (2008), *A functionally oriented vessel data model used as basis for classification*, 7th Conf. Computer and IT Applications in the Maritime Industries (COMPIT), Liège, pp.60-69

Evaluation of Surrogate Models of Internal Energy Absorbed by Oil Tanker Structure during Collision

Pero Prebeg, University of Zagreb, Zagreb/Croatia, pero.prebeg@fsb.hr
Smiljko Rudan, University of Zagreb, Zagreb/Croatia, smiljko.rudan@fsb.hr
Jerolim Andrić, University of Zagreb, Zagreb/Croatia, jerolim.andric@fsb.hr

Abstract

The main purpose of the research presented in this paper is to evaluate the quality of surrogate models of collision energy absorbed by an oil tanker during collision accident, in order to evaluate appropriateness of their usage in a ship structural optimization process. The motivation for research is investigation of possibility to include ship crashworthiness as an additional objective in a ship structural optimization in a preliminary or even a concept design phase. Numerical simulations were executed in LS Dyna using simulation models generated by an in-house made model generator.

1. Introduction

Modern optimization methods, developed in the areas of naval architecture, aerospace, mechanical engineering etc. are capable of validating innovative vessels concepts as well as generating competitive designs for standard ship types. ISSC (2012) report contains a section on the design requirements, mathematical models of required fidelity for design phases (concept, preliminary and detail), basic taxonomy, applicable optimization methods, formulations including safety as design objective etc. The methods presented help designers to achieve significant savings for the shipyard and the ship owner: increase of deadweight; decrease in the price and weight of construction steel; production costs and lead time improvements; increase of safety (and robustness); savings regarding life cycle cost (LCC) etc.

As shown in Zanic *et al.* (2013), numerical analysis methods for contemporary complex engineering systems, like CFD or FEM, can be computationally very demanding and despite of steady advances in computing power, the expense of running many analysis calculations remains nontrivial. Single analysis of one design solution can take from seconds to hours or even much longer for e.g. non-laminar and non-stationary 3D CFD problems. Therefore, direct use of some analysis methods is not possible in optimization because optimization demands several hundreds or even thousands analysis of different variants. To address such a challenge, surrogate or metamodeling techniques are often used. An application of surrogate modeling as approximations of expensive computer analysis codes can result in significant savings in both number of analysis and total time in which satisfactory optimal solutions are obtained. Due to the wide usage of this approach in many research fields, it can be found under various names like: surrogate (or metamodel) assisted optimization, surrogate (or metamodel) driven design optimization, surrogate (or metamodel) based design optimization, optimization using surrogate models (or metamodels), etc.

There are various criteria that can be used for assessment of the effects of optimization in designing ship and offshore structures. An optimally shaped structure can be compared to a design made by an experienced designer. For a certain typical simple structures, the optimization effects amount to a few percent, whereas for more complex and untypical structures such effects may amount to a dozen or so percent.

One of the main objectives of the national research project DATAS (www.fsb.unizg.hr/datas), is to investigate possible improvements in tanker structural design that could lead to the reduction of consequences for tanker ship accidents in Adriatic Sea. Of course the, the improved methodology for the tanker structural design needs to be incorporated in the ship design methodology and as such it is under the time constraints relevant to the ship design process, which can range from several weeks to several months.

Overall objective of a standard oil tanker structural design process is to simultaneously increase the ship-owner's profit and reduce shipyard production cost, while satisfying all rules prescribed by IACS Harmonized Common Structural Rules for Bulkers and Oil Tankers. The goal of DATAS project is to investigate possibilities of introducing additional structural safety measures as additional objectives. The primary focus is on the measures capable of identification of hull structural integrity (ship crashworthiness, hull girder ultimate strength). Selected design parameters, having significant effect on design solution, have to be identified and discussed with the stake-holders as a part of DeSS formulated for concept (CDP) and preliminary (PDP) design phases, where the most far-reaching decisions are made.

Outline of the proposed overall procedure is shown in Fig 1. The first three blocks are part of CDP, while the last is PDP. The main purpose of the Block 1 is a generation of the response surface model of internal energy E_i absorbed during collision as a measure of crashworthiness. The second block is used to perform multi-objective optimization with weight and structural safety measures (crashworthiness, hull girder ultimate strength) as objectives. The optimization will be done with constraints/requirements prescribed by the CSR Harmonized Rules for Bulkers and Oil Tankers. Block 3, where the preliminary design variant is selected from the set of non-dominated solutions, is the last block in CDP, but it could also be seen as a first block in PDP. The three hold FEM model is used in Block 4 to verify accuracy of the CDP model, and to dimension parts of structure like transverse bulkheads and double bottom that cannot be adequately dimensioned with the models used in CDP.

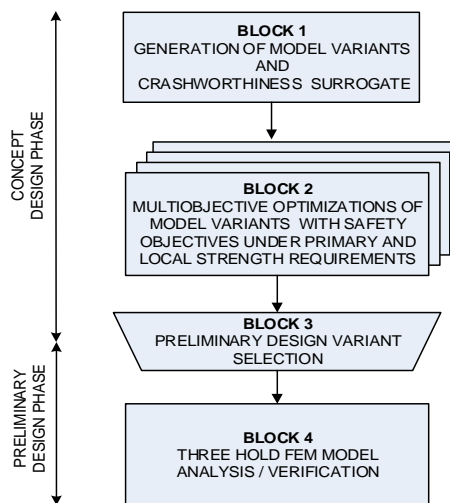


Fig. 1: Proposed tanker structural design procedure

The main purpose of the research presented in this paper is to evaluate the quality of surrogate models of internal energy absorbed by an oil tanker during collision accidents, in order to evaluate appropriateness of their usage in a ship structural optimization process. The motivation for that is an investigation of possibility of inclusion of ship crashworthiness measure as an additional objective in a ship structural optimization in a preliminary or even a concept design phase.

Crashworthiness (collision and grounding) analysis models are one of the most complex and the most time consuming ship structural analysis models. Depending on the level of details modeled and the extent of the model (partial model to full ship model), nonlinear finite element analysis of a single variant could take from an hour to several days. Even the simplest possible model are usually too demanding for direct usage in structural optimization during preliminary design phase and especially during a concept design phase.

The possible solution is a creation of appropriate surrogate models that could replace demanding nonlinear numerical models in structural optimization. Since an inclusion of surrogate models in optimization process requires execution of analysis runs that are necessary to train those surrogates,

special considerations are necessary to reduce number of analysis runs for the training to an acceptable level, while maintaining a level of accuracy acceptable for the optimization process.

2. Surrogate modelling

Surrogate / approximation / metamodeling, is the key to surrogate assisted optimization. It can be stated that surrogate modelling actually evolves from classical Design of Experiments (DOE) theory, in which polynomial functions are used as response surfaces, or surrogate models. One of the most cited handbooks with detail overview of DOE for classical (physical) experiments is *Montgomery (2001)*, while the overview of surrogate modeling for deterministic computer experiments (DACE – design and analysis of computer experiments) can be found in e.g. *Fang et al. (2006)*, *Simpson et al. (2001)*.

The main difference between “classical” and computer experiments is nonexistence of random error for deterministic computer experiments, which according to *Sacks et al. (1989)* leads to the conclusion that surrogate model adequacy is determined solely by systematic bias and that the classical notions of experimental blocking, replication and randomization are irrelevant. In depth review of surrogate modeling for computer based engineering design can be found in *Simpson et al. (2001)* and *Wang and Shan (2007)*. Steps necessary for generation of surrogate models includes: planning of experiments or sampling, Fig. 2, execution of simulations with original analysis methods, generation or creation of selected surrogate model and validation of surrogate model adequacy.

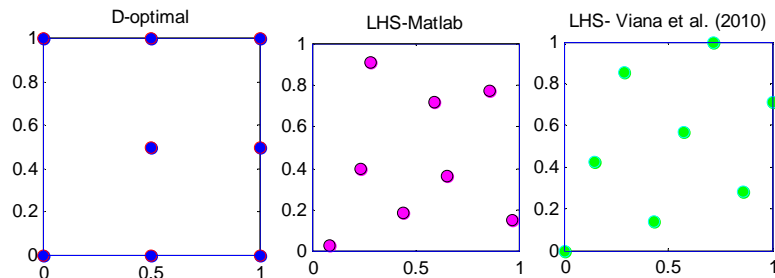


Fig. 2: Preview of D-optimal design and two different space filling LHS designs

After selecting an appropriate experimental design according to appropriate criteria, *Goel et al. (2008)*, *Viana et al. (2010)*, and performing the necessary computer runs, the next step is to choose a surrogate model type and corresponding fitting method. Many alternative models and methods exist, and there is no clear answer which is better. The selection of appropriate surrogate model depends mostly on characteristic of physical phenomenon that is approximated. Some of widely used surrogate models in engineering include: Response Surfaces (RS), *Fang et al. (2006)*, *Kaufman et al. (1996)*, *Montgomery (2001)*, *Roux et al. (1996)*, Kriging, *Koch et al. (2002)*, *Martin and Simpson (2005)*, *Simpson et al. (2001)*, Radial basis functions (RBF), *Fang et al. (2006)*, *Powell (1992)*, *Regis and Shoemaker (2007)*, Artificial Neural Network (ANN), *Miralbes and Castejon (2012)*, *Park et al. (2013)*, *Patnaik et al. (2005)*, Support Vector Machine (SVM), *Collobert and Bengio (2001)*, *Rivas-Perea et al. (2013)*, Multivariate Adaptive Regression Splines (MARS), *Friedman (1991)*.

Generally, the value of a target criteria response y at some location x can be written as:

$$y(\mathbf{x}) = \hat{y}(\mathbf{x}) + \varepsilon_b \quad (1)$$

where $\hat{y}(\mathbf{x})$ is surrogate model of response y , while ε_b is a surrogate model error or bias. As already stated, one of the characteristics of deterministic computer experiments is nonexistence of random error ε_r , and that is the reason why it is not included in Eq.(1).

In this research, RS method will be used as surrogate modelling method, so it's basic theoretical background is given in the following subchapter

2.1. Response surfaces (RS)

Probably the most widely used surrogate modeling method is response surfaces (RS) that approximates criteria functions using low order polynomials, mostly simple linear and quadratic or some specific polynomials like orthogonal Legendres polynomials.

General matrix formulation of this model can be written as:

$$\hat{y}_{RS} = \mathbf{B}^T \boldsymbol{\beta} \quad (2)$$

where \mathbf{B} is a k-tuple of a used polynomial functions, while $\boldsymbol{\beta}$ is a k-touple of unknown corresponding coefficients. If a mostly linear polynomial is used, \mathbf{B} i $\boldsymbol{\beta}$ are:

$$\mathbf{B}^T = \{1 \ x_1 \dots \ x_i \dots \ x_k\} \quad (3)$$

$$\boldsymbol{\beta}^T = \{\beta_0 \ \beta_1 \dots \ \beta_i \dots \ \beta_k\} \quad (4)$$

The unknown coefficients $\boldsymbol{\beta}$ are usually determined using least square regression analysis by fitting the response surface approximation into existing data:

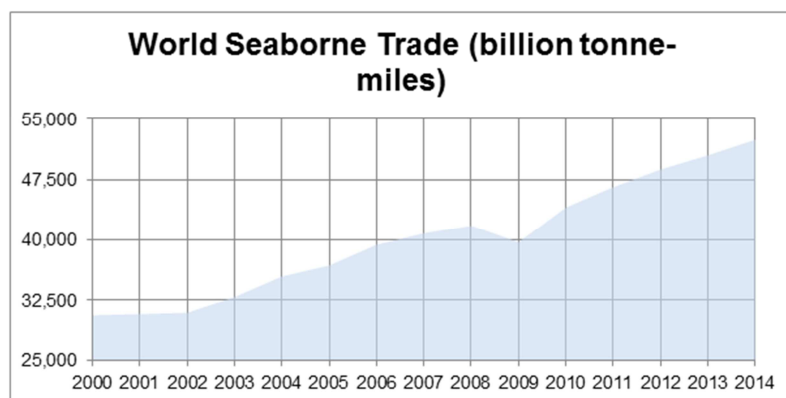
$$\boldsymbol{\beta} = (\mathbf{B}_{1-n} \mathbf{B}_{1-n}^T)^{-1} \mathbf{B}_{1-n} \mathbf{y}_{1-n} \quad (5)$$

where \mathbf{y}_{1-n} is n-tuple of n known response values, while \mathbf{B}_{1-n} is $k \times n$ matrix with the calculated values of selected basis functions at locations 1-n.

RS popularity for modeling of a deterministic computer experiments, besides its good characteristics for certain type of problems, is due to the fact that surrogate modeling itself evolves from classical Design of Experiments theory where RS was used for the description of physical phenomena, *Montgomery (2001)*. Discussion of the statistical pitfalls associated with the application of RS to deterministic computer experiments can be found in *Sacks et al. (1989)* and *Simpson et al. (2001)*. Some of the applications in engineering includes: structural optimization, *Arai and Shimizu (2001)*, *Prebeg (2014)*, *Vitali et al. (2002)*, and Pareto front generation, *Goel et al. (2007)*, *Lian and Liou (2005)*.

2. NFEM ship collision analysis

Ship collisions are high-energy marine accidents leading sometimes to catastrophic consequences: loss of human lives, loss of a cargo or a ship itself and environmental pollution on which closed seas are extremely sensitive. Due to that, a number of measures were taken to prevent or reduce the consequences of ship collisions and groundings. However, such accidents still occur worldwide.



Source: UNCTAD Review of Maritime Transport, 2014

Fig. 3: World Seaborne Trade, www.ics-shipping.org

It was in 1987 when one of the most catastrophic collisions occurred when "MT Vector", carrying 8800 barrels of gasoline collided with "MV Doña Paz" off the coast of Dumali Point, Mindoro, in the Philippines. More than 4000 people died in that incident, becoming so the deadliest ferry disaster ev-

er. More recently, on January 2012, the "Costa Concordia" collided with the rock formation near the cost of Isla del Giglio and grounded nearby. Due to the size of damage 32 people lost their lives and a ship was completely lost. A number of collision and grounding events occur during the year but, fortunately, the catastrophic events are rare and their number is being constantly reduced. On the other hand, maritime traffic is increasing and the number of ships transporting goods worldwide is growing, Fig. 3, and so is the risk of collision.

2.1 Adriatic Sea collision scenario

Adriatic Sea is a semi-enclosed narrow sea stretching from north-west to south-east mainly between two countries, Italy and Croatia. Other countries having the access to Adriatic Seas are all on its east coast: Slovenia, Bosnia and Hercegovina, Montenegro and Albania. The closest point between Italy and Albania defines the Otrant Strait which is the only entrance to the Adriatic Sea from the Mediterranean Sea. In this way, Adriatic Sea is rather closed sea and any risk of ship collision and related marine environment pollution in that area has to be considered seriously as the regenerating capacity of the sea is limited and the impact on surrounding industry, particularly tourism, may be dramatic.

Due to shape of the Sea two most important traffic routes are north-west to south-east or longitudinal routes and west to east, or transversal routes, Fig. 4. Commonly large merchant ships are sailing over longitudinal routes to bring the cargo to large northern harbours in Koper, Rijeka, Trieste, Venice etc. while ferries and leisure ships are sailing over transversal routes, connecting large cities on both west and east cost of Adriatic. Due to the nature of such trafficking an orthogonal collision of a tanker and a ferry was assumed to be a reasonable collision scenario for Adriatic.



Fig. 4: Maritime traffic in the Adriatic, Zec et al. (2009)

2.1 Numerical model

In order to study consequences of specified collision scenario a calculation model in commercial software package LS-Dyna was set. It consists of two ships in concern:

- A struck ship, being an Aframax class tanker
- A striking ship, being a typical international ferry of the Adriatic Sea.

Due to the complexity of the problem, both ship models are reduced in order to enable the study of all most important physical aspects of their collision and yet at the same time to enable the reasonably fast calculation. The main struck and striking ship particulars are listed in Table 1.

Table 1: Main struck and striking ship particulars

Struck ship (tanker)		Striking ship (ferry)	
Lpp	236 m	Length over all	121.83 m
B	42 m	Ship mass	4730 t
D	21 m	Ship with cargo mass (assumed)	6889 t
Scantling draught	15.1 m	Draft aft	5.25 m
Displacement	133000 t	Draft fore	5.30 m
Max. service speed	15.3 kn	Middle draft	5.28 m
Long. center of gravity (from L/2)	5.599 m	Ship centre of gravity height	8.38 m
Ship center of gravity height	12.050 m	Ship centre of gravity length	61.08 m

Struck ship model is being generated using an in-house software code enabling the quick generation of FE models by changing their geometric parameters like double side width, number of web frames, number and position of side stringers, etc. Since fine mesh is required in the collision zone the size of the finite elements in that area is approx. 100x100 mm. Struck ship model consists of the portside cargo hold and it is entirely made of fine mesh plate finite elements. The rest of the ship is taken into account by the concentrated ship mass (less the portside cargo hold) modelled using eight solid elements and located at the exact location of the ship centre of gravity.

Striking ship model is made in detail in the bow section while the rest of the ship is modelled using simple beam elements with appropriate mass. In this way, bow shape realistically affects the penetration in the struck ship side, while the rest of ship (inertia) is adequately taken into account. Finally, both models are presented in Fig.5, where the orthogonal collision scenario is set: portside cargo hold of a tanker is being subjected to the impact of a ferry bow.

The following scenario lists the reference collision scenario parameters:

- Ferry is located in front of the middle cargo hold of a tanker,
- Collision is orthogonal,
- Speed of a tanker is 0 m/s,
- Speed of the ferry is 8 m/s,
- Draft of the tanker is 15.1 m,
- Draft of the ferry is 5.3m.

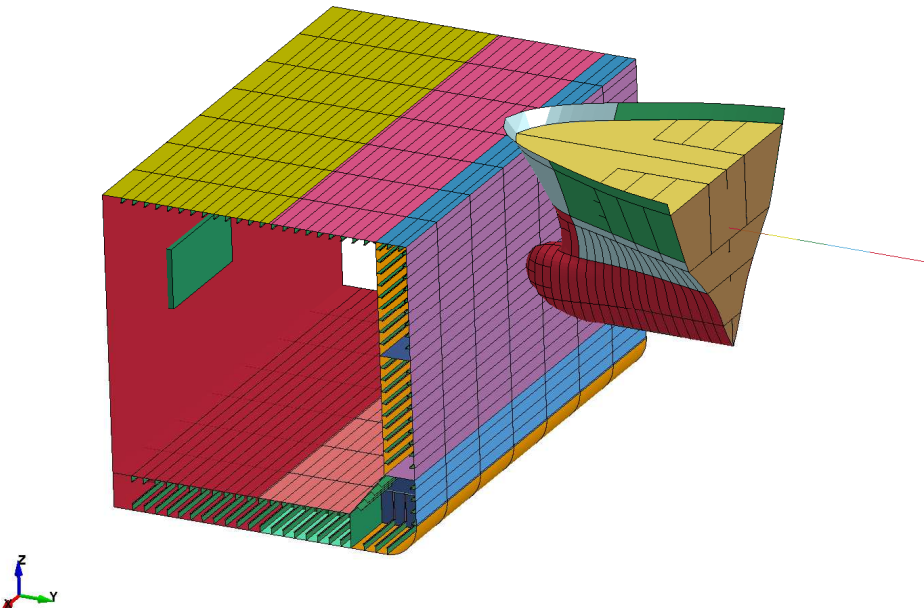


Fig. 5: Calculation model: portside cargo hold of a tanker and a ferry bow in orthogonal collision

2.3 Numerical analysis

FEM analysis is being performed using explicit LS-Dyna solver considering both non-linear material model properties and a contact between the models. Mesh size parameter is taken into account by applying Peschmann method of correcting the failure criteria, i.e. critical strain. Contact between the striking and the struck ship is defined using LS-Dyna keyword *CONTACT_AUTOMATIC_SURFACE_TO_SURFACE. Both static and dynamic friction is defined for steel-to-steel situation and chosen values are 0.74 and 0.57, respectively. Material models used for ship models are defined by keywords *MAT_RIGID and *MAT_PIECEWISE_LINEAR_PLASTICITY.

As a result of collision a typical structural damage occurs as presented in Fig. 6. In all of the collision calculations, one for each variation of struck ship structural parameters, a tanker hull is breached, suggesting that impact of such energy would lead to cargo spill. Two main sets of data characterise collision event, namely contact force and deformation energy (both elastic and plastic).

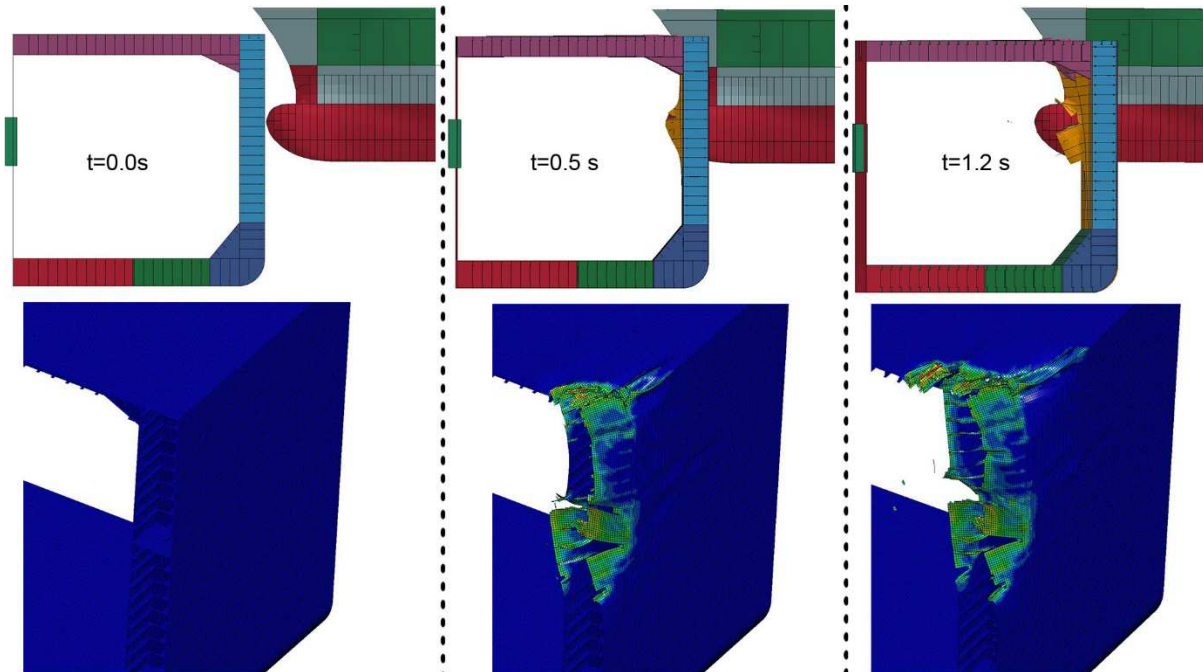


Fig. 6: Progress of collision on one of the tested models

3. Ship crashworthiness surrogate models

In order to prepare surrogate models of struck ship crashworthiness, first it is necessary to select the relevant measures of crashworthiness. Internal energy absorbed by the structure during collision is usually used as a crashworthiness criterion, e.g. Klanac *et al.* (2009), Ehlers (2010). Usually, maximal internal energy is used, however, for practical purposes, maximal internal energy is substituted with Internal energy absorbed during the first 1.2 s $E_{it=1.2}$.

One of the most important parts in preparation of surrogate models is the selection of relevant control parameters that influences the selected surrogate model responses. Based on the previous work, the relevant parameters that influence the struck ship crashworthiness includes:

- topology parameters like number of web frames, number of side stringers, side stiffener spacing
- geometry parameters like double side width, height of web / breadth of flange of longitudinal and transfer stiffeners
- scantlings like outer shell thickness, inner hull thickness, side stringer thickness, and off course web / flange thickness of longitudinal and transfer stiffeners.

In order to enable simple generation of models that combine all of those parameters, it has been decided to prepare in-house model generator, since it has been estimated that preparation of few hundreds different topology/geometry model combinations would take more time than preparation of an in-house model generator.

The preliminary study presented in this paper includes two control parameters: one geometry parameter (double side width) and one scantling parameter (thickness of the side shell). Both parameters were tested on three levels, Table 2.

Table 2: Preliminary study control parameters

Parameters	Level 1	Level 2	Level 3
Double side width	2000 mm	2100 mm	2200 mm
Side shell thickness	13.5 mm	15.5 mm	17.5 mm

In order to study influence of all effects, including removal of experiments, full factorial design is used, which result with the total of 9 experiments, Table 3. Since full quadratic model for two parameters have 6 unknowns, that requires 6 experiments for their determination, the remaining experiments are used for the evaluation of model error.

3.2. Numerical analysis results

The numerical experiments have been executed on IBM x240 (Xeon E5-2680 v3/ 32GB RAM) using 8 cores for each experiment. Average time for each simulation was 36 hours. Figs. 7 and 8 present time-domain results for C20 and A20 models, respectively. Main results for all the models are listed in Table 3. Fig. 7 presents C20 model energy distribution typical for long-time, i.e. $t=1.9s$ collision simulations. Only models B20 and C20 were subjected to prolonged simulation. Figure 8 presents A20 model energy distribution, typical for short-time, i.e. $t=1.2s$ simulations. Two different run times were chosen for the following reasons. Short-time simulation was chosen to save the cost of the calculation and at the same time to reach the inner hull breach confidently. Long-time simulation was chosen to examine the results after the moment when internal collision energy has reached the maximum.

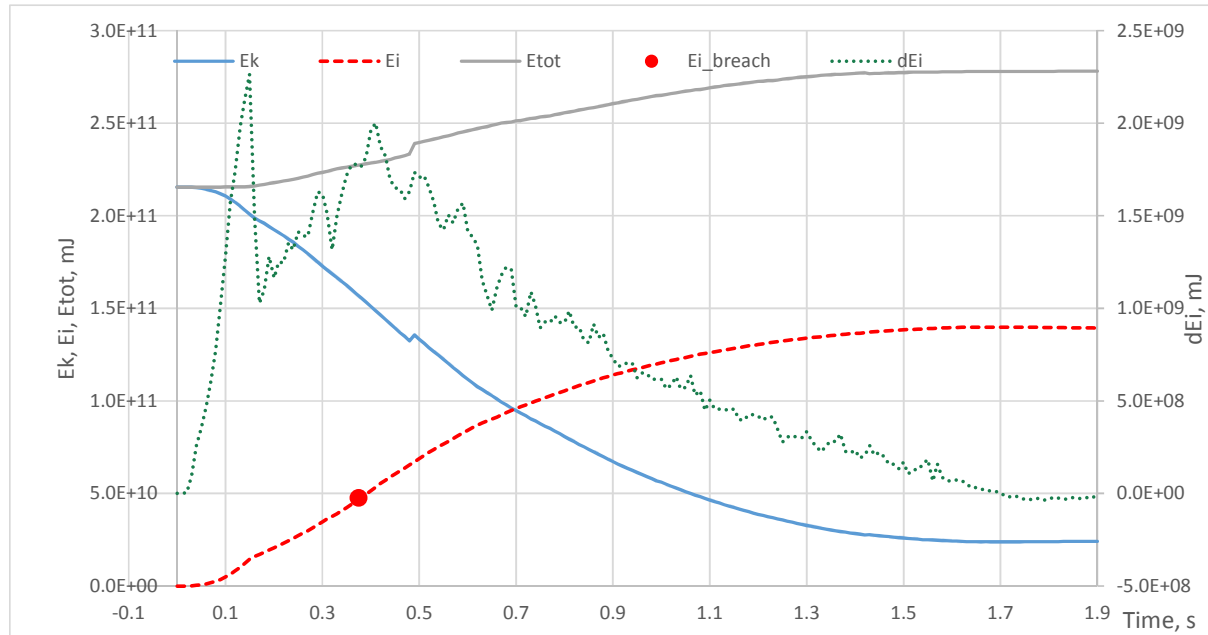


Fig. 7: Model C20 Results

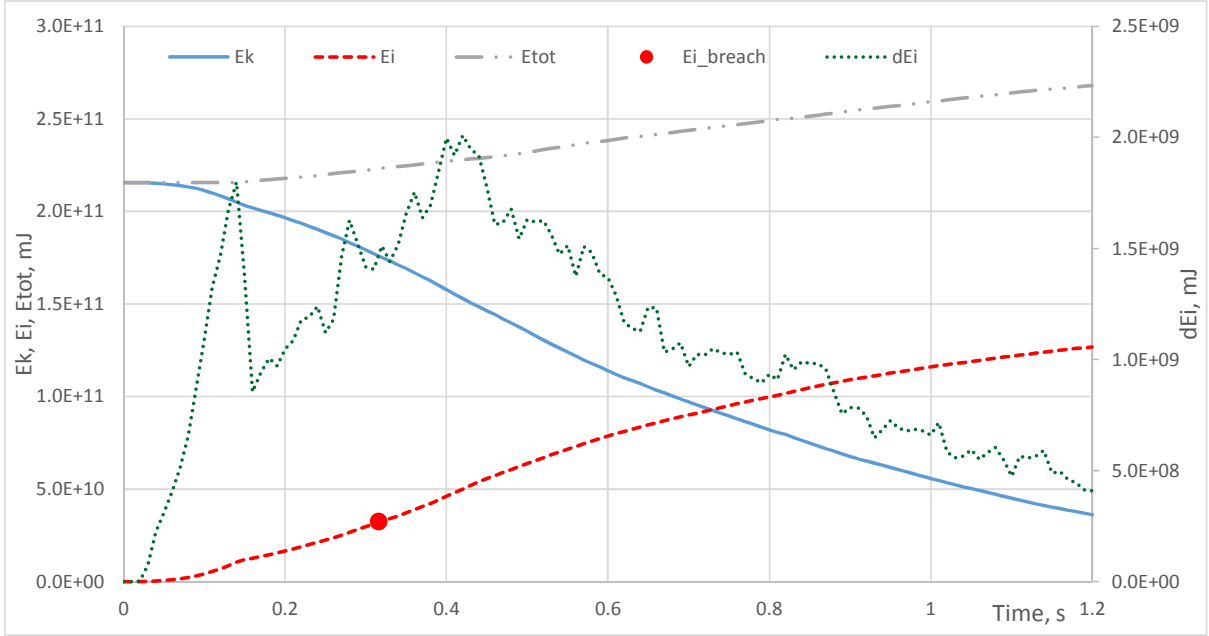


Fig. 8: Model A20 Results

On both Fig. 7 and 8 the following is presented:

- Blue line presents the kinetic energy in the system. As the struck ship is not moving, kinetic energy in the system is generated by the speed and mass of the striking ship, namely a 6889 t ferry with an initial speed of 8 m/s. Once the contact between ships occurs, available kinetic energy is transformed into internal energy, as well as being lost by friction during the contact.
- Red line presents the internal energy, being the energy generated by elastic and plastic deformation of the structure, both for the struck and the striking ship. Each finite element deformation is measured and the related energy is calculated until the critical strain is detected and element erased from further calculation. A sum of internal energy is a measure of damage on both ships.
- Grey line presents the total energy in the system and in the LS-Dyna it is a sum of initial total energy plus the external work, which is in this case mostly the contact energy.
- Finally, green line presents time-step distribution of internal energy, indicating the gradients of internal energy during the collision.

Table 3: Experiment results

Model	t_s, mm	b_s, mm	t_{breach}, s	$E_{i, breach}, \text{mJ}$	$E_{i, t=1.2}, \text{mJ}$
A20	13.5	2000	0.3158	3.26 E+10	1.267 E+11
B20	15.5	2000	0.3774	4.55 E+10	1.297 E+11
C20	17.5	2000	0.3750	4.77 E+10	1.308 E+11
A21	13.5	2100	0.3922	4.57 E+10	1.245 E+11
B21	15.5	2100	0.3513	4.01 E+10	1.265 E+11
C21	17.5	2100	0.3871	4.76 E+10	1.277 E+11
A22	13.5	2200	0.3807	4.18 E+10	1.253 E+11
B22	15.5	2200	0.4129	5.09 E+10	1.269 E+11
C22	17.5	2200	0.4237	5.50 E+10	1.275 E+11

3.3. Surrogate model of an internal energy

As given above, an internal energy absorbed during the first 1.2 s $E_{i,t=1.2}$ is used instead the maximal internal energy. Full quadratic response surrogate model have been used as a starting model.

Backward elimination procedure was planned to be used for exclusion of members that have been marked as not significant (F test value greater than 0.1). However, $E_{i,t=1.2}$ response surface model for obtained experiment responses have resulted with full quadratic model, since all model factor, including interaction of control parameters were significant. Final analysis of variance (ANOVA) for this model is given in upper part of Table 5, while the model equation and some basic statistic measures are given in lower part of the table. Adjusted R² is high and in very good correlation with Predicted R².

Some of the surrogate model diagnostics plots, Residuals vs Predicted and Predicted vs Actual, are presented in Fig. 9. Fig. 10 shows resulting surrogate model in 3D plot together with the numerical experiments used for the generation (marked with spheres).

Table 5: Surrogate model statistics

Source	Sum of Squares	df	Mean Square	F Value	p-value Prob > F	
Model	6.33E+19	5	1.27E+19	800.9	< 0.0001	significant
A-TPL	3.06E+19	1	3.06E+19	1936.5	< 0.0001	
B-Width	1.9E+19	1	1.9E+19	1200.9	< 0.0001	
AB	1.82E+18	1	1.82E+18	115.08	< 0.0001	
A ²	1.37E+18	1	1.37E+18	86.98	< 0.0001	
B ²	1.05E+19	1	1.05E+19	665.07	< 0.0001	
Residual	1.9E+17	3	1.58E+16			
Lack of Fit	1.9E+17	3	6.32E+16			
$R^2=0.9970$, Adjusted $R^2=0.9958$, Predicted $R^2=0.9936$, Adequate Precision=90.24						
$E_{i,t=1.2} = 7.426E+11 + 1.034E+10 t_s - 6.563E+8 b_s - 2.383E+6 t_s b_s - 1.465E+8 * t_s^2 + 1.620E+5 b_s^2$						

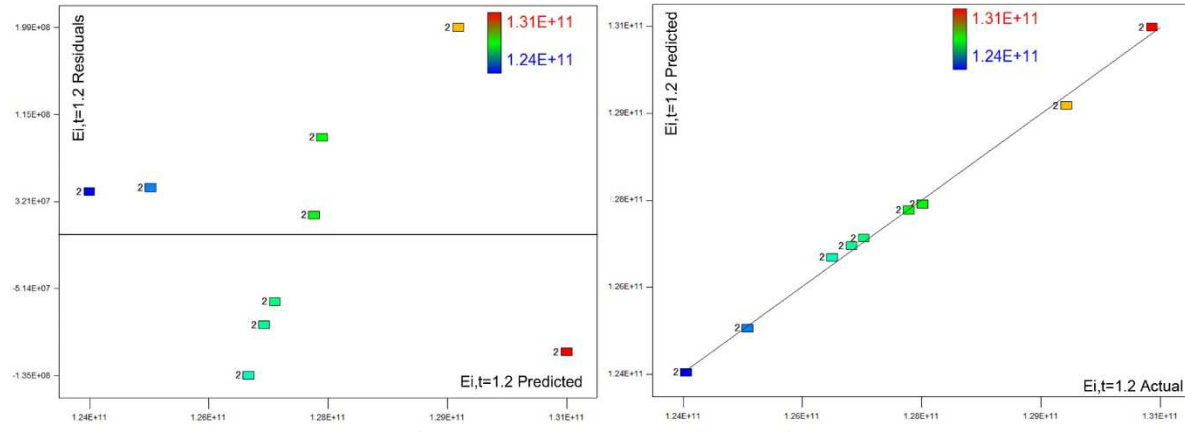


Fig. 9: Surrogate model diagnostic

Based on the presented surrogate model statistics and diagnostic plots, it is reasonable to conclude that the internal energy surrogate model is in a very good agreement with simulation results, and that its usage in optimization is reasonable, of course inside of used control parameters interval. However, as indicated above, those are just preliminary results on two control parameters. The study continues with inclusion of other relevant control parameters, and it is expected that the complete study will be finished by the end of 2016. Also, the further study will include modelling of other possible crashworthiness measures that sounds reasonable (e.g. internal energy absorbed until the inner hull breach, size of the hull rupture after collision, etc.). The first step will be to extend simulation time to at least 2 second in order to catch maximal internal energy.

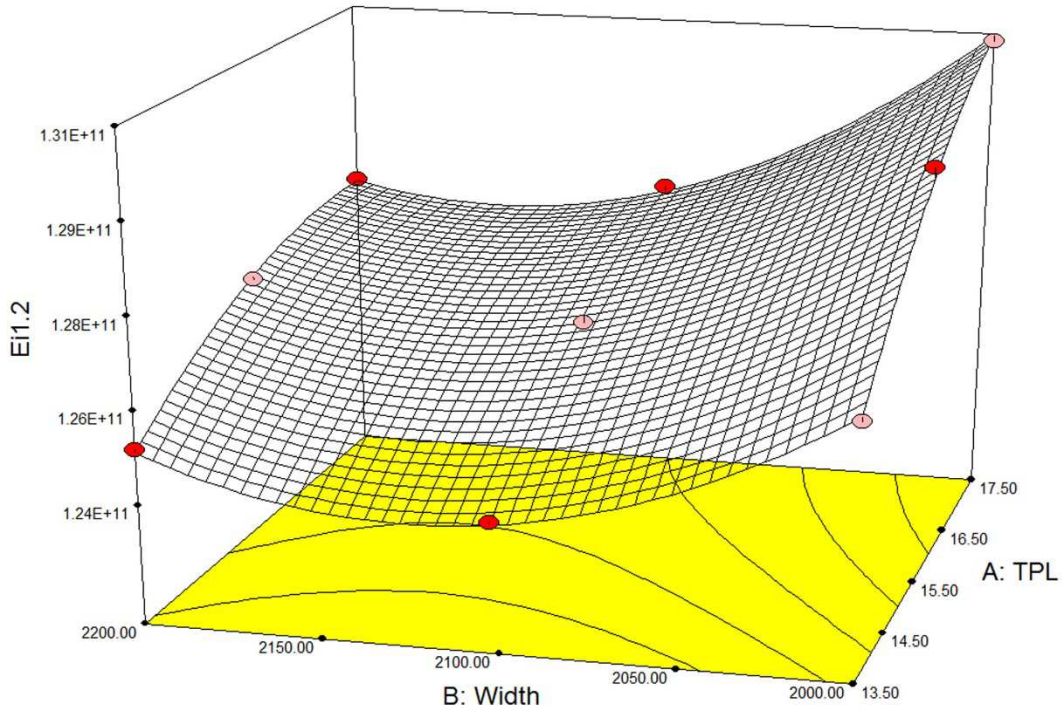


Fig. 10: Surrogate model 3D plot

4. Conclusions

The design of a ship structure falls within the category of large scale problems characterized by several design objectives, hundreds of design variables and tens of thousands of design constraints. The objective of the research partially presented in this paper is to evaluate ship crashworthiness surrogate modelling possibilities in order to evaluate suitability of their usage in the improved tanker structural design process. The preliminary results presented here show that the accuracy of an internal energy surrogate model with respect to the used control parameters is more than adequate for use in optimization. This is a very good motivation for the continuation of research and preparation and evaluation of surrogate model that will include all other relevant control parameters.

Acknowledgment

This work has been supported in part by Croatian Science Foundation under the project 8658.

References

- ARAI, M.; SHIMIZU, T. (2001), *Optimization of the design of ship structures using response surface methodology*, 8th Int. Symp. Practical Design of Ships and Other Floating Structures, Shanghai
- COLLOBERT, R.; BENGIO, S. (2001), *SVMTorch: support vector machines for large-scale regression problems*, J. Mach. Learn. Res. 1, pp.143-160
- FANG, H.B.; HORSTEMEYER, M. (2006a), *Global response approximation with radial basis functions*, Eng. Optimization 38, pp.407-424
- FANG, K.T.; LI, R.; SUDJANTO, A. (2006b), *Design and modeling for computer experiments*, Chapman & Hall
- FRIEDMAN, J. H. (1991), *Multivariate Adaptive Regression Splines*, Annals of Statistics 19, pp.1-67

EHLERS, S. (2010), *A procedure to optimize ship side structures for crashworthiness*, J. Eng. for the Maritime Environment 224(1), pp.1-11

GOEL, T.; HAFTKA, R.T.; SHYY, W.; WATSON, L.T. (2008), *Pitfalls of using a single criterion for selecting experimental designs*, Int. J. Numerical Methods in Engineering 75, pp.127-155

GOEL, T.; VAIDYANATHAN, R.; HAFTKA, R.T.; SHYY, W.; QUEIPO, N.V.; TUCKER, K. (2007), *Response surface approximation of Pareto optimal front in multi-objective optimization*, Computer Methods in Applied Mechanics and Engineering 196, pp.879-893

ISSC (2012), *Report of Technical Committee IV.2 - Design Methods*, 18th Int. Ship and Offshore Structures Congress

KAUFMAN, M.; BALABANOV, V.; GIUNTA, A.A.; GROSSMAN, B.; MASON, W.H.; BURGEE, S.L.; HAFTKA, R.T.; WATSON, L.T. (1996), *Variable-complexity response surface approximations for wing structural weight in HSCT design*, Computational Mechanics 18, pp.112-126

KLANAC, A.; EHLERS, S.; JELOVICA, J. (2009), *Optimization of crashworthy marine structures*, Marine Structures 22(4), pp.670-690

KOCH, P.; WUJEK, B.; GOLOVIDOV, O.; SIMPSON, T. (2002), *Facilitating probabilistic multidisciplinary optimization using Kriging approximation models*, 9th AIAA/ISSMO Symp. Multi-disciplinary Analysis and Optimization

LIAN, Y.; LIOU, M.S. (2005), *Multiobjective optimization using coupled response surface model and evolutionary algorithm*, AIAA J. 43, pp.1316-1325

MARTIN, J.D.; SIMPSON, T.W. (2005), *Use of Kriging models to approximate deterministic computer models*, AIAA J. 43, pp.853-863

MIRALBES, R.; CASTEJON, L. (2012), *Structural design and optimization using neural networks and genetic algorithms of a tanker vehicle*, J. Chinese Institute of Engineers 35, pp.181-192

MONTGOMERY, D.C. (2001), *Design and analysis of experiments*, Wiley

PARK, K.H.; JUN, S.O.; BAEK, S.M.; CHO, M.H.; YEE, K.J.; LEE, D.H. (2013), *Reduced-order model with an artificial neural network for aerostructural design optimization*, J. Aircraft 50, pp.1106-1116

PATNAIK, S.N.; CORONEOS, R.M.; GUPTILL, J.D.; HOPKINS, D.A. (2005), *Subsonic aircraft design optimization with neural network and regression approximators*, J. Aircraft 42, pp.1347-1350

POWELL, M.J.D. (1992), *The theory of radial basis functions approximation*, Advances in Numerical Analysis, Oxford University Press

PREBEG, P.; ZANIC V.; VAZIC B. (2014), *Application of a surrogate modeling to the ship structural design*, Ocean Engineering 84, pp.259-272

REGIS, R.G.; SHOEMAKER, C.A. (2007), *Parallel radial basis function methods for the global optimization of expensive functions*, Eur. J. Operational Research 182, pp.514-535

RIVAS-PEREÀ, P.; COTA-RUIZ, J.; CHAPARRO, D.; VENZOR, J.; CARREÓN, A.; ROSILES, J. (2013), *Support vector machines for regression: A succinct review of large-scale and linear programming formulations*, Int. J. Intelligence Science 3, pp.5-14

ROUX, W.; STANDER, N.; HAFTKA, R. (1996), *Response surface approximations for structural optimization*, 6th Symp. Multidisciplinary Analysis and Optimization

SACKS, J.; WELCH, W.J.; MITCHELL, T.J.; WYNN, H.P. (1989), Design and analysis of computer experiments, *Statistical Science* 4, pp.409-423

SIMPSON, T.W.; MAUERY, T.M.; KORTE, J.J.; MISTREE, F. (2001a), *Kriging models for global approximation in simulation-based multidisciplinary design optimization*, *AIAA J.* 39, pp.2233-2241

SIMPSON, T.W.; POPLINSKI, J.D.; KOCH, P.N.; ALLEN, J.K. (2001b), *Metamodels for computer-based engineering design: Survey and recommendations*, *Eng. with Computers* 17, pp.129-150.

VIANA, F.A.C.; VENTER, G.; BALABANOV, V. (2010), *An algorithm for fast optimal Latin hypercube design of experiments*, *Int. J. Num. Methods in Eng.* 82, pp.135-156

VITALI, R.; PARK, O.; HAFTKA, R.T.; SANKAR, B.V.; ROSE, C.A. (2002), Structural optimization of a hat-stiffened panel using response surfaces, *J. Aircraft* 39, pp.158-166

WANG, G.G.; SHAN, S. (2007), *Review of metamodeling techniques in support of engineering design optimization*, *J. Mechanical Design* 129, pp.370-380

ZANIC, V.; ANDRIC, J.; PREBEG, P. (2013), *Design synthesis of complex ship structures*, *Ships and Offshore Structures* 8(3-4), pp.383-403

ZEC, D.; MAGLIĆ, L.; ŠIMIĆ HLAČA, M. (2009), *Maritime transport and possible accidents in the Adriatic sea*, 17th Annual Conf. Eur. Environment and Sustainable Development Advisory Councils EEAC, Dubrovnik

Enhancing Performance through Continuous Monitoring

Stefan Gunnsteinsson, Marorka, Reykjavik/Iceland, stefan.gunnsteinsson@marorka.com
Jacob Wiegand Clausen, Marorka DK, Copenhagen/Denmark, jacob.clausen@marorka.com

Abstract

With raised economic and environmental awareness through market pressure and stricter regulations (e.g. SEEMP, ECA, MRV), the need for relevant and reliable performance data has become increasingly important. Noon reporting is currently the preferred way of monitoring fuel consumption in the shipping industry. It is argued that the level of sophistication in performance systems has to be raised to be competitive in the coming years. Business decisions are currently being made based on indicators derived from different combinations of measured data, without estimating sensor uncertainty and how it propagates. The paper shows how the sampling method and frequency impacts accuracy of data-based decisions, first by illustrating the difference in accuracy of performance indicators and models, and secondly through operational analysis by comparing noon-reported and continuously-logged data for the same vessel and period. The results highlight areas where noon-reported data comes up short and where higher resolution data sets have the potential to increase quality and reduce the effort required to make data-based business decisions.

1. Introduction

A large set of variables is needed to describe a ship's propulsion performance at any given time - this includes speed over ground, speed through water, loading condition, weather observation, fuel consumption, shaft power and many more, depending on the purpose and detail. Currently, ships have a wide range of variability in terms of quantity and quality of available measuring equipment. Best practice should be to focus not only on the measured value of a performance indicator, but also on the degree of uncertainty associated with that value. This is especially important when making business decisions based on a defined set of key performance indicators (KPIs), all of which are derived from one or more measurements, each with its own degree of uncertainty. In statistics, the term propagation of uncertainty or error, is used when estimating the resulting uncertainty of a function based on the uncertainty of the individual variables.

Shipping companies and operators currently rely largely on noon-reported data as the primary way of collecting vessel energy performance data, *Rojon et al. (2014)*). A noon report is a data set provided by a ship and transmitted to shore every 24 hours with information required to assess weather conditions and the ship's performance. Noon-reported data gives, among other things, a confirmed estimate (although dependent on human error and inconsistency) of accumulated fuel consumption and total distance travelled along with a snapshot of weather observations. With increasing economic and environmental incentives (SEEMP, ECA, MRV), it is becoming more and more apparent for ship-owners and operators that they must have a better and more accurate understanding of how their vessels are performing. This need has been identified, *Aldous et al. (2015), Poulsen et al. (2016)*.

This paper examines how the sampling method and frequency impact on data-based decisions in the following twofold approach: firstly, by illustrating the difference in monitoring and accuracy of performance indicators and models; secondly, through operational analysis and quantification of the benefits of continuous monitoring by comparing noon-reported and continuously-logged data for the same vessel and period.

2. Key Performance Indicators for Efficient Shipping

The term Key Performance Indicator (KPI) is used in all businesses in all industries. Its main goal is to set a benchmark and be able to track success over time. The shipping sector applies groups of performance indicators such as crew performance, health and safety, environmental management,

energy efficiency and more. Every organization should select a small number (typically less than 10) of KPIs which have the important feature that positive movement of the indicator affects the business in a positive way. Selecting the right KPIs might take some time and several iterations but the key is that they must be measured frequently and acted upon by relevant stakeholders with clear responsibilities.

Using KPIs effectively is one of the approaches currently being used to successfully drive and improve the energy performance of a fleet of vessels. Monitoring changes over time and studying what affects ships brings a new dimension of advanced operational knowledge to shipping operations. However, this knowledge generation is highly dependent on trust and transparency. If the foundation, Fig. 1, in terms of data availability, data reliability and data accuracy, is in place, then there is something to build on. A certain investment and discipline is required to reach and maintain good data quality; this process is in practice most often underestimated by shipping companies.

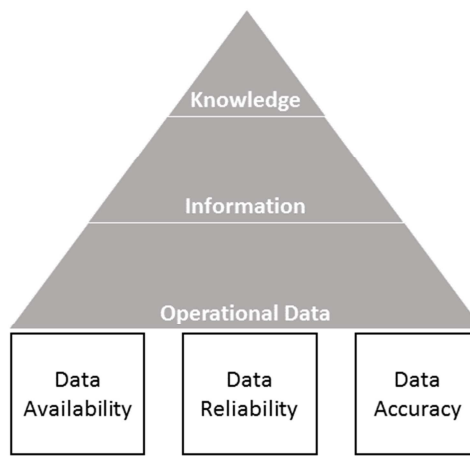


Fig. 1: Knowledge is created when information can be trusted and monitored over time

One quality indicator of a data set is the availability of all relevant variables. The frequency of missing data points can be mitigated by having processes in place that can use other sources to estimate the missing data. In some cases, statistical methods can be used. This is one of the challenges in the upcoming MRV regulations, which require all reporters to clearly describe how to create surrogate data which compensates for any missing data. Reliability of a data set refers to the consistency of reported values; manual reporting is affected by human factors; automatic data collection is vulnerable to various sensor issues (drift, spikes, frozen). A point which should be taken into account is that manual reporting most often entails reading from sensors, which could be drifting or frozen without the reporter noticing.

Accuracy, when referring to the quality of measurements, is a word that is often misused, and according to the standard definition (ISO 5725-1), the term accuracy only tells half the story. Formally, it describes only the closeness of a measurement to the true value, while precision describes the closeness among a set of values. The combination of these two errors is called the uncertainty (or total error) of any measurement. The former is often referred to as systematic errors, which can result from a non-calibrated sensor or by applying the wrong measuring technique. In both cases, the result will be a systematic deviation from the true value (true value = exact physical value, which is attempted to be measured). Proper equipment and processes can help avoid and eliminate this type of error. Random errors are the variability around the true value due to the precision limitations of the measuring device. Random errors can be evaluated using statistical analysis and can be reduced by increasing sample size.

A performance indicator that is calculated by applying mathematical operations to combine various individual measurements or quantities also has its own level of uncertainty. In statistics, the term

propagation of uncertainty is used to describe the effect which uncertainty of individual measurements has on the uncertainty of the indicator (or function) based on those measurements.

For addition or subtraction, if:

$$Q = a + b + c + \dots - (x + y + z)$$

then the resulting uncertainty in Q , let's call it δQ , will be:

$$\delta Q = \sqrt{(\delta a)^2 + (\delta b)^2 + (\delta c)^2 + \dots + (\delta x)^2 + (\delta y)^2 + (\delta z)^2}$$

And for multiplication or division if:

$$Q = \frac{a \cdot b \cdot \dots \cdot c}{x \cdot y \cdot \dots \cdot z}$$

then the resulting uncertainty in Q will be:

$$\frac{\delta Q}{|Q|} = \sqrt{\left(\frac{\delta a}{a}\right)^2 + \left(\frac{\delta b}{b}\right)^2 + \left(\frac{\delta c}{c}\right)^2 + \dots + \left(\frac{\delta x}{x}\right)^2 + \left(\frac{\delta y}{y}\right)^2 + \left(\frac{\delta z}{z}\right)^2}$$

But these only apply if a, b, c, \dots, x, y, z are statistically independent. Other rules apply if you are raising a variable to a power. To keep the discussion relevant to shipping, let's take an example of an indicator now widely used in the shipping industry: the Energy Efficiency Operational Index (EEOI). Here is the formal (IMO) definition to calculate EEOI for a voyage:

$$EEOI = \frac{\sum_j FC_j \times CF_j}{m_{cargo} \times D}$$

where:
 j fuel type
 FC_j mass of consumed fuel per fuel type j
 CF_j fuel mass to CO_2 conversion factor for fuel j
 m_{cargo} cargo carried (tonnes)
 D distance in nautical miles

Assuming an uncertainty of 1–3% for FC (individual sensors are more accurate but this refers to the fuel-system uncertainty), 1–3% for distance (state-of-the-art is currently 1% at ideal condition but many factors will influence this in operation) and 2–5% for cargo carried, the range of uncertainty in the final EEOI is 2.5–6.6%. For a typical 8000 TEU container vessel with an EEDI reference of 18.62 g CO_2 /ton-mile, the conservative uncertainty range in EEOI is +/- 1.2 g CO_2 /ton-mile.

3. Performance Reporting

A noon report (NR) is a data set provided by a ship and transmitted to shore every 24 hours with information required to assess weather conditions and the ship's performance. The content of noon reports typically includes vessel name, voyage number, date, time, position, average speed, average rpm, snapshot of weather condition (wind direction and speed, sea and swell condition) and fuel oil/lube oil/water remaining on board (R.O.B.). In terms of assessing propulsion efficiency, the noon report gives a confirmed estimate of accumulated fuel consumption used for propulsion and total distance travelled along with a snapshot of weather conditions. If the vessel is equipped with a torque meter on the propulsion shaft(s), then the average shaft power is typically provided as well.

Although the noon report is confirmed and signed by the officers on board, it is susceptible to manual

errors. Anytime a human is asked to read a value from a sensor, record the time and write it manually into a report, there will be inconsistencies. Frequent crew changes make this a particular on-board vulnerability, during each 24 hours period and also in the long term. Inconsistencies can be greatly reduced with clear guidelines, processes and training. Processes to cross-check reported values and follow-up with crew should be in place. Crew members might report at different times of the day, assess sea-state conditions differently, sensors in a different order or forget that the vessel crossed a time-zone.

Another source of error in manual reporting is the incentive for misreporting. According *Poulsen et. al. (2016)* on energy consumption monitoring in shipping companies one of the challenges identified is the problem of misreporting because the “logic of good energy consumption monitoring practices conflicts with common business practices in shipping companies”. An example of one of these conflicts is the over-reporting of daily fuel consumption by crew to make up for under-supplied bunker fuel deliveries. Usually, the crew realizes too late that the delivery note and fuel status don't match, and the incentive for over-reporting is to avoid legal actions from a port state control. Another example is time charter agreements where maximum daily fuel consumption is stated in the charter party agreement. To avoid any claims from the charterer, the crew might be asked to under-report on a specific day and make up for it in the coming days.

A survey by the UCL institute from 2014 reveals that noon reports were the most widespread monitoring tool (63%) among the 94 companies that participated. Automated data logging accounts for 56% of the respondents with 21% using automated continuous onboard monitoring, 12% automated continuous monitoring communicated to shore-based offices and 22% selected both options. It is likely that every respondent has his own ideas of what continuous monitoring (CM) of vessel performance data entails, but it should at least mean considerably higher frequency data collection than noon reporting (at least once every hour) and main automatic digital storing of data. Commercial providers of higher frequency data collection systems for shipping usually refer to their products as “performance monitoring systems”; there is room within that scope for both noon reports and higher resolution data collection.

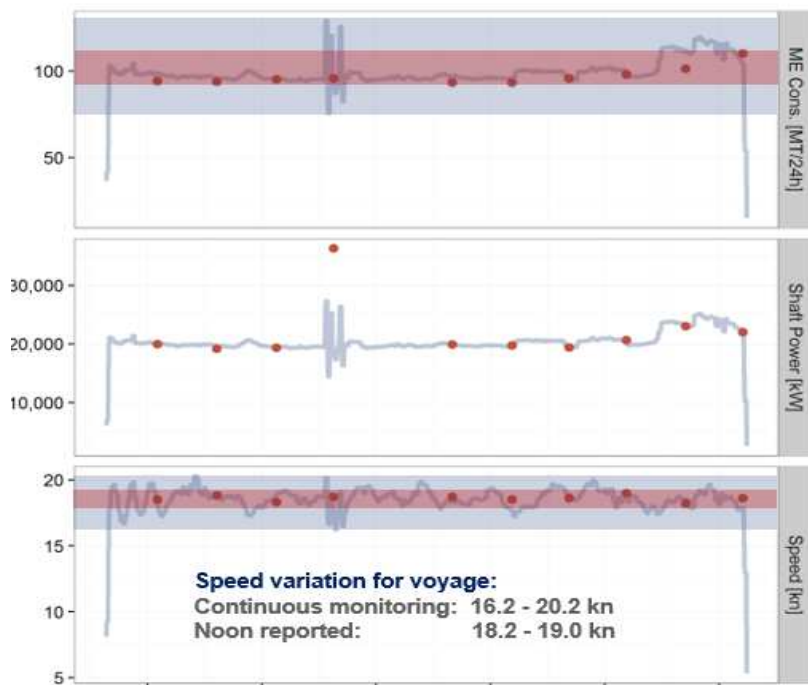


Fig. 2: Trend plots of main engine consumption, shaft power and speed through water for a 10-day voyage sailed by a post-panamax container vessel showing both noon reported values (points) and higher frequency (15 min resolution) values as continuous lines.

With the increasing economic and environmental pressure (SEEMP, EEDI, MRV) it is becoming increasingly important for ship owners and operators to have a near real-time and precise picture of their vessels performance. Although fully acknowledging the day-to-day and historical importance of the noon-report, it must be realized that in terms of performance reporting and analysis, this data set has its limitations. Low-resolution data collection means that variability in vessel speed and weather is not captured over the 24-hour period. Among the variables that affect vessel performance speed, weather and sea conditions usually have the largest impact on a vessel's total resistance. Since the correlation between these parameters and vessel performance is non-linear, inaccuracy will only increase the error and therefore scatter the noon-reported data set.

Fig. 2 shows trend plots of main engine consumption, shaft power and speed-through-water for a recent 10-day voyage sailed by a direct diesel driven post-panamax container vessel. Each trend-plot includes data from two sources – noon reports and continuous monitoring with a 15-minute frequency. The speed variations (range +/- 2 knots) captured with the higher resolution data are averaged out for the noon values (range +/- 0.4 knots). In addition, inconsistent reporting is apparent in both power and fuel consumption trends, but what is more important is that the variation is not captured. The true variation in fuel consumption based on the variation in speed is 4–5 times larger than the variation based on the noon-reported speed values, Fig. 3a. To clearly demonstrate how those variables do not correlate, Fig. 3b shows results from two legs sailed by the same post-panamax vessel, where the total fuel consumption has been summarized in three ways. Estimating consumption based on the reported speed gives total fuel consumption values 27% and 18% higher than the average of the reported consumption.

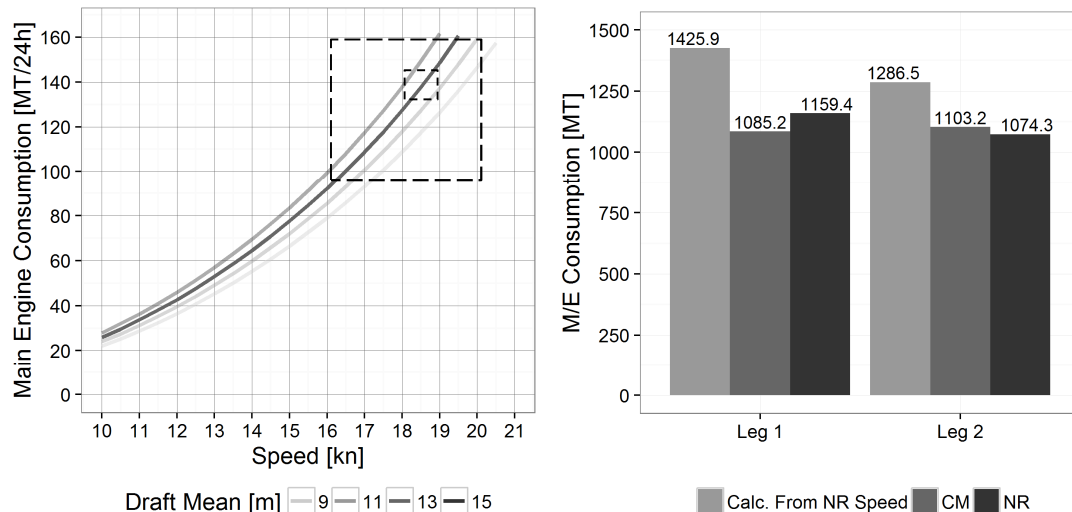


Fig. 3: (a): Speed – M/E consumption relationship for a range of drafts in calm weather conditions. The two boxes on the plot represent the window of speed variation captured for CM (larger box) and NR (small box). (b): Comparison of estimates of total fuel consumption for two legs sailed – 1) sum of NR values 2) sum of CM values 3) sum of estimated consumption using NR speed as input into propulsion model.

Human cognitive biases are tendencies to think in a certain way that can lead to systematic deviations from reality. One such bias is called confirmation bias, which is the “tendency to search, interpret, favour and recall information that confirm one’s beliefs or hypotheses” (www.sciencedaily.com – Confirmation bias). In relation to performance reporting from ships, this means that there is most probably a tendency to report values closer to the target or expected values. Therefore, a ship’s officer who is informed about speed targets is more likely to be biased when reporting average speed in noon reports. This cognitive bias also translates to repetitive reporting, meaning that if the reporter has no reason to believe an operation has changed, he will most likely report yesterday’s values again today. This pattern is seen again and again when comparing noon-reported data sets with automatically

collected data. Fig. 4 shows histograms of speed and draft for sister vessels. One of these vessels is equipped with both continuous monitoring and noon reporting, while the other sister reports using only noon reports. It is apparent from the noon reported histograms (middle row) that certain values are favoured and that the natural spread seen in the continuous monitored set (top row) is not visible in the lower-frequency data set. The same pattern where a few favourable values are most often reported can be seen in the sister vessel's data set (bottom row).

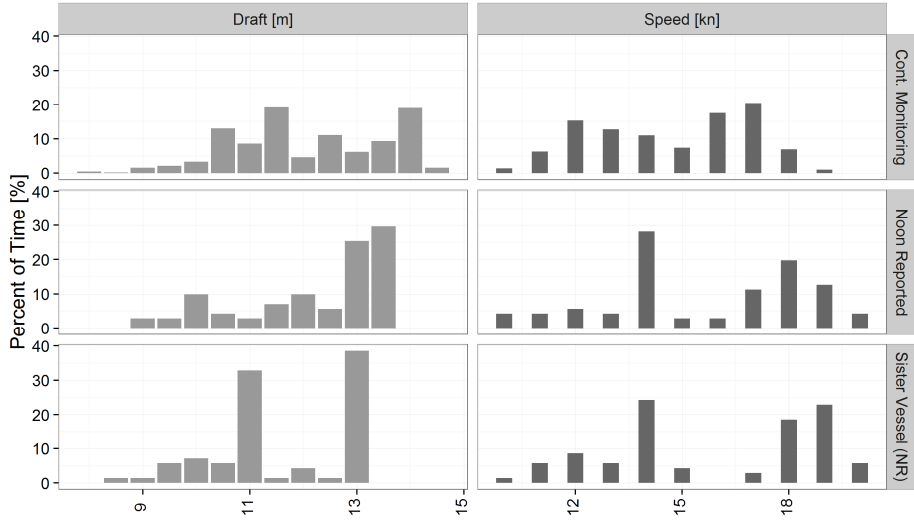


Fig. 4: Operational profile (mean draft and log speed) for post-panamax sister vessels, one equipped with both CM and NR systems, while the bottom row is a sister vessel sailing the same route only with NR system.

In shipping the prices for transporting goods from one port to another are negotiated in the freight market. Freight rates are dependent on demand and have historically been highly volatile. On the other hand, the supply of tonnage is much slower (it takes time to build new vessels). This is especially apparent in the voyage (spot) charter market. There agreements are made on a voyage basis where the ship owner (or his management company) estimates voyage costs (fuel cost, port cost and daily operating costs) of delivering the cargo from port A to B. In the long term, the success of this business model relies heavily on the success of making accurate cost estimates, where the largest variable cost is the price of fuel. The inconsistencies in reporting, as shown in Fig. 4, also translate to information on fuel consumption. Fig. 5 shows two tables created from NR and CM data sets for the same vessel over a full-year. Comparing the tables there is a natural continuity in the CM table where, as expected, fuel consumption used for propulsion increases with speed and draft, but the same is not apparent for the NR table. Adding the effect of weather will only exaggerate this difference.

Continuous Monitoring MT/24h		Draft				
		10	11	12	13	14
Speed	12	46	44	48	53.1	68.2
	14	52.5	59.2	65.5	68.6	80.9
	16	93.9	92.5	89.1	94.3	99.5
	18	114.2	116.2	111.6	119.9	113.8

Noon Reported MT/24h		Draft				
		10	11	12	13	14
Speed	12	26.2	41.9	34.1	51.3	40.7
	14	66.4	52.1	51	46.5	55.5
	16	94.4	62	70.3	107.3	-
	18	82.5	104.4	103.5	107.3	105.4

Fig. 5: Tables showing how fuel consumption for propulsion changes with respect to speed and draft using data from two different sources for the same vessel and period.

4. Benefits of higher frequency and automation

Performance indicators as introduced in chapter 2 are often distinguished as leading or lagging indicators (actionable and directional synonymous). The main difference between the groups is the time delay until it is practical or even possible for relevant stakeholder to act based on their value. The absolute value of this time delay depends on the type of business. In shipping, a typical lagging indicator is calculated and presented on a voyage, weekly, monthly or quarterly basis. Leading indicators are those which can be calculated and acted upon in the short term, even down to an hour and minute basis. There are various operations and processes on board that have shorter time spans than 24 hours, and they are a challenge for ship management to monitor and follow up. One of these areas worth mentioning is diesel generator operation, where unnecessary running of too many generators is often seen. This translates into both less efficient production of the required electricity and increased maintenance cost (since most operators make maintenance and overhaul plans based on running hours). Another example is soot-blowing procedures, which are infrequent in normal operation but typically increase in frequency when slow-steaming. When diesel engines are run far outside their design condition for longer periods, engine designers recommend that the load on the engine is increased at fixed intervals with the purpose of “cleaning” soot deposits and other particles that build up in the exhaust system and exhaust gas boiler. The crew is therefore directed to carry out this operation at a set load, frequency and period.

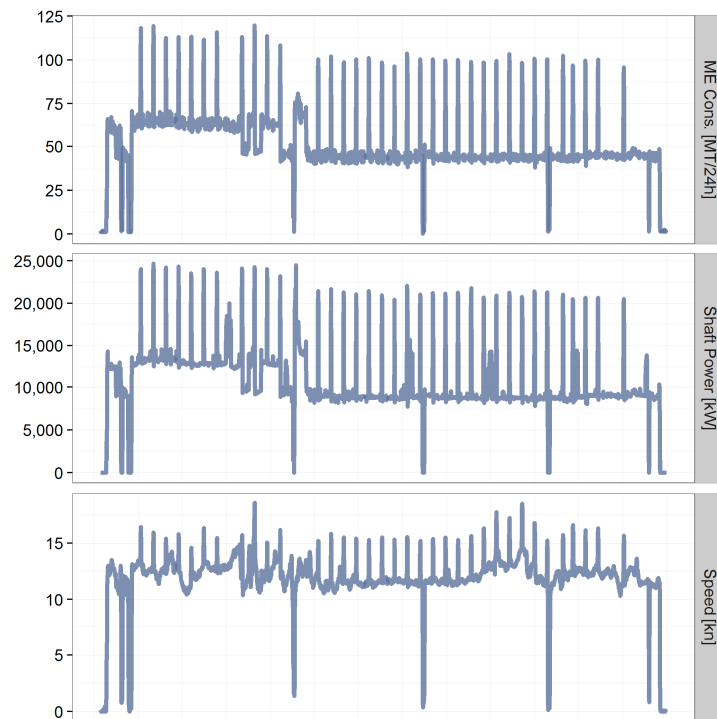


Fig. 6: Trend plots of main engine consumption, shaft power and speed through water for a 43-day voyage sailed by a VLCC where soot blowing of main engine was instructed once per day.

Fig. 6 is an example with visualized trends showing how soot blowing affects main engine consumption, shaft power and speed through water for a VLCC aboard which the crew were instructed to carry out soot blowing on a daily basis for a period of one hour. This is a 43-day voyage with 38 soot blowing incidents. In this case, the MT/24h consumption typically doubles (from 45 to 85 MT/day) during a soot blowing procedure which in most cases lasted for between 2 and 3 h. The average cost of each incident was 4–5 MT, making a total of 178 MT for the voyage. This is a significant amount (8%) of the total fuel consumed for propulsion for the whole voyage. When the ship management was challenged on these procedures and informed that the duration was longer than necessary, they consulted the engine designer and agreed to reduce soot-blowing to a weekly 1-h event, potentially reducing fuel consumption on this voyage by 6.5%.

One area where day-to-day variability plays a larger role in terms of fuel savings is monitoring vessel speed in relation to voyage execution. The IMO estimated, *Bazari et al. (2011)*, that voyage execution (combination of speed profile optimization and weather routing) has the greatest potential for gains apart from speed reduction and hull condition monitoring. As mentioned earlier, speed and weather variability over 24 h are not captured in daily reports, and due to the non-linear correlation between speed and consumption, it is difficult to grade how well a voyage was executed using noon-reported values alone. With higher frequency data collection, it is possible to identify unnecessary speed variations, for instance so-called sprint-loiter operations where navigators tend to speed up at the beginning of a voyage to make sure they will arrive in port on time. This early “sprint” is understandable due to the fact that the uncertainty of predicting the best for the target is substantial and the cost of arriving late bears a huge penalty. However, these risks can be reduced with more reliable, accurate information and feedback. On a longer term basis, comparing the time series data for the voyage with an optimal execution and filtering or normalizing for weather effects will allow for the creation of a summarized estimate of the potential savings which can be fed back to the crew in a retrospective analysis. The aim, with proper training and follow-up, would be to reduce potential for savings through voyage execution improvements. Fig. 7 illustrates a trend in reduced potential for a New Panamax container vessel over a full year period.

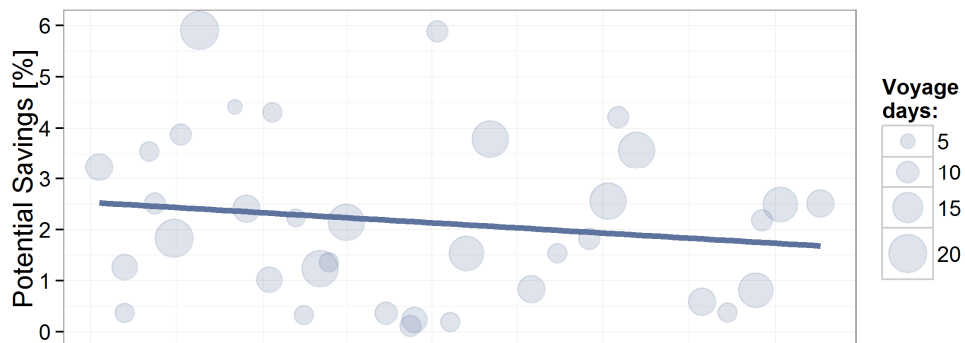


Fig.7: Reduction in fuel saving potential as function of time with each dot representing a voyage

Another type of performance indicator is the comparison of an operational value to a physical baseline where the difference is tracked over time and/or between sister vessels. In some cases these indicators can be treated as leading indicators (e.g. engine maintenance that can be done on-board), although this is usually considered over a longer term. For a diesel engine, this baseline is typically the official shop test specific fuel oil consumption (SFOC) curve. For a hull and propeller performance, it is usually the official sea trial speed-power curve. A KPI which moves outside a certain range would normally trigger an investigation followed by a maintenance action. Hull and propeller performance is often evaluated in terms of an annual speed drop conservatively ranging from 1–5%. The potential for considerable gains in this area means that a great deal of effort and development has been put into antifouling technologies. Ship owners have to decide on the best coating system depending on ship type, condition of waters it will operate in and the foreseen operational profile. An ongoing process has been initiated, mainly by paint suppliers, to standardize a method (ISO 19030) and establish a common method to guarantee performance for both parties. However, the need for a more short-term solution has been identified, *Aldous et al. (2015)*.

Currently, many ship operators rely on noon-reported data sets to plan underwater hull and propeller inspections, potentially followed by cleaning events. Due to the non-linear relationship between vessel speed and shaft power (or fuel consumption) and the way the noon-report is created, inconsistent data points will prevail. Corrections and normalizations for differences in loading conditions, sea state and weather (such normalization has been standardized in ISO 15016) are applied to reduce scatter. However, there is no mention of the level of confidence of these normalization methods in the standard, and it is hard to know whether or not they will just increase the scatter instead of coming closer to an informed decision.

A principal statement in probability and statistics, called the law of large numbers, states that confidence increases as sample size grows. Typical resolutions for systems with continuous monitoring are in minutes or even seconds, which means 100 – 5000 more data points than the noon report every day. Fig. 8 compares the percentage speed drop for the same vessel for a 4.5 month period using two different reporting methods. The upper plot is based on noon reports, while the lower plot is based on automatically collected data with 15-minutes' resolution. As shown, the statistical confidence in the slope of the trend line is much greater in the case of the higher resolution. The higher frequency data provides a better basis for making qualified decision within the same time period. Alternatively, it could reduce the time for building up the same confidence level and thus reduce the decision time. This is the key to transforming indicators that were previously lagging indicators into leading indicators with acceptable levels of confidence.

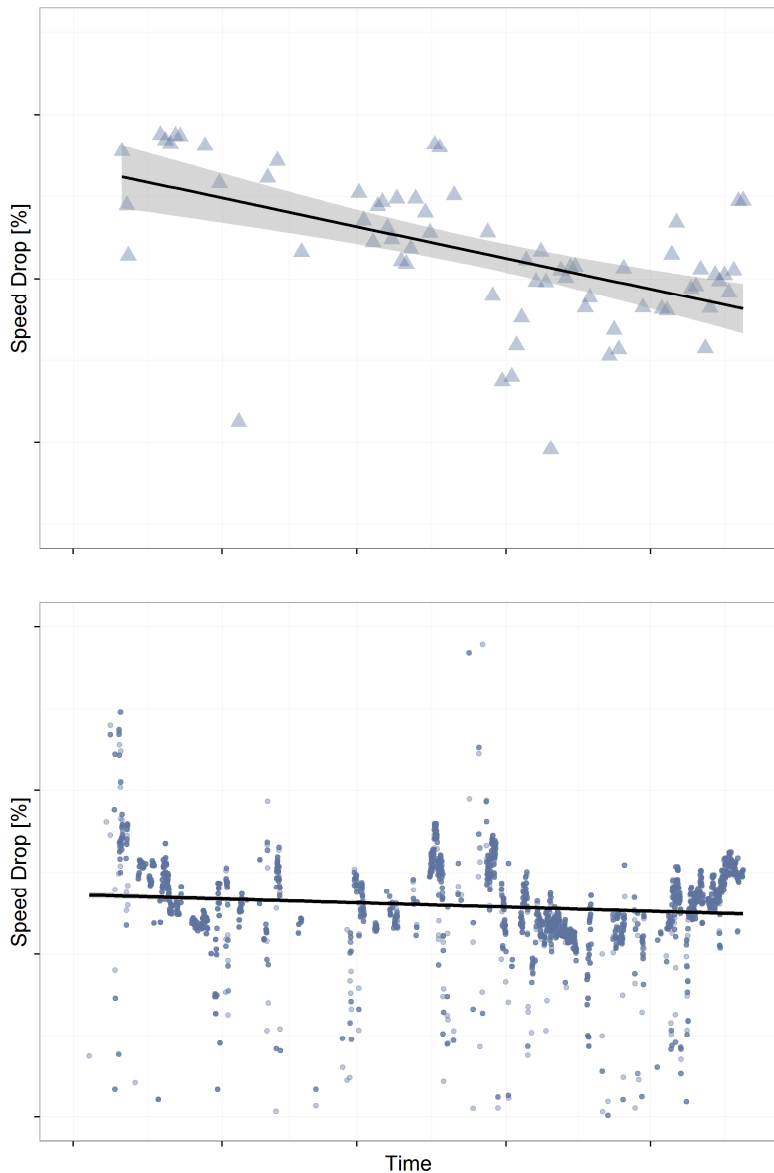


Fig. 8: Comparison of the confidence in percentage speed drop trend line over a 4.5 month period based on NR data set (top) and CM data set (below).

5. Conclusion

Various researchers, Acciaro *et al.* (2013); Jafarzadeh and Utne (2014); Johnson and Andersson (2011), have touched upon the energy efficiency gap or barriers where the different areas halting implementation of best energy management practices have been identified and scrutinized. In one of

the more recent publications, *Poulsen and Johnson (2016)* look further to try to find the “context of action in which decisions on energy efficiency take place” by extensively interviewing professionals from shipping companies and classification societies. Among the many problems highlighted as effecting energy consumption monitoring were: 1) lack of real-time data; 2) unclear manual reporting procedures; 3) crew incentives for misreporting; 4) lack of trust regarding data quality. These points underline the importance of the methodology introduced in chapter 2 and illustrated in chapter 3 where it is argued that lack of trust in the available information makes it difficult for decision makers to create and follow up on procedures and prioritize project initiatives.

Increased frequency, automation and communication between crew and shore is essential in certain technical areas of the shipping business. Chapter 4 shows this with examples which commonly rely on capturing variations in all parameters so that confidence in data collection is established over a relatively short period. The results highlight areas where noon-reported data comes up short and where higher resolution data sets have the potential to increase quality and reduce the effort required to make data-based business decisions. More leading indicators can be defined and used to identify operational behaviours and excess consumption. They can be addressed within hours rather than days. The greater potential that can be addressed and the reduced time to respond are leading to an advancement in performance management which cannot be achieved with noon-report data.

References

- ACCIARO, M.; HOFFMANN, P.N.; EIDE, M.S. (2013), *The energy efficiency gap in maritime transport*, J. Shipping and Ocean Engineering 3, pp.1-10
- ALDOUS, L.; SMITH, T. (2013), *Noon report data uncertainty*, Low Carbon Shipping Conf., London
- BAZARI, Z.; LONGVA, T. (2011), *Assessment of IMO Mandated Energy Efficiency Measures for International Shipping*, Int. Maritime Org., London
- ISO 5725-1 (1994), *Accuracy (trueness and precision) of measurement methods and results*, Int. Office for Standardization, Geneva
- JAFARZADEH, S.; UTNE, I.B. (2014), *A framework to bridge the energy efficiency gap in shipping*, Energy Volume 69, pp.603-612
- JOHNSON, H., ANDERSSON, K. (2011), *The energy efficiency gap in shipping - barriers to improvement*, Int. Association of Maritime Economists (IAME) Conf., Santiago de Chile
- POULSEN, R.T.; JOHNSON, H. (2016), *The logic of business vs. the logic of energy management practice: understanding the choices and effects of energy consumption monitoring systems in shipping companies*, J. Cleaner Production 112, pp.3785-3797
- ROJON, L.; SMITH, T. (2014), *On the attitudes and opportunities of fuel consumption monitoring and measurement within the shipping industry and the identification and validation of energy efficiency and performance interventions*, UCL Energy Institute, London

Fuzzy Logic Single-Objective Optimization Using Multiple Criteria to Understand Human Factors on Early Stage Design

Seth Fireman, University of Michigan, Ann Arbor, Michigan/USA, sfireman@umich.edu

Angela Lossa, Colombian Navy, Ann Arbor, Michigan/USA, alossa@umich.edu

David Singer, University of Michigan, Ann Arbor, Michigan/USA, djsinger@umich.edu

Abstract

The ultimate goal in early stage design is to uncover and identify interdependencies that will impact the performance of the final produced product. While most early stage design is focused on traditional performance metrics such as hydrodynamic efficiency, seakeeping performance, production cost and traditional hydrostatic measures, non-traditional operational performance evaluations are usually not considered. In reality the success of the final product is a marriage between the performance of the vessel and the performance of the people who operate it. For naval ships this marriage is even more critical. The goal of this paper is to demonstrate the use of a fuzzy logic human factors system in a single-objective multi-criteria formulation solved with a particle swarm optimizer as a means to understand how we to incorporate human factors implications for a naval vessel under a variety of Sea State conditions, mission profiles, and ship parameters in early stage design. The single objective multiple criteria optimization structure evaluates the ship's ability to maintain speed through various sea-states while taking into account the heave effects on sea-state, and the overall crew effectiveness utilizing a modified Subjective Workload Assessment Technique (SWAT).

1. Introduction

The incorporation of human factors into early stage design has always been a challenge. Traditional methods for evaluating human factors require detailed design information. For example, when discrete event modelling is used to evaluate a ship's fire egress not only is a full CAD model of the general arrangements needed the time to develop and run the event model is extensive, *Rigterink (2014)*. The execution time pushes this type of analysis to late stage design and thus egress simply is evaluated for a completed design versus being a driver in the early stage design decisions.

The human element is key within the design process of any vessel or marine vehicle. Knowing that Human error causes 80-85% of marine accidents, *Baker (2005)*, this issue becomes relevant to take into account especially on early stages of the design process for vessels that rely on people for their operations.

2. Methodology

The overarching goal of this research initiative was to identify using only preliminary design tools how a hull behaved at a given Sea State and speed in order to find what heading would give the maximum human performance of the crew. This goal led to the development of a single-objective optimization using multiple criteria conducted through the use of sub functions calculating disciplines of interest. The top-level objective function was optimized with MATLAB's particle swarm optimizer within the fuzzy logic toolbox.

The objective function was developed with sub functions calculating individual features of interest of the vessel performance. Sub functions included: calm water resistance, ship motions due to various sea-state conditions, and a human factors evaluation module. These sub functions are then individually calculated. Results of the calculations were incorporated together using fuzzy logic rules to create an overall crew effectiveness value. Effectiveness values were used in the optimization in order to determine what headings at given Sea States the ship would be most effective and thus the true performance of the vessel in various sea-states. While traditionally seakeeping is simply evaluated in early stage design and the naval architect interprets if those motions are acceptable the method

presented in the paper attempts to remove the subjectivity of ship motions and frame them into the construct of human performance.

2.1. Resistance

Resistance and powering calculations were conducted through utilization of the University of Michigan's Powering Prediction Program (PPP). PPP calculates a vessel's resistance using a regression-based approach to the Holtrop & Mennen Method. PPP is used extensively in the University of Michigan's senior design courses: NA 470/475. Calculations were conducted on speeds ranging from 14 kn to 28 kn in order to identify all operating ranges for the notional vessel. PPP requires that the following conditions be met in order to conduct calculations:

$$\begin{aligned} 0.55 \leq C_p \leq 0.85 \\ 3.90 \leq L/B \leq 14.9 \\ 2.10 \leq \frac{B}{T} \leq 4.00 \\ 0.05 \leq F_n \leq 1.00 \end{aligned}$$

PPP requires the user to input: vessel length, beam, draft, block coefficient, midship coefficient, waterplane coefficient, analysis speed, approximate propeller diameter, and approximate propeller pitch/drag ratio, *Parsons (1998)*. Best engineering judgement is to be used where data was available.

2.2. Seakeeping

Seakeeping calculations were conducted using the University of Michigan's in house Seakeeping Prediction Program (SPP). SPP utilizes the five-degree of freedom SCORES program using strip theory. SPP was chosen for use because of its fast run speed and because detailed hull geometry is not required for the analysis. This research prioritized identifying how early stage design calculations would lead to a final human performance, thus tools chosen needed to require only the minimum information known at the early design stage, *Parsons, et al. (1998)*.

The Pierson-Moskowitz spectrum was chosen as the wave spectrum to be used in the analysis. 0.3 Hz to 3.0 Hz were used as bounding frequencies during calculations in order to capture the energy within the Pierson-Moskowitz spectrum. Analysis was performed on seas from Sea State 0 through Sea State 6. Sea State 6 served as the upper limit for calculations as beyond Sea State 6, analysis of human performance is trivial and sure to lead to poor performance. The Beaufort scale of Sea States was used for analysis. Sea State vs. wind, significant wave height, wave period, and wavelength can be found in Table 1, *Newman (1977)*.

Table 1: Beaufort Scale of Sea States

SS	Wind Speed	$H_{1/3}$	T_{MP}	Wave Length
2	10 kn	0.6 m	2.7 s	22 m
4	20 kn	2.2 m	5.3 s	89 m
6	30 kn	5.0 m	8.0 s	200 m
7	40 kn	8.9 m	10.7 s	355 m
8	50 kn	13.9 m	13.4 s	554 m

SPP requires the user to input: length, beam, draft, prismatic coefficient, maximum section coefficient, waterplane coefficient, longitudinal center of buoyancy, longitudinal center of flotation, displacement, vertical center of gravity, % parallel midbody, roll radius of gyration (K_{11}), desired wave spectrum specific parameters, and evaluation frequency. Fewer parameters are required if detailed hull geometry is available. Where parameters were unavailable, best engineering judgement is to be used.

2.3. Human Performance

In the development of this research program the team wanted to include Human Factors to the optimization process, addressing one of the three possible areas which in accordance with the information reviewed in documents by ASTM, ABS, IMO, ISO, RINA and the U.S. Navy, were identified to increase crew comfort, reduce crew fatigue and increase their general well-being. The main areas addressed in the standards stated above are:

- Physical environment related to indoor climate, noise, whole body vibrations.
- Material handling which deals with body posture and ergonomics on board.
- Mental Workload, related to the executions of the tasks on board and the accurate response of the crew depending on the conditions.

For the purpose of this study, Mental Workload (MWL) was selected as the main area to investigate. MWL considers that for the personnel on board, a stressor is either high or low mental workload. These stressors lead to a decrease in the performance of the operators, their comfort, and thus the safety of the ship. Important aspects of MWL are shown in Fig. 1.

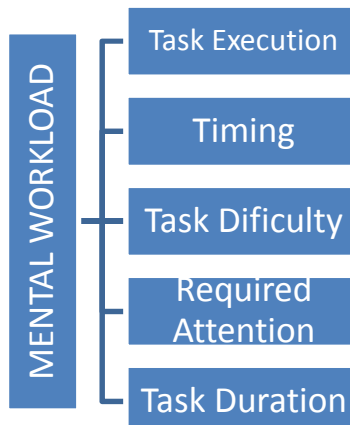


Fig. 1: Mental Workload Categories

MWL has a close connection with fatigue, which is one of the negative results of a poor ship design without ergonomic considerations. Mental fatigue causes some of the following symptoms: shortened attention span, inability to concentrate, decreased vigilance, lethargy, itchy eyes, uneven reaction times, increased difficulty in performing a task effectively, decrease short term memory, micro sleep episodes of up to 15 seconds during which a person uncontrollably falls asleep, impaired decision making skills, moodiness, decreased multitasking ability, and decreased motivation, *BUMED (1989), Calhoun (1999), McCallum (2003), MoDSTD 00-25-17, NAVMED P-6410, Parker (1998), Paul (2001,2003)*. These negative symptoms lead to poor performance and a high risk of accidents. For military ships MWL impacts the ability for the crew to perform missions such as search and rescue, surveillance and warfighting.

On the other hand, among the causes of mental fatigue are issues like bothersome conditions when the workplaces have not been designed with the appropriate environment to perform a task. These issues include: being too noisy, poor visibility, or high vibrations. In the same way, boredom and mental under-load produced for a very low level of stimulation especially when the interaction with the equipment or other members of the crew is little, will cause a significant decrease in the alertness and in the response time of the operators in the moment of a sudden emergency situation. Emergencies on board and bad weather (e.g. severe storms) are situations that will cause mental overload.

Current early stage design methods do not provide designers solutions that enable them to mitigate the negative effects that increase mental fatigue. Naval Architects need to understand the implications of the hull design decisions and its impact on motions on the crew. Some of these issues can be

mitigated by placing working areas near the center of the ships for reduced accelerations or far from the machinery rooms for issues such as high temperatures and noise. All spaces should be designed with enough lighting, good HVAC system, and appropriate thermal and acoustic insulation, Ross (2009). While rule-of-thumb information exists they are not often used and require the designer to have knowledge in these areas. The method created puts these concerns into the hands of less experienced designers or even experienced designers that have not designed many heavily crewed vessels.

For this project, several MWL measurement tools were reviewed in order to identify how they are already applied in different fields including for: pilots, drivers, astronauts, and military personnel. There are several ways to measure MWL, the team reviewed the most common types of evaluations as follows:

- Subjective assessment techniques and self-report measures
- Physiological measures: where some functions of the human body like heart rate, blood pressure, eye movement, respiration and pupil diameter are assessed in order to find some answers.

For the purpose of this study the physiological measures technique was discarded since this research did not intend to study the clinical aspects of the Mental Workload of the members of the crew. On the contrary the information of the self-report measures was considered useful to obtain a real context and to understand all the design implications of this research.

Several techniques are available to measure mental effort through self-report techniques. This project focuses on only two of the most common: Subjective Workload Assessment Technique (SWAT) and the NASA Task Load Index (NASA-TLX), both were reviewed in order to select the conditions that will apply on board.

In the SWAT technique, three different aspects are covered, all of them were considered to be included in the simulations as follows:

- (1) Time load, which reflects the amount of spare time available in planning, executing, and monitoring a task;
- (2) Mental effort load, which assesses how much conscious mental effort and planning are required to perform a task;
- (3) Psychological stress load, which measures the amounts of risk, confusion, frustration, and anxiety associated with task performance.

From the NASA-TLX, only two out of five factors were selected, these are: (1) physical demand regarding all the required activities and their level of difficulty and (2) temporal demand, related to the pace of the task (slow or rapid) and the time pressure experienced by the crew members.

Table 2: Expert opinion determined human factor effectiveness values for given operational stances.
Each Category is Evaluated out of a 20 for Maximum Effectiveness where the larger the number the more effective the human is.

	Baseline Operations	Heightened Operations	Slow Operations
Time Demand	20	8	20
Mental Demand	10	5	19
Physiological Demand	18	4	20
Temporal Demand	15	5	19
Physical Demand	15	7	5

The team used the expert opinion of Mrs. Angela Lossa, former Director of the Research Program in Ergonomics and Human Factors in Cotecmar Shipyard (Colombia 2006-2012) in order to determine reasonable human performance effectiveness values for each of the five factors evaluated. Table 2 shows these values that were input into the fuzzy logic human performance vs. Sea State system.

2.4 Fuzzy Logic

Prior work completed at the University of Michigan use a Fuzzy Logic System to decouple difficult and complex coupling issues associated with heave, pitch and roll. *Cuneo (2013)* included a Fuzzy Logic system in order to incorporate the outputs from the sub functions of the objective function into a useable and relatable output that enabled the evaluation of seasickness into early stage design.

2.4.1 Seakeeping Fuzzy Logic System

In the research presented, first seakeeping output motions are fed into a seakeeping fuzzy logic system. The goal of the seakeeping fuzzy logic system is to merge coupled motions. Motions in heave, pitch, and roll were evaluated with respect to membership functions. In general, heave is used traditionally as the standard for seasickness. However, in addition to providing for poor working conditions, when coupled heave, pitch, and roll can cause seasickness even then the individual motions do not, *Wertheim (1998)*.

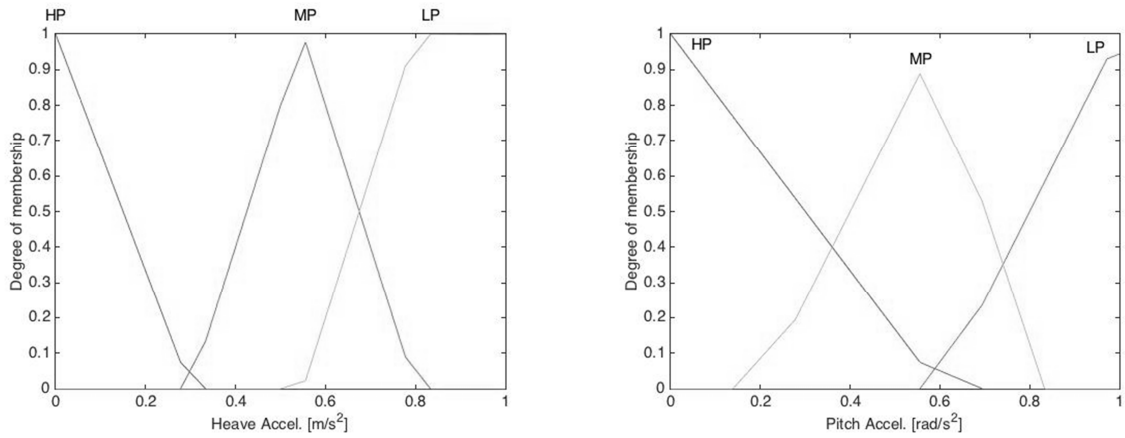


Fig. 2: (L) Heave seakeeping fuzzy logic input membership functions. (R) Pitch and roll fuzzy logic input membership functions.

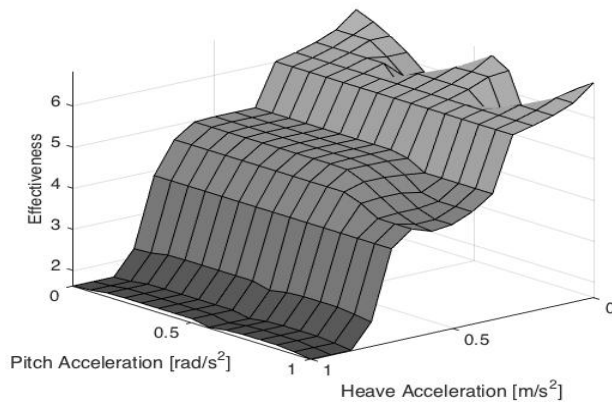


Fig. 3: Rule evaluation for heave, pitch, and roll accelerations vs. effectiveness

As heave, pitch, and roll, are each important in the analysis but evaluating these coupled motions can prove to be difficult. Fuzzy Logic provides the ability to emulate the impacts of coupled motions without having to solve the coupled motions problem. Fig. 2 provides an example of a fuzzy logic

heave input membership functions. There are three membership functions in this example: One where heave accelerations are less than 0.33, a second where heave accelerations between 0.28 and 0.82, and one where heave accelerations greater than 0.5. In this example the first membership function is given high preference, the second is given a medium preference, and the third is given the lowest preference. These preference function assignments relate to the potential for extreme coupling activities. The ranges and shape of each individual membership functions were created using human expert opinion of coupling effects.

After fuzzification of input parameters to the seakeeping factor model, the system was evaluated according to the Fuzzy Logic rule surface shown in Fig. 3. Maximum values on this surface are preferred as they indicate the least coupled motion. Seakeeping output effectiveness was generated on a 0-10 scale following evaluation of the fuzzy logic rule surface where 10 is of highest preference for lowest motion and 0 is lowest preference. Fig. 4 shows the output membership function used to generate a crisp overall seakeeping value.

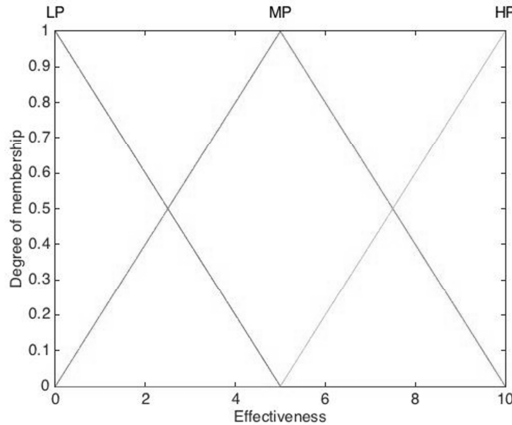


Fig. 4: Seakeeping Fuzzy Logic system output membership function

2.4.2 Human Factors Fuzzy Logic System

The human factors fuzzy logic models were developed to input the crisp seakeeping effectiveness value and an individual human factor value based on present vessel operational stance (baseline, heightened, slow). In total, five fuzzy logic human factor models were developed: time demand, mental demand, physiological demand, temporal demand, and physical workload. All five human factor models used the same membership functions to enable fuzzification. Fig. 5L shows a sample human factor input membership function. Fig. 5R shows the input membership function for seakeeping effectiveness generated as the result of the seakeeping fuzzy logic system.

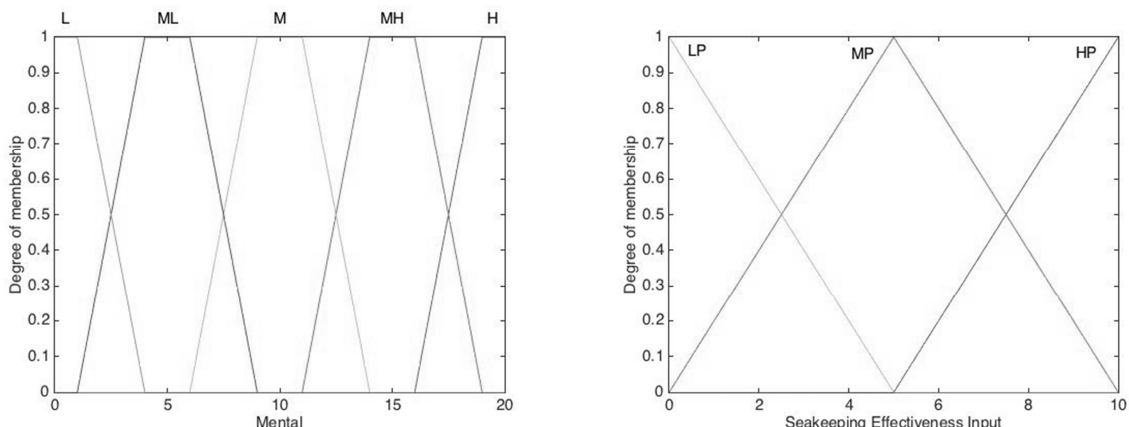


Fig. 5: (L) Sample human factor membership function, (R) Seakeeping effectiveness input membership function

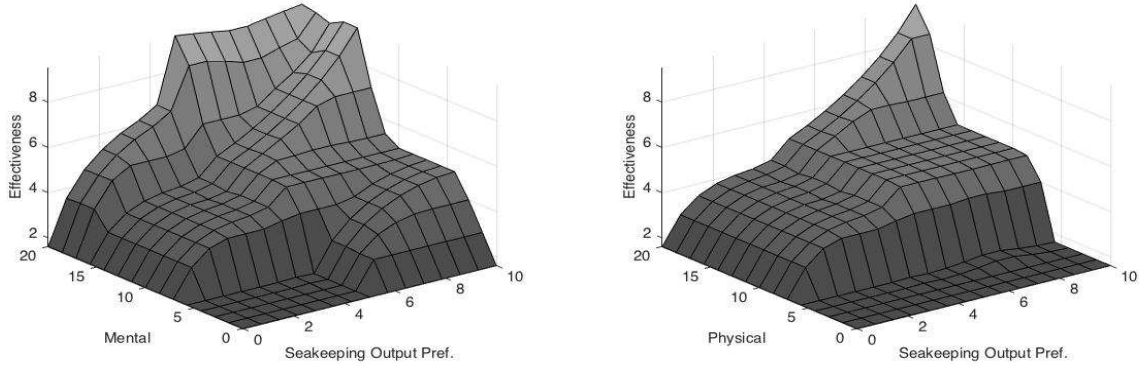


Fig. 6: (L) Fuzzy logic rule surface for mental workload vs. vessel seakeeping response. (R) Rule surface for physical workload vs. vessel seakeeping response

After fuzzification of input parameters to the human factor models, human factors were evaluated according to the Fuzzy Logic rule surfaces. Two of the surfaces are shown as a sample in Fig. 6. Finally, all human factor fuzzy logic models were evaluated to generate crisp output values. The geometric mean was then taken of all of the crisp outputs to generate an overall human performance metric on a 1 to 10 scale.

2.5 Particle Swarm Optimization

A single objective optimization using multiple criteria was conducted utilizing a Particle Swarm Optimization (PSO). Human performance at a given heading was used as the objective to be optimized. Multiple criteria are present with the single objective optimization as the human performance is derived from both the operational stance of the vessel as well as the seakeeping performance. The operational stance of the vessel and the seakeeping performance of the vessel were taken into account in the fuzzy logic system to create the overall human performance value fed into the optimizer.

MATLAB's PSO was used to conduct the optimization. For the optimization, heading was used as a dynamic variable and Sea State was a static variable. Sea State was pre-defined for each run of the optimization in order to provide better resolution into the results. To initialize a PSO, an initial random population is generated where each individual is assigned a velocity. Each of the members of the population is then computed with the objective function. The algorithm continues until the population converges. Velocity for the particles is generated according to the following equation

$$\begin{aligned} v &= W * v + y_1 * u_1 * (p - x) + y_2 * u_2 * (g - x) \\ x &= x + v \end{aligned}$$

Where x is the particle's current position, W is the inertia of the particle, y_1 is the self-adjusted weight of the particle, y_2 is the social adjusted weight of the particle, $(p-x)$ is defined as the difference between the particle's current location and the best location it has seen, $(g-x)$ is defined as the difference between the particle's current position and the best position in the particle's current area, and v is the particle's newly calculated velocity. Large values of the y_1 term will encourage the particle to head toward the best place it has already traveled and large values of the y_2 term will encourage the particle to head toward the best position in the particle's current area. Finally, the particle's position is updated using the new v and the process is repeated (Mathworks). The algorithm continues to progress until relative change between the best objective function value is minimal.

3. Case Study

A case study was developed to demonstrate with the algorithm and method described. The case study conducted analysis of a small fast combatant vessel which is likely to be traveling at speed during

times which Sea States and human performance become vital aspects of the vessel's ability to do its mission. To account for real environments the vessel could encounter, a hybrid between the SWAT and NASA-TLX human factor evaluation methods were chosen. These factors were computed across all chosen Sea States.

Vessel motions increase drastically beyond Sea State 6. As such, results of the analysis would become uninteresting beyond this point. Therefore, Sea State 6 served as an upper bound to this research. The notional fast combatant chosen for analysis had the following key parameters shown in Table 3.

Table 3: Key Parameters for Analysis Vessel

Length	108.90 m	V_{sprint}	28 kn
Beam	14.75 m	C_B	0.6
Δ	3813 t	C_P	0.6
Draft	3.80 m		

In order for simplicity of calculations, several parameters were estimated from *Parsons (2007)*. These estimated parameters included: the vertical center of gravity (VCG), roll radius of gyration (k_{11}), and water plane coefficient.

$$VCG = 1.1 \times T$$

$$K_{11} = \frac{1}{2} \left(0.746 + 0.046 \left(\frac{B}{T} \right) - 0.086 \left(\frac{L}{100} \right) \right) \times B$$

$$C_{wp} = \frac{C_b}{0.471 + 0.551 * C_B}$$

The optimization was then conducted in order to identify which heading produced the optimal human performance metric and thus the true operational performance of the vessel.

4. Results / Conclusions

The results from the 28 knot analysis of operations in Sea State 0, 2, 4, and 6 show that a maximum human performance value of 7.1/10 is found at Sea State 0 under standard baseline operations. The Sea State 0 baseline operation case can be seen in Fig. 7L. At Sea State 0 under “slow operations” human performance is not the maximum and is in fact 5% lower, 6.68/10, than in the baseline operations condition. The Sea State 0 slow operations human performance can be seen in Fig. 7R

On the surface it is not intuitive that lesser workload produces lesser human performance as in the case of slow operations. As was explained in the human factors methodology section, when an individual is bored or trying to keep themselves occupied because no work is present, it becomes difficult for the sailor to focus and successfully do their job and accomplish his or her part of the mission. This results in a crew wide reduction in performance.

Sea State 4 operations, shown in Fig. 8, show the influence of how motions at different headings influence the overall human performance. Fig. 8R shows that the heightened operational stance has a overall subtraction effect on the human performance values. However, waves from astern in the 0°-40° have the largest heightened operations human performance values. These larger human performance values at these headings are due to relative magnitudes of the heave, pitch, and roll motions being smaller. The beam sea headings at this Sea States have large heave and roll motions thereby reducing the performance value.

Sea State 6 analysis shows an even further reduction of human performance than when compared with Sea State 4. At Sea State 6, vessel motions become severe enough that effectiveness in the baseline operational stance is condensed to a value of 4.3/10, 40% less than baseline operations at Sea State 0. Fig. 9 shows the Sea State 6 baseline human performance.

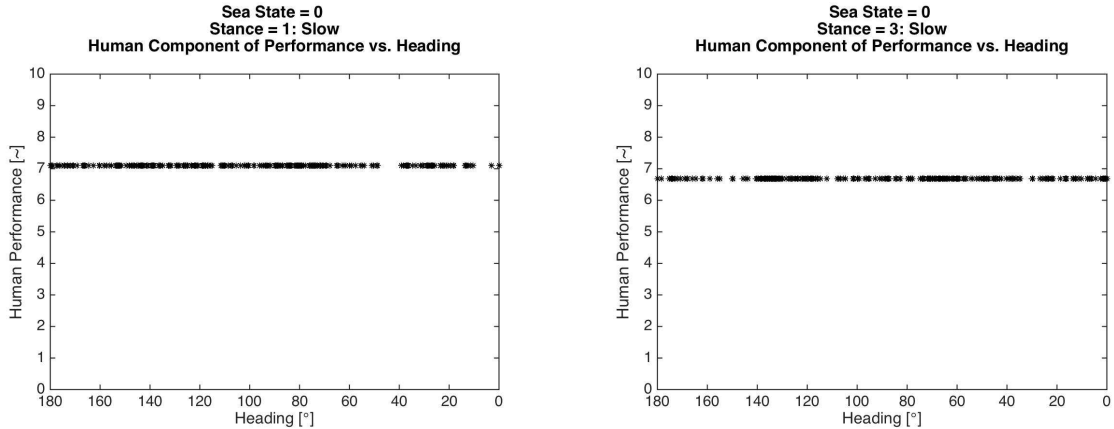


Fig. 7: Zero wave condition, results as expected (L) baseline operations. (R) Slow operations.

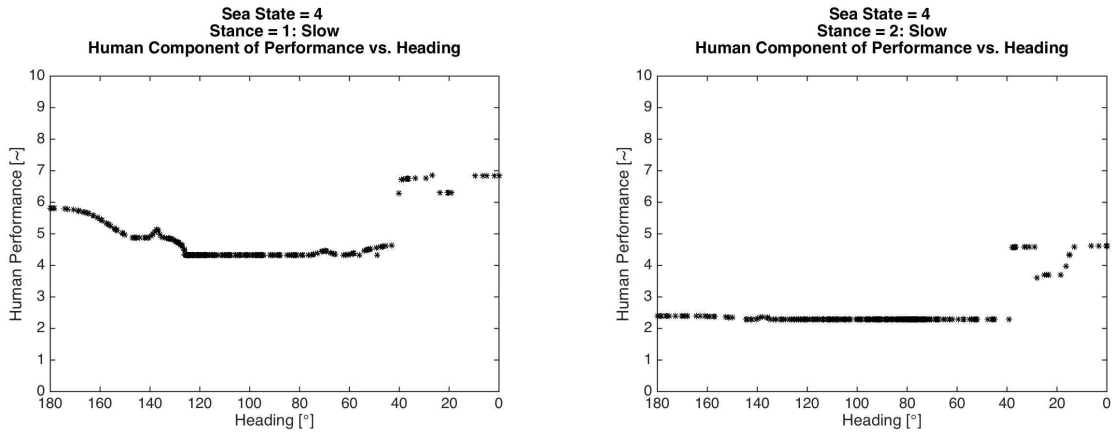


Fig. 8: Sea State 4 Operational Conditions. (L) Shows Baseline Operational Stance. (R) Shows Heighted Operational Stance.

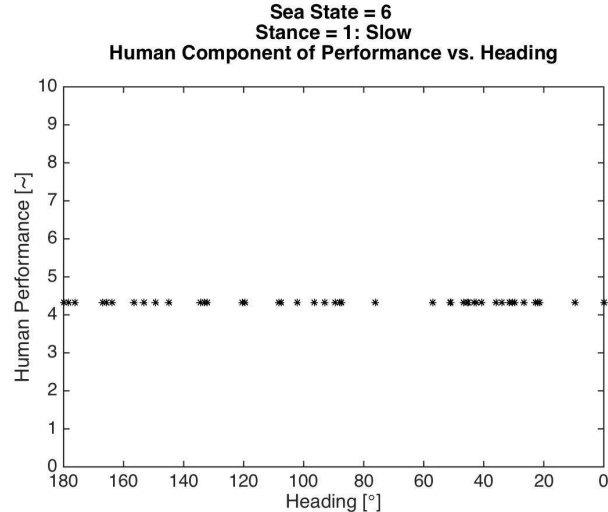


Fig. 9: Sea State 6 Baseline Human Performance

5. Conclusion

Sailing at different headings during increasing Sea States can have a large impact on overall human performance on board the vessel. Ships regularly travel in seaways with varying Sea State conditions and in the past, little attention has been paid in the early stage design process to how vessel motions will affect crew operations in other than calm water. This paper conducted an analysis on a notional

small fast combatant vessel in order to identify how the human component is affected at varying Sea States and with varying operational stances and thus providing an evaluation of the true total performance of the vessel.

Future work for this project includes diving deeper into how changes in the principal dimensions affects overall vessel performance and human operations. Additionally, a sensitivity analysis should be conducted on the input stance criteria used in the analysis. Since this data was derived generally from expert opinion, changing it will likely affect the final results. The current data, however, provides a starting point from which different vessel designs/speeds can be compared in order provide better insight and understanding into what the sailors are enduring on the deck plates.

References

- ABS (2014), *Guidance Notes on The Application of Ergonomics to Marine Systems*, ABS Publ. 86
- BAKER, C.C.; McCAFFERTY, D.B. (2005), *Accident database review of human element concerns: What do the results mean for classification?*, Human Factor in Ship Design, Safety and Operations Symp., London
- BUMED (1989), *U.S. Naval Fight Surgeon's Manual*, Bureau of Med. and Surgery, Dept of the Navy
- CALHOUN, S.R. (1999), *Human factors in ship design: preventing and reducing shipboard operator fatigue*, NAME, University of Michigan
- CUNEO, B.J. (2013), *Development of a human centric multidisciplinary design optimization method using fuzzy logic systems and controllers*, PhD Thesis, University of Michigan
- The Mathworks Inc. (2016), *Particle Swarm Optimization Algorithm*, The Mathworks Inc. Web
- McCALLUM, M.; SANQUIST, T.; MITLER, M.; KRUEGER, G. (2003), *Commercial Transportation Operator Fatigue Management Reference*, U.S. Dept. Transportation Research and Special Programs Administration
- MoD STD 00-25-19 (2004), *Human factors for designers of systems: Personnel domain – Technical guidance and data*, Defence Standard 00-25 Part 17, Issue 1, Ministry of Defence
- NEWMAN, J. N. (1977), *Marine Hydrodynamics*, MIT Press
- PARKER, A.W.; HUBINGER (1998), *On tour analyses of the work and rest patterns of Great Barrier Reef pilots: Implications for fatigue management*, Australian Maritime Safety Authority
- PARSONS, M.G. (2007), *University of Michigan NA 470 Course Pack*, Univ. of Michigan
- PARSONS, M.G.; LI, J.; SINGER, D.J. (1998), *Michigan conceptual ship design software environment - User's manuals*, Rep. 338, Dept NAME, Univ. of Michigan
- RAO, S.S. (2009), *Engineering Optimization: Theory and Practice*, John Wiley
- RIGTERINK, D.; PIKS, R.; SINGER, D.J. (2014), *The use of network theory to model disparate ship design information*, Int. J. Naval Architecture and Ocean Engineering 6, pp.484-495
- ROSS, J. (2009), *Human Factors for Naval Marine Vehicle Design and Operation*, Ashgate
- WICKENS, C.D.; LEE, J.D.; LIU, Y. (2003), *An Introduction to Human Factors Engineering*, Prentice Hall

Index by Authors

Amaya	401	Garcia	84	Ortiz	84
Andrews	339	Gaspar	410	Patterson	186
Andric	458	Gentile	146	Pawling	339
Ang	264	Gentzsch	218	Perera	361
Bernhard	84	Gernez	392	Perez	19
Berrini	255	Goh	264	Pinardi	161
Bertram	33	Gordon	387	Piperakis	339
Bhuiyan	280	Gunnsteinsson	471	Prebeg	458
Bibuli	99	Haraldsson	302	Purwanto	218
Bonnin	84	Harries	204	Ramsden	439
Bons	420	Heilig	110	Ranieri	99
Borresen	392	Heslop	240	Renton	280
Bradbury	75	Hijazi	288	Reyer	218
Britton	130	Hopman	130	Rødseth	361
Broerstrup	204	Husteli	448	Roermond	439
Bruschi	146	Ivancsics	316	Roskilly	240
Bruzzone	99	Jamt	448	Roth	195
Button	75	Jean	255	Roux	255
Caccia	99	Jensen	51	Rudan	458
Caharija	280	Koch	84	Sabra	130
Campana	8	Korbetis	374	Saggini	99
Carter	280	Lelliot	439	Sayers	353
Chatzimoisiadis	374	Li	264	Sciberras	240
Chaves	410	Lind	302	Serani	8
Chiarelli	99	Lossa	481	Singer	481
Clausen	471	Ludvigsen	448	Siwe	302
Cleophas	316	Lundh	123	Smith	280
Company	84	Lützen	51	Smogeli	448
Coppini	161	MacKinnon	75,123	Stern	8
Coraddu	316	MacPherson	204	Stewart	172
Daeffler	130	Mallam	123	Thomason	439
Dalén	302	Mallol	33	Thomson	387
Dalhaug	42	Mannarini	161	Vatteroni	64
Danese	223	Matsuo	234	Vichi	146
Dausendschön	331	Mediavilla	280	Vindoy	42
Del Toro	33	Mellegård	302	Voß	110
De Masi	146	Merad	288	Vugt	240
De Nucci	130	Mestl	331	Waldie	223
De Vries	240	Mikkelsen	51	Webb	186
Diez	8	Mo	361	Wirdum	420
Drap	288	Morais	223	Yoshida	401
Drougkas	374	Mourrain	255	Zereik	99
Dudka	204	Naeem	280	Zerem	302
Duncan	172	Natarajan	84		
Etienne	353	Nawaf	288		
Fireman	481	Nordby	392		
Fontaine	255	Odetti	99		
Furustam	430	Oneto	316		
Gabetta	146	Orihara	401		

16th Conference on
Computer Applications and Information Technology in the Maritime Industries
COMPIT'17
Cardiff / UK, 15-17 May 2017

Topics: Artificial Intelligence / CAX Techniques / PLM / Decision Support Systems / Simulations / Robotics / Virtual & Augmented Reality / Web Technology / Big Data
In Design, Production and Operation of Maritime Systems

Organiser: Volker Bertram (volker.bertram@dnvgl.com)

Advisory Committee:

Volker Bertram	Tutech, Germany	Stein Ove Erikstad	NTNU, Norway	Darren Larkins	SSI, Canada
Marcus Bole	AVEVA, UK	Augusto Gomez	SENER, Spain	Samuel Saltiel	BETA CAE Systems, Greece
Andrea Caiti	Univ Pisa, Italy	Michael Harper	ONR Global, UK	Giampiero Soncini	SpecTec, Cyprus
Nick Danese	NDAR, France	Stefan Harries	Friendship Systems, Germany	Bastiaan Veele	SARC, Netherlands

Venue: The conference will be held at the Angel Hotel in Cardiff; conference dinner in Cardiff Castle



Format: Papers to the above topics are invited and will be selected by a committee. There will be hard-cover black+white book with ISBN produced in addition to the online pdf version in colour. Papers may have up to 15 pages.

Deadlines: anytime Optional “early warning” of intent to submit paper
19.12.2016 First round of abstract selection (1/3 of available slots)
20.1.2017 **Final round of abstract selection** (remaining 2/3 of slots)
25.3.2017 Payment due for authors
25.3.2017 Final papers due (50 € surcharge for late submission)

Fees: **600 € / 300 €** regular / PhD student – early registration (by 25.3.2017)
700 € / 350 € regular / PhD student – late registration

Fees are subject to VAT (reverse charge mechanism in Europe)
Fees include proceedings, lunches, coffee breaks and conference dinner

Sponsors: Aveva, Beta CAE Systems, CD-adapco, DNV GL, Sener, SpecTec, SSI
(further sponsors to be announced)

Information: www.compit.info